frontiers | Research Topics

Optimized gene-engineering and combination therapies to boost γδt cell immunotherapeutic performance

Edited by
Jonathan Fisher, Daniel Abate-Daga and Marta Barisa

Published in
Frontiers in Immunology

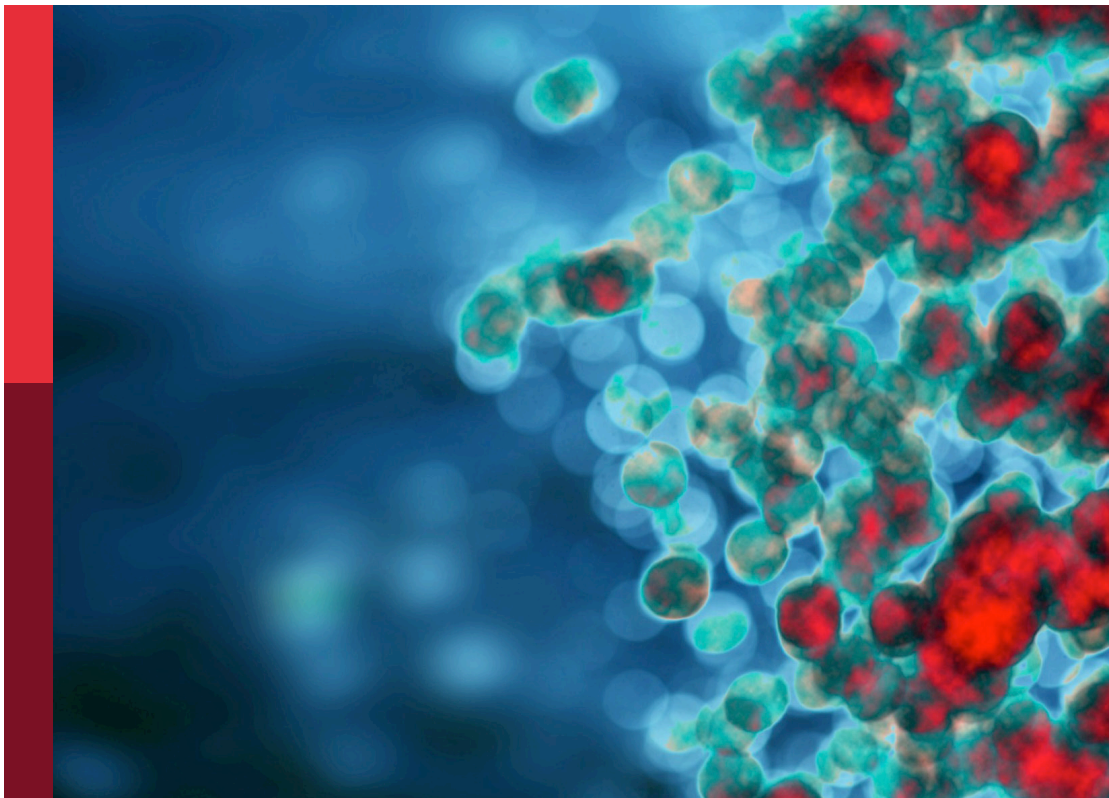

ISSN 1664-8714
ISBN 978-2-8325-4842-4
DOI 10.3389/978-2-8325-4842-4

About Frontiers

Frontiers is more than just an open access publisher of scholarly articles: it is a pioneering approach to the world of academia, radically improving the way scholarly research is managed. The grand vision of Frontiers is a world where all people have an equal opportunity to seek, share and generate knowledge. Frontiers provides immediate and permanent online open access to all its publications, but this alone is not enough to realize our grand goals.

Frontiers journal series

The Frontiers journal series is a multi-tier and interdisciplinary set of open-access, online journals, promising a paradigm shift from the current review, selection and dissemination processes in academic publishing. All Frontiers journals are driven by researchers for researchers; therefore, they constitute a service to the scholarly community. At the same time, the *Frontiers journal series* operates on a revolutionary invention, the tiered publishing system, initially addressing specific communities of scholars, and gradually climbing up to broader public understanding, thus serving the interests of the lay society, too.

Dedication to quality

Each Frontiers article is a landmark of the highest quality, thanks to genuinely collaborative interactions between authors and review editors, who include some of the world's best academicians. Research must be certified by peers before entering a stream of knowledge that may eventually reach the public - and shape society; therefore, Frontiers only applies the most rigorous and unbiased reviews. Frontiers revolutionizes research publishing by freely delivering the most outstanding research, evaluated with no bias from both the academic and social point of view. By applying the most advanced information technologies, Frontiers is catapulting scholarly publishing into a new generation.

What are Frontiers Research Topics?

Frontiers Research Topics are very popular trademarks of the *Frontiers journals series*: they are collections of at least ten articles, all centered on a particular subject. With their unique mix of varied contributions from Original Research to Review Articles, Frontiers Research Topics unify the most influential researchers, the latest key findings and historical advances in a hot research area.

Find out more on how to host your own Frontiers Research Topic or contribute to one as an author by contacting the Frontiers editorial office: frontiersin.org/about/contact

Optimized gene-engineering and combination therapies to boost γδt cell immunotherapeutic performance

Topic editors

Jonathan Fisher — University College London, United Kingdom

Daniel Abate-Daga — Department of Immunology, Moffitt Cancer Center, United States

Marta Barisa — University College London, United Kingdom

Citation

Fisher, J., Abate-Daga, D., Barisa, M., eds. (2024). *Optimized gene-engineering and combination therapies to boost γδt cell immunotherapeutic performance*. Lausanne: Frontiers Media SA. doi: 10.3389/978-2-8325-4842-4

Table of contents

frontiers | Frontiers in Immunology

TYPE Editorial
PUBLISHED 18 April 2024
DOI 10.3389/fimmu.2024.1414812

OPEN ACCESS

EDITED AND REVIEWED BY
Peter Brossart,
University of Bonn, Germany

*CORRESPONDENCE
Marta Barisa
m.barisa@ucl.ac.uk

RECEIVED 09 April 2024
ACCEPTED 10 April 2024
PUBLISHED 18 April 2024

CITATION
Barisa M, Abate-Daga D and Fisher J (2024) Editorial: Optimized gene-engineering and combination therapies to boost γδT cell immunotherapeutic performance. *Front. Immunol.* 15:1414812. doi: 10.3389/fimmu.2024.1414812

Editorial: Optimized gene-engineering and combination therapies to boost γδT cell immunotherapeutic performance

Marta Barisa[1]*, Daniel Abate-Daga[2] and Jonathan Fisher[1]

[1]Developmental Biology & Cancer Department, University College London Great Ormond Street Institute of Child Health, University College London, London, United Kingdom, [2]Department of Immunology, H. Lee Moffitt Cancer Center & Research Institute, Tampa, FL, United States

KEYWORDS

γδT cell, immunotherapy, oncology, CAR-T, BiTe, checkpoint blockade (ICB) therapy

Editorial on the Research Topic
Optimized gene-engineering and combination therapies to boost γδT cell immunotherapeutic performance

This collection of original research articles, reviews and perspectives summarizes the state-of-the-art in γδT cell immunotherapy, and examines it in the broader context of allogeneic chimeric antigen receptor (CAR-T) therapies for cancer. The topics covered include a review of specific γδT cell clinical trials, alone or in the context of alternative allogeneic cellular immunotherapy approaches, and a range of pre-clinical studies that focus on γδT cell combination with checkpoint blockade, modulators of the cholesterol biosynthesis pathway, bispecific T cell engagers (BiTes), angiogenic blockers, as well as γδT cell therapeutic homing, enhanced methods of γδT cell product manufacture, and, finally, an overview of the latest in γδT cell synthetic engineering.

Interest in cancer immunotherapy using non-canonical lymphocytes has grown steadily since the early 2000s (1, 2). Much of this interest is driven by the perception of specific limitations of the more widely adopted gene-modified αβT cell therapies (3), which have produced transformative shifts in the treatment of $CD19^+$ and $BCMA^+$ B cell malignancies, but have yet to produce similar breakthroughs in the treatment of other leukaemia types or solid tumours. Additionally, the major histocompatibility complex (MHC) recognition-driven alloreactivity of peripheral αβT cells has restricted their use predominantly to autologous adoptive transfer, which is accompanied by high cost and complex logistics of product manufacture (4).

γδT cells, natural killer T cells (NKT) and NK cells are all alternative cytotoxic lymphocyte (CTL) sources that are MHC non-restricted and do not cause graft *versus* host disease (GvHD). All are further easily accessible in the peripheral blood of healthy donors, from which they can be expanded and genetically modified using GMP-compatible methods. γδT cells offer a particularly attractive route for cellular immunotherapy development, as their phenotype combines features of a range of the afore-mentioned cells. Like classical αβT cells as well as NKT cells, γδT cells express a T cell receptor (TCR). What defines the γδT cell subset is its expression of TCRγ/δ as opposed to TCRα/β heterodimers. While different TCRγ/δ clones have been found to engage various atypical

MHCs loaded with sulfatide or lipid antigens, as well as butyrophilin and butyrophilin-like molecules, TCRγ/δ biology and ligand recognition remain poorly understood (5).

In addition to the TCR, γδT cells express a range of receptors that are also expressed by NK cells. These are activated by ligand patterns of cellular stress and transformation, and include NKG2D, DNAM-1, NKp30 and NKp44. Both NK and γδT cells can further express receptors that engage humoral immunity, including Fc receptor CD16. Upon target engagement, human γδT cells can exhibit prolific Th1-type cytokine production and cytotoxicity. Murine γδT cells further appear to present with a thymically-determined Th1/Th17 functional dichotomy characterised by IFN-γ and IL-17 production, respectively, though the degree to which this is relevant for primate γδT cell biology remains unknown (6).

Olofsson et al. open this Research Topic by exploring γδT cell anti-tumour functionality in their article on Vγ9Vδ2 cell tumour antigen cross-presentation to αβT cells. Vγ9Vδ2 cells are the most common peripheral γδT cell subset, and their ability to cross-present antigens has been described in several contexts (7, 8). This unique aspect of their biology represents a significant additional route of immune response modulation that γδT cells possess in contrast to αβT cells or NK cells.

Despite this range of features that make them attractive for cellular oncoimmunotherapy, clinical trials testing γδT cell adoptive transfer interventions have produced mixed results. Ling Ma et al. provide a comprehensive overview of the data that has been published on a range of γδT cell adoptive immunotherapy trials. Smirnov et al. then expand on this further with their review, placing γδT cell studies in the broader context of allogeneic CAR-T clinical efforts at large, where γδT cells are considered alongside TCR-knockout or otherwise modified αβT cells, virus-specific CTLs and induced pluripotent stem cells. Lv et al. continue this theme with their review, which explores current approaches to overcome allogeneic cellular immunotherapy GvHD and host rejection. Their review considers γδT cell immunotherapy alongside that of NK cells, NKT cells, mucosal invariant T cells and pluripotent stem cells.

The most sizeable portion of the Research Topic focuses on pre-clinical data reports that examine γδT cell therapeutic combinations. In all cases, the type of γδT cell discussed is the peripherally-dominant Vγ9Vδ2 subset. Liou et al. describe a novel approach to modulating TCR engagement by increasing tumour cell accumulation of the Vγ9Vδ2-TCR ligand, isopentenyl pyrophosphate (IPP). They achieved this by knocking out the IPP-catalyzing enzyme, farnesyl diphosphate synthase, using short-hairpin RNA. This work is followed by a range of studies examining Vγ9Vδ2 cell checkpoint receptor expression and blockade, with a compelling if complex set of results.

Ridgley et al. examined Vγ9Vδ2 T cell checkpoint receptor expression following phosphoantigen challenge, and found that, in the context of their THP-1 acute myeloid leukaemia model, TIM-3, LAG-3 and NKG2A, but not PD-1, were promising targets for checkpoint blockade. Curiously, however, they reported that – despite the substantial upregulation of these receptors upon T cell challenge – the team were unable to identify a cytotoxic or cytokine benefit of applying checkpoint blockers, speculating instead that these may play a more important role in de-repressing T cell proliferation. This was in some contrast to a report by Lui et al., where PD-1 blockade was efficacious at enhancing Vγ9Vδ2 cell immunotherapy against mesothelioma *in vitro* and *in vivo*, especially against PD-L1 high tumours, but not in a manner that was dependent on pyroptosis. Giannotta et al., meanwhile, reported that, in the context of multiple myeloma, PD-1^{+} bone marrow Vγ9Vδ2 T cells exhibited phenotypic, functional alterations that are consistent with chronic exhaustion and immune senescence. Importantly, they found that PD-1, TIM-3 and LAG-3 checkpoints were upregulated on Vγ9Vδ2 cells in a hierarchical manner, and that the blockade of specific combinations of these could exacerbate, rather than rescue, γδT cell dysfunction. Their data indicated that a PD-1/LAG-3 blockade combination is the most effective in the context of multiple myeloma. The group concluded that immune checkpoint blockade should be tailored to the disease to enhance the positive and minimise the negative effects - an observation that is likely relevant for all γδT cell therapeutic combinations.

Yang et al. evaluated Vγ9Vδ2 cell checkpoint interactions in the context of targeting with BiTes, specifically anti-PD-L1 x anti-CD3 BiTes. A therapeutic combination of expanded Vγ9Vδ2 cells with BiTe was efficacious against models of PD-L1-expressing non-small cell lung carcinoma. Branella et al. took an alternative approach to Vγ9Vδ2 cell BiTes. The group developed an acute myeloid leukaemia-targeting CAR-γδT cell that also secreted a BiTe against c-kit, both knocked in via transient transfection. The CAR/BiTe-modified γδT cells moderately extended survival of NSG mice engrafted with disseminated AML, but therapeutic efficacy was limited by a lack of γδT cell homing to murine bone marrow. This report was followed by a second report from the same group (Trent Spencer, Emory), where Parwani et al. examined the lack of Vγ9Vδ2 cell homing to NSG mouse bone marrow in greater detail. Interestingly, while they showed that total body irradiation of the animals could increase human γδT cell migration to the bone marrow, this was passive accumulation rather than homing. γδT cell homing could be induced by providing sources of CCL-2 within the tumour microenvironment.

Bold et al. reported a new way to manufacture Vγ9Vδ2 cells in a GMP-compatible manner, by switching from RPMI1640-based media to CTS OpTmizer-based media, and increasing both zoledronic acid and IL-2 concentrations, as well as extending expansion period, in order to achieve greater cytotoxic efficacy of their products.

Zhang et al. reported an unexpected finding in murine models of breast cancer, whereby low-dose VEGFR2 mAb or VEGFR2-tyrosine kinase inhibitors were efficacious, while high-dose VEGFR2 mAb was not. The mechanism they identified for this was that high-dose anti-VEGFR2 mAb treatment elicited IL-17A expression in resident γδT cells via VEGFR1-PI3K-AKT pathway activation, and that this then promoted N2-like neutrophil polarization and consequent shaping of the tumour microenvironment to a suppressive state. While compelling, given

the species differences, it remains unclear how directly this applies to human γδT cells and breast cancer.

To conclude the Research Topic, Yuan et al. summarize and critically evaluate the latest developments in γδT cell synthetic engineering, covering topics like CAR-T, TCR gene transfer and combination with γδT cell engagers. The team then discuss the implications of these latest engineering strategies, and the challenges that lie ahead for engineered γδT cell monotherapy and combinatorial approaches. As this collection of articles highlights, much exciting pre-clinical and clinical exploration of γδT cell combinatorial and gene-modified approaches is taking place. The coming decade of clinical trial data will shape the direction of the γδT cell immunotherapy field within oncology and beyond.

Author contributions

MB: Writing – original draft, Writing – review & editing. DA-D: Writing – review & editing. JF: Writing – review & editing.

Funding

The author(s) declare financial support was received for the research, authorship, and/or publication of this article. MB is supported by Stand Up To Cancer, the UCL Technology Fund and the UKRI Developmental Pathway Funding Scheme (DPFS). JF is supported by the UCL Technology Fund, the Little Princess Trust, the GOSH Charity, The Wellcome Trust and by a UKRI Future Leaders Fellowship. DA-D is supported by the Moffit Cancer Centre, the NCI, and the NIH.

Conflict of interest

MB, JF, and DA-D are all inventors on patents that pertain to gene-modified cellular immunotherapy development and use. DA-D is a member of the scientific advisory board of Anixa Biosciences and receives or has received research funding from Celgene/BMS, bluebird bio, and Intellia Therapeutics. MB is a member of the scientific advisory board of LAVA Therapeutics.

Publisher's note

References

1. Mensurado S, Blanco-Domínguez R, Silva-Santos B. The emerging roles of γδ T cells in cancer immunotherapy. *Nat Rev Clin Oncol*. (2023) 20(3):178–191. doi: 10.1038/s41571-022-00722-1

2. Dolgin E. Unconventional γδ T cells 'the new black' in cancer therapy. *Nat Biotechnol*. (2022) 40:805–8. doi: 10.1038/s41587-022-01363-6

3. Labanieh L, Mackall CL. CAR immune cells: design principles, resistance and the next generation. *Nature*. (2023) 614:635–48. doi: 10.1038/s41586-023-05707-3

4. Harrison RP, Zylberberg E, Ellison S, Levine BL. Chimeric antigen receptor–T cell therapy manufacturing: modelling the effect of offshore production on aggregate cost of goods. *Cytotherapy*. (2019) 21:224–33. doi: 10.1016/j.jcyt.2019.01.003

5. Willcox BE, Willcox CR. γδ TCR ligands: the quest to solve a 500-million-year-old mystery. *Nat Immunol*. (2019) 20:121–8. doi: 10.1038/s41590-018-0304-y

6. Silva-Santos B, Ribot JC, Adams EJ, Willcox BE, Eberl M. γδ T cell explorations seek terra firma. *Nat Immunol*. (2023) 24:1606–1609. doi: 10.1038/s41590-023-01606-x

7. Brandes M, Willimann K, Bioley G, Levy N, Eberl M, Luo M, et al. Cross-presenting human γδ T cells induce robust CD8+ αβ T cell responses. *Proc Natl Acad Sci*. (2009) 106:2307–12. doi: 10.1073/pnas.0810059106

8. Capsomidis A, Benthall G, Van Acker HH, Fisher J, Kramer AM, Abeln Z, et al. Chimeric antigen receptor-engineered human gamma delta T cells: enhanced cytotoxicity with retention of cross presentation. *Mol Ther*. (2018) 26:354–65. doi: 10.1016/j.ymthe.2017.12.001

frontiers in Immunology

ORIGINAL RESEARCH
published: 10 May 2021
doi: 10.3389/fimmu.2021.654080

Bispecific Antibody PD-L1 x CD3 Boosts the Anti-Tumor Potency of the Expanded Vγ2Vδ2 T Cells

Rui Yang[1,2], Susu Shen[1,2], Cheng Gong[1], Xin Wang[1], Fang Luo[1], Fengyan Luo[1], Yang Lei[1], Zili Wang[1], Shasha Xu[1], Qian Ni[1], Yan Xue[1], Zhen Fu[1], Liang Zeng[1], Lijuan Fang[1], Yongxiang Yan[1], Jing Zhang[1], Lu Gan[2], Jizu Yi[1] and Pengfei Zhou[1]**

[1] Research and Development Department, Wuhan YZY Biopharma Co., Ltd, Wuhan, China, [2] National Engineering Research Center for Nanomedicine, College of Life Science and Technology, Huazhong University of Science and Technology, Wuhan, China

Vγ2Vδ2 T cell-based immunotherapy has benefited some patients in clinical trials, but the overall efficacy is low for solid tumor patients. In this study, a bispecific antibody against both PD-L1 and CD3 (PD-L1 x CD3), Y111, could efficiently bridge T cells and PD-L1 expressing tumor cells. The Y111 prompted fresh CD8+ T cell-mediated lysis of H358 cells, but spared this effect on the fresh Vδ2+ T cells enriched from the same donors, which suggested that Y111 could bypass the anti-tumor capacity of the fresh Vγ2Vδ2 T cells. As the adoptive transfer of the expanded Vγ2Vδ2 T cells was approved to be safe and well-tolerated in clinical trials, we hypothesized that the combination of the expanded Vγ2Vδ2 T cells with the Y111 would provide an alternative approach of immunotherapy. Y111 induced the activation of the expanded Vγ2Vδ2 T cells in a dose-dependent fashion in the presence of PD-L1 positive tumor cells. Moreover, Y111 increased the cytotoxicity of the expanded Vγ2Vδ2 T cells against various NSCLC-derived tumor cell lines with the releases of granzyme B, IFNγ, and TNFα *in vitro*. Meanwhile, the adoptive transferred Vγ2Vδ2 T cells together with the Y111 inhibited the growth of the established xenografts in NPG mice. Taken together, our data suggested a clinical potential for the adoptive transferring the Vγ2Vδ2 T cells with the Y111 to treat PD-L1 positive solid tumors.

Keywords: [CD3xPD-L1], Vγ2Vδ2 T cells, adoptive transfer, immunotherapy, NSCLC

OPEN ACCESS

Edited by:
John - Maher, King's College London, United Kingdom

Reviewed by:
Massimo Fantini, Precision Biologics, Inc., United States
Christian Peters, Christian-Albrechts-Universität, Germany

***Correspondence:**
Pengfei Zhou
pfzhou@yzybio.com
Jizu Yi
yijizu@yzybio.com

Specialty section:
This article was submitted to Cancer Immunity and Immunotherapy, a section of the journal Frontiers in Immunology

Received: *15 January 2021*
Accepted: *26 April 2021*
Published: *10 May 2021*

Citation:
Yang R, Shen S, Gong C, Wang X, Luo F, Luo F, Lei Y, Wang Z, Xu S, Ni Q, Xue Y, Fu Z, Zeng L, Fang L, Yan Y, Zhang J, Gan L, Yi J and Zhou P (2021) Bispecific Antibody PD-L1 x CD3 Boosts the Anti-Tumor Potency of the Expanded Vγ2Vδ2 T Cells. Front. Immunol. 12:654080. doi: 10.3389/fimmu.2021.654080

INTRODUCTION

Vγ2Vδ2 T cells, accounting for about 90% of total γδ T cells in the peripheral bloodstreams of healthy adults, appear to be a fast-acting and non-conventional T-cell population that contributes to both innate and adaptive immune responses to microbial infections and cancers (1). Due to their unique biological functions, Vγ2Vδ2 T cells have been widely used for adoptive cell immunotherapy

Abbreviations: ADCC, antibody-dependent cell-mediated cytotoxicity; ATCC, American Type Culture Collection; BsAb, bispecific antibody; CBA, cytometric bead array; CFSE, carboxyfluorescein succinimidyl ester; EGFR, epidermal growth factor receptor; Fab, antigen-binding fragment; ICS, intracellular cytokine staining; IHC, Immunohistochemistry; IFNγ, interferon Gamma; NPG, NOD.Cg-Prkdc^{scid} IL2rg^{tm1Vst}/Vst; NSCLC, non-small cell lung cancer; PBMCs, peripheral blood mononuclear cells; PD1, programmed cell death protein 1; PD-L1, programmed death-ligand 1; PI, propidium iodide; TNFα, tumor necrosis factor alpha; SDS-PAGE, sodium dodecyl sulfate-polyacrylamide gel electrophoresis; scFv, single-chain variable fragment.

in clinical trials to treat a broad range of cancer patients who have been resistant to the standard therapies (2). In the past decades, the phase I/II clinical trials demonstrated that the adoptive Vγ2Vδ2 T cell-based therapy was safe, but showed limited efficacy (3). The poor infiltration of the transfused Vγ2Vδ2 T cells into the tumor sites and the anti-tumor activities of Vγ2Vδ2 T cells impaired in the tumor microenvironment may cause the failure of the current therapy (4, 5).

There is an unmet need for the development of novel strategies to improve the therapeutic efficiency of the current Vγ2Vδ2 T cell-based immunotherapy (6). Over three decades ago, Ferrini et al. initially proposed the concept that bispecific antibodies (bsAbs) targeting the γδ TCR and a folate binding protein enhanced the cytotoxic activity of the γδ T cells against human ovarian carcinoma cells (7). Several studies exploited the synergic effects of bsAbs and the Vγ2Vδ2 T cells on fighting tumors in recent years. The combination of bispecific antibodies, (Her2 x CD3) or (Her2 x Vγ2) (8, 9), together with the transferred Vγ2Vδ2 T cells in the presence of IL2, achieved a delay in the growth of pancreatic ductal adenocarcinoma tumor in murine models (10). Another bispecific VHH construct (namely 7D12-5GS-6H4), targeting epidermal growth factor receptor (EGFR) and Vδ2-TCR, was also reported to activate Vγ2Vδ2 T cells (11), and to prolong significantly the survival time of xenograft bearing mice in the presence of the transfused Vγ2Vδ2 T cells with the repeated injections of IL2 (12). Moreover, a recent study demonstrated that the combination of anti-Tim3 mAb, T-cell redirecting bispecific antibody MT110 (EpCAM x CD3), and IL2 could further enhance the anti-tumor effects of the transfused Vγ2Vδ2 T cells in tumor-bearing nude mice (13). However, these bispecific molecules were either originally from mice, which raised the risks of the immunogenicity in human beings, or in a form of VHH structure, which could have a short half-life time in the blood (14). Thus, an IgG-like bispecific antibody would display better pharmacokinetics comparing to those antibody fragments. Although these studies showed that the γδ TCR-based bispecific antibodies displayed modest activities of tumor growth inhibitions with the co-administration of IL2 (7–13), these approaches seemed less attractive than the exploring of CD3-targeting bsAbs. We hypothesized that a tumor associated antigen and CD3-targeting bispecific antibody, rather than targeting to only γδ TCR, would enhance the anti-tumor effects of the transfused Vγ2Vδ2 T cells even without administration of phosphoantiens and IL2 into the animals.

Lung cancer is still the leading cause of the deaths of cancer patients worldwide (15). The clinical response rates to the current first or second-line treatment of non-small cell lung cancer (NSCLC) patients, which accounts for approximately 85% of the total lung cancers, are still unsatisfying (16, 17). The adoptive transfer of Vγ2Vδ2 T cells could reduce the growth of NSCLC cell line-derived xenografts and prolong the survival of tumor-bearing mice (18, 19). Yet, this immunotherapy failed in its efficacy evaluation of clinical trials during the past decades (20–22). Meanwhile, the landscape-changing "Magacurve" for advanced NSCLC showed the therapeutic successes of PD1/PD-L1 blockade (23), even though the monotherapy of anti-PD1/PD-L1 mAb resulted in positive response of only ~ 15-30% of NSCLC patients (24). Hence, a combination strategy of the Vγ2Vδ2 T cells-based adoptive transfer therapy together with PD-L1-targeted therapy is worth to be explored for the NSCLC treatment.

In this study, we designed a novel IgG-like bispecific antibody Y111, targeting both PD-L1 and CD3, on the format of Y-body® in which the anti-PD-L1 half antibody maintains its binding affinity to the PD-L1-positive tumor cells while the anti-CD3 scFv may reduce its binding affinity to the T cells (25, 26). Y111 could bridge the T cells and PD-L1 expressing tumor cells, and prompted fresh CD8+ T cell-mediated lysis of H358 cells but spared this effect on the fresh γδ T cells enriched from the same donors, which suggested that Y111 could bypass the anti-tumor capacity of the fresh Vγ2Vδ2 T cells. We then found that Y111 could selectively trigger the activation of the expanded and purified Vγ2Vδ2 T cells dependent on the presence of PD-L1-positive tumor cells. Furthermore, Y111 enhanced the cytotoxicity of Vγ2Vδ2 T cells against various NSCLC cell lines with the secretion of IFNγ, TNFa, and Granzyme B. Furthermore, the combination of Y111 and transfused Vγ2Vδ2 T cells displayed effective inhibitory effects on the growth of the established xenograft in immunodeficient NPG mice. Taken together, our data demonstrated a new strategy for potentially efficient Vγ2Vδ2 T cell-based immunotherapy for NSCLC and other types of cancers.

MATERIALS AND METHODS

Expression and Purification of Bispecific Antibody

The Y111 is a recombinant anti-PD-L1 and anti-CD3 (PD-L1 x CD3) bispecific antibody (**Figure 1A**) generated from the CHO cell expression system. The anti-PD-L1 monovalent unit was from the drug bank website (https://go.drugbank.com/drugs/DB11595). The anti-PD-L1 sequence was reversely translated into the DNA sequence, and the anti-CD3 single-chain DNA sequence was reversely translated from the protein sequences of anti-CD3 monoclonal antibody 2A5 (27). These coding gene sequences were synthesized, inserted into the pEASY-T1 vector (Transgene, Beijing, China), and verified by sequencing the entire vectors by Huada Gene (Wuhan, China). The control molecule, CD3 Isotype, targeting both CD3 and fluorescein [derived from Clone 4-4-20 (28)] was similarly constructed (**Supplementary Figure 1**). Subsequently, these expression vectors were transfected into the CHO cells (Invitrogen, Carsbad, USA) using Fecto PRO Reagent (Ployplus, New York, USA) according to the manufacturer's protocols. After culturing for 7-days, the supernatant was collected and purified serially by Sepharose Fast Flow protein A affinity chromatography column (GE, Milwaukee, USA), Fab Affinity KBP Agarose High Flow Resin (ACROBio systems, Newark, USA), and SP cation exchanged chromatography column (GE, Milwaukee, USA).

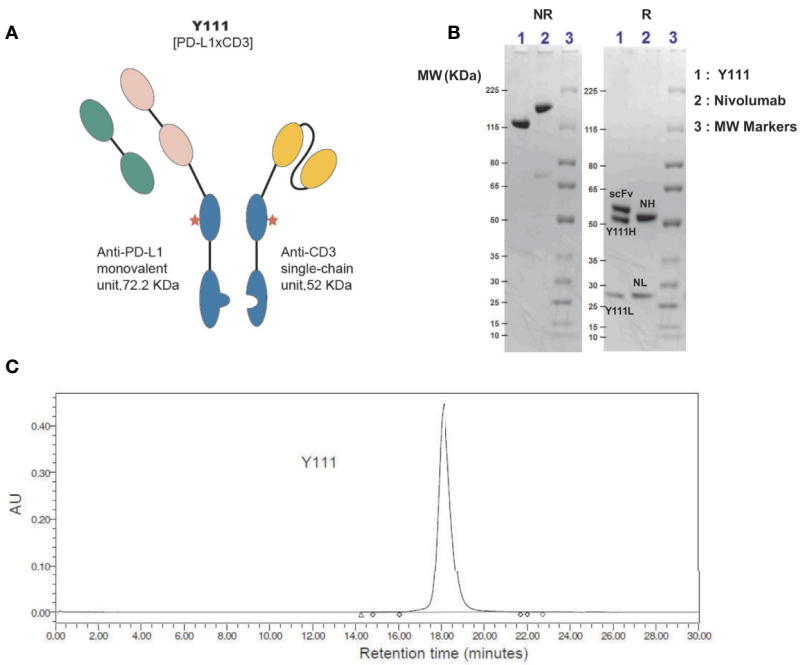

FIGURE 1 | Generation and purification of Y111, a bispecific antibody targeting both CD3 and PD-L1. **(A)** Schematic diagram of bispecific antibody Y111, which consists of a monovalent unit adapted from Tecentriq, a monoclonal antibody targeting PD-L1, and a single-chain variable fragment (scFv) from 2A5 (27), a monoclonal antibody for CD3 activation. The red asterisk indicates N297Q mutation for precluding Fc receptor-mediated crosslinking. **(B)** SDS-PAGE analysis of the purified Y111 under non-reducing (NR, left) and reducing (R, right) conditions. Nivolumab is a monoclonal antibody used as a control. Molecular weight (MW) is indicated in KDa. The MW of Y111 is a little smaller than the monoclonal antibody Nivolumab as indicated from NR gel. There are 3 and 2 bands for Y111and Nivolumab in reducing gel respectively as expected. Please note that the nominal MW of Y111H is 48.850 KDa, Y111L is 23.365 KDa, scFv is 52.057 KDa, and intact Y111 is 124.272 KDa as predicted by their protein sequences. The predicted nominal MW of Nivolumab is 143.597 KDa, the predicted MW of heavy (NH) and light (NL) chain of Nivolumab is 48.422 KDa and 23.359 KDa, respectively. **(C)** Size-exclusion chromatograms of Y111 purified by Protein-A and ion-exchange chromatography. The purity for this Y111 sample is 99.63%.

Cancer Cell Lines

Four human NSCLC cell lines, including NCI-H1975 (human adenocarcinoma epithelial cell line, CRL-5908), NCI-H358 (human lung bronchioalveolar carcinoma cell line, CRL-5807), A549 (human adenocarcinoma epithelial cell line, CRL-185), and NCI-H1299 (human NSCLC metastatic cell line, CRL-5803) were purchased from ATCC. Cells were cultured in RPMI 1640 medium (Gibco, New York, USA) supplemented with 10% FBS (ExCell, Clearwater, USA) except for A549, which was cultured in F-12K medium (Gibco, New York, USA) supplemented with 10% FBS. Before culture, the viability and density of cells were determined by the Vi-Cell counter (Beckman Coulter, Indianapolis, USA). All cell lines in use were routinely tested to make sure free of Mycoplasma infection using a 16s-based PCR kit (Vazyme, Nanjing, China), and new cultures were established monthly from frozen stocks as described previously (29).

Cell Binding and Co-Binding Assays

Cells were incubated in the presence of serially diluted antibodies for 1 hour at room temperature. Subsequently, the cells were washed twice in PBS buffer (PBS+2%FBS+ 2 mM EDTA) and stained for 25 minutes with PE-conjugated anti-human IgG Fc antibody (HP6017, Biolegend, San Diego, USA) diluted in 1:100 into PBS buffer. The bound antibodies were measured using flow cytometry.

To determine the cell-to-cell association mediated by Y111, CFSE-stained H1975 cells were co-cultured with PKH26-labeled Jurkat cells at a ratio of 1:1 with specified concentrations of the Y111 or CD3 Isotype for 1-hour in a 96-well-plate. The samples were measured with a FACSelesta instrument (BD, San Jose, USA) and analyzed with FlowJo software (BD, San Jose, USA). Co-binding% of two cells mediated by bispecific antibodies was indicated as the percentages of both CFSE and PKH26 double-positive cells among the total cells.

Ex Vivo Expansion of PBMCs and Purification of Vγ2Vδ2 T Cells and Other T Cell Subsets

Human peripheral blood mononuclear cells (PBMCs) were first isolated from the fresh blood of randomized healthy donors (LDEBIO, Guangzhou, China) by density gradient centrifugation using Ficoll-Hypaque PLUS (GE, Milwaukee, USA). The purified PBMCs were frozen in liquid nitrogen to mimic the clinic situation in which the frozen PBMCs was usually utilized as the starting point for evaluating the anti-cancer efficiency of the Vγ2Vδ2 T cells. After quick thawing, the cell numbers were

counted using AO/PI after staining with Cellometer K2 Fluorescent Cell Viability Counter (Nexcelom Bioscience, Lawrence, USA), and the PBMCs were cultured in RPMI 1640 medium supplemented with 10% FBS, 2.5 μM Zoledronic Acid (Sigma Aldrich, Darmstadt, Germany), and 1000 IU/mL IL2 (Sihuan Pharma, Beijing, China) at 2×10^6 cells/mL seeded in 6-well-plate as described (30). Every 3 days, half the volume of the culture media was removed and replaced with fresh cell-culture media containing 1000 IU/mL IL2. During days 12-14, Vγ2Vδ2 T cells were purified from the expanded PMBCs by negative selection using the TCR γ/δ + T Cell Isolation Kit (Miltenyi Biotech, Teterow, Germany). The Vγ2Vδ2 T cells purity was assessed by flow cytometry, and the purified (>96%) Vγ2Vδ2 T cells were further cultured in RPMI 1640 medium supplemented with 10% FBS overnight for rest. Then, these Vγ2Vδ2 T cells were used for functional analyses by *in vitro* assays and *in vivo* anti-tumor studies (**Supplementary Figure 2**). In some assays, the T cell subsets were purified from freshly-collected PBMC using the respective negative isolation kits (Miltenyi Biotech, Teterow, Germany) according to the manufacturer's instructions.

Intracellular Cytokine Staining (ICS) for T Cell Functional Evaluation

Flow cytometry was performed as described in the previous reports (31, 32). H1975 cells were firstly plated in a 24-wells plate. On the next day, expanded and negatively enriched Vγ2Vδ2 T cells were added into each of the wells with doses of Y111 or CD3 Isotype together with BV510-anti-CD107a (H4A3, Biolegend, San Diego, USA) and BFA (Golgi Plug, BD, San Jose, USA). After co-cultured for 6 hours, the cells were stained with Zombie Fixable Viability Kit (Biolegend, San Diego, USA), followed by incubation with APC-anti-CD3 (SP34-2, BD, San Jose, USA), PE-anti-Vδ2 (B6, Biolegend, San Diego, USA) for 20 min at room temperature in dark. The cells were permeabilized for 30 min at 4 degrees (Cytofix/Cytoperm, BD, San Jose, USA). After wash, the cells were incubated fixation buffer with BV650-anti-IFNγ (4S.B3; Biolegend, San Diego, USA), BV421-anti-TNFα (Mab11, Biolegend, San Diego, USA) for 30 min at room temperature in dark. Then cells were washed and collected by a BD FACSelesta flow cytometry.

In Vitro Tumor Cell Killing Assay

On the first day of the cytotoxicity assay, $2X10^4$ CFSE-labeled target cells were seeded and co-cultured with the enriched- and expanded- Vγ2Vδ2 T cells at an E: T ratio of 1:1, or with the T cell subsets at 1:10 with various doses of indicated antibodies. The cells were incubated at 37°C for 12 h in a humidified CO_2 incubator. Flow cytometry was used to determine antibody-induced cytotoxic activity-mediated by Vγ2Vδ2 T cells. The percentages of CFSE and PI double-positive cells among the total of target cells (CFSE+) were defined as "Cytotoxicity %".

Cytometric Bead Array Method

To measure the cytokines released from Vγ2Vδ2 T cells, the supernatants were harvested from the samples co-cultured with the T cells and tumor cells. Flex Set kits (BD, San Jose, USA) were used to measure the human IFNγ, TNFα, and Granzyme B according to the manufacturer's instructions. To determine the production of cytokines induced by the antibodies, the raw values were subtracted from the values of E+T groups in the absence of the tested antibodies.

In Vivo Mice Tumor Model Analysis

Female Nonobese diabetic/severe combined immunodeficiency mice (NOD. Cg-Prkdc^{scid} IL2rg^{tm1Vst}/Vst, NPG) were obtained from the VITALSTAR (Beijing, China) at ages of 6-8 weeks and housed in the central laboratory in Hubei Province Food and Drug Safety Evaluation Center. 5 x10^6 H1975 cells were injected *s.c.* into NPG mice for xenotransplantation on Day 0. On Day 15 when tumor volumes reached about 220 mm^3, mice were randomly divided into four groups (n = 7 per group). On Day 17, the grouped mice were injected *i.v.* with 1 x10^6 purified Vγ2Vδ2 T cells with 1 mg/kg or 4 mg/kg Y111 or PBS as the control. This injection was repeated on Day 20, 24, and 27 (twice a week for 2 weeks).

For each treatment, the purified Vγ2Vδ2 T cells displayed the mature phenotype of the T cells indicated by that the IL2 treatment increased the expressions of CD86, CD69, and HLA-DR (**Supplementary Figure 2**). Tumor volumes were measured with a digital caliper three times a week and calculated using the formula: Tumor Volume (mm^3) = (a x b^2)/2, where "a" is the longitudinal length and "b" is the transverse width.

IHC Analysis

To assess the infiltration and accumulation of transferred Vγ2Vδ2 T cells *in vivo*, mice were sacrificed on Day 39. The tumor tissues were immediately removed, cut into small pieces, and embedded in 4% paraformaldehyde for fixation. Then these tumor pieces were sectioned, stained staining with a rabbit-anti-human CD3 antibody (SP7, Abcam, Cambridge, USA), and examined on a Nikon microscope (Tokyo, Japan). Positive cells were counted in five randomly selected microscopic fields (magnification 20X) and supplied for further quantification analysis.

Statistical Analyses

Statistical analyses were performed with Prism 6.0 (GraphPad, San Diego, USA) and data were shown as mean± SEM. Non-linear regression methods were applied for analyses of cell binding, co-binding, activation, and cell-based killing activities, and the results were plotted as "Dose-Response Curves". *P* values were assessed by student's t-test, nonparametric Mann–Whitney U test, one-way or two-way ANOVA, and Dunnett test or Tukey multiple comparisons as appropriate. *P* values <0.05 were considered significant.

RESULTS

Characterization of Y111

Y111 (PD-L1 x CD3), a both PD-L1- and CD3-targeting bispecific antibody, that redirected T cells to attack PD-L1-

expressing cancer cells, was designed under the Y-body® platform (25, 26). Y111 consisted of a Fab structure targeting PD-L1, a single-chain variable fragment (scFv) targeting CD3 originated from a monoclonal antibody 2A5 (27) for activating T cells, and a modified Fc region (**Figure 1A**) from human IgG1. The Fc region of Y111 was engineered with the mutations for both "Knob-into-Hole" match for the favorable formation of the heterodimer between the heavy chains and the single chain, and the deficiency of ADCC activity (25). The molecular weight of the Y111 generated from CHO expression was verified by non-reduced and reduced SDS-PAGE analyses (**Figure 1B**). As expected, under reducing conditions the three bands in the gel demonstrated the three chains of Y111, i.e., heavy chain (Y111H: ~ 52 kDa), light chain (Y111L: ~ 28 kDa), and single-chain (scFv: ~ 57 kDa) (**Figure 1B**), while a monoclonal antibody Nivolumab displayed two bands consisting of the heavy (NH) and light (NL) chains (**Figure 1B**). The purity of the Y111 was determined by size-exclusion chromatograms-HPLC (SEC-HPLC) to be > 99% (**Figure 1C**).

Binding Properties of Y111

We assessed the affinity of Y111 at the anti-CD3 moiety on Jurkat cells by flow cytometry. With the structural change to sFv from Fab, it was not surprising that the affinity of Y111 was 360-folds lower than that of 2A5 (the parental CD3 mAb of Y111) to Jurkat cells, with the dissociation constants (Kd) of Y111 and 2A5 binding to the Jurkat cells being 711.4 nM and 1.96 nM, respectively (**Figure 2A**), which were consistent with previous reports (14, 25). The K_D values of the Y111 bispecific antibody and its parental PD-L1 mAb binding to H1975 cells were 0.84 nM and 0.21 nM, respectively (**Figure 2B**). The results demonstrated that the tumor cell-based affinity of Y111 to PD-L1 was equivalent to its parental mAb.

CD3-targeting bispecific antibody mediating T cells recruitment to cancer cells is considered to be its critical mechanism of action (MOA) (14). We, therefore, investigated whether Y111 could bridge T cells to tumor cells through its dual binding arms. To this end, Jurkat cells stained with CFSE were incubated with H1975 cells labeled with PKH26 for 1 hour, then the proportion of double-positive cells was measured to represent the bridging activity of Y111 (25). In the presence of the CD3 Isotype (fluorescein x CD3) at 10 μg/mL, the double-positive cell population was 1.79% (**Figure 2C**). In the presence of Y111 at the same concentration the double-positive cell population was 34.6% (**Figure 2C**),

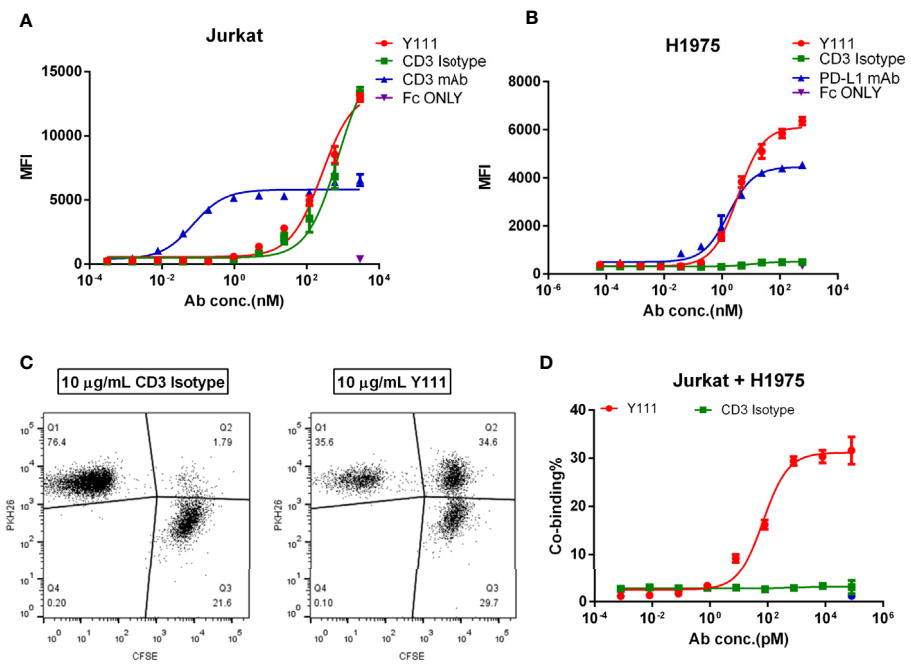

FIGURE 2 | Cell binding activities of Y111. **(A, B)** The binding affinity of Y111 to the CD3 expressed on the Jurkat cells **(A)**, and the PD-L1 expressed on the H1975 cells **(B)**. Flow cytometry was used to assess the geometric mean fluorescence (MFI) of the PE channel, and data were analyzed using the "One Site-Specific binding" method through the least-squares fitting. Plotted dots were the means ± SEM of the triplicate wells from one of three independent experiments. **(C, D)** Y111 bridged the tumor cell and T cells in a dose-dependent manner. CFSE-stained H1975 cells were co-cultured with PKH26-labeled Jurkat cells with a dose of Y111 or CD3 Isotype for 1hour. Co-binding% was indicated as percentages of the CFSE and PKH26 double-positive cells (Q2) among cells. Representative co-binding dot plots were shown in **(C)**, a nonlinear regression depicting dose-dependent-association modulated by Y111was shown in **(D)** Data in **(D)** were represented as mean ± SEM pooled from four independent experiments, and were analyzed using the "log (agonist) vs. response (three parameters)" method through an ordinary fitting. Y111, a bispecific antibody targeting CD3 and PD-L1; CD3 Isotype, a control bispecific antibody targeting CD3 and fluorescein; CD3 mAb and PD-L1 mAb, the parental monoclonal antibody targeting CD3 and PD-L1; Fc only, adding the PE-hFc only.

suggesting that the Y111 significantly bridges the T cell and tumor cell. This function of Y111 in inducing the tumor cell to T-cell association displayed a dose-dependent manner with EC_{50} ~ 72.1 pM, while the CD3 Isotype control was unable to induce this cell-to-cell association (**Figure 2D**). Taken together, these results demonstrated the unique binding activities of Y111 by the anti-PD-L1 moiety to the tumor cells and by the anti-CD3 moiety to the T cells.

Y111 Failed to Enhance the Cytotoxicity of the Fresh γδT Cells

As the crosslinking of PD-L1 positive target cells with T cells mediated by the Y111 bispecific antibody was expected to cause the effector T-cell–dependent lysis of the target cells (14), we checked whether Y111 redirected the fresh T cells to kill PD-L1 positive tumor cells. To this end, two T-cell subsets including CD8+ and Vδ2+ T cells were negatively isolated from the same PBMCs samples, and co-cultured individually with H358 cells in a ratio of 1:10 (E: T) in the presence of Y111 (**Figure 3A**). Interestingly, we did not observe an elevated effect of Y111 on the cytotoxicity of the fresh Vδ2 T cells, but Y111 increased the effects of CD8+ T cells on lysing the H358 cells in a Y111 dose-dependent fashion (**Figure 3B**). This finding of the difference between the two T-cell subsets was consistent with a previous study using a bispecific antibody targeting Her2 and CD3. These data showed that Y111 prompted the lysis of H358 cells mediated by the fresh CD8+ T cells but spared this effect on the fresh Vδ2 T cells enriched from the same donors, which suggested that Y111 could bypass the anti-tumor capacity of the fresh Vγ2Vδ2 T cells.

The Activation of the Expanded and Purified Vγ2Vδ2 T Cells by Y111 Was Dependent on the Presence of PD-L1 Expressing Tumor Cells

As the adoptive transfer of the expanded and purified Vγ2Vδ2 T cells has been shown a safe and well-tolerated therapy (20–22), we tested the concept of the combination of the purified Vγ2Vδ2 T cells with Y111 in the following study. Firstly, we investigated whether Y111 could bridge the expanded Vγ2Vδ2 T cells and tumor cells. To this end, we measured the Y111-mediated co-binding to the tumor cells and Vγ2Vδ2 T cells and found that the Y111 efficiently prompted the double-positive population in the co-culture system with the two types of cells (**Supplementary Figure 3**). Next, the purified Vγ2Vδ2 T cells (the purity and quality of Vγ2Vδ2 T cells were shown in **Supplementary Figure 2**) were cultured with/without tumor cells in the presence of the Y111 in a serial concentrations for 6 hours. We then measured the cell surface expression of CD107a to assess the degranulation of cytotoxic molecules (33), and the intracellular expression of IFNγ and TNFα (34). With the stimulation of both Y111 and tumor cells, a higher proportion of Vγ2Vδ2 T cells displayed potent effector functions and degranulation at 1 μg/mL (~ 8.05 nM), which was not the case for CD3 Isotype (**Figure 4A**, **Supplementary Figure 4**). Furthermore, the considerably unregulated expression of TNFα, IFNγ, and CD107a was aborted in the absence of tumor cells even under the stimulation by Y111 (**Figure 4A**). These data indicated that the activation of Vγ2Vδ2 T cells was controlled jointly by both Y111 and tumor cells. Moreover, this specific activation was in an Y111 dose-depended manner (**Figures 4B–D**). Multifunctional Vγ2Vδ2 T cells have been reported to play central roles in controlling intracellular bacterial infection and killing transformed tumor cells (1, 35). Indeed, we found the co-stimulation of Y111 and H1975 cells induced larger percentages of effector cells to produce multiple cytokines simultaneously (**Figure 4E**). At last, we also observed a dose-depended increase of these multifunctional Vγ2Vδ2 T cells after co-incubation of both the Y111 and tumor cells (**Supplementary Figure 5**). Taken together, these data demonstrated that the efficient activation of Vγ2Vδ2 T cells was dependent on the simultaneous binding of the Y111 to both Vγ2Vδ2 T cells and PD-L1 positive tumor cells.

Y111 Increased the Killing of PD-L1-Positive NSCLC Cell Lines Mediated by the Expanded and Purified Vγ2Vδ2 T Cells

We chose four NSCLC cell lines including A549, H1299, H358, and H1975 cells, as these four types of cancer cells express high levels of PD-L1 (**Supplementary Figure 6**). When CFSE-stained tumor cells were co-cultured with purified Vγ2Vδ2 T cells at a ratio of 1:1 and a range of serially diluted Y111 antibody for 12 hours, tumor cells were killed efficiently by Y111 in a dose-dependent manner, but not at all by CD3 Isotype or PD-L1 mAb at any tested concentration (**Figure 5**). As Y111 alone did not affect the viability of tumor cells (**Supplementary Figure 7**), it was believed that the observed high cytotoxicity was directly elicited by Y111-induced T cells. Although the anti-PD-L1 activity of Y111 may block the PD1/PD-L1 interaction and act as a checkpoint inhibitor, our data showed that the PDL1-antibody alone had little effect on the killing ability of the Vγ2Vδ2 T cells against PDL1-positive tumor cells (**Figure 5).** We noticed that only four pair dots might not provide meaningful correlations, but we indeed found a negative trend between the Y111-induced killing ability (EC50 values) and the PD-L1 positive percentages (**Supplementary Table 1**). Furthermore, Y111 plus the expanded Vγ2Vδ2 T cells did not attack the normal cells (such as PBMCs) from other donors (**Supplementary Figure 8**), suggesting the safety of the combination of the Y111 and the expanded Vγ2Vδ2 T cells in its potential clinical applications.

The Secretion of IFNγ, TNFα, and Granzyme B From Vγ2Vδ2 T Cells Was Enhanced by Y111 Along With the Killing of the Tumor Cells

The killing ability of Vγ2Vδ2 T cells induced by Y111 prompted us to check the production of killing cytokines, including IFNγ and TNFα, and cytotoxic mediator granzyme B in the co-culture of the T cell and tumor cells. We found Y111, but not CD3 Isotype or PD-L1 mAb could significantly enhance the secretions of IFNγ, TNFα, and granzyme B from

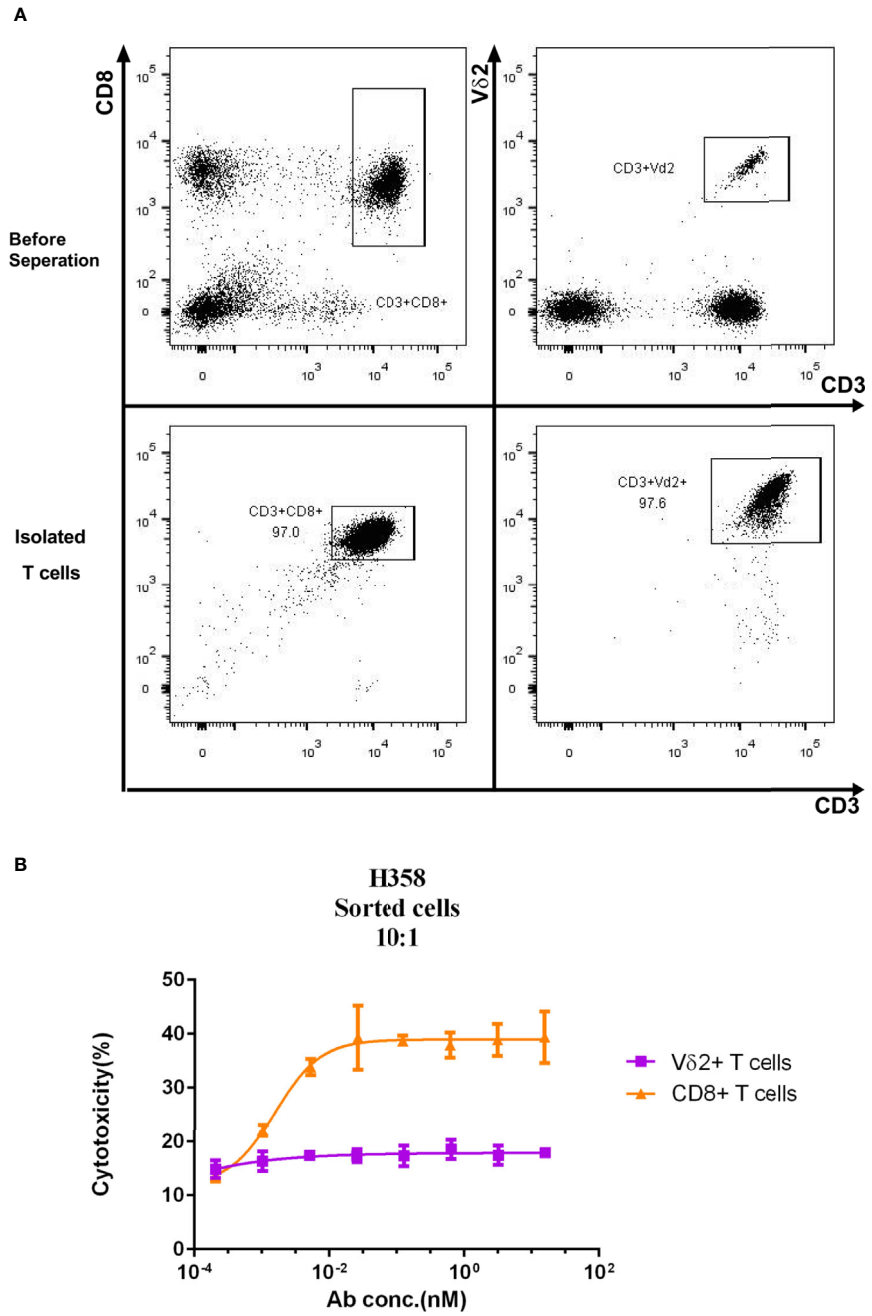

FIGURE 3 | Differential cytotoxicity of fresh CD8+ and Vδ2+ T cells induced by Y111. **(A)** Representative plots show the purity of CD8+, and Vδ2+ T cells enriched from PBMC by negatively magnetic beads separation. **(B)** The purified T-cell subsets from PBMC were co-cultured with CFSE-stained H358 in the presence of serial dilutions of the Y111 for the indicated time, then the proportions of killed target cells (PI+CFSE+) were plotted along with antibody concentration. The dots shown were from 3 independent experiments with T cells obtained from 5 healthy subjects. Data were analyzed using the "log (agonist) vs. response (three parameters)" method through an ordinary fitting.

the expanded Vγ2Vδ2 T cells in the presence of tumor cells (**Figure 6A**). Moreover, the evaluated releases of IFNγ and TNFα, and granzyme B were consistent with the enhanced killing ability of the Vγ2Vδ2 T cells mediated by Y111, as inferred from the significant correlation coefficients between the secreted amounts of IFNγ, TNFα, and granzyme B and the cytotoxicity activities (**Figure 6B**). However, there is no obvious increase of IFNγ and TNFα in the co-cultures of the expanded and purified Vγ2Vδ2 T cells and PBMCs from other donors in the presence of Y111 (**Supplementary Figure 8**).

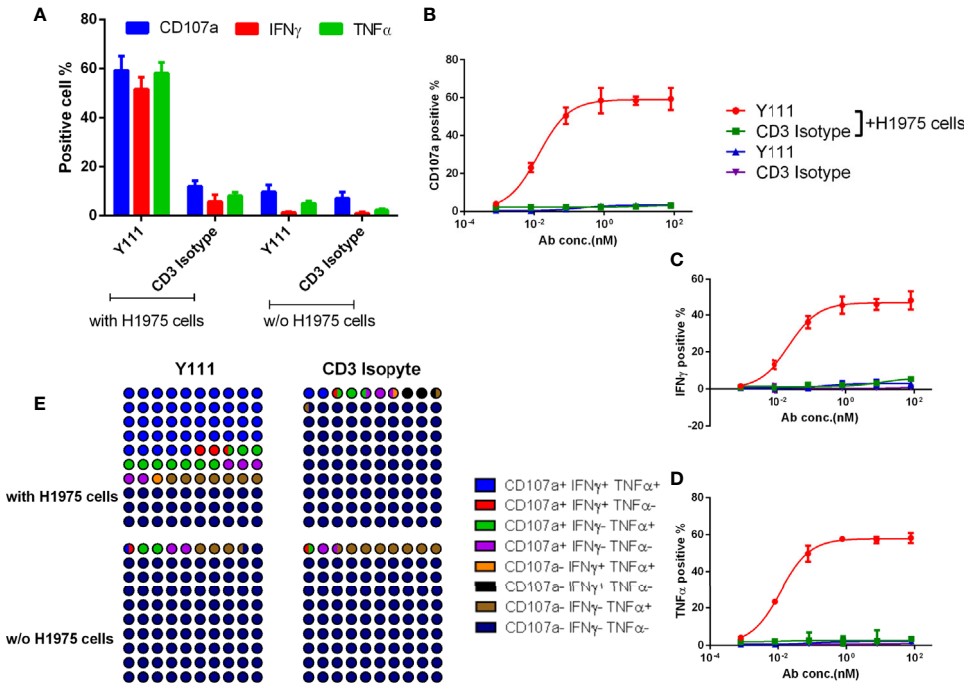

FIGURE 4 | Y111 selectively triggered the cytokine production and degranulation of Vγ2Vδ2 T cells in the presence of target tumor cells. **(A-D)** Y111 efficiently enhanced the activation of Vγ2Vδ2 T cells to produce IFNγ, TNFα, and up-regulate CD107a in tumor cell-dependent fashion. Vγ2Vδ2 T cells were stimulated by Y111 or CD3 Isotype (1 μg/mL of each) **(A)**, and indicated concentration ranges of Y111 or CD3 Isotype **(B–D)** in the presence/absence of H1975 cells in a 1:1 ratio for 6 hours. **(E)** Part of the whole graph shown the co-expression signatures of Vγ2Vδ2 T cells treated by Y111 or CD3 Isotype (1 μg/mL of each) in the presence or absence of H1975 cells. After gating cytokine-positive population (**Supplementary Figure 4**), the boolean analysis was utilized to determine the percentages of multi-functional effector subsets of Vγ2Vδ2 T cells. Bar graph data shown in **(A)** were represented as means ± SEM pooled from three experiments involving 9 healthy donors, dots in **(B–D)** were the means of these individual donors. The data in **(B)** were analyzed using the "log (agonist) vs. response (three parameters)" plot through an ordinary fitting.

Adoptive Transfer of the Purified and Expanded Vγ2Vδ2 T Cells With Y111 Displayed Potent Anti-Tumor Efficacy in NPG Mice

To assess the therapeutic potential of transfusing Vγ2Vδ2 T cells with bispecific antibody Y111, we utilized the H1975-NPG model to check whether this combination treatment could fight against the established xenograft in mice model (**Figure 7A**). Adoptive transfer of the *ex vivo* expanded and purified Vγ2Vδ2 T cells alone had no effect on the growth of the established H1975-derived xenograft, similar to the control group (**Figures 7B, C**, **Supplementary Figure 9A**). In contrast, the supplementation of the Y111 combined with Vγ2Vδ2 T cells purified from the same donor significantly delayed the malignant progression, comparing to the control or the T cells alone groups (**Figures 7B, C** and **Supplementary Figures 9A**). These significant inhibitory effects of tumor growth started on Day 27 after tumor cell inoculation in the mice received both Vγ2Vδ2 T cells and 4 mg/kg Y111 (**Figure 7B** and **Supplementary Figure 9A**). Moreover, 4 mg/kg Y111 elicited superior suppressive effects with a greater extent of delaying tumor growth of this group than 1 mg/kg Y111 group (**Figures 7B, C** and **Supplementary Figure 9A**). The observed inhibitory effects were associated with significant increases in the infiltration and accumulation of transfused Vγ2Vδ2 T cells induced by Y111 (**Figures 7D, E**). During the study, the Y111 treatment resulted in no or little weight loss in mice (**Supplementary Figure 9B**). All of these results demonstrated that Y111 enhanced the anti-tumor efficacy of transfused Vγ2Vδ2 T cells, suggesting a potential safety and efficient therapy of the combination of the expanded Vγ2Vδ2 T cells with the Y111 bsAb.

DISCUSSION

Since the discovery of the Vγ2Vδ2 T cells in the late 1980s, a significant amount of knowledge has been accumulated concerning its vital roles in killing tumor cells and controlling tumor growth, raising the possibility of its potential for anti-cancer therapeutics (35–37). The currently available results of clinical trials using the transferred Vγ2Vδ2 T cells against both hematological malignancies and solid tumors were proved to be safe but ineffective (35, 38). The low efficacy results could be due to the failure of the transfused Vγ2Vδ2 T cells infiltrating into tumor sites or due to the suppression of the killing activity of the transfused Vγ2Vδ2 T cells by the tumor microenvironment (4, 39). In this study, the transfused Vγ2Vδ2 T cell was redirected into tumor sites by a novel anti-CD3 and anti-PD-L1 bsAb, Y111. This proof-of-concept study

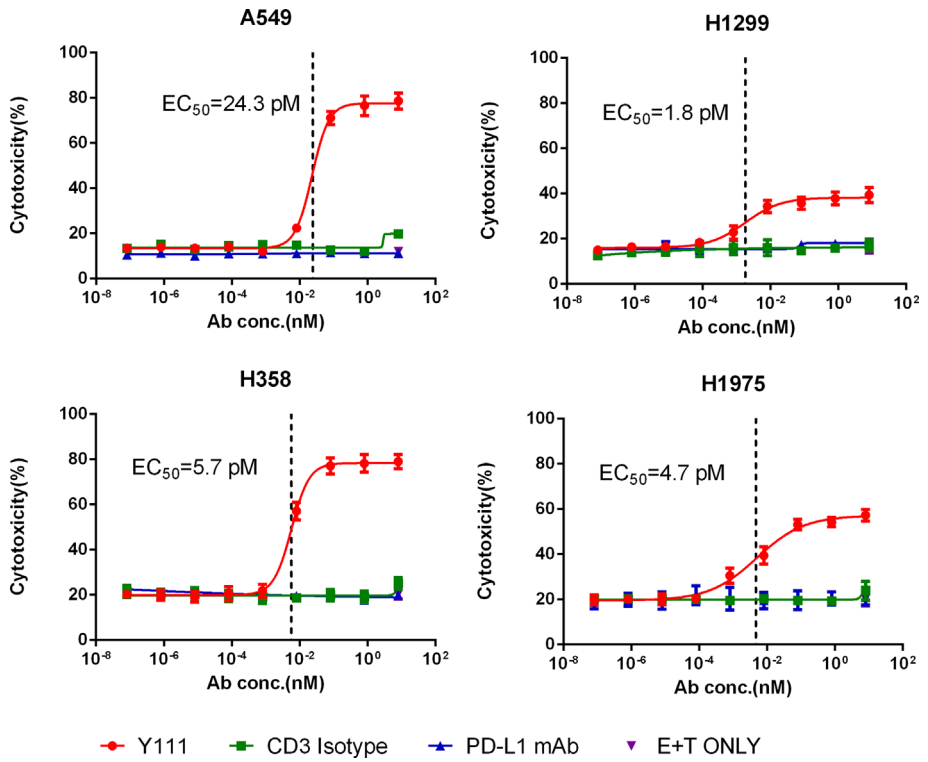

FIGURE 5 | Y111 redirected Vγ2Vδ2 T cells to kill PD-L1 positive NSCLC cell lines *in vitro*. The expanded and purified Vγ2Vδ2 T cells were incubated with four NSCLC cell lines, including A549, H1299, H1975, and H358, in a 1:1 ratio with the Y111 in a range of concentrations, CD3 Isotype or PD-L1 mAb for 12 hours. Then the proportions of killed target cells were plotted against the antibody concentrations. These cell lines were PD-L1 positive shown in **Supplementary Figure 6**. The calculated EC_{50} values were shown. The data points in were represented as mean ± SEM among 9 individual subjects for the analysis.

also verified the value of the bsAb-based immunotherapy to leverage the potent anti-tumor capacity of Vγ2Vδ2 T cells, and suggested that the combination of the Vγ2Vδ2 T cells and Y111 could be applied for PD-L1+ cancer therapies.

With the obligatory ability in two binding specificities simultaneously, bispecific antibodies are progressing into clinical developments for a wide variety of tumors (14, 26). In this study, we generated a PD-L1 X CD3 bsAb Y111, based on the Y-body® technological platform, which was characterized as an asymmetric format for easy purification, with the modified Fc fragment to abolish Fc-mediated effector functions (25, 26). The observed MW of Y111 was larger than the theoretical MW, as a result of its N-linked glycosylation, which prompted its stability (25). Moreover, the Y111 retained a relatively weaker binding affinity to the CD3 molecule, comparing to its parent monoclonal antibody 2A5, but displayed a similar affinity to PD-L1 as that of its parental mAb. The reduced affinity for CD3 of Y111 was desired for clinical applications as several previous studies had shown that a lower affinity of the anti-CD3 moiety of a T cells-redirecting bsAb contributed to the efficient tumor infiltration of the T cells without rapid CD3-modulated plasma clearance (40–42), and to lowing the risk of cytokine release syndrome (CRS) (25, 26). Indeed, our data indicated that Y111 could prompt T cell infiltration into tumor sites *in vivo* and induced high potential cytotoxicity against tumor cells *in vitro*.

The different susceptibility of fresh CD8+ and Vδ2 T cells-, and the expanded Vγ2Vδ2 T cells-modulated the killing activities of tumor cells induced by Y111 may be attributed to the various action mechanisms of the TCR activation by these cells (43, 44). The observation in this study indicated that the cytotoxicity of the fresh Vγ2Vδ2 T cells would not be enhanced by Y111. As the adoptive transfer of the expanded Vγ2Vδ2 T cells was proved to be safe and well-tolerated in clinical evaluation, here we showed that the combination of the expanded Vγ2Vδ2 T cells and Y111 would improve the efficacy of the current therapy. Indeed, our data demonstrated that Y111 triggered the up-regulated expression of CD107a on the surfaces of Vγ2Vδ2 T cells and selectively provoked their production of IFNγ and TNFα in the presence of PD-L1 expressing tumor cells. Moreover, the observed killing of PD-L1 expressing NSCLC cell lines was not affected by gene variations in these tumor cell lines, including the mutations of KRAS (A549 and H358 cells) or EGFR (H1975 cells), and the loss of P53 activities (H358 and H1299 cells). This gene variation-ignored killing mechanism of our approach further proved the potential anti-tumor nature of the Vγ2Vδ2 T cells (35, 36, 45). Yet, the Y111-induced cytotoxicity of the Vγ2Vδ2 T cells was dependent on the cross-linkage of the T cells and PD-L1-positive cells (**Figure 5**). However, the combination of the Y111 plus the Vγ2Vδ2 T cells did not lyse PBMCs from the unrelated healthy donors (**Supplementary Figure 8**); no

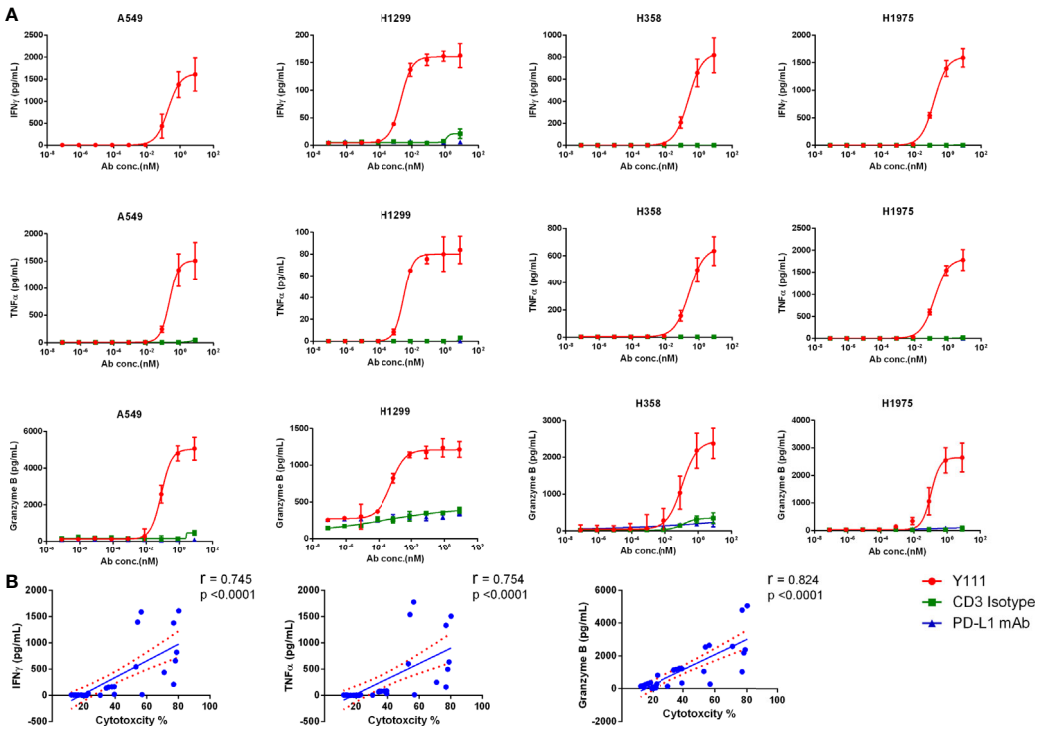

FIGURE 6 | Y111 prompted the release of IFNγ, TNFα, and granzyme B from Vγ2Vδ2 T cells. **(A)** The increased cytokine secretion by Vγ2Vδ2 T cells after co-culture for 12 h with tumor cells with Y111 or control antibodies (as indicated in **Figure 4**) analyzed by the CBA method. Please note that the values were the results of raw values subtracted E+T only groups. The data points in **Figure 5** were represented as mean ± SEM among 9 healthy subjects. **(B)** The correlations of the enhanced cytotoxicity induced by Y111 with the increased production of IFNγ, TNFα, and granzyme **(B)** The spearman's r and two-tailed p values were calculated by GraphPad prism 6. The blue line indicated the best-fit line, and the red line indicated the 95% confidence band of the best-fit line.

significant change of the body weights in the Y111 + Vγ2Vδ2 T cells treated mice was observed (**Supplementary Figure 9B**). These results suggested that the safety of the combination approach reminded as that of the adoptive transferred Vγ2Vδ2 T cells therapy (35, 38).

While expanding a large scale of autologous Vγ2Vδ2 T cells from a cancer patient *ex vivo* still represents a critical clinical challenge (37), we explored the antitumor activity of a modified protocol by transferring a small amount of Vγ2Vδ2 T cells together with Y111 into NPG mice bearing tumor cell line derived xenograft. The approach seems particularly promising given the potential of controlling the growth of established tumors in mice model, while the therapy of the transfused Vγ2Vδ2 T cells alone was not effective. This better efficacy *in vivo* result was consistent with the increased cytotoxicity of this treatment *in vitro*.

It is not feasible to directly using syngeneic mouse tumor models to evaluate Vγ2Vδ2 T cell-based anti-cancer therapy since the Vγ2Vδ2 T cell subset exists only in human and non-human primates, but not in rodents (46). Due to the limitation of immunodeficiency of NPG mice used in this study, we could not probe whether our strategy could modulate suppressive tumor microenvironment. Previous study showed that Treg cell, which has a strong immunosuppressive function in tumor microenvironment, could regulate phosphoantigen-induced proliferation of Vγ2Vδ2 T cell *ex vivo*, but did not suppress the cytokine production or cytotoxic effector functions of Vγ2Vδ2 T cell (47).However, phosphoantigen+IL2-expanded Vγ2Vδ2 T cells could antagonize the expansion and functions of CD4 +CD25+ regulatory T cells both *in vivo* and *in vitro* (48), and even overcome TGFβ immunosuppressive functions (49). Moreover, the clinical trials did not offer evidence of Treg-exerting immunosuppression to Vγ2Vδ2 T cells, as the repeated administration of IL2 was regarded as a standard operation (50). Thus, based on these previous reports, we believed that Tregs did not impair the killing function of the expanded Vγ2Vδ2 T cells in the presence of Y111. Recently, a series of studies have probed the cross-talk of the tumor resistance mechanisms and Vγ2Vδ2 T cells, and concluded that a combination therapy of adoptively transferred Vγ2Vδ2 T cells and bispecific T cell engagers is a possible future directions to overcome the immunosuppressive tumor microenvironment [reviewed in 5]. Consistent with this concept, we found Y111 could increase the trafficking of the transferred Vγ2Vδ2 T cells into the tumor site (**Figure 6D**) even for 12 days after the last cell transfer. Comparing to other studies using bispecific antibodies or anti-TIM3 monoclonal antibodies with the Vγ2Vδ2 T cells (7–13), our combination approach was demonstrated to be effective and safe without the additional administrations of IL2 or aminobisphoshponates or pyrophosphates for sensitizing the tumor cells.

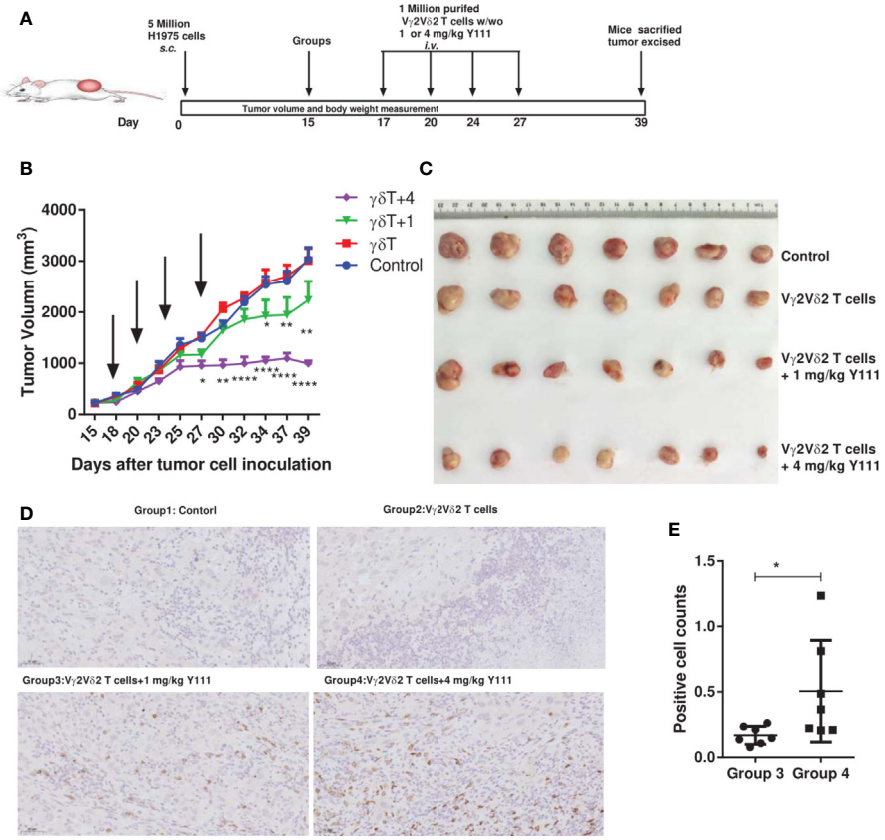

FIGURE 7 | The combined usage of transfused Vγ2Vδ2 T cells with Y111 significantly inhibited tumor growth *in vivo*. **(A)** Experimental schema of protocols for establishing xenograft in NPG mice and evaluating the anti-tumor therapeutic efficacy of different treatments. Immunodeficient NPG mice were *s.c.* inoculated with H1975 NSCLC cells on Day 0. After seventeen days, mice were treated with *i.v.* transfused Vγ2Vδ2 T cells w/wo 1 or 4 mg/kg Y111. These treatments were repeated twice per week for 2 weeks. Mice treated PBS were used as control. **(B)** The pooled tumor growth curves for NPG mice in four groups. The black arrows indicated the treatment time point. Data are mean ± SEM with 7 mice per group, $^{****}p < 0.0001$, $^{**}p < 0.01$, $^{*}p < 0.05$ versus control group, two-way ANOVA followed by Dunnett test. **(C)** Inspection of tumor tissues excised from each group at the end of the study. **(D)** Representative IHC photomicrographs of tumors excited from mice stained with the anti-human CD3 antibody. Magnification, 20X. **(E)** Infiltrated and accumulated T-cell counts at the tumor sites for mice received purified Vγ2Vδ2 T cells with 1 or 4 mg/kg Y111. Quantitative analysis of Vγ2Vδ2 T cells was done by counting positive dots in a total of 70 fields from 14 mice. We did not find the accumulation of Vγ2Vδ2 T cells in the other two groups. Each dot represented one mouse. Data were presented as mean ± SEM, $^{*}p < 0.05$, Mann Whitney U test.

In conclusion, this study demonstrated that bispecific antibody Y111, targeting the CD3 on Vγ2Vδ2 T cells and the PD-L1 on the tumor cells, could harness the anti-tumor potential of the Vγ2Vδ2 T cells to kill the cancer cells *in vitro* and inhibit the growth of the established xenograft tumors *in vivo*. The study provides new evidence to support the hypothesis that a CD3-targeting bispecific antibody has the potential to enhance the Vγ2Vδ2 T cells-based anti-tumor efficacy. The combination immunotherapy of the Y111 and the expanded Vγ2Vδ2 T cells is worth for further clinical evaluation for its benefit to cancer patients.

DATA AVAILABILITY STATEMENT

The raw data supporting the conclusions of this article will be made available by the authors, without undue reservation.

ETHICS STATEMENT

The studies involving human participants were reviewed and approved by Institutional Animal Care and Use Committee at Huazhong University of Science and Technology (Wuhan, China). The patients/participants provided their written informed consent to participate in this study. The animal study was reviewed and approved by Institutional Animal Care and Use Committee at Huazhong University of Science and Technology (Wuhan, China).

AUTHOR CONTRIBUTIONS

RY, LG, JY, and PZ designed the project. JZ, YY, LF, and LZ supervised the project. RY, SS, ZF, YX, CG, XW, FL, ZW, LY, and FYL performed the experiments. RY, LG, JY, and PZ analyzed the data and jointly wrote the manuscript. All authors contributed to the article and approved the submitted version.

FUNDING

This work was supported by the National Natural Science Foundation of China (Grant No. 81901607).

SUPPLEMENTARY MATERIAL

The Supplementary Material for this article can be found online at: https://www.frontiersin.org/articles/10.3389/fimmu.2021.654080/full#supplementary-material

Supplementary Figure 1 | The schematic diagrams of antibodies used in this study and the MOA of Y111. **(A)** Schematic diagrams of bispecific antibody Y111, PD-L1 mAb, and CD3 Isotype. Y111, a bispecific antibody targeting both PD-L1 and CD3; PD-L1 mAb, the parental monoclonal antibody targeting PD-L1; CD3 Isotype, a control bispecific antibody targeting CD3 and fluorescein (Clone 4420). **(B)** The proposed model for the mechanism of action (MOA) in this study. Y111 bridges the PD-L1 positive tumor cells to the Vγ2Vδ2 T cells to form the immune synapse, resulting in the release of cytolytic granzyme B, IFNγ, and TNFα.

Supplementary Figure 2 | The quality of expanded Vγ2Vδ2 T cells for *in vitro* and *in vivo* assays. **(A, B)** Kinetics of population and absolute numbers of Vγ2Vδ2 T cells during the expansion (n=9). **(C)** The expression levels of PD-L1 on Vγ2Vδ2 T cells and dead cells (PI-positive) among Vγ2Vδ2 T cells at day 14 (n=9). **(D)** Representative flow cytometry plots showed the population of Vγ2Vδ2 T cells at day 0-, day 14-PBMC cultures. Then, Vγ2Vδ2 T cells were negatively isolated from the day 14-cultures. The purity of enriched Vγ2Vδ2 T cells was assessed by flow cytometry. **(E)** The expression levels of the co-stimulatory molecule CD86, the activation associated marker CD69, and antigen-presenting molecule HLA-DR on Vγ2Vδ2 T cells at day 0 (red lines) and day 14 (blue lines). The black line represents isotype controls. These enriched cells were used for either binding or killing and functional assay *in vitro* or assessing anti-tumor activity *in vivo*.

Supplementary Figure 3 | Y111 bridged the tumor cell and the Vγ2Vδ2 T cells in a dose-dependent fashion. CFSE-stained H1975 cells were co-cultured with PKH26-labeled Vγ2Vδ2 T cells in the presence of Y111 or CD3 Isotype for 30 mins. Co-binding% was indicated as the percentages of the CFSE and PKH26 double-positive cells (Q2) of the total cells. Representative co-binding dot plots were shown in **(A)**, and a nonlinear regression depicting the dose-dependent association of Y111 was shown in **(B)**.

Supplementary Figure 4 | Representative contour plots showing the production of various cytokines by Vγ2Vδ2 T cells activated by 1 μg/mL of Y111 or CD3 Isotype with or without tumor cells. The gating strategies of positive cytokines were based on the biology control with the expanded Vγ2Vδ2 T cells treated by CD3 Isotype (the third column).

Supplementary Figure 5 | Multi-functional phenotypes of Vγ2Vδ2 T cells activated by Y111 or CD3 Isotype in the absence/presence of H1975 cells. After gating cytokine positive population (**Supplementary Figure 2**), the boolean analysis was utilized to check the percentages of multi-functional effector subsets (three-, or two-positive cytokines producing cells) of Vγ2Vδ2 T cells. Then the percentages of these multi-functional effector subsets of Vγ2Vδ2 T cells from four groups were plotted along with serially diluted antibodies. The shown data were the means of nine individuals of healthy subjects.

Supplementary Figure 6 | The expressions of PD-L1 on four cell lines. The surface expression of PD-L1 (clone: 29E.2A3, Biolegend, San Diego, USA) on four tumor cell lines (H358, H1975, H1299, and A549) was depicted as histograms from one representative assay. The PD-L1 positive percentages of these four cell lines were 23.9%, 34.0%, 91.9%, and 93.0%, respectively. The PD-L1 positive percentages displayed a positive correlation with the Y111-induced killing ability (see **Figure 5**).

Supplementary Figure 7 | Antibodies alone did not influence the viability of tumor cells. Bar graph showing Y111, CD3 Isotype, and PD-L1 mAb at 10 μg/mL exerted no effect on the growth of tumor cells. Data were from 3 independent experiments, and compared to the blank control there was no significant difference of these groups analyzed by one-way ANOVA.

Supplementary Figure 8 | Y111 induced minimal lysis of PBMC mediated by the expanded and purified Vγ2Vδ2 T cells. **(A)** Vγ2Vδ2 T cells were co-cultured with CFSE-labeled unrelated PBMC in the presence of antibodies at indicated concentrations for 12 hours. Then, the killed PBMC was determined by PI staining. **(B)** Y111 failed to induce significant release of cytokines at any tested concentrations. This experiment was performed three times involving the PBMCs from four unrelated subjects as target cells.

Supplementary Figure 9 | The combination usage of the transfused Vγ2Vδ2 T cells together with Y111 inhibited significantly the tumor growth *in vivo*. **(A)** Curves of tumor burden for the individual mouse from the control group against the Vγ2Vδ2 T cells only group, the Vγ2Vδ2 T cells plus 1 mg/kg of Y111 group, or the Vγ2Vδ2 T cells plus 4 mg/kg of Y111 group. **(B)** Curves of body weight changes for each group. The black arrows indicated the treatment time point. Data are the mean ± SEM with 7 mice per group.

Supplementary Table 1 | The negative trend between Y111-induced killing ability (EC_{50}) and PD-L1 positive percentages of tumor cell lines. a. The Pearson's r and p-value was calculated as rMFI and EC_{50}, PD-L1 positive percentages and EC_{50}.

REFERENCES

1. Shen L, Huang D, Qaqish A, Frencher J, Yang R, Shen H, et al. Fast-Acting Gammadelta T-cell Subpopulation and Protective Immunity Against Infections. *Immunol Rev* (2020) 298(1):254–63. doi: 10.1111/imr.12927
2. Beetz S, Marischen L, Kabelitz D, Wesch D. Human Gamma Delta T Cells: Candidates for the Development of Immunotherapeutic Strategies. *Immunol Res* (2007) 37(2):97–111. doi: 10.1007/BF02685893
3. Yazdanifar M, Barbarito G, Bertaina A, Airoldi I. γδ T Cells: The Ideal Tool for Cancer Immunotherapy. *Cells* (2020) 9(5):1305. doi: 10.3390/cells9051305
4. Lo Presti E, Pizzolato G, Corsale AM, Caccamo N, Sireci G, Dieli F, et al. Gammadelta T Cells and Tumor Microenvironment: From Immunosurveillance to Tumor Evasion. *Front Immunol* (2018) 9:1395. doi: 10.3389/fimmu.2018.01395
5. Wesch D, Kabelitz D, Oberg HH. Tumor Resistance Mechanisms and Their Consequences on γδ T Cell Activation. *Immunol Rev* (2020) 298(1):84–98. doi: 10.1111/imr.12925
6. Garber K. γδ T Cells Bring Unconventional Cancer-Targeting to the Clinic - Again. *Nat Biotechnol* (2020) 38(4):389–91. doi: 10.1038/s41587-020-0487-2
7. Ferrini S, Prigione I, Mammoliti S, Colnaghi MI, Ménard S, Moretta A, et al. Re-Targeting of Human Lymphocytes Expressing the T-cell Receptor Gamma/Delta to Ovarian Carcinoma Cells by the Use of Bispecific Monoclonal Antibodies. *Int J Cancer* (1989) 44(2):245–50. doi: 10.1002/ijc.2910440210
8. Oberg HH, Kellner C, Gonnermann D, Peipp M, Peters C, Sebens S, et al. γδ T Cell Activation by Bispecific Antibodies. *Cell Immunol* (2015) 296(1):41–9. doi: 10.1016/j.cellimm.2015.04.009
9. Oberg HH, Peipp M, Kellner C, Sebens S, Krause S, Petrick D, et al. Novel Bispecific Antibodies Increase γδ T-cell Cytotoxicity Against Pancreatic Cancer Cells. *Cancer Res* (2014) 74(5):1349–60. doi: 10.1158/0008-5472.Can-13-0675
10. Oberg HH, Kellner C, Gonnermann D, Sebens S, Bauerschlag D, Gramatzki M, et al. Tribody [(HER2)(2)Xcd16] Is More Effective Than Trastuzumab in Enhancing γδ T Cell and Natural Killer Cell Cytotoxicity Against Her2-

Expressing Cancer Cells. *Front Immunol* (2018) 9:814. doi: 10.3389/fimmu.2018.00814
11. de Bruin RCG, Lougheed SM, van der Kruk L, Stam AG, Hooijberg E, Roovers RC, et al. Highly Specific and Potently Activating Vγ9vδ2-T Cell Specific Nanobodies for Diagnostic and Therapeutic Applications. *Clin Immunol* (2016) 169:128–38. doi: 10.1016/j.clim.2016.06.012
12. de Bruin RCG, Veluchamy JP, Lougheed SM, Schneiders FL, Lopez-Lastra S, Lameris R, et al. A Bispecific Nanobody Approach to Leverage the Potent and Widely Applicable Tumor Cytolytic Capacity of Vγ9vδ2-T Cells. *Oncoimmunology* (2017) 7(1):e1375641. doi: 10.1080/2162402x.2017.1375641
13. Guo Q, Zhao P, Zhang Z, Zhang J, Zhang Z, Hua Y, et al. TIM-3 Blockade Combined With Bispecific Antibody MT110 Enhances the Anti-Tumor Effect of γδ T Cells. *Cancer Immunol Immunother* (2020) 69(12):2571–87. doi: 10.1007/s00262-020-02638-0
14. Labrijn AF, Janmaat ML, Reichert JM, Parren P. Bispecific Antibodies: A Mechanistic Review of the Pipeline. *Nat Rev Drug Discovery* (2019) 18(8):585–608. doi: 10.1038/s41573-019-0028-1
15. Barta JA, Powell CA, Wisnivesky JP. Global Epidemiology of Lung Cancer. *Ann Glob Health* (2019) 85(1):8. doi: 10.5334/aogh.2419
16. Garon EB, Ciuleanu TE, Arrieta O, Prabhash K, Syrigos KN, Goksel T, et al. Ramucirumab Plus Docetaxel Versus Placebo Plus Docetaxel for Second-Line Treatment of Stage IV non-Small-Cell Lung Cancer After Disease Progression on Platinum-Based Therapy (REVEL): A Multicentre, Double-Blind, Randomised Phase 3 Trial. *Lancet* (2014) 384(9944):665–73. doi: 10.1016/S0140-6736(14)60845-X
17. Masters GA, Temin S, Azzoli CG, Giaccone G, Baker SJr., Brahmer JR, et al. Systemic Therapy for Stage Iv Non-Small-Cell Lung Cancer: American Society of Clinical Oncology Clinical Practice Guideline Update. *J Clin Oncol* (2015) 33(30):3488–515. doi: 10.1200/JCO.2015.62.1342
18. Dokouhaki P, Han M, Joe B, Li M, Johnston MR, Tsao MS, et al. Adoptive Immunotherapy of Cancer Using Ex Vivo Expanded Human Gammadelta T Cells: A New Approach. *Cancer Lett* (2010) 297(1):126–36. doi: 10.1016/j.canlet.2010.05.005
19. Kang N, Zhou J, Zhang T, Wang L, Lu F, Cui Y, et al. Adoptive Immunotherapy of Lung Cancer With Immobilized anti-TCRgammadelta Antibody-Expanded Human Gammadelta T-cells in Peripheral Blood. *Cancer Biol Ther* (2009) 8(16):1540–9. doi: 10.4161/cbt.8.16.8950
20. Kakimi K, Matsushita H, Masuzawa K, Karasaki T, Kobayashi Y, Nagaoka K, et al. Adoptive Transfer of Zoledronate-Expanded Autologous Vgamma9Vdelta2 T-Cells in Patients With Treatment-Refractory non-Small-Cell Lung Cancer: A Multicenter, Open-Label, Single-Arm, Phase 2 Study. *J Immunother Cancer* (2020) 8(2):e001185. doi: 10.1136/jitc-2020-001185
21. Sakamoto M, Nakajima J, Murakawa T, Fukami T, Yoshida Y, Murayama T, et al. Adoptive Immunotherapy for Advanced non-Small Cell Lung Cancer Using Zoledronate-Expanded gammadeltaTcells: A Phase I Clinical Study. *J Immunother* (2011) 34(2):202–11. doi: 10.1097/CJI.0b013e318207ecfb
22. Nakajima J, Murakawa T, Fukami T, Goto S, Kaneko T, Yoshida Y, et al. A Phase I Study of Adoptive Immunotherapy for Recurrent non-Small-Cell Lung Cancer Patients With Autologous Gammadelta T Cells. *Eur J Cardiothorac Surg* (2010) 37(5):1191–7. doi: 10.1016/j.ejcts.2009.11.051
23. Brahmer J, Borghaei H, Ramalingam SS, Horn L, Holgado E, Pluzanski A, et al. Abstract CT195: Long-Term Survival Outcomes With Nivolumab (NIVO) in Pts With Previously Treated Advanced non-Small Cell Lung Cancer (NSCLC): Impact of Early Disease Control and Response. *Cancer Res* (2019) 79(13 Supplement): CT195–5. doi: 10.1158/1538-7445.am2019-ct195
24. Sui H, Ma N, Wang Y, Li H, Liu X, Su Y, et al. Anti-PD-1/PD-L1 Therapy for Non-Small-Cell Lung Cancer: Toward Personalized Medicine and Combination Strategies. *J Immunol Res* (2018) 2018:6984948. doi: 10.1155/2018/6984948
25. Yu S, Zhang J, Yan Y, Yao X, Fang L, Xiong H, et al. A Novel Asymmetrical anti-HER2/CD3 Bispecific Antibody Exhibits Potent Cytotoxicity for HER2-positive Tumor Cells. *J Exp Clin Cancer Res* (2019) 38(1):355. doi: 10.1186/s13046-019-1354-1
26. Zhang J, Yi J, Zhou P. Development of Bispecific Antibodies in China: Overview and Prospects. *Antibody Ther* (2020) 3(2):126–45. doi: 10.1093/abt/tbaa011
27. Zhang J, Fang L, Yan Y, Zeng L, Zhou P. (2020). CD3 ANTIGEN BINDING FRAGMENT AND APPLICATION THEREOF 2020: China.
28. Kranz DM, Voss EWJr. Partial Elucidation of an Anti-Hapten Repertoire in BALB/c Mice: Comparative Characterization of Several Monoclonal Anti-Fluorescyl Antibodies. *Mol Immunol* (1981) 18(10):889–98. doi: 10.1016/0161-5890(81)90012-2
29. Yang R, Yang E, Shen L, Modlin RL, Shen H, Chen ZW. Il-12+Il-18 Cosignaling in Human Macrophages and Lung Epithelial Cells Activates Cathelicidin and Autophagy, Inhibiting Intracellular Mycobacterial Growth. *J Immunol* (2018) 200(7):2405–17. doi: 10.4049/jimmunol.1701073
30. Yang R, Yao L, Shen L, Sha W, Modlin RL, Shen H, et al. Il-12 Expands and Differentiates Human Vγ2vδ2 T Effector Cells Producing Antimicrobial Cytokines and Inhibiting Intracellular Mycobacterial Growth. *Front Immunol* (2019) 10:913(913). doi: 10.3389/fimmu.2019.00913
31. Yang E, Yang R, Guo M, Huang D, Wang W, Zhang Z, et al. Multidrug-Resistant Tuberculosis (MDR-TB) Strain Infection in Macaques Results in High Bacilli Burdens in Airways, Driving Broad Innate/Adaptive Immune Responses. *Emerg Microbes Infect* (2018) 7(1):207. doi: 10.1038/s41426-018-0213-z
32. Fan L, Shen H, Huang H, Yang R, Yao L. Impairment of Wnt/beta-catenin Signaling in Blood Cells of Patients With Severe Cavitary Pulmonary Tuberculosis. *PloS One* (2017) 12(3):e0172549. doi: 10.1371/journal.pone.0172549
33. Yang R, Peng Y, Pi J, Liu Y, Yang E, Shen X, et al. A CD4+CD161+ T-Cell Subset Present in Unexposed Humans, Not Tb Patients, are Fast Acting Cells That Inhibit the Growth of Intracellular Mycobacteria Involving Cd161 Pathway, Perforin, and IFN-γ/Autophagy. *Front Immunol* (2021) 12:599641. doi: 10.3389/fimmu.2021.599641
34. Hoeres T, Holzmann E, Smetak M, Birkmann J, Wilhelm M. PD-1 Signaling Modulates Interferon-Gamma Production by Gamma Delta (Gammadelta) T-Cells in Response to Leukemia. *Oncoimmunology* (2019) 8(3):1550618. doi: 10.1080/2162402X.2018.1550618
35. Silva-Santos B, Mensurado S, Coffelt SB. Gammadelta T Cells: Pleiotropic Immune Effectors With Therapeutic Potential in Cancer. *Nat Rev Cancer* (2019) 19(7):392–404. doi: 10.1038/s41568-019-0153-5
36. Silva-Santos B, Serre K, Norell H. Gammadelta T Cells in Cancer. *Nat Rev Immunol* (2015) 15(11):683–91. doi: 10.1038/nri3904
37. Hoeres T, Smetak M, Pretscher D, Wilhelm M. Improving the Efficiency of Vgamma9Vdelta2 T-Cell Immunotherapy in Cancer. *Front Immunol* (2018) 9:800. doi: 10.3389/fimmu.2018.00800
38. Sebestyen Z, Prinz I, Dechanet-Merville J, Silva-Santos B, Kuball J. Translating Gammadelta (Gammadelta) T Cells and Their Receptors Into Cancer Cell Therapies. *Nat Rev Drug Discovery* (2020) 19(3):169–84. doi: 10.1038/s41573-019-0038-z
39. Lo Presti E, Dieli F, Meraviglia S. Tumor-Infiltrating Gammadelta T Lymphocytes: Pathogenic Role, Clinical Significance, and Differential Programing in the Tumor Microenvironment. *Front Immunol* (2014) 5:607. doi: 10.3389/fimmu.2014.00607
40. Mandikian D, Takahashi N, Lo AA, Li J, Eastham-Anderson J, Slaga D, et al. Relative Target Affinities of T-Cell-Dependent Bispecific Antibodies Determine Biodistribution in a Solid Tumor Mouse Model. *Mol Cancer Ther* (2018) 17(4):776–85. doi: 10.1158/1535-7163.MCT-17-0657
41. List T, Neri D. Biodistribution Studies With Tumor-Targeting Bispecific Antibodies Reveal Selective Accumulation At the Tumor Site. *MAbs* (2012) 4(6):775–83. doi: 10.4161/mabs.22271
42. Bortoletto N, Scotet E, Myamoto Y, D'Oro U, Lanzavecchia A. Optimizing anti-CD3 Affinity for Effective T Cell Targeting Against Tumor Cells. *Eur J Immunol* (2002) 32(11):3102–7. doi: 10.1002/1521-4141(200211)32:11<3102::AID-IMMU3102>3.0.CO;2-C
43. Alarcon B, De Vries J, Pettey C, Boylston A, Yssel H, Terhorst C, et al. The T-cell Receptor Gamma chain-CD3 Complex: Implication in the Cytotoxic Activity of a CD3+ Cd4- CD8- Human Natural Killer Clone. *Proc Natl Acad Sci U.S.A.* (1987) 84(11):3861–5. doi: 10.1073/pnas.84.11.3861
44. Dopfer EP, Hartl FA, Oberg HH, Siegers GM, Yousefi OS, Kock S, et al. The CD3 Conformational Change in the Gammadelta T Cell Receptor is Not Triggered by Antigens But can be Enforced to Enhance Tumor Killing. *Cell Rep* (2014) 7(5):1704–15. doi: 10.1016/j.celrep.2014.04.049

45. Vantourout P, Hayday A. Six-of-the-Best: Unique Contributions of Gammadelta T Cells to Immunology. *Nat Rev Immunol* (2013) 13(2):88–100. doi: 10.1038/nri3384
46. Adams EJ, Gu S, Luoma AM. Human Gamma Delta T Cells: Evolution and Ligand Recognition. *Cell Immunol* (2015) 296(1):31–40. doi: 10.1016/j.cellimm.2015.04.008
47. Kunzmann V, Kimmel B, Herrmann T, Einsele H, Wilhelm M. Inhibition of Phosphoantigen-Mediated Gammadelta T-cell Proliferation by CD4+ Cd25+ FoxP3+ Regulatory T Cells. *Immunology* (2009) 126(2):256–67. doi: 10.1111/j.1365-2567.2008.02894.x
48. Gong G, Shao L, Wang Y, Chen CY, Huang D, Yao S, et al. Phosphoantigen-Activated V Gamma 2V Delta 2 T Cells Antagonize IL-2-induced Cd4+Cd25 +Foxp3+ T Regulatory Cells in Mycobacterial Infection. *Blood* (2009) 113 (4):837–45. doi: 10.1182/blood-2008-06-162792
49. Capietto AH, Martinet L, Cendron D, Fruchon S, Pont F, Fournié JJ. Phosphoantigens Overcome Human TCRVgamma9+ Gammadelta Cell Immunosuppression by TGF-beta: Relevance for Cancer Immunotherapy. *J Immunol* (2010) 184(12):6680–7. doi: 10.4049/jimmunol.1000681
50. Fournié JJ, Sicard H, Poupot M, Bezombes C, Blanc A, Romagné F, et al. What Lessons can be Learned From γδ T Cell-Based Cancer Immunotherapy Trials? *Cell Mol Immunol* (2013) 10(1):35–41. doi: 10.1038/cmi.2012.39

Conflict of Interest: L.G declares no financial conflicts of interest. Others in the authorship are employees of Wuhan YZY Biopharma Co., Ltd.

The remaining author declares that the research was conducted in the absence of any commercial or financial relationships that could be construed as a potential conflict of interest.

frontiers in Immunology

ORIGINAL RESEARCH
published: 02 June 2021
doi: 10.3389/fimmu.2021.645131

Vγ9Vδ2 T Cells Concurrently Kill Cancer Cells and Cross-Present Tumor Antigens

Gitte Holmen Olofsson[1], Manja Idorn[1,2], Ana Micaela Carnaz Simões[1], Pia Aehnlich[1], Signe Koggersbøl Skadborg[1], Elfriede Noessner[3], Reno Debets[4], Bernhard Moser[5], Özcan Met[1,6] and Per thor Straten[1,6]*

[1] National Center for Cancer Immune Therapy, CCIT-DK, Department of Oncology, Copenhagen University Hospital Herlev, Herlev, Denmark, [2] Department of Biomedicine, Aarhus University, Aarhus, Denmark, [3] Helmholtz Zentrum München, Germany Research Center for Environmental Health, Immunoanalytics, Research Group Tissue control of immunocytes, Munich, Germany, [4] Laboratory of Tumor Immunology, Department of Medical Oncology, Erasmus MC-Cancer Center, Rotterdam, Netherlands, [5] Division of Infection & Immunity, Cardiff University School of Medicine, Cardiff, United Kingdom, [6] Department of Immunology and Microbiology, Faculty of Health and Medical Sciences, University of Copenhagen, Copenhagen, Denmark

OPEN ACCESS

Edited by:
Jonathan Bramson, McMaster University, Canada

Reviewed by:
John Anderson, University College London, United Kingdom
Ye Li, University of Texas MD Anderson Cancer Center, United States

***Correspondence:**
Gitte Holmen Olofsson
gitte.holmen.olofsson@regionh.dk; per.thor.straten@regionh.dk

Specialty section:
This article was submitted to Cancer Immunity and Immunotherapy, a section of the journal Frontiers in Immunology

Received: *22 December 2020*
Accepted: *13 May 2021*
Published: *02 June 2021*

Citation:
Holmen Olofsson G, Idorn M, Carnaz Simões AM, Aehnlich P, Skadborg SK, Noessner E, Debets R, Moser B, Met Ö and thor Straten P (2021) Vγ9Vδ2 T Cells Concurrently Kill Cancer Cells and Cross-Present Tumor Antigens. Front. Immunol. 12:645131. doi: 10.3389/fimmu.2021.645131

The human Vγ9Vδ2 T cell is a unique cell type that holds great potential in immunotherapy of cancer. In particular, the therapeutic potential of this cell type in adoptive cell therapy (ACT) has gained interest. In this regard optimization of *in vitro* expansion methods and functional characterization is desirable. We show that Vγ9Vδ2 T cells, expanded *in vitro* with zoledronic acid (Zometa or ZOL) and Interleukin-2 (IL-2), are efficient cancer cell killers with a trend towards increased killing efficacy after prolonged expansion time. Thus, Vγ9Vδ2 T cells expanded for 25 days *in vitro* killed prostate cancer cells more efficiently than Vγ9Vδ2 T cells expanded for 9 days. These data are supported by phenotype characteristics, showing increased expression of CD56 and NKG2D over time, reaching above 90% positive cells after 25 days of expansion. At the early stage of expansion, we demonstrate that Vγ9Vδ2 T cells are capable of cross-presenting tumor antigens. In this regard, our data show that Vγ9Vδ2 T cells can take up tumor-associated antigens (TAA) gp100, MART-1 and MAGE-A3 - either as long peptide or recombinant protein – and then present TAA-derived peptides on the cell surface in the context of HLA class I molecules, demonstrated by their recognition as targets by peptide-specific CD8 T cells. Importantly, we show that cross-presentation is impaired by the proteasome inhibitor lactacystin. In conclusion, our data indicate that Vγ9Vδ2 T cells are broadly tumor-specific killers with the additional ability to cross-present MHC class I-restricted peptides, thereby inducing or supporting tumor-specific αβTCR CD8 T cell responses. The dual functionality is dynamic during *in vitro* expansion, yet, both functions are of interest to explore in ACT for cancer therapy.

Keywords: γδ or gamma delta T cells, Vγ9Vδ2 T cells, APC or antigen presenting cells, antigen cross-presentation, cancer, cancer killing

INTRODUCTION

Conventional T cells expressing αβ T cell receptors (TCR) have been characterized in detail with regards to antigen recognition, differentiation, and function (1). γδ T cells are less well characterized, less abundant, and exist as several subtypes with the common feature that they express a dimeric TCR consisting of a γ- and a δ-chain. The dominant γδ T cell subtype in peripheral blood are Vγ9Vδ2 T cells which are only found in humans, higher primates and the alpaca (2), and constitute 0.5-10% of lymphocytes in human blood (3). Most Vγ9Vδ2 T cells are double negative (DN) for the co-receptors CD4 and CD8, approx. 20-30% are single positive CD8 and 0.1-7% express CD4 (4, 5). The functional role of these co-receptors in the context of γδ T cells is however unknown, since Vγ9Vδ2 T cells recognize antigen in an HLA independent fashion. To this end, Vγ9Vδ2 T cells recognize a group of non-peptide antigens called phosphoantigens (pAgs) (6), examples of these are the bacterial metabolite ((E)-4-hydroxy-3-methyl-but-2-enylpyrophosphate (HMBPP)) (7) and isopentenyl pyrophosphate (IPP), which is a by-product of the mevalonate isoprenoid pathway. The interaction between pAgs and the butyrophilin proteins BTN3A1 (8, 9) and BTN3A2 (10, 11) leads to extracellular changes in conformation (12), allowing for proper recognition of the Vγ9Vδ2 TCR (13). Normal or healthy cells have low levels of IPP, which does not activate Vγ9Vδ2 T cells. In contrast, stressed cells and cancer cells show increased IPP levels, although in most cases not enough in itself for recognition by Vγ9Vδ2 T cells (14, 15). However, the activation of Vγ9Vδ2 T cells by pAgs can be exploited using drugs such as zoledronic acids (ZOL) (16). ZOL is an aminobisphosphonate that inhibits the enzyme farnesyl pyrophosphate synthase in the mevalonate pathway, which induces an accumulation of IPP in the cell (17, 18). ZOL can be used for selective expansion of Vγ9Vδ2 T cells from blood samples, and also to sensitize cancer cells to Vγ9Vδ2 T cell-mediated killing. Thus, the addition of ZOL to cultures of PBMC along with interleukin-2 (IL-2) leads to a selective expansion of Vγ9Vδ2 T cells, which are in turn highly efficacious killers of cancer cells upon sensitization of cancer cells with ZOL. Induction of effector function is not solely governed by recognition of pAgs, but also influenced by expression of receptors traditionally attributed to NK cells, such as NKG2D and DNAM-1 (3, 19).

An additional characteristic of Vγ9Vδ2 T cells is the capacity to cross-present antigen, i.e., to act as antigen presenting cells (APCs) (20). The term APC is normally used to refer to a group of innate cells that mediate cellular immune responses by processing and presenting antigens to aβ T cells. Classical APCs include dendritic cells (DCs) and macrophages, but Vγ9Vδ2 T cells have also been shown to cross-present viral and tumor antigen (21). Cross-presentation of the melanoma-associated antigen MART-1 was demonstrated using long synthetic peptide (22), and uptake of cellular protein upon killing of cancer cells has also been reported (23). However, in the latter case, efficient cross-presentation only took place when cancer cells were opsonized (24), and involvement of the proteasome was not investigated. Although some antigens have been shown to be cross-presented independently of proteasomal degradation, in most cases the proteasome is crucial for cross-presentation (25).

In the past decade, immunotherapy has revolutionized treatment of cancer and given new hope to patients with metastatic disease (26). Adoptive cell therapy (ACT) with tumor infiltrating lymphocytes (TILs) or T cells equipped with chimeric antigen receptors (CARs) have yielded impressive results in melanoma, and hematological malignancies, respectively (27). To the former, administration of *in vitro* expanded TILs is associated with 50% objective and 20% complete responses (28). Concerning ACT using CARs, administration of CAR T cells recognizing CD19 are now approved for the treatment of acute lymphoblastic leukemia (ALL) and diffuse large B-cell lymphoma (DLBCL) (29). In particular, CAR therapy is a highly promising broadly applicable strategy with the potential to develop patient tailored, off the shelf treatments. Great advances have been made over the past few years (30), but much need to be learned, in particular, in terms of optimal targets and best suited cell types for ACT.

The majority of studies on ACT, including FDA/EMA approved CAR therapies (31), are based on the use of conventional αβ-T cells as effector cells, largely, because these are well-studied effector cells in natural anti-cancer immunity with proven success in treatment settings (30). NK cells and γδ T cells have been tested as well in ACT treatments, with demonstrable pros and cons. NK and γδ T cells are capable of killing cancer cells in an HLA unrestricted manner, with the potential of efficacy in the absence of graft-versus-host disease (GvHD), and can be used as an off-the-shelf cellular source even in an allogenic setting (32). NK cells are problematic in terms of expansion of primary cells, conversely, Vγ9Vδ2 T cells are easily expanded to high cell numbers using ZOL and IL-2. Several clinical trials based on administration of *in vitro* expanded Vγ9Vδ2 T cells have been carried out with encouraging data, including good tolerability and little or no toxicity. But studies included too few patients to draw conclusions on clinical response (33). The combined capacity to kill cancer cells and cross-present antigen to CD8 T cells – even when equipped with a CAR (22) - represents another feature in favor of future testing of *in vitro* expanded Vγ9Vδ2 T cells in ACT in cancer. We describe that Vγ9Vδ2 T cells expanded with ZOL and IL-2 are capable of killing cancer cells as well as cross-presenting tumor antigens. Moreover, we show the dynamic change of this dual functionality over time in culture, a characteristic that should be considered in clinical application.

Abbreviations: ACT, adoptive cell therapy; APC, antigen presenting cell; HMB-PP, 4-Hydroxy-3-methyl-but-2-enyl pyrophosphate; IPP, isopentenyl pyrophosphate; ZOL, zoledronic acid.

MATERIALS AND METHODS

Samples From Patients and Healthy Donors

Peripheral blood mononuclear cells (PBMC) from healthy donors were obtained from the blood bank at Rigshospitalet, Copenhagen, Denmark. Processing was completed within < 6 h

for all sample specimens. PBMC were isolated by centrifugation with Lymphoprep™ (Axis-Shield PoC) (30 minutes at 1200 RPM) and cryopreserved at -150°C in fetal bovine serum (FBS) (GibcoBRL) + 10% dimethylsulfoxide (DMSO) (Sigma-Aldrich) using a CoolCell® (Bioscision) gradual freezing device. Cells were thawed in pre-warmed 37°C RPMI and counted after thawing using trypan blue staining and a microscope.

Cancer Cell Cultures

Cancer cell lines A2058 (melanoma), MDA-MB-231 (breast cancer), PC-3 (prostate cancer), U266 (myeloma) and K562 (chronic myelogenous leukemia) were all purchased from the American Type Culture Collection (ATCC). The FM55-1 (melanoma, ESTDAB-012) and FM86 (melanoma, ESTDAB-028) cancer cell lines were obtained from European Searchable Tumor Cell Line and Data Bank (ESTDAB) (http://www.ebi.ac.uk/ipd/estdab/). All cancer cells were grown in RPMI 1640 GlutaMAX-I™ medium (RPMI, Gibco) supplemented with 10% FBS (R10). Prior to cytotoxicity assays, the cancer cells were left untreated or pre-treated with 10 μM ZOL for 24 h.

Expansion of Vγ9Vδ2 T Cells

Vγ9Vδ2 T cells were cultured in X-vivo 15 medium (Lonza) supplemented with 5% human serum (X-vivo +5% HS) (Sigma-Aldrich). Vγ9Vδ2 T cells were expanded from thawed PBMC. On day zero, $1x10^6$ PBMC were cultured in a 24 well plate with 2 ml X-vivo + 5% HS and stimulated with 10 μM zoledronic acid (ZOL, Zometa 4 mg/5ml, Novartis). On day 2, 1000 U/ml IL-2 (Preprotech) was added, and every second or third day onwards, the cultures were supplemented with 1 ml fresh medium and 1000 U/ml IL-2. Purity of the Vγ9Vδ2 T cells was tested at day 9 by flow cytometry. We are aware that different groups use different amount of ZOL and IL-2. In our hands, we found expansion of Vγ9Vδ2 T cells to be most efficient when using 10μM ZOL, combined with either high IL-2 (1000U/ml) or low IL-2 + low IL-15 (100U/ml IL-2 + 100U/ml IL-15) (34). We have also tested 1μM ZOL combined with 100U/ml IL-2, but our data gave a less efficient and less pure expansion of Vγ9Vδ2 T cells (data not published).

Establishment of CMV Peptide Specific T Cell Cultures

αβTCR T-cell culture specific for CMV (CMV short) was generated from healthy donor (HD220) by stimulating with irradiated CMV-peptide-loaded Vγ9Vδ2 T cells (as an alternative to DCs, which are used in other protocols [32]). The following day, 40 U/ml IL-7 and 20 U/ml IL-12 (PeproTech) were added. Stimulation of the cultures was carried out every 8 days with CMV-peptide–loaded irradiated autologous Vγ9Vδ2 T cells. The day after peptide stimulation, 120 U/ml IL-2 (PeproTech) was added. Specificity of the T cell culture was tested by chromium release assays and IFNγ ELISPOT.

mRNA Transfection of PBMC for the Generation of gp100 Specific αβTCR T Cells

T cells expressing αβTCR specific for gp100 (gp100 short) were generated by mRNA transfection. The coding sequence of the $gp100_{280-288}$-specific TCR 296 (35) α and β chain was *de novo* synthesized and cloned into the $pCIpA_{102}$ plasmid (kindly provided Dr. G. Gaudernack, The Norwegian Radium Hospital, Oslo, Norway). Plasmids were linearized, purified (Wizard DNA Clean-Up System (Promega, Oslo, Norway), and *in vitro* transcribed 36, and used for electroporation of PBMC from healthy donors. PBMC were washed twice in OptiMEM medium (Invitrogen) and adjusted to a final cell density of 1×10^8 cells/ml in the same media. The cell suspension was pre-incubated for 5 min on ice and gp100 TCR encoding mRNA (100 μg/ml final concentration) was added to PBMCs before transfer to a 4-mm gap electroporation cuvette. Cells were pulsed using a BTX 830 square-wave electroporator (Harvard Apparatus, Holliston MA, USA), adjusted to a single pulse, 500 V, 5 ms. After electroporation, cells were transferred to pre-warmed culture medium and incubated in humidified atmosphere with 5% CO_2. Mock-(H_2O) transfected PBMCs were used as controls. Specificity of the T cell culture was tested by chromium release assays and IFNγ ELISPOT.

Retroviral Transduction for the Generation of MART-1 Specific T Cells

TCRα and β sequences of the HLA-A2-restricted MART-1-specific A42 T cell clone (37) were codon optimized and murinized by exchanging the constant regions by their murine counterparts then linked by a P2A element to yield the transgene cassette 5'-TCRvß4.2J2.7-P2A-TCRvα29J42.01-3' (IMGT nomenclature). The cassette was cloned into the retroviral vector MP71-PRE (38) using NotI and EcoRI restriction sites. This vector was designated MP71-TCR-A42.

Transgenic TCR expression in T cells was achieved as described (38). Briefly, PBMCs were plated into 24-well plates at a cell density of 1×10^6/ml per well in RPMI1640 supplemented with 10% human serum, 1% L-glutamine, 1% non-essential amino acids, 1% sodium pyruvate, 1% penicillin/streptomycin (all Invitrogen) and 100 U/ml IL-2 (Cancernova). Then, cells were activated with 5 μg/ml OKT3 (provided by E. Kremmer, Helmholtz Center Munich, Germany) and 1 μg/ml anti-CD28 (BD Pharmingen) for 2 days.

Amphotrophic TCR-A42-encoding retroviruses were generated as described (39) using TransIT®-LT1 Reagent (Mirus) according to the manufacturer's protocol. Virus supernatant was harvested after 48 h and bound to RetroNectin® (10 μg/ml, Takara) coated plates by centrifugation.

PBMCs, which were activated for 2 days, were added to virus-coated plates for 24 h, then split to freshly virus-coated plates and cultivated for another 3 days. Transduced PBMCs were transferred to uncoated plates and cultivated for at least 12 additional days, reducing the amount of IL-2 to 50 U/ml. TCR-A42 surface expression was determined at day 12 after transduction using anti-mouse TCRß-constant region-Pacific Blue (BioLegend) and anti-human CD8α-V500 (BD Pharmingen) antibodies. Furthermore, specificity of the T cell culture was also tested by chromium release assays and IFNγ ELISPOT.

Lentiviral Transduction for the Generation of MAGE-A3 Specific T Cells

Lentiviral vector containing the high affinity MAGE-A3^{a3a} TCR (40) and corresponding packaging and envelope plasmids (VSVG, REV and gag/pol) was generously provided by Dr Andrew Gerry and Dr. Bent Jakobsen, Adaptimmune, Ltd. (Oxfordshire, UK) (41).

Lentivirus were produced and T cells transduced as previously described (42). In brief, 293T human embryonic kidney cells cultured in DMEM (BioWhittaker, Rockville MD, USA), 10% FBS, were transfected using 1 μg of pMAGE-A3^{a3a} TCR and 0.5 μg of corresponding packaging and envelope plasmids, together with TurboFect Transfection Reagent (Thermo Fisher Scientific). After 48 h, lentiviral supernatant was harvested. T cells were transduced by incubation with filtered lentiviral supernatant + 1000 U/ml rhIL-2 for 72 h before sorting using a FACSAria cell sorter (BD Biosciences, San Jose CA, USA).

1-2 x 10^5 of the transduced and sorted T cells were put into a rapid expansion protocol (REP) consisting of feeder cells (a mix of three HD PBMCs, which were gamma irradiated with 40 Gy) at a ratio of 1:200 in T25 tissue culture flasks (Corning, #430168), 20 ml x-vivo medium + 5% human serum, 30 ng/ml anti-CD3 (OKT-3, eBioscience, #14-0037-82) and 6000 U/ml rhIL-2. On day 14 of REP, T cells were harvested and routine assays for receptor expression *via* flow cytometry and mycoplasma were conducted. Furthermore, specificity of the T cell culture was tested by chromium release assays and IFNγ ELISPOT.

Flow Cytometry

Flow cytometry was used to study expression of surface- and intracellular markers on cells. In short, cells were washed twice in FACS buffer (PBS +2%FCS) before and after staining. Antibodies were mixed to a total volume of 50 μl, and cells were stained for 30 minutes at 4°C. **Table 1**, provides an overview of antibodies used in this paper. Near-Infrared fixable dead cell stain from Invitrogen (Carlsbad, California, USA). The gating analysis was either performed with BD FACSDiva™ software or NovoExpress® software from ACEA biosciences.

TABLE 1 | List of antibodies used in this study.

Antibody	Fluorochrome	Clone	Company
CCR7	PE-Cy7	3D12	BD bioscience, New Jersey, USA
CD3	PE-Cy7	UCTH1	BD bioscience, New Jersey, USA
CD3	BV421	UCTH1	Biolegend, San Diego, California, USA
CD16	FITC	3G8	Biolegend, San Diego, California, USA
CD56	FITC	L307.4	Biolegend, San Diego, California, USA
CD56	PE	NCAM16.2	BD bioscience, New Jersey, USA
CD86	APC	IT2.2	Biolegend, San Diego, California, USA
CD161	BV421	DX12	BD bioscience, New Jersey, USA
DNAM	PerCP-Cy5.5	11A8	Biolegend, San Diego, California, USA
GPR56	PE	4C3	Biolegend, San Diego, California, USA
HLA-ABC	BV711	G46-2.6	BD bioscience, New Jersey, USA
HLA-DR	HV500	G46-6	BD bioscience, New Jersey, USA
IFNγ	BV510	4S.B3	Biolegend, San Diego, California, USA
IL-2	PE	MQ1-17H12	BD bioscience, New Jersey, USA
NKG2D	BV510	1D11	Biolegend, San Diego, California, USA
TNFα	PE-CF594	Mab11	BD bioscience, New Jersey, USA
TCRγ/δ	FITC	11F2	BD bioscience, New Jersey, USA
Vγ9	PC5	IMMU360	Beckmann Coulter, Brea, California, USA

Intracellular Staining (ICS)

Vγ9Vδ2 cells were co-cultured with PC3 cells (cancer cells), either non-stimulated or stimulated with 10 μM ZOL, at a ratio (1:1). The cells were incubated for 5 hours in the presence of Brefeldin A (BioLegend). Addition of cell culture medium served as a negative control, while 5 ng/ml PMA (Sigma Aldrich) plus 75 nM Ionomycin (Sigma Aldrich) were used as a positive control. After incubation, cells were centrifuged and washed twice with PBS + 2% FBS. Staining with surface antibodies was performed as described above. Then cells were fixed and permeabilized as described in detail in the manual of the Intracellular Fixation & Permeabilization Buffer Set (eBioscience). In short, cells were fixed overnight at 4°C in 200 μl Fixation Buffer per well. After centrifugation, cells were washed twice with 150 μl Permeabilization Buffer per well. Staining with intracellular antibodies was then performed in the same manner as the surface antibody staining. Subsequently, cells were washed twice with Permeabilization buffer, resuspended in 150 μl PBS + 2% FBS and acquired on the NovoCyte Quanteon.

Cell Sorting

Sorting was used to purify αβTCR-specific cultures and was performed on the FACS Aria(BD bioscience). For sorting, the MAGE-A3 transduced T cell cultures were first stained with HLA-A1 tetramers for 30 minutes at 37°C. For that, 20 ng of PE- and APC-conjugated MAGE-A3 specific tetramers were added to1 x 10^6 T cells in 50 mL of 1x PBS, 0.5% bovine serum albumin (BSA, Sigma Aldrich) and 2 mM EDTA. After the tetramer staining, CD3-BV421 (Biolegend), in a volume of 50 μl, was added directly into the tetramer/cell mix and incubated for 20–30 minutes in the dark and on ice. The transduced MAGE-A3 (also named MAGE-A3a3a) tetramer positive T cells were sorted directly into a rapid expansion protocol (REP) for further culturing. All antibodies, buffers and procedures were kept under sterile conditions to ensure aseptic sorting of cells for further culturing.

Rapid Expansion Protocol (REP)

To expand the MAGE-A3 positive T cells cells into high cells number, the rapid expansion protocol (REP) was used. For this, a REP mix was generated which included: feeder cells, 6000 U/ml IL-2 (Proleukin) (Peprotech) and 0,6 μg/20 ml anti-CD3 (clone OKT3) (ebioscience, Thermo Fisher). Detailed protocol was described elsewhere (43, 44), but in short; feeder cells were irradiated at 30 Gy and counted to the concentration of 20x10^6 PBMCs/20 ml medium (X-vivo + 5% HS) to which IL-2 and anti-CD3 was added. The REP mix was then ready for the tetramer sorted MAGE-A3 positive T cells to be added. From here, the cells were given fresh IL-2 (3000 U/ml) and medium (X-vivo + 5% HS) three times a week, until the γδ T cells started growing, allowing for further analysis.

^{51}Cr-Release Assay

Conventional ^{51}Cr-release assays for cell-mediated cytotoxicity was carried out as described elsewhere (10). Briefly, target cells (cancer cells) were labeled with 100 mCi 51Cr (Perkin Elmer, Skovlunde, Denmark) in 100 µL R10 for 1 h at 37°C. After washing, the target cells were incubated with effector cells (Vγ9Vδ2 T cells) at different effector:target (E:T) ratios for 4 h at 37°C. Subsequently, the amount of radioactivity in the supernatant was measured using a gamma cell counter (Perkin Elmer Wallac Wizard 1470 Automatic gamma counter). Target cells were the cancer cell lines FM55-1 (melanoma), FM86 (melanoma), A2058 (melanoma), MDA-MB-231 (breast cancer), PC-3 (prostate cancer), U266 (myeloma) and K562 (chronic myelogenous leukemia). Also, allogeneic PBMCs (lymphocytes) from five healthy donors (HD) were thawed and rested ON and used as target cells.

Prior to cytotoxicity assays, the cancer cells or lymphocytes were left untreated or pre-treated with 10 µM ZOL for 24 hs. The rationale for pre-stimulating cancer cells with ZOL, is to make them more prone to killing by Vγ9Vδ2 T cells. ZOL inhibits farnesyl pyrophosphate synthase (FPPS), an enzyme downstream of IPP within the mevalonate pathway, which leads to accumulations off IPP intracellular making them more prone to recognition by Vγ9Vδ2 T cells. This has been shown repeatedly and the potential clinical application is being tested (45).

xCELLigence Assay

To measure the cytotoxicity of Vγ9Vδ2 T cells against cancer cell over an extended period, the xCELLigence system was used. This assay is composed of one station with an E96 plate (xCELLigence-specific 96 well plate; ACEA biosciences, San Diego, USA), which is stored within a standard tissue culture incubator (37°C and 5% CO_2). Its high-density electrode array, covering the bottom of E96 plates, allows this system to measure the variation in impedance throughout time. This measurement is then converted into a cell index, which can be translated into cytotoxicity.

Optimal seeding density was optimized (data not shown) and each target cell was plated out in E96 plates (10 000 cells/well for PC-3, A2058 and MDA-MD-231) and incubated for 6-24 h to promote adhesion and initial proliferation without reaching full confluency. Vγ9Vδ2 T cells were then added to each well, at a titrated 3:1, 1:1 effector-to-target ratio. The cell index was continuously measured for the next 24 h. To determine minimum impedance, 100 µl of 10% TritonX-100 (Sigma-Aldrich) was added to separate wells. Additionally, wells with Vγ9Vδ2 T cells alone were included to account for the effector cells' contribution to the cell index. Data was analyzed with the immunotherapy module of the 185 xCELLigence RTCA Software Pro (ACEA Biosciences) as reported previously (46, 47).

Several things were considered to rule out batch differences. All cytotox assays were conducted with Vγ9Vδ2 T cell cultures expanded from three to five different donors. Also, two different approaches were tested in cytotox assays with PC3 as a target: first the cytotox assays were conducted at the specific day of expansion, while the Vγ9Vδ2 T cells were 'in culture', meaning that cytotox was done on day 9, then waited 5 days to setup another cytotox on day 14, and again on day 25. The same days as the cytotox assay were performed, Vγ9Vδ2 T cells 'in culture' were also cryopreserved. The second approach was then to thaw cells, frozen at day 9, 14 and 25, and perform a cytotox assay in one setup. Both approaches showed similar results and representative data are shown in **Figures 1B, C**. For cytotox assay with A2058 and MDA-MB-231 as targets, only frozen Vγ9Vδ2 T cell cultures were used as effector cells.

Antigen Cross-Presentation Assay

Vγ9Vδ2 T cells were expanded *in vitro* for 9-11 days prior to the APC assay. The setup for the APC assay was as following: *Day 1*, Vγ9Vδ2 T cells were stimulated with 1 µM ZOL and 100 U/mL IL-2. *Day 2*, Vγ9Vδ2 T cells were exposed to either a long peptide or protein and incubated 24 h to allow for cross-presentation of antigens. *Day 3*, Vγ9Vδ2 T cells were carefully washed twice with PBS to remove excess peptide or protein within the supernatant. Antigen cross-presentation was measured by IFNγ or TNFα release, using ELISPOT assay (see overview in **Figure 3**). The effector cells were either CMV-specific αβTCR T cells, or αβTCR T cells specific for gp100, MART-1 or MAGE-A3. Vγ9Vδ2 T cells and the antigen specific αβTCR T effector cells (also called 'Teff' in **Figures 3** and **4**), was added to the ELISPOT plate in a ratio of 4:1 ('γδ': 'Teff'). This was followed by a 24 h incubation and development of the ELISPOT (see below). As a positive control, the Vγ9Vδ2 T cells were incubated with corresponding short peptide and co-cultured with the Teff. cells.

Peptide and proteins were added at the following concentrations: 0.5 µM long CMV peptide, 0.5 µM long gp100 peptide, 1.25 nM MART-1 recombinant protein and 27 nM MAGE-A3 recombinant protein. All short peptides were added as 5 nM.

Blocking of Antigen Cross-Presentation by the Proteasome Inhibitor Lactacystin

To test if antigen cross-presentation involved the proteasome, the proteasome inhibitor Lactacystin (Sigma Aldrich) was added to Vγ9Vδ2 T cells. In short, on 'Day 2' of the antigen cross-presentation assay: 50µM of Lactacystin was added to the Vγ9Vδ2 T cells. After two hours of incubation at 37°C, 5% CO_2, cells were washed twice in RPMI medium. From here, the long peptide or protein was added as described above. This means that lactacystin was added after the initial ZOL stimulation on day 1, but prior to addition of the peptide/protein on day 2. The idea was to ensure blocking of proteasome before addition of peptide/protein, to allow blocking of antigen cross-presentation.

Peptides and Proteins Used for the APC Assay

Overview of peptides and proteins used for the APC assay can be found in **Table 2**. All peptides were obtained from KJ Ross Petersen, with a purity >70%. All proteins were obtained from Abcam.

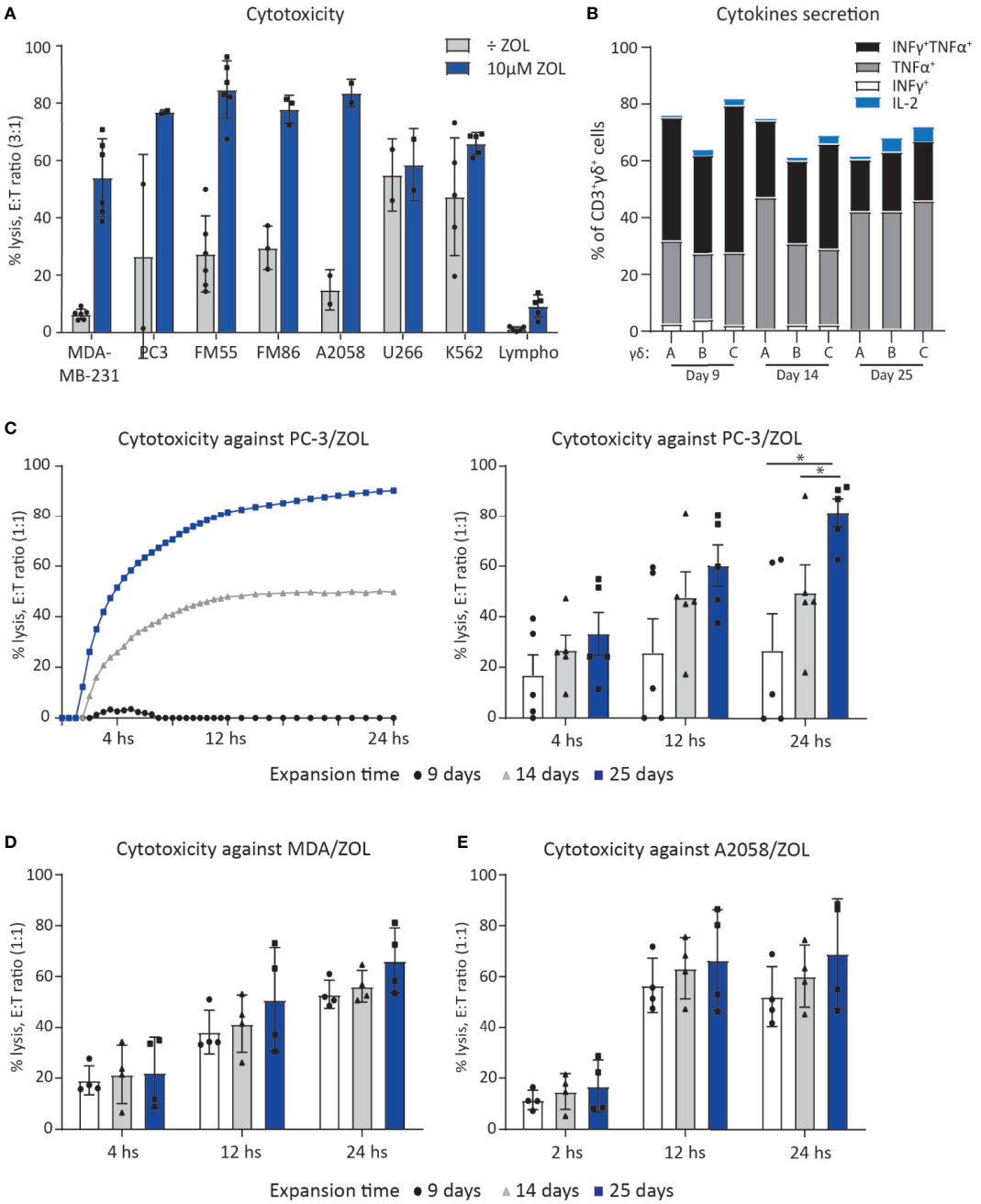

FIGURE 1 | Vγ9Vδ2 T cell can efficiently kill cancer cells. **(A)** Chromium release assay (4 h) was used to test Vγ9Vδ2 T cell ability to kill cancer cell lines of various origins. Vγ9Vδ2 T cells were expanded from healthy donors (n =2-6). Effector cell (E:T) Target cell ratio (3:1). Breast cancer cell line = MDA-MB-231, Prostate cancer cell line = PC-3. Melanoma cells lines = FM55, FM86 and A2058. Hematological cancer cells lines = U266 and K562. Lymphocytes (lympho) were thawed and rested overnight prior to the assay. Vγ9Vδ2 T cell cultures used in these assays had been in culture for 14-30 days prior to the chromium release assays. Purity >90% for Vγ9Vδ2 T cell cultures was verified by flow cytometry (data not shown, see gating strategy in **Supplementary Figure 1A**). **(B)** Cytokine expression of day 9, 14 and 24 expanded Vγ9Vδ2 T cells was determined by gating on positive cells in PC-3/ZOL co-cultured with Vγ9Vδ2 T cells. Gates were set according to PC-3 co-cultured control. Three different Vγ9Vδ2 T cell cultures were analyzed, named A, B and C **(C)** Vγ9Vδ2 T cells ability to kill PC-3/ZOL cancer cell line was compared between cultures expanded for 9, 14 or 25 days, using a 24 h xCELLigence assay at effector-target cell ratio (1:1). The left graph depict one donor, showing the full 24 h xCELLigence assay, and the right graph summarizes the data from five donors (n=5 donors, repeat three times) **(D)** Comparison of percentage cytolysis at effector-target cell ratio (1:1) in xCELLigence assay, assessing Vγ9Vδ2 T cells expanded for 9, 14 or 25 days, targeting MDA-MD-231/ZOL (MDA). (n=3 donors, repeat twice) **(E)** Comparison of percentage cytolysis at effector-target cell ratio (1:1) in xCELLigence assay, assessing Vγ9Vδ2 T cells expanded for 9, 14 or 25 days, targeting A2058/ZOL (MDA). (n=3 donors, repeat twice). Statistical significance was determined by a paired T-test. *P ≤ 0.05. Error bars indicated standard error of mean (SD).

TABLE 2 | List of short peptides, long peptides and proteins used in this study.

Name	ID	HLA restriction	Size	Peptide sequence
HIV short	HIV	HLA-A*01.01	9aa	GSEELRSLY
HIV short	HIV	HLA-A*02.01	9aa	ILKEPVHGV
CMV short	CMV_nlv	HLA-A*02.01	9aa	NLVPMVATV
CMV long	CMV_480	–	40aa	VFTWPPWQAGILARNLVPMVATV QGQNLKYQEFFWDANDI
Gp100 short	Gp100_280	HLA-A*02.01	9aa	YLEPGPVTA
Gp100 long	Gp100 long	–	29aa	SRALVVTHTYLEPGPVTA QVVLQAAIPLT
MART-1 short	MART_27-36	HLA-A*02.01	10aa	ELAGIGILTV
Recombinant MART-1 protein	–	–	118aa	N- ELAGIGILTV- N
MAGE-A3 short	MAGE-A3_199-209	HLA-A*01.01	9aa	EVDPIGHLY
Recombinant MAGE-A3 protein	–	–	314aa	N- EVDPIGHLY- N

ELISPOT Assay

ELISPOT assay was used to measure cross-presentation of antigens by Vγ9Vδ2 T cells. In brief, ELISPOT plates (nitrocellulose bottomed 96-well plates by MultiScreen MAIP N45; Millipore) were coated ON with IFNγ capture antibody (Ab) (Mabtech) and afterwards blocked by X-vivo medium. Vγ9Vδ2 T cells (target cells) were placed in the ELISPOT plate (setup in triplicates) and short control peptides were added at 5 nM (see sequence above), with and without Teff. cells. The effector cells were either CMV, gp100, MART-1 or MAGE-A3 specific αβTCR T cells. The cells were then incubated ON, after which, the plates were washed off and secondary biotinylated Ab (Mabtech) was added. After 2 h incubation, unbound secondary antibody was washed off and streptavidin conjugated alkaline phosphatase (Mabtech) was added for 1 h. Finally, unbound conjugated enzyme was washed off and the assay developed by adding BCIP/NBT substrate (Mabtech). Developed ELISPOT plates were analyzed on CTL ImmunoSpot S6 Ultimate-V analyzer using Immunospot software v5.1.

Criteria for standard protocol guidelines as well as determination of ELISPOT responses have been a challenge. In this regard, these ELISPOT assays were conducted according to the guidelines provided by CIP (48). Significance was determined by using the nonparametric distribution-free resampling (DFR) test which gives a way of formally comparing antigen-stimulated wells with negative control wells (49).

Apoptosis Staining

To detect apoptotic and dead cells after incubation with proteasome inhibitor Lactacystin, 0.5 x 10^6 day-9 expanded Vγ9Vδ2 T cells were seeded in a round-bottom 96-well plate in X-vivo + 5% HS. Lactacystin (Sigma Aldrich) was dissolved in sterile H_2O and added to the wells at final concentrations of 0 μM, 1 μM, 10 μM, 25 μM, 50 μM and 100 μM. After two hours of incubation at 37°C, 5% CO_2, cells were washed twice with PBS + 2% FBS and stained with the following extracellular antibodies in a total volume of 50 μl for 20 min at 4°C: anti-CD3 PE-Cy7, anti-TCRγ/δ FITC and anti-HLA-ABC BV711. After two washes with PBS + 2% FBS, apoptotic and dead cells were marked by staining with the Pacific Blue™ Annexin V/SYTOX™ AADvanced™ Apoptosis Kit (Invitrogen™). Annexin V binds to phosphatidylserine exposed on the outer membrane of apoptotic cells and SYTOX™ AADvanced™ Dead Cell Stain detects necrotic cells due to their loss of membrane integrity. A stain master mix was prepared by diluting Pacific Blue™ Annexin V and SYTOX™ AADvanced™ in 1X Annexin binding buffer. Cells were stained with 100 μl stain master mix per well for 30 min at 4°C and acquired on a NovoCyte Quanteon (ACEA Biosciences) without further washes.

Statistical Analysis

Statistical analyses were conducted using Graph-Pad Prism 7 (San Diego, USA). Differences between groups were determined by a paired T test. ELISPOT responses were analyzed using distribution free resampling (DFR) method, described by Moodie et al. for statistical analysis of ELISPOT responses (49, 50). The DFR method described here was used for statistical analysis of triplicates. DFR, $p \leq 0.05$ (*) were considered statistically significant. Statistical analysis was performed using Rstudio (RStudio Team (2016). RStudio: Integrated Development for R. RStudio, Inc., Boston, MA URL http://www.rstudio.com/).

RESULTS

Vγ9Vδ2 T Cells Cytotoxic Capacity Increases With Culturing Time

Vγ9Vδ2 T cells ability to kill cancer cell lines of various origins, was tested in a 4 h chromium release assay. Expanded Vγ9Vδ2 T cells from 2-5 healthy donors were used as effector cells to kill target cells, with or without sensitization with ZOL (**Figure 1A**). Effective killing when sensitized with ZOL was demonstrated in three melanoma cells lines (FM55, FM86 and A2058), a prostate cancer (PC-3) and a breast cancer cell line (MDA-MB-231) reaching 60-80% lysis. Two hematological cancer cell lines, myeloma (U266) and chronic myelogenous leukemia (K562), were also efficiently killed by Vγ9Vδ2 T cells varying from 50-70% lysis, even in the absence of ZOL sensitization. To test if Vγ9Vδ2 T cells would also kill normal healthy cells, allogeneic PBMCs (called lympho), were used as target cells. The data showed that the killing of PBMCs was below 15%, even after sensitized with ZOL (5-15%) (**Figure 1A**). Thus, while Vγ9Vδ2 T

cells efficiently killed cancer cells, healthy lymphocytes were mainly left untouched.

For deeper characterization of the killing capacity, we performed long-term killing over the course of 24 h using the xCELLigence assay and additionally assessed the cytotoxic abilities of Vγ9Vδ2 T cells at different time-points of expansion. Vγ9Vδ2 T cells cultured from five healthy donor, expanded for 9, 14 or 25 days, were compared in their killing potential of PC-3 sensitized with ZOL, at an effector cell (E):(T) target cell ratio of 1:1. Exemplified in **Figure 1C**, the killing of PC-3/ZOL cancer cells by Vγ9Vδ2 T cells increased with expansion time; with Vγ9Vδ2 T cells expanded for 25 days being most efficient reaching almost 100% lysis, compared to ~45% lysis and ~0-5% lysis forVγ9Vδ2 T cells expanded for 14 days or 9 days, respectively. **Figure 1C** also summarizes the data of all five Vγ9Vδ2 T cell cultures, showing a significant higher cancer cell killing capacities for cultures that were expanded the longest in culture. The enhanced killing capacity was most evident at 24 h of co-culture, with Vγ9Vδ2 T cell cultures expanded for 25 days reaching on average ~90% lysis, compared to ~50% lysis and ~30% lysis for T cells expanded for 14 days or 9 days, respectively. Importantly, when increasing the E:T ratio to 3:1, all Vγ9Vδ2 T cell cultures had comparable ability to kill prostate cancer cells (data not shown), irrespective of expansion time. In similar setups, the ability of Vγ9Vδ2 T cells to kill A2058 and MDA-MB-231, sensitized with ZOL, was tested (**Figures 1D, E**). A tendency towards a higher cancer cell killing capacities for Vγ9Vδ2 T cell cultures that were expanded the longest in culture, could also been observed here (**Figures 1D, E**). Together, all Vγ9Vδ2 T cell cultures were capable of cancer cell killing even those of short-term expansion, but cytotoxic capacity seems to increase over expansion time, with differences depending on the cells targeted.

Finally, we setup an ICS assay, to investigate the activation of Vγ9Vδ2 T cells upon tumor engagement. Vγ9Vδ2T cells were co-cultured with PC-3 with or without ZOL, for 5 hours, and expression of IFNγ, TNFα and IL-2 was measured (**Figure 1B**). Altogether, 60-80% Vγ9Vδ2 T cells expressed one or more of the cytokines upon engagement with PC-3/ZOL – this was compared to Vγ9Vδ2 T cells cocultured with PC-3 without ZOL. IL-2 expression was generally below 5% for all conditions. No significant difference was observed between 9, 14 or 25 expansion days, and hence, the difference observed in killing, could not be explained by expression of the cytokines IFNγ, TNFα and IL-2.

Phenotype Analysis of Vγ9Vδ2 T Cell Cultures

The phenotype dynamics of Vγ9Vδ2 T cell cultures over time was analyzed by flow cytometry. Vγ9Vδ2 T cell cultures were expanded from PBMCs of three healthy donors using 10 μM ZOL and 1000 U/ml IL-2. Initially only 0.5-5% of CD3-postive cells were Vγ9Vδ2 T cells (see **Figure 2E**). After 11 days of expansion, frequency of CD3-positive T cells was above 90% for all cultures and more than 95% of these cells were Vγ9 positive). Of the remaining cells in the cultures, NK cells constituted between 2-7% at day 9-11, but continued to decline to below 2% from day 19 (**Figure 2A**). The expression of the co-stimulatory markers CD80, CD86 and CCR7 was highest in the initial expansion phase (**Figure 2B**), in particular for CCR7 where the expression by day 9 varied from ~30-60% and dropped to zero at day 15. CD80 and CD86 were more widely expressed reaching 80-100%, and a decline starting around day 13 or 15, though at a less rapid decrease. In contrast, HLA-DR expression stayed above 90% throughout the expansion period (**Figure 1C**).

It has previously been described that expanded Vγ9Vδ2 T cells can express NK cell markers involved in killing such as NKG2D (51, 52). The data in **Figure 2C** shows, that NKG2D expression increased rapidly after day 9 and reached >80% from day 19 and onwards. The expression of the adhesion molecule CD56, increased steadily with time and reached >90% expression at day 28. CD16, a molecule involved in antibody dependent cell cytotoxicity (ADCC), was also expressed but a high degree of variance (20-60%) was observed between the Vγ9Vδ2 T cell cultures – though an increase in expression from day 9 and onwards, was observed. Finally, DNAM-1 stayed above 90% throughout the expansion period (**Figure 1C**). Notably, contrary to the decreased expression of co-stimulatory markers over time, the expression of NK markers increased with time (**Figures 2B, C**).

Other markers, such as CD161 and the GPR56, has also been suggested as markers of a cytotoxic phenotype for Vγ9Vδ2 T cells. CD161 is a C-type lectin, proposed to be involved in increased IFNγ production during γδTCR activation or in response to IL-12 and IL-18 (53). GPR56 is a G protein-coupled receptor, that although still poorly defined, appears to be involved or associated with a cytotoxic phenotype of T cells (54). We found, that both CD161 and GPR56 was expressed on almost 100% of the Vγ9Vδ2 T cells from day 9-28 (see **Supplementary Figure 1D**). For transparency, the expression of both molecules is here depicted by MFI. As for GPR56 we observed an increase in MFI during culturing time, and for CD161 the opposite, a slight decrease (see **Figure 1D**). The biological relevance of these change compared to percentage expression is unknown. A similar trend was observed for HLA class I, with a decrease in expression during culturing time, a change that was difficult to observe when only looking a percentage expression (**Figure 2D** and **Supplementary Figure 1D**). The overall gating strategy for phenotype analysis of Vγ9Vδ2 T cells is shown in **Supplementary Figure 1**.

Cross-Presentation of Virus-Specific Antigens by Vγ9Vδ2 T Cells

We next set out to test the ability of Vγ9Vδ2 T cells to cross-present tumor antigens, because Vγ9Vδ2 T cells in the early expansion (day 7-13) express co-stimulatory markers (**Figure 2A**) and previously has been shown to cross-present virus peptides (23). To verify findings by Brandes et al. (23), and to validate our assays, we first tested Vγ9Vδ2 T cells' ability to cross-present a virus antigen. Our experimental setup is illustrated in **Figure 3**; Vγ9Vδ2 T cells were expansion for 9-11 days after which the long peptide or protein, and minimal peptide for positive control was added for 24 hs. This was followed by analysis of Vγ9Vδ2 T cells (written as 'γδAPC') as targets for specific αβTCR T effector cells ('Teff.') using ELISPOT assay. IFNγ secretion was used as a measurement for specific target recognition and hence

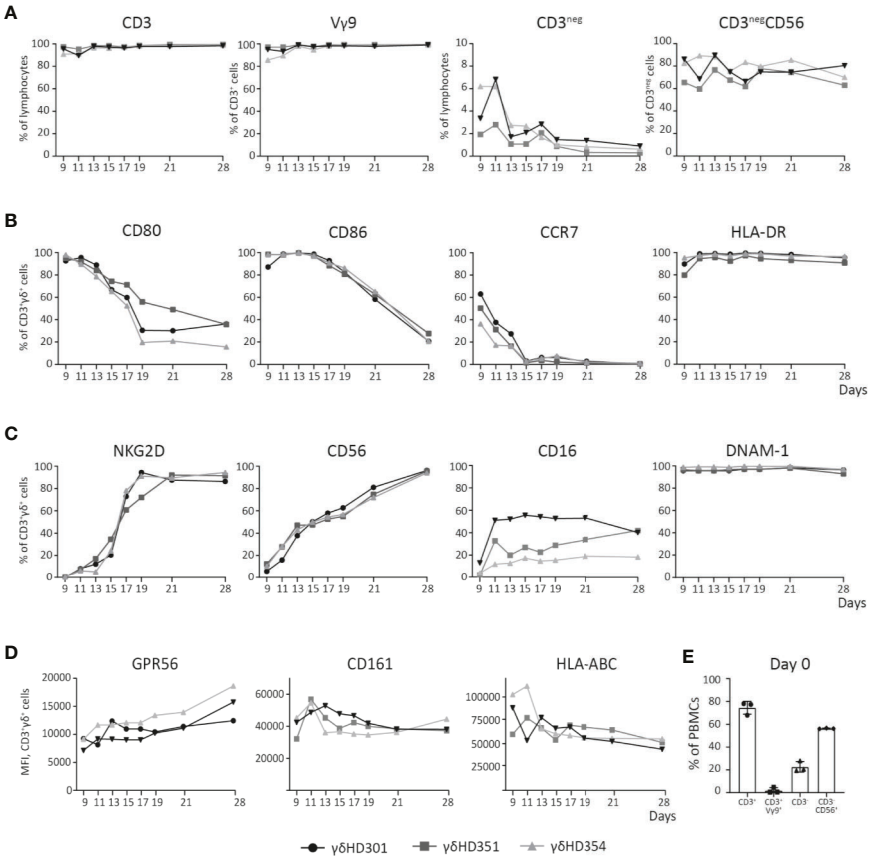

FIGURE 2 | Phenotype analysis of Vγ9Vδ2 T cell cultures over time. Vγ9Vδ2 T cells cultures were expanded from three different healthy donors (HD), and analyzed by flow cytometry during culturing time *in vitro* up to 28 days. **(A)** Purity of the Vγ9Vδ2 T cell cultures is shown, by looking at both $CD3_{pos}$ and Vγ9Vδ2 (Vγ9) T cells, but also $CD3_{neg}$ and NK ($CD3_{neg}CD56$) cells. **(B)** Vγ9Vδ2 T cell percentage expression of CD80, CD86, CCR7 and HLA-DR is shown. **(C)** Vγ9Vδ2 T cell percentage expression of NKG2D, CD56, CD16, and DNAM-1 is shown. **(D)** Finally, Vγ9Vδ2 T cells expression of GPR56, CD161 and HLA-ABC is shown by MFI values. **(E)** Purity analysis on day 0 of the PBMCs used for expansion to Vγ9Vδ2 T cells cultures. Complete gating strategies can be found in **Supplementary Figure 1**. (n=3).

antigen cross-presentation. In **Supplementary Figure 2A**, successful antigen cross-presentation of the CMV epitope was demonstrated in ELISPOT as the long (40aa) CMV peptide reached ~50% of IFNγ secretion compared to the positive control with short CMV peptide, which is loaded on the HLA-molecules extracellularly. This successfully supported previously data and validated the assay.

Cross-Presentation of Tumor Antigens by Vγ9Vδ2 T Cells

The ability of Vγ9Vδ2 T cells to cross-present tumor antigens was investigated using three tumor-antigen specific $CD8^+$ αβTCR T effector cells (Teff.) that recognized, gp100 or MART-1 in an HLA-A*02:01-restricted manner, or MAGE-A3 with HLA-A*01:01 restriction. These were generated by either transfection or transduction of the TCR into αβ T cells (see material and methods). The specificity of the three αβTCR T effector cells (Teff.) was established using IFNγ ELISPOT upon recognition of the minimal gp100, MART-1, or MAGE-A3 peptide (**Table 2**) compared to reactivity to a minimal HIV peptide as negative control (The grey bars of **Figures 4A–C**). Specificity of these transfected/transduced αβTCR T effector cells (Teff.) was also confirmed in chromium release assay (data not shown).

To test cross-presentation of tumor antigens by Vγ9Vδ2 T cells, expanded Vγ9Vδ2 T cells were incubated for 24 hs with; the long gp100 peptide (29aa) which contains the minimal epitope flanked on both sides by several amino acids (**Table 2**); or the recombinant MART-1 protein; or the MAGE-A3 protein. Antigen-exposed Vγ9Vδ2 T cells were used as APC (γδ-APC), and recognition by Teff. was analyzed by IFNγ ELISPOT. Specific recognition was observed for all three antigens yielding roughly 50% of the spot count in the cross-presentation situation (blue bars) compared to the peptide-loaded condition (black bar) (**Figures 4A–C**). As an additional control for Teff. potential reactivity to long peptide, we also setup an ELISPOT with only Teff., added either short HIV peptide, short gp100 peptide or long gp100 peptide. Reactivity was only observed against the short gp100 peptide (compared to the short HIV peptide), and also not against the long gp100 peptide (see **Supplementary Figure 2B**). In conclusion, our data show that Vγ9Vδ2 T cells

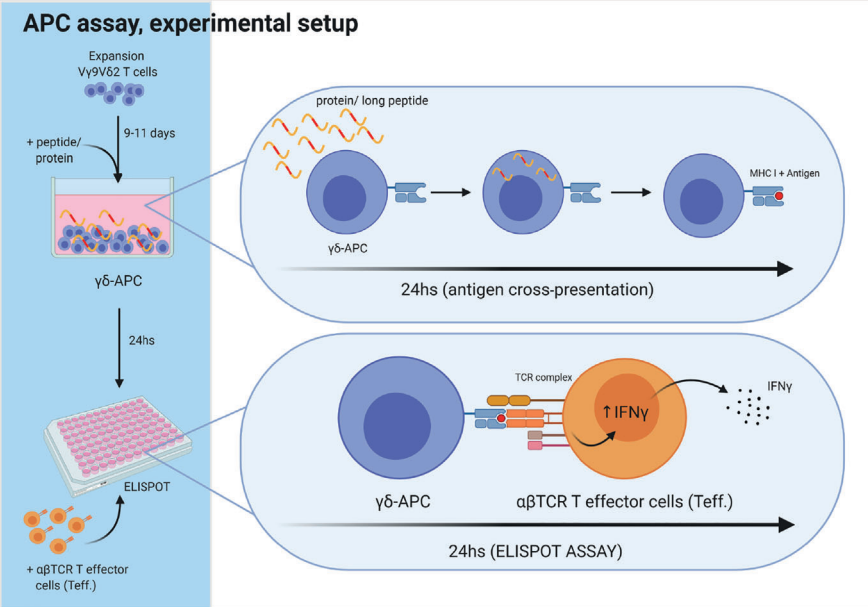

FIGURE 3 | Experimental setup for antigen cross-presenting assay. The ability of Vγ9Vδ2 T cells to cross-present antigens was tested as schematically outlined. Vγ9Vδ2 T cells were expanded for 9-11 days, as described in the method section. Next, long peptide or protein was added to wells with Vγ9Vδ2 T cells, followed by 24 h incubation, to allow antigen uptake and cross-presentation. Then, the Vγ9Vδ2 T cells were washed twice to remove excess long peptide or protein. Next, Vγ9Vδ2 T cells were transferred to the ELIPOT plate and antigen specific αβTCR T effector cells (Teff) were added. IFNγ secretion following specific target recognition was measured by IFNγ ELISPOT assay. Vγ9Vδ2 T cells alone were used as negative controls. For positive controls, short peptide was added to wells containing both Vγ9Vδ2 T cells and Teff leading to maximal recognition and associated cytokine secretion by Teff.Figure is created with Biorender.

can cross-present the tumor-associated antigens (TAA) gp100, MART-1 and MAGE-A3.

Cross-Presentation of Tumor Antigen Is Proteasome Dependent

To further strengthen these results, we included a proteasome inhibitor, lactacystin. To ensure that lactacystin was not toxic to the cells, an apoptosis assay was performed (**Supplementary Figure 3**), confirming that addition of 50μM lactacystin did not result in significant increase of either dead or apoptotic cells, nor a decrease in living cells. Analysis of HLA class I expression in response to lactacystin, showed no significant difference in expression. For the antigen cross-presentation assay, the lactacystin was added after the initial ZOL stimulation on day 1, but prior to addition of the peptide/protein on day 2. The rationale was to ensure blocking of the proteasome before addition of long-peptide/protein, to allow blocking of antigen cross-presentation. Addition of lactacystin, in the cross-presentation assay reduced the number of IFN-γ spots significantly (bars with stripes), emphasizing that cross-presentation by Vγ9Vδ2 T cells is, at least in part, mediated by the proteasome (**Figure 4C**).

DISCUSSION

Vγ9Vδ2 T cells as well as αβ T cells are known to recognize infected and cancerous cells, but by very different mechanisms. αβ T cells recognize peptides bound to HLA molecules, whereas Vγ9Vδ2 T cells recognize pAg independently of HLA. As a consequence, Vγ9Vδ2 T cells recognize and kill cancer cells independently of tissue type, and its specificity is broader compared to αβ T cells at the clonal level. Most of the target molecules recognized by Vγ9Vδ2 T cells are broadly expressed on cancer cells (55). Our results support this notion by showing that Vγ9Vδ2 T cells can kill cancer cells of various histotypes, ranging from breast cancer, prostate cancer, melanoma to hematological cancers. Furthermore, the killing capacity of Vγ9Vδ2 T cells can be significantly increased upon sensitization with ZOL, with the exception of the hematological cancer cell lines, which were killed quite efficiently in the absence of sensitization.

Data from several studies have shown that Vγ9Vδ2 T cells can express both co-stimulatory and NK markers. To our knowledge, previous comparisons have merely been restricted to single time points (20, 56), stimuli dependent expression (57) or comparison of NK markers (58). Here, we aimed to observe the expression of these markers over an extended period, to obtain a better understanding of the dynamics of the phenotype over time during *in vitro* generation of Vγ9Vδ2 T cell cultures. We observed that co-stimulatory markers CD80, CD86 and CCR7 are highly expressed in the initial expansion phase, followed by a decrease, while expression of NK markers tended to increase over time. This seems to especially involve an increase in NKG2D, CD56, to a minor extent CD16 and GPR56. These markers have also been suggested by others in describing cytotoxic phenotype

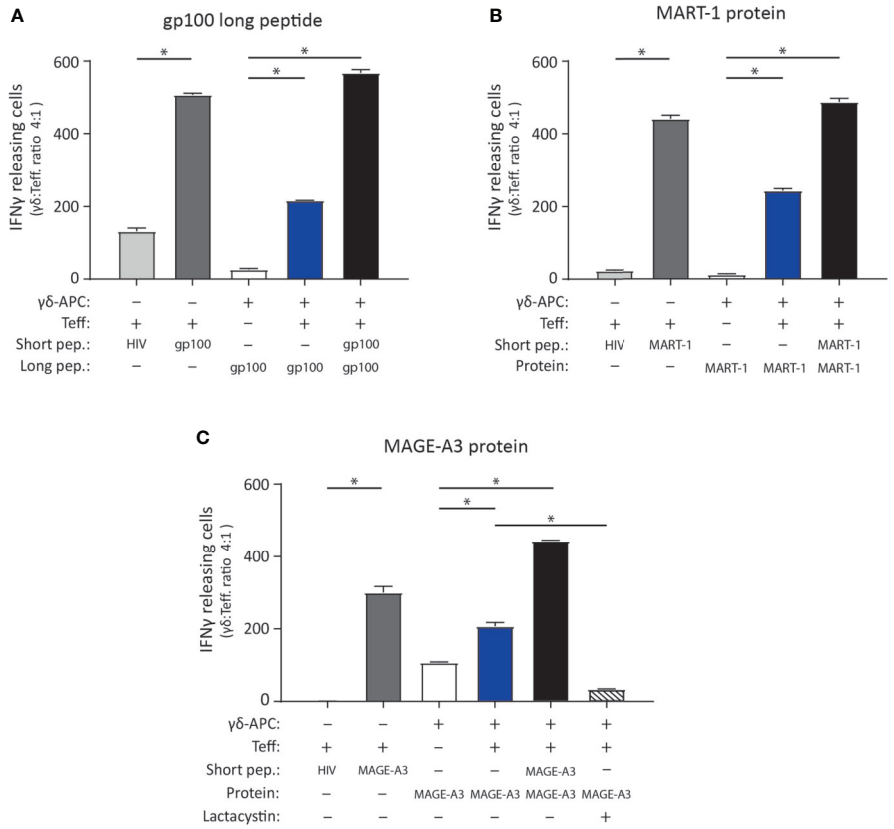

FIGURE 4 | Vγ9Vδ2 T cells can cross-present tumor antigen from long tumor peptides and tumor proteins. To test the ability of Vγ9Vδ2 T cells to cross-present tumor antigen, the experimental APC setup illustrated in **Figure 3** was used. **(A–C)** Specificity of the tumor antigen specific CD8$^+$ αβTCR T cells which were used as effector cells in the APC assay, is shown by ELISPOT assay. This includes three different αβTCR T effecter cells (called 'Teff'), being specific for either gp100 (YLEPGPVTA, HLA-A*02.01-restricted), MART-1 (ELAGIGILTV, HLA-A*02.01-restricted) or MAGE-A3 peptide (EVDPIGHLY, HLA-A*01.01-restricted). Short peptides for gp100, MART-1 or MAGE-A3 peptides, were added to the ELISPOT wells as a positive control (5 nM) and confirmed specificity (dark grey bars) by comparison the unspecific short HIV peptide (ILKEPVHGV), used as negative control (light grey bars in figure a, b and c). Peptide concentration was 5 nM. (n=3, triplicates). **(A)** Tumor antigen cross-presentation was measured using IFNγ ELISPOT assay. Cross-presentation of a long gp100 peptide (29aa, 0.5 μM), recognized by gp100 specific αβTCR cells (Teff.) (n=3 triplicates). **(B)** Cross-presentation of MART-1 recombinant protein (118aa, 1.25 nM), recognized by MART-1 specific αβTCR effector cells (T.eff) (n=3 triplictes). **(C)** Cross-presentation of MAGE-A3 recombinant protein (314aa, 27 nM), recognized by MAGE-A3 specific αβTCR effector cells (Teff). Additionally, inhibition of cross-presentation of the MAGE-A3 recombinant protein was shown by addition of 50 μM lactacystin (proteasome inhibitor) (n=3, repeated in 4 independent experiments). γδ-APC refers to the Vγ9Vδ2 T cells that served as APC for antigen presentation, Teff refers to the αβTCR T effector cells, pep = peptide. All experiments were carried out in triplicates, and distribution free resampling (DFR) method was used for statistical analysis. P-value ≤ 0.05 (*) were considered statistically significant. Error bars indicated SD.

for Vγ9Vδ2 T cells (22, 59, 60). To investigate whether these phenotypic changes actually corresponded to changes in functionality, we compared the cytotoxic capacity of Vγ9Vδ2 T cells expanded for 9 days *versus* those expanded for 14 or 25 days. Vγ9Vδ2 T cells, independent of duration of expansion, were able to kill cancer cells. However, a significant difference in killing efficiency could be observed between the γδ T cell populations at low EC : TC ratio; with Vγ9Vδ2 T cells expanded for more than 25 days being the most efficient cancer cell killers. This was most pronounced when targeting the prostate cancer cell PC-3, whereas only a tendency could be observed when targeting MDA-MB-231 or A2058. Overall, this supports our findings that Vγ9Vδ2 T cell cultures switch from a co-stimulatory phenotype into a more effector cell type during prolonged expansion times *in vitro*.

Expression of co-stimulatory markers has traditionally been described for professional APC, such as DCs, and has been shown to be essential for priming of naïve αβ T cells (61). A comparison of antigen presenting capacity of Vγ9Vδ2 T cells with DCs has been reported elsewhere. In short, Brandes and colleagues demonstrated that *in vitro* Vγ9Vδ2 T cells are equal to DCs in their ability to present virus antigen and activate αβ T cells (20). The same study also showed that Vγ9Vδ2 T cells are capable of cross-presenting virus antigens, and as study by Capsomidis et al, showed antigen cross-presentation of a long MART-1 peptide (25 amino acids long) (22). In further consideration of tumor antigens, Himoudi et al., demonstrated that Vγ9Vδ2 T cells can cross-present long peptide as well as cancer cell derived protein, the latter requiring opsonization of target cells (24). We show cross-presentation by Vγ9Vδ2 T cells

for three different tumor antigens; gp100, MART1 and MAGE-A3, as long peptide or recombinant protein and restricted by two different HLA molecules (**Figure 4**). The exact mechanism of how antigens are cross-presented is still under investigation, and cross-presentation without the involvement of the proteasome and transporter associated with antigen processing (TAP) has been described (62). However, most studies have demonstrated a mandatory requirement for proteasomal activity (25). To substantiate this notion, we took advantage of the proteasome inhibitor lactacystin which led to a highly reduced IFNγ response of MAGE-A3-specific CD8 T cells (see **Figure 4C**), strongly suggesting that the proteasome is indeed involved in cross-presentation of antigens by Vγ9Vδ2 T cells. Minor variation in efficacy can be observed between the three Teff. cells, but this has also been described elsewhere, for example by Morel et al. (63) and we still find the antigen cross-presentation to be solid for all three Teff.

Collectively, our data support the role of Vγ9Vδ2 T cells as an antigen presenting cells *in vitro*. Whether this is a physiological relevant function *in vivo* is still unknown and we do not know the exact mechanism of antigen uptake. The study of Himoudi et al., could demonstrate a significantly improved uptake of cells upon opsonisation (24). We tested uptake of protein but did not test uptake of cells in our system, but Vγ9Vδ2 T cells have been shown to take up antigen by phagocytosis (64) as well as trogocytosis (65) and it seems likely that antibody binding could possibly improve both. Based on our results, it is clear that Vγ9Vδ2 T cells can take up antigen regardless of opsonization, and cross-present the antigen to CD8 T cells.

We were able to demonstrate a shift in phenotype and cytotoxic capacity associated with culture time. However, even at early time points when the cells are highly capable of antigen cross-presentation – the cells are efficient killers. This is in agreement with previous studies showing that Vγ9Vδ2 T cells can cross-present antigens from target cells which they just had killed (24). At this stage, the Vγ9Vδ2 T cells should still express CCR7 and supposedly migrate to lymph nodes to initiate or support CD8 T cell activation. This notion is currently purely speculative, although it has been shown that Vγ9Vδ2 T cells have a supportive role for antitumor responses performed by αβ T cells (66).

Vγ9Vδ2 T cells have been tested in ACT, and the condition used for expansion of Vγ9Vδ2 T cells in the present study should be relevant for the generation of such cells for clinical application. The presented data reveal important information regarding dynamic changes during prolonged time in culture and highlight the possibility that the change in function to some extent can be monitored by changes in phenotype. Given the knowledge that *in vitro* expanded Vγ9Vδ2 T cells –do not present antigen in the absence of added tumor antigen –, the most rational setup for maximal cytotoxic effector function in ACT would be to use Vγ9Vδ2 T cells that do not express CCR7, e.g. have been expanded for 14 days or more. Alternatively, tumor antigen could be added for uptake and cross-presentation very early during the expansion, and cells be administered while they still express CCR7 on the surface, however, in that case much fewer cells. Potentially concurrent administration of IL-2 or IL15 could aid *in vivo* expansion and persistence (34, 67).

In conclusion, we show that *in vitro* expanded Vγ9Vδ2 T cells can kill cancer cells across a broad range of histotypes, cross-present tumor antigens in a proteasome-dependent manner and become more cytotoxic with culture time. We believe these dynamics of function and phenotype should be considered prior to clinical application.

DATA AVAILABILITY STATEMENT

The original contributions presented in the study are included in the article/**Supplementary Material**. Further inquiries can be directed to the corresponding author.

AUTHOR CONTRIBUTIONS

GHO: study design, development of methodology, data acquisition, analysis and interpretation, and writing of the manuscript. MI, AMCS, PA and SKS: data acquisition, analysis and interpretation, and revision of the manuscript. EN, RD, BM and ÖZ: development of methodology and data interpretation. PS: study supervision and design, development of methodology, data analysis and interpretation, and writing of the manuscript. All authors contributed to the article and approved the submitted version.

FUNDING

The project was supported by grants from The Danish Cancer Society (R72-A4396-13-S2), The Aase and Ejnar Danielsen Foundation, The Dagmar Marshalls Foundation, the A.P. Moller foundation, The Danish Council for Independent Research (DFF – 1331 – 00095B), and Dansk Kræftforskningsfond.

ACKNOWLEDGMENTS

We would like to acknowledge Dr. Andrew Gerry and Dr. Bent Jakobsen of Adaptimmune Ltd. (Oxfordshire, UK) for supplying us with lentiviral vectors for high affinity MAGE-A3^{a3a} TCR transduction and Dr. Niels Schaft (Universitätsklinikum Erlangen, Germany) for helpful suggestions in transfection setup.

SUPPLEMENTARY MATERIAL

The Supplementary Material for this article can be found online at: https://www.frontiersin.org/articles/10.3389/fimmu.2021.645131/full#supplementary-material

REFERENCES

1. Davis MM. T Cell Receptor Gene Diversity and Selection. *Annu Rev Biochem* (1990) 59:475–96. doi: 10.1146/annurev.bi.59.070190.002355
2. Karunakaran MM, Göbel TW, Starick L, Walter L, Herrmann T. Vγ9 and Vδ2 T Cell Antigen Receptor Genes and Butyrophilin 3 (BTN3) Emerged With Placental Mammals and are Concomitantly Preserved in Selected Species Like Alpaca (Vicugna Pacos). *Immunogenetics* (2014) 66:243–54. doi: 10.1007/s00251-014-0763-8
3. Ribeiro ST, Ribot JC, Silva-Santos B. Five Layers of Receptor Signaling in γδ T-cell Differentiation and Activation. *Front Immunol* (2015) 6:15. doi: 10.3389/fimmu.2015.00015
4. Kabelitz D. Human Gd T Cells: From a Neglected Lymphocyte Population to Cellular Immunotherapy: A Personal Reflection of 30 Years of Gd T Cell Research. *Clin Immunol* (2016) 172:90–7. doi: 10.1016/j.clim.2016.07.012
5. Holmen Olofsson G, Pedersen SR, Aehnlich P, Svane IM, Idorn M, Thor Straten P. The Capacity of CD4+ Vγ9vδ2 T Cells to Kill Cancer Cells Correlates With Co-Expression of CD56. *Cytotherapy* (2021) 0:1–8. doi: 10.1016/j.jcyt.2021.02.003
6. Belmant C, Decise D, Fournié JJ. Phosphoantigens and Aminobisphosphonates: New Leads Targeting γδ T Lymphocytes for Cancer Immunotherapy. *Drug Discovery Today Ther Strateg* (2006) 3:17–23. doi: 10.1016/j.ddstr.2006.02.001
7. Gu S, Borowska MT, Boughter CT, Adams EJ. Butyrophilin3A Proteins and Vγ9vδ2 T Cell Activation. *Semin Cell Dev Biol* (2018) 84:65–74. doi: 10.1016/j.semcdb.2018.02.007
8. Harly C, Guillaume Y, Nedellec S, Peigné C, Mönkkönen H, Mönkkönen J, et al. Key Implication of CD277/butyrophilin-3 (BTN3A) in Cellular Stress Sensing by a Major Human γδ T-cell Subset. *Blood* (2012) 120:2269–79. doi: 10.1182/blood-2012-05-430470
9. Vavassori S, Kumar A, Wan GS, Ramanjaneyulu GS, Cavallari M, El Daker S, et al. Butyrophilin 3A1 Binds Phosphorylated Antigens and Stimulates Human γδ T Cells. *Nat Immunol* (2013) 14:908–16. doi: 10.1038/ni.2665
10. Rigau M, Ostrouska S, Fulford TS, Johnson DN, Woods K, Ruan Z, et al. Butyrophilin 2A1 is Essential for Phosphoantigen Reactivity by Gd T Cells. *Sci (80-)* (2020) 367:1–24. doi: 10.1126/science.aay5516
11. Karunakaran MM, Willcox CR, Salim M, Paletta D, Fichtner AS, Noll A, et al. Butyrophilin-2A1 Directly Binds Germline-Encoded Regions of the Vγ9vδ2 TCR and Is Essential for Phosphoantigen Sensing. *Immunity* (2020) 52:487–98. doi: 10.1016/j.immuni.2020.02.014. e6.
12. Sandstrom A, Peigné CM, Léger A, Crooks J, Konczak F, Gesnel MC, et al. The Intracellular B30.2 Domain of Butyrophilin 3A1 Binds Phosphoantigens to Mediate Activation of Human Vγ9vδ2t Cells. *Immunity* (2014) 40:490–500. doi: 10.1016/j.immuni.2014.03.003
13. Willcox BE, Willcox CR. γδ TCR Ligands: The Quest to Solve a 500-Million-Year-Old Mystery. *Nat Immunol* (2019) 20:121–8. doi: 10.1038/s41590-018-0304-y
14. Altincicek B, Moll J, Campos N, Foerster G, Beck E, Hoeffler JF, et al. Cutting Edge: Human Gamma Delta T Cells are Activated by Intermediates of the 2-C-methyl-D-erythritol 4-Phosphate Pathway of Isoprenoid Biosynthesis. *J Immunol* (2001) 166:3655–8. doi: 10.4049/jimmunol.166.6.3655
15. Hintz M, Reichenberg A, Altincicek B, Bahr U, Gschwind RM, Kollas AK, et al. Identification of (E)-4-hydroxy-3-methyl-but-2-enyl Pyrophosphate as a Major Activator for Human Gammadelta T Cells in Escherichia Coli. *FEBS Lett* (2001) 509:317–22. doi: 10.1016/s0014-5793(01)03191-x
16. Kondo M, Izumi T, Fujieda N, Kondo A, Morishita T, Matsushita H, et al. Expansion of Human Peripheral Blood γδ T Cells Using Zoledronate. *J Vis Exp* (2011) 2:6–11. doi: 10.3791/3182
17. Thompson K, Rogers MJ. Statins Prevent Bisphosphonate-Induced Gamma, delta-T-cell Proliferation and Activation. *Vitro J Bone Miner Res* (2004) 19:278–88. doi: 10.1359/JBMR.0301230
18. Roelofs AJ, Jauhiainen M, Mönkkönen H, Rogers MJ, Mönkkönen J, Thompson K. Peripheral Blood Monocytes are Responsible for Gammadelta T Cell Activation Induced by Zoledronic Acid Through Accumulation of IPP/DMAPP. *Br J Haematol* (2009) 144:245–50. doi: 10.1111/j.1365-2141.2008.07435.x
19. Lança T, Correia DV, Moita CF, Raquel H, Neves-Costa A, Ferreira C, et al. The MHC Class Ib Protein ULBP1 is a Nonredundant Determinant of Leukemia/Lymphoma Susceptibility to Gammadelta T-cell Cytotoxicity. *Blood* (2010) 115:2407–11. doi: 10.1182/blood-2009-08-237123
20. Brandes M, Willimann K, Moser B. Professional Antigen-Presentation Function by Human Gammadelta T Cells. *Science* (2005) 309:264–8. doi: 10.1126/science.1110267
21. van Endert P. Intracellular Recycling and Cross-Presentation by MHC Class I Molecules. *Immunol Rev* (2016) 272:80–96. doi: 10.1111/imr.12424
22. Capsomidis A, Benthall G, Van Acker HH, Fisher J, Kramer AM, Abeln Z, et al. Chimeric Antigen Receptor-Engineered Human Gamma Delta T Cells: Enhanced Cytotoxicity With Retention of Cross Presentation. *Mol Ther* (2018) 26:354–65. doi: 10.1016/j.ymthe.2017.12.001
23. Brandes M, Willimann K, Bioley G, Lévy N, Eberl M, Luo M, et al. Cross-Presenting Human Gammadelta T Cells Induce Robust CD8+ Alphabeta T Cell Responses. *Proc Natl Acad Sci USA* (2009) 106:2307–12. doi: 10.1073/pnas.0810059106
24. Himoudi N, Morgenstern DA, Yan M, Vernay B, Saraiva L, Wu Y, et al. Professional Antigen Presentation by Interaction Human γδ T Lymphocytes Are Licensed for With Opsonized Target Cells. *J Immunol* (2012) 188:1708–16. doi: 10.4049/jimmunol.1102654
25. Embgenbroich M, Burgdorf S. Current Concepts of Antigen Cross-Presentation. *Front Immunol* (2018) 9:1643. doi: 10.3389/fimmu.2018.01643
26. Decker WK, da Silva RF, Sanabria MH, Angelo LS, Guimarães F, Burt BM, et al. Cancer Immunotherapy: Historical Perspective of a Clinical Revolution and Emerging Preclinical Animal Models. *Front Immunol* (2017) 8:829. doi: 10.3389/fimmu.2017.00829
27. Ahmad A, Uddin S, Steinho M. CAR-T Cell Therapies: An Overview of Clinical Studies Supporting Their Approved Use Against Acute Lymphoblastic Leukemia and Large B-Cell Lymphomas. *Int J Mol Sci* (2020) 21:1–9. doi: 10.3390/ijms21113906
28. Rosenberg SA, Yang JC, Sherry RM, Kammula US, Hughes MS, Phan GQ, et al. Durable Complete Responses in Heavily Pretreated Patients With Metastatic Melanoma Using T-cell Transfer Immunotherapy. *Clin Cancer Res* (2011) 17:4550–7. doi: 10.1158/1078-0432.CCR-11-0116
29. Mohty M, Gautier J, Malard F, Aljurf M, Bazarbachi A, Chabannon C, et al. CD19 Chimeric Antigen Receptor-T Cells in B-cell Leukemia and Lymphoma: Current Status and Perspectives. *Leukemia* (2019) 33:2767–78. doi: 10.1038/s41375-019-0615-5
30. Met Ö, Jensen KM, Chamberlain CA, Donia M, Svane IM. Principles of Adoptive T Cell Therapy in Cancer. *Semin Immunopathol* (2019) 41:49–58. doi: 10.1007/s00281-018-0703-z
31. European Medicines Agency. *First Two CAR-T Cell Medicines Recommended for Approval in the European Union | European Medicines Agency* (2018). Available at: https://www.ema.europa.eu/news/first-two-car-t-cell-medicines-recommended-approval-european-union.
32. Wilhelm M, Smetak M, Schaefer-Eckart K, Kimmel B, Birkmann J, Einsele H, et al. Successful Adoptive Transfer and *In Vivo* Expansion of Haploidentical γδ T Cells. *J Transl Med* (2014) 12:45. doi: 10.1186/1479-5876-12-45
33. Künkele K-P, Wesch D, Oberg H-H, Aichinger M, Supper V, Baumann C. Vγ9vδ2 T Cells: Can We Re-Purpose a Potent Anti-Infection Mechanism for Cancer Therapy? *Cells* (2020) 9:829. doi: 10.3390/cells9040829
34. Aehnlich P, Carnaz Simões AM, Skadborg SK, Holmen Olofsson G, Thor Straten P. Expansion With Il-15 Increases Cytotoxicity of Vγ9vδ2 T Cells and Is Associated With Higher Levels of Cytotoxic Molecules and T-Bet. *Front Immunol* (2020) 11:1868. doi: 10.3389/fimmu.2020.01868
35. Schaft N, Willemsen RA, de Vries J, Lankiewicz B, Essers BWL, Gratama J-W, et al. Peptide Fine Specificity of Anti-Glycoprotein 100 CTL Is Preserved Following Transfer of Engineered TCR Genes Into Primary Human T Lymphocytes. *J Immunol* (2003) 170:2186–94.
36. Met Ö, Balslev E, Flyger H, Svane IM. High Immunogenic Potential of p53 mRNA-Transfected Dendritic Cells in Patients With Primary Breast Cancer. *Breast Cancer Res Treat* (2011) 125:395–406. doi: 10.1007/s10549-010-0844-9
37. Cole DJ, Weil DP, Shamamian P, Rivoltini L, Kawakami Y, Topalian S, et al. Identification of MART-1-Specific T-Cell Receptors: T Cells Utilizing Distinct T-Cell Receptor Variable and Joining Regions Recognize the Same Tumor Epitope. *Cancer Res* (1994) 54:5265–8.
38. Leisegang M, Engels B, Meyerhuber P, Kieback E, Sommermeyer D, Xue S-A, et al. Enhanced Functionality of T Cell Receptor-Redirected T Cells is Defined

by the Transgene Cassette. *J Mol Med (Berl)* (2008) 86:573–83. doi: 10.1007/s00109-008-0317-3
39. Leisegang M, Turqueti-Neves A, Engels B, Blankenstein T, Schendel DJ, Uckert W, et al. T-Cell Receptor Gene-Modified T Cells With Shared Renal Cell Carcinoma Specificity for Adoptive T-Cell Therapy. *Clin Cancer Res* (2010) 16:2333–43. doi: 10.1158/1078-0432.CCR-09-2897
40. Cameron BJ, Gerry AB, Dukes J, Harper JV, Kannan V, Bianchi FC, et al. Identification of a Titin-Derived HLA-A1-Presented Peptide as a Cross-Reactive Target for Engineered MAGE A3-Directed T Cells. *Sci Transl Med* (2013) 5:197ra103. doi: 10.1126/scitranslmed.3006034
41. Li Y, Moysey R, Molloy PE, Vuidepot A-L, Mahon T, Baston E, et al. Directed Evolution of Human T-cell Receptors With Picomolar Affinities by Phage Display. *Nat Biotechnol* (2005) 23:349–54. doi: 10.1038/nbt1070
42. Idorn M, Olsen M, Halldórsdóttir HR, Skadborg SK, Pedersen M, Høgdall C, et al. Improved Migration of Tumor Ascites Lymphocytes to Ovarian Cancer Microenvironment by CXCR2 Transduction. *Oncoimmunology* (2017) 7: e1412029. doi: 10.1080/2162402X.2017.1412029
43. Ellebaek E, Iversen TZ, Junker N, Donia M, Engell-Noerregaard L, Met Ö, et al. Adoptive Cell Therapy With Autologous Tumor Infiltrating Lymphocytes and Low-Dose Interleukin-2 in Metastatic Melanoma Patients. *J Transl Med* (2012) 10:1–12. doi: 10.1186/1479-5876-10-169
44. Riddell SR, Greenberg PD. Rapid Expansion Method ("Rem") For in Vitro Propagation of T Lymphocytes. *United States Patent* (1998) 11182:3080–6.
45. Das H, Wang L, Kamath A, Bukowski JF. Vgamma2Vdelta2 T-cell Receptor-Mediated Recognition of Aminobisphosphonates. *Blood* (2001) 98:1616–8. doi: 10.1182/blood.v98.5.1616
46. Peper JK, Schuster H, Löffler MW, Schmid-Horch B, Rammensee HG, Stevanovic S. An Impedance-Based Cytotoxicity Assay for Real-Time and Label-Free Assessment of T-cell-mediated Killing of Adherent Cells. *J Immunol Methods* (2014) 405:192–8. doi: 10.1016/j.jim.2014.01.012
47. Solly K, Wang X, Xu X, Strulovici B, Zheng W. Application of Real-Time Cell Electronic Sensing (RT-CES) Technology to Cell-Based Assays. *Assay Drug Dev Technol* (2004) 2:363–72. doi: 10.1089/adt.2004.2.363
48. CIP Guidelines. Cip Assay Guidelines Guideline for Analyzing Antigen-Specific CD8 + T Cells With Interferon-Gamma ELISPOT Assay. *CIMT Immunoguiding Program* (2011) 4–7.
49. Moodie Z, Price L, Janetzki S, Britten CM. Handbook of ELISPOT. *Springer* (2012) 792:185–96. doi: 10.1007/978-1-61779-325-7
50. Moodie Z, Price L, Gouttefangeas C, Mander a, Janetzki S, Löwer M, et al. Response Definition Criteria for ELISPOT Assays Revisited. *Cancer Immunol Immunother* (2010) 59:1489–501. doi: 10.1007/s00262-010-0875-4
51. Shibuya A, Campbell D, Hannum C, Yssel H, Franz-Bacon K, McClanashan T, et al. Dnam-1, a Novel Adhesion Molecule Involved in the Cytolytic Function of T Lymphocytes. *Immunity* (1996) 4:573–81. doi: 10.1016/S1074-7613(00)70060-4
52. Lança T, Correia DV, Moita CF, Raquel H, Neves-Costa A, Ferreira C, et al. The MHC Class Ib Protein ULBP1 is a Nonredundant Determinant of Leukemia/Lymphoma Susceptibility to γ δ T-Cell Cytotoxicity. *Blood* (2011) 115:2407–11. doi: 10.1182/blood-2009-08-237123
53. Tian Y, Babor M, Lane J, Schulten V, Patil VS, Seumois G, et al. Unique Phenotypes and Clonal Expansions of Human CD4 Effector Memory T Cells Re-Expressing CD45RA. *Nat Commun* (2017) 8:1473. doi: 10.1038/s41467-017-01728-5
54. Peng Y-M, van de Garde MDB, Cheng K-F, Baars PA, Remmerswaal EBM, van Lier RAW, et al. Specific Expression of GPR56 by Human Cytotoxic Lymphocytes. *J Leukoc Biol* (2011) 90:735–40. doi: 10.1189/jlb.0211092
55. Sun L, Li Y, Jiang Z, Zhang J, Li H, Li B, et al. Vγ9vδ2 T Cells and Zoledronate Mediate Antitumor Activity in an Orthotopic Mouse Model of Human Chondrosarcoma. *Tumour Biol* (2016) 37:7333–44. doi: 10.1007/s13277-015-4615-4
56. Khan MWA, Curbishley SM, Chen HC, Thomas AD, Pircher H, Mavilio D, et al. Expanded Human Blood-Derived Gdt Cells Display Potent Antigen-Presentation Functions. *Front Immunol* (2014) 5:344. doi: 10.3389/fimmu.2014.00344
57. Mao C, Mou X, Zhou Y, Yuan G, Xu C, Liu H, et al. Tumor-Activated Tcrγδ+ T Cells From Gastric Cancer Patients Induce the Antitumor Immune Response of Tcrαβ+ T Cells *Via* Their Antigen-Presenting Cell-Like Effects. *J Immunol Res* (2014) 2014:593562. doi: 10.1155/2014/593562
58. Rincon-Orozco B, Kunzmann V, Wrobel P, Kabelitz D, Steinle A, Herrmann T. Activation of V 9V 2 T Cells by NKG2D. *J Immunol* (2005) 175:2144–51. doi: 10.4049/jimmunol.175.4.2144
59. Nussbaumer O, Thurnher M. Functional Phenotypes of Human Vγ9vδ2 T Cells in Lymphoid Stress Surveillance. *Cells* (2020) 9:772. doi: 10.3390/cells9030772
60. Fisher JPH, Yan M, Heuijerjans J, Carter L, Abolhassani A, Frosch J, et al. Neuroblastoma Killing Properties of Vδ2 and Vδ2-Negative γδt Cells Following Expansion by Artificial Antigen-Presenting Cells. *Clin Cancer Res* (2014) 20:5720–32. doi: 10.1158/1078-0432.CCR-13-3464
61. Kershaw MH, Westwood JA, Darcy PK. Gene-Engineered T Cells for Cancer Therapy. *Nat Rev Cancer* (2013) 13:525–41. doi: 10.1038/nrc3565
62. Shen L, Sigal LJ, Boes M, Rock KL. Important Role of Cathepsin S in Generating Peptides for TAP-independent MHC Class I Crosspresentation. *Vivo Immun* (2004) 21:155–65. doi: 10.1016/j.immuni.2004.07.004
63. Morel S, Lévy F, Burlet-Schiltz O, Brasseur F, Probst-Kepper M, Peitrequin AL, et al. Processing of Some Antigens by the Standard Proteasome But Not by the Immunoproteasome Results in Poor Presentation by Dendritic Cells. *Immunity* (2000) 12:107–17. doi: 10.1016/s1074-7613(00)80163-6
64. Wu Y, Wu W, Wong WM, Ward E, Thrasher AJ, Goldblatt D, et al. Human γδ T Cells: A Lymphoid Lineage Cell Capable of Professional Phagocytosis. *J Immunol* (2009) 183:5622–9. doi: 10.4049/jimmunol.0901772
65. Poupot M, Pont F, Fournié J-J. Profiling Blood Lymphocyte Interactions With Cancer Cells Uncovers the Innate Reactivity of Human γδ T Cells to Anaplastic Large Cell Lymphoma. *J Immunol* (2005) 174:1717–22. doi: 10.4049/jimmunol.174.3.1717
66. Chen H-C, Joalland N, Bridgeman JS, Alchami FS, Jarry U, Khan MWA, et al. Synergistic Targeting of Breast Cancer Stem-Like Cells by Human γδ T Cells and CD8+ T Cells. *Immunol Cell Biol* (2017) 95(7):620–9. doi: 10.1038/icb.2017.21
67. Van Acker HH, Anguille S, Willemen Y, Van den Bergh JM, Berneman ZN, Lion E, et al. Interleukin-15 Enhances the Proliferation, Stimulatory Phenotype, and Antitumor Effector Functions of Human Gamma Delta T Cells. *J Hematol Oncol* (2016) 9:101. doi: 10.1186/s13045-016-0329-3

Conflict of Interest: The authors declare that the research was conducted in the absence of any commercial or financial relationships that could be construed as a potential conflict of interest.

frontiers in Immunology

ORIGINAL RESEARCH
published: 15 October 2021
doi: 10.3389/fimmu.2021.699478

"γδT Cell-IL17A-Neutrophil" Axis Drives Immunosuppression and Confers Breast Cancer Resistance to High-Dose Anti-VEGFR2 Therapy

Zhigang Zhang[1,2†], Chenghui Yang[3†], Lili Li[2,4], Ying Zhu[1], Ke Su[2], Lingyun Zhai[1], Zhen Wang[2,5] and Jian Huang[2,5,6*]*

[1] Department of Gynecology, The Second Affiliated Hospital, Zhejiang University School of Medicine, Zhejiang University, Hangzhou, China, [2] Key Laboratory of Tumor Microenvironment and Immune Therapy of Zhejiang Province, The Second Affiliated Hospital, Zhejiang University School of Medicine, Hangzhou, China, [3] Department of Breast Surgery, The First Affiliated Hospital, Wenzhou Medical University, Wenzhou, China, [4] Department of Medical Oncology, The Second Affiliated Hospital, Zhejiang University School of Medicine, Hangzhou, China, [5] Department of Breast Surgery, The Second Affiliated Hospital, Zhejiang University School of Medicine, Hangzhou, China, [6] Cancer Center, Zhejiang University, Hangzhou, China

OPEN ACCESS

Edited by:
Karine Rachel Prudent Breckpot,
Vrije University Brussel, Belgium

Reviewed by:
Damya Laoui,
Vrije University Brussel, Belgium
Kevin Van der Jeught,
Indiana University School of Medicine, United States
Yuanzhang Fang,
Indiana University, United States

***Correspondence:**
Jian Huang
drhuangjian@zju.edu.cn
Zhen Wang
tonywang@zju.edu.cn

[†]These authors have contributed equally to this work and share first authorship

Specialty section:
This article was submitted to Cancer Immunity and Immunotherapy, a section of the journal Frontiers in Immunology

Received: 23 April 2021
Accepted: 17 September 2021
Published: 15 October 2021

Citation:
Zhang Z, Yang C, Li L, Zhu Y, Su K, Zhai L, Wang Z and Huang J (2021) "γδT Cell-IL17A-Neutrophil" Axis Drives Immunosuppression and Confers Breast Cancer Resistance to High-Dose Anti-VEGFR2 Therapy. Front. Immunol. 12:699478. doi: 10.3389/fimmu.2021.699478

Angiogenesis is an essential physiological process and hallmark of cancer. Currently, antiangiogenic therapy, mostly targeting the vascular endothelial growth factor (VEGF)/VEGFR2 signaling axis, is commonly used in the clinic for solid tumors. However, antiangiogenic therapies for breast cancer patients have produced limited survival benefits since cancer cells rapidly resistant to anti-VEGFR2 therapy. We applied the low-dose and high-dose VEGFR2 mAb or VEGFR2-tyrosine kinase inhibitor (TKI) agents in multiple breast cancer mouse models and found that low-dose VEGFR2 mAb or VEGFR2-TKI achieved good effects in controlling cancer progression, while high-dose treatment was not effective. To further investigate the mechanism involved in regulating the drug resistance, we found that high-dose anti-VEGFR2 treatment elicited IL17A expression in γδ T cells *via* VEGFR1-PI3K-AKT pathway activation and then promoted N2-like neutrophil polarization, thus inducing $CD8^+$ T cell exhaustion to shape an immunosuppressive microenvironment. Combining anti-VEGFR2 therapy with immunotherapy such as IL17A, PD-1 or Ly-6G mAb therapy, which targeting the immunomodulatory axis of "γδT17 cells-N2 neutrophils" *in vivo*, showed promising therapeutic effects in breast cancer treatment. This study illustrates the potential mechanism of antiangiogenic therapy resistance in breast cancer and provides synergy treatment for cancer.

Keywords: γδT cell, neutrophil, anti-VEGFR2 therapy, breast cancer, IL17A, therapy resistance

INTRODUCTION

Pathological angiogenesis is a key feature of cancer and is involved in multiple stages of cancer development (1). Neovascularization can be enacted by a number of different mechanisms and multiple proangiogenic factors in the tumor microenvironment (such as VEGF and ANG-2) (2). Currently, antiangiogenic therapies, mostly targeting the VEGF/VEGFR2 signaling, are widely

applied in the clinic and considered as a major treatment for a wide range of advanced or metastatic tumors, including breast, colon, lung and gynecological cancers (3, 4). Interestingly, the efficacy of antiangiogenic drugs in the treatment of breast cancer is inconsistent. Clinical trials found that antiangiogenic therapy achieved only modest gains in progression-free survival and had no effect on overall survival (5, 6). Thus, the clinical guideline recommendations may not be universally applicable. The relapse mechanisms under antiangiogenic therapy remain unclear.

Antiangiogenic therapy cannot kill tumor cells directly, but works by changing the tumor microenvironment, such as restoring tumor perfusion and proper oxygenation to limit tumor cell invasion. Studies have also revealed that many factors in the tumor microenvironment can influence the effects of antiangiogenic drugs (7–9). Evidence suggests that myeloid cells, the largest population of innate immune cells, are crucial for resistance to antiangiogenic therapies *via* their immunosuppressive pathways (10). Previous studies have reported that neutrophils produce VEGF, MMP9, and Bv8 to sustain tumor angiogenesis (11–13). However, how neutrophils are functionally differentiated during antiangiogenic therapy remains unknown.

γδ T cells are a subtype of innate-like T lymphocytes that perform critical functions in the immune system and are conducive to either the immune response or immune regulation depending on their environment (14, 15). In the tumor microenvironment, γδ T cells are a remarkably heterogeneous population. Their antitumor effects are mediated by direct tumor cell killing *via* secreting interferon (IFN)-γ but they can also secret IL17A to promote tumor growth (16). Coffelt's research showed that, in a breast cancer mouse model, IL17A-producing γδ T cells induced neutrophil expansion and polarization, which created a premetastatic immunosuppressive microenvironment (17). However, it has not been reported whether γδ T cells are involved in antiangiogenic tumor therapy.

In this study, to clarify the mechanism of resistance to high-dose anti-VEGFR2 therapy, we applied different doses of VEGFR2 mAb and VEGFR2-tyrosine kinase inhibitor (TKI) in various breast cancer mouse models. Our results revealed that γδ T cells and neutrophils were actively involved in tumor resistance to high-dose anti-VEGFR2 therapy. Furthermore, we found that high-dose VEGFR2-TKI induced γδ T cells to produce IL17A *via* VEGFR1-PI3K-AKT pathway activation, which in turns promoted N2-like neutrophil polarization. N2 neutrophils accelerrated the CD8+ T cells exhaustion and then shaped an immunosuppressive microenvironment. Finally, we uncovered the "γδ T17 cells- N2 neutrophils" immunomodulatory axis that instigates resistance to high-dose anti-VEGFR2 therapy.

MATERIALS AND METHODS

Cell Lines

The 4T1 mammary tumor cell line was obtained from the Shanghai Institute of Cell Biology of the Chinese Academy of Science (SIBS, Shanghai, China), and the EMT6 mammary tumor cell lines were obtained from FuDan IBS Cell Center (FDCC, Shanghai, China). Both cell lines were authenticated by STR profiling and incubated in a humidified incubator with 5% CO_2 at 37°C. They were cultured in RPMI-1640 complete medium supplemented with 10% FBS (Gibco, USA) and 1:100 penicillin-streptomycin (Gibco).

Mice

Female wild-type BALB/c mice were provided by Slaccas Co. (Shanghai, China), and FVB/N-Tg (MMTV-PyMT) mice were provided by Gempharmatech (Nanjing, China). All mice were housed in the specific pathogen-free conditions of Zhejiang Chinese Medical University Laboratory Animal Research Center. All mouse protocols and procedures were reviewed and approved by the Ethics Review Committee of the Second Affiliated Hospital of the Zhejiang University School of Medicine.

In order to establish the 4T1 or EMT6 tumor-bearing mouse model, BALB/c mice were anesthetized with 0.8% sodium pentobarbital (80 mg/kg) intraperitoneal (*i.p.*) and inoculated with a suspension of $1x10^5$ 4T1 or EMT6 cells in the right fourth mammary fat pad.

VEGFR2 Tyrosine Kinase Inhibitors (TKI) and VEGFR2 Monoclonal Antibody (mAb) Treatment

The VEGFR2-TKI YN968D1 (apatinib) that inhibited VEGFR2 was obtained from Jiangsu Hengrui Medicine Co. (Nanjing, China) (18). Anti-mouse VEGFR2 mAb was obtained from BioXCell (clone DC101). VEGFR2-TKI YN968D1 was intragastric (*i.g.*) administrated for mice (low dose: 100mg/kg/day, high dose: 200mg/kg/day) and Anti-mouse VEGFR2 mAb was *i.p.* administrated for mice (low dose: 2mg/kg/twice a week, high dose: 10mg/kg/twice a week). The details of the strategy are shown in **Supplementary Figures S1A**, **S2A**. The primary tumor CD31 expression level, primary tumor size and tumor weight, spleen weight, and numbers of lung metastatic nodules were measured to evaluate the therapeutic effect of VEGFR2-TKI and VEGFR2 mAb (**Figure 1** and **Supplementary Figure S1**).

Specimen Acquisition and Processing

The spleen was ground on 100-μm nylon mesh (BD Falcon, #352360) into single cells. The splenocyte suspensions were lysed for 1 min (BD Bioscience, #349202) before subsequent detection or culture. Bone marrow cells were obtained from the hind limbs and then filtered into single cells. Primary tumors were cut into small pieces after excluding connective tissue and digested in digestion medium containing RPMI-1640 with 1 mg/ml collagenase IV (Sigma-Aldrich, #V900893) in a 37°C shaker for 1-2 h until digestion was complete. The single-cell suspension was further filtered through 40-μm nylon mesh (BD Falcon, #352340) to effectively remove impurities.

Flow Cytometry Analysis and Sorting

For cell surface marker staining, primary tumor cells, bone marrow cells and splenocytes were isolated as described

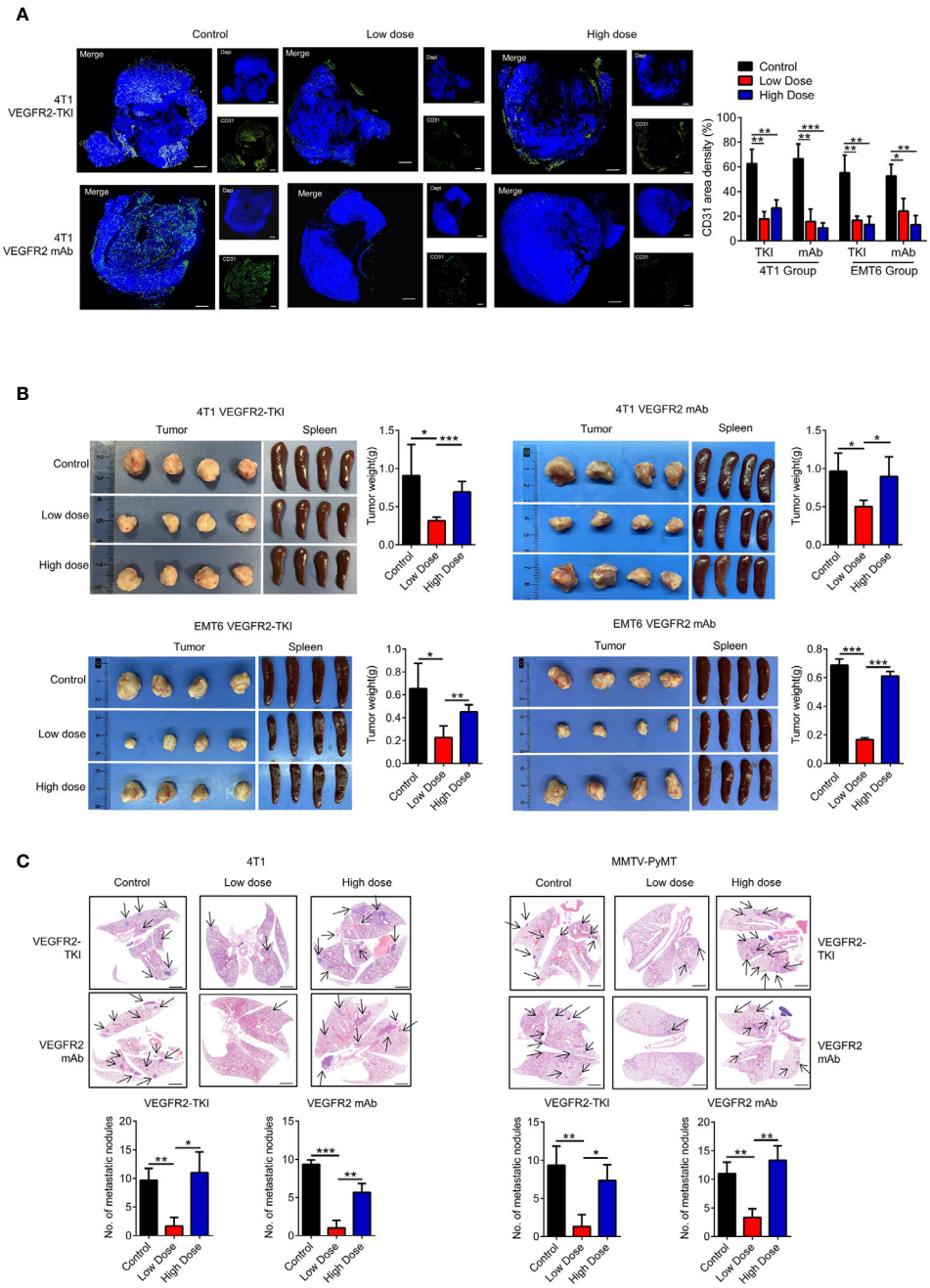

FIGURE 1 | High doses of anti-VEGFR2 therapy are not effective at controlling breast cancer progression. **(A)** Immunofluorescence and quantification of CD31 on breast cancer tissue after anti-VEGFR2 therapy in 4T1 model. Bar=200 μm. Green, CD31; blue, DAPI. **(B)** Representative size and weight of tumor and spleen after anti-VEGFR2 therapy. **(C)** H&E staining and quantification of lung metastasis in the 4T1 model (Black arrow) and MMTV-PyMT model (Black arrow) after anti-VEGFR2 therapy. Bar=1 mm. Data are presented as the means ± SD from one representative experiment. Similar results were obtained from three independent experiments, n=4 mice each group, unless indicated otherwise. Statistical analysis was performed by one-way ANOVA. *p < 0.05, **p < 0.01, and ***p < 0.001. See also **Supplementary Figures S1**, **S2**.

previously (19) and incubated with Zombie Red™ Fixable Viability Kit (Biolegend, #423109, to assess live vs. dead status of cells) for 30 min at room temperature (RT) and then washed with PBS. Cell suspension was then stained with anti-CD16/32 (clone S17011E, to block non-specific binding of immunoglobulin to the Fc receptors) for 10 min and then with the following fluorochrome-conjugated mAbs for 30 min at 4°C: anti-CD45 (clone 30-F11), anti-CD3ϵ (clone 145-2C11),

anti-CD4 (clone RM4-5), anti-CD8a (clone 53-6.7), anti-TCRγ/δ (clone GL3), anti-TCRβ (clone H57-597), anti-CD11b (clone M1/70), anti-Ly6G (clone 1A8), anti-EpCAM (clone G8.8), anti-PD-1 (clone RMP1-30), anti-PD-L1 (clone 10F.9G2), anti-VEGFR2 (clone 89B3A5), anti-CD14 (clone Sa14-2), anti-Ly6C (clone HK1.4) (all from BioLegend) and anti-VEGFR1/Flt-1 (clone 141522), anti-VEGFR3/Flt-4 (Polyclonal) (from R&D Systems). Isotype controls are applied as negative controls.

For intracellular staining, the cell density was adjusted to 5×10^6/ml, and a cell stimulation cocktail plus protein transport inhibitors (eBioscience, #00-4975-03) was added to the plate and incubated for 4-6 h. Cell surface marker staining was performed as described above, and the cells were then fixed and permeabilized using a fixation buffer (BioLegend, #420801) and permeabilization wash buffer (BioLegend, #421002). Subsequently, the cells were stained with fluorophore-conjugated antibodies against IFN-γ (clone XMG1.2, BioLegend) and IL17A (clone TC11-18H10.1, BioLegend).

For detecting the ROS level of indicated neutrophils, cells were harvested and Reactive Oxygen Species Assay Kit (Beyotime, #S0033) was used for staining.

Data were obtained from a FACSCanto II flow cytometer (BD Biosciences, San Jose, CA) and analyzed with FlowJo software (V10, Tree Star Inc., Ashland, OR). For flow cytometry sorting, a single-cell suspension was sorted with a FACSAria II cell sorter (BD Bioscience). The cell sorting strategy was as follows: ① CD45-APC/Cy7, CD3ϵ-PerCP/Cy5.5, and TCRγ/δ-APC; ② CD45-APC/Cy7, CD11b-PE/Cy7, and Ly-6G-APC.

Mouse Neutrophil Magnetic Isolation

Mouse neutrophil MACS isolation was performed using a Mouse Neutrophil Isolation Kit (Miltenyi, #130-097-658). Briefly, single-cell suspensions from mice bone marrow or tumor tissue were acquired, and erythrocytes were lysed before magnetic labeling. Then, 50 μl of Neutrophil Biotin-Antibody Cocktail was added per 200 μL of cell suspension ($5x10^7$ total cells) and incubated for 15 min on ice. After washing, 100 μl of Anti-Biotin MicroBeads was added per 400 μl of cell suspension. An LS column and a MidiMACS separator (Miltenyi) were used for subsequent magnetic sorting.

Biochemical Characterization Detection of Neutrophil

Arginase1, Prostaglandin E2 (PGE2), nitric oxide (NO) levels were measured to evaluate the indicated neutrophils' cellular immunosuppressive function. Arginase Activity Assay Kit (Sigma-Aldrich, #MAK112), Prostaglandin E2 Assay (R&D Systems, #KGE004B), Nitric Oxide Assay Kit (Beyotime, #S0021) were applied. The procedures were performed according to the manufacturers' protocol.

Tissue Culture Supernatant Collection

Primary tumor tissue was cut into small pieces using sterile ophthalmic scissors. Then, the samples were placed in a 6-well plate with RPMI-1640 medium. The culture supernatant was harvested after 24 h and centrifuged at 300xg for 5 min for further purification.

Neutrophil and γδ T Cells Induction *In Vitro*

Mouse bone marrow-derived neutrophils were obtained as previously described. Neutrophils were plated in plate bottom 96-well plates with different concentration of VEGFR2-TKI, tissue culture supernatant, IL17A mAb (1μg/mL, Biolegend, #506945), IFN-γ mAb (1μg/mL, Biolegend, #505833) and cells were harvested after 4h. The neutrophils cellular marker staining procedure is described above. For co-culture assay (**Figures 4D, E**), tumor-infiltrating γδ T cells were obtained from primary tumors *via* single-cell FACS sorting. γδ T cells and neutrophils (cell ratio 1:1) suspended in complete RPMI-1640 medium containing Ultra-LEAF-purified anti-mouse CD3ϵ mAb (BioLegend, #100340) were plated in U-bottom 96-well plates separated with 0.4μm transwell chamber (Corning, #3381).

For γδ T induction *in vitro* (**Figures 3B, D** and **Supplementary Figure S3G**), mouse spleen-derived γδ T cells were obtained by MACS isolation. γδ T cells suspended in complete RPMI-1640 medium containing purified anti-mouse CD3ϵ mAb were plated in U-bottom 96-well plates and different concentration of VEGFR2-TKI (**Figures 3B, D**) and YS-49 (**Supplementary Figure S3G**).

$CD8^+$ T Cell Detection and Co-Culture System *In Vitro*

$CD8^+$ T cells were isolated from naive BALB/c mouse spleens using a positive $CD8^+$ T cell isolation kit (BioLegend, #100704). For T cell proliferation assays, MACS-isolated $CD8^+$ T cells were firstly labeled with CFSE (1 μM, BioLegend, #423801) in a 37°C cell culture incubator for 10 min and thoroughly washed 3 times with pre-warmed complete RPMI-1640 medium.

For exploring $CD8^+$ T cells proliferation (**Figures 6A**, **Supplementary Figures S6B, D**) and PD-1 expression (**Figures 6B**, **Supplementary Figures S6C, E**), cells were suspended in complete RPMI-1640 medium with Ultra-LEAF-purified anti-mouse CD3ϵ mAb, anti-mouse CD28 mAb (BioLegend, #102115) and recombinant IL-2 (PeproTech, #210-12). For detecting $CD8^+$ T cells change under the VEGFR2-TKI intervention *in vitro*, different dose VEGFR2-TKI was added in the culture system for 3 days and evaluated *via* flow cytometry. For detecting $CD8^+$ T cells change under the influence of tumor-infiltrating neutrophils or γδ T cells, tumor-infiltrating neutrophils or γδ T cells were obtained from primary tumors (low dose VEGFR2-TKI treated, high does VEGFR2-TKI treated or untreated mice) *via* single-cell FACS sorting. γδ T cells or neutrophils were co-cultured with $CD8^+$ T cells (cell ratio 10:1) for 3 days and evaluated *via* flow cytometry.

For investigating the γδ T-neutrophil-$CD8^+$ T cells axis and the effect of IL17A, The schedule was operated and showed in **Figure 6C**. Briefly, tumor-infiltrating γδ T cells from high does VEGFR2-TKI treated mice primary tumors were plated into upper chamber (0.4μm transwell chamber) and $CD8^+$ T cells with or without naive neutrophils were plated into the lower chamber with complete RPMI-1640 medium containing Ultra-LEAF-purified anti-mouse CD3ϵ mAb, anti-mouse CD28 mAb and recombinant IL-2 (γδ T cells: neutrophil: $CD8^+$ T cells ratio =10:10:1). IgG control

(1μg/mL, Biolegend, #400431) or anti-IL17A mAb (1μg/mL) was added in the coculture system.

PI3K Activator and Inhibitor Treatment

In order to evaluate the PI3K pathway in tumor development, BALB/c mice were inoculated 4T1 cells in the right fourth mammary fat pad and divided into 5 groups as shown in **Supplementary Figure S3F**: 1. PBS group, 2. low-dose VEGFR2-TKI group, 3. low-dose VEGFR2-TKI with PI3K inhibitor Copanlisib (MCE, #HY-15346, intravenous (*i.v.*) 100 μg/mouse/every other days) group, 4. high-dose VEGFR2-TKI group, 5. high-dose VEGFR2-TKI with PI3K activator YS-49 (MCE, #HY-15346, *i.p.* 100 μg/mouse/every other days) group. Intervention was started two weeks after 4T1 cells inoculation.

Therapeutic mAb Treatment

Two weeks after 4T1 cell inoculation in the right fourth mammary fat pad, the combination treatment of high-dose VEGFR2-TKI and a mAb was performed for 2 weeks. Anti-IL17A mAb (clone 17F3), anti-Ly-6G mAb (clone 1A8), anti-PD-1 mAb (clone J43), mouse IgG1 (clone MOPC-21) (All from BioXCell, i.v., 100 μg/mouse/every three days) or PBS as control was applied. The mAb deleting efficiency was proved by obtain PB at the end of the treatment and stained with anti-CD45, anti-CD11b, anti-Ly6G *via* flow cytometry.

Western Blot

Sorted γδ T cells from primary tumor or spleen-derived γδ T cells after *in vitro* treatment were harvested and lysed in pre-cooled RIPA Lysis Buffer (Beyotime, #P0013B) with a cocktail of protease and phosphatase inhibitor (Thermo Fisher, #78445). A bicinchoninic acid (BCA) assay kit (Thermo Fisher, #23227) was used for protein concentration measurement. The proteins were separated by sodium dodecyl sulfatepolyacrylamide gel electrophoresis (SDS-PAGE) and then transferred onto a polyvinylidene difluoride (PVDF) membrane (Bio-Rad). After blocking with 5% (w/v) fat-free milk (BD Biosciences, #232100) at RT for 1 h, the membrane was incubated with the corresponding primary antibodies overnight at 4°C followed by the appropriate horseradish peroxidase (HRP)-conjugated secondary antibodies. Immunoreactive bands were identified using enhanced chemiluminescence (Thermo Fisher Pierce, #32109). Primary antibody, including anti-AKT (1:1000, Cell Signaling Technology, #4685S), anti-Phospho-Akt (Ser473, 1:1000, Cell Signaling Technology, #4058S), anti-PI3 Kinase (p85, 1:1000, Cell Signaling Technology, #4257S), anti-PI3 Kinase p85 (Tyr458)/p55 (Tyr199) (1:1000, Cell Signaling Technology, #4228S), and anti-β-actin (1:2000, HuaBio, #EM21002), was applied. Secondary antibodies, including anti-mouse (1:5000, HuaBio, #G1006-1) and anti-rabbit (1:5000, HuaBio, #HA1001), were applied. Quantification of WB images was conducted by ImageJ software (version 1.48).

Tissue Immunofluorescence Staining

Mouse tissue was obtained, fixed with 4% paraformaldehyde for 24 h and then embedded in paraffin for sectioning. After dewaxing and dehydration, sections were incubated with a primary antibody overnight. A fluorophore-labeled secondary antibody was added and incubated for 2 h at RT. Finally, the sections were stained with DAPI and imaged. Primary Abs specific for CD31 (Polyclonal, Proteintech, #28083-1-AP) were applied. CD31 area density (%) was calculated by dividing the CD31-positive staining area with the total total tissue area. Quantification of immunofluorescence images was conducted by ImageJ software.

Giemsa Staining

Collected neutrophils were adjusted to a cell concentration of $1x10^6$/mL. Then, 50 μL of cell suspension was added to a cytospin, and the cells were attached to the slide. Then, the cells were fixed for 20 min in 4% paraformaldehyde, stained with a Giemsa solution (Solarbio, 0.4 w/v, #G1015) for 10 min and washed with ddH_2O. Cell nuclear morphology was observed under an optical light microscopy by two independent researchers (Chenghui Yang AND Ke Su). 5 fields of view are randomly selected for each sample and cells with nucleus segmentation ≥3 are deemed as N1 type neutrophil while cells with round nucleus are deemed as N2 type neutrophil.

Statistical Analysis

All statistical analyses were performed using GraphPad Prism (V6.0, GraphPad Software, Inc. La Jolla, CA). The results are expressed as the mean values ± SD. The significance of variations between two groups was determined by an unpaired two-tailed Student's t test, and one-way ANOVA was also used for the multiple groups comparisons. Repeated-Measures ANOVA was performed for changes over time in the groups. Statistical significance was assumed at $p<0.05$. The following symbols were applied in figures: $^*p<0.05$, $^{**}p<0.01$, and $^{***}p<0.001$.

RESULTS

High-Dose Anti-VEGFR2 Therapy Is Not Effective at Controlling Breast Cancer Progression

Previous studies suggested that anti-VEGFR2 treatment inhibit angiogenesis and tumor growth in dose-dependent pattern (20, 21). In order to investigate the changes in intratumoral vessels and tumor through the treatment, we treated the breast cancer mice with administration of an anti-VEGFR2 antibody (clone DC101) or YN968D1 (Apatinib), a small molecule tyrosine kinase inhibitor (TKI) that selectively inhibits VEGFR2.

According to previous studies, 50 to 200mg/kg/day of VEGFR2-TKI (YN968D1) has an anti-tumor effect in different tumor mouse models (18). Combined with the sensitivity of breast cancer to antiangiogenic therapy and related mouse studies, we selected 200mg/kg/day as the high-dose group, and 100mg/kg/day was the relatively low-dose control group. In addition, the optimal biotherapeutic dose of VEGFR2 mAb (DC101) remains controversial and fluctuates widely among mouse strains and tumor types, with a maximum of 50mg/kg, 3 times a week (22, 23). Studies have found that the treatment

efficiency is the highest at 6mg/kg dose of DC101, the highest at 13-16mg/kg dose, and then decreases with the increase of dose and duration (24). Combining the published literatures with our former experiments, we selected 10mg/kg twice-weekly intraperitoneal injection as the high-dose group and 2mg/kg twice-weekly as the low-dose control group.

Various breast cancer mice models were conducted in our experiments. We used the metastatic (4T1) and less invasive (EMT6) mammary cell lines in a syngeneic (Balb/c) mouse xenograft model. Murine 4T1 cells were originally derived from a spontaneous breast cancer in the Balb/c strain and have been reported as metastatic, which are largely similar to human basal/triple-negative breast cancer (TNBC) cell lines. Conversely, the EMT6 murine cell lines have been shown to be less invasive and exhibit the characteristics of human Luminal breast cancer subtype. To test the efficacy of VEGFR2-TKI (YN968D1) and VEGFR2 mAb (DC101) in the treatment of breast cancer with different invasive potentials, we established following treatment groups (**Supplementary Figure S1A**). Tumor angiogenesis was effectively reduced with different doses of VEGFR2-TKI and VEGFR2 mAb treatment (**Figure 1A** and **Supplementary Figure S1B**). However, the inhibitory effects of anti-VEGFR2 therapy on tumor growth were evident in the low-dose group but not significant in the high-dose group (**Figures 1B**, **Supplementary Figures S1C, D**). Furthermore, the same VEGFR2 treatment was also given to MMTV-PyMT mouse model (**Supplementary Figure S2A**), a spontaneous breast cancer model, and the low-dose group reduced the primary tumor as well as lung metastasis, while no effect was found in the high-dose group (**Figures 1C** and **Supplementary Figures S2B**). This is consistent with current reports that high-dose anti-VEGFR2 therapy is not effective for breast cancer treatment.

High-Dose VEGFR2-TKI Therapy Contributes to the Polarization of IL17A-Producing γδ T Cells Rather Than IFN-γ-Producing γδ T Cells

Our study and previous studies found that the onset of VEGFR2-TKI (YN968D1) response and relapse is similar to that observed with VEGFR2 mAb (DC101) (22, 25), supporting the notion that VEGFR2-TKI predominantly blocks the VEGFR2 pathway in breast cancer. Therefore, VEGFR2-TKI was used to explore the resistance mechanism.

While exploring the immunological factors involved in the resistance mechanism of high-dose VEGFR2-TKI on tumor progression, we found that the therapeutic target VEGFR2 was expressed at significantly higher levels in T lymphocytes than in myeloid cells (**Figure 2A** and **Supplementary Figure S2C**), and γδ T cells exhibited higher VEGFR2 expression than αβ T cells (**Figure 2B**). We also found that neither low dose nor high dose affected the proportion of γδ T cells infiltrating the tumor in the 4T1 model, while the high-dose group in EMT6 was abundant in infiltrating γδ T cells (**Figure 2C**). Importantly, IFN-γ-producing γδ T cells were predominant with the low-dose treatment, while IL17A-producing γδ T cells were predominant with the high-dose treatment that induced drug resistance (**Figure 2D**). From these results, we speculated that VEGFR2-TKI acts on γδ T cells directly *via* VEGFR-2, thereby affecting γδ T cell polarization.

High-Dose VEGFR2-TKI Treatment Activates the "VEGFR1-PI3K-AKT" Pathway to Promote Polarization of γδT17 Cells

VEGFR is divided into R1, R2 and R3. We found that VEGFR2-TKI therapy effectively reduced the expression of VEGFR2 on γδ T cells (**Supplementary Figure S3A**), while high dose treatment increased the VEGFR1 expression without affecting VEGFR3 expression (**Figure 3A** and **Supplementary Figure S3B**). Furthermore, with the increase of VEGFR2-TKI concentration, the VEGFR1 expression of naive γδ T cells gradually increasing *in vitro* (**Figure 3B**), while VEGFR2 expression was opposite (**Supplementary Figure S3C**). Previous studies demonstrated that the PI3K signaling pathway can be activated by VEGFR2 or VEGFR1 (26, 27). We found that the PI3K-AKT pathway was significantly inhibited in γδ T cells sorted from tumors of the low-dose VEGFR2-TKI treatment group. On the contrary, γδ T cells from the high-dose and control groups had activated PI3K-AKT pathway (**Figure 3C** and **Supplementary Figure S3D**). In addition, we treated naive γδ T cells with VEGFR2-TKI *in vitro* and found progressively increased IL17A-secreting γδ T cells and decreased IFN-γ-producing γδ T cells with increasing drug concentration gradients (**Figure 3D**). Published studies discovered that activation of the PI3K-AKT pathway effectively promotes the secretion of IL17A (28, 29). Therefore, we speculated that the exchange of γδ T cell subtypes with different doses was attributed to the activation status of the PI3K-AKT pathway. We found that PI3K-AKT was also gradually activated in a dose-dependent manner of VEGFR2-TKI treatment (**Figure 3E** and **Supplementary Figure S3E**). Thus, we hypothesized that IL17A-producing γδ T cells are maintained by activated VEGFR2-PI3K-AKT signaling in the absence of treatment. However, activation of the VEGFR1-PI3K-AKT-IL17A pathway and the subsequent increased IL17A-producing γδ T cells accounts for the resistance to high-dose VEGFR2-TKI. To further prove the hypothesis, we designed *in vivo* experiments in which the PI3K-AKT agonist YS-49 was given to the low-dose group and the PI3K-AKT inhibitor Copanlisib was given to the high-dose group (**Supplementary Figure S3F**). We found that low-doses VEGFR2-TKI with YS-49 increased tumor size slightly, while the tumor from high-dose with Copanlisib group was significantly reduced, indicating that inhibiting the PI3K-AKT signaling pathway could reverse tumor resistance induced by high-dose treatment (**Figure 3F**). Further detection of tumor infiltrating γδT cells showed that low dose VEGFR2-TKI with YS-49 increased IL17A secretion, while high-dose VEGFR2-TKI with Copanlisib had the opposite effect (**Figure 3G**). PI3K signaling pathway is crucial for tumor cell (30) and tumor microenvironments (31–33). In order to further illustrate the role of PI3K on γδT cells, *in vitro* PI3K agonist treatment on naive γδT cells was operated and found that IL17A secreting increased gradually in accordance with PI3K agonist concentration (**Supplementary Figure S3G**). These results further confirmed the possibility of γδT cells-PI3K-IL17A pathway.

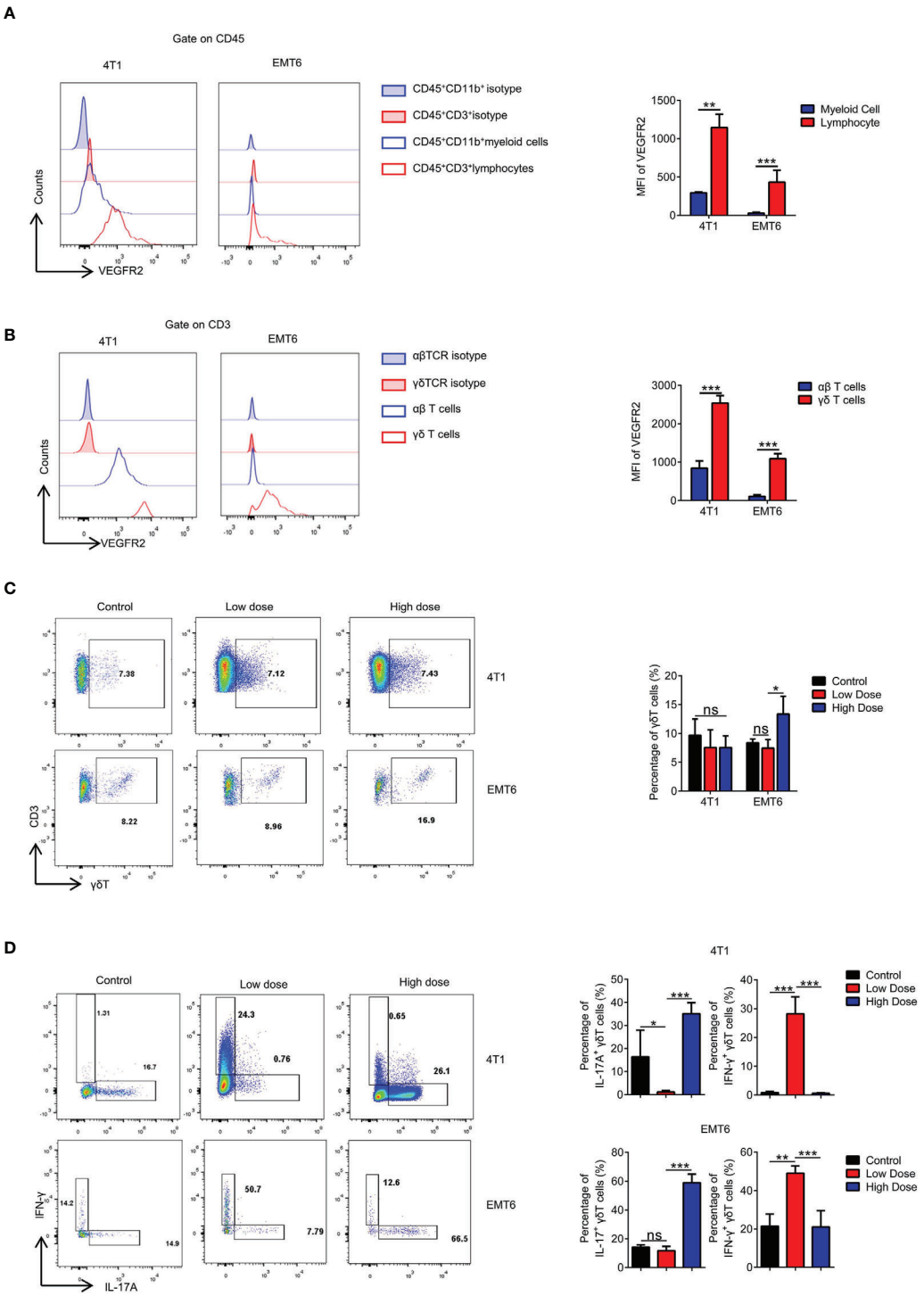

FIGURE 2 | High-dose VEGFR2-TKI therapy contributes to differentiation into IL17A-producing γδT cells rather than IFN-γ producing γδT cells. **(A)** Flow cytometry analysis of VEGFR2 expression of myeloid cells ($CD45^+CD11b^+$) and lymphocytes ($CD45^+CD3^+$). **(B)** Flow cytometry analysis of VEGFR2 expression of αβT cells ($CD45^+CD3^+TCR\beta^+$) and γδT cells ($CD45^+CD3^+TCR\gamma\delta^+$). **(C)** Frequency of γδT cells in the tumor after anti-VEGFR2 therapy. **(D)** Intracellular IFN-γ and IL17A expression of γδT cells from tumors *in vivo*. Data are presented as the means ± SD from one representative experiment. Similar results were obtained from three independent experiments, n=4 mice each group, unless indicated otherwise. Statistical analysis was performed by two-tailed unpaired Student's t test. ns, not significant, *$p < 0.05$, **$p < 0.01$, and ***$p < 0.001$. See also **Supplementary Figure S3**.

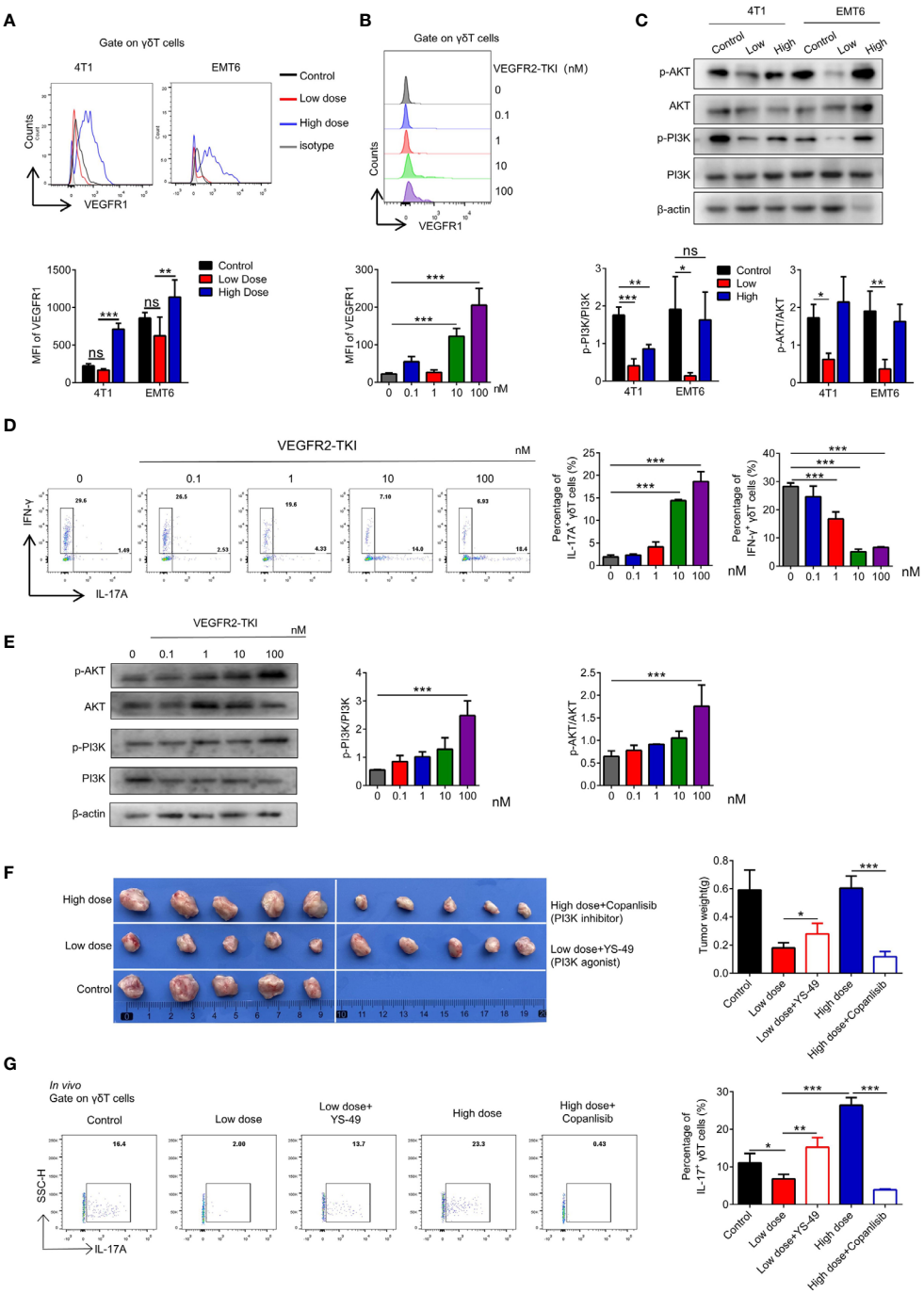

FIGURE 3 | High-dose VEGFR2-TKI therapy induce γδT cells producing IL17A *via* VEGFR1-PI3K-AKT pathway. **(A)** Flow cytometry analysis of VEGFR1 expression of γδT cells ($CD45^+CD3^+TCR\gamma\delta^+$) in the tumor. **(B)** Flow cytometry analysis of VEGFR1 expression of γδT cells derived from naive spleen treated with different doses of VEGFR2-TKI *in vitro*. **(C)** Western blot analysis of the PI3K and AKT pathways in γδT cells from tumors with different dose of VEGFR2-TKI therapy (γδT cells were sorted from 4 tumors as one donor). **(D)** Flow cytometry analysis of intracellular IFN-γ and IL17A expression of γδT cells derived from naive spleens treated with different doses of VEGFR2-TKI *in vitro*. **(E)** Western blot analysis of PI3K and AKT pathways in γδT cells derived from naive spleens treated with different doses of VEGFR2-TKI *in vitro* (γδT cells were sorted from 9 naive spleens as one donor). **(F)** Representative size of primary tumor after different dose VEGFR2-TKI therapy combined with PI3K agonist or inhibitor *in vivo* (n=5). **(G)** Intracellular IL17A expression of γδT cells from tumors after different dose VEGFR2-TKI therapy combined with PI3K agonist or inhibitor *in vivo* (n=5). Data are presented as the means ± SD from one representative experiment. Similar results were obtained from three independent experiments, n=4 mice each group, unless indicated otherwise. Statistical analysis was performed by one-way ANOVA. ns, not significant, *$p < 0.05$, **$p < 0.01$, and ***$p < 0.001$. See also **Supplementary Figure S3**.

High-Dose VEGFR2-TKI Therapy Facilitates "N2-Like" Neutrophil Differentiation Induced by IL17A-Producing γδ T Cells

Previous studies have shown that both IFN-γ and IL17A have effects on the development of neutrophils (34), and we found that neutrophil numbers were significantly increased after VEGFR2-TKI treatment regardless of the therapeutic dose (**Figure 4A**). Fridlender (35) reported that neutrophils can be classified into an antitumorigenic type (called the "N1 phenotype") and a protumorigenic type (the "N2 phenotype"). To assess the morphology of tumor-associated neutrophils, intratumoral $CD45^+CD11b^+Ly6G^+Ly6C^-$ cells were isolated. We observed that neutrophils in the low-dose group were more lobulated and hypersegmented. While in the high-dose group, neutrophils appeared to have characteristically circular nuclei (immature morphology) (**Figure 4B**). Production of reactive oxygen species (ROS), the key anti-tumor product of N1 neutrophils, was higher in neutrophils of the low-dose group than in those of the high-dose group (**Figure 4C**). Furthermore, we treated neutrophils with different doses of VEGFR2-TKI *in vitro* and found that the nucleus segmentation and ROS production of the neutrophils were not affected by the drug concentration (**Supplementary Figures S4A, B**). We also isolated γδ T cells from tumors treated with low-dose or high-dose VEGFR2-TKI and then cocultured them indirectly with naive neutrophils in a transwell chamber. The γδ T cells from low dose group could effectively promote the maturation of neutrophils and the secretion of ROS, while the γδ T cells from high-dose group did not have this ability (**Figures 4D, E** and **Supplementary Figure S4C**). To further demonstrate that neutrophils differ depending on the cytokines secreted in the tumor, we extracted culture supernatants from tumor tissues after treatment with different doses for induction of naive neutrophils, and an anti-IL17A mAb and anti-IFN-γ mAb were given as appropriate. The results showed that the anti-IL17A mAb could inhibit N2-phenotype induction in neutrophils mediated by high-dose tumor culture supernatant, while the anti-IFN-γ mAb could induce the transformation of neutrophils from the N1 phenotype to the N2 phenotype (**Figures 4F, G** and **Supplementary Figure S4D**). The above results illustrate that low doses of VEGFR2-TKI induce γδ T cells to secrete IFN-γ to promote neutrophil differentiation into the N1 phenotype, while at high-dose VEGFR2-TKI treatment, γδ T cells secrete IL17A to promote neutrophil differentiation into the N2 phenotype.

High-Dose VEGFR2-TKI Therapy Exhausts $CD8^+$ T Cells in Tumors

To further clarify the proposed "γδ T cells- IL17A- N2 neutrophils- immunosuppression" hypothesis, we examined functional changes in T cells in the tumor microenvironment. The proportion of $CD3^+$ T cells was independent of the therapeutic dose (**Figure 5A**). However, the CD4/CD8 ratio changed markedly, which was reflected by a significant decrease in the number of $CD8^+$ T cells after high-dose treatment (**Figure 5B**). Further tests showed that PD-1 expression was increased on $CD8^+$ T cells after high-dose treatment (**Figure 5C**). We also detected PD-L1 expression on tumor cells and found that it did not change with the different VEGFR2-TKI doses (**Supplementary Figures S5A, B**), indicating that the PD-1 expression on $CD8^+$ T cells was upregulated for other reasons.

Exhaustion of $CD8^+$ T Cells Is Attributed to Neutrophils After High-Dose VEGFR2-TKI Therapy

It has been suggested that N2 neutrophils play an immunosuppressive role in the tumor microenvironment (36). Therefore, we examined the key molecules reported to play immunosuppressive function of N2 neutrophils, including Arginase, NO and PGE2, and found that PGE2 significantly increased in the high-dose treatment group, which may be the mechanism of immunosuppressive function (**Supplementary Figure S6A**). We cocultured neutrophils from tumors treated with different doses of VEGFR2-TKI with naive $CD8^+$ T cells and found that only the neutrophils from the high-dose treatment group had immunosuppressive effects and significantly upregulated PD-1 expression on the $CD8^+$ T cells (**Supplementary Figures S6A, B**). Furthermore, changes in the proportion and function of $CD8^+$ T cells were not affected by γδ T cells in tumors treated with different therapeutic doses (**Supplementary Figures S6B, C**) or by the dose of VEGFR2-TKI (**Supplementary Figures S6D, E**). Therefore, we hypothesized that the drug resistance observed with high-dose VEGFR2-TKI treatment was due to the secretion of IL17A by γδ T cells, polarizing neutrophils into the N2 phenotype. N2 neutrophils play an immunosuppressive role, which reduces the number of $CD8^+$ T cells and increases the expression level of PD-1, leading to the progression of breast cancer. In order to confirm the hypothesis, we designed co-culture system *in vitro* (**Supplementary Figure S6C**). We found that tumor-infiltrating γδT cells in the high-dose treatment group can only exert immunosuppressive effects in the presence of neutrophils, and this effect can be antagonized by IL17A mAb (**Figures 6D, E**).

Combination With a mAb Can Restore the Efficacy of High-Dose VEGFR2-TKI Therapy

To corroborate our pathway hypothesis, in 4T1 orthotopic breast cancer mice model, VEGFR2-TKI was treated alone or in combination with multiple immunotherapy, including an anti-IL17A mAb, anti-PD-1 mAb and anti-Ly6G mAb. Anti-Ly6G mAb can remove neutrophils from mouse body (**Supplementary Figure S7A**). We found that mAb combination was effective, especially in the anti-IL17A mAb group (**Figure 7A** and **Supplementary Figure S7B**). Notably, application of the anti-IL17A mAb, anti-PD-1 mAb or anti-Ly6G mAb alone may not be sufficient for tumor growth inhibition. What's more, VEGFR2-TKI in combination with immunotherapy was seen to reduce lung metastasis (**Supplementary Figure S7C**), although it cannot be ruled out that it is affected by the reduction of primary tumor burden. More importantly,

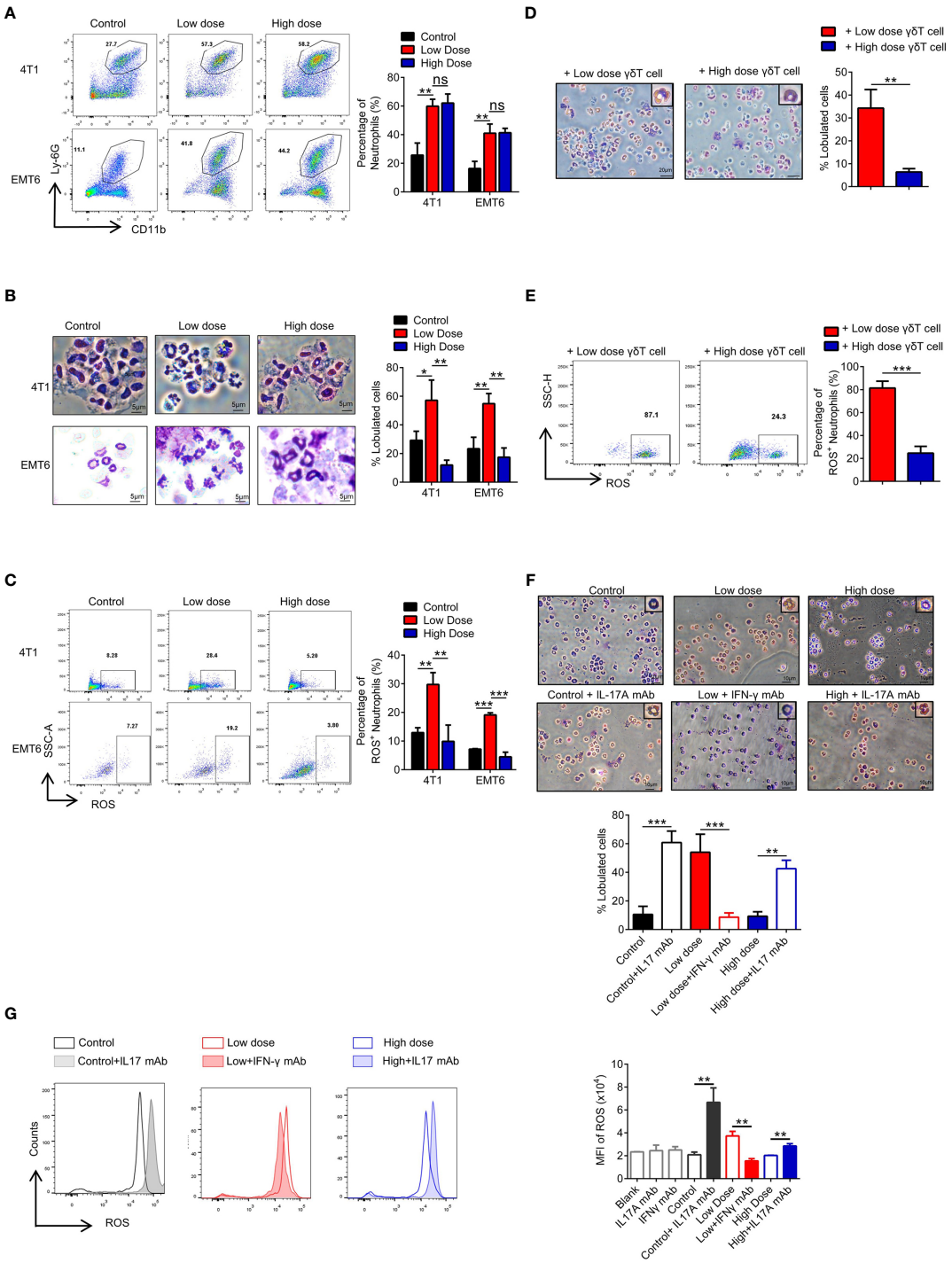

FIGURE 4 | High-dose VEGFR2-TKI therapy facilitates N2-like neutrophils by IL17A-producing γδT cells. **(A)** Flow cytometry analysis of the percentage of neutrophils ($CD45^+CD11b^+Ly\text{-}6G^+$) in the tumor after VEGFR2-TKI therapy. **(B)** Giemsa-stained neutrophils from the tumor after VEGFR2-TKI therapy *in vivo*. Bar=5 μm. **(C)** Reactive oxygen species (ROS) production of neutrophils in the tumor after VEGFR2-TKI therapy *in vivo*. **(D, E)** Representative images of Giemsa nuclear morphology analysis **(D)** and Frequency of ROS expression **(E)** of naive bone marrow (BM)-derived neutrophils, which were co-cultured with γδT cells sorted from tumors after different dose of VEGFR2-TKI therapy. Bar=20 μm. **(F, G)** Representative images of Giemsa nuclear morphology analysis **(F)** and MFI of ROS expression by flow cytometry analysis **(G)** in BM-derived neutrophils co-cultured with different tumor culture supernatants after VEGFR2-TKI therapy and (or) IL17 mAb or IFN-γ mAb added *in vitro*. Bar=10 μm. Data are presented as the means ± SD from one representative experiment. Similar results were obtained from three independent experiments, n=4 mice each group, unless indicated otherwise. Statistical analysis was performed by two-tailed unpaired Student's t test **(A–E)** and one-way ANOVA **(F, G)**. ns, not significant, *$p < 0.05$, **$p < 0.01$, and ***$p < 0.001$. See also **Supplementary Figure S4**.

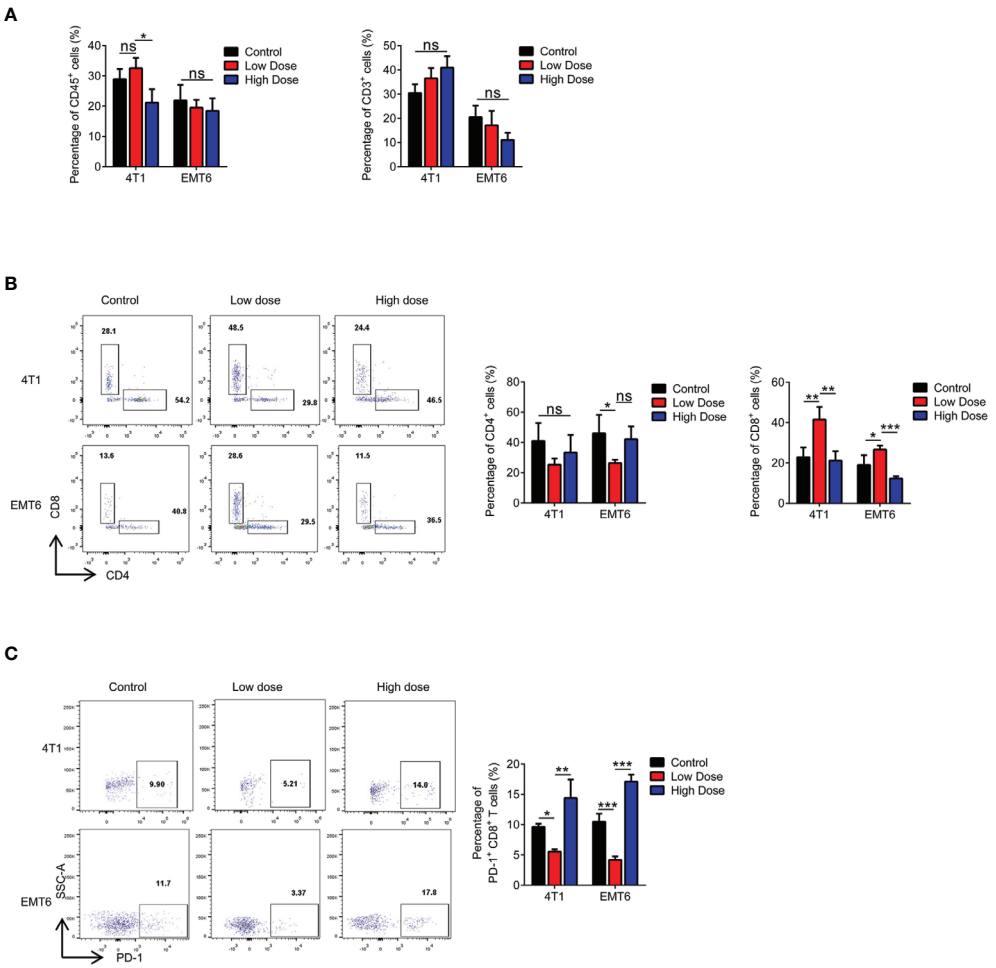

FIGURE 5 | High-dose VEGFR2-TKI therapy exhausts $CD8^+$ T cells in the tumor. **(A)** Flow cytometry analysis of immune cells ($CD45^+$) and T cells ($CD45^+CD3^+$) in the tumor after VEGFR2-TKI therapy. **(B)** Frequency of $CD4^+$ T cells ($CD45^+CD3^+CD4^+$) and $CD8^+$ T cells ($CD45^+CD3^+CD8^+$) in the tumor. **(C)** Frequency of PD-1 expression on $CD8^+$ T cells in the tumor after VEGFR2-TKI therapy. Data are presented as the means ± SD from one representative experiment. Similar results were obtained from three independent experiments, n=4 mice each group, unless indicated otherwise. Statistical analysis was performed by two-tailed unpaired Student's t test, ns, not significant, *$p < 0.05$, **$p < 0.01$, and ***$p < 0.001$. See also **Supplementary Figure S5**.

VEGFR2-TKI combined with the anti-IL17A mAb and anti-Ly6G mAb restored the percentage of $CD8^+$ T cells and effectively reduced the expression of PD-1 (**Figures 7B, C**). In addition, the anti-IL17A mAb restored the ROS production of neutrophils in the tumor (**Figure 7D**). In general, high-dose of VEGFR2-TKI therapy combined with immunotherapy can relieve tumor drug resistance induced by high-dose therapy and is closely associated with γδT cells-IL17-neutrophils.

DISCUSSION

In orthotopic breast cancer models of 4T1 and EMT6 and the MMTV-PyMT model of spontaneous breast cancer, high-dose anti-VEGFR2 treatment was found to cause resistance to VEGFR2 monoclonal antibody and VEGFR2-TKI. We determined that intratumoral γδ T cells and neutrophils are involved in driving responsiveness and resistance to antiangiogenic therapy with a VEGFR2-TKI therapy. High-dose VEGFR2-TKI treatment induced IL17A production by tumor-infiltrating γδ T cells through the VEGFR1-PI3K-AKT pathway, while IL17A promoted "N2" neutrophil polarization, driving immunosuppression and conferring resistance to anti-VEGFR2 treatment (**Figure 8**).

VEGFR2 is widely expressed in blood vessels, especially tumor microvessels. Furthermore, VEGFR2 has been detected on various types of immune cells, such as macrophages, T cells and dendritic cells (37). It is an effective therapeutic target for tumor angiogenesis, but drug resistance caused by high-dose treatment is the current limitation of clinical treatment. Our study found that VEGFR2 expression was higher in T cells than in myeloid cells. Previous studies revealed that regulatory T cells (Tregs) are the most common VEGFR2-expressing T cells (38). However, T cells can be classified by T cell receptors (TCRs) into

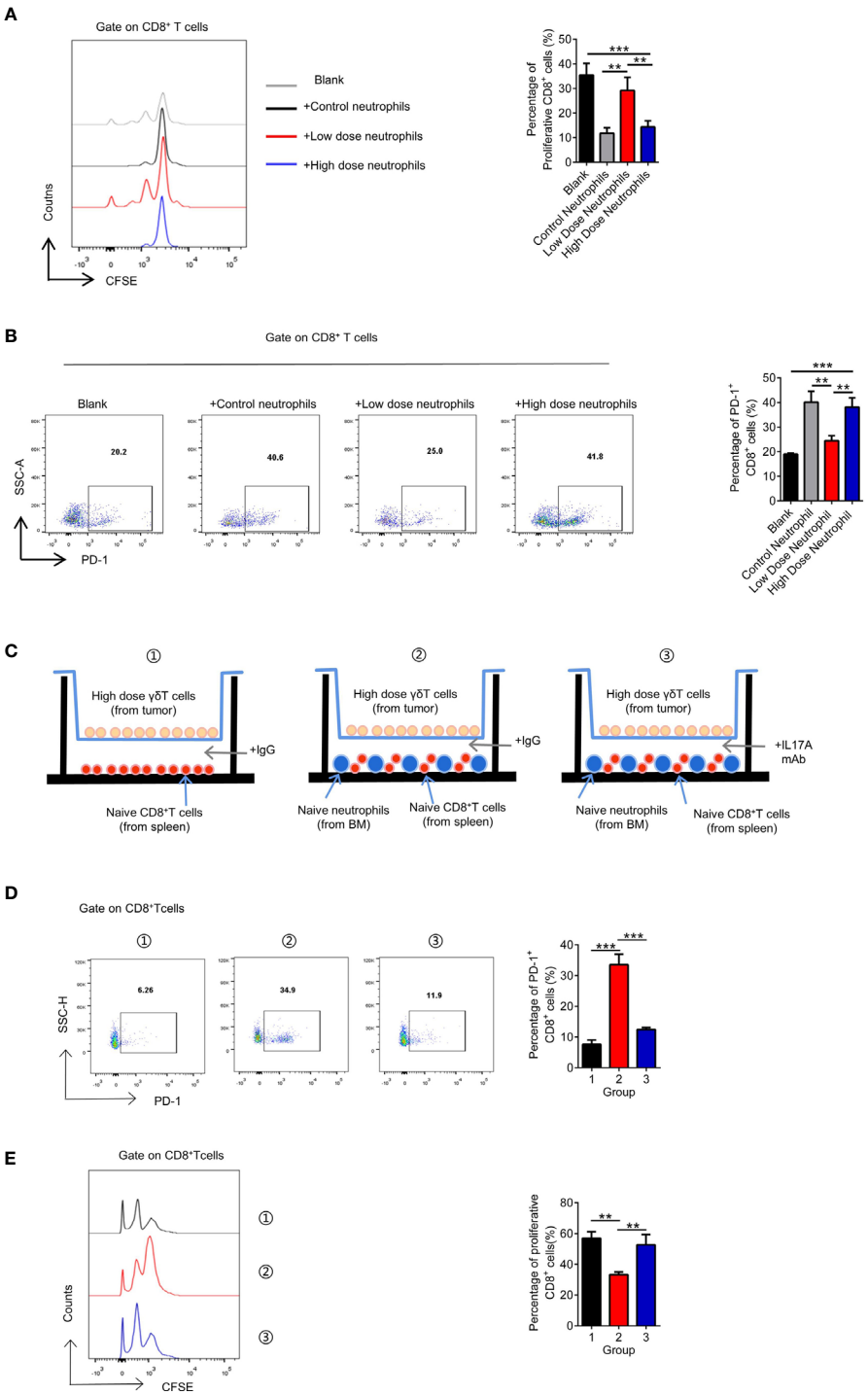

FIGURE 6 | The exhaustion of $CD8^+$ T cells is attributed to neutrophils after high-dose VEGFR2-TKI therapy. **(A, B)** Quantification of proliferation of $CD8^+$ T cells ($CFSE^{low}CD8^+$) **(A)** and PD-1 expression on $CD8^+$ T cells **(B)** after co-culture with different groups of neutrophils sorted from the tumor after VEGFR2-TKI therapy. $CD8^+$ T cells were derived from naive spleens. **(C)** Schematic illustration of $CD8^+$ T cells and neutrophils indirect co-cultrured with high dose of γδT cells sorted from the tumor after VEGFR2-TKI therapy shown in 6D and 6E. $CD8^+$ T cells were derived from naive spleens. Neutrophils were derived from bone marrow. Transwell chamber=0.4μm. **(D, E)** Quantification of PD-1 expression on $CD8^+$ T cells **(D)** and proliferation of $CD8^+$ T cells ($CFSE^{low}CD8^+$) **(E)** after co-cultured with neutrophils and high dose of γδT cells sorted from the tumor after VEGFR2-TKI therapy shown in 6C. Data are presented as the means ± SD from one representative experiment. Similar results were obtained from three independent experiments, n=4 mice each group, unless indicated otherwise. Statistical analysis was performed by one-way ANOVA. $^{**}p < 0.01$, and $^{***}p < 0.001$. See also **Supplementary Figure S6**.

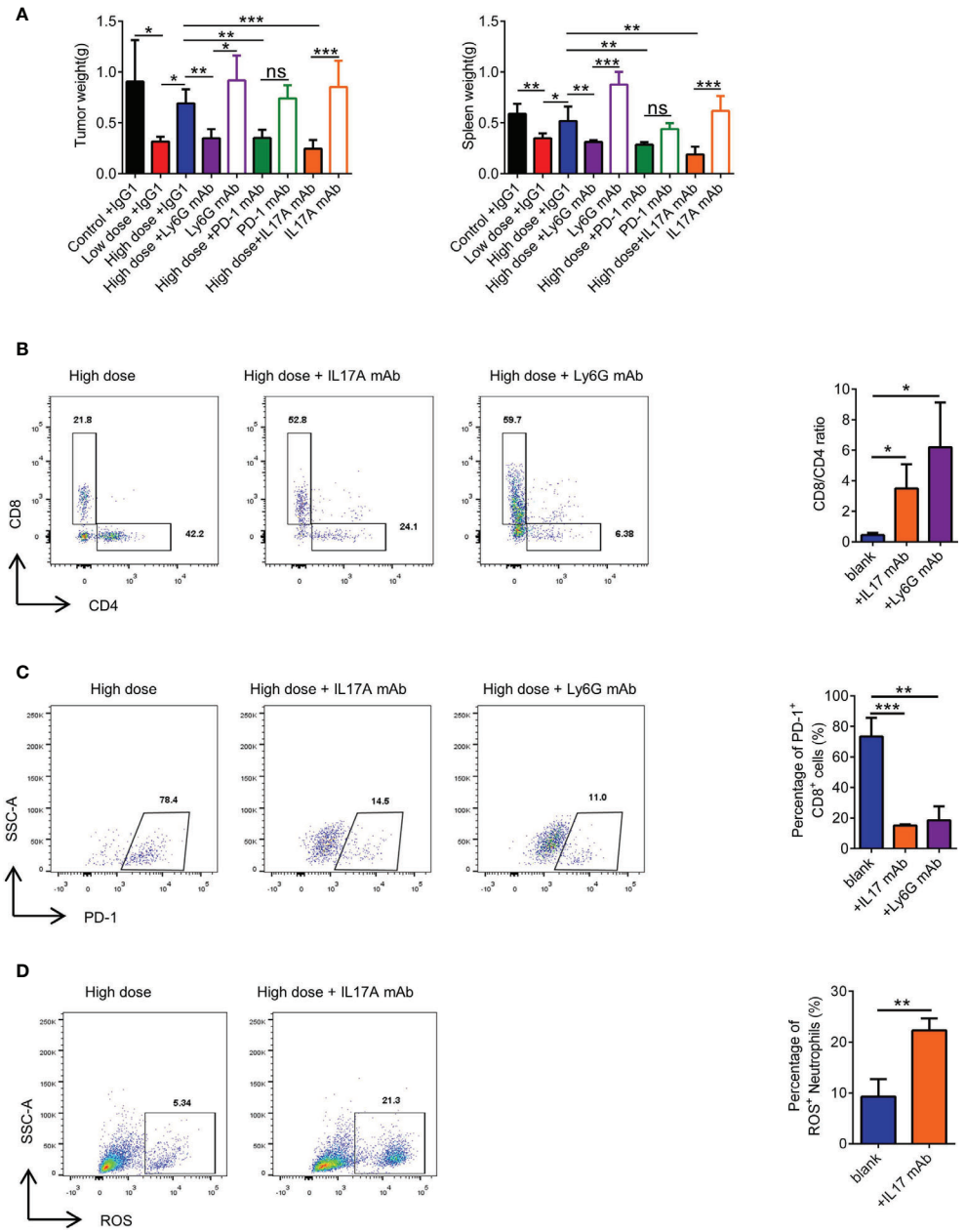

FIGURE 7 | Combination with immunotherapeutic monoclonal antibody can rescue high-dose VEGFR2-TKI therapy. **(A)** Representative weight of primary tumor and spleen after high-dose VEGFR2-TKI therapy and(or) IL17A mAb, PD-1 mAb or Ly6G mAb. **(B)** Frequency of $CD4^+$ T cells and $CD8^+$ T cells in the tumor after high-dose VEGFR2-TKI therapy and(or) IL17A mAb or Ly6G mAb. **(C)** Frequency of PD-1 expression on $CD8^+$ T cells in the tumor after high-dose VEGFR2-TKI therapy and(or) IL17A mAb or Ly6G mAb. **(D)** The expression of ROS in neutrophils after high-dose VEGFR2-TKI therapy and (or) IL17A mAb. Data are presented as the means ± SD from one representative experiment. Similar results were obtained from three independent experiments, n=5 mice each group, unless indicated otherwise. Statistical analysis was performed by two-tailed unpaired Student's t test **(D)** and one-way ANOVA **(A–C)**. ns, not significant, *$p < 0.05$, **$p < 0.01$, and ***$p < 0.001$. See also **Supplementary Figure S7**.

structural subsets, including αβ and γδ T cells (39). In the mouse breast cancer model, γδ T cells exhibited the highest VEGFR2 expression among all immune cells, implying that anti-VEGFR2 therapy may influence the function of γδ T cells. Nevertheless, the role of γδ T cells has not been studied in anti-VEGFR2 therapy resistance. Furthermore, we found that γδ T cells polarized into cytotoxic IFN-γ-producing subsets in "response" phases, while in "relapse" phases, γδ T cells polarized into suppressive IL17A-producing subsets. Further study found that, in "relapse" phases, mobilized VEGFR1 activated the PI3K-AKT pathway and then elicited IL17A secretion despite VEGFR2 inhibition. These results suggest that the PI3K-AKT pathway is likely to be the switch for

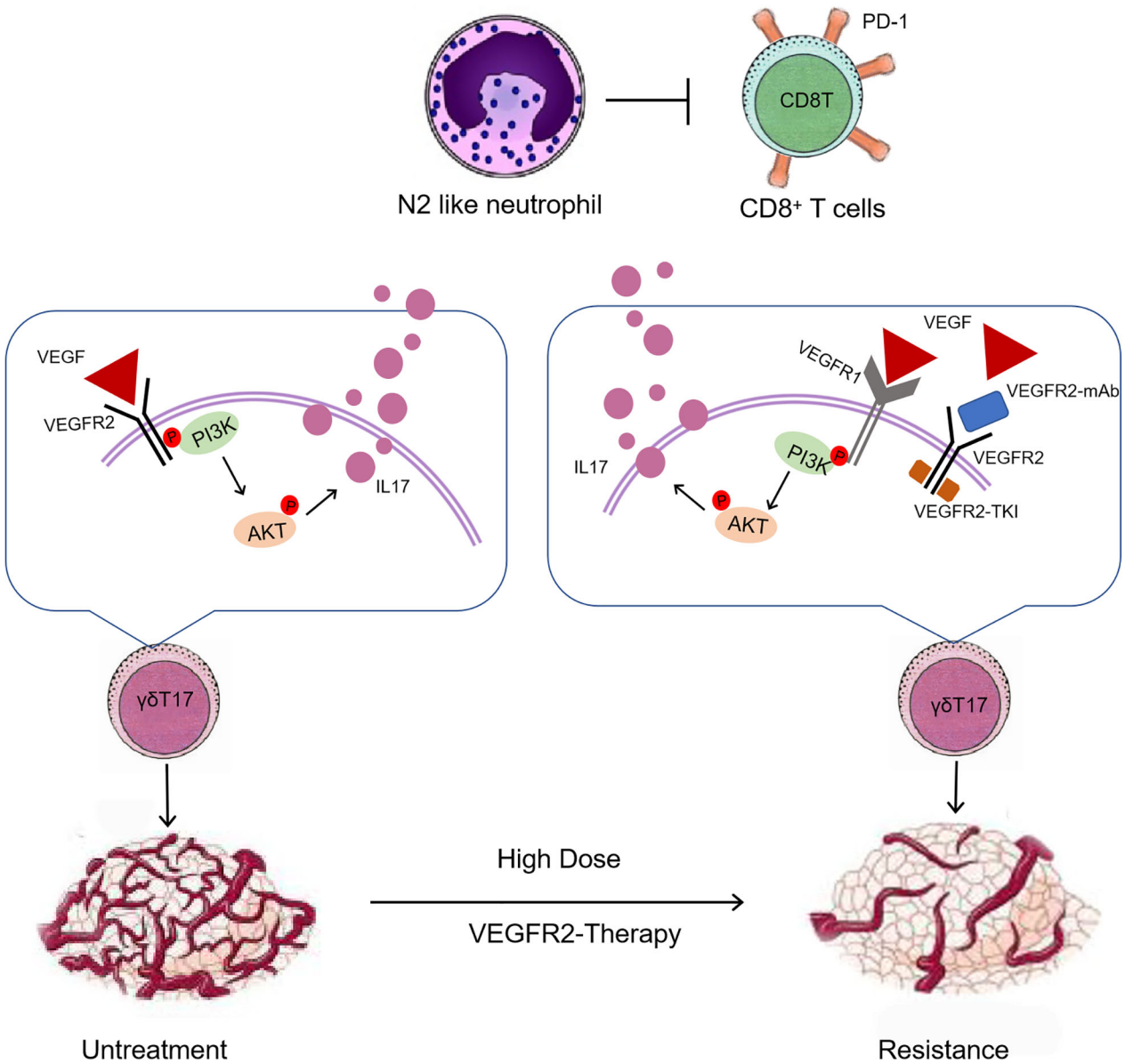

FIGURE 8 | An overview schematic demonstrating that high-dose anti-VEGFR2 treatment modifies the tumor immunosuppression microenvironment *via* "γδT cell-IL17A-neutrophil" axis.

conversion among γδ T cell subsets, and the upregulation of VEGFR1 in γδ T cells may exert major drug resistance in breast cancer.

Studies have reported that myeloid cells, including monocytes, macrophages and neutrophils, play a key role in the tumor microenvironment and promote tumor growth and metastasis (40). Myeloid cells promote tumor angiogenesis and are also involved in responsiveness and resistance to antiangiogenic therapy (25, 41). Anti-VEGF therapy facilitates $Ly6C^{lo}$ monocyte infiltration *via* the CX3CL1-CX3CR1 pathway, and $CX3CR1^{+}Ly6C^{lo}$ monocytes create an immunosuppressive microenvironment that mediates resistance to antiangiogenic therapy (42). Previous study showed that anti- VEGFR2 treatment resistance is concerned with the accumulated myeloid-derived suppressor cells recruited by GM-CSF in ovarian cancer (43). Other studies have also found that macrophages actively contribute to resistance to antiangiogenic therapy in ovarian cancer (44). Considering quite different component of tumor microenvironment among diverse tumor types, and the role of neutrophils in conferring resistance to antiangiogenic therapy never been studied, the mechanism of antiangiogenic therapy resistance in breast cancer needs to be studied in depth.

Fridlender's study verified that tumor-associated neutrophils are a heterogeneous set of immune cells, which can be classified as antitumorigenic (the "N1" phenotype) or protumorigenic (the "N2" phenotype) (35). N1 neutrophils exert antitumor activities by secreting more immunoactivating cytokines, producing more ROS and expressing lower levels of arginase, while N2 neutrophils play an immunosuppressive role. We found that neutrophils in "response" phases had a mature neutrophil-like morphology and "N1" function, while in "relapse" phases, neutrophils had an immature neutrophil-like morphology and "N2" function.

In the tumor microenvironment, immune cells undergo dramatic phenotypic changes induced by various stimuli and exhibit different functions (45). In our study, IL17A induced neutrophil N2 polarization, and nuclear morphological analysis revealed characteristics of immature neutrophils. A recent study demonstrated that IL17A-producing γδ T cells can polarize neutrophils into an immunosuppressive phenotype. Unfortunately, we did not find a specific surface marker for N1/N2 conversion from the anti-VEGFR2 therapy resistance models, as only morphological and immunosuppressive functions are involved. Further experiments, especially single-cell sequencing, are needed to focus on the effect of IL17A and IFN-γ on neutrophil phenotypes.

Our findings implied that immunosuppression, rather than angiogenesis, in the breast cancer microenvironment is the crucial mechanism conferring resistance to anti-VEGFR2 therapy exerted by γδT cells and neutrophils. Previous studies have shown that combining antiangiogenic therapy with immunotherapies has potential translational significance for cancer therapy (46). Moreover, most studies suggest low doses of anti-VEGFR2 therapy can induce vascular normalization and improve antitumor immunity, and improve immunotherapeutic efficacy (22, 47). But, according to the "therapy window" of vascular normalization, the low dose and treatment duration is difficult in clinical practice (46). Indeed, the therapeutic dose of anti-VEGFR2 drug currently applied in the clinic is often considered as a full or high dose. The clinical trials, like KEYNOTE-426 and IMbrave 150, found that full or high dose anti-VEGFR2 therapy plus PD-1 inhibitor significantly longer survival in some tumor types, which implied that high dose anti-VEGFR2 therapy closely related to the inhibitory immune microenvironment (48, 49). Our data also provide compelling evidence for optimized therapeutic strategies, when high-dose anti-VEGFR2 monotherapy evolve resistance. By remodeling inhibitory immune microenvironment via targeting the multiple points of "γδT cell-IL17A-neutrophil" axis (such as an anti-IL17 mAb), which can resensitize resistant tumors to antiangiogenic therapy and generate relatively durable effects. The mechanism of resistance caused by changes in the immune microenvironment provided by our research provides a possible solution for resistance to anti-vascular therapy, that is, while paying attention to the anti-vascular effect, the immune microenvironment should also be paid attention to, besides, combining with high-dose anti-vascular therapy and immunotherapy may provide new strategy for therapy in breast cancer treatment.

CONCLUSION

Our study provides a novel rationale for the immunomodulatory effects involved in anti-VEGFR2 therapy, like VEGFR2-TKI antiangiogenic therapy. VEGFR2-TKI can directly act on γδ T cells and increase the inhibitory effects of N2-like neutrophils on T cell function in the tumor microenvironment, providing potential antitumor strategies in aggressive breast cancer. It will be important to perform clinical trials to test the usefulness of anti-VEGFR2 therapy combined with immunotherapy.

DATA AVAILABILITY STATEMENT

The original contributions presented in the study are included in the article/**Supplementary Material**. Further inquiries can be directed to the corresponding authors.

ETHICS STATEMENT

The animal study was reviewed and approved by the Ethics Committee of the Second Affiliated Hospital of Zhejiang University School of Medicine in accordance with the Declaration of Helsinki. Written informed consent was obtained from the owners for the participation of their animals in this study.

AUTHOR CONTRIBUTIONS

Conception and design, JH and ZW. Development of methodology, ZZ and CY. Acquisition of data (provided animals, acquired and managed patients, provided facilities, etc.), ZZ and CY. Analysis and interpretation of data (e.g., statistical analysis, biostatistics, computational analysis), ZZ, CY, and LZ. Writing, review, and/or revision of the manuscript, ZZ and LL. Administrative, technical, or material support (i.e., reporting or organizing data, constructing databases), YZ and KS. Study supervision, ZW. All authors contributed to the article and approved the submitted version.

FUNDING

This work was supported by grants from the National Natural Science Foundation of China (81930079, 81872317, 81902981, 81902626) and Health Commission of Zhejiang Province (WKJ-ZJ-1803).

ACKNOWLEDGMENTS

The authors would like to thank our research group for discussion and editing the manuscript.

SUPPLEMENTARY MATERIAL

The Supplementary Material for this article can be found online at: https://www.frontiersin.org/articles/10.3389/fimmu.2021.699478/full#supplementary-material

Supplementary Figure S1 | related to **Figure 1**. **(A)** Schematic illustration of VEGFR2-TKI and VEGFR2 mAb of different therapeutic doses in 4T1 and EMT6 breast cancer models. i.g., intragastric administration. i.p., intraperitoneal injection. **(B)** Immunofluorescence of CD31 on breast cancer tissue after anti-VEGFR2 therapy in EMT6 model. Bar=200 μm. Green, CD31; blue, DAPI. **(C)** Analysis weight of spleens after different doses of anti-VEGFR2 therapy in 4T1 and EMT6 models. **(D)** Tumor growth curve of 4T1 and EMT6 breast cancer tissue after anti-VEGFR2 therapy. Data are presented as the means ± SD from one representative experiment. Similar results were obtained from three independent experiments, n=4 mice each group, unless indicated otherwise. Statistical analysis was performed by one-way ANOVA **(C)** and repeated-measures ANOVA **(D)**. ns, not significant, *p<0.05, **p<0.01, and ***p<0.001.

Supplementary Figure S2 | related to **Figure 1** and **Figure 2**. **(A, B)** Schematic illustration **(A)** and anatomy results **(B)** for anti-VEGFR2 treatment in the MMTV-PyMT breast cancer model. i.g., intragastric administration. i.p., intraperitoneal injection. **(C)** Flow cytometry gate strategy of tumor-infiltrating myeloid cell and lymphocyte detection. Data are presented as the means ± SD from one representative experiment. Similar results were obtained from three independent experiments, n=4 mice each group, unless indicated otherwise. Statistical analysis was performed by one-way ANOVA **(B)**. ns, not significant, *p<0.05, **p<0.01, and ***p<0.001.

Supplementary Figure S3 | related to **Figure 3**. **(A, B)** Flow cytometry analysis of VEGFR2 **(A)** and VEGFR3 **(B)** expression of γδT cells ($CD45^+CD3^+TCR\gamma\delta^+$) in tumors after different dose of VEGFR2-TKI therapies. **(C)** Flow cytometry analysis of VEGFR2 expression of γδT cells derived from naive spleens treated with different doses of VEGFR2-TKI *in vitro*. **(D)** Western blot analysis of PI3K/actin and AKT/actin in γδ T cells from tumors with different dose of VEGFR2-TKI therapies (γδT cells were sorted from 4 tumors as one donor). **(E)** Western blot analysis of PI3K/actin and AKT/atin in γδ T cells derived from naive spleens treated with different doses of VEGFR2-TKI *in vitro* (γδ T cells were sorted from 9 naive spleens as one donor). **(F)** Schematic illustration of VEGFR2-TKI of different therapeutic doses combined with YS-49 (PI3K agoist) and Copanlisib (PI3K inhibitor) in 4T1 breast cancer models. *i.g.*, intragastric administration. *i.p.*, intraperitoneal injection. Qd, once a day. Qod once every other one day. **(G)** Flow cytometry analysis of IL17 expression of γδT cells derived from naive spleens treated with different doses of YS-49 *in vitro*. Data are presented as the means ± SD from one representative experiment. Similar results were obtained from three independent experiments, n=4 mice each group, unless indicated otherwise. Statistical analysis was performed by one-way ANOVA. ns, not significant, *p<0.05, **p<0.01, and ***p<0.001.

Supplementary Figure S4 | related to **Figure 4**. **(A)** Giemsa-stained naive BM-derived neutrophils treated with different concentrations of VEGFR2-TKI *in vitro*. **(B)** Flow cytometry analysis of ROS expression of neutrophils treated with different concentrations of VEGFR2-TKI *in vitro*. **(C)** Giemsa-stained naive BM-derived neutrophils without any treatment. **(D)** Giemsa-stained neutrophils treated with or without IL17A mAb or IFN-γ mAb. Data are presented as the means ± SD from one representative experiment. Similar results were obtained from three independent experiments, n=4 mice each group, unless indicated otherwise. Statistical analysis was performed by one-way ANOVA. ns, not significant, *p<0.05, **p<0.01, and ***p<0.001.

Supplementary Figure S5 | related to **Figure 5**. **(A)** Flow cytometry gating strategy of tumor cells. **(B)** Frequency of PD-L1 expression on tumor cells ($CD45^-EpCAM^+$) in the tumor after VEGFR2-TKI therapy. Data are presented as the means ± SD from one representative experiment. Similar results were obtained from three independent experiments, n=4 mice each group, unless indicated otherwise. Statistical analysis was performed by one-way ANOVA. ns, not significant, *p<0.05, **p<0.01, and ***p<0.001.

Supplementary Figure S6 | related to **Figure 6**. **(A)** Compared biochemical parameters associated with immunosuppressive characterization of neutrophils including arginase (Functional kit), NO (Content detection kit) and PGE2 (ELISA) in tumor-infiltrating neutrophils after different dose of VEGFR2-TKI therapies. **(B, C)** Flow cytometry analysis of proliferation **(B)** and PD-1 expression **(C)** of $CD8^+$ T cells after co-culturing with the different group of γδT cells sorting from the tumor after VEGFR2-TKI therapy. $CD8^+$ T cells were derived from naive spleen. **(D, E)** Flow cytometry analysis of proliferation of $CD8^+$ T cells ($CFSE^{low}CD8^+$) **(D)** and PD-1 expression of $CD8^+$ T cells **(E)** treated with different concentrations of VEGFR2-TKI *in vitro*. Data are presented as the means ± SD from one representative experiment. Similar results were obtained from three independent experiments, n=4 mice each group, unless indicated otherwise. Statistical analysis was performed by one-way ANOVA. ns, not significant, *p<0.05, **p<0.01, and ***p<0.001.

Supplementary Figure S7 | related to **Figure 7**. **(A)** Flow cytometry analysis of neutrophils in the PB of the 4T1 model treated with Ly-6G mAb. **(B)** Representative of primary tumor after high-dose VEGFR2-TKI therapy and(or) IL17A mAb, PD-1 mAb or Ly6G mAb. **(C)** H&E staining and quantification of lung metastasis in the 4T1 model (Black arrow) after multiple treatments. Bar=1 mm. Data are presented as the means ± SD from one representative experiment. Similar results were obtained from three independent experiments, n=4 mice each group, unless indicated otherwise. Statistical analysis was performed by one-way ANOVA. ns, not significant, *p<0.05, **p<0.01, and ***p<0.001.

REFERENCES

1. Hanahan D, Weinberg Robert A. Hallmarks of Cancer: The Next Generation. *Cell* (2011) 144(5):646–74. doi: 10.1016/j.cell.2011.02.013
2. De Palma M, Biziato D, Petrova TV. Microenvironmental Regulation of Tumour Angiogenesis. *Nat Rev Cancer* (2017) 17(8):457–74. doi: 10.1038/nrc.2017.51
3. Yihai C, Jack A, D'Amato RJ, D'Amore PA, Ingber DE, Kerbel R, et al. Forty-Year Journey of Angiogenesis Translational Research. *Sci Transl Med* (2011) 3 (114):114rv3. doi: 10.1126/scitranslmed.3003149
4. Jayson GC, Kerbel R, Ellis LM, Harris AL. Antiangiogenic Therapy in Oncology: Current Status and Future Directions. *Lancet* (2016) 388 (10043):518–29. doi: 10.1016/s0140-6736(15)01088-0
5. Robert NJ, Dieras V, Glaspy J, Brufsky AM, Bondarenko I, Lipatov ON, et al. RIBBON-1: Randomized, Double-Blind, Placebo-Controlled, Phase III Trial of Chemotherapy With or Without Bevacizumab for First-Line Treatment of Human Epidermal Growth Factor Receptor 2-Negative, Locally Recurrent or Metastatic Breast Cancer. *J Clin Oncol* (2011) 29(10):1252–60. doi: 10.1200/JCO.2010.28.0982
6. Kathy Miller MW, Gralow J, Dickler M, Cobleigh M, Perez EA, Shenkier T, et al. Paclitaxel Plus Bevacizumab Versus Paclitaxel Alone for Metastatic Breast Cancer. *N Engl J Med* (2007) 357(26):2666–76. doi: 10.1056/NEJMoa072113
7. Shojaei F, Ferrara N. Role of the Microenvironment in Tumor Growth and in Refractoriness/Resistance to Anti-Angiogenic Therapies. *Drug Resist Updat* (2008) 11(6):219–30. doi: 10.1016/j.drup.2008.09.001
8. Rapisarda A, Melillo G. Overcoming Disappointing Results With Antiangiogenic Therapy by Targeting Hypoxia. *Nat Rev Clin Oncol* (2012) 9(7):378–90. doi: 10.1038/nrclinonc.2012.64
9. Iwamoto H, Abe M, Yang Y, Cui D, Seki T, Nakamura M, et al. Cancer Lipid Metabolism Confers Antiangiogenic Drug Resistance. *Cell Metab* (2018) 28 (1):104–17.e5. doi: 10.1016/j.cmet.2018.05.005
10. Shojaei F, Ferrara N. Refractoriness to Antivascular Endothelial Growth Factor Treatment: Role of Myeloid Cells. *Cancer Res* (2008) 68(14):5501–4. doi: 10.1158/0008-5472.CAN-08-0925
11. Shaul ME, Fridlender ZG. Tumour-Associated Neutrophils in Patients With Cancer. *Nat Rev Clin Oncol* (2019) 16(10):601–20. doi: 10.1038/s41571-019-0222-4
12. Powell DR, Huttenlocher A. Neutrophils in the Tumor Microenvironment. *Trends Immunol* (2016) 37(1):41–52. doi: 10.1016/j.it.2015.11.008
13. Campbell EL. Hypoxia-Recruited Angiogenic Neutrophils. *Blood* (2015) 126 (17):1972–3. doi: 10.1182/blood-2015-09-666578

14. Silva-Santos B, Serre K, Norell H. γδ T Cells in Cancer. *Nat Rev Immunol* (2015) 15(11):683–91. doi: 10.1038/nri3904
15. Silva-Santos B, Mensurado S, Coffelt SB. Gammadelta T Cells: Pleiotropic Immune Effectors With Therapeutic Potential in Cancer. *Nat Rev Cancer* (2019) 19(7):392–404. doi: 10.1038/s41568-019-0153-5
16. Fleming C, Morrissey S, Cai Y, Yan J. Gammadelta T Cells: Unexpected Regulators of Cancer Development and Progression. *Trends Cancer* (2017) 3 (8):561–70. doi: 10.1016/j.trecan.2017.06.003
17. Coffelt SB, Kersten K, Doornebal CW, Weiden J, Vrijland K, Hau CS, et al. IL-17-Producing Gammadelta T Cells and Neutrophils Conspire to Promote Breast Cancer Metastasis. *Nature* (2015) 522(7556):345–8. doi: 10.1038/nature14282
18. Tian S, Quan H, Xie C, Guo H, Lü F, Xu Y, et al. YN968D1 Is a Novel and Selective Inhibitor of Vascular Endothelial Growth Factor Receptor-2 Tyrosine Kinase With Potent Activity *In Vitro* and *In Vivo*. *Cancer Sci* (2011) 102(7):1374–80. doi: 10.1111/j.1349-7006.2011.01939.x
19. Wu P, Wu D, Ni C, Ye J, Chen W, Hu G, et al. Gammadeltat17 Cells Promote the Accumulation and Expansion of Myeloid-Derived Suppressor Cells in Human Colorectal Cancer. *Immunity* (2014) 40(5):785–800. doi: 10.1016/j.immuni.2014.03.013
20. Huang Y, Yuan J, Righi E, Kamoun WS, Ancukiewicz M, Nezivar J, et al. Vascular Normalizing Doses of Antiangiogenic Treatment Reprogram the Immunosuppressive Tumor Microenvironment and Enhance Immunotherapy. *Proc Natl Acad Sci USA* (2012) 109(43):17561–6. doi: 10.1073/pnas.1215397109
21. Huang Y, Goel S, Duda DG, Fukumura D, Jain RK. Vascular Normalization as an Emerging Strategy to Enhance Cancer Immunotherapy. *Cancer Res* (2013) 73(10):2943–8. doi: 10.1158/0008-5472.CAN-12-4354
22. Li Q, Wang Y, Jia W, Deng H, Li G, Deng W, et al. Low-Dose Anti-Angiogenic Therapy Sensitizes Breast Cancer to PD-1 Blockade. *Clin Cancer Res* (2020) 26 (7):1712–24. doi: 10.1158/1078-0432.CCR-19-2179
23. Bono F, De Smet F, Herbert C, De Bock K, Georgiadou M, Fons P, et al. Inhibition of Tumor Angiogenesis and Growth by a Small-Molecule Multi-FGF Receptor Blocker With Allosteric Properties. *Cancer Cell* (2013) 23 (4):477–88. doi: 10.1016/j.ccr.2013.02.019
24. Guido B, Man S, Green SK, Francia G, Ebos JML, du Manoir JM, et al. Increased Plasma Vascular Endothelial Growth Factor (VEGF) as a Surrogate Marker for Optimal Therapeutic Dosing of VEGF Receptor-2 Monoclonal Antibodies. *Cancer Res* (2004) 64(18):6616–25. doi: 10.1158/0008-5472.CAN-04-0401
25. Rivera Lee B, Meyronet D, Hervieu V, Frederick Mitchell J, Bergsland E, Bergers G. Intratumoral Myeloid Cells Regulate Responsiveness and Resistance to Antiangiogenic Therapy. *Cell Rep* (2015) 11(4):577–91. doi: 10.1016/j.celrep.2015.03.055
26. Wang X, Bove AM, Simone G, Ma B. Molecular Bases of VEGFR-2-Mediated Physiological Function and Pathological Role. *Front Cell Dev Biol* (2020) 8:599281. doi: 10.3389/fcell.2020.599281
27. Zheng Z, Zhao C, Wang L, Cao X, Li J, Huang R, et al. A VEGFR1 Antagonistic Peptide Inhibits Tumor Growth and Metastasis Through VEGFR1-PI3K-AKT Signaling Pathway Inhibition. *Am J Cancer Res* (2015) 5(10)::3149–61.
28. Chen X, Guo Y, Han R, Liu H, Ding Y, Shi Y, et al. Class I PI3K Inhibitor ZSTK474 Attenuates Experimental Autoimmune Neuritis by Decreasing the Frequency of Th1/Th17 Cells and Reducing the Production of Proinflammatory Cytokines. *Cell Immunol* (2018) 329:41–9. doi: 10.1016/j.cellimm.2018.04.011
29. Huang L, Wang M, Yan Y, Gu W, Zhang X, Tan J, et al. OX40L Induces Helper T Cell Differentiation During Cell Immunity of Asthma Through PI3K/AKT and P38 MAPK Signaling Pathway. *J Trans Med* (2018) 16(1):74. doi: 10.1186/s12967-018-1436-4
30. Yang Q, Jiang W, Hou P. Emerging Role of PI3K/AKT in Tumor-Related Epigenetic Regulation. *Semin Cancer Biol* (2019) 59:112–24. doi: 10.1016/j.semcancer.2019.04.001
31. Liu X, Xu Y, Zhou Q, Chen M, Zhang Y, Liang H, et al. PI3K in Cancer: Its Structure, Activation Modes and Role in Shaping Tumor Microenvironment. *Future Oncol (London England)* (2018) 14(7):665–74. doi: 10.2217/fon-2017-0588
32. Zhang J, Li H, Wu Q, Chen Y, Deng Y, Yang Z, et al. Tumoral NOX4 Recruits M2 Tumor-Associated Macrophages via ROS/PI3K Signaling-Dependent Various Cytokine Production to Promote NSCLC Growth. *Redox Biol* (2019) 22:101116. doi: 10.1016/j.redox.2019.101116
33. Zhao R, Song Y, Wang Y, Huang Y, Li Z, Cui Y, et al. PD-1/PD-L1 Blockade Rescue Exhausted CD8+ T Cells in Gastrointestinal Stromal Tumours via the PI3K/Akt/mTOR Signalling Pathway. *Cell Prolif* (2019) 52(3):e12571. doi: 10.1111/cpr.12571
34. Mollinedo F. Neutrophil Degranulation, Plasticity, and Cancer Metastasis. *Trends Immunol* (2019) 40(3):228–42. doi: 10.1016/j.it.2019.01.006
35. Fridlender ZG, Sun J, Kim S, Kapoor V, Cheng G, Ling L, et al. Polarization of Tumor-Associated Neutrophil Phenotype by TGF-β: "N1" Versus "N2" TAN. *Cancer Cell* (2009) 16(3):183–94. doi: 10.1016/j.ccr.2009.06.017
36. Shaul ME, Levy L, Sun J, Mishalian I, Singhal S, Kapoor V, et al. Tumor-Associated Neutrophils Display a Distinct N1 Profile Following TGFbeta Modulation: A Transcriptomics Analysis of Pro- vs. antitumor TANs. *Oncoimmunology* (2016) 5 (11):e1232221. doi: 10.1080/2162402X.2016.1232221
37. Zhu P, Hu C, Hui K, Jiang X. The Role and Significance of VEGFR2(+) Regulatory T Cells in Tumor Immunity. *Onco Targets Ther* (2017) 10:4315–9. doi: 10.2147/OTT.S142085
38. Ziogas AC, Gavalas NG, Tsiatas M, Tsitsilonis O, Politi E, Terpos E, et al. VEGF Directly Suppresses Activation of T Cells From Ovarian Cancer Patients and Healthy Individuals via VEGF Receptor Type 2. *Int J Cancer* (2012) 130(4):857–64. doi: 10.1002/ijc.26094
39. Kisielow J, Kopf M. The Origin and Fate of gammadeltaT Cell Subsets. *Curr Opin Immunol* (2013) 25(2):181–8. doi: 10.1016/j.coi.2013.03.002
40. Hinshaw DC, Shevde LA. The Tumor Microenvironment Innately Modulates Cancer Progression. *Cancer Res* (2019) 79(18):4557–66. doi: 10.1158/0008-5472.CAN-18-3962
41. Shojaei F, Wu X, Malik AK, Zhong C, Baldwin ME, Schanz S, et al. Tumor Refractoriness to Anti-VEGF Treatment Is Mediated by CD11b+Gr1+ Myeloid Cells. *Nat Biotechnol* (2007) 25(8):911–20. doi: 10.1038/nbt1323
42. Jung K, Heishi T, Khan OF, Kowalski PS, Incio J, Rahbari NN, et al. Ly6Clo Monocytes Drive Immunosuppression and Confer Resistance to Anti-VEGFR2 Cancer Therapy. *J Clin Invest* (2017) 127(8):3039–51. doi: 10.1172/jci93182
43. Horikawa N, Abiko K, Matsumura N, Baba T, Hamanishi J, Yamaguchi K, et al. Anti-VEGF Therapy Resistance in Ovarian Cancer Is Caused by GM-CSF-Induced Myeloid-Derived Suppressor Cell Recruitment. *Br J Cancer* (2020) 122(6):778–88. doi: 10.1038/s41416-019-0725-x
44. Dalton HJ, Pradeep S, McGuire M, Hailemichael Y, Ma S, Lyons Y, et al. Macrophages Facilitate Resistance to Anti-VEGF Therapy by Altered VEGFR Expression. *Clin Cancer Res* (2017) 23(22):7034–46. doi: 10.1158/1078-0432.ccr-17-0647
45. Morgan A, Giese LEH, Huttenlocher A. Neutrophil Plasticity in the Tumor Microenvironment. *Blood* (2019) 133(20):2159–67. doi: 10.1182/blood-2018-11-844548
46. Fukumura D, Kloepper J, Amoozgar Z, Duda DG, Jain RK. Enhancing Cancer Immunotherapy Using Antiangiogenics: Opportunities and Challenges. *Nat Rev Clin Oncol* (2018) 15(5):325–40. doi: 10.1038/nrclinonc.2018.29
47. Zhao S, Ren S, Jiang T, Zhu B, Li X, Zhao C, et al. Low-Dose Apatinib Optimizes Tumor Microenvironment and Potentiates Antitumor Effect of PD-1/PD-L1 Blockade in Lung Cancer. *Cancer Immunol Res* (2019) 7(4):630–43. doi: 10.1158/2326-6066.CIR-17-0640
48. Finn RS, Qin S, Ikeda M, Galle PR, Ducreux M, Kim TY, et al. Atezolizumab Plus Bevacizumab in Unresectable Hepatocellular Carcinoma. *N Engl J Med* (2020) 382(20):1894–905. doi: 10.1056/NEJMoa1915745
49. Rini BI, Plimack ER, Stus V, Gafanov R, Hawkins R, Nosov D, et al. Pembrolizumab Plus Axitinib Versus Sunitinib for Advanced Renal-Cell Carcinoma. *N Engl J Med* (2019) 380(12):1116–27. doi: 10.1056/NEJMoa1816714

Conflict of Interest: The authors declare that the research was conducted in the absence of any commercial or financial relationships that could be construed as a potential conflict of interest.

this article, or claim that may be made by its manufacturer, is not guaranteed or endorsed by the publisher.

frontiers in Immunology

REVIEW
published: 15 December 2021
doi: 10.3389/fimmu.2021.780145

Strategies to Circumvent the Side-Effects of Immunotherapy Using Allogeneic CAR-T Cells and Boost Its Efficacy: Results of Recent Clinical Trials

Sergei Smirnov[1†], *Alexey Petukhov*[1,2*†], *Ksenia Levchuk*[1], *Sergey Kulemzin*[1,3], *Alena Staliarova*[4], *Kirill Lepik*[5,6], *Oleg Shuvalov*[2], *Andrey Zaritskey*[1], *Alexandra Daks*[1,2] *and Olga Fedorova*[1,2]

[1] Almazov National Medical Research Centre, Personalized Medicine Centre, Saint Petersburg, Russia, [2] Institute of Cytology, Laboratory of Gene Expression Regulation, Russian Academy of Sciences, Saint Petersburg, Russia, [3] Institute of Molecular and Cellular Biology SB Russian Academy of Science (RAS), Department of Molecular Immunology, Laboratory of Immunogenetics, Novosibirsk, Russia, [4] Belarusian Research Center for Pediatric Oncology, Hematology and Immunology, Oncological Department 3, Borovliani, Minsk Region, Belarus, [5] RM Gorbacheva Research Institute of Pediatric Oncology, Hematology and Transplantation, Chemotherapy and Bone Marrow Transplantation Department, Saint Petersburg, Russia, [6] Pavlov University, Department of Hematology, Transfusiology and Transplantology, Saint Petersburg, Russia

Despite the outstanding results of treatment using autologous chimeric antigen receptor T cells (CAR-T cells) in hematological malignancies, this approach is endowed with several constraints. In particular, profound lymphopenia in some patients and the inability to manufacture products with predefined properties or set of cryopreserved batches of cells directed to different antigens in advance. Allogeneic CAR-T cells have the potential to address these issues but they can cause life-threatening graft-versus-host disease or have shorter persistence due to elimination by the host immune system. Novel strategies to create an "off the shelf" allogeneic product that would circumvent these limitations are an extensive area of research. Here we review CAR-T cell products pioneering an allogeneic approach in clinical trials.

Keywords: chimeric, allogeneic, clinical, trials, GvHD, receptor, T cell, CAR (chimeric antigen receptor)

OPEN ACCESS

Edited by:
John Maher,
King's College London,
United Kingdom

Reviewed by:
Christopher Daniel Chien,
National Cancer Institute (NCI),
United States
Xi Zhang,
Xinqiao Hospital, China

****Correspondence:***
Alexey Petukhov
alexeysakhalin@gmail.com

†These authors have contributed equally to this work and share first authorship

Specialty section:
This article was submitted to Cancer Immunity and Immunotherapy, a section of the journal Frontiers in Immunology

Received: *20 September 2021*
Accepted: *22 November 2021*
Published: *15 December 2021*

Citation:
Smirnov S, Petukhov A, Levchuk K, Kulemzin S, Staliarova A, Lepik K, Shuvalov O, Zaritskey A, Daks A and Fedorova O (2021) Strategies to Circumvent the Side-Effects of Immunotherapy Using Allogeneic CAR-T Cells and Boost Its Efficacy: Results of Recent Clinical Trials. Front. Immunol. 12:780145. doi: 10.3389/fimmu.2021.780145

1 INTRODUCTION

Recently, therapy using chimeric antigen receptor T cells (CAR-T cells) has emerged as a powerful tool for patients with certain subtypes of B-cell lymphoma and leukemia. CAR-T cells are designed to selectively target a predefined tumor-associated antigen. This is achieved by the expression of a chimeric antigen receptor (CAR) on the surface of immune cells, typically T cells or natural killer (NK) cells (1).

CARs are composed of an antigen-binding domain (e.g., a single-chain variable fragment (scFv) derived from a monoclonal antibody) and a signaling domain (e.g., the intracellular portion of the cluster of differentiation (CD)3ζ subunit of the T-cell receptor) that are linked together *via* a transmembrane and an optional hinge domain. This design allows for major histocompatibility

complex (MHC) molecule-independent antigen binding, which launches downstream signaling events culminating in a cytotoxic response and destruction of the target cell (2). Second- and third generation CAR-T cells carry additional co-stimulatory domains such as those derived from CD28 or 4-1BB (3). For instance, recent studies have shown that CAR-T cells with a CD28 costimulatory domain exhibit rapid activation of CAR-T cells followed by exhaustion (4, 5). By contrast, incorporation of a 4-1BB-based co-stimulatory domain ensures prolonged endurance of CAR-T cells by diminishing expression of exhaustion-related genes (6), which enhances the capacity for oxidative metabolism and central memory differentiation (7). However, large-cohort clinical data have demonstrated that CAR-T cells with CD28 or 4-1BB costimulatory domains can mediate long-lasting remission and have shown comparable results against B cell lymphomas (8, 9) and acute lymphoblastic leukemia (10–13). Considering many differences except from co-stimulatory domains in trials performed up to date (8–10, 12, 14), an additional trial could clarify the possible superiority of CD28 or 4-1BB domains.

More advanced designs of "armored" CAR-T cells have been developed to modify the immunosuppressive tumor microenvironment, and also to enhance T-cell functioning/trafficking and ameliorate CAR-T cell-associated toxicities (15, 16). For instance, interleukin (IL)-7 has been shown to play an essential part in the antigen-driven expansion of naive and activated T cell populations (17) whereas C–C motif chemokine ligand CCL21 is a chemokine implicated in attracting naive T cells and antigen-presenting cells, and coordinating their interaction and consequent tumor antigen-specific immune response (18). The co-expression of IL-7 and CCL21 along with a CAR has led to significant improvement in the proliferation of CAR-T cells *in vitro* and boosted therapeutic activity *in vivo* (18). Antigen-driven signaling *via* second- and third-generation CARs has been described to induce proliferation of CAR-T cells. Excessive immune stimulation, however, can manifest as increased serum levels of cytokines such as IL-6, interferon-γ, and tumor necrosis factor (TNF). This action may lead to uncontrolled systemic inflammation, and is one of the most frequent side-effects of CAR-T cell therapy, referred to as "cytokine release syndrome" (CRS) (19). The second common adverse effect of therapy using CAR-T cells is known as an "immune effector cell-associated neurotoxicity syndrome" (ICANS), which results from increased cytokine levels and their penetration across the blood–brain barrier (20).

In patients with hematological malignancies, most clinical trials have focused on an autologous approach that utilizes T cells isolated from the patient's peripheral blood. However, in spite of remarkable clinical outcomes (10, 21, 22), this strategy is endowed with several important limitations, namely, very high treatment costs and individual manufacturing processes (23) with possible issues (24–27), reaching 9% in Kymriah pivotal trial (28). Despite comparable time burdens of autologous and allogeneic manufacturing processes, the key difference is that allogeneic CAR-T cells represent an "off the shelf product" that can be administered without delay, which is very important for patients with highly proliferative diseases such as acute leukemia. In addition, T-cell dysfunction and a reduction in the number of naive and central memory T-cell subsets due to chemotherapy (29) or the tumor microenvironment (30) impair *ex vivo* expansion and the persistence of autologous CAR-T cells (31, 32).

CAR-T cells produced from the material of allogeneic donors have three main advantages compared with therapies using autologous CAR-T cells. First, allogeneic CAR-T cells can be produced in advance and delivered without delay according to the established treatment program of the individual patient. Second, allogeneic donor-derived T cells are not exposed to multiple rounds of anti-leukemia therapy, so they are more amenable to *ex vivo* manipulation (33). Third, products based on autologous CAR-T cells cannot be manufactured 3 for some patients because of their profound lymphopenia, which is not an issue with products based on allogeneic CAR-T cells.

Despite the numerous advantages of therapy using allogeneic CAR-T cells, this technology comes with two major disadvantages. First, the recipient's cells appear "foreign" to the native T cell receptors (TCRs) of the administered CAR-T cells, which may induce their activation and result in acute graft-versus-host disease (GvHD). Second, CAR-T cells are foreign to the host immune system, which may cause their rapid elimination from the circulation, and a lack of durable persistence of CAR-T cells in turn has been demonstrated to be associated with poor patient responses in an autologous setting (34).

T cells used for the manufacture of allogeneic CAR-T cells are derived mainly from peripheral blood mononuclear cells, particularly cells that have a TCR consisting of an α and β chain (αβ T cell subsets), which constitute ~90% of circulating T cells in healthy donors (35). On the one hand, due to their relative abundance in peripheral blood and ability to proliferate rapidly, αβ T cells represent an attractive target for the manufacture of allogeneic CAR-T cells. On the other hand, this subset of cells has been shown to play a major part in the pathogenesis of acute and chronic GvHD due to an inherent immunologic mismatch between the patient and donor. In autologous settings, the T cells of patients that undergo negative selection in the thymus are used, thereby comprising a population that is non-responsive to self-peptides in a complex with MHC-I molecules (36). By contrast, in allogeneic settings, the administered cells can recognize healthy recipient's tissues *via* TCRs in an MHC molecule-dependent manner, with subsequent induction of apoptosis of healthy cells and GvHD manifestation (37–39).

The manufacturing processes of allogeneic CAR-T cells comprise all the production steps of the autologous products that have been reviewed elsewhere (40) with additional, more sophisticated gene-editing steps that will not be discussed in detail here. Turtle et al. pointed out that the defined ratio of CD8+ and CD4+ T-cell subsets is essential for the *in vivo* expansion and persistence of CAR-T cells (41). However, CAR-T cells so far have been administered in both defined (41) and undefined (10, 21, 22) CD4/8 ratios without any loss of efficacy. In an autologous setting, the endurance and efficacy of CAR-T cells have been found to correlate with the numbers of less differentiated CD8+ and CD4+ T-cell subsets in the final

product (42). In particular, Xu et al. (43) discovered that the expansion of CD19-redirected T cells was dependent upon the frequency of CD8+CD45RA+CCR7+ subsets corresponding to stem cell-like memory and naive T-cell phenotypes. Conversely, patients after previous lines of therapy often suffer from lymphopenia and have higher quantities of effector memory T cells (42): an allogeneic approach could circumvent this issue because the cells are derived from the peripheral blood mononuclear cells of a healthy donor. In addition, in autologous and allogeneic settings, the number of T cells can be amplified in more defined subsets *via* modulation of the culture conditions. Yang et al. showed that supplementing media with IL-15 and IL-7 during *ex vivo* expansion increased the number of naive T cells (43).

Herein, we review relevant clinical data on the use of therapies based on allogeneic CAR-T cells. We discuss the outcomes of strategies aiming to mitigate GvHD and also the other side-effects associated with therapy using allogeneic CAR-T cells described in recent clinical trials.

2 SOURCES OF ALLOGENEIC CAR-T CELLS

Building upon clinical experience, the ability of allogeneic CAR-T cells to eliminate tumor cells is dependent upon the initial expansion, duration of persistence, absence of GvHD and also on the ability of the host immune system to reject these cells. When devising strategies for administering allogeneic CAR-T cells, different approaches to reduce the risk of GvHD (e.g., selection of T-cell subsets, use of virus-specific memory T cells or gene editing) could be implemented.

2.1 Genetically Modified αβ T Cells

In addition to the introduction of the "CAR-encoding cassette" most commonly delivered by lentiviral and gamma-retroviral vectors (44), we can distinguish two major types of T-cell genetic modifications to obtain allogeneic CAR-T cells with a reduced risk of GvHD and alloimmunization (**Figure 1**).

2.1.1 Disruption of TCRs

The first modification aimed to limit GvHD is the disruption of TCRs. This can be undertaken in three distinct ways: expression of the inhibitory protein(s); by knockout (KO) of the genes encoding TCR chains with site-specific nucleases such as transcription activator-like effector nucleases (TALENS) or clustered regularly interspaced short palindromic repeats/CRISPR associated protein 9 (CRISPR/Cas9); and by short hairpin (sh)RNA-mediated silencing of transcribed messenger (m)RNA.

For instance, the very first technology utilized to remove αβTCR expression was based on TALENs targeting the T cell

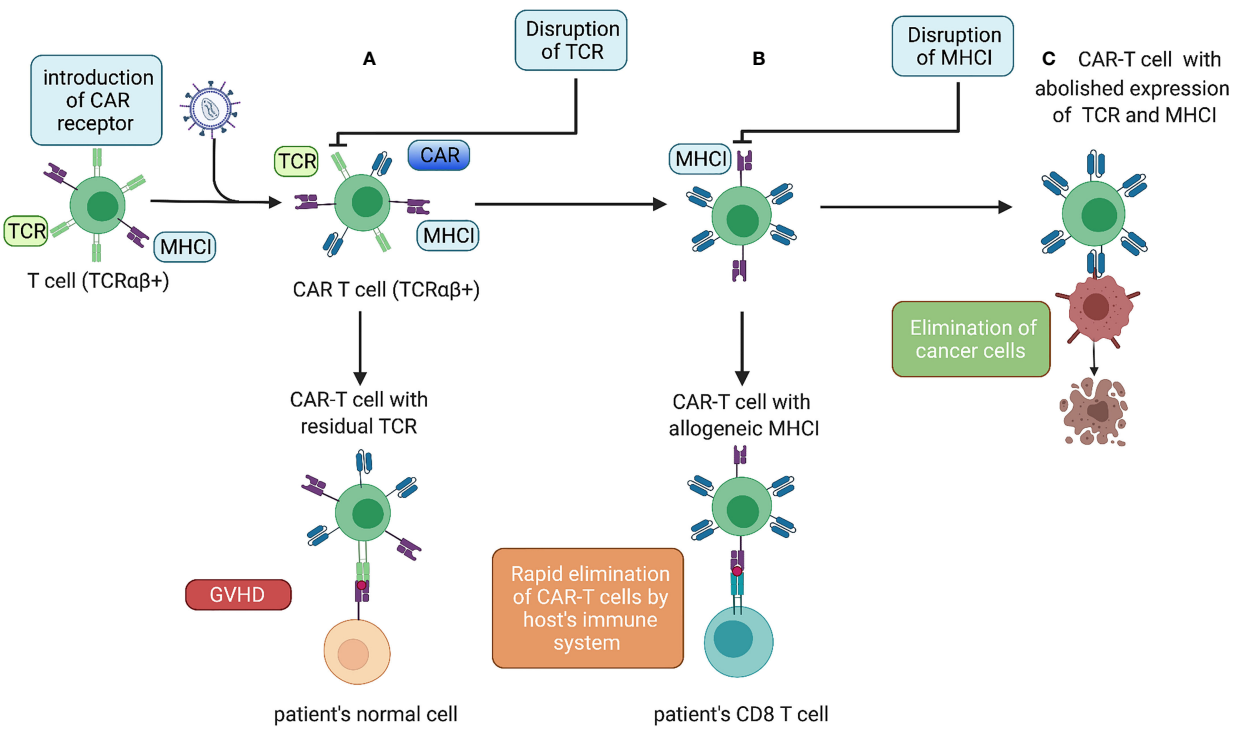

FIGURE 1 | Genetic modifications of allogeneic CAR-T cells. **(A)** Lentiviral transduction of allogeneic T cells with a CAR. Donor CAR-T cells with allogeneic TCRs administered to a patient causing GvHD. **(B)** After an additional gene-editing step to disrupt TCR expression, the cells do not cause GvHD but can be eliminated rapidly by the host immune system. **(C)** The next gene-editing step abolishes expression of MHC-I molecules, thereby ensuring the prolonged endurance and persistence of allogeneic CAR-T cells.

receptor alpha chain TRAC gene (**Figure 2A**), and efficiency of TCR elimination of 78% was recorded (45). The CRISPR/Cas9 efficiency of TCR KO was estimated to be 70% by Eyquem and colleagues (46). The use of zinc finger nucleases (ZFNs) to disrupt TCRs was first reported by Torikai and coworkers. Cells with anti-CD19 CAR were electroporated with ZFN mRNA targeting TCR alpha constant (*TRAC*) and *TRBC*, which abolished TCR signaling in 60 and 20% of cells, respectively (47). To generate their allogeneic CAR-T cell product PBCAR019 (particularly *via* insertion of the gene that encodes an anti-CD19 CAR into the *TRAC* locus), Precision BioSciences (Durham, NC, USA) used the ARCUS platform based on the engineered I-CreI homing endonuclease with the subsequent step of elimination of residual TCR+ cells. The engineered I-CreI homing endonuclease has shown 60% efficiency for TCR elimination previously (48).

Gilham and colleagues developed an approach leveraging a truncated dominant-negative CD3ζ protein (TIM). This protein acts as a competitive inhibitor to the component of TCR-CD3ζ, thereby interfering with TCR signaling (**Figure 2B**) and lowering the risk of GvHD (49). This approach was also used to disrupt TCRs in CYAD-101-CAR-T cells that target NKG2D. *In vivo* models assessing the efficiency of TCR inhibition showed a reduction in CD3-mediated stimulation and cytokine secretion in TIM-transduced T cells as well as no GvHD in mice in contrast with that in alloreactive control cells.

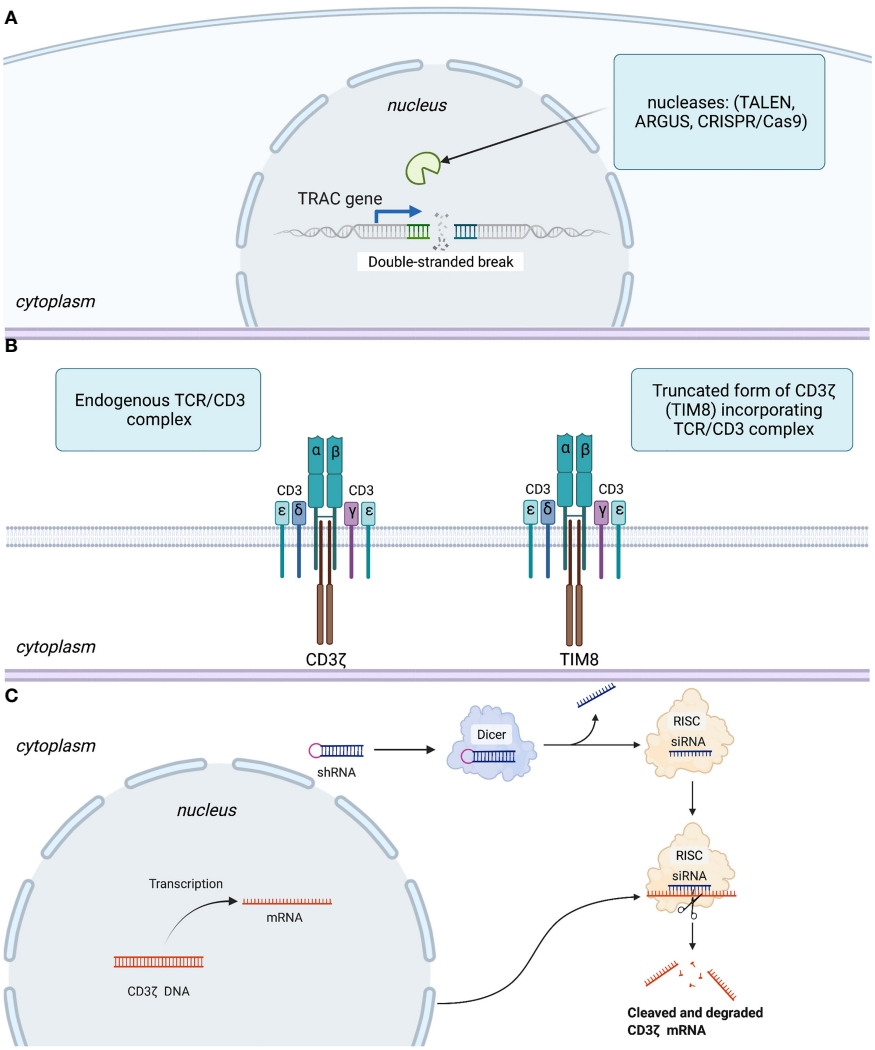

FIGURE 2 | Three basic strategies to disrupt expression or signaling of TCRs. **(A)** Abolishing TCR expression by introduction of a double-stranded break in *TRAC gene.* ***(B)*** Interfering with TCR signaling using a competitive inhibitor of CD3ζ-TIM8. **(C)** Leveraging an RNA interference regulatory mechanism to silence mRNA coding for the CD3ζ component of the TCR. More specifically, RNase III endonuclease (Dicer) cuts the loop of the introduced shRNA homologous to the target within the CD3ζ genome. Furthermore, a guide strand (siRNA) is incorporated in the RNA-induced silencing complex (RISC), with subsequent transcriptional silencing of the target gene.

2.1.2 Disruption of MHC-I Molecules

To increase the persistence of allogeneic CAR-T cells, the genetic abrogation of key mediators of immune rejection, MHC-I molecules (50), can be considered (**Figure 1**). This is best achieved by the disruption of a gene encoding β-microglobulin. Toricai et al. reported that transient expression of ZFNs specific for β-microglobulin resulted in the elimination of human leukocyte antigen (HLA)-A expression in ≤52% of the T-cell population (51). With a subsequent single round of depletion of HLA-A+ cells with antibody-coated paramagnetic beads, the fraction of HLA-A− cells increased up to 95%. Due to concern that cells without MHC-I molecules could be eliminated by host NK cells, Toricai et al. validated the approach to prevent NK cell-mediated cytotoxicity against MHC-I− allogeneic CAR-T cells. They ascertained that recognition by NK cells could be circumvented by enforced expression of HLA-E or HLA-G (51). Recently, it was shown that genetic abrogation of TCRs, as well as MHC-I (β2-microglobulin KO) and MHC-II (CIITA KO) molecules, ensured prolonged persistence of allogeneic CAR-T cells compared with that in cells with only TCR KO and MHC-I KO in a mouse model of cancer (52). Among allogeneic CAR-T cells products that include the disruption of the *β2m* locus alone with abrogation of TCR expression only CTX110 is at the clinical-trial stage (NCT04035434).

2.1.3 Depletion of αβTCR+ Cells

None of the approaches described above remove 100% TCRαβ from a cell population. Hence, additional depletion of residual TCRαβ+ cells is an essential part of the manufacture of allogeneic CAR-T cells which, to a large extent, determines the absence of GvHD and therapy efficacy. The most advanced approach for eliminating TCRαβ+ cells is based on the CliniMACS™ device, which is described in detail elsewhere (53). In short, after introducing the CAR and TCR elimination, T cells are incubated first with biotinylated anti-TCRαβ antibodies followed by incubation with an anti-biotin antibody conjugated to magnetic microbeads. Thereafter, residual TCR+ cells are depleted by CliniMACS. Schumm et al. reported a median 0.00097% of residual TCRαβ cells after depletion using CliniMACS (53). Qasim et al. determined 0.7% of cells with detectable cell-surface TCRs after magnetic bead-mediated depletion (54).

Alexandre et al. investigated whether the transient expression of CARs targeting CD3 *via* mRNA electroporation would result in depletion of residual TCRαβ+ cells (55). To accomplish this goal, the authors first electroporated mRNA that encoded a TALEN targeting *TRAC*, followed by electroporation of an anti-CD3 CAR 49 h later. They observed that the minimum residual CD3+ TCRαβ+ population was 0.25%, which is comparable with results (0.7%) obtained with magnetic bead-mediated depletion of residual TCRαβ+ cells (54).

2.1.4 Possible Genotoxicity of Gene-Editing Tools

If elucidating different approaches of genome editing, one should consider possible off-target events such as insertions, deletions, and chromosomal translocations (56). TALENs and ZFNs are dependent upon DNA–protein interactions, which are highly specific (57). In contrast, CRISPR/Cas9 is reliant on RNA–DNA interactions, which permit some mismatches, and therefore, lead to an increased risk of off-target events (58). However, Stadtmauer et al. reported chromosomal translocations and rearrangements after gene editing with CRISPR-Cas9 in a comparable percentage of cells (4%) as with gene editing using TALENs (59). They also mentioned that the efficiency and number of side effects using CRISPR/Cas9 correlated with a particular single guide (sg)RNA. Thus, optimization in preclinical evaluations *via* an accurate selection of suitable sgRNAs for gene targeting was possible. Hence, off-target events should be monitored *via* i*n silico* prediction with subsequent next-generation sequencing. Furthermore, we could speculate that, because the number of off-target events correlates with the number of gene edits, reducing the latter during the manufacture of CAR-T cells by insertion of a CAR directly into *TRAC* or gene silencing *via* shRNA could be essential to mitigate possible genotoxicity.

Stadtmauer et al. reported their experience with CRISPR/Cas9 to enhance antitumor activity in patients receiving autologous rather than allogeneic T cells engineered by lentiviral transduction to express cancer-specific (NY-ESO-1) TCRs (59). That report is interesting in terms of assessment of safety and possible genotoxicity. In particular, CRISPR/Cas9 was used to disrupt two genes encoding endogenous TCR chains (*TRAC* and *TRBC*), as well as programmed cell death protein 1. They reported chromosomal translocations and rearrangements (that declined *in vivo* and were at the limit of detection or not detected depending on the patient 30–170 days after infusion) in 4% of cells, which is similar to that employing genetic editing using TALENs (54). Off-target mutations were identified for *TRAC* sgRNA in chloride intracellular channel-2 (not expressed in T cells) and for *TRBC* sgRNA in transcriptional regulator ZNF609 and LINC00377 (long intergenic non-protein-coding RNA) (59). They mentioned more durable persistence of CRISPR-Cas9-edited T cells (up to 9 months) in contrast with cells that retained expression of the endogenous TCR and PD-1. A more recent single case of chromosomal abnormality was reported by Allogene Therapeutics (San Francisco, CA, USA) that was followed by a clinical hold of phase 2 ALLO-501A trial by the Food and Drug Administration (FDA) (60). The manufacturing process of these allogeneic CAR-T cells includes TALEN-mediated KO of TRAC and CD52 genes. As of October 7, 2021, the investigation is underway to clarify the potential relationship to gene editing and estimate the evidence of possible clonal expansion (60).

2.2 CAR-T Cells Based on Virus-Specific T Cells

Beyond genome-editing methods, one of the strategies to mitigate GvHD is to use CAR-T cells based on virus-specific T cells that combine the profound anti-tumor activity of the CAR and reduced risk of GvHD. GvHD risk corresponds to TCR diversity, therefore GvHD absence after infusion of virus-specific memory T cells is likely to be due to the restricted *repertoire* of TCRs in virus-specific memory T cells (61). For instance, the

peptide GLCTLVAML is one of the most immunogenic T cell targets derived from the Epstein–Barr virus (EBV). Hence, T cell subsets with TCRα and β chains that specifically recognize this antigen on MHC complexes could be used in allogeneic settings without additional gene-editing steps to disrupt TCR expression. One of the possible *caveats* of this strategy could be the initial low numbers of virus-specific memory T cells. In peripheral blood during latent infection with EBV, T cells specific for this peptide constitute 0.5–2.2% of total CD8+ T cells (62).

2.3 γδ T Cells

Donor-derived αβ T cells recognize antigen bound to MHC molecules. Donor-derived γδ T cells recognize multiple tumor antigens by utilizing their innate receptors in an MHC molecule independent manner, and could be applied in an allogeneic setting without TCR elimination. Moreover, upon activation, they can, in turn, exert a further adaptive immune response by facilitating the function of other immune cells. Rozenbaum et al. investigated the possible use of donor-derived γδ T cells as the carriers of the CAR for the production of allogeneic CAR-T cells (63). They hypothesized that, in addition to functioning across MHC molecule-barriers without causing GvHD, γδ T cells could overcome the major issue of therapy using CAR-T cells: the loss of antigen on cancer cells. They reported encouraging results showing that, in addition to *in vivo* activity against tumor CD19+ cells, γδ CAR-T cells utilizing various surface receptors exhibited *in vitro* activity against CD19− clones (63). The Vγ9Vδ2 T-cell subset prevailing among γδ-T cells constitutes 2–4% of T cells in peripheral blood. Efficient expansion of this cell subset has been devised (64, 65). A phase-I clinical trial in 132 patients with late-stage cancer showed the feasibility and clinical safety of allogeneic Vγ9Vδ2 T cells (65). Hence, γδ T cells could be candidates for cellular tumor immunotherapy for metastatic and progressive solid malignancies that can address the tumor microenvironment.

2.4 Induced Pluripotent Stem Cells (iPSCs) as a Source for Allogeneic CAR-T Cells

Another option validated by Themeli et al. relies on the production of CAR-T cells from iPSCs (66). Briefly, the authors generated iPSCs from peripheral-blood T lymphocytes by transduction with retroviral vectors encoding reprogramming factors. Thereafter, multiple iPSC clones were screened to select the clone that was subsequently transduced with a lentiviral vector encoding an anti-CD19 CAR. Upon differentiation into a T-lymphoid lineage, the authors detected TCRαβ+ cells harboring the same rearrangements in TCRβ and γ chains as in the parental clone. The CAR-T cells of this origin are generated from one clonal pluripotent cell line, so we can conclude that they are phenotypically defined. To better describe the phenotype of iPSC-derived CAR-T cells, the authors turned to microarray analysis of gene expression and uncovered that the CAR-T cells generated from iPSCs resembled those in peripheral-blood γδ T cells (66). The authors also pointed out lower levels of CAR expression and shorter survival in an immunodeficient xenograft mouse model than those in CAR-T cells derived from the TCRαβ subset in peripheral blood (66). By contrast, more recent *in vivo* results in a disseminated xenograft model of lymphoblastic leukemia of FT819 (an anti-CD19 CAR-T-cell product derived from a clonal engineered iPSC line by insertion of genes encoding for novel 1XX CAR into the *TRAC* locus) showed enhanced clearance of tumor as compared with that in control anti-CD19 cells (67). Signal transduction by TCRs is initiated by phosphorylation of conserved immunoreceptor tyrosine-based activation motifs (68), and strong activation of T cells can drive exhaustion (69). Feucht et al. investigated whether the impaired redundancy of CD28 and CD3ζ signaling enhanced the therapeutic properties of CAR-T cells. They estimated that mutation in the 1XX tyrosine residue that impedes phosphorylation and downstream signaling increases persistence and extends the effector function of T cells (70). TFT819 was generated from a single clonal line with the bi-allelic disruption of TCRs with a minimum likelihood of GvHD. Functional assessment of FT819 showed potent cytolytic activity against leukemia and lymphoma lines and the inability to produce GvHD (67). However, the efficacy of FT819 warrants further clinical investigation that is being initiated by Fate Therapeutics (La Jolla, CA, USA) for patients with relapsed/refractory (r/r) B-cell malignancies (71). Overall iPSCs derived from CAR-T cells, despite some limitations, hold the potential of uniform and mass-produced CAR-T cells.

2.5 NK-92 Cell Line

Given the success of therapies using CAR-T cells for hematological malignancies, many researchers have sought to develop CAR-engineered NK cells. In contrast to CAR-T cells, CAR-NK cells cause minimal CRS or ICANS in autologous settings (72). However, there are technical challenges to obtain them because NK cells represent only ~10% of lymphocytes. In addition, in autologous settings, the function of NK cells can be impaired in patients with malignant disorders. Specifically, tumors employ upregulation of inhibitory ligands such as MHC-I molecules (HLA-G, HLA-E, and HLA-ABC) (73). Similarly, an immunosuppressive cancer microenvironment comprising regulatory T cells and myeloid-derived suppressor cells could decrease expression of activating receptors such as NKG2D and enhance expression of inhibitory receptors (NKG2A), thereby restricting the cytotoxicity of NK cells (74). Furthermore, autologous NK cells are functionally silenced upon encountering a self-MHC antigen. Conversely, blood-derived NK cells can carry the risk of GvHD in allogeneic settings because they may contain contaminating T cells (75). In this context, a clonal immortalized cell line from a patient with NK-cell lymphoma (NK-92) that could be expanded in the presence of IL-2 appears as a valuable alternative.

There are three main reasons why CAR-expressing NK cell lines such as NK-92 are of interest as allogeneic effectors for cell therapy.

- All cells used in the preparation originate from a single cell, so their properties are strictly determined and there is no product heterogeneity. In this regard, standardization is also simplified;
- There are no restrictions on the scale of cell modification. For example, multiple sequential transductions or rounds of

genomic editing can be carried out to obtain a product with desired properties;
- NK-92 cells can be produced in any volume, up to multi-ton bioreactors, so this reduces (by several orders of magnitude) the cost of production significantly (76).

However, NK-92 are cancer cells, so they must be lethally irradiated before being injected into a patient to eliminate the chance of their engraftment or development of NK lymphoma. The latter, and the fact that the irradiated cells appear to be eliminated rapidly by the patient's immune system, raise serious concerns about the feasibility of using CAR-NK-92 cells (77).

3 TRANSLATION OF ALLOGENEIC CAR-T CELLS INTO CLINICAL USE

The sources of allogeneic CAR-T cells described above are summarized in **Table 1**. This section focuses on products pioneering the technology of allogeneic CAR-T cells in the clinic.

3.1 ALLO-715 Anti-BCMA CAR-T Cells (NCT04093596 Trial)

Allogene Therapeutics reported the results of a study on ALLO-715 anti-BCMA CAR-T cells. This was a phase-1 clinical trial (NCT04093596) in adults with r/r multiple myeloma who had ≥3 prior lines of therapy and were refractory to the last treatment line. As of October 2020, 31 patients had enrolled in the safety population. The efficacy population comprised 26 patients across four dosing levels of cells (40, 160, 320, and 480 × 106 CARs), with a median follow-up of 3.2 months (78). The CAR-T-cell receptor of ALLO-715 includes a single-chain variable anti-BCMA fragment with a 4-1BB costimulatory domain. To prevent graft rejection and allow for selective lymphodepletion without affecting ALLO-715 CAR-T cells, KOs of *CD52* and *TRAC* were introduced (79). Patients received lymphodepletion consisting of fludarabine plus cyclophosphamide and anti-CD52 antibody ALLO-647 in a set of different dosing regimens (**Table 2**). The overall response rate (ORR) across all dosing cohorts and lymphodepletion regimens among 26 patients evaluated for efficacy was 42% (11 patients) (78). The superior anti-cancer activity was observed among the 10 patients treated with 320 × 106 cells (dose level 3) of ALLO-715. For this cohort, the ORR was 60% (6/10 cases), which included a very good partial-plus response in four patients (40%).

CRS was reported in 45% (14/31) patients. One grade-5 episode in a patient who developed non-neutropenic fever and multifocal pneumonia one day after ALLO-715 infusion led to respiratory failure and death. The authors considered this episode to be related to progressive myeloma and the conditioning regimen with cyclophosphamide and ALLO-647 (79). The authors reported that infectious diseases developed during therapy in 42% (13/31) patients, including grade 3 infections in 13% of patients. Cases of GvHD or ICANS were not observed (**Table 3**).

3.2 ALLO-501 Anti-CD19 CAR-T Cells (NCT03939026 Trial)

According to a recent report, ALLO-501 (Allogene Therapeutics) showed positive results in a trial (NCT03939026) for patients with relapsed/refractory non-Hodgkin lymphoma (r/r NHL) who had ≥3 prior lines of therapy (82). As of April 19, 2021, 41 patients had received ALLO-501, 41 patients had enrolled in the safety population and the efficacy population included 32 patients across three dosing levels of cells (40, 120 and 360 × 106 CARs). The ALLO-501 CAR-T receptor is based on murine CD19 specific (4G7) scFv. In addition, TALEN-mediated KO of TRAC and CD52 genes were introduced.

Therapy comprised prior lymphodepletion including fludarabine plus cyclophosphamide (**Table 2**) with ALLO-647 and infusion of ALLO-501 CAR-T cells. The ORR was 75% (24/32 patients), with 50% (16/32) cases having a complete response (CR).

The authors reported mild-to-moderate CRS in 11 (27%) patients, one (2%) case of grade-3 neurotoxicity, and no GvHD among enrolled patients. The prevalence of infection was 61%

TABLE 1 | Allogeneic CAR-T cells sources.

CAR-T cells source	Therapy target	Necessity of gene editing
1. αβ T cells subsets	PBCAR0191 (CD19)	Insertion of CD19- specific CAR into the TRAC locus using versatile genome editing 785 platform ARGUS
	ALLO-715 (CD19)	TALEN-mediated CD52 and TRAC gene knockout
	ALLO-715 (BCMA)	TALEN-mediated CD52 and TRAC gene knockout
	UCART19 (CD19)	TALEN-mediated CD52 and TRAC gene knockout
	CTX110 (CD19)	CRISPR/Cas9 mediated insertion of CD19 CAR into TRAC locus and disruption of the *β2m* locus
	CYAD-101 (NKGD2D)	Gene editing of TCR is not needed due signaling inhibition (TIM)
	CYAD-211 (BCMA)	shRNA-mediated silencing of TCR signal is used
2. γδ T-cells subset	Kiromic announces submission of applications for PD1 γδ T cells CAR-T cell Therapy with the FDA	Gene editing or TCR is not needed due the absence of αβTCR
3. Virus specific memory T cells	ATA3219 (CD19)	Gene editing of TCR is not needed due restricted repertoire
4. Induced pluripotent stem cells	FT819 (CD19)	CAR targeting CD19 inserted into the TRAC locus *via* CRISPR/Cas9

TABLE 2 | Conditioning regimes administered in clinical trials of autologous and allogeneic CAR-T products.

Product and corresponding clinical trial	Conditioning regimen
501 ALPHA (ALLO-501)	Fludarabine 30 mg/m^2/day and cyclophosphamide 300 mg/m^2/day given on 3 days with ALLO-647 (from 13 to 30 mg daily given for 3 days). The starting of lymphodepletion 5 days before the infusion ALLO-501.
UNIVERSAL (ALLO-715)	Fludarabine 30 mg/m^2/day and cyclophosphamide 300 mg/m2/day given on the fifth, fourth, and third days before infusion ALLO-715 with ALLO-647 (13–30 mg × 3 days) or cyclophosphamide (300 mg/m^2/day) given on the fifth, fourth, and third days before infusion ALLO-715 with ALLO-647 (13–30 mg × 3 days).
CARBON (CTX)	Fludarabine 30 mg/m^2 and cyclophosphamide 500 mg/m^2 given daily on the third, second, and first days before infusion CTX110. Infusion of CTX110 after completion of lymphodepleting chemotherapy.
PBCAR0191 (PBCAR0191)	Fludarabine 30 mg/m^2/day and cyclophosphamide 500 mg/m^2/day given on 3 days or fludarabine 30 mg/m^2/day for 4 days and cyclophosphamide 1,000 mg/m^2/day for 3 days. Infusion of PBCAR0191 after completion of lymphodepleting chemotherapy.
CARCIK (CARCIK—CD19)	Fludarabine 30 mg/m^2/day × 4 days and cyclophosphamide 500 mg/m^2/day × 2 days starting with the first dose of fludarabine. Infusion of CARCIK—CD19 from 2 to 14 days after completion of lymphodepleting chemotherapy.
PALL (UCART19)	Combining cyclophosphamide 60 mg/kg/day for 2 days, fludarabine 30 mg/m^2/day for 5 days and alemtuzumab 0.2 mg/kg/day for 5 days starts during the week preceding UCART19 infusion (from Days 7 to 1).
CALM (UCART19)	Combining cyclophosphamide (1,500 mg/m^2) and fludarabine (90 mg/m^2) without (FC) or with alemtuzumab (FCA) (1 mg/kg) was administered one week before UCART19 infusion.
ELIANA (KYMRIAH): Pediatric and Young Adult Relapsed or Refractory (r/r) B cell Acute Lymphoblastic Leukemia (ALL):	Fludarabine 30 mg/m^2 IV daily for 4 days and cyclophosphamide 500 mg/m^2 IV daily for 2 days starting with the first dose of fludarabine.
ELIANA (KYMRIAH): Adult Relapsed or Refractory (r/r) Diffuse Large B cell lymphoma (DLBCL)	Fludarabine 25 mg/m^2 daily for 3 days and cyclophosphamide 250 mg/m^2 IV daily for 3 days starting with the first dose of fludarabine. Infuse KYMRIAH from 2 to 14 days after completion of the lymphodepleting chemotherapy.
ZUMA-5 (Yescarta)	Fludarabine 30 mg/m^2/day and cyclophosphamide 500 mg/m^2/day given on the fifth, fourth, and third days before infusion YESCARTA
TRANSCEND NHL 001 (BREYANZI; lisocabtagene maraleucel; liso-cel)	Fludarabine 30 mg/m^2/day and cyclophosphamide 300 mg/m^2/day for 3 days. Infuse BREYANZI from 2 to 7 days after completion of lymphodepleting chemotherapy.
ZUMA-2 (TECARTUS; Brexucabtagene Autoleucel; KTEX19): Mantle Cell Lymphoma.	Fludarabine 30 mg/m^2 daily for 3 days, and cyclophosphamide 500 mg/m^2 daily for 3 days.
ZUMA-2 (TECARTUS; Brexucabtagene Autoleucel; KTEX19): Acute lymphoblastic leukemia.	Fludarabine 25 mg/m^2 iv on the fourth, third, and second days and cyclophosphamide 900 mg/m^2 on the second day before infusion of TECARTUS.

TRANSCEND NHL 001 clinical trial (80), ZUMA-2 clinical trial (81), ELIANA clinical trial (10), ZUMA-5 clinical trial (22).

(25/41 cases), which was similar to the prevalence observed in trials using autologous CAR-T cells (82).

3.3 UCART19 Anti-CD19 CAR-T Cells (PALL and CALM Trials)

Another CAR-T cell product based on lentiviral transduction of CAR19 and the use of TRAC/CD52 specific TALENs is UCART19 (54). TALENs are used to introduce KOs in genes encoding the α constant chain of TCRs and CD52 to minimize GvHD risk and to confer resistance to the anti-CD52 monoclonal antibody alemtuzumab (54). Residual TCR+ cells were removed by magnetic beads [CliniMACS (53)] and only 0.7% of cells had detectable cell-surface TCRs. The vector also incorporates a 2A peptide-linked sort/suicide gene (RQR8), which includes CD34 and CD20 epitopes for cell enrichment, and rituximab is used for *in vivo* depletion in case of adverse effects (83). Unexpectedly, RQR8 expression was further detected by flow cytometry in only 19.9% of cells, despite linked transcription and translation through a self-cleaving 2A peptide configuration of RQR8 with highly expressed (85% of cells) CAR19 (54). More than 64% of cells also exhibited a CD52− phenotype. The authors revealed a high representation of the CD8-phenotype subset together with "naive-like" phenotypes. If using gene-editing nucleases such as TALENs, one should consider possible off-target events (nonhomologous end-joining, insertions, deletions). Using next-generation sequencing, the authors detected <0.18% off-target events at 15 *in silico*-predicted off-target TALEN sites.

The efficacy of therapy with UCART19 was first evaluated in two infants with relapsed B cell acute lymphoblastic leukemia. The complete protocol of this therapy is described elsewhere (54). Summing up, before UCART19 infusion, lymphodepletion (fludarabine, cyclophosphamide, and alemtuzumab) was administered (54). The authors reported no infusion-related toxicities and no evidence of CRS. Grade 2 skin GvHD was observed by histology in one patient at 9 weeks and resolved after corticosteroids treatment. Finally, to correct aplasia and accelerate reconstitution, the TCRαβ-depleted allograft from the original mismatched unrelated donor was administered. Patients were in complete remission after eradication of UCART19 and transplantation.

The safety and efficacy of UCART19 were further evaluated in the PALL trial in seven children and in the CALM trial in 14 adults. Patients had to have evidence of CD19+ B cell acute lymphoblastic leukemia with >5% blasts in bone marrow or a minimal residual

TABLE 3 | Efficacy and adverse events associated with allogeneic and autologous CAR T cell therapy.

Product	Allogenic CAR-T						Autologous CAR-T	
	ALLO-715	**ALLO-501**	**UCART19**	**CTX110**	**PBCAR0191**	**CARCIKCD19**	**Kymriah**	**Yescarta**
Clinical trial	UNIVERS AL (NCT04093596)	ALLO-501 ALPHA NCT03939026	CALM/PALL NCT02746952/ NCT02808442	CARBON NCT04035434	PBCAR0191 NCT036660 00	CARCIK NCT03389035	ELIANA NCT02435849	ZUMA-5 NCT03105336
Number of patients that received CAR-T	31 patients	41 patients	21 patients	11 patients	27 patients	13 patients	75 patients	146 patients
Disease	Relapsed/ Refractory Multiple Myeloma	Relapsed/Refractory large B cell lymphoma and follicular lymphoma	Refractory or relapsed B cell ALL	Refractory or relapsed non-Hodgkin lymphoma Refractory or relapsed B cell ALL	Refractory or relapsed non-Hodgkin lymphoma Refractory or relapsed B cell ALL	Relapsed or refractory adult and pediatric B cell precursor ALL after HSCT	Refractor y or relapsed B cell ALL	Relapsed or Refractor y large B-cell lymphoma
ECOG	0–1	0–1	<2	0–1	0–1	N/D	N/D	0–1
Adverse Events of Interest, pts	31	41	21	11	27	13	75	146
CRS	Gr 1–2: 14 (45%) ≥Gr 3 absent	Gr 1–2: 11 (27%) ≥Gr 3 absent	Gr 1–2 16 (76%) ≥3 Gr 3 3(16%)	Gr 1–2: Gr 3 absent	≥3 Gr absent	Gr 1–2: 3 (23%) ≥Gr 3 absent	Gr 1–2: 23 (31%) ≥Gr 3:35 (46%)	119/146 (81,5%) ≥Gr 3:7%
ICANS	absent	Gr 3 1(2%)	Gr 1–2: 8 (38%) ≥Gr3 absent	Gr 1–2: 1 (9%)	≥ Gr 3 single case	absent	Gr 1–2: 20 (27%) Gr3: 10 (13%)	87/146 (59,6%) including ≥Gr3: 19%
Infections	13 (42%)	25 (61%)	13 (62%)	3 (27%)	4/18 (22%) NHL	4(30%)	32 (43%)	16%
GvHD	absent	absent	2 (10%) Skin 1Gr	absent	absent	absent	–	–
Efficacy, pts	26	32	21	11	27	13	75	104
*ORR, n (%)	11(42%)	24 (75%)	–	4 (36%)	15 (55%)	–	81%	92%
*CR, n (%)	–	16 (50%)	14(67%) 82% (AL)	4 (36%)	10 (37%) 75% (IL)	8 (61.5%)	60%	76%

**ORR and CR is shown for patients among all dosing cohorts and lymphodepletion regimes according to recently published results of allogeneic CAR-T cells trials described above and results of clinical trials of autologous products Kymriah (10) and Yescarta (22).*

AL, patients with alemtuzumab-containing lymphodepletion.

IL, (patients with relapsed or refractory non-Hodgkin lymphoma who received enhanced lymphodepletion regimen).

ND, not detected.

disease of 1×10^{-3} cells as assessed by flow cytometry or quantitative polymerase chain reaction. Before UCART19 infusion, all the patients underwent lymphodepletion: 17 patients (81%) with fludarabine, cyclophosphamide, and alemtuzumab, and four (19%) with fludarabine and cyclophosphamide (**Table 2**).

Children in the PALL trial received UCART19 ($1.1–2.3 \times 10^6$ per kg) and the CALM trial included a dose-escalating phase (6×10^6 cells, $6–8 \times 10^7$ cells, or $1.8–2.4 \times 10^8$ cells) (84). The ORR was 67% (14/21) and 82% (14/17) for patients receiving alemtuzumab-containing lymphodepletion (84). Ten (71%) of the 14 patients achieved a complete response (CR) and proceeded to allogeneic hematopoietic stem cell transplantation (HSCT). The authors reported that, at the data cutoff of August 2019, 10 (71%) of the 14 patients who achieved a CR or CR with incomplete hematologic recovery (including patients who underwent SCT) had subsequently relapsed or died. Progression free survival at 6 months was 27% (95%CI 10–47). All but one of these relapsing patients were CD19+.

The adverse effects observed with UCART19 seem similar to those reported for autologous antiCD19 CAR-T cells. CRS was the most common adverse event associated with the UCART19 treatment (91% of patients). CRS of grade ≥3 was documented in three patients. Other adverse events were neurotoxicity of grade 1 in seven patients and grade 2 in one patient that lasted at a median duration of 3 days and did not require specific treatment. Only two patients (10%) developed grade 1 GvHD after UCART19 infusion. One death in the CALM trial reported as the dose-limiting toxicity

of UCART19 was caused by neutropenic sepsis with grade 3 CRS, and the other death was caused by pulmonary hemorrhage occurring in the context of infection and grade 4 cytopenia. Although, reactivation of infection by cytomegalovirus, adenovirus and EBV was observed particularly in patients receiving high doses of alemtuzumab (anti-CD52 monoclonal antibody), omitting alemtuzumab abolished UCART19 expansion. Therefore, subsequently, the dose of alemtuzumab was reduced to prevent severe viral infections and enable UCART19 expansion.

Benjamin and colleagues (84) stated that grade 4 cytopenia in 32% of patients during therapy was probably associated with an intensive lymphodepletion regimen required to overcome HLA barriers (alemtuzumab in combination with fludarabine and cyclophosphamide). Of note, 3–6% of TALENedited UCART19 cells used in the trials had translocation-associated karyotype abnormalities with yet unrevealed adverse effects (84). Despite initial concern, residual infused TCR+ cells after expansion did not cause transfusion-associated GvHD during the CALM and PALL trials. Both could have been due to ablation of residual UCART19 cells before allogeneic HSCT (84).

3.4 CTX110 Anti-CD19 CAR-T Cells (NCT04035434 Trial)

UCART19 and other CAR-T cells use randomly integrating viruses to deliver genes encoding CAR constructs to T cell DNA. CRISPR Therapeutics (Cambridge, MA, USA) inserted a CAR construct precisely into the *TRAC* locus using CRISPR/Cas9. Hence, TCR KO and the introduction of the CAR are achieved in one step. CRISPR/Cas9 is also used to disrupt the *β2m* locus, thus eliminating the expression of MHC-1 molecules.

The results from CRISPR Therapeutics' ongoing phase-1 CARBON trial (NCT04035434) evaluating the safety and efficacy of CTX110 in 11 patients with r/r NHL who had ≥2 prior lines of treatment have been announced. CTX110 targets CD19+ B-cell malignancies. Eleven patients were infused with CTX110 cells at four dose levels (30, 100, 300 or 600 × 10^6) after lymphodepletion consisting of fludarabine and cyclophosphamide (**Table 2**). Among the patients who received 30–300 × 10^6 CTX110 cells, the authors reported no cases of GvHD despite a high HLA mismatch between donors and patients, three cases of grade ≤2 CRS (30%) and one case of grade 2 ICANS (10%) (85). A patient who received 600 × 10^6 CTX110 cells experienced grade 2 CRS, febrile neutropenia, and developed short-term memory loss and confusion (which later progressed to significant obtundation), reactivation of HHV-6 (Human Herpes Virus), and HHV-6 encephalitis (85). A complete response was achieved in 36% (four) of patients at 100, 300, and 600 × 106 CTX110 cells. At 300 × 106 CTX110 cells, two out of four patients had a complete response (85).

3.5 PBCAR0191 Anti-CD19 CAR-T Cells (NCT03666000 Trial)

Precision BioSciences makes the allogeneic product PBCAR0191. It is created by the insertion of a CD19-specific CAR into the *TRAC* locus using the versatile genome-editing platform ARCUS, which is based on I-CreI homing endonuclease (86). Then, cells undergo a D3 elimination step, followed by expansion and freezing (87). Preliminary data are from the phase-I study of PBCAR0191 cells from 27 patients (16 with r/r NHL, 11 with r/r B-cell acute lymphoblastic leukemia) who had ≥2 previous lines of treatment (88). PBCAR0191 treatment was undertaken at dose level 1 (3 × 105 cells), dose level 2 (1 × 10^6 cells), dose level 3 (3 × 10^6 cells), and a split dose level 4 (two doses at 3 × 10^6 cells employed after standard lymphodepletion consisting of fludarabine plus cyclophosphamide). PBCAR0191 was also dosed in an enhanced lymphodepletion regimen consisting of PBCAR0191 at dose level 3 (3 × 10^6 cells) or dose level 4 (two doses at 3 × 10^6 cells plus fludarabine (30 mg/m2/day for 4 days) and cyclophosphamide (1,000 mg/m^2/day for 3 days).

The ORR and complete response across all dosing cohorts and lymphodepletion regimens was 55% (15/27 cases) and 37% (10/27 cases), respectively. The authors reported an 83% ORR at day-28 or later for patients with NHL or B-cell acute lymphoblastic leukemia who received PBCAR0191 when coupled with enhanced lymphodepletion. On day-28 or later, 75% of patients with r/r NHL who received PBCAR0191 with enhanced lymphodepletion achieved a complete response, versus only 33% across dose level 2 (1 × 10^6) and dose level 3 (3 × 10^6 cells) using standard lymphodepletion (88). Hirayama et al. sought to identify the biomarkers associated with a complete response and progression-free survival in patients with aggressive B cell NHL after autologous anti-CD19 CAR-T cell therapy. Patients receiving high-intensity lymphodepletion had a higher probability of achieving a favorable cytokine profile (IL-7 and serum monocyte chemoattractant protein-1) that correlated with a better complete response and progression-free survival compared with that in patients receiving low-intensity lymphodepletion (89).

More recently, Shah et al. (90) published clinical trial results concerning patients cohort to whom the PBCAR0191 was dosed at level 3 (3 × 10^6 cells) and coupled with enhanced lymphodepletion (fludarabine 30 mg/m^2/day × 4 days plus cyclophosphamide 1,000 mg/m^2/day × 3 days). Twenty one patients were enrolled, including 16 patients with NHL and 5 patients with B-ALL with measurable CD19+ R/R B-ALL or NHL disease after two or more prior treatment regimens. The authors reported profoundly improved PBCAR0191 kinetics compared to patients to whom standard lymphodepletion was administered. The treatment efficiency was assessed in 13 patients with NHL and in 5 subjects with ALL. The overall response was 83% (15/18) patients, including 85% (11/13) patients with NHL and 80% (4/5) ALL subjects, with 50% (12/18) cases having a complete response (CR/CRi) including 62% (8/13) patients with NHL and 80% (4/5) ALL subjects. Most adverse events were mild. The authors reported that ICANS Grade 3 was observed in one patient with NHL, grade 3 infections observed in 31% (5/16) patients with NHL, and 80% (4/5) patients with B-ALL. No evidence of GvHD was observed.

3.6 CYAD-101 (CYAD-211 Trials)

Celyad Oncology manufactures CYAD-101. This product combines a human full-length NKG2D receptor that binds eight different ligands expressed by cancer cells of different origins in an MHC molecule-independent fashion (91) and a TCR inhibitory peptide that interferes with signaling by the endogenous TCR. CYAD-101 was evaluated in the alloSHRINK phase-I study in patients with

unresectable metastatic colorectal cancer (NCT03692429). After standard preconditioning chemotherapy (FOLFOX), 15 patients received one of three dose levels (1×10^8, 3×10^8 or 1×10^9 cells per infusion). The authors reported no dose-limiting toxicity or GvHD. CYAD-101 at 1×10^9 cells per injection post-FOLFOX chemotherapy was used. Out of 15 patients, two (13%) patients achieved a partial response and nine (60%) cases had stable disease (92).

In parallel, Celyad Oncology investigated (93) another approach to prevent GvHD by leveraging shRNA to silence the mRNA coding for the CD3ζ component of the TCR (**Figure 2C**). In particular, their new product, CYAD-211, which is designed to express anti-BCMA CAR and shRNA interfering with CD3ζ expression, is being evaluated in the phase-I IMMUNICY-1 trial (NCT04613557) for the treatment of patients with r/r multiple myeloma. The authors pointed out a high percentage of shRNA-CD3ζ knockdown comparable with that using CRISPRs targeting CD3ζ to inhibit TCR expression.

3.7 Cytokine-Induced Killer (CIK) Anti-CD19 Cells (NCT03389035 Trial)

Magnani et al. proposed a nonviral engineering of allogeneic CAR-T cells based on a "Sleeping Beauty" transposon system to produce CIK cells with CARs (94). According to the CIK-cell protocol, cells were stimulated to differentiate to a subpopulation of memory T cells (95). Cells were derived from four matched unrelated donors, six haploidentical donors and three siblings with identical HLAs. During multicenter clinical studies (NCT03389035), CARCIK-CD19 cells were administered to 13 patients with B cell acute lymphoblastic leukemia who had relapsed after HSCT. The authors reported no cases of ICANS or GvHD even in patients who experienced GvHD after initial HSCT (**Table 3**). The only severe adverse events were two cases of grade 1 and grade 2 CRS in patients receiving the highest dose. A complete response was noted in 61.5% of patients whereas, among the six patients receiving the two highest doses, a complete response was noted in 85.7% of cases. The authors pointed out that the absence of manageable GvHD after the infusion of CIK cells was associated with the acquisition of MHC molecule-independent NK-like cytotoxicity during stimulation with interferon-γ, CD3, and differentiation in the presence of IL-2 (96). The insertions of Sleeping Beauty did not appear to trigger clonal dominance, while in rare cases, the insertion of *CAR* with a lentiviral vector might alter T-cell regulatory pathways due to preferable integration into highly expressed genes triggering clonal expansion [e.g., vector insertion within the CBL oncogene (97) and disruption of the TET2 allele (98)].

3.8 ATA188 and the NCT03283826 Trial

Prockop et al. revealed that EBV-targeted T cells demonstrated a favorable safety and limited risks of GvHD or CRS in 46 recipients with rituximab-refractory EBV-associated lymphoma (99). Curran et al. reported a complete response in 70% (7/10 patients with r/r B-cell malignancies) and an absence of ICANS, CRS, or GvHD above grade 2 after treatment with a CD19-specific CAR developed by transducing EBV-specific donor cells (100).

Preliminary results utilizing EBV-specific subsets of T cells were demonstrated by Atara Biotherapeutics in a phase-I trial using ATA188 (NCT03283826). GvHD or CRS after the infusion of ATA188 cells was not documented. The authors reported that ATA188 was well-tolerated in patients with progressive multiple sclerosis, and dose-limiting toxicities were not reported. ATA188 was manufactured from lymphocytes specific for the EBV antigens of an unrelated (but partially HLA-matched) donor. Atara Biotherapeutics also developed EBV-specific T cells with a CAR targeting CD19. Their product (Allo-EBV-CD19-CAR-T) expresses an anti-CD19 CAR and maintains the expression of the native EBV TCR (101). Allo-EBV-CD19-CAR-T demonstrates a robust killing of antigen+ cells, antigen-specific proliferation in the presence of EBV and CD19+ cells, an enriched central memory phenotype (with higher frequency expression of CD62L, CCR7, and CD45RO), and provides a framework for developing next-generation allogeneic CAR-T cells: ATA3219.

3.9 Vγ9Vδ2 T Cells

Xu et al. published the results of the clinical trials of allogeneic Vγ9Vδ2 T-cell therapy for 132 patients with late-stage malignant liver ((NCT03183232), lung (NCT03183219), pancreatic (NCT03183206) or breast (NCT03180437) cancer. The details of the protocol and results are described elsewhere (65). Significant adverse events (CRS, GvHD) were not reported after infusion of allogeneic Vγ9Vδ2 T cells.

3.10 NK Cells

NK cells are candidates for engineering allogeneic CAR-NK cells for cancer treatment. Liu et al. reported the results of phase-I and -II trials in which HLA-mismatched anti-CD19 CAR-NK cells derived from cord blood were administered to 11 patients with r/r NHL or chronic lymphocytic leukemia (102). NK cells were transduced with a retroviral vector encoding an anti-CD19 CAR, IL-15 and inducible caspase 9 (to trigger apoptosis of CAR-NK cells in case of unacceptable toxic effects). The authors reported a median of 0.01% contaminating CD3+ T cells in the final product and the absence of CRS, ICANS, and GvHD (102). The authors mentioned stable levels of the proinflammatory cytokines IL-6, interferon-γ, and TNF. All patients had reversible hematologic toxic events, mainly associated with lymphodepletion. At a median follow-up of 13.8 months, seven patients (64%) had a complete response.

In the sole completed CAR-NK-92 trial (CD33-specific for patients with acute myeloid leukemia), cells were injected thrice at doses 3×10^8, 6×10^8 and 1×10^9 cells on days 1, 3, and 5, respectively (103). Of the three patients in the trials, two patients experienced mild pyrexia and one episode of pyrexia up to 40°C that resolved in 2 days. Tang et al. (103) reported only two cases of grade-I CRS and no cases of GvHD after the infusion of CD33-CAR NK-92 cells. Hence, CAR NK-92 cells (at least with this particular CAR) were as safe as the unmodified parental NK-92 cell line (104). Unfortunately, two patients relapsed and one had no response to treatment. CAR-T-cell therapy in patients with acute myeloid leukemia remains challenging because antigens (e.g., CD123) used as a target for CAR-T cells are also expressed

in normal hematopoietic stem cells and myeloid cells, which can cause severe CRS, neurotoxicity and off-target events (105, 106). Therefore, in terms of side effects, NK-92 cells as CAR carriers appear to be safe, but cases of a complete response after their injection have not been described.

4 DISCUSSION

Presently, all FDA-approved CAR-T cell therapies are based on the autologous T cells isolated from the patient. Clearly, the use of a CAR-T cell product derived from a healthy donor appears advantageous, given that it would be less dependent on the immune status of the patient, be more standardized and greatly expand the patient access to the therapy due to lower production costs. It must also be taken into account that upon rapid disease progression the time required for autologous CAR-T cell manufacturing becomes a critical factor. During this time, tumor burden increases which may translate into a lower survival rate. Furthermore, a fraction of patients may ultimately never receive the autologous CAR-T cell product of decent quality and therapeutically meaningful quantity. In contrast, allogeneic

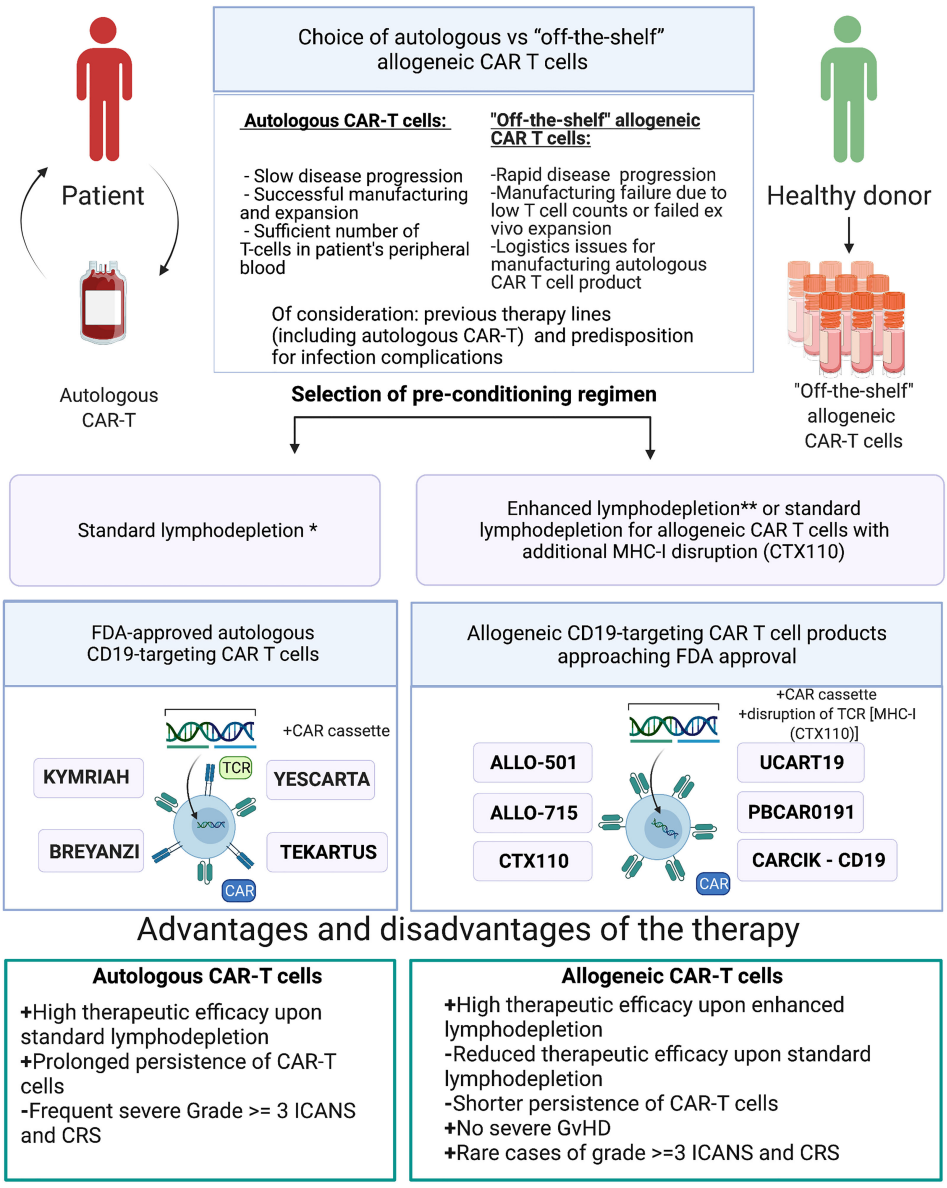

FIGURE 3 | Choice of either autologous or allogeneic CAR-T cell therapy. *Standard lymphodepletion—conditioning regimen in which intermediate doses of chemotherapy drugs are applied. **Enhanced lymphodepletion—conditioning regimen in which high doses of chemotherapy drugs and/or additional biologic medications (monoclonal antibody, including allo-647) are applied.

CAR-T cells produced from healthy donors may display significantly better cellular fitness at the time of infusion, and by default, such CAR-T cell products would be free of contaminating tumor cells, unlike in the autologous format. In this regard, similarly to BiTEs (107), allogeneic CAR-T cell products are "off-the-shelf" and combine the advantages of both platforms. Nonetheless, these formats are not exactly interchangeable, and each of them has its own niche. Depending on the clinical presentation, BiTEs, autologous CAR-T, and allogeneic CAR-T cell products can be successfully used consecutively and even target the same antigen.

There are several scenarios when allogeneic CAR-T cells can and should be used in place of or in combination with the autologous CAR-T cells: i) logistics issues preventing the manufacturing of the autologous product; ii) manufacturing failure, wherein the allogeneic product may substitute the autologous one without delaying the scheduled infusion; iii) infusion of the allogeneic CAR-T cell product when the autologous product fails to expand in the patient; iv) autologous CAR-T cell product cannot be manufactured upfront due to low T cell numbers in the patient and/or rapidly progressing disease; v) allogeneic CAR-T cell product serves as a bridge to hematopoietic stem cell transplantation by design; and vi) dose-adjusted infusion of allogeneic CAR-T cells with a low chance of engraftment to achieve progressive tumor de-bulking, thereby reducing the chance and magnitude of adverse side effects by the time of infusion of autologous CAR T cell product (**Figure 3**).

Allogeneic CAR-T cells may cause GvHD and may themselves be rejected by the immune system of the recipient. The frequency of such adverse effects is associated with the fine details of the manufacturing protocols and the procedures of how such cells are rendered universal to avoid allorejection. One avenue to avoid destruction of the allogeneic CAR-T cell product is to induce immunosuppression in the patient, but this must be finely balanced and closely monitored to reduce the risk of life-threatening infections. In most clinical trials of allogeneic CAR-T cells, GvHD never progressed beyond stage I, and only skin involvement was observed (**Table 3**). Therefore, we arrived into the conclusion that gene editing and subsequent cell-processing steps (depletion of TCR+ cells using magnetic beads) enable nearly complete elimination of residual TCRαβ+ cells (<1%) below the thresholds that might cause clinically significant GvHD. Therapy toxicity evaluation of the reviewed allogeneic CAR-T clinical trials revealed single cases of severe (≥3 grade) CRS and ICANS (**Table 3**), while more frequent development of severe (≥3 grade) CRS and ICANS was observed in patients who received autologous CAR-T therapy (clinical trials ELIANA, ZUMA-5). Higher doses of allogenic CAR-T cells and/or enhanced lymphodepletion were associated with higher efficacy of allogeneic CAR-T cells comparable with efficacy of autologous products (**Tables 2**, **3**). Under standard lymphodepletion, allogeneic CAR T cells had inferior efficacy and response rates compared to the autologous CAR-T cells, which is largely attributable to their lower persistence. This can be viewed as a surmountable issue. Furthermore, this can be considered as a safety advantage in the long run, particularly in the context of CAR T cells targeting the molecules present on the healthy tissues and organs. In fact, multiple autologous CAR T cell infusions have similarly been reported (e.g., NKG2D-CAR) as a means to counteract relatively short persistence. Finally, in the absence of contraindications enhancing the lymphodepletion regimen prior to CAR T cell infusion may ultimately obviate the need for such multiple infusions.

The limitation of this review is that data concerning clinical trials of ALLO-715, ALLO-501, CTX110, and PBCAR0191 are based on press releases, published by the corresponding companies. Notwithstanding this limitation, all studies showed the feasibility of administering allogeneic CAR-T cells and provide a path for more widespread and efficacious anticancer therapy.

AUTHOR CONTRIBUTIONS

All authors listed have made a substantial, direct, and intellectual contribution to the work and approved it for publication.

FUNDING

This work was financially supported by the Ministry of Science and Higher Education of the Russian Federation (075-15-2020-901).

REFERENCES

1. Caldwell KJ, Gottschalk S, Talleur AC. Allogeneic CAR Cell Therapy—More Than a Pipe Dream. *Front Immunol* (2021) 11(3466). doi: 10.3389/fimmu.2020.618427
2. Hartmann J, Schüßler-Lenz M, Bondanza A, Buchholz CJ. Clinical Development of CAR T Cells-Challenges and Opportunities in Translating Innovative Treatment Concepts. *EMBO Mol Med* (2017) 9 (9):1183–97. doi: 10.15252/emmm.201607485
3. Sadelain M, Brentjens R, Rivière I. The Basic Principles of Chimeric Antigen Receptor Design. *Cancer Discov* (2013) 3(4):388–98. doi: 10.1158/2159-8290.CD-12-0548
4. Salter AI, Ivey RG, Kennedy JJ, Voillet V, Rajan A, Alderman EJ, et al. Phosphoproteomic Analysis of Chimeric Antigen Receptor Signaling Reveals Kinetic and Quantitative Differences That Affect Cell Function. *Sci Signal* (2018) 11(544):eaat6753. doi: 10.1126/scisignal.aat6753
5. Ying Z, He T, Wang X, Zheng W, Lin N, Tu M, et al. Parallel Comparison of 4-1BB or CD28 Co-Stimulated CD19-Targeted CAR-T Cells for B Cell Non-Hodgkin's Lymphoma. *Mol Ther - Oncolytics* (2019) 15:60–8. doi: 10.1016/j.omto.2019.08.002
6. Long AH, Haso WM, Shern JF, Wanhainen KM, Murgai M, Ingaramo M, et al. 4-1BB Costimulation Ameliorates T Cell Exhaustion Induced by Tonic Signaling of Chimeric Antigen Receptors. *Nat Med* (2015) 21(6):581–90. doi: 10.1038/nm.3838
7. Kawalekar OU, O'Connor RS, Fraietta JA, Guo L, McGettigan SE, Posey AD, et al. Distinct Signaling of Coreceptors Regulates Specific Metabolism Pathways and Impacts Memory Development in CAR T Cells. *Immunity* (2016) 44(2):380–90. doi: 10.1016/j.immuni.2016.01.021
8. Neelapu SS, Locke FL, Bartlett NL, Lekakis LJ, Miklos DB, Jacobson CA, et al. Axicabtagene Ciloleucel CAR T-Cell Therapy in Refractory Large B-Cell Lymphoma. *N Engl J Med* (2017) 377(26):2531–44. doi: 10.1056/NEJMoa1707447
9. Schuster SJ, Bishop MR, Tam CS, Waller EK, Borchmann P, McGuirk JP, et al. Tisagenlecleucel in Adult Relapsed or Refractory Diffuse Large B-Cell Lymphoma. *New Engl J Med* (2018) 380(1):45–56. doi: 10.1056/NEJMoa1804980

10. Maude SL, Laetsch TW, Buechner J, Rives S, Boyer M, Bittencourt H, et al. Tisagenlecleucel in Children and Young Adults With B-Cell Lymphoblastic Leukemia. *N Engl J Med* (2018) 378(5):439–48. doi: 10.1056/NEJMoa1709866
11. Park JH, Rivière I, Gonen M, Wang X, Sénéchal B, Curran KJ, et al. Long-Term Follow-Up of CD19 CAR Therapy in Acute Lymphoblastic Leukemia. *New Engl J Med* (2018) 378(5):449–59. doi: 10.1056/NEJMoa1709919
12. Locke FL, Ghobadi A, Jacobson CA, Miklos DB, Lekakis LJ, Oluwole OO, et al. Long-Term Safety and Activity of Axicabtagene Ciloleucel in Refractory Large B-Cell Lymphoma (ZUMA-1): A Single-Arm, Multicentre, Phase 1-2 Trial. *Lancet Oncol* (2019) 20(1):31–42. doi: 10.1016/S1470-2045(18)30864-7
13. Zhang X, Lu XA, Yang J, Zhang G, Li J, Song L, et al. Efficacy and Safety of Anti-CD19 CAR T-Cell Therapy in 110 Patients With B-Cell Acute Lymphoblastic Leukemia With High-Risk Features. *Blood Adv* (2020) 4 (10):2325–38. doi: 10.1182/bloodadvances.2020001466
14. Cappell KM, Kochenderfer JN. A Comparison of Chimeric Antigen Receptors Containing CD28 Versus 4-1BB Costimulatory Domains. *Nat Rev Clin Oncol* (2021) 18(11):715–27. doi: 10.1038/s41571-021-00530-z
15. Yeku OO, Purdon TJ, Koneru M, Spriggs D, Brentjens RJ. Armored CAR T Cells Enhance Antitumor Efficacy and Overcome the Tumor Microenvironment. *Sci Rep* (2017) 7(1):10541. doi: 10.1038/s41598-017-10940-8
16. Webster B, Xiong Y, Hu P, Wu D, Alabanza L, Orentas RJ, et al. Self-Driving Armored CAR-T Cells Overcome a Suppressive Milieu and Eradicate CD19 + Raji Lymphoma in Preclinical Models. *Mol Ther* (2021) 29(9):2691–706. doi: 10.1016/j.ymthe.2021.05.006
17. Fry TJ, Mackall CL. Interleukin-7: Master Regulator of Peripheral T-Cell Homeostasis? *Trends Immunol* (2001) 22(10):564–71. doi: 10.1016/S1471-4906(01)02028-2
18. Luo H, Su J, Sun R, Sun Y, Wang Y, Dong Y, et al. Coexpression of IL7 and CCL21 Increases Efficacy of CAR-T Cells in Solid Tumors Without Requiring Preconditioned Lymphodepletion. *Clin Cancer Res* (2020) 26 (20):5494–505. doi: 10.1158/1078-0432.CCR-20-0777
19. Lee DW, Gardner R, Porter DL, Louis CU, Ahmed N, Jensen M, et al. Current Concepts in the Diagnosis and Management of Cytokine Release Syndrome. *Blood* (2014) 124(2):188–95. doi: 10.1182/blood-2014-05-552729
20. Gust J, Hay KA, Hanafi LA, Li D, Myerson D, Gonzalez-Cuyar LF, et al. Endothelial Activation and Blood-Brain Barrier Disruption in Neurotoxicity After Adoptive Immunotherapy With CD19 CART Cells. *Cancer Discov* (2017) 7(12):1404–19. doi: 10.1158/2159-8290.CD-17-0698
21. Lee DW, Kochenderfer JN, Stetler-Stevenson M, Cui YK, Delbrook C, Feldman SA, et al. T Cells Expressing CD19 Chimeric Antigen Receptors for Acute Lymphoblastic Leukaemia in Children and Young Adults: A Phase 1 Dose-Escalation Trial. *Lancet* (2015) 385(9967):517–28. doi: 10.1016/S0140-6736(14)61403-3
22. Jacobson C, Chavez JC, Sehgal AR, William BM, Munoz J, Salles G, et al. Primary Analysis of Zuma-5: A Phase 2 Study of Axicabtagene Ciloleucel (Axi-Cel) in Patients With Relapsed/Refractory (R/R) Indolent Non-Hodgkin Lymphoma (iNHL). *Blood* (2020) 136(Supplement 1):40–1. doi: 10.1182/blood-2020-136834
23. Jacobson CA, Farooq U, Ghobadi A. Axicabtagene Ciloleucel, an Anti-CD19 Chimeric Antigen Receptor T-Cell Therapy for Relapsed or Refractory Large B-Cell Lymphoma: Practical Implications for the Community Oncologist. *Oncol* (2020) 25(1):e138–e46. doi: 10.1634/theoncologist.2019-0395
24. Porter DL, Hwang WT, Frey NV, Lacey SF, Shaw PA, Loren AW, et al. Chimeric Antigen Receptor T Cells Persist and Induce Sustained Remissions in Relapsed Refractory Chronic Lymphocytic Leukemia. *Sci Transl Med* (2015) 7(303):303ra139. doi: 10.1126/scitranslmed.aac5415
25. Schuster SJ, Svoboda J, Chong EA, Nasta SD, Mato AR, Anak Ö, et al. Chimeric Antigen Receptor T Cells in Refractory B-Cell Lymphomas. *N Engl J Med* (2017) 377(26):2545–54. doi: 10.1056/NEJMoa1708566
26. Haydu JE, Abramson JS. CAR T-Cell Therapies in Lymphoma: Current Landscape, Ongoing Investigations, and Future Directions. *J Cancer Metastasis Treat* (2021) 7:36. doi: 10.20517/2394-4722.2021.39
27. Tambaro FP, Singh H, Jones E, Rytting M, Mahadeo KM, Thompson P, et al. Autologous CD33-CAR-T Cells for Treatment of Relapsed/Refractory Acute Myelogenous Leukemia. *Leukemia* (2021) 35(11):3282–6. doi: 10.1038/s41375-021-01232-2
28. U.S. Food & Drug Administration. *KYMRIAH (Tisagenlecleucel)* (2017). Available at: https://www.fda.gov/vaccines-blood-biologics/cellular-gene-therapy-products/kymriahtisagenlecleucel.
29. Das RK, Vernau L, Grupp SA, Barrett DM. Naïve T-Cell Deficits at Diagnosis and After Chemotherapy Impair Cell Therapy Potential in Pediatric Cancers. *Cancer Discov* (2019) 9(4):492–9. doi: 10.1158/2159-8290.CD-18-1314
30. Thommen DS, Schumacher TN. T Cell Dysfunction in Cancer. *Cancer Cell* (2018) 33(4):547–62. doi: 10.1016/j.ccell.2018.03.012
31. Klebanoff CA, Scott CD, Leonardi AJ, Yamamoto TN, Cruz AC, Ouyang C, et al. Memory T Cell-Driven Differentiation of Naive Cells Impairs Adoptive Immunotherapy. *J Clin Invest* (2016) 126(1):318–34. doi: 10.1172/JCI81217
32. Fraietta JA, Lacey SF, Orlando EJ, Pruteanu-Malinici I, Gohil M, Lundh S, et al. Determinants of Response and Resistance to CD19 Chimeric Antigen Receptor (CAR) T Cell Therapy of Chronic Lymphocytic Leukemia. *Nat Med* (2018) 24(5):563–71. doi: 10.1038/s41591-018-0010-1
33. Qasim W. Allogeneic CAR T Cell Therapies for Leukemia. *Am J Hematol* (2019) 94(S1):S50–4. doi: 10.1002/ajh.25399
34. Finney OC, Brakke HM, Rawlings-Rhea S, Hicks R, Doolittle D, Lopez M, et al. CD19 CAR T Cell Product and Disease Attributes Predict Leukemia Remission Durability. *J Clin Invest* (2019) 129(5):2123–32. doi: 10.1172/JCI125423
35. Kreslavsky T, Gleimer M, Garbe AI, von Boehmer H. αβ Versus γδ Fate Choice: Counting the T-Cell Lineages at the Branch Point. *Immunol Rev* (2010) 238(1):169–81. doi: 10.1111/j.1600-065X.2010.00947.x
36. Starr TK, Jameson SC, Hogquist KA. Positive and Negative Selection of T Cells. *Annu Rev Immunol* (2003) 21:139–76. doi: 10.1146/annurev.immunol.21.120601.141107
37. Dai H, Zhang W, Li X, Han Q, Guo Y, Zhang Y, et al. Tolerance and Efficacy of Autologous or Donor-Derived T Cells Expressing CD19 Chimeric Antigen Receptors in Adult B-ALL With Extramedullary Leukemia. *Oncoimmunology* (2015) 4(11):e1027469. doi: 10.1080/2162402X.2015.1027469
38. Hu Y, Wang J, Wei G, Yu J, Luo Y, Shi J, et al. A Retrospective Comparison of Allogenic and Autologous Chimeric Antigen Receptor T Cell Therapy Targeting CD19 in Patients With Relapsed/Refractory Acute Lymphoblastic Leukemia. *Bone Marrow Transplant* (2019) 54(8):1208–17. doi: 10.1038/s41409-018-0403-2
39. Zhang C, Wang X-Q, Zhang R-L, Liu F, Wang Y, Yan Z-L, et al. Donor-Derived CD19 CAR-T Cell Therapy of Relapse of CD19-Positive B-ALL Post Allotransplant. *Leukemia* (2021) 35(6):1563–70. doi: 10.1038/s41375-020-01056-6
40. Vormittag P, Gunn R, Ghorashian S, Veraitch FS. A Guide to Manufacturing CAR T Cell Therapies. *Curr Opin Biotechnol* (2018) 53:164–81. doi: 10.1016/j.copbio.2018.01.025
41. Turtle CJ, Hanafi LA, Berger C, Gooley TA, Cherian S, Hudecek M, et al. CD19 CAR-T Cells of Defined CD4+:CD8+ Composition in Adult B Cell ALL Patients. *J Clin Invest* (2016) 126(6):2123–38. doi: 10.1172/JCI85309
42. Sommermeyer D, Hudecek M, Kosasih PL, Gogishvili T, Maloney DG, Turtle CJ, et al. Chimeric Antigen Receptor-Modified T Cells Derived From Defined CD8+ and CD4+ Subsets Confer Superior Antitumor Reactivity *In Vivo*. *Leukemia* (2016) 30(2):492–500. doi: 10.1038/leu.2015.247
43. Xu Y, Zhang M, Ramos CA, Durett A, Liu E, Dakhova O, et al. Closely Related T-Memory Stem Cells Correlate With *In Vivo* Expansion of CAR.CD19-T Cells and Are Preserved by IL-7 and IL-15. *Blood* (2014) 123(24):3750–9. doi: 10.1182/ blood-2014-01-552174
44. Bonifant CL, Jackson HJ, Brentjens RJ, Curran KJ. Toxicity and Management in CAR T-Cell Therapy. *Mol Ther - Oncolytics* (2016) 3:16011. doi: 10.1038/mto.2016.11
45. Poirot L, Philip B, Schiffer-Mannioui C, Le Clerre D, Chion-Sotinel I, Derniame S, et al. Multiplex Genome-Edited T-Cell Manufacturing Platform for "Off-The-Shelf" Adoptive T-Cell Immunotherapies. *Cancer Res* (2015) 75(18):3853–64. doi: 10.1158/0008-5472.CAN-14-3321
46. Eyquem J, Mansilla-Soto J, Giavridis T, van der Stegen SJ, Hamieh M, Cunanan KM, et al. Targeting a CAR to the TRAC Locus With CRISPR/Cas9 Enhances Tumour Rejection. *Nature* (2017) 543(7643):113–7. doi: 10.1038/nature21405
47. Torikai H, Reik A, Liu PQ, Zhou Y, Zhang L, Maiti S, et al. A Foundation for Universal T-Cell Based Immunotherapy: T Cells Engineered to Express a

CD19-Specific Chimeric-Antigen-Receptor and Eliminate Expression of Endogenous TCR. *Blood* (2012) 119(24):5697–705. doi: 10.1182/blood-2012-01-405365
48. MacLeod DT, Antony J, Martin AJ, Moser RJ, Hekele A, Wetzel KJ, et al. Integration of a CD19 CAR Into the TCR Alpha Chain Locus Streamlines Production of Allogeneic Gene-Edited CAR T Cells. *Mol Ther* (2017) 25 (4):949–61. doi: 10.1016/j.ymthe.2017.02.005
49. Gilham DE, Michaux A, Breman E, Mauen S, Bolsée J, Huberty F, et al. TCR Inhibitory Molecule as a Promising Allogeneic NKG2D CAR-T Cell Approach. *J Clin Oncol* (2018) 36(15_suppl):e15042–e. doi: 10.1200/JCO.2018.36.15_suppl.e15042
50. Wang D, Quan Y, Yan Q, Morales JE, Wetsel RA. Targeted Disruption of the β2-Microglobulin Gene Minimizes the Immunogenicity of Human Embryonic Stem Cells. *Stem Cells Trans Med* (2015) 4(10):1234–45. doi: 10.5966/sctm.2015-0049
51. Torikai H, Reik A, Soldner F, Warren EH, Yuen C, Zhou Y, et al. Toward Eliminating HLA Class I Expression to Generate Universal Cells From Allogeneic Donors. *Blood* (2013) 122(8):1341–9. doi: 10.1182/blood-2013-03-478255
52. Kagoya Y, Guo T, Yeung B, Saso K, Anczurowski M, Wang CH, et al. Genetic Ablation of HLA Class I, Class II, and the T-Cell Receptor Enables Allogeneic T Cells to Be Used for Adoptive Tcell Therapy. *Cancer Immunol Res* (2020) 8(7):926–36. doi: 10.1158/2326-6066.CIR-18-0508
53. Schumm M, Lang P, Bethge W, Faul C, Feuchtinger T, Pfeiffer M, et al. Depletion of T-Cell Receptor Alpha/Beta and CD19 Positive Cells From Apheresis Products With the CliniMACS Device. *Cytotherapy* (2013) 15 (10):1253–8. doi: 10.1016/j.jcyt.2013.05.014
54. Qasim W, Zhan H, Samarasinghe S, Adams S, Amrolia P, Stafford S, et al. Molecular Remission of Infant B-ALL After Infusion of Universal TALEN Gene-Edited CAR T Cells. *Sci Transl Med* (2017) 9(374):eaaj2013. doi: 10.1126/scitranslmed.aaj2013
55. Juillerat A, Tkach D, Yang M, Boyne A, Valton J, Poirot L, et al. Straightforward Generation of Ultrapure Off-The-Shelf Allogeneic CAR-T Cells. *Front Bioeng Biotechnol* (2020) 8(678). doi: 10.3389/fbioe.2020.00678
56. Shuvalov O, Petukhov A, Daks A, Fedorova O, Ermakov A, Melino G, et al. Current Genome Editing Tools in Gene Therapy: New Approaches to Treat Cancer. *Curr Gene Ther* (2015) 15(5):511–29. doi: 10.2174/1566523215666150818110241
57. Cornu TI, Mussolino C, Cathomen T. Refining Strategies to Translate Genome Editing to the Clinic. *Nat Med* (2017) 23(4):415–23. doi: 10.1038/nm.4313
58. Ernst MPT, Broeders M, Herrero-Hernandez P, Oussoren E, van der Ploeg AT, Pijnappel WWMP. Ready for Repair? Gene Editing Enters the Clinic for the Treatment of Human Disease. *Mol Ther - Methods Clin Dev* (2020) 18:532–57. doi: 10.1016/j.omtm.2020.06.022
59. Stadtmauer EA, Fraietta JA, Davis MM, Cohen AD, Weber KL, Lancaster E, et al. CRISPRengineered T Cells in Patients With Refractory Cancer. *Science* (2020) 367(6481):eaba7365. doi: 10.1126/science.aba7365
60. Cassiano C. *Allogene Therapeutics Reports FDA Clinical Hold of AlloCAR T Trials Based on a Single Patient Case in ALPHA2 Trial*. South Sam Francisco: Allogene Therapeutics: Allogene Therapeutics, Inc. (2021).
61. Depil S, Duchateau P, Grupp SA, Mufti G, Poirot L. 'Off-The-Shelf' Allogeneic CAR T Cells: Development and Challenges. *Nat Rev Drug Discovery* (2020) 19(3):185–99. doi: 10.1038/s41573-019-0051-2
62. Nguyen TH, Bird NL, Grant EJ, Miles JJ, Thomas PG, Kotsimbos TC, et al. Maintenance of the EBV-Specific CD8(+) Tcrαβ Repertoire in Immunosuppressed Lung Transplant Recipients. *Immunol Cell Biol* (2017) 95(1):77–86. doi: 10.1038/icb.2016.71
63. Rozenbaum M, Meir A, Aharony Y, Itzhaki O, Schachter J, Bank I, et al. Gamma-Delta CART Cells Show CAR-Directed and Independent Activity Against Leukemia. *Front Immunol* (2020) 11:1347. doi: 10.3389/fimmu.2020.01347
64. Meraviglia S, Eberl M, Vermijlen D, Todaro M, Buccheri S, Cicero G, et al. *In Vivo* Manipulation of Vgamma9Vdelta2 T Cells With Zoledronate and Low-Dose Interleukin-2 for Immunotherapy of Advanced Breast Cancer Patients. *Clin Exp Immunol* (2010) 161(2):290–7. doi: 10.1111/j.1365-2249.2010.04167.x
65. Xu Y, Xiang Z, Alnaggar M, Kouakanou L, Li J, He J, et al. Allogeneic Vgamma9Vdelta2 Tcell Immunotherapy Exhibits Promising Clinical Safety and Prolongs the Survival of Patients With Latestage Lung or Liver Cancer. *Cell Mol Immunol* (2021) 18(2):427–39. doi: 10.1038/s41423-020-0515-7
66. Themeli M, Kloss CC, Ciriello G, Fedorov VD, Perna F, Gonen M, et al. Generation of Tumortargeted Human T Lymphocytes From Induced Pluripotent Stem Cells for Cancer Therapy. *Nat Biotechnol* (2013) 31 (10):928–33. doi: 10.1038/nbt.2678
67. Mandal M, Clarke R, van der Stegen S, Chang C-W, Lai Y-S, Witty A, et al. Abstract 3245: FT819 Path to IND: First-Of-Kind Off-the-Shelf CAR19 T-Cell for B Cell Malignancies. *Cancer Res* (2020) 80(16 Supplement):3245–. doi: 10.1158/1538-7445.AM2020-3245
68. Love PE, Hayes SM. ITAM-Mediated Signaling by the T-Cell Antigen Receptor. *Cold Spring Harb Perspect Biol* (2010) 2(6):a002485. doi: 10.1101/cshperspect.a002485
69. Wherry EJ, Kurachi M. Molecular and Cellular Insights Into T Cell Exhaustion. *Nat Rev Immunol* (2015) 15(8):486–99. doi: 10.1038/nri3862
70. Feucht J, Sun J, Eyquem J, Ho YJ, Zhao Z, Leibold J, et al. Calibration of CAR Activation Potential Directs Alternative T Cell Fates and Therapeutic Potency. *Nat Med* (2019) 25(1):82–8. doi: 10.1038/s41591-018-0290-5
71. Park JH, Jain N, Chen A, McGuirk JP, Diaz M, Valamehr B, et al. A Phase I Study of FT819, a First-Of-Kind, Off-The-Shelf, iPSC-Derived TCR-Less CD19 CAR T Cell Therapy for the Treatment of Relapsed/Refractory B-Cell Malignancies. *Blood* (2020) 136(Supplement 1):15–6. doi: 10.1182/blood-2020-142423
72. Xie G, Dong H, Liang Y, Ham JD, Rizwan R, Chen J. CAR-NK Cells: A Promising Cellular Immunotherapy for Cancer. *EBioMedicine* (2020) 59:102975. doi: 10.1016/j.ebiom.2020.102975
73. Lee N, Llano M, Carretero M, Ishitani A, Navarro F, López-Botet M, et al. HLA-E is a Major Ligand for the Natural Killer Inhibitory Receptor CD94/NKG2A. *Proc Natl Acad Sci USA* (1998) 95(9):5199–204. doi: 10.1073/pnas.95.9.5199
74. Veluchamy JP, Kok N, van der Vliet HJ, Verheul HMW, de Gruijl TD, Spanholtz J. The Rise of Allogeneic Natural Killer Cells As a Platform for Cancer Immunotherapy: Recent Innovations and Future Developments. *Front Immunol* (2017) 8:631. doi: 10.3389/fimmu.2017.00631
75. Shah NN, Baird K, Delbrook CP, Fleisher TA, Kohler ME, Rampertaap S, et al. Acute GvHD in Patients Receiving IL-15/4-1BBL Activated NK Cells Following T-Cell-Depleted Stem Cell Transplantation. *Blood* (2015) 125 (5):784–92. doi: 10.1182/blood-2014-07-592881
76. Klingemann H, Boissel L, Toneguzzo F. Natural Killer Cells for Immunotherapy - Advantages of the NK-92 Cell Line Over Blood NK Cells. *Front Immunol* (2016) 7:91. doi: 10.3389/fimmu.2016.00091
77. Rezvani K, Rouce RH. The Application of Natural Killer Cell Immunotherapy for the Treatment of Cancer. *Front Immunol* (2015) 6:578. doi: 10.3389/fimmu.2015.00578
78. Rosa K, *FDA Grants CAR T-Cell Therapy ALLO-715 Orphan Drug Status for Multiple Myeloma*. San Francisco, California: Christine Cassiano, Allogene Therapeutics (2021).
79. Mailankody S. 129 Universal: An Allogeneic First-In-Human Study of the Anti-Bcma ALLO-715 and the Anti-CD52 ALLO-647 in Relapsed/Refractory Multiple Myeloma. In: *American Society of Hematology Annual Meeting and Exposition*. Washington: American Society of Hematology (2020). Virtual2020.
80. Abramson JS, Palomba ML, Gordon LI, Lunning MA, Wang M, Arnason J, et al. Lisocabtagene Maraleucel for Patients With Relapsed or Refractory Large B-Cell Lymphomas (TRANSCEND NHL 001): A Multicentre Seamless Design Study. *Lancet* (2020) 396(10254):839–52. doi: 10.1016/S0140-6736(20)31366-0
81. Wang M, Munoz J, Goy A, Locke FL, Jacobson CA, Hill BT, et al. KTE-X19 CAR T-Cell Therapy in Relapsed or Refractory Mantle-Cell Lymphoma. *New Engl J Med* (2020) 382(14):1331–42. doi: 10.1056/NEJMoa1914347
82. Cassiano C. *Allogene Therapeutics Presents Positive Phase 1 Data on ALLO-501 and ALLO-501A in Relapsed/Refractory Non-Hodgkin Lymphoma at the 2021 Annual Meeting of the American Society of Clinical Oncology*. San Francisco, California: Christine Cassiano, Allogene Therapeutics (2021).
83. Philip B, Kokalaki E, Mekkaoui L, Thomas S, Straathof K, Flutter B, et al. A Highly Compact Epitope-Based Marker/Suicide Gene for Easier and Safer T-Cell Therapy. *Blood* (2014) 124(8):1277–87. doi: 10.1182/blood-2014-01-545020

84. Benjamin R, Graham C, Yallop D, Jozwik A, Mirci-Danicar OC, Lucchini G, et al. Genomeedited, Donor-Derived Allogeneic Anti-CD19 Chimeric Antigen Receptor T Cells in Paediatric and Adult B-Cell Acute Lymphoblastic Leukaemia: Results of Two Phase 1 Studies. *Lancet* (2020) 396(10266):1885–94. doi: 10.1016/S0140-6736(20)32334-5
85. Cassiano C. *CRISPR Therapeutics Reports Positive Top-Line Results From Its Phase 1 CARBON Trial of CTX110™ in Relapsed or Refractory CD19+ B-Cell Malignancies*. Zug Switzerland: CRISPR Therapeutics (2020).
86. Chevalier BS, Stoddard BL. Homing Endonucleases: Structural and Functional Insight Into the Catalysts of Intron/Intein Mobility. *Nucleic Acids Res* (2001) 29(18):3757–74. doi: 10.1093/nar/29.18.3757
87. Jacobson CA, Herrera AF, Budde LE, DeAngelo DJ, Heery C, Stein A, et al. Initial Findings of the Phase 1 Trial of PBCAR0191, a CD19 Targeted Allogeneic CAR-T Cell Therapy.. *Blood* (2019) 134(Supplement_1):4107. doi: 10.1182/blood-2019-128203
88. Messier M. *Precision BioSciences Reports Positive Interim Results From PBCAR0191 Phase 1/2a Trial in Relapsed/Refractory (R/R) Non-Hodgkin Lymphoma (NHL) and R/R B-Cell Acute Lymphoblastic Leukemia (B-ALL)* Durham, N.C.: Precision BioSciences in GlobeNewswire (2020).
89. Hirayama AV, Gauthier J, Hay KA, Voutsinas JM, Wu Q, Gooley T, et al. The Response to Lymphodepletion Impacts PFS in Patients With Aggressive Non-Hodgkin Lymphoma Treated With CD19 CAR T Cells. *Blood* (2019) 133(17):1876–87. doi: 10.1182/blood-2018-11-887067
90. Shah BD. Allogeneic CAR-T PBCAR0191 With Intensified Lymphodepletion Is Highly Active in Patients With Relapsed/Refractory B-Cell Malignancies. In: *ASH Annual Meeting & Exposition*. Washington, USA: American Society of Hematology (2021).
91. Sallman DA, Brayer J, Sagatys EM, Lonez C, Breman E, Agaugue S, et al. NKG2D-Based Chimeric Antigen Receptor Therapy Induced Remission in a Relapsed/Refractory Acute Myeloid Leukemia Patient. *Haematologica* (2018) 103(9):e424–e6. doi: 10.3324/haematol.2017.186742
92. Prenen H, Dekervel J, Hendlisz A, Anguille S, Awada A, Cerf E, et al. Updated Data From alloSHRINK Phase I First-in-Human Study Evaluating CYAD-101, An Innovative Non-Gene Edited Allogeneic CAR-T in mCRC. *J Clin Oncol* (2021) 39(3_suppl):74–. doi: 10.1200/JCO.2021.39.3_suppl.74
93. Gilham DE, Bornschein S, Springuel L, Michaux A, Steklov M, Breman E, et al. Single Vector Multiplexed shRNA Provides a Non-Gene Edited Strategy to Concurrently Knockdown the Expression of Multiple Genes in CAR T Cells. *J Clin Oncol* (2020) 38(15_suppl):3103–. doi: 10.1200/JCO.2020.38.15_suppl.3103
94. Magnani CF, Gaipa G, Lussana F, Belotti D, Gritti G, Napolitano S, et al. Sleeping Beauty– Engineered CAR T Cells Achieve Antileukemic Activity Without Severe Toxicities. *J Clin Invest* (2020) 130(11):6021–33. doi: 10.1172/JCI138473
95. Introna M, Lussana F, Algarotti A, Gotti E, Valgardsdottir R, Mic C, et al. Phase II Study of Sequential Infusion of Donor Lymphocyte Infusion and Cytokine-Induced Killer Cells for Patients Relapsed After Allogeneic Hematopoietic Stem Cell Transplantation. *Biol Blood Marrow Transplant* (2017) 23(12):2070–8. doi: 10.1016/j.bbmt.2017.07.005
96. Nishimura R, Baker J, Beilhack A, Zeiser R, Olson JA, Sega EI, et al. *In Vivo* Trafficking and Survival of Cytokine-Induced Killer Cells Resulting in Minimal GvHD With Retention of Antitumor Activity. *Blood* (2008) 112 (6):2563–74. doi: 10.1182/blood-2007-06-092817
97. Shah NN, Qin H, Yates B, Su L, Shalabi H, Raffeld M, et al. Clonal Expansion of CAR T Cells Harboring Lentivector Integration in the CBL Gene Following Anti-CD22 CAR T-Cell Therapy. *Blood Adv* (2019) 3(15):2317–22. doi: 10.1182/bloodadvances.2019000219
98. Fraietta JA, Nobles CL, Sammons MA, Lundh S, Carty SA, Reich TJ, et al. Disruption of TET2 Promotes the Therapeutic Efficacy of CD19-Targeted T Cells. *Nature* (2018) 558(7709):307–12. doi: 10.1038/s41586-018-0178-z
99. Prockop S, Doubrovina E, Suser S, Heller G, Barker J, Dahi P, et al. Off-The-Shelf EBVspecific T Cell Immunotherapy for Rituximab-Refractory EBV-Associated Lymphoma Following Transplantation. *J Clin Invest* (2020) 130 (2):733–47. doi: 10.1172/JCI121127
100. Curran KJ, Sauter CG, Kernan NA, Prockop SE, Boulad F, Perales M, et al. Durable Remission Following Infusion «Off-the-Shelf» Chimeric Antigen Receptor (CAR) T-Cells in Patients With Relapse/Refractory (R/R) B-Cell Malignancies. *Transplant Cell Ther Meet* (2020) 26(3):S89. doi: 10.1016/j.bbmt.2019.12.590
101. Shen RR, Pham CD, Wu M, Munson DJ, Aftab BT. CD19 Chimeric Antigen Receptor (CAR) Engineered Epstein-Barr Virus (EBV) Specific T Cells – An Off-the-Shelf, Allogeneic CAR T-Cell Immunotherapy Platform. *Cytotherapy* (2019) 21(5, Supplement):S11. doi: 10.1016/j.jcyt.2019.03.569
102. Liu E. Use of CAR-Transduced Natural Killer Cells in CD19-Positive Lymphoid Tumors. *N Engl J Med* (2020) 382:545–53. doi: 10.1056/NEJMoa1910607
103. Tang X, Yang L, Li Z, Nalin AP, Dai H, Xu T, et al. First-In-Man Clinical Trial of CAR NK-92 Cells: Safety Test of CD33-CAR NK-92 Cells in Patients With Relapsed and Refractory Acute Myeloid Leukemia. *Am J Cancer Res* (2018) 8(6):1083–9.
104. Arai S, Meagher R, Swearingen M, Myint H, Rich E, Martinson J, et al. Infusion of the Allogeneic Cell Line NK-92 in Patients With Advanced Renal Cell Cancer or Melanoma: A Phase I Trial. *Cytotherapy* (2008) 10(6):625–32. doi: 10.1080/14653240802301872
105. Ehninger A, Kramer M, Röllig C, Thiede C, Bornhäuser M, von Bonin M, et al. Distribution and Levels of Cell Surface Expression of CD33 and CD123 in Acute Myeloid Leukemia. *Blood Cancer J* (2014) 4(6):e218. doi: 10.1038/bcj.2014.39
106. Gill S, Tasian SK, Ruella M, Shestova O, Li Y, Porter DL, et al. Preclinical Targeting of Human Acute Myeloid Leukemia and Myeloablation Using Chimeric Antigen Receptor–Modified T Cells. *Blood* (2014) 123(15):2343–54. doi: 10.1182/blood-2013-09-529537
107. Goebeler M-E, Bargou RC. T Cell-Engaging Therapies — BiTEs and Beyond. *Nat Rev Clin Oncol* (2020) 17(7):418–34. doi: 10.1038/s41571-020-0347-5

Conflict of Interest: The authors declare that the research was conducted in the absence of any commercial or financial relationships that could be construed as a potential conflict of interest.

frontiers | Frontiers in Immunology

TYPE Original Research
PUBLISHED 05 October 2022
DOI 10.3389/fimmu.2022.1012051

OPEN ACCESS

EDITED BY
Maurizio Chiriva-Internati,
University of Texas MD Anderson Cancer Center, United States

REVIEWED BY
Martin John Cannon,
University of Arkansas for Medical Sciences, United States
Ilan Bank,
Sheba Medical Center, Israel

*CORRESPONDENCE
Tyler Lahusen
tylerlah@gmail.com

†These authors have contributed equally to this work

SPECIALTY SECTION
This article was submitted to Cancer Immunity and Immunotherapy, a section of the journal Frontiers in Immunology

RECEIVED 05 August 2022
ACCEPTED 20 September 2022
PUBLISHED 05 October 2022

CITATION
Liou M-L, Lahusen T, Li H, Xiao L and Pauza CD (2022) Reducing farnesyl diphosphate synthase levels activates Vγ9Vδ2 T cells and improves tumor suppression in murine xenograft cancer models.
Front. Immunol. 13:1012051.
doi: 10.3389/fimmu.2022.1012051

Reducing farnesyl diphosphate synthase levels activates Vγ9Vδ2 T cells and improves tumor suppression in murine xenograft cancer models

Mei-Ling Liou[1†], Tyler Lahusen[1*†], Haishan Li[1,2], Lingzhi Xiao[1] and C. David Pauza[1,2]

[1]American Gene Technologies International Inc., Rockville, MD, United States, [2]Viriom Inc., Rockville, MD, United States

Human Vγ9Vδ2 T cells are attractive candidates for cancer immunotherapy due to their potent capacity for tumor recognition and cytolysis of many tumor cell types. However, efforts to deploy clinical strategies for Vγ9Vδ2 T cell cancer therapy are hampered by insufficient potency. We are pursuing an alternate strategy of modifying tumors to increase the capacity for Vγ9Vδ2 T cell activation, as a means for strengthening the anti-tumor response by resident or ex vivo manufactured Vγ9Vδ2 T cells. Vγ9Vδ2 T cells are activated *in vitro* by non-peptidic antigens including isopentenyl pyrophosphate (IPP), a substrate of farnesyl diphosphate synthase (FDPS) in the pathway for biosynthesis of isoprenoids. In an effort to improve *in vivo* potency of Vγ9Vδ2 T cells, we reduced FDPS expression in tumor cells using a lentivirus vector encoding a short-hairpin RNA that targets FDPS mRNA (LV-shFDPS). Prostate (PC3) or hepatocellular carcinoma (Huh-7) cells transduced with LV-shFDPS induced Vγ9Vδ2 T cell stimulation *in vitro*, resulting in increased cytokine expression and tumor cell cytotoxicity. Immune deficient mice implanted with LV-shFDPS transduced tumor cells showed dramatic responses to intraperitoneal injection of Vγ9Vδ2 T cells with strong suppression of tumor growth. *In vivo* potency was increased by transducing tumor cells with a vector expressing both shFDPS and human IL-2. Tumor suppression by Vγ9Vδ2 T cells was dose-dependent with greater effects observed in mice injected with 100% LV-shFDPS transduced cells compared to mice injected with a mixture of 50% LV-shFDPS transduced cells and 50% control (no vector) tumor cells. Delivery of LV-shFDPS by intratumoral injection was insufficient to knockdown FDPS in the majority of tumor cells, resulting in insignificant tumor suppression by Vγ9Vδ2 T cells. Thus, Vγ9Vδ2 T cells efficiently targeted and suppressed tumors expressing shFDPS in mouse xenotransplant models. This proof-of-concept study demonstrates the potential for suppression of genetically modified tumors by human Vγ9Vδ2 T cells and indicates that co-expression of cytokines may boost the anti-tumor effect.

KEYWORDS

T-cell, gamma delta T-cell, cancer, tumor, immunotherapy, shRNA, FDPS

10.3389/fimmu.2022.1012051

Introduction

Human Vγ9Vδ2 (hereinafter referred to as Vδ2) T cells are a unique population in peripheral blood with frequencies ranging from 0.5-10% of peripheral blood mononuclear cells (PBMC). Due to unique features of their T cell receptor, these are often considered to have features representing both innate and adaptive immunity (1). The T cell receptor (TCR) on Vδ2 T cells is composed of V gamma 9), a specific J segment (JP) and the V delta 2 chains capable of responding to non-peptide antigens independently of antigen presentation by major histocompatibility complex proteins (MHC) (2, 3). Non-peptide antigens capable of stimulating Vδ2 T cells are known as phosphoantigens (PAgs) include (E)-4-hydroxy-3-methyl-but-2-enyl pyrophosphate (HMBPP) found in bacterial, fungal and protozoan pathogens, and isopentenyl pyrophosphate (IPP), an intermediate metabolite in the mevalonate pathway for biosynthesis of isoprenoids (Supplementary Figure 1) (4–7).

PAg recognition depends on cell surface molecules from the butyrophilin family, most importantly 3A1 and 3A2 (8, 9). In our current understanding, butyrophilin binds PAg *via* a cytoplasmic domain, resulting in a conformational change to the ectodomain that is recognized by Vδ2 T cells (10–12). Considering that butyrophilins are widely expressed and tumor cells upregulate the mevalonate pathway to meet an increasing need for membrane synthesis (13, 14), Vδ2 T cells respond to many types of malignant cells and may participate in tumor immunosurveillance through their recognition of PAg (15–17). The common expression of butyrophilins and upregulation of the mevalonate/cholesterol pathway allows for broad recognition of tumors by Vδ2 T cells (18–20). Accordingly, Vδ2 T cells are increasingly appreciated as a key component in natural tumor immunity and a potential target for cell-based therapy against cancers due to their ability to recognize malignant cells, infiltrate tumors, and release cytotoxic and pro-inflammatory cytokines (21–24). Both adoptive transfer and *in vivo* activation of Vδ2 T cells have been safe during clinical trials making them a promising cell therapy against various tumors such as lymphoma, myeloma (25), hepatocellular, and colorectal carcinoma (26), and prostate (23), lung (27), colon (28), breast (24), and ovary cancers (29).

Vδ2 T lymphocytes can be activated by PAg producing accessory cells, such as immune presenting cells and tumor cells, or self-activate through exogenous PAgs (30). The activated Vδ2 T cells are cytolytic against tumor cells, secrete the inflammatory cytokines TNFα and IFNγ among others, release cytolytic proteins perforin and granzyme B, and are effector cells for antibody-dependent cell mediated cytotoxicity (ADCC) (31).

Nitrogen-containing-bisphosphonates (NBPs) have immunomodulatory properties including activation of Vδ2 T cells. NBPs are inhibitors of farnesyl diphosphate synthase (FDPS), an enzyme in the mevalonate pathway (Supplementary Figure 1). NBPs compete for IPP binding on FDPS leading to competitive enzyme inhibition, IPP accumulation and Vδ2 T cell activation (32–34). NBPs are used clinically to treat osteoporosis and osteolytic bone lesions. Pharmaceutical NBPs, such as zoledronic acid (Zomata), pamidronate (Aredia) and Alendronic acid (Fosamax) are used to treat osteoporosis and are reported to have anti-tumor effects in metastatic bone cancer patients (35–37). Given the anti-tumor effect exhibited by NBPs, in addition to the fact that some tumors overproduce IPP, *in vitro* data showed that treatment of tumor cells with NBPs leads to activation of Vδ2 T cells and increased cytolytic responses against tumor cells (38).

Existing approaches for exploiting Vδ2 T cells in cancer therapy utilize soluble activators of Vδ2 T cells such as NBPs or PAg to increase the potency of Vδ2 T cells against tumor cell targets (39). Another approach to activating Vδ2 T cells uses RNA interference with a small hairpin RNA (shRNA) stem-loop structure to knockdown FDPS mRNA in tumor cells, thus causing IPP accumulation and Vδ2 T cell activation (6, 40, 41). As a proof of concept, we delivered shFDPS to cancer cells using a lentivirus vector. The large carrying capacity of lentiviral vectors also allowed us to co-express shFDPS and immune-stimulating factors on individual lentivirus vector constructs. Several cytokines are known to enhance Vδ2 T cell activation or increase Vδ2 T cell expansion. IL2 and IL15 increase the activity of Vδ2 T cells in response to PAg or NBPs (42, 43) and IL2 increases the expansion of Vδ2 T cells in response to zoledronic acid (44, 45). Expressing IL2 in addition to FDPS shRNA in a lentiviral vector might enhance the potency of Vδ2 T cells against cancer (24).

The combination of NBPs and Vδ2 T cell treatments used in xenograft mouse models were tested in several human tumor types including melanoma (46), glioma (47), neuroblastoma (48), pancreatic (46, 49), and prostate cancer (49). However, there are two limitations to using NBPs for activating Vδ2 T cells *in vivo*. One is that soluble NBPs are absorbed by binding to hydroxyapatite on the bone surface, thus reducing bioavailability, and the second is that NBPs cannot be targeted to the tumors. Consequently, we constructed a lentiviral vector expressing shFDPS (LV-shFDPS) to determine if reducing FDPS mRNA and protein expression in prostate and hepatocellular tumors ex vivo or *in vivo* would lead to tumor suppression by Vδ2 T cells from healthy human donors. We also tested whether FDPS knockdown in addition to NBP treatment could increase the activation and cytolytic activity of Vδ2 T cells and whether this would be enhanced further with concurrent tumor cell expression of IL2.

Materials and methods

Isolation and cryopreservation of human PBMC

Leukopaks from anonymous donors were obtained from the New York Blood Center (New York, NY, USA). PBMC were isolated using density gradient centrifugation using a Ficoll-Paque Plus gradient (Sigma-Aldrich, St. Louis, MO, USA). The PBMC were transferred to a new tube and washed twice with PBS. The resulting cell pellet was resuspended in culture medium composed of RPMI 1640 complete medium: RPMI 1640 medium (Thermo Fisher Scientific, Burlington, MA, USA), 10% Fetal Bovine Serum (FBS) (Gemini, Sacramento, CA, USA), and 10,000 U/mL Penicillin-Streptomycin (Thermo Fisher Scientific). PBMC were cryopreserved in 90% FBS + 10% DMS0 (Sigma-Aldrich) at a final concentration of 3 X 10^7 cells/mL. The PBMC were placed at -80°C for overnight and then transferred to liquid nitrogen for long term storage.

Expansion of Vδ2 T cells from cryopreserved human PBMC

3 X 10^7 cryopreserved PBMC were thawed in a 37°C water bath and washed with RPMI 1640 medium. The PBMC were resuspended at a concentration of 1 X 10^7cells/mL in 10 mL RPMI 1640 medium supplemented with 1 μM zoledronic acid (ZA) (Sigma-Aldrich) and 0.1 mg/mL recombinant human IL2 (Thermo Fisher Scientific). The cells were expanded in T25 or T75 tissue culture flasks (Greiner Bio, VWR, Radnor, PA, USA) for a minimum of two weeks prior to use for *in vitro* and *in vivo* experiments. During the first 10 days of expansion, the medium was supplemented with 0.1 mg/mL of recombinant human IL2 twice in the first week after which IL2 supplementation was continued at 0.01 mg/mL. After a minimum of two weeks in culture, the mixed cell population contained 20-90% Vδ2 T cells as determined by flow cytometry.

Cultivation of cancer cell lines

PC3 prostate carcinoma cells were obtained from the American Type Culture Collection (ATCC, Manassas, VA, USA) and Huh-7 liver hepatocellular carcinoma cells were obtained from the Japanese Collection of Research Bioresources (JCRB Cell Bank, Osaka, Japan). The cells were thawed and passaged in DMEM complete medium: DMEM (Thermo Fisher Scientific), 10% FBS (Gemini), and 10,000 U/mL Penicillin-Streptomycin (Thermo Fisher Scientific). Cells were seeded into T-75 flasks (Greiner Bio, VWR) and cultured in a 37°C incubator with 5% CO_2.

Transduction of cancer cells and coculture with Vδ2 T cells

PC3 or Huh-7 cells were seeded at 0.5 X 10^6 cells/well in a 6-well plate followed by incubation overnight. The next day, when the cells had reached around 50% confluency, the cells were transduced with LV control, LV-shFDPS or LV-shFDPS-IL2 using a multiplicity of infection (MOI) of 5 or 10. Three days after transduction, the transduced PC3 or Huh-7 cells were collected, centrifuged, and resuspended in fresh, complete DMEM medium. The PC3 or Huh-7 cells were added at 5 X 10^5 cells/100 μL in wells of 96-well U-bottom plates. Next, 1 X 10^6/100 μL Vδ2 T cells were added to the wells and cytokine secretion was arrested by adding the GolgiPlug reagent per the manufacturer's instructions (BD Biosciences, Franklin Lakes, NJ, USA). The coculture was incubated in a 37°C cell incubator for 4 h, whereupon cells were collected and cytokine expression was measured by flow cytometry.

Measuring FDPS expression by immunoblotting

293T cells were seeded at 8 X 10^5 cells in each well of a 6-well plate and cultured in 1.5 mL of complete DMEM medium in a 37°C incubator at 5% CO_2 overnight. The next day, lentivirus vector was added to the cells at a MOI of 2.5, 5, 10 or 20 for 48 h. For PC3 cells, in addition to lentivirus, polybrene (Sigma-Aldrich) was added to the cell medium at a concentration of 2 μg/mL. Cells were lysed in 1% NP-40 lysis buffer containing a Pierce Protease Inhibitor Tablet (Thermo Fisher Scientific). Protein lysates were prepared in 1x NuPAGE LDS sample buffer (Thermo Fisher Scientific), samples were heated for 10 min at 70°C, and proteins were separated with 4-12% NuPAGE Bis-Tris gels (Thermo Fisher Scientific). Proteins were transferred to polyvinylidene fluoride (PVDF) membranes (MilliporeSigma) and probed with the antibodies anti-FDPS (Bethyl Laboratories Fortis Life Sciences, Waltham, MA, USA) and β-actin (MilliporeSigma). Anti-mouse or rabbit secondary antibody conjugated with horseradish peroxidase (HRP) (Bio-Rad, Hercules, CA, USA) was visualized with the Immobilon Western HRP substrate (MilliporeSigma) and detected with the LI-COR C-DiGit Blot Scanner (Lincoln, NE, USA).

Measurement of IL2 by ELISA

PC3 cells were transduced with lentivirus at 5 MOI in addition to 2 μg/mL of polybrene. The cell medium was changed after 6 h and then collected after 3 days whereupon

IL2 expression was determined with a human IL2 ELISA kit (Thermo Fisher Scientific).

Reverse transcriptase (RT) PCR and real-time qPCR

Cells were collected and RNA was extracted with the RNeasy kit (Qiagen, Germantown, MD, USA). The reverse transcription reaction was done using 1.4 µg of RNA and the Vilo SuperScript cDNA synthesis kit (Thermo Fisher Scientific) on a Veriti 96-well thermal cycler (Thermo Fisher Scientific). The PCR steps were according to the following: 25°C for 10 min, 42°C for 60 min, and 85°C for 5 min. For the Real-Time qPCR assays, 1.5 µL of the RT-PCR reaction was mixed with 1 µL of FDPS (Fwd: 5"-GTGCTGACTGAGGATGAGATG-3', Rev: 5"-CCGGT TATACTTGCCTCCAAT-3", Fam probe: 5'-TAGCTCTCC TATCTCTGGGTGCCC-3') and actin (Fwd: 5'-GGACC TGACTGACTACCTCAT-3", Rev: 5'-CGTAGCACAGCT TCTCCTTAAT-3", Yakima probe: 5'-AGCGGGAAAT CGTGCGTGAC-3') primers and probes at 0.5 µM and the reaction components of the TaqMan Fast Advanced Master Mix (Thermo Fisher Scientific). The qPCR reactions were performed on a QuantStudio3 Real-Time PCR system (Thermo Fisher Scientific) according to the following steps: 50°C for 2 min, 95°C for 20 secs, 40 cycles of 95°C for 1 sec and 60°C for 20 secs. Data were collected and analyzed with QuantStudio Design and Analysis software (Thermo Fisher Scientific).

Flow cytometry analysis

The 96-well U-bottom plate containing the co-cultured cells was centrifuged, followed by removal of the supernatant and resuspension in 50 µL of flow staining buffer (1X PBS magnesium/calcium depleted + 1% FBS) containing PE-labeled anti-human Vδ2 antibody (BioLegend, San Diego, CA, USA). Next, the cells were treated with 50 µL of fixation buffer (BD Biosciences) before washing with 1X perm/wash solution (BD Biosciences). Then cells were resuspended in 50 µL of APC-labeled anti-human TNFα or IFNγ (BioLegend). The cells were incubated at 4°C for 20 min in the dark and washed 2 times with 250 µL of 1X perm/wash solution. Flow cytometry data were acquired on a FACS Calibur (BD Biosciences) and analyzed using FlowJo software.

Labeling of cancer cells with calcein AM

PC3 or Huh-7 cells were seeded in 6-well plates at 4 X 10^5 cells per well and incubated overnight. The next day, the cells were transduced with lentiviral vector stocks at a MOI of 5 or 10. For PC3 cells, in addition to lentivirus, polybrene was added to the cell medium at a concentration of 2 µg/mL. After 48 h, the medium was changed with or without 1 µM ZA for overnight incubation. The next day, 5 µM of Calcein AM (Thermo Fisher Scientifc) were added to the medium and cells were placed in a 37°C cell incubator for 20 min. Next, the cells were washed with culture medium. Finally, the labeled cells were resuspended to a concentration of 5 X 10^5 cells/mL.

Cytotoxicity assay

Serial dilutions of expanded Vδ2 T cells were prepared with 1 X 10^6/mL, 5 X 10^5/mL, 2.5 X 10^6/mL, and 1.625 X 10^6/mL cell concentrations. 100 µL of each dilution of PBMC enriched for Vδ2 T cells were added to 5 X 10^4/100 µL of the Calcein AM-labeled PC3 or Huh-7 cells which resulted in effector to target cell ratios (E:T) of 20:1, 10:1, 5:1, 2.5:1, and 1.25:1; the ratio indicates numbers of enriched PBMC (Effector) and were not corrected for the percentage of Vδ2 T cells in each cell preparation. All co-cultures were performed in triplicate. The cocultures were incubated in a 96-well U-bottom plate in a 37°C cell incubator for 4 h. To account for spontaneous cell lysis, 5 X 10^4 of the cells were cultured without Vδ2 T cells. To determine maximum cell lysis, 5 X 10^4 cells cultured without Vδ2 T cells were completely lysed by the addition of 1% Triton-X-100 (Sigma-Aldrich) to the culture medium. After 4 h, 75 µL of supernatant from each well of the 96-well plate were transferred to a new 96-well black plate with a clear bottom and lid (VWR). Cell lysis was measured by the level of fluorescent Calcein AM detected in the supernatant using a fluorescent spectrophotometer (Biotek/Agilent, Santa Clara, CA, USA). The percentage of specific lysis was calculated with the following formula: % specific lysis = (Co-culture lysis–spontaneous lysis)÷(Maximum lysis–spontaneous lysis) X 100.

Tumor xenograft and Vδ2 T cell treatments in mice

PC3 or Huh-7 cells were seeded in a T75 flask. When the cells were 80% confluent, they were transferred to a T175 flask. PC3 or Huh-7 cells were transduced when the cells had reached 50% confluency by replacing the medium with lentiviral vector stocks diluted in medium to result in a MOI of 5 or 10. For PC3 cells, in addition to lentivirus, polybrene was added to the cell medium at a concentration of 2 µg/mL. Three days following cell seeding, the cells were collected by trypsinization and washed twice in complete medium for inoculation into mice. For each treatment, 5-8 NSG or NRG mice were inoculated subcutaneously with 3 X 10^6 cells/0.1 mL PC3 or Huh-7 cell plus 0.05 mL Matrigel (Corning, Corning, NY, USA) into the right flank of each mouse. Mice were weighed and tumor

10.3389/fimmu.2022.1012051

volumes were measured twice a week using a caliper. Tumor volume was calculated using the following equation: Tumor volume (mm^3)=d^2 (d=the shortest diameter) X (D/2) (D=the longest diameter). Mice were euthanized when tumor volume reached approximately 2000 mm^3, followed by excision and weighing of the tumor. 5-8 X 10^6 Vδ2 T cells expanded from PBMC were administered by intraperitoneal injection (IP) when the average tumor volume reached 200-300 mm^3. Vδ2 T cells were injected by IP route every week for a total of 4 injections. ZA was administered to mice by IP injection with a dose of 100 mg/kg the day prior to each injection of Vδ2 T cells.

Statistical analysis

The data was presented as the mean ± SEM where applicable and statistical analysis was performed with GraphPad Prism. Statistical analysis of the data from *in vivo* tumor studies was performed with the unpaired t test.

Results

Lentiviral vector LV-shFDPS decreases FDPS mRNA and protein expression

The lentiviral vector with a small hairpin (shFDPS) stem loop structure (Figure 1A upper panel) was used to reduce FDPS mRNA levels. The specific guide sequence used in LV-shFDPS was selected from several predicted targets after head-to-head comparisons based on mRNA levels (not shown). The ability of LV-shFDPS to reduce FDPS expression was evaluated by Real-Time qPCR or Western blot analysis in the presence of 0, 5, 10, 20 or 25 MOI of LV-shFDPS lentiviral vector in the PC3 metastatic human prostate adenocarcinoma cell line and in the Huh-7 human hepatocellular carcinoma cell line. The FDPS mRNA levels were reduced in a dose-dependent manner as compared with no LV treatment levels (100%) in PC3 cells at 5 MOI (67.9 ± 4.6%), 10 MOI (49.5 ± 2.4%), and 25 MOI (25.6 ± 2.1%) (Figure 1B). In Huh-7 cells, there was a decrease in FDPS

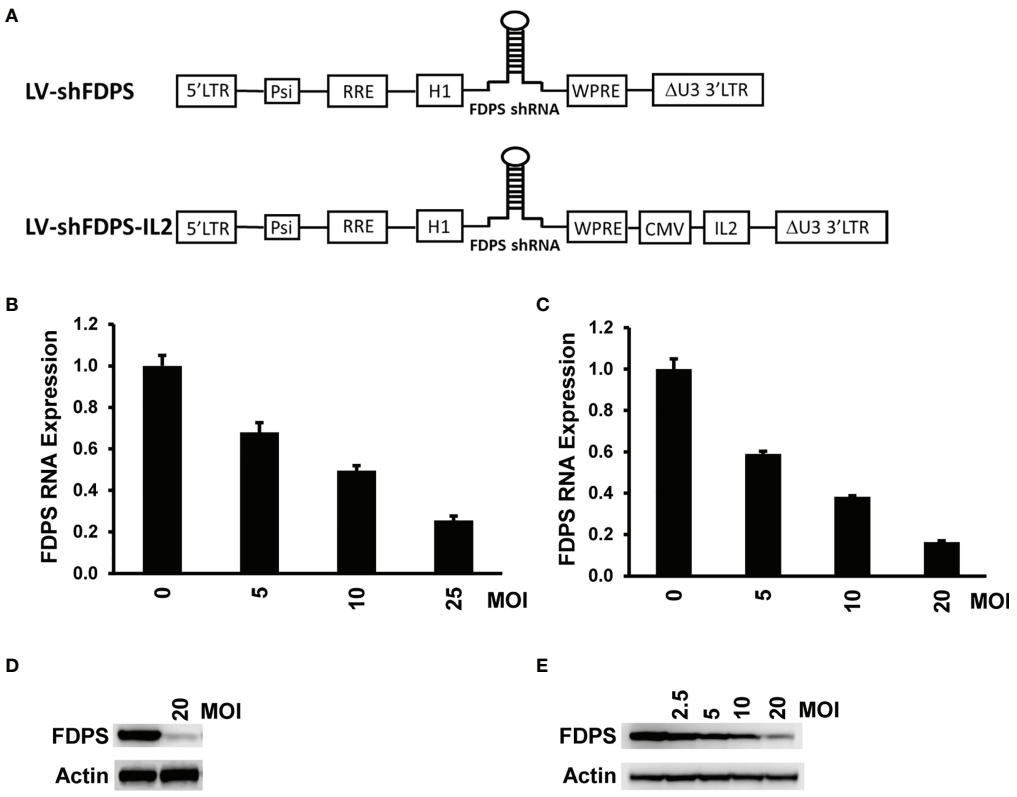

FIGURE 1
A lentivirus expressing a short-hairpin RNA (shRNA) targeting farnesyl diphosphate synthase (FDPS) reduces its expression in cancer cells. **(A)** Schematic diagram of the lentivirus vectors LV-shFDPS and LV-shFDPS-IL2. Additionally, the vectors may express the luciferase and GFP gene. **(B, C)** Real-time qPCR analysis of FDPS RNA from PC3 prostate and Huh-7 hepatocellular carcinoma cells transduced with LV-shFDPS at a MOI of 5, 10, and 20 or 25. In PC3 cells at a MOI of 25, FDPS expression was reduced by 74% and in Huh-7 cells at a MOI of 20, FDPS expression was reduced by 84%. **(D, E)** Immunoblot analysis of FDPS protein from PC3 and Huh-7 cells transduced with LV-shFDPS.

mRNA at 5 MOI (59.1 ± 1.2%), 10 MOI (38.2 ± 0.6%), and 20 MOI (16.3 ± 0.7%) (Figure 1C). FDPS protein expression was similarly reduced in a dose-dependent manner in PC3 and Huh-7 cells, respectively (Figures 1D, E). These results showed that LV-shFDPS specifically targeted FDPS mRNA resulting in a reduction in both mRNA and protein levels. IL2 is an important cytokine forVδ2 T cell activation and proliferation, therefore we generated another lentiviral vector expressing both shFDPS and secretory human IL2 and showed it also reduced FDPS mRNA and protein in a dose-dependent manner in PC3 cells (Figure 1A lower panel; Supplementary Figure 4).

Vδ2 T cell cytotoxicity against PC3 and Huh-7 cancer cell lines transduced with the lentiviral vector LV-shFDPS and treated with zoledronic acid (ZA)

To determine whether transduction of cancer cells with the lentiviral vector LV-shFDPS can activate Vδ2 T cells, we measured cytokine production and cell lysis by Vδ2 T cells co-cultured with LV-shFDPS transduced PC3 and Huh-7 cells. Activation of Vδ2 T cells was indicated by increased production of the proinflammatory cytokines IFNγ or TNFα. PC3 or Huh-7 cells were transduced with either LV-shFDPS or LV-Control (LV) for 48 h followed by ZA (1 μM) treatment for 24 h. The ZA dose of 1 μM was used because this is in the range of vivo bioavailability (50). The cell lines were co-cultured with Vδ2 T cells for 4 h and analyzed subsequently for Vδ2 and TNFα expression. By gating IFNγ positive cells among the Vδ2 population, activation of Vδ2 T cells was indicated by IFNγ expression. In PC3 cells, the percentage of IFNγ producing cells was 9.59 (LV (control vector) + ZA), 1.28 (LV-shFDPS) and 30.9 (LV-shFDPS + ZA) (Figure 2A upper panel).

In Huh-7 cells, the percent positive of IFNγ producing cells was 38.9 (LV + ZA), 49.3 (LV-shFDPS), and 76.3 (LV-shFDPS + ZA) (Figure 2A lower panel). Donor-specific variation was controlled by testing expanded Vδ2 T cells (60-80%) from multiple, unrelated donors. The activity of LV-shFDPS and ZA treatment was evaluated by co-culture of Vδ2 T cells with PC3 and Huh-7 cells for 4 h, followed by flow cytometry analysis for Vδ2 and TNFα expression. The data represents a summary of assays using Vδ2 T cells from multiple donors (PC3, N=56; Huh-7, N=39). Each dot represents the percentage of Vδ2 and TNFα positive cells from an individual donor. In PC3 cells, the average percent positive of TNFα producing cells was 12 ± 10.9% (LV + ZA), 4.8 ± 4.3% (LV-shFDPS), and 38.6 ± 16.3% (LV-shFDPS + ZA) (Figure 2B). In Huh-7 cells, the average percentage of cells positive for TNFα expression was 16.1± 15.9% (LV + ZA), 20 ± 10.8% (LV-shFDPS), and 36.9± 23.1% (LV-shFDPS + ZA) (Figure 2C). The results show that treatment of PC3 and Huh-7 cells with either LV-shFDPS or ZA alone was insufficient to fully activate Vδ2 T cells and the highest levels of cell activation occurred with the combined treatments. Similar results were seen with HepG2, MDA-MB-231, MiaPaCa, A549, and FaDu cells (Supplementary Figure 2).

The cytolytic activity of Vδ2 T cells by LV-shFDPS and ZA treatment of PC3 and Huh-7 cells was tested using a Calcein AM assay. PC3 or Huh-7 cells were treated with LV-shFDPS or ZA alone or in combination and then loaded with Calcein AM before incubating with Vδ2 T cells in various effector to target ratios (E: T) for 4 h. The supernatant from these co-cultures was evaluated for the presence of Calcein AM, which is indicative of tumor cell lysis. The results were analyzed, and the percent specific lysis values were calculated. At an E:T ratio of 2.5:1 for Vδ2 T cells to PC3 cells, the percent lysis was 22.2 ± 1.1% (LV), 45.1 ± 1.4% (LV + ZA), 38.8 ± 2.8% (LV-shFDPS), and 70.9 ± 3.1% (LV-shFDPS + ZA) (Figure 2D). At an E:T ratio of 2.5:1 for Vδ2 T cells to Huh-7 cells, % lysis was 15.6 ± 5.6% (LV), 31.0 ± 1.0% (LV + ZA), 37.3 ± 1.4% (LV-shFDPS), and 48.4 ± 6.1% (LV-shFDPS + ZA) (Figure 2E). Vδ2 T cells showed the highest cytokine production and cytotoxicity against PC3 and Huh-7 cells treated with both LV-shFDPS and ZA as compared with each alone.

The effect of Vδ2 T cells on PC3 tumors modified by the lentiviral vector LV-shFDPS in immunodeficient mice

A xenotransplant mouse tumor model using NSG immunodeficient mice was used to evaluate the anti-tumor activity of Vδ2 T cells against PC3 tumors transduced with LV-shFDPS at an MOI of 5. PC3 cells were injected into the flanks of mice and grown to a size of 200-300 mm^3. Expanded Vδ2 T cells (6-10 X $10^{6)}$ were injected weekly by intraperitoneal (IP) delivery. One group of mice additionally received ZA injections also given by IP. Mice were monitored for health and tumor volume was measured twice weekly until conclusion of the study. LV-shFDPS transduced tumors grew slower than the LV-Control (LV) tumors, but at the end of the study reached a similar average tumor volume which was not significantly different (ns p=0.5967, N=8) (Figure 3A). PC3 cells transduced with LV-shFDPS significantly suppressed tumor growth with or without ZA treatment after Vδ2 T cell injections (* p=0.0155, ** p=0.0037, N=8). At the end of the study, 36 days post 1st Vδ2 injection, the average tumor volume for LV-shFDPS was 1680 ± 166 mm^3 which was reduced to 795 ± 193 mm^3 when combined with Vδ2 treatment (Figure 3A). Therefore, LV-shFDPS alone decreased the growth of PC3 tumors, but this was further increased when combined with Vδ2 T cells.

A Kaplan Meier survival analysis was done with the end point being the number of days after the initial injection of Vδ2 T cells before the tumor reached 2000 mm^3. There was a significant survival advantage in mice with PC3 tumors transduced with LV-shFDPS and treated with Vδ2 T cells as

10.3389/fimmu.2022.1012051

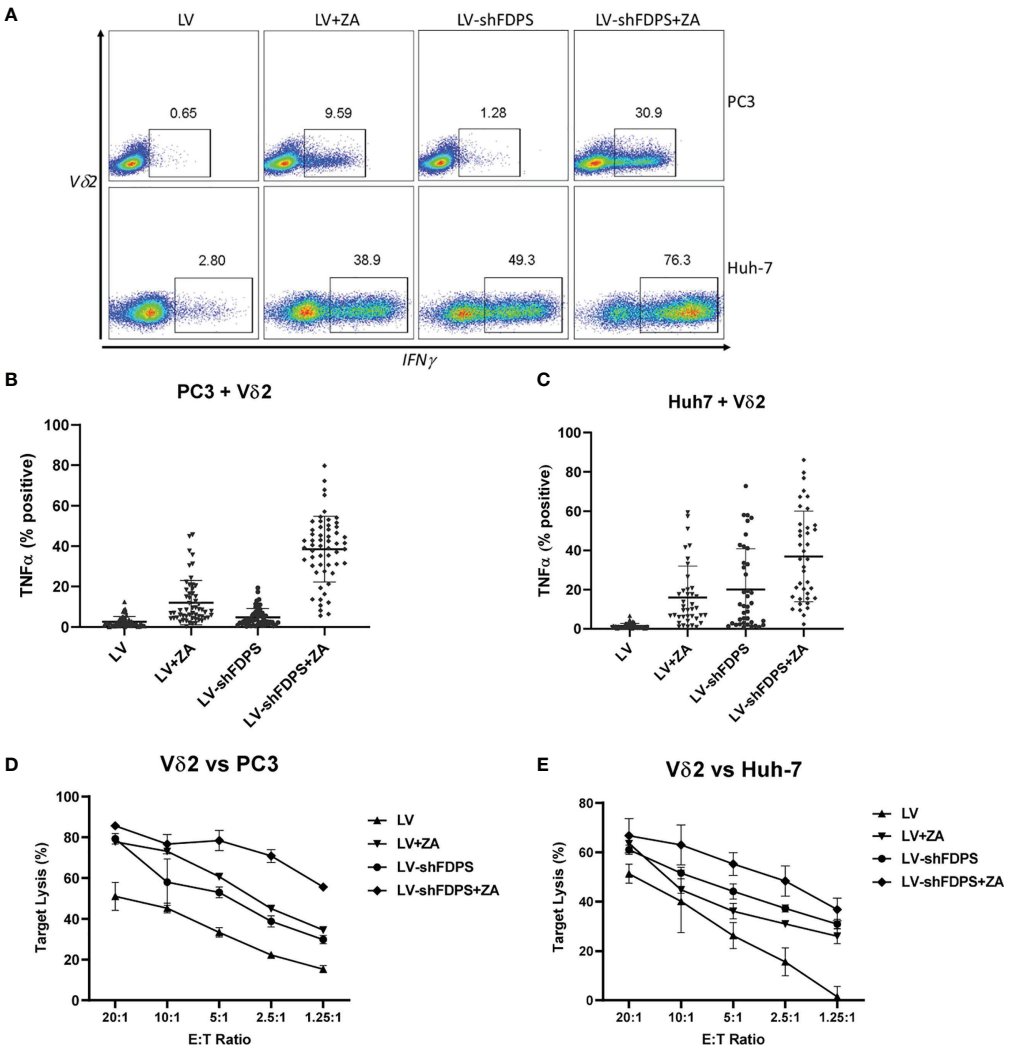

FIGURE 2
Vδ2 T cells increase cytokine production and cytotoxic activity when cultured with cancer cells treated with low-dose zoledronic acid (ZA) and transduced with shFDPS. **(A)** Representative flow cytometry dot plots from PC3 and Huh-7 cells transduced with LV-shFDPS in the presence or absence of ZA for overnight, followed by co-culture with Vδ2 T cells for 4 h. The gated region indicates the Vδ2 and IFNγ positive population. In PC3 cells, the percent positive of IFNγ producing cells was 9.59 (LV + ZA), 1.28 (LV-shFDPS), and 30.9 (LV-shFDPS + ZA). In Huh-7 cells, the percent positive of IFNγ producing cells was 38.9 (LV + ZA), 49.3 (LV-shFDPS), and 76.3 (LV-shFDPS + ZA). **(B, C)** LV-shFDPS transduced PC3 and Huh-7 cells were treated either with or without ZA for overnight, followed by co-culture with Vδ2 T cells for 4 h. The cells were analyzed by flow cytometry for Vδ2 and TNFα expression. The data represents a summary of assays using Vδ2 T cells from multiple donors (PC3, N=56; Huh-7, N=39). Each dots represents the percentage of Vδ2 and TNFα positive cells from an individual donor. In PC3 cells, the percent positive of TNFα producing cells was 12 ± 10.9% (LV + ZA), 4.8 ± 4.3% (LV-shFDPS), and 38.6 ± 16.3% (LV-shFDPS + ZA). In Huh-7 cells, the percent positive of TNFα producing cells was 16.1 ± 15.9% (LV + ZA), 20 ± 10.8% (LV-shFDPS), and 36.9 ± 23.1% (LV-shFDPS + ZA). **(D, E)** LV or LV-shFDPS transduced PC3 and Huh-7 were treated either with or without ZA for overnight as the target cells and labeled with calcein AM. This was followed by culturing the target cells with a serial dilution of Vδ2 effector cells in target ratios (E/T) for 4 h. All co-cultures were performed in triplicate. Cell lysis was measured by the level of fluorescent calcein AM detected in the supernatant.

compared with no Vδ2 T cells (**** $p<0.0001$, N=8) (Figure 3B). All mice with LV (control) transduced PC3 tumors with or without treatment of Vδ2 T cells had been euthanized by day 22. In mice implanted with LV-shFDPS transduced PC3 tumors, mice survived to day 44, and with Vδ2 T cell treatment all mice were still alive on day 60 (Figure 3B).

Since the lentiviral vectors used in this mouse study also carried the firefly luciferase gene, bioluminescence imaging could be used to monitor tumor growth. Bioluminescence images of LV-shFDPS transduced PC3 tumors were captured on days 11 and 28 after the initial injection of Vδ2 T cells (Figure 3C). By day 11, mice had been injected twice with Vδ2 T cells but there were no differences in photon levels between the

10.3389/fimmu.2022.1012051

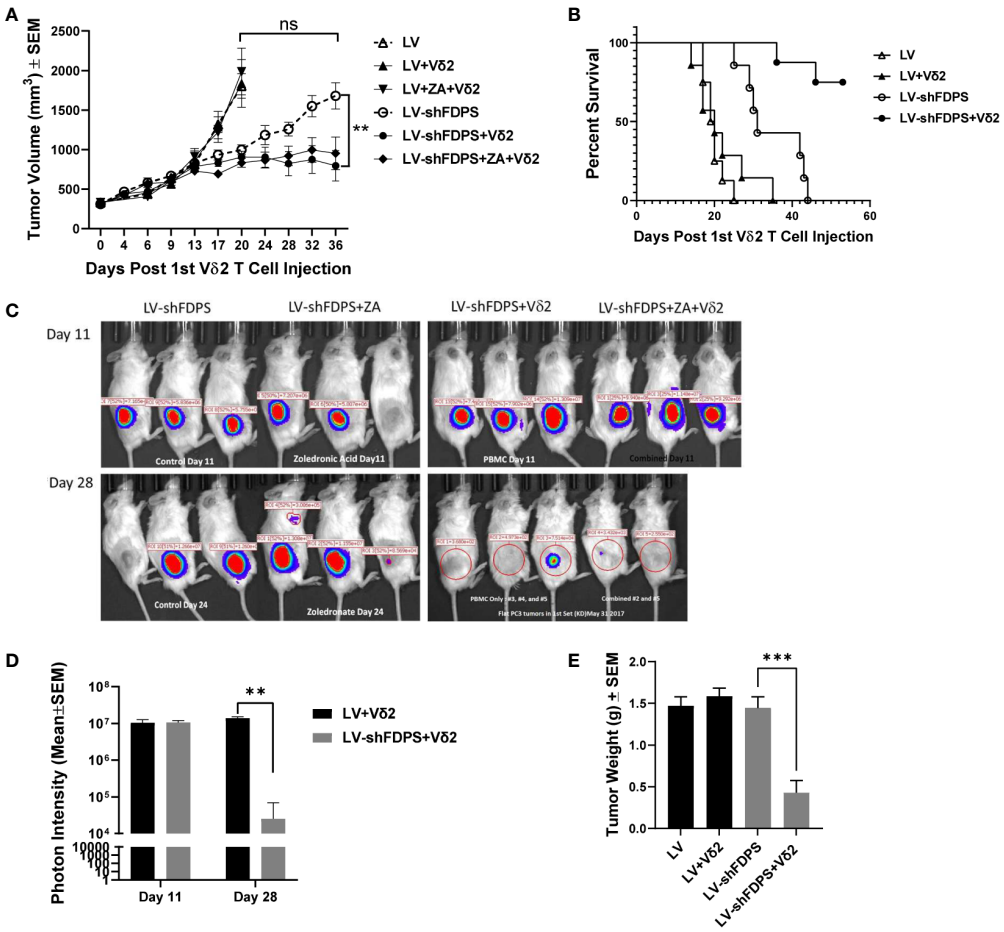

FIGURE 3
Vδ2 T cells suppress the growth of PC3 prostate carcinoma tumors transduced with a lentivirus expressing a shRNA targeting FDPS. **(A)** Vδ2 T cells significantly suppressed the growth of PC3 tumors transduced with LV-shFDPS as compared with LV (**p<0.0037, N=8). At the end of the study, 36 days post Vδ2 injection, the average tumor volume for LV-shFDPS was 1680 ± 166 mm^3 which was reduced to 795 ± 193 mm^3 when combined with Vδ2 treatment. There was minimal effect on tumor volume with ZA treatment with or without LV-shFDPS. **(B)** An analysis using a Kaplan-Meier survival curve was based on the end event being when the tumor size reached 2000 mm^3. There was a significant survival advantage in mice with PC3 tumors transduced with LV-shFDPS and treated with Vδ2 T cells as compared with no Vδ2 T cells (****$p < 0.0001$, N=8). All mice with LV transduced PC3 tumors with or without treatment of Vδ2 T cells were sacrificed up to day 22. In mice with LV-shFDPS transduced PC3 tumors, mice survived up to day 44, and with Vδ2 T cell treatment all mice survived up to day 60. **(C, D)** Mice were imaged for luciferase expression with a Xenogen IVIS200 bioluminescent imager. All tumor groups showed a similar photon intensity 11 days after the initial injection of Vδ2 T cells. On day 28, in the mice injected four times with Vδ2 T cells, the photon intensity of LV-shFDPS transduced PC3 tumors as compared with LV was significantly decreased from 1.4 X 10^7 to 2.5 X 10^4 photon units (**p=0.002, N=6). **(E)** Comparison of LV and LV-shFDPS transduced PC3 tumors in combination with Vδ2 T cell treatment. At the end of the study, each group of mice (N=7 or 8) were euthanized, tumors were extracted and weighed. In mice injected four times with Vδ2 T cells, the tumor weight of LV-shFDPS transduced PC3 tumors was significantly decreased as compared with LV from 1.5 to 0.5 g (***p=0.0002, N=8). ns, not significant.

LV and LV-shFDPS tumor groups. On day 28, the mice had been injected 4 times with Vδ2 T cells and there was a significant reduction in photon levels from 1.4 X 10^7 to 2.5 X 10^4 in the LV tumors compared with tumors bearing the LV-shFDPS (** p=0.002, N=6) (Figure 3D).

At the end of the study, all mice were sacrificed when PC3 tumors reached 2000 mm^3; tumors were collected and weighed. There were significantly lower weights for the LV-shFDPS tumors; from 1.5 to 0.5 g (3-fold decrease) in mice treated with Vδ2 T cells (*** p=0.0002, N=8) (Figure 3E). The results demonstrated that treatment of PC3 tumors with LV-shFDPS and Vδ2 T cells lead to PC3 tumor growth suppression. Tumors were also analyzed by flow cytometry for the presence of Vδ2 T cells. Vδ2 T cells were detected in both LV-shFDPS transduced tumors after an injection of 8 million Vδ2 T cells (Supplementary Figure 3).

10.3389/fimmu.2022.1012051

Effects of Interleukin-2 (IL2) on the anti-tumor activity of Vδ2 T cells against PC3 tumors modified by the lentiviral vector LV-shFDPS in immunodeficient mice

IL2 is used frequently to increase the activation and proliferation of Vδ2 T cells. We tested if adding an IL2 gene to LV-shFDPS and expressing both in a tumor cell line, would increase Vδ2 T cell activity in a coculture assay. PC3 cells were transduced with 5 MOI of LV-shFDPS-IL2 lentiviral vector and secreted IL2 was detected in cell culture medium by ELISA. The mean concentration of IL2 in culture medium was 52 ng/mL from 4 replicates as determined with a standard curve (Figure 4A). Next, we determined if LV-shFDPS-IL2 produced active IL2. We compared LV-shFDPS and LV-shFDPS-IL2 transduced PC3 cells for the ability to stimulate IFNγ expression in co-cultured Vδ2 T cells. The frequency of Vδ2 T cells expressing IFNγ was higher when tumor cells were cultured with LV-shFDPS-IL2 (16.6%) compared to tumor cells transduced with LV-shFDPS (10.7%) (Figure 4B).

Expressing IL2 from LV-shFDPS transduced PC3 tumors impacted the growth of tumors in NSG mice treated with Vδ2 T cells. Mice were inoculated with 3 X 10^6 LV-shFDPS or LV-shFDPS-IL2 transduced PC3 cells. Once tumor volumes reached 200-300 mm^3, each group of mice were distributed into two subgroups. One subgroup (N=8) was injected intraperitoneally with 6-10 X 10^6 Vδ2 T cells and the other group was injected with vehicle (N=8). One group of mice was injected with Vδ2 T cells once a week for a total of four weeks. Mouse body weights and tumor volumes were measured twice a week and the animals were euthanized when tumors reached 2000 mm^3 or at the end of the study. At the end of the study, 39 days after the 1st Vδ2 T cell injection, the average tumor volume for LV-shFDPS and LV-shFDPS-IL2 was 1835 ± 289 and 1900 ± 210 mm^3 which was reduced to 356 ± 140 mm^3 and 116 ± 55 mm^3 when combined with Vδ2 T cell treatment, respectively (Figure 4C). In mice treated with Vδ2 T cells, the growth of PC3 tumors transduced with LV-shFDPS or LV-shFDPS-IL2 were significantly suppressed compared with mice that did not receive Vδ2 T cells (**** p=0.0001, *** p=0.001, N=8) (Figure 4C). However,

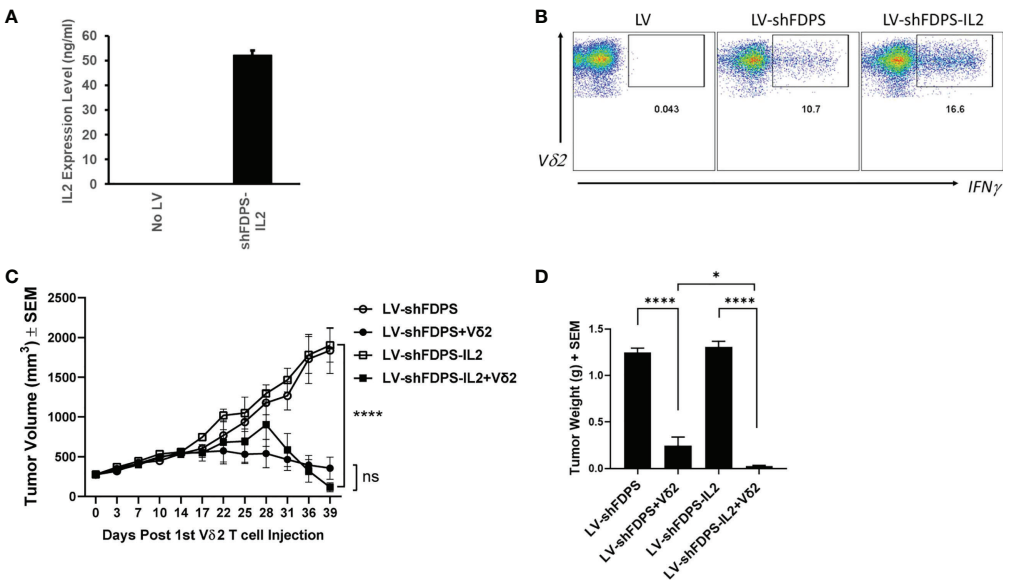

FIGURE 4
Vδ2 T cells suppress the growth of PC3 prostate carcinoma tumors transduced with a lentivirus expressing IL-2 and a shRNA targeting FDPS. **(A)** ELISA analysis of secreted IL2 expression by PC3 cells transduced with LV-shFDPS-IL2. **(B)** Representative flow cytometry dot plots from PC3 cells transduced with LV-shFDPS or LV-shFDPS-IL2, followed by co-culture with Vδ2 T cells for 4 h. The gated region indicates the Vδ2 and IFNγ positive population. The percent positive of IFNγ producing cells was 10.7 (LV-shFDPS) and 16.6 (LV-shFDPS-IL2). **(C)** Tumor volume of PC3 cells transduced with LV-shFDPS or shFDPS-IL2. In mice treated with Vδ2 T cells, the tumor volume of PC3 cells transduced with LV-shFDPS was significantly decreased at the end of the study from 1900 mm^3 to 356 mm^3 and with LV-shFDPS-IL2 from 1835 mm^3 to 116 mm^3 (****p=0.0001, ***p=0.001, N=8). There was no significant difference when comparing LV-shFDPS and LV-shFDPS-IL2 (ns p=0.743, N=8). **(D)** Comparison of LV, LV-shFDPS, and LV-shFDPS-IL2 transduced PC3 tumors in combination with Vδ2 T cell treatment. At the end of the study, each group of mice (N=8) were euthanized, tumors were extracted and weighed. There was a significant decrease in tumor weight of PC3 tumors transduced with LV-shFDPS when treated with Vδ2 T cells from 1.25 g to 0.23 g (5.5-fold decrease, ****p<0.0001, N=8). The addition of IL2 in the LV-shFDPS vector also significantly decreased tumor weight in mice treated with Vδ2 T cells as compared with LV-shFDPS-IL2 alone from 1.31 g to 0.04 g. There was also a significant 6-fold decrease in the tumor weight of LV-shFDPS-IL2 vs LV-shFDPS groups with Vδ2 T cells (* p=0.012, N=8). ns= not significant.

there was no significant difference in tumor volume when comparing LV-shFDPS and LV-FDPS-IL2 (ns p=0.743, N=8) (Figure 4C). Tumor weights were determined for excised tumors collected during necropsy. There was a significant decrease in tumor weight for the LV-shFDPS vs LV-shFDPS + Vδ2 groups from 1.25 to 0.23 g (5.5-fold decrease) and 1.31 to 0.04 g (32-fold decrease) for the LV-shFDPS-IL2 vs LV-shFDPS-IL2 + Vδ2 groups (**** p<0.0001, **** p<0.0001, N=8) (Figure 4D). There was also a significant 6-fold decrease in the tumor weight of LV-shFDPS-IL2 + Vδ2 vs LV-shFDPS + Vδ2 groups (* p=0.012, N=8) (Figure 4D). Therefore, IL2 enhanced Vδ2 T cell activity and suppressed the growth of PC3 tumors when FDPS expression was reduced by shRNA. Notably, 4 out of 8 mice bearing LV-shFDPS-IL2 modified tumors lost weight and died 3 weeks after the initial injection of Vδ2 T cells. The cause of death was suspected to be a form of tumor lysis syndrome, but the pathology was not definitive. Tumor volume measurements for the mice that died were included up to the point of death and only 4 surviving mice to the end of the study were included in the tumor weight measurements.

Effects of Vδ2 T cells on LV-shFDPS transduced Huh-7 tumors in immunodeficient mice

Next, we examined the effect Vδ2 T cells have on another xenotransplant model, this time using Huh-7 hepatocellular carcinoma tumor cells transduced with LV-shFDPS and implanted in NRG mice. The Huh-7 cells were transduced with either LV or LV-shFDPS and cells were injected into the flanks of NRG mice in the following numbers: 2 X 10^6 LV (N=10), 2 X 10^6 LV-shFDPS (N=10), or a 1:1 mixture of 1 X 10^6 LV + 1 X 10^6 LV-shFDPS (N=10; designated 50% transduced mice). A week after injection, all mice were injected once a week with 7 X 10^6 Vδ2 T cells by IP delivery and half of the mice received ZA treatment for 5 weeks. There was a significant decrease in tumor volume in mice with 100% LV-shFDPS transduced cells and treated with ZA as compared with LV transduced cells (** p=0.001, N=5) (Figure 5A). Additionally, there was a significant decrease in the volume of tumors containing 100% LV-shFDPS transduced cells without ZA as compared with LV transduced cells (* p=0.014, N=5) (Figure 5A). The tumor volumes in mice implanted with 100% LV-shFDPS transduced cells were significantly lower than in mice who received 50% transduced cells (* p=0.024, N=5) (Figure 5A). The Kaplan Meier survival curve was based upon the event when tumors reached 2000 mm^3. There was a significant survival advantage for mice with Huh-7 tumors transduced with LV-shFDPS as compared with LV in the presence of Vδ2 T cells (**** p<0.0001, N=5). Additionally, there was a significant survival advantage for mice with 100% versus 50% LV-shFDPS transduced tumors in the presence or absence of ZA. (** p=0.0089, ** p=0.0048, N=5). The survival curve showed that mice with LV transduced tumors were sacrificed 21 days after the initial injection of Vδ2 T cells and mice with 100% and 50% LV-shFDPS transduced tumors remained alive at the end of the study on day 37 (Figure 5B). At the end of the study, 23 days following the initial Vδ2 T cell injections, mice were euthanized, and tumors were removed and weighed. The average tumor weights were 2.3 ± 0.4 g (LV), 1.9 ± 0.2 g (50% LV-shFDPS) 1.6 ± 0.4 g (50% LV-FDPS + ZA), 1.0 ± 0.3 g (100% LV-shFDPS), and 0.4 ± 0.1 g (100% LV-FDPS + ZA) (Figure 5C). The tumor weights of the 100% LV-shFDPS and 100% LV-shFDPS + ZA group were significantly decreased by 2.3 and 5.75-fold, respectively, compared with LV (* p=0.045, ** p=0.003, N=5) (Figure 5C). The tumor weights of the 100% LV-shFDPS + ZA group also showed a significant decrease compared with 50% LV-shFDPS + ZA (* p=0.0237, N=5) (Figure 5C). In rough terms, the therapeutic effects among animals with 50% transduced tumors were half the levels observed for animals with 100% uniformly transduced tumors.

Effects of Vδ2 T cells on Huh-7 tumors by intra-tumoral (IT) injection of LV-shFDPS

The possibility of using a lentiviral vector for *in vivo* treatment of human cancer will depend on the efficiency of IT injection. To mimic the clinical procedure, we performed a pilot experiment using intratumoral (IT) injection of LV-shFDPS in Huh-7 tumors in combination with Vδ2 T cells. NSG mouse were injected subcutaneously with 2 X 10^6 Huh-7 cells in the right flank. Three weeks after injection, the average tumor sizes ranged from 100-900 mm^3; mice were placed into two groups with roughly equal distribution of starting tumor sizes. One group of tumors (N=8) were injected daily with 60 µL of LV and the other group (N=8) with 60 µL of LV-shFDPS for three consecutive days. Five days after IT injection of LV or LV-shFDPS, mice were injected with 7 X 10^6 Vδ2 T cells twice a week for a total of 4 weeks. Although the LV-shFDPS tumors (1934 ± 181 mm^3) grew slower than LV tumors (2785 ± 447. mm^3), the overall tumor volume showed no significant differences between LV and LV-shFDPS at the end of the study (ns p=0.108, N=8) (Figure 5D). It may be due to an insufficient amount of LV-shFDPS injected into the tumors that the effect of treatment on tumor growth with Vδ2 T cells was limited. Since LV and LV-shFDPS contain the luciferase gene, the injected lentiviral vector could be detected by bioluminescence imaging. Bioluminescent imaging demonstrated that tumors injected with LV-shFDPS showed an average decrease in photon intensity from 8.8 X 10^6 to 5.6 X 10^6 from day 34 to day 42 but this was not significant (ns p=0.107, N=8) (Figure 5E).

10.3389/fimmu.2022.1012051

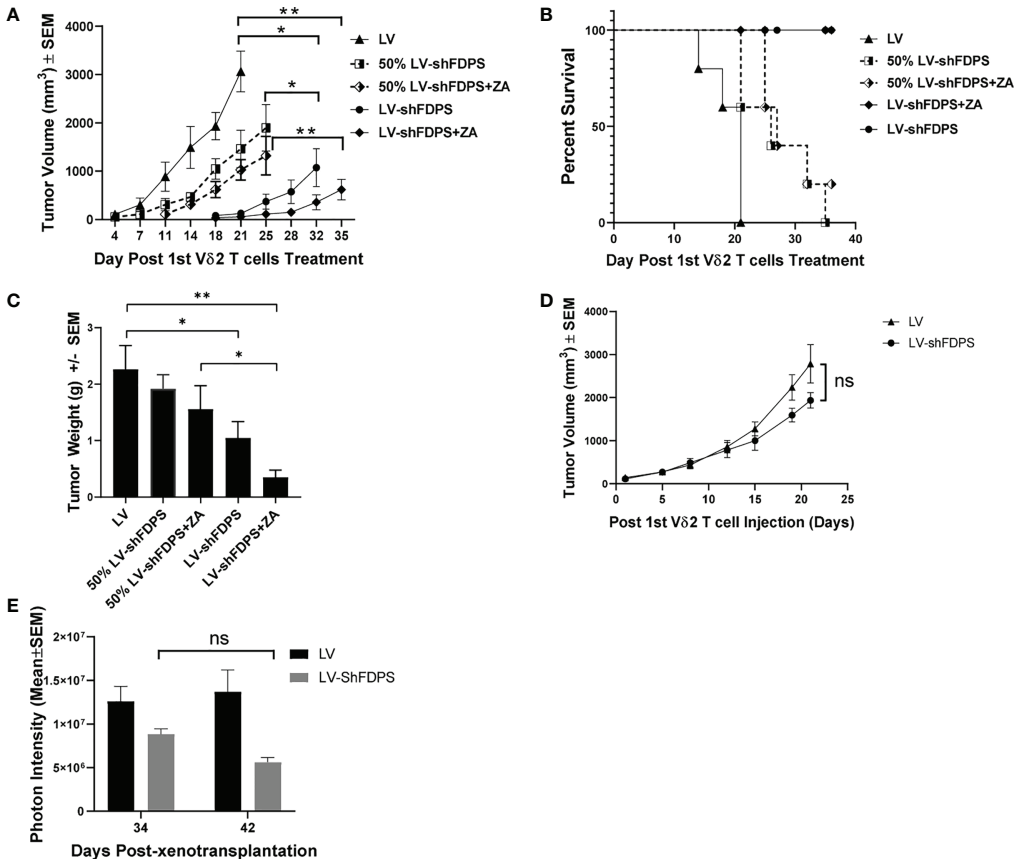

FIGURE 5
Vδ2 T cells suppress the growth of Huh-7 hepatocellular tumors transduced with a lentivirus expressing a shRNA targeting FDPS. **(A)** Tumor volume in mice with LV, 100% LV-shFDPS or 50% LV-shFDPS transduced Huh-7 cells in the presence or absence of ZA. The tumor volume of 100% LV-shFDPS and 50% LV-shFDPS tumors was decreased as compared with LV tumors in the presence or absence of ZA. There was a significant decrease in tumor volume in mice with 100% LV-shFDPS and treated with ZA or without ZA as compared with LV tumors (** p=0.001, *p=0.014, N=5). The tumor volumes in mice implanted with 100% LV-shFDPS transduced cells were significantly lower than in mice who received 50% transduced cells (*p=0.024, N=5). **(B)** A Kaplan-Meier survival curve of mice which were transplanted with LV, LV-shFDPS, or 50% LV-shFDPS transduced Huh-7 cells in the presence or absence of ZA. Each group of mice (N=5) was euthanized when tumors reached 2000 mm^3. The survival of mice with LV transduced tumors was reduced versus mice with LV-shFDPS and 50% LV-shFDPS transduced tumors in the presence or absence of ZA. There was a significant survival advantage for mice with Huh-7 tumors transduced with LV-shFDPS as compared with LV (****p<0.0001, N=5). Additionally, there was a significant survival advantage for mice with 100% versus 50% LV-shFDPS transduced tumors in the presence or absence of ZA. (**p=0.0089, **p=0.0048, N=5). **(C)** Tumor weight of mice with LV, 100% LV-shFDPS or 50% LV-shFDPS transduced Huh-7 cells in the presence or absence of ZA. Each group of mice (N=5) were euthanized and tumors were extracted and weighed. The tumor weight of 100% LV-shFDPS and 50% LV-shFDPS tumors was decreased versus LV tumors in the presence and absence of ZA. The tumor weights of the 100% LV-shFDPS and 100% LV-shFDPS + ZA group were significantly decreased by 2.3 and 5.75-fold, respectively, compared with LV (* p=0.045, ** p=0.003, N=5). The tumor weights of the 100% LV-shFDPS + ZA group also showed a significant decrease compared with 50% LV-shFDPS + ZA (* p=0.0237, N=5). **(D)** Volume of Huh-7 tumors in mice injected intratumorally with LV and LV-shFDPS. At the end of the study, 22 days post Vδ2 injections, the tumor volume decreased from 2785 ± 181 mm^3 to 1934 ± 447 mm^3 in LV versus LV-shFDPS injected tumors (ns p=0.108, N=8). **(E)** Mice were imaged for luciferase expression with a Xenogen IVIS200 bioluminescent imager. The photon intensity of tumors injected with LV was not significantly different from day 34 to 42 after treatment with Vδ2 T cells, whereas there was a decrease in the photon intensity of tumors injected with LV-shFDPS from 8.8 X 10^6 to 5.6 X 10^6 from day 34 to 42 (ns p=0.107, N=8). ns, not significant.

Discussion

A distinguishing feature of human Vδ2 T cells is the capacity for T cell receptor-dependent sensing of metabolic changes in malignant tissues, specifically the upregulation of mevalonate pathway flux signaled by increased levels of IPP. Several groups have appreciated the potential for exploiting the unique specificity of Vδ2 T cells for cancer therapy. Here, we explored the potential for enhanced recognition and destruction of tumors following direct genetic manipulation of tumor cells to increase IPP levels. We demonstrated significantly enhanced potency of Vδ2 T cells from healthy donors for suppressing growth of genetically modified as compared to unmodified tumor cells *in vivo*. We further

demonstrated the dose dependence of Vδ2 T cell tumor suppression, by varying the proportion of tumor cells expressing shFDPS needed to increase IPP levels. The inefficient suppression of tumor growth after intratumoral injection of the lentivirus vector may be a further demonstration of dose dependency, although the pilot studies presented here are not conclusive. Lastly, we confirmed that dual targeting of FDPS activity, by reducing mRNA and protein levels plus adding the competitive enzyme inhibitor zoledronic acid, increased the potency for Vδ2 T cells suppression of tumor cell growth. These findings provide insight into the possibility of combining genetic and small molecule therapies with, *ex vivo* expanded Vδ2 T cells, in a cancer therapy regimen.

There are several limitations to these studies. While group sizes were generally sufficient at 8-10 mice per group, we did not explore a broad range of mixed tumors (cells with or without shFDPS expression) and definitive conclusions about the relationship between vector dose and tumor suppression are not warranted at this time. Experiments with lentivirus vectors expressing both shFDPS and IL2 were limited in numbers and the precise cause of animal deaths was uncertain, although we note that the vector construct was not toxic as animal deaths occurred only after infusing Vδ2 T cells. In this context we did not test mixtures of individual vectors (LV-shFDPS + LV-shFDPS-IL2 in varying ratios) to see whether a lower proportion of IL2 producing tumor cells would support Vδ2 T cells effects without the associated toxicity. Finally, the intratumoral injection pilot studies are likely to require multiple repetitions and perhaps alternate delivery sites or methods.

Our key findings are that genetic manipulation of tumor cells increases the potential for Vδ2 T cell activation and tumor suppression *in vivo*. Tumor suppression occurred in the absence of IL-2 treatment, although co-expressing IL-2 with shFDPS on the same vector appears to have increased potency. Dual targeting of FDPS activity, using LV-shFDPS plus ZA increased tumor suppression but the added benefit of adding ZA was modest compared to what was observed for dual targeting *in vitro*.

Several published studies explored the effects of N-bisphosphonate (NBP) treatment in combination with Vδ2 T cells in mouse models. For example, Kabelitz et al. tested whether NBP alendronate plus IL2 suppressed the growth of the melanoma cell line MeWo in NSG mice treated with Vδ2 T cells (46). Santolaria et al. tested the NBP pamidronate plus Vδ2 T cells on the prostate adenocarcinoma cell line PC3 in NSG mice (51). These studies demonstrated decreased tumor growth when Vδ2 T cells were administered to NBP treated mice and the effect was greater with repeated treatment of both NBP and Vδ2 T cells. The therapeutic effect of Vδ2 T cells on LV-shFDPS modified PC3 or Huh-7 tumors was at least as potent as treating mice with Vδ2 T cells and alendronate plus IL-2 (46) or pamidronate (51). In most cases, mouse survival was better and tumor weights were reduced more in mice with LV-shFDPS modified tumors treated with Vδ2 T cells; with or without the NBP zoledronic acid had little impact on tumor growth and mouse survival.

The cytokine IL2 stimulates expansion and Vδ2 T cell cytotoxic activity. We observed that PC3 cells transduced with LV-shFDPS-IL2 as compared with LV-shFDPS stimulated more IFNγ production. Additionally the growth of PC3 tumors with LV-shFDPS-IL2 was decreased as compared with LV-FDPS in combination with Vδ2 T cells. However, we observed weight loss in some mice with LV-FDPS-IL2 transduced tumors, which may be caused by a supraphysiological level of circulating IL2 in the mice. In mice injected with a mixture of cells, 50% LV-FDPS-IL2 + 50% LV, there was no weight loss or deaths observed (data not shown). This suggests that the optimum level of IL2 can enhance the activity of Vδ2 T cell activity without causing toxicity. In the current vector, IL2 expression is being controlled by the strong CMV promoter, but weaker promoters or promoter regulatory units could be engineered into the vector for future studies.

Several groups have conducted exploratory clinical trials to evaluate the potential for activating Vδ2 T cells for cancer therapy. Zoledronic acid plus IL-2 therapy was tested in male patients with hormone-refractory prostate cancer (23). A similar approach was used to treat patients with advanced renal cell carcinoma (52) along with many other studies summarized in recent reviews. Recent reports evaluated Vδ2 T cell therapies providing positive outcomes in late-stage lung or liver cancer (53), treatment refractory lung cancer (54), cholangiocarcinoma (55), and gastric carcinoma (56). A meta-analysis of 13 clinical trials involving Vδ2 T cell therapy, either adoptive transfer of ex vivo expanded Vδ2 T cells or *in vivo* activation of these cells using PAg or bisphosphonate compounds, showed a significant event rate for Vδ2 T cell therapies and no significant association with severe adverse events (57). These studies affirm an overall view that Vδ2 T cell therapies involving ex vivo or *in vivo* cell activation and expansion, can provide positive therapeutic benefit but overall have modest potency.

Our approach was to improve upon these preclinical results by genetically targeting FDPS to further increase IPP levels in tumor cells and promote their subsequent destruction by Vδ2 T cells (41). Thus, we are exploring the utility of a new tool for manipulating the Vδ2 T cell capacity for tumor suppression and believe it can be combined with PAg or bisphosphonate stimulation, IL-2 treatment and ex vivo expanded autologous or allogeneic effector cells in a continuing effort to develop potent treatment strategies.

Several major obstacles must be overcome to realize the potential for gamma delta T cell-based cancer therapy. Use of bisphosphonates drugs for *in vivo* stimulation of Vδ2 T cells is inefficient, possibly due to the unusual pharmacodynamics of these drugs which precipitate in bone (58, 59) and cytokine supplementation, using IL-2 or others, has inherent toxicity.

Activating Vδ2 T cells by targeting butyrophilin complexes on tumor cell membranes is an area of intense interest (60, 61) and has potential for combining with a genetic approach to achieve higher potency for tumor cell killing. The value for genetic modification of tumor cells was demonstrated in our studies but we recognize the potential for alternative approaches based on the same underlying concept of decreasing FDPS enzyme activity in tumor cells. Alternate approaches might involve the use of tumor-specific oncoviruses expressing the shRNA specific for FDPS, and direct delivery of shRNA to tumor cells is another possibility for increasing treatment potency. By modifying tumor cells through multiple, concurrent methods including genetic modification, drug treatment and agonist antibodies or antibody-like molecules, we hope to increase potency and fully operationalize the power of Vδ2 T cells and their capacity for broad recognition of multiple tumor types.

Data availability statement

The raw data supporting the conclusions of this article will be made available by the authors, without undue reservation.

Ethics statement

The animal study was reviewed and approved by University of Maryland School of Medicine-Institutional Review Board.

Author contributions

M-LL is the first author of the manuscript, designed, performed, and analyzed the *in vivo* studies and cellular assays, and wrote the initial version of the paper; TL is a shared first author of the manuscript, supervised the project, contributed to molecular and cellular assays, data analysis, and revision and preparation of the manuscript; HL contributed to study design and cellular assays; LX contributed to molecular assays; CDP supervised the project and contributed to revising the main text of the manuscript; TL is the corresponding author of the manuscript. All authors contributed to the article and approved the submitted version.

Conflict of interest

The authors M-LL, TL, and LX are employed by American Gene Technologies and HL and CDP are former employees of American Gene Technologies and currently employed by Viriom, Inc.

Publisher's note

All claims expressed in this article are solely those of the authors and do not necessarily represent those of their affiliated organizations, or those of the publisher, the editors and the reviewers. Any product that may be evaluated in this article, or claim that may be made by its manufacturer, is not guaranteed or endorsed by the publisher.

Supplementary material

The Supplementary Material for this article can be found online at: https://www.frontiersin.org/articles/10.3389/fimmu.2022.1012051/full#supplementary-material

References

1. Hayday AC. [gamma][delta] cells: a right time and a right place for a conserved third way of protection. *Annu Rev Immunol* (2000) 18:975–1026. doi: 10.1146/annurev.immunol.18.1.975

2. Sturm E, Braakman E, Fisch P, Vreugdenhil RJ, Sondel P, Bolhuis RL. Human V gamma 9-V delta 2 T cell receptor-gamma delta lymphocytes show specificity to daudi burkitt's lymphoma cells. *J Immunol* (1990) 145(10):3202–8.

3. Halary F, Pitard V, Dlubek D, Krzysiek R, de la Salle H, Merville P, et al. Shared reactivity of V{delta}2(neg) {gamma}{delta} T cells against cytomegalovirus-infected cells and tumor intestinal epithelial cells. *J Exp Med* (2005) 201(10):1567–78. doi: 10.1084/jem.20041851

4. Hintz M, Reichenberg A, Altincicek B, Bahr U, Gschwind RM, Kollas AK, et al. Identification of (E)-4-hydroxy-3-methyl-but-2-enyl pyrophosphate as a major activator for human gammadelta T cells in escherichia coli. *FEBS Lett* (2001) 509(2):317–22. doi: 10.1016/S0014-5793(01)03191-X

5. Wesch D, Marx S, Kabelitz D. Comparative analysis of alpha beta and gamma delta T cell activation by mycobacterium tuberculosis and isopentenyl pyrophosphate. *Eur J Immunol* (1997) 27(4):952–6. doi: 10.1002/eji.1830270422

6. Wang H, Sarikonda G, Puan KJ, Tanaka Y, Feng J, Giner JL, et al. Indirect stimulation of human Vgamma2Vdelta2 T cells through alterations in isoprenoid metabolism. *J Immunol* (2011) 187(10):5099–113. doi: 10.4049/jimmunol.1002697

7. Gober HJ, Kistowska M, Angman L, Jeno P, Mori L, De Libero G. Human T cell receptor gammadelta cells recognize endogenous mevalonate metabolites in tumor cells. *J Exp Med* (2003) 197(2):163–8. doi: 10.1084/jem.20021500

8. Harly C, Guillaume Y, Nedellec S, Peigne CM, Monkkonen H, Monkkonen J, et al. Key implication of CD277/butyrophilin-3 (BTN3A) in cellular stress sensing by a major human gammadelta T-cell subset. *Bloodγ* (2012) 120(11):2269–79. doi: 10.1182/blood-2012-05-430470

9. Palakodeti A, Sandstrom A, Sundaresan L, Harly C, Nedellec S, Olive D, et al. The molecular basis for modulation of human Vgamma9Vdelta2 T cell responses by CD277/butyrophilin-3 (BTN3A)-specific antibodies. *J Biol Chem* (2012) 287 (39):32780–90. doi: 10.1074/jbc.M112.384354

10. Gu S, Sachleben JR, Boughter CT, Nawrocka WI, Borowska MT, Tarrasch JT, et al. Phosphoantigen-induced conformational change of butyrophilin 3A1 (BTN3A1) and its implication on Vgamma9Vdelta2 T cell activation. *Proc Natl Acad Sci U S A.* (2017) 114(35):E7311–E20. doi: 10.1073/pnas.1707547114

11. Yang Y, Li L, Yuan L, Zhou X, Duan J, Xiao H, et al. A structural change in butyrophilin upon phosphoantigen binding underlies phosphoantigen-mediated Vgamma9Vdelta2 T cell activation. *Immunityγ* (2019) 50(4):1043–53 e5. doi: 10.1016/j.immuni.2019.02.016

12. Vavassori S, Kumar A, Wan GS, Ramanjaneyulu GS, Cavallari M, El Daker S, et al. Butyrophilin 3A1 binds phosphorylated antigens and stimulates human gammadelta T cells. *Nat Immunol* (2013) 14(9):908–16. doi: 10.1038/ni.2665

13. Thurnher M, Nussbaumer O, Gruenbacher G. Novel aspects of mevalonate pathway inhibitors as antitumor agents. *Clin Cancer Res* (2012) 18(13):3524–31. doi: 10.1158/1078-0432.CCR-12-0489

14. Freed-Pastor WA, Mizuno H, Zhao X, Langerod A, Moon SH, Rodriguez-Barrueco R, et al. Mutant p53 disrupts mammary tissue architecture *via* the mevalonate pathway. *Cellγ* (2012) 148(1-2):244–58. doi: 10.1016/j.cell.2011.12.017

15. Silva-Santos B, Serre K, Norell H. Gammadelta T cells in cancer. *Nat Rev Immunol* (2015) 15(11):683–91. doi: 10.1038/nri3904

16. Kato Y, Tanaka Y, Miyagawa F, Yamashita S, Minato N. Targeting of tumor cells for human gammadelta T cells by nonpeptide antigens. *J Immunol* (2001) 167 (9):5092–8. doi: 10.4049/jimmunol.167.9.5092

17. Kabelitz D, Wesch D, Pitters E, Zoller M. Potential of human gammadelta T lymphocytes for immunotherapy of cancer. *Int J Cancer.* (2004) 112(5):727–32. doi: 10.1002/ijc.20445

18. Holmen Olofsson G, Idorn M, Carnaz Simoes AM, Aehnlich P, Skadborg SK, Noessner E, et al. Vgamma9Vdelta2 T cells concurrently kill cancer cells and cross-present tumor antigens. *Front Immunol* (2021) 12:645131. doi: 10.3389/fimmu.2021.645131

19. Song Y, Liu Y, Teo HY, Liu H. Targeting cytokine signals to enhance gammadeltaT cell-based cancer immunotherapy. *Front Immunol* (2022) 13:914839. doi: 10.3389/fimmu.2022.914839

20. Cairo C, Surendran N, Harris KM, Mazan-Mamczarz K, Sakoda Y, Diaz-Mendez F, et al. Vgamma2Vdelta2 T cell costimulation increases NK cell killing of monocyte-derived dendritic cells. *Immunologyγ* (2014) 144, 422–30. doi: 10.1111/imm.12386

21. Kabelitz D, Serrano R, Kouakanou L, Peters C, Kalyan S. Cancer immunotherapy with gammadelta T cells: many paths ahead of us. *Cell Mol Immunol* (2020) 17(9):925–39. doi: 10.1038/s41423-020-0504-x

22. Cordova A, Toia F, La Mendola C, Orlando V, Meraviglia S, Rinaldi G, et al. Characterization of human gammadelta T lymphocytes infiltrating primary malignant melanomas. *PloS One* (2012) 7(11):e49878. doi: 10.1371/journal.pone.0049878

23. Dieli F, Vermijlen D, Fulfaro F, Caccamo N, Meraviglia S, Cicero G, et al. Targeting human {gamma}delta} T cells with zoledronate and interleukin-2 for immunotherapy of hormone-refractory prostate cancer. *Cancer Res* (2007) 67 (15):7450–7. doi: 10.1158/0008-5472.CAN-07-0199

24. Meraviglia S, Eberl M, Vermijlen D, Todaro M, Buccheri S, Cicero G, et al. *In vivo* manipulation of Vgamma9Vdelta2 T cells with zoledronate and low-dose interleukin-2 for immunotherapy of advanced breast cancer patients. *Clin Exp Immunol* (2010) 161(2):290–7. doi: 10.1111/j.1365-2249.2010.04167.x

25. Dudley ME, Wunderlich JR, Yang JC, Sherry RM, Topalian SL, Restifo NP, et al. Adoptive cell transfer therapy following non-myeloablative but lymphodepleting chemotherapy for the treatment of patients with refractory metastatic melanoma. *J Clin Oncol* (2005) 23(10):2346–57. doi: 10.1200/JCO.2005.00.240

26. Bouet-Toussaint F, Cabillic F, Toutirais O, Le Gallo M, Thomas de la Pintiere C, Daniel P, et al. Vgamma9Vdelta2 T cell-mediated recognition of human solid tumors. potential for immunotherapy of hepatocellular and colorectal carcinomas. *Cancer Immunol Immunother.* (2008) 57(4):531–9. doi: 10.1007/s00262-007-0391-3

27. Kang N, Zhou J, Zhang T, Wang L, Lu F, Cui Y, et al. Adoptive immunotherapy of lung cancer with immobilized anti-TCRgammadelta antibody-expanded human gammadelta T-cells in peripheral blood. *Cancer Biol Ther* (2009) 8(16):1540–9. doi: 10.4161/cbt.8.16.8950

28. Corvaisier M, Moreau-Aubry A, Diez E, Bennouna J, Mosnier JF, Scotet E, et al. V Gamma 9V delta 2 T cell response to colon carcinoma cells. *J Immunol* (2005) 175(8):5481–8. doi: 10.4049/jimmunol.175.8.5481

29. Wilhelm M, Kunzmann V, Eckstein S, Reimer P, Weissinger F, Ruediger T, et al. Gammadelta T cells for immune therapy of patients with lymphoid malignancies. *Bloodγ* (2003) 102(1):200–6. doi: 10.1182/blood-2002-12-3665

30. Laplagne C, Ligat L, Foote J, Lopez F, Fournie JJ, Laurent C, et al. Self-activation of Vgamma9Vdelta2 T cells by exogenous phosphoantigens involves TCR and butyrophilins. *Cell Mol Immunol* (2021) 18(8):1861–70. doi: 10.1038/s41423-021-00720-w

31. Tokuyama H, Hagi T, Mattarollo SR, Morley J, Wang Q, So HF, et al. V Gamma 9 V delta 2 T cell cytotoxicity against tumor cells is enhanced by monoclonal antibody drugs–rituximab and trastuzumab. *Int J Cancer.* (2008) 122(11):2526–34. doi: 10.1002/ijc.23365

32. Kavanagh KL, Guo K, Dunford JE, Wu X, Knapp S, Ebetino FH, et al. The molecular mechanism of nitrogen-containing bisphosphonates as antiosteoporosis drugs. *Proc Natl Acad Sci U S A.* (2006) 103(20):7829–34. doi: 10.1073/pnas.0601643103

33. Dunford JE, Kwaasi AA, Rogers MJ, Barnett BL, Ebetino FH, Russell RG, et al. Structure-activity relationships among the nitrogen containing bisphosphonates in clinical use and other analogues: time-dependent inhibition of human farnesyl pyrophosphate synthase. *J Med Chem* (2008) 51(7):2187–95. doi: 10.1021/jm7015733

34. Tsoumpra MK, Muniz JR, Barnett BL, Kwaasi AA, Pilka ES, Kavanagh KL, et al. The inhibition of human farnesyl pyrophosphate synthase by nitrogen-containing bisphosphonates. Elucidating the role of active site threonine 201 and tyrosine 204 residues using enzyme mutants. *Bone* (2015) 81:478–86. doi: 10.1016/j.bone.2015.08.020

35. Caraglia M, Santini D, Marra M, Vincenzi B, Tonini G, Budillon A. Emerging anti-cancer molecular mechanisms of aminobisphosphonates. *Endocr Relat Cancer.* (2006) 13(1):7–26. doi: 10.1677/erc.1.01094

36. Mattarollo SR, Kenna T, Nieda M, Nicol AJ. Chemotherapy and zoledronate sensitize solid tumour cells to Vgamma9Vdelta2 T cell cytotoxicity. *Cancer Immunol Immunother.* (2007) 56(8):1285–97. doi: 10.1007/s00262-007-0279-2

37. Naoe M, Ogawa Y, Takeshita K, Morita J, Shichijo T, Fuji K, et al. Zoledronate stimulates gamma delta T cells in prostate cancer patients. *Oncol Res* (2010) 18(10):493–501. doi: 10.3727/096504010x12671222663638

38. Miyagawa F, Tanaka Y, Yamashita S, Minato N. Essential requirement of antigen presentation by monocyte lineage cells for the activation of primary human gamma delta T cells by aminobisphosphonate antigen. *J Immunol* (2001) 166 (9):5508–14. doi: 10.4049/jimmunol.166.9.5508

39. Saura-Esteller J, de Jong M, King LA, Ensing E, Winograd B, de Gruijl TD, et al. Gamma delta T-cell based cancer immunotherapy: Past-Present-Future. *Front Immunol* (2022) 13:915837. doi: 10.3389/fimmu.2022.915837

40. Li J, Herold MJ, Kimmel B, Muller I, Rincon-Orozco B, Kunzmann V, et al. Reduced expression of the mevalonate pathway enzyme farnesyl pyrophosphate synthase unveils recognition of tumor cells by Vgamma9Vdelta2 T cells. *J Immunol* (2009) 182(12):8118–24. doi: 10.4049/jimmunol.0900101

41. Pauza CD, Liou ML, Lahusen T, Xiao L, Lapidus RG, Cairo C, et al. Gamma delta T cell therapy for cancer: It is good to be local. *Front Immunol* (2018) 9:1305. doi: 10.3389/fimmu.2018.01305

42. Casetti R, Perretta G, Taglioni A, Mattei M, Colizzi V, Dieli F, et al. Drug-induced expansion and differentiation of V gamma 9V delta 2 T cells *in vivo*: the role of exogenous IL-2. *J Immunol* (2005) 175(3):1593–8. doi: 10.4049/jimmunol.175.3.1593

43. Van Acker HH, Anguille S, Willemen Y, Van den Bergh JM, Berneman ZN, Lion E, et al. Interleukin-15 enhances the proliferation, stimulatory phenotype, and antitumor effector functions of human gamma delta T cells. *J Hematol Oncol* (2016) 9(1):101. doi: 10.1186/s13045-016-0329-3

44. Nussbaumer O, Gruenbacher G, Gander H, Komuczki J, Rahm A, Thurnher M. Essential requirements of zoledronate-induced cytokine and gammadelta T cell proliferative responses. *J Immunol* (2013) 191(3):1346–55. doi: 10.4049/jimmunol.1300603

45. Domae E, Hirai Y, Ikeo T, Goda S, Shimizu Y. Cytokine-mediated activation of human ex vivo-expanded Vgamma9Vdelta2 T cells. *Oncotargetγ* (2017) 8 (28):45928–42. doi: 10.18632/oncotarget.17498

46. Kabelitz D, Wesch D, Pitters E, Zoller M. Characterization of tumor reactivity of human V gamma 9V delta 2 gamma delta T cells *in vitro* and in SCID mice *in vivo*. *J Immunol* (2004) 173(11):6767–76. doi: 10.4049/jimmunol.173.11.6767

47. Beck BH, Kim H, O'Brien R, Jadus MR, Gillespie GY, Cloud GA, et al. Dynamics of circulating gammadelta T cell activity in an immunocompetent mouse model of high-grade glioma. *PloS One* (2015) 10(5):e0122387. doi: 10.1371/journal.pone.0122387

48. Di Carlo E, Bocca P, Emionite L, Cilli M, Cipollone G, Morandi F, et al. Mechanisms of the antitumor activity of human Vgamma9Vdelta2 T cells in combination with zoledronic acid in a preclinical model of neuroblastoma. *Mol Ther* (2013) 21(5):1034–43. doi: 10.1038/mt.2013.38

49. Oberg HH, Peipp M, Kellner C, Sebens S, Krause S, Petrick D, et al. Novel bispecific antibodies increase gammadelta T-cell cytotoxicity against pancreatic cancer cells. *Cancer Res* (2014) 74(5):1349–60. doi: 10.1158/0008-5472.CAN-13-0675

50. Weiss HM, Pfaar U, Schweitzer A, Wiegand H, Skerjanec A, Schran H. Biodistribution and plasma protein binding of zoledronic acid. *Drug Metab Dispos* (2008) 36(10):2043–9. doi: 10.1124/dmd.108.021071

51. Santolaria T, Robard M, Leger A, Catros V, Bonneville M, Scotet E. Repeated systemic administrations of both aminobisphosphonates and human Vgamma9Vdelta2 T cells efficiently control tumor development *in vivo*. *J Immunol* (2013) 191(4):1993–2000. doi: 10.4049/jimmunol.1300255

52. Kobayashi H, Tanaka Y, Yagi J, Toma H, Uchiyama T. Gamma/delta T cells provide innate immunity against renal cell carcinoma. *Cancer Immunol Immunother.* (2001) 50(3):115–24. doi: 10.1007/s002620100173

53. Xu Y, Xiang Z, Alnaggar M, Kouakanou L, Li J, He J, et al. Allogeneic Vgamma9Vdelta2 T-cell immunotherapy exhibits promising clinical safety and prolongs the survival of patients with late-stage lung or liver cancer. *Cell Mol Immunol* (2021) 18(2):427–39. doi: 10.1038/s41423-020-0515-7

54. Kakimi K, Matsushita H, Masuzawa K, Karasaki T, Kobayashi Y, Nagaoka K, et al. Adoptive transfer of zoledronate-expanded autologous Vgamma9Vdelta2 T-cells in patients with treatment-refractory non-small-cell lung cancer: a multicenter, open-label, single-arm, phase 2 study. *J Immunother Cancer* (2020) 8(2):1-13. doi: 10.1136/jitc-2020-001185

55. Alnaggar M, Xu Y, Li J, He J, Chen J, Li M, et al. Allogenic Vgamma9Vdelta2 T cell as new potential immunotherapy drug for solid tumor: a case study for cholangiocarcinoma. *J Immunother Cancer.* (2019) 7(1):36. doi: 10.1186/s40425-019-0501-8

56. Cui J, Li L, Wang C, Jin H, Yao C, Wang Y, et al. Combined cellular immunotherapy and chemotherapy improves clinical outcome in patients with gastric carcinoma. *Cytotherapyγ* (2015) 17(7):979–88. doi: 10.1016/j.jcyt.2015.03.605

57. Buccheri S, Guggino G, Caccamo N, Li Donni P, Dieli F. Efficacy and safety of gammadeltaT cell-based tumor immunotherapy: a meta-analysis. *J Biol Regul Homeost Agents.* (2014) 28(1):81–90.

58. Drake MT, Clarke BL, Khosla S. Bisphosphonates: mechanism of action and role in clinical practice. *Mayo Clin Proc* (2008) 83(9):1032–45. doi: 10.4065/83.9.1032

59. Sato M, Grasser W, Endo N, Akins R, Simmons H, Thompson DD, et al. Bisphosphonate action. alendronate localization in rat bone and effects on osteoclast ultrastructure. *J Clin Invest.* (1991) 88(6):2095–105.

60. Gay L, Mezouar S, Cano C, Foucher E, Gabriac M, Fullana M, et al. BTN3A targeting Vgamma9Vdelta2 T cells antimicrobial activity against coxiella burnetii-infected cells. *Front Immunol* (2022) 13:915244. doi: 10.3389/fimmu.2022.915244

61. Starick L, Riano F, Karunakaran MM, Kunzmann V, Li J, Kreiss M, et al. Butyrophilin 3A (BTN3A, CD277)-specific antibody 20.1 differentially activates Vgamma9Vdelta2 TCR clonotypes and interferes with phosphoantigen activation. *Eur J Immunol* (2017) 47(6):982–92. doi: 10.1002/eji.201646818

frontiers | Frontiers in Immunology

TYPE Original Research
PUBLISHED 20 December 2022
DOI 10.3389/fimmu.2022.1073227

OPEN ACCESS

EDITED BY
Alessandro Poggi,
San Martino Hospital (IRCCS), Italy

REVIEWED BY
David Vermijlen,
Université libre de Bruxelles, Belgium
Zheng Xiang,
The University of Hong Kong, Hong Kong SAR, China
Chiara Agrati,
Bambino Gesù Pediatric Hospital (IRCCS), Italy

*CORRESPONDENCE
Massimo Massaia
massimo.massaia@unito.it

†These authors have contributed equally to this work and share first authorship

SPECIALTY SECTION
This article was submitted to Cancer Immunity and Immunotherapy, a section of the journal Frontiers in Immunology

RECEIVED 18 October 2022
ACCEPTED 29 November 2022
PUBLISHED 20 December 2022

CITATION
Giannotta C, Castella B, Tripoli E, Grimaldi D, Avonto I, D'Agostino M, Larocca A, Kopecka J, Grasso M, Riganti C and Massaia M (2022) Immune dysfunctions affecting bone marrow Vγ9Vδ2 T cells in multiple myeloma: Role of immune checkpoints and disease status. *Front. Immunol.* 13:1073227. doi: 10.3389/fimmu.2022.1073227

Immune dysfunctions affecting bone marrow Vγ9Vδ2 T cells in multiple myeloma: Role of immune checkpoints and disease status

Claudia Giannotta[1†], Barbara Castella[1,2†], Ezio Tripoli[1,2], Daniele Grimaldi[2], Ilaria Avonto[3], Mattia D'Agostino[4], Alessandra Larocca[4], Joanna Kopecka[5], Mariella Grasso[2], Chiara Riganti[5] and Massimo Massaia[1,2*]

[1]Laboratorio di Immunologia dei Tumori del Sangue (LITS), Centro Interdipartimentale di Biotecnologie Molecolari "Guido Tarone", Dipartimento di Biotecnologie Molecolari e Scienze della Salute, Università degli Studi di Torino, Torino, Italy, [2]Struttura Complessa (SC) Ematologia, Azienda Ospedaliera (AO) S.Croce e Carle, Cuneo, Italy, [3]Servizio Interdipartimentale di Immunoematologia e Medicina Trasfusionale, Azienda Ospedaliera (AO) S.Croce e Carle, Cuneo, Italy, [4]Struttura Complessa (SC) Ematologia, Azienda Ospedaliero-Universitaria (AOU) Città della Salute e della Scienza di Torino, Torino, Italy, [5]Dipartimento di Oncologia, Università degli Studi di Torino, Torino, Italy

Introduction: Bone marrow (BM) Vγ9Vδ2 T cells are intrinsically predisposed to sense the immune fitness of the tumor microenvironment (TME) in multiple myeloma (MM) and monoclonal gammopathy of undetermined significance (MGUS).

Methods: In this work, we have used BM Vγ9Vδ2 T cells to interrogate the role of the immune checkpoint/immune checkpoint-ligand (ICP/ICP-L) network in the immune suppressive TME of MM patients.

Results: PD-1+ BM MM Vγ9Vδ2 T cells combine phenotypic, functional, and TCR-associated alterations consistent with chronic exhaustion and immune senescence. When challenged by zoledronic acid (ZA) as a surrogate assay to interrogate the reactivity to their natural ligands, BM MM Vγ9Vδ2 T cells further up-regulate PD-1 and TIM-3 and worsen TCR-associated alterations. BM MM Vγ9Vδ2 T cells up-regulate TIM-3 after stimulation with ZA in combination with αPD-1, whereas PD-1 is not up-regulated after ZA stimulation with αTIM-3, indicating a hierarchical regulation of inducible ICP expression. Dual αPD-1/αTIM-3 blockade improves the immune functions of BM Vγ9Vδ2 T cells in MM at diagnosis (MM-dia), whereas single PD-1 blockade is sufficient to rescue BM Vγ9Vδ2 T cells in MM in remission (MM-rem). By contrast, ZA stimulation

10.3389/fimmu.2022.1073227

induces LAG-3 up-regulation in BM Vγ9Vδ2 T cells from MM in relapse (MM-rel) and dual PD-1/LAG-3 blockade is the most effective combination in this setting.

Discussion: These data indicate that: 1) inappropriate immune interventions can exacerbate Vγ9Vδ2 T-cell dysfunction 2) ICP blockade should be tailored to the disease status to get the most of its beneficial effect.

KEYWORDS

Vγ9Vδ2 T cells, immune checkpoints (ICP), tumor microenvironment, multiple myeloma, chronic exhaustion, immune senescence

Introduction

The discovery of immune checkpoints (ICP) and their role as therapeutic targets has revitalized immunotherapy in cancer (1). However, clinical results have been discontinuous with major achievements in some diseases and negligible or disappointing results in others (2–5). Both primary and acquired resistance have been reported to hamper the efficacy of ICP blockade, but the underlying mechanisms have only partially been elucidated. Multiple myeloma (MM) is a paradigm disease in which the immune system and the tumor microenvironment (TME) play a major role in disease progression (6–8). Several phenotypic and functional alterations have been reported in innate and adaptive immune effector cells, including the expression of ICP/ICP ligands in myeloma cells and bystander cells in the TME (9–11). Despite these favourable premises, single αPD-1 treatment has fallen short of clinical expectations in MM, whereas clinical studies of αPD-1 in combination with immunomodulatory drugs (IMiDs) have been terminated ahead of time because of unexpected toxicity in the experimental arm. These unsuccessfully immune interventions have led to the premature termination of alternative studies targeting the ICP/ICP-L network and generated some reluctance in further pursuing this approach due to the complexity of the tumor-host interactions in MM (12).

Vγ9Vδ2 T cells from the bone marrow (BM) are excellent tools to monitor the immune suppressive commitment and decode the ICP/ICP-L network in MM patients (13). Vγ9Vδ2 T-cells are non-conventional T cells half-way between adaptive and innate immunity with a natural inclination to react against malignant B cells, including myeloma cells (14). This intrinsic susceptibility is due to the enhanced cell surface expression of stress-induced self-ligands and the intense production of phosphorylated metabolites generated by the mevalonate (Mev) pathway (14). Isopentenyl pyrophosphate (IPP) is the prototypic Mev metabolite recognized by Vγ9Vδ2 T cells *via* the combination of two immunoglobulin superfamily members, butyrophilin 2A1 (BTN2A1) and BTN3A1. The former directly binds the Vγ9+ domain of the T cell receptor (TCR), whereas the latter binds the Vδ2 and γ-chain regions on the opposite side of the TCR (15–18). IPP is structurally related to the phosphoantigens (pAgs) generated by bacteria and stressed cells that are patrolled by Vγ9Vδ2 T cells as part of their duty to act as first-line defenders against infections and stressed cell at risk of malignant transformation (19). By interrogating the reactivity of BM MM Vγ9Vδ2 T cells to IPP generated by monocytes or dendritic cells (DC) after stimulation with zoledronic acid (ZA), we have revealed a very early and long-lasting dysfunction of BM Vγ9Vδ2 T cells which is already detectable in monoclonal gammopathy of undetermined significance (MGUS) and not fully reverted in clinical remission after autologous stem cell transplantation (9). Multiple cell subsets [myeloma cells, myeloid-derived suppressor cells (MDSC), regulatory T cells (Tregs), BM-derived stromal cells (BMSC)] are involved in Vγ9Vδ2 T-cell inhibition *via* several immune suppressive mechanisms including PD-1/PD-L1 expression (9, 10). Previous work from our lab has shown that single PD-1 blockade improved ZA-induced proliferation of BM MM Vγ9Vδ2 T cells from MM at diagnosis (MM-dia). PD-1 blockade also increased CD107 expression suggesting improved effector functions, but both proliferation and CD107 expression remained far from standard values observed in BM Vγ9Vδ2 T cells from controls (Ctrl) (9).

Recently, it has been reported that the expression of additional ICP on immune effector cells can be involved in acquired resistance to single ICP blockade. PD-1 and TIM-3 co-expression has been reported in conventional T cells from patients with solid cancers (20–23), AML (24), and MM (25–27). PD-1 and TIM-3 co-expression has also been reported in Vγ9Vδ2 T cells chronically exposed to infectious agents (28) or to cancer cells in solid (29, 30) and blood tumors (31). Exhaustion and immune senescence are other T-cell dysfunctions which can potentially contribute to resistance to ICP blockade (32–35).

10.3389/fimmu.2022.1073227

The aim of this work was to investigate the contribution of ICP expression, exhaustion, and immune senescence to the dysfunction of BM MM Vγ9Vδ2T cells and to envisage possible interventions, correlated with the disease status, to overcome the immune suppressive commitment operated by the ICP/ICP-L network in the TME of MM patients.

Methods

Samples collection

Bone marrow mononuclear cells (BMMC) from BM aspirates and autologous peripheral blood mononuclear cells (PBMC) from MM patients at different stages of disease (diagnosis: MM-dia; remission: MM-rem; relapse: MM-rel) were used for the study. All experiments were performed with BM samples from MM-dia unless otherwise specified. BMMC from patients with hematological malignancies in unmaintained molecular remission, frozen human normal BMMC purchased from Stem Cell Technologies, and PBMC from healthy donors attending the local Blood Bank were used as control (Ctrl). The study was approved by institutional regulatory boards (n.176-19 December 11, 2019).

Cell surface and intracellular flow cytometry

The monoclonal antibodies (mAbs) used in the study are listed in Supplemental Table I. Cell surface and intracellular flow cytometry were performed as previously reported (9). Vγ9Vδ2 T cells were identified with αTCR Vγ9 mAb conjugated with the appropriate fluorochrome (FITC, PE, APC) depending on the multicolor staining combination (see Supplemental Table I). We have intentionally focused on Vγ9Vδ2 T cells because this is the only γδ T-cell subset directly activated by pAgs or indirectly activated by ZA stimulation (36–38). Moreover, Vδ2 chain is the only one to combine with the Vγ9 chain confirming that αTCR Vγ9 mAbs are reliable tools to identify Vγ9Vδ2 T cells (39). Cytofluorimetric analyses were performed with FACS Calibur Cell Sorter and FlowJo software (Becton Dickinson, Mountain View, CA).

Vγ9Vδ2 T-cell proliferation, cytokine release and degranulation

Cryopreserved or freshly isolated PBMC or BMMC from MM patients and Ctrl were cultured for 7 days with 10 IU/ml IL-2, and 1 μM ZA+10 IU/ml IL2. In selected experiments, cells were cultured in the presence of αPD1 (10 μg/ml), αTIM-3 (10 μg/ml), αLAG-3 (10 μg/ml), or a combination thereof. Proliferation was evaluated by calculating total counts of viable Vγ9Vδ2 T cells on day 7 with the trypan blue staining assay and flow cytometry after gating for CD3 in combination with appropriate αVγ9 mAb. IL-17 production was evaluated in freshly isolated BMMC after incubation with PMA (50 ng/ml)/Ionomycin (1 μg/ml) for 4 hours at 37°C and 5% CO2 with brefeldin (500 ng/ml) added during the last hour. IFN-γ, and CD107 expression were evaluated as previously reported (9).

Conventional T- cell proliferation

Conventional T-cell proliferation was measured by carboxyfluorescein-diacetate-succinimidyl-ester (CFSE) dilution assay. BMMC were suspended in warmed PBS at a concentration of 10×10^6 cells/ml and labeled with 1 μM CFSE at 37°C for 15 min in the dark. After quenching with FCS for 10 minutes in dark at 37°C and washing with RPMI medium, cells were seeded at 1×10^6 cells/ml in 96-well flat-bottom plate and stimulated with αCD3 (1 μg/ml - BioLegend) and αCD28 (2 μg/ml - BioLegend) antibodies for 72 h at 37°C. After 3 days, conventional T cells where harvested and identified with αCD8 and αCD4 rather than αCD3 given the down-modulation induced by αCD3/αCD28 stimulation and the lineage discrimination capacity of CD4 and CD8 expression (40). In selected experiments, the proliferation of BM CD4 and CD8 T cells with αCD3 and αCD28 was performed in the presence (BMMC) or absence of γδ T cells (BMMC-γδ-). Depletion was performed by immune magnetic separation using Anti-pan-γδ-conjugated magnetic microbeads (Miltenyi Biotec, Germany #130-050-701).

Western blots

For Western blot experiments, γδ T cells were purified by immune magnetic separation using Anti-pan-γδ-conjugated magnetic microbeads (Miltenyi Biotec, Germany #130-050-701). Purity was always > 90% by FITC-conjugated-Hapten MicroBeads staining (Miltenyi Biotec, Germany #130-050-701). After ZA stimulation, Vγ9Vδ2 T cells were the predominant population also in MM patients who did not respond to ZA stimulation (Supplemental Figure 1). Cells were lysed in a MLB buffer (125 mM Tris-HCl, 750 mM NaCl, 1% v/v NP40, 10% v/v glycerol, 50 mM MgCl2, 5 mM EDTA, 25 mM NaF, 1 mM NaVO4, 10 μg/ml leupeptin, 10 μg/ml pepstatin, 10 μg/ml aprotinin, 1 mM phenylmethylsulphonyl fluoride, pH 7.5), sonicated and centrifuged at 13,000 × g for 10 min at 4°C. Twenty μg of proteins from cell lysates were subjected to Western blotting and probed with the antibodies listed in Supplemental Table II. The proteins were detected by enhanced chemiluminescence (Bio-Rad Laboratories). The band density analysis was performed using the ImageJ software (https://imagej.nih.gov/ij/) and expressed as arbitrary units. The ratio band density of each protein/band density of

tubulin (as housekeeping protein) was calculated in each experimental condition. For untreated/baseline/unstimulated cells, the band density ratio was considered 1. For the other experimental conditions, the ratio was expressed as proportion towards the ratio obtained in untreated cells.

ELISA

Supernatants (S/N) from Ctrl and MM BMMC stimulated for 7 days with 10 IU/ml IL2, 1 μM ZA+10 IU/ml IL2 in the presence or absence of αPD1 were collected and stored at -80°C. The concentration of human IL27 was quantified in S/N by enzyme-linked immunosorbent assay (ELISA) technology with the IL-27 Human ELISA kit (Invitrogen; Catalogue number: # BMS2085) according to manufacturer's instructions.

Statistical analysis

The results are expressed as mean ± SE. Differences between the groups have been evaluated with the one-way analysis of variance, and the Wilcoxon–Mann–Whitney non-parametric test for paired or unpaired samples as appropriate and considered to be statistically significant for p values <0.05. Correlation analyses have been performed with the non-parametric Spearman Rank Order test with a cut-off p value <0.05.

Results

Dual PD-1/TIM-3 expression, functional exhaustion, and immune senescence are intertwined in BM MM Vγ9Vδ2 T cells

Figure 1A shows PD-1, TIM-3, LAG-3 and CTLA-4 expression in resting PB and BM Vγ9Vδ2 T cells from Ctrl and MM patients. PD-1 and TIM-3 expression was significantly higher in BM of MM patients than in Ctrl samples. After ZA stimulation, BM MM Vγ9Vγ2 T cells further increased PD-1 (9) and TIM-3 expression (Figure 1B), while the increase in BM Ctrl Vγ9Vδ2 T cells was limited and significantly lower (Figure 1B). Cytofluorometric analysis from one representative MM shows

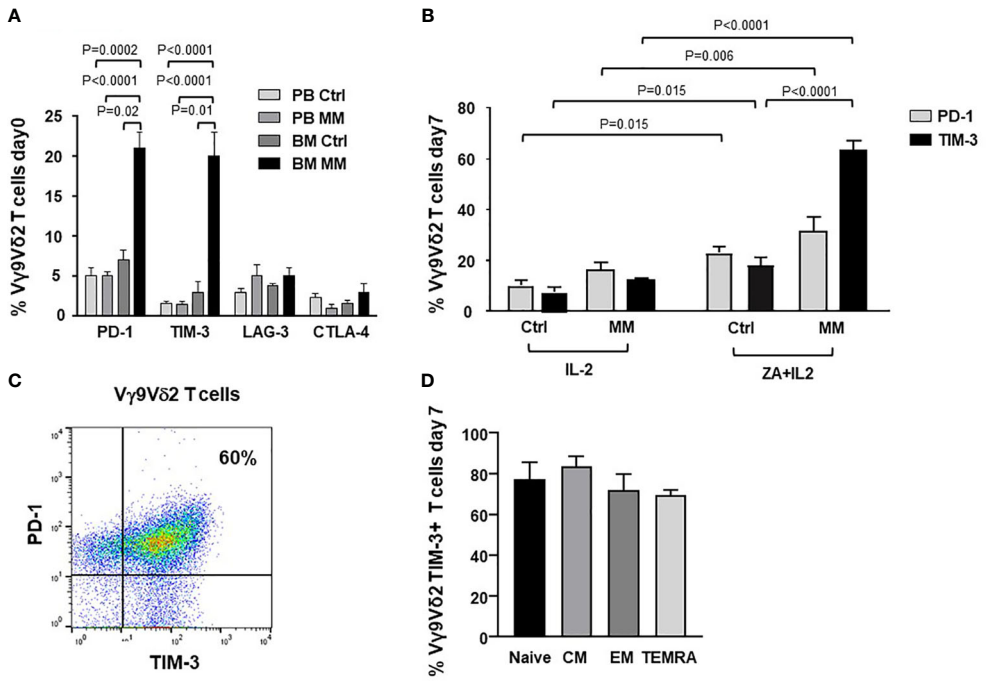

FIGURE 1
ICP expression and subset distribution in resting and ZA-stimulated BM MM Vγ9Vδ2 T cells. **(A)** PD-1, TIM-3, LAG-3 and CTLA-4 expression in resting PB and BM Vγ9Vδ2 T cells from healthy subjects (Ctrl) and MM at diagnosis. Bars represent mean values ± SE from 5 (BM Ctrl) to 30 (BM MM) experiments. **(B)** PD-1 and TIM-3 expression are significantly increased after ZA stimulation in MM BM Vγ9Vδ2 T cells. Bars represent mean values ± SE from 7 (BM Ctrl) to 30 (BM MM) experiments; **(C)** Cytofluorimetric analysis of PD-1 and TIM-3 co-expression in BM MM Vγ9Vδ2 T cells from one representative MM after ZA stimulation. **(D)** TIM-3 expression in naive (CD27+ CD45RA+), central memory (CM) (CD27+ CD45RA-), effector memory (EM) (CD27- CD45RA-), and terminally differentiated effector memory (TEMRA) (CD27- CD45RA+) BM MM Vγ9Vδ2 T cells after ZA stimulation. CM BM MM Vγ9Vδ2 T cells show the highest TIM-3 expression. Bars represent mean values ± SE of 3 experiments.

that PD-1 and TIM-3 are co-expressed by approximately 60% of BM MM Vγ9Vδ2 T cells after ZA stimulation (Figure 1C). In freshly isolated Vγ9Vδ2 T cells we have previously shown that central memory (CM) Vγ9Vδ2 T cells display the highest PD-1 expression (9). After ZA stimulation, TIM-3 up-regulation was documented in all Vγ9Vδ2 T-cell subsets with CM and naïve Vγ9Vδ2 T cells showing slightly higher levels than effector memory (EM) and terminally differentiated effector memory (TEMRA) Vγ9Vδ2 T cells (Figure 1D). The gating strategy used to investigate TIM-3 expression in Vγ9Vδ2 T-cell subsets is shown in Supplemental Figure 2.

Figure 2A compares the expression of immune senescence markers (33, 41, 42) in BM Ctrl and MM Vγ9Vδ2 T cells. BM MM Vγ9Vδ2 T cells showed significantly higher CD57 and CD160, and lower CD28 expression than BM Ctrl Vγ9Vδ2 T cells, even if differences were not statistically significant. The highest CD160 expression was observed in CM BM Vγ9Vδ2 T cells which is the cell subset with the highest PD-1 (9) and TIM-3 expression (Figure 2B). Cytofluorometric analysis of CD160 and PD-1 co-expression in BM MM Vγ9Vδ2 T cells from one representative sample is shown in Figure 2B (right panel).

Phosphorylated-γH2AX (p-γH2AX) is an early marker of DNA damage associated to immune senescence (43). p-γH2AX expression in BM Ctrl and MM-dia Vγ9Vδ2 T cells is shown in Figure 2C (one representative experiment) and Figure 2D (pooled data). These experiments were performed on purified γδ T cells. Both Vδ1 and Vγ9Vδ2 subsets can be represented in variable proportions in freshly purified γδ T cells (day 0), whereas after ZA stimulation Vγ9Vδ2 T cells become predominant (Supplemental Figure 1) and any change should be referred to these because they are the only γδ T-cell subset sensitive to ZA stimulation. In freshly isolated BM γδ T cells, p-γH2AX expression was slightly higher in MM than Ctrl, but the difference was not statistically significant. After ZA stimulation,

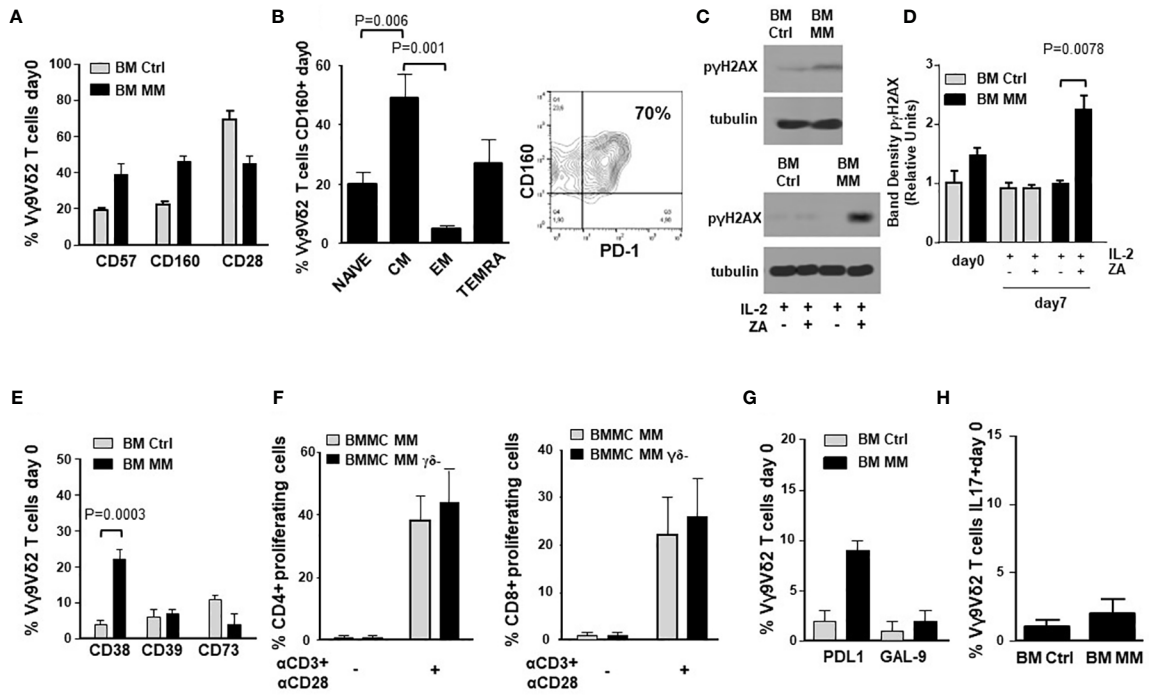

FIGURE 2
ICP expression in BM MM Vγ9Vδ2 T cells is associated with chronic exhaustion and immune senescence markers. **(A)** CD57, CD160 and CD28 expression in BM Ctrl and BM MM Vγ9Vδ2 T cells. Bars represent mean values ± SE from 3 (BM Ctrl) to 50 (BM MM) experiments. Differences are not statistically significant. **(B)** *left:* CM is the BM MM Vγ9Vδ2 T-cell subset with the highest CD160 expression. Bars represent mean values ± SE of 8 experiments; *right:* cytofluorometric analysis of CD160 and PD-1 co-expression in BM MM Vγ9Vδ2 T cells from one representative sample. **(C)** Western blot analysis of p-γH2AX expression in resting (upper panel) and ZA-stimulated (lower panel) Vγ9Vδ2 T cells from one representative BM Ctrl and MM sample. Tubulin expression is shown to confirm equal protein loading per lane. **(D)** Densitometric analysis of pooled p-γH2AX expression data in resting (day 0) and ZA-stimulated (day 7) BM Ctrl and MM Vγ9Vδ2 T cells. Bars represent mean values ± SE from 1 (BM Ctrl and BM MM d0) to 4 (BM MM) experiments. **(E)** CD38, CD39, and CD73 expression in resting BM Ctrl and BM MM Vγ9Vδ2 T cells. Bars represent mean values ± SE from 8 (BM Ctrl) to 40 (BM MM) experiments. **(F)** CFSE-based analysis of BM MM CD4+ and CD8+ proliferation after 72-hour stimulation with αCD3 + αCD28 in the presence (BMMC) or absence (BMMC- γδ- T-cell depleted) of BM Vγ9Vδ2 T cells. Bars represent mean values ± SE of 3 experiments. **(G)** PD-L1 and GAL-9 expression in resting BM Ctrl and MM Vγ9Vδ2 T cells. Bars represent mean values ± SE from 4 (BM Ctrl) to 16 (BM MM) experiments. **(H)** Intracellular IL-17 expression in resting BM Ctrl and MM Vγ9Vδ2 T cells after PMA+ ionomycin stimulation. Bars represent mean values ± SE from 3 (BM Ctrl) to 15 (BM MM) experiments.

p-γH2AX expression was significantly increased in BM MM only (Figures 2C, D).

IL-7 has been reported to mitigate the induction of immune senescence of conventional T cells exposed to tumor cells (44, 45). We have investigated whether exogenous IL-7 could relieve the immune dysfunction of BM MM Vγ9Vδ2 T cells, but we have not observed any beneficial effect (data not shown).

Accumulating evidences indicate that Vγ9Vδ2 T cells can exert different functions depending on the local microenvironment, including the ability to promote tumor progression *via* the acquisition of regulatory or pro-tumoral functions (46). Figure 2E shows the expression of CD38, CD39, and CD73 in BM Vγ9Vδ2 T cells from Ctrl and MM patients. These molecules cooperate in the induction of the immune suppressive TME in MM *via* adenosine production (47). Only CD38 was significantly up-regulated in MM compared with Ctrl, whereas no differences were observed in CD39 and CD73 expression. The adenosine circuitry operated by CD38, CD39, and CD73 is well known to contribute to the establishment of the immune suppressive contexture in the TME of MM (47), but our data indicate that Vγ9Vδ2 T cells are not directly involved in this immune suppressive circuitry.

Lastly, BM MM Vγ9Vδ2 T cells did not show any phenotypic and/or functional features consistent with suppressor and/or pro-tumoral functions. The proliferation of CD4+ and CD8+ T cells after αCD3/αCD28 stimulation was similar in the presence or absence of γδ T cells (Figure 2F). Supplementary Figure 3A shows that proliferation of BM MM CD4+ and CD8+ cells was similar or even better compared with PB Ctrl CD4+ and CD8+ cells. Unlike BM Vγ9Vδ2 T cells, CD4 + and CD8+ cell proliferation was not influenced by the disease status (Supplementary Figure 3B), confirming the unique BM MM Vγ9Vδ2 T-cell susceptibility to the immune suppressive TME contexture.

The expression of PD-L1, GAL-9 and IL-17 characterizes Vγ9Vδ2 T cells with pro-tumoral functions in the TME (48). As shown in Figures 2G, H, the expression of GAL-9 and cytoplasmic IL-17 was similar in BM Ctrl and MM Vγ9Vδ2 T cells except for PD-L1 expression, which was slightly increased in the former, but the difference was not statistically significant. Representative dot plots of IL-17 expression in BM MM and Ctrl Vγ9Vδ2 T cells are shown in Supplemental Figure 4.

Altered expression of TCR-associated molecules in BM MM Vγ9Vδ2 T cells

ICP expression and immune senescence in T cells are associated with defective intracellular TCR signaling (49, 50). Figure 3A shows the expression of selected TCR-associated molecules in purified BM γδ T cells from one representative Ctrl and MM patient on day 0 and after ZA-stimulation (day 7). As reported above, both Vδ1 and Vγ9Vδ2 cells are represented in freshly purified γδ T cells (day 0), whereas Vγ9Vδ2 T cells are predominant on day 7 and they are the only γδ T-cell subset engaged by ZA (Supplemental Figure 1). Pooled data are shown in Figure 3B showing that BM MM Vγ9Vδ2 T cells had significantly lower pAKT, higher PTEN, and lower pSTAT-1 expression on day 7 compared to BM Ctrl Vγ9Vδ2 T cells.

ZAP-70 and CD3-ζ chain are other TCR-associated molecules defectively expressed in T cells from the TME of mice and humans (51). ZAP-70 expression was significantly lower in resting BM MM Vγ9Vδ2 T cells compared with PB and BM Ctrl Vγ9Vδ2 T cells, but also with PB MM Vγ9Vδ2 T cells (Figure 3C), further confirming the striking difference between circulating *vs* TME-resident Vγ9Vδ2 T cells. Representative dot plots are shown in Figure 3D. Paired analyses of Vγ9Vδ2+ and CD3+ Vγ9Vδ2- cells showed that the mean ZAP-70 expression was also significantly down-regulated in BM CD3+ Vγ9Vδ2- T cells of MM patients with a wide range of expression in individual samples (Supplemental Figure 5). A slight increase was observed after ZA stimulation in Vγ9Vδ2 T cells from 3 MM patients with low ZAP-70 expression at baseline, but values remained inferior to Ctrl values (Figure 3E). Unlike ZAP-70, the proportion and MFI of CD3-ζ chain expression were not different in PB and BM Ctrl and MM Vγ9Vδ2 T cells (Supplemental Figure 6).

PD-1/TIM-3 cross-talk in BM MM Vγ9Vδ2 T cells

It has been reported that TIM-3 up-regulation is involved in the acquired resistance to PD-1 blockade (31, 52, 53). Thus, we have investigated whether TIM-3 was involved in the incomplete recovery of BM MM Vγ9Vδ2 T cells after ZA stimulation and single PD-1 blockade. Figure 4A shows that both TIM-3 expression and MFI values were significantly up-regulated in BM MM Vγ9Vδ2 T cells in the presence of αPD-1, whereas PD-1 expression was slightly down-regulated after ZA stimulation in the presence of αTIM-3, but the decrease was not statistically significant. Representative cytofluorometric analyses of increased TIM-3 up-regulation and PD-1 down-regulation are shown in Figure 4A (right panel) and Figure 4B (right panel).

Next, we investigated whether dual PD1-/TIM-3 blockade was more effective than single blockade. We evaluated the proliferation (Figure 4C), IFN-γ production (Figure 4D) and CD107 expression (Figure 4E) in BM MM Vγ9Vδ2 T cells after ZA stimulation in the presence of αPD-1, αTIM-3, and the combination thereof. Representative cytofluorometric analyses of increased IFN-γ and CD107 expression in BM MM Vγ9Vδ2 T cells after dual blockade are shown in Figure 4D (right panel) and Figure 4E (right panel). Our results indicate that dual blockade PD-1/TIM-3 blockade is more effective than single PD-1 or TIM-3 blockade in MM-dia to mitigate BM MM Vγ9Vδ2 T-cell dysfunctions.

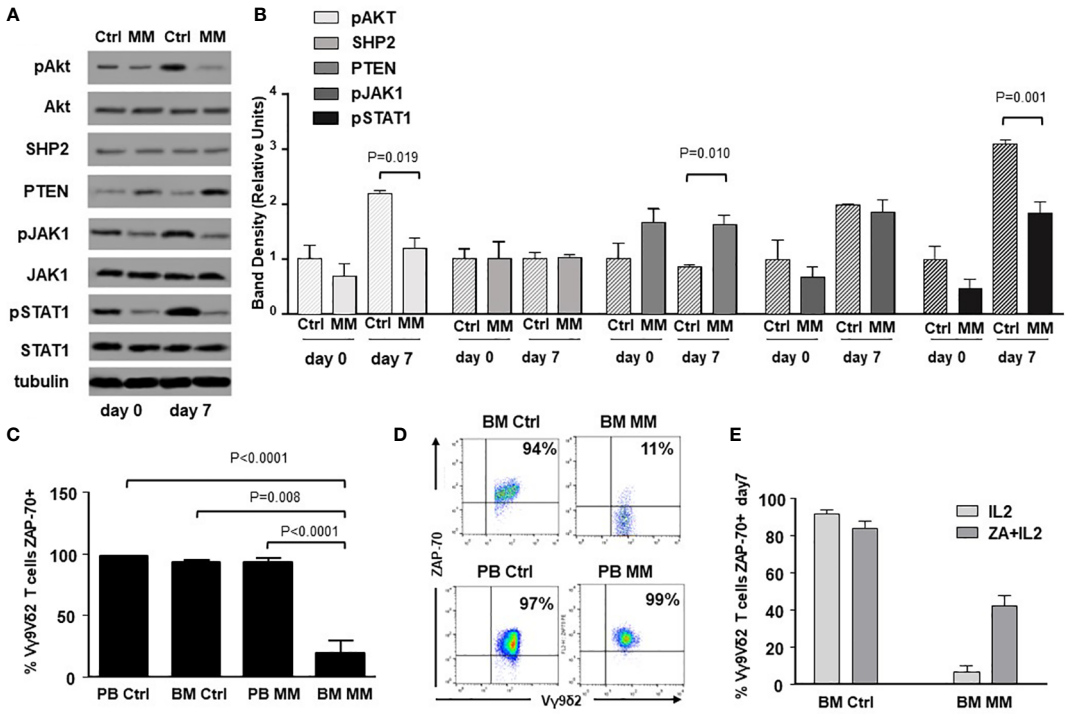

FIGURE 3
Alterations of TCR-associated molecules in BM MM Vγ9Vδ2 T cells. **(A)** Western blot analysis of selected TCR-associated molecules (pAKT, AKT, SHP2, PTEN, pJAK-1, JAK-1, pSTAT-1, STAT-1) in purified resting (day 0) and ZA-stimulated (day 7) BM γδ T cells from one representative Ctrl and MM. pAKT, pJAK and pSTAT-1 are down-regulated, whereas PTEN is up-regulated in resting BM MM γδ T cells. These differences are amplified after ZA stimulation (day 7). Tubulin expression is shown to confirm equal protein loading per lane. **(B)** Densitometric analysis of pooled data from ZA-stimulated BM Ctrl and BM MM γδ T cells confirms lower expression of pAKT, and pSTAT1, and higher PTEN expression in BM MM γδ T cells *vs* BM Ctrl γδ T cells. Bars represent mean values ± SE from 1 (BM Ctrl d0 and BM MM d0) to 14 experiments (BM MM). **(C)** ZAP-70 expression in resting PB and BM Vγ9Vδ2 T cells from Ctrl and MM patients. Bars represent mean values ± SE from 3 (BM Ctrl) to 25 experiments (BM MM); **(D)** cytofluorimetric analysis of ZAP-70 expression in Vγ9Vδ2 T cells from BM and PB MM Vγ9Vδ2 T cells and BM and PB Ctrl; **(E)** ZAP-70 expression after ZA stimulation in Ctrl and MM BM Vγ9Vδ2T cells. Bars represent mean values ± SE from 2 (BM Ctrl) to 3 experiments (BM MM).

Dual PD-1/TIM-3 blockade was also associated with a partial recovery of TCR-associated alterations. Data from one representative Ctrl and MM are shown in Figure 5A, while pooled data from 2 paired experiments are shown in Figure 5B. αPD-1 partially normalized pAKT and PTEN expression, whereas αTIM-3 partially normalized pJAK1 and pSTAT1 expression. No antagonist, additive or synergistic effect was observed suggesting that αPD-1 and αTIM-3 target mutually exclusive TCR-associated molecules in BM MM Vγ9Vδ2 T cells. Supplementary Figure 8 shows pooled data from unpaired experiments after αPD-1 treatment only.

Intracellular PD-1/TIM-3 cross-talk is not mediated by the IL-27/pSTAT1/T-bet or the PI3K-AKT pathways

Next, we looked for possible intersections between the intracellular pathways triggered by αPD-1 and αTIM-3. Previous work from Zhu C. et al. (54) has reported a cross-talk between TIM-3 and PD-1 mediated by the IL-27/pSTAT1/T-bet axis. BM MM Vγ9Vδ2 T cells showed the lowest T-bet (Figure 6A), and the highest IL-27R expression (Figure 6B). This pattern has recently been reported in severely exhausted T cells from the BM of patients with AML in relapse after allogeneic transplantation (55). αPD-1 treatment did not increase T-bet and/or IL-27R expression in ZA-stimulated BM Vγ9Vδ2 T cells (Figures 6C, D). Moreover, low IL-27 levels were detected in the supernatants of BM MM Vγ9Vδ2 T cells which were not modified by αPD-1 (Figure 6E).

The PI3K/Akt axis is another intracellular signalling pathway connecting PD-1 and TIM-3 in tumor-infiltrating lymphocytes from patients with head and neck cancer (53). In these cells, TIM-3 up-regulation induced by αPD-1 can be abrogated with LY294002, a broad PI3K inhibitor (53). Thus, we evaluated whether αPD-1-induced TIM-3 up-regulation in BM MM Vγ9Vδ2 T cells could be inhibited by single pSTAT-1 inhibition with fludarabine monophosphate (FAMP) (56), single PI3K inhibition with LY294002, or the combination thereof.

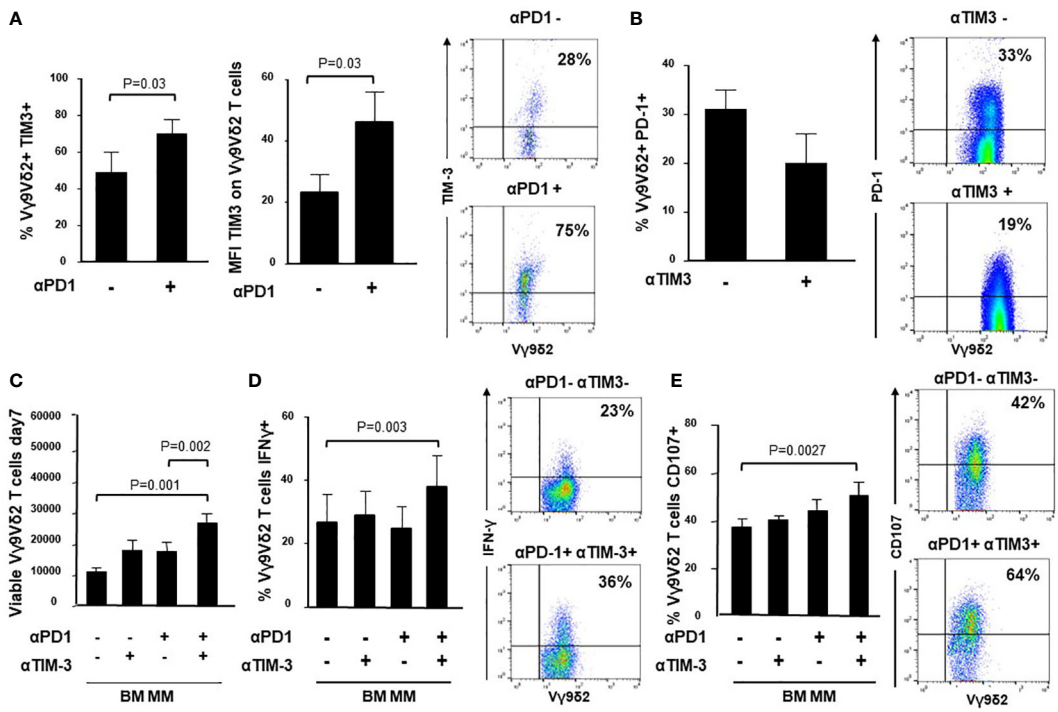

FIGURE 4
Intracellular cross-talk between PD-1 and TIM-3 in BM MM Vγ9Vδ2 T cells. **(A)** *left:* Percentage and MFI of TIM-3+ cells are significantly up-regulated in BM MM Vγ9Vδ2 T cells after ZA stimulation in the presence of αPD1. Bars represent mean values ± SE of 6 experiments; *right:* cytofluorimetric analysis of TIM-3 expression after ZA stimulation in the absence (upper panel) or in the presence (lower panel) of αPD-1 in one representative experiment; **(B)** *left:* PD-1 expression is slightly down-regulated in BM MM Vγ9Vδ2 T cells after ZA stimulation in the presence of αTIM-3, but the difference is not statistically significant. PD-1 expression is significantly up-regulated after ZA stimulation as already reported in Figure 1B. Bars represent mean values ± SE of 5 experiments; *right:* cytofluorimetric analysis of PD-1 expression after ZA stimulation in the absence (upper panel) or in the presence (lower panel) of αTIM-3 in one representative experiment; **(C)** ZA-induced BM MM Vγ9Vδ2 T-cell proliferation in the absence or in the presence of αPD-1, αTIM-3 and the combination thereof. Bars represent mean values ± SEM of 5 experiments. **(D)** *left:* intracellular IFN-γ production by ZA-stimulated BM MM Vγ9Vδ2 in the absence or in the presence of αPD-1, αTIM-3 and the combination thereof. Bars represent mean values ± SEM of 4 experiments; *right:* cytofluorimetric analyses of IFN-γ production in BM MM Vγ9Vδ2 T cells after ZA stimulation in the absence (upper panel) or in the presence (lower panel) of dual PD1/TIM-3 blockade. **(E)** *left:* CD107 expression in ZA-stimulated BM MM Vγ9Vδ2 in the absence or in the presence of αPD-1, αTIM-3, and the combination thereof. Bars represent mean values ± SE of 6 experiments; *right:* cytofluorimetric analyses of CD107 expression in BM MM Vγ9Vδ2 T cells after ZA stimulation in the absence (upper panel) or in the presence (lower panel) of dual blockade PD1/TIM-3 blockade.

Results shown in Figure 6F indicate that these pathways are not druggable to prevent αPD-1-induced TIM-3 up-regulation in BM MM Vγ9Vδ2 T cells.

Improved efficacy by tailoring ICP blockade to the disease status

Next, we investigated whether the ICP/ICP-L immune suppressive circuitry was influenced by the disease status. PD-1 expression was significantly higher in MM-rel than in MM-dia, while MM-rem showed intermediate values. By contrast, no differences were observed in TIM-3 expression between MM-dia, MM-rem, and MM rel (Figure 7A). We investigated whether αPD-1 treatment induced TIM-3 up-regulation also in MM-rem and MM-rel. Figure 7B shows that TIM-3 was up-regulated in MM-dia only, but not in MM-rem and MM-rel.

The effect of single or dual PD-1/TIM-3 blockade on ZA-induced proliferation in BM MM Vγ9Vδ2 T cells in MM-dia, MM-rem and MM-rel is shown in Figure 7C. BM Vγ9Vδ2 T cells from MM-rem were the only ones to reach normal proliferation values with single PD-1 or TIM-3 blockade, the former being slightly more effective than the latter. Dual PD-1/TIM-3 blockade was not superior to single blockade in MM-rem. By contrast dual PD-1/TIM-3 blockade was more effective than single blockade in MM-dia, the only clinical setting in which αPD-1 induces TIM-3 up-regulation. BM Vγ9Vδ2 T cells from MM-rel showed the worst anergy to single and dual blockade, even if TIM-3 expression was similar to MM-dia and MM-rem and was not up-regulated by αPD-1 (Figures 7A, B).

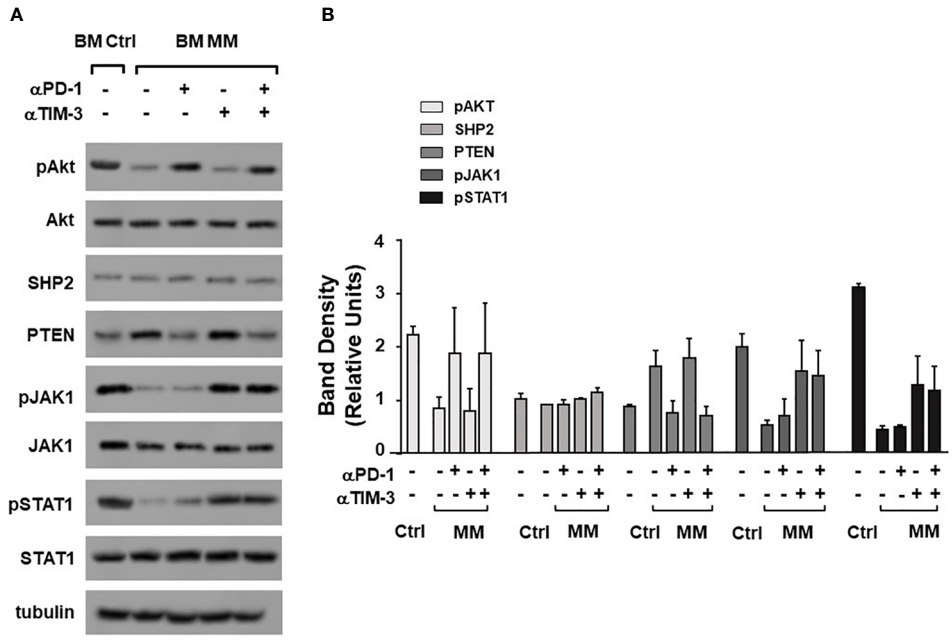

FIGURE 5
Alterations of TCR-associated molecules are mitigated by αPD-1 and/or αTIM-3. **(A)** Western blot analysis of pAKT, AKT, SHP2, PTEN, pJAK-1, JAK-1, pSTAT-1, and STAT-1 expression in BM Ctrl and BM MM γδ T cells from one representative experiment after ZA stimulation in the absence or in the presence of αPD1, αTIM-3, and the combination thereof. Tubulin expression is shown to confirm equal protein loading per lane. **(B)** Densitometric analysis of pooled data. Bars represent mean values ± SE of 2 experiments.

These findings prompted us to investigate the expression of additional ICP on BM MM Vγ9Vδ2 T cells in MM-rel. Figure 7D shows that LAG-3 expression was similar in resting (day 0) BM Vγ9Vδ2 T cells from MM-dia, MM-rem, and MM-rel. After ZA stimulation, LAG-3 expression was slightly increased in MM-dia, unmodified in MM-rem, and increased in MM-rel, even if the differences was not statistically significant. Next, we determined which PD-1/TIM-3/LAG-3 combination was more effective to mitigate the anergy of BM Vγ9Vδ2 T cells in MM-rel. Results shown in Figure 7E indicate that dual PD-1/LAG-3 blockade was more effective than dual PD-1/TIM-3, dual TIM-3/LAG-3, and even triple PD-1/TIM-3/LAG-3 blockade, but still inferior to that reached in MM-rem after single PD-1 or TIM-3 blockade, or MM-dia after dual PD-1/TIM-3 blockade.

These data confirm that the relapse is the most challenging setting, and immune-based strategies should be delivered in remission, when the immune suppressive TME commitment is partially relieved.

Discussion

In this work, we have used Vγ9Vδ2 T cells as cellular decoders to investigate the role played by the ICP/ICP-L network in the TME of MM patients. A significant proportion of resting BM MM Vγ9Vδ2 T cells showed PD-1 and TIM-3 co-expression, as previously reported in Vγ9Vδ2 T cells chronically exposed to infectious agents (28) or to cancer cells in solid (29, 30) and blood tumors (31). PD-1 and TIM-3 co-expression is considered a phenotypic hallmark of functional exhaustion (24, 26). However, multiple ICP expression is not sufficient per se to identify functionally exhausted cells. One reason is that immune competent T cells can also express ICP after activation, but in this case ICP expression is transient and finalized to dampen T-cell activation to prevent uncontrolled immune reactions and autoimmunity. In contrast, ICP expression on chronically activated T cells reflects a dysfunctional state induced by the long-term exposure to antigens in the context of an inappropriate microenvironment. We have previously shown that BM MM Vγ9Vδ2 T cells are exposed to supra-physiological IPP concentrations released in large amounts by BMSC and, to a lower extent by myeloma cells (57). Thus, BM MM Vγ9Vδ2 T cells fulfil the operational criteria of functionally exhausted cells because: 1) PD-1/TIM-3 co-expression is associated with functional dysfunctions; 2) functional dysfunctions are observed after challenging the normal counterpart (i.e., BM Ctrl Vγ9Vδ2 T cells) with the same antigen (i.e., ZA) in the same microenvironment (i.e., BM) (58). After ZA stimulation, BM MM Vγ9Vδ2 T cells further up-regulated PD-1 and TIM-3 expression. In mice, functionally exhausted cells are

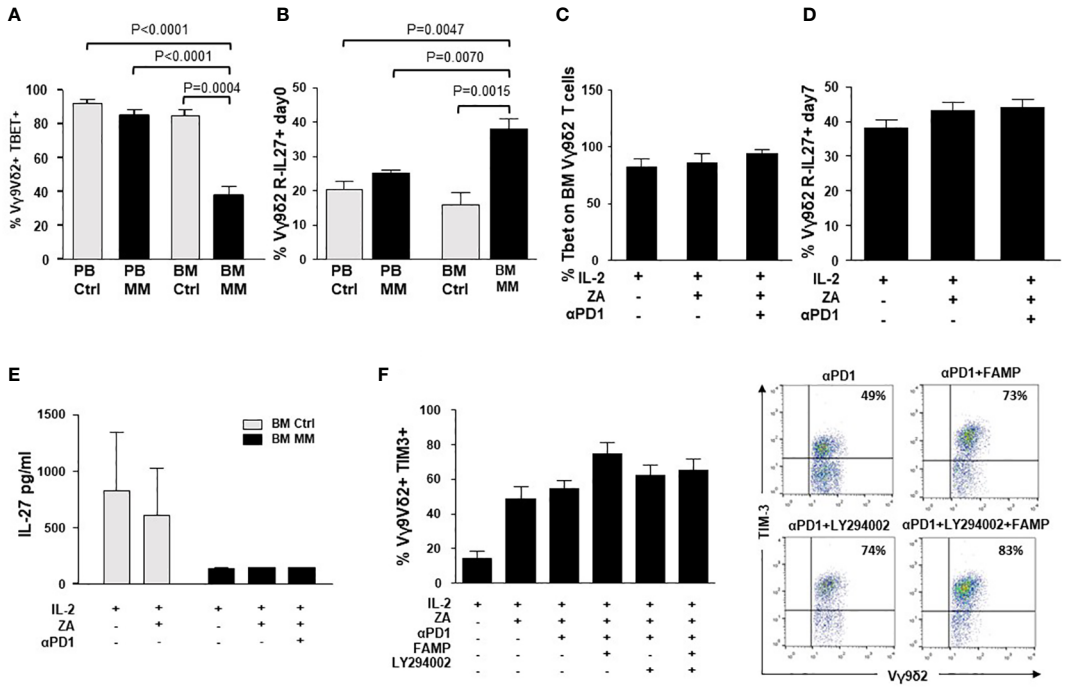

FIGURE 6
Intracellular PD-1/TIM-3 cross-talk is not mediated by the IL-27/pSTAT1/T-bet or PI3K-AKT axes. **(A)** T-bet and MFI expression in resting PB and BM Ctrl and MM Vγ9Vδ2 T cells. Bars represent the mean values ± SE from 6 (BM Ctrl) to 25 experiments (BM MM); **(B)** IL-27R expression in resting PB and BM Ctrl and MM Vγ9Vδ2 T cells. Bars represent the mean values ± SE from 6 (BM Ctrl) to 25 experiments (BM MM). **(C)** T-bet and **(D)** IL-27R expression in ZA-stimulated BM MM Vγ9Vδ2 T cells with or without αPD1. Bars represent mean values ± SE from 4 (Tbet) to 6 (IL-27R) experiments **(E)** IL-27 concentrations in the supernatants (S/N) of ZA-stimulated BMMC from Ctrl and MM patients. Bars represent the mean values ± SE from 3 (BM Ctrl) to 4 experiments (BM MM). **(F)** *Left*: TIM-3 expression in ZA-stimulated BM MM Vγ9Vδ2 T cells without or with αPD1 in the presence of LY294002 (PI3K inhibitor), fludarabine monophosphate (FAMP) (p-STAT1 inhibitor), and the combination thereof. Bars represent the mean values ± SE of 7 experiments. *Right*: cytofluorimetric analysis of TIM-3 expression in ZA-stimulated BM MM Vγ9Vδ2 T cells without or with α-PD-1 and PI3K and/or pSTAT-1 inhibitors from one representative MM.

hierarchically organized from progenitor to terminally differentiated exhausted T cells (58), the latter being more difficult to rescue than the former. Our data indicate that inadvertent or inappropriate engagement of immune effector cells can worsen functional exhaustion also in humans.

PD-1+ TIM-3+ BM MM Vγ9Vδ2 T cells expressed immune senescence markers (33, 41, 42). Vγ9Vδ2 T cells from normal individuals are particularly resistant to immune senescence due to their peculiar capacity to adapt to life-long stimulation (59). In MM, the immune suppressive TME turns off the capacity of Vγ9Vδ2 T cells to resist life-long stimulation. CD160 expression was mainly restricted to CM and TEMRA BM MM VγVδ2 T cells, which is the subset with the highest ICP expression. Interestingly, the loss of CD27 and CD28 and the expression of TIM-3 and CD57 on T cells has been associated with resistance to ICP blockade (35).

Immune senescence of BM MM Vγ9Vδ2 T cells was confirmed by the expression of pγH2AX. A weak pγH2AX expression was already detectable in freshly isolated BM γδ T cells, but significantly increased after ZA stimulation, whereas no expression was detected in resting or ZA-stimulated BM Ctrl samples. γH2AX phosphorylation is used by mammalian cells to prevent genomic instability after DNA breakage induced by genotoxic stress or senescence (60). Our data indicate that pγH2AX quantification can be used to predict the functional outcome of immune effector cells after stimulation, and not only to screen the genotoxic profile of drugs and to identify senescent cells in aging and disease (61).

The functional plasticity of Vγ9Vδ2 T cells embedded in the immune suppressive TME can lead to the acquisition of regulatory or pro-tumoral functions (46). We have not found any phenotypic or functional evidence to support a regulatory/pro-tumoral shift of BM Vγ9Vδ2 T cells in MM, unlike colon, breast and other solid cancers in which immune senescent γδ T cells have been reported to suppress the proliferation of conventional T cells (62–65).

Exhaustion and immune senescence of BM MM Vγ9Vδ2 T cells were associated with alterations in the TCR signaling

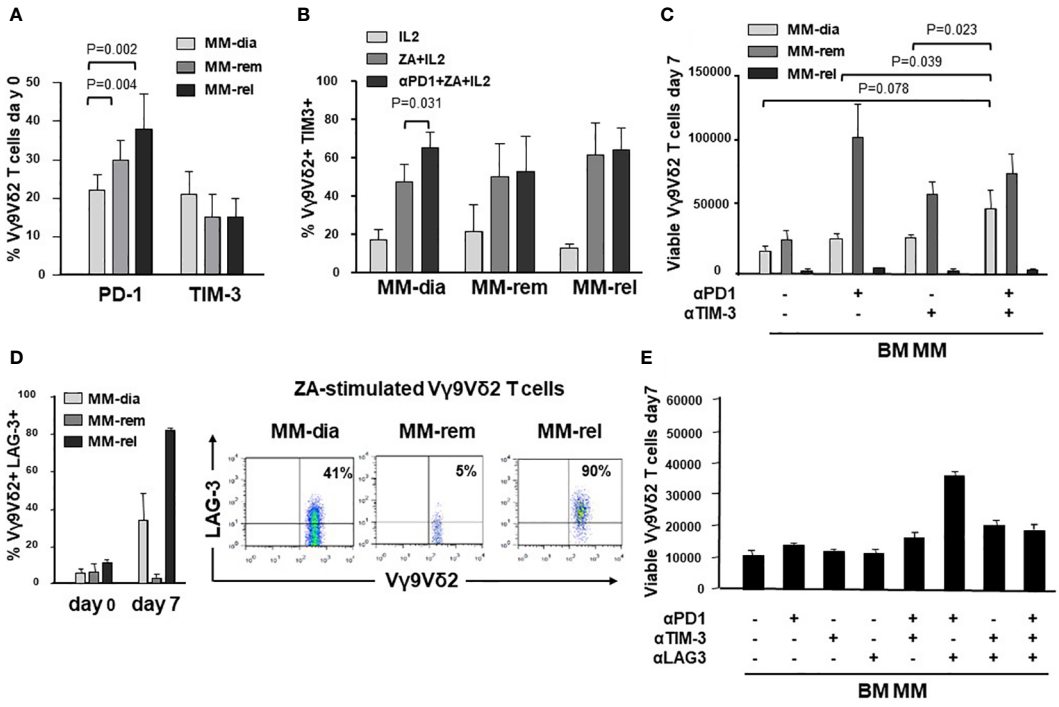

FIGURE 7
The ICP/ICP-L network is dynamically shaped by the disease status. **(A)** PD-1 and TIM-3 expression in resting BM Vγ9Vδ2 T cells from MM patients at different stages of disease (MM-dia, MM-rem and MM-rel). Bars represent the mean values ± SE from 7 (MM-rel) to 50 (MM-dia). **(B)** TIM-3 expression in BM MM Vγ9Vδ2 T cells after 7-day ZA stimulation in the presence or absence of αPD1. Bars represent the mean values ± SE from 3 (MM-rem) to 6 (MM-dia). **(C)** BM MM Vγ9Vδ2 T-cell proliferation in MM-dia, MM-rem and MM-rel after 7-day ZA stimulation in the presence of αPD1, αTIM-3, and the combination thereof. Bars represent the mean values ± SE from 4 (MM-rem) to 8 (MM-dia). **(D)** *left:* LAG-3 expression in resting (day 0) or ZA-stimulated BM Vγ9Vδ2 T cells from MM patients at different stages of disease (MM-dia, MM-rem and MM-rel). Bars represent the mean ± SE from 4 (MM-rel) to 5 (MM-dia) experiments; *right:* cytofluorimetric analyses of LAG-3 expression in ZA-stimulated Vγ9Vδ2 T cells from one representative MM-dia, MM-rem, and MM-rel. **(E)** BM MM Vγ9Vδ2 T-cell proliferation in MM-rel after 7-day ZA stimulation in the presence αPD1, αTIM-3, and αLAG-3 as single agents or in combination. Bars represent the mean ± SE of 3 experiments.

pathway. pAKT, pSTAT1, pJAK1, and ZAP-70 were down-regulated, while PTEN was up-regulated in MM BM Vγ9Vδ2 T cells. ZAP-70 was also down-regulated in BM CD3+ Vγ9Vδ2- T cells of MM patients. The significantly lower ZAP-70 expression in BM compared further confirms how powerful is the immune conditioning exerted by the prolonged exposure to tumor cells in the TME. In contrast, we have not observed CD3-ζ chain down-modulation in Vγ9Vδ2 T cells and CD3+ Vγ9Vδ2- T cells unlike previous reports (51). Increasing evidence suggests that ZAP-70 down-regulation in T cells and NK cells can contribute to impairment of anti -tumor immune responses and bias the efficacy of immunotherapy (66). We are currently investigating whether ZAP-70 expression is correlated with Vγ9Vδ2 T-cell dysfunctions in MM.

TIM-3 was significantly up-regulated after ZA stimulation in the presence of αPD1, whereas PD-1 was not up-regulated after ZA stimulation in the presence of αTIM3, indicating a one-way rather than two-way cross-talk between these molecules. TIM-3 up-regulation after PD-1 blockade in conventional T cells is considered a potential mechanism of adaptive resistance to αPD-1 *in vitro* (52, 53, 67) and *in vivo* (52, 53, 68).

Dual PD-1/TIM-3 blockade was more effective than single ICP blockade to partially recover proliferation, IFN-γ production, and CD107 expression in BM Vγ9Vδ2 T cells, and to mitigate the altered expression of TCR-associated molecules. Dual PD-1/TIM-3 blockade has also been reported to up-regulate IFN-γ and TNF-α production in PB Vγ9Vδ2 T cells of AML patients after pAg stimulation (31).

Dual ICP blockade is currently carried on in the clinical setting using mAb combinations willing to improve response rates and/or overcome acquired resistance to single ICP blockade (69). However, this strategy is burdened by clinical and financial toxicities (70), and alternative approaches are under investigation (69, 71). One alternative approach could be the identification of druggable intracellular intersections between these pathways. To this end, we have investigated the IL-27/pSTAT1/T-bet, and the PI3K/AKT pathways that have been reported to connect PD-1 and TIM-3 in tumor-bearing

mice and patients with head and neck squamous cell carcinomas (53, 54), but we have not found any evidence of PD-1/TIM-3 cross-talk *via* these pathways in BM MM Vγ9Vδ2 T cells.

Interestingly, T-bet expression was low in resting BM MM Vγ9Vδ2 T cells as recently shown in the BM of patients with AML. In these patients, the emergence of severely exhausted (i.e., T-bet^{low}, PD-1+) T cells has been reported to predict disease relapse after allogeneic transplantation (55). By contrast, IL-27R expression was high in BM MM Vγ9Vδ2 T cells, whereas soluble IL-27 levels were low and did not increase after ZA stimulation. We speculate that BM MM Vγ9Vδ2 T cells are equipped with a high number of IL-27R to catch the small amount of IL-27 available in the TME to eventually improve their fitness, and not to up-regulate TIM-3.

This is the first report comparing the role of ICP/ICP-L and their blockade in the TME of MM-dia, MM-rem and MM-rel. PD-1 expression in BM MM Vγ9Vδ2 T cells was significantly higher in MM-rel than in MM-rem and MM-dia, whereas TIM-3 expression was not different. Interestingly, MM-rem showed significantly higher PD-1 expression than MM-dia, indicating that it is not trivial for BM MM Vγ9Vδ2 T cells to get rid of the immune suppressive imprinting operated by the TME. Single or dual blockade PD-1/TIM-3 showed different efficacy according to the disease status. MM-rem showed the best recovery in the presence of the αPD-1 or αTIM-3: the former was slightly better than the latter, whereas the combination did not show any additive or synergistic effect. Dual PD-1/TIM-3 blockade showed an additive effect in MM-dia, whereas MM-rel were totally refractory, no matter single or dual PD-1/TIM-3 blockade was applied. It remains to be determined in MM-rel whether the immune dysfunction anticipates the myeloma cell regrowth or vice-versa.

Our data confirm that the refractory/relapse setting remains the most difficult challenge for immune-based interventions. Paradoxically, this is also the clinical setting usually selected for first-in-man or phase I/II studies, including MM (72), with the risk to jeopardize future investigation since results will rarely meet clinical expectations. Interestingly, BM Vγ9Vδ2 T cells from MM-rel significantly up-regulated LAG-3 after ZA stimulation in addition to PD-1 and TIM-3. In the MC38 mouse tumor model, dual PD-1/TIM-3 blockade increases the expression of LAG-3 in T cells, and LAG-3 expression confers resistance to αPD-1/αTIM-3 treatment (73). Increased LAG-3 expression in T cells of patients with non-small cell lung cancer (NSCLC) has been associated with resistance to αPD-1 treatment and shorter progression-free survival (22). Likewise, co-expression of PD-1, TIM-3, and LAG-3 in TILs of patients clear cell renal cell carcinoma (CCRC) has been associated with high risk of early progression (23).

Dual PD-1/LAG-3 blockade was the most effective combination to improve the proliferative responses to ZA stimulation in MM-rel, confirming the profound immune suppressive TME commitment in this setting. Triple PD-1/TIM-3/LAG-3 blockade has been proposed to overcome this barrier in syngeneic mouse tumor models (73), but in our hands triple blockade was less effective than dual PD-1/LAG-3 blockade. Alternative strategies can be dual ICP blockade after lymphodepletion by whole body radiation, as reported in the 5T33 murine MM model (74), or after the addition of TGF-β inhibitors as reported by Kwon et al. (25), but these strategies are not easy to apply to humans.

In conclusion, the immune suppressive TME contexture in MM is under dynamic evolution and ICP blockade should be individually tailored to gain the maximum efficacy. The remission phase remains the most favorable setting to deliver Vγ9Vδ2 T-cell-based immune interventions.

Data availability statement

The original contributions presented in the study are included in the article/Supplementary material. Further inquiries can be directed to the corresponding author.

Ethics statement

The studies involving human participants were reviewed and approved by Comitato Etico Interaziendale A.O. Santa Croce e Carle di Cuneo AA. SS. LL. Cuneo 1, Cuneo 2, Asti. n.176-19 December 11, 2019. The patients/participants provided their written informed consent to participate in this study.

Author contributions

CG, BC, and JK performed the experiments, analyzed the data, and contributed to the manuscript writing and editing; MM and CR designed and supervised the experiments, analyzed the data and wrote the manuscript; ET, IA, MDA, and AL managed samples collection, analyzed and correlated clinical data, and contributed to the manuscript editing. All authors contributed to the article and approved the submitted version.

Funding

This study received funding from the Italian Association for Cancer Research (AIRC) (IG21744 to MM and IG21408 to CR), Sanofi Research-to-Care (MM), CRT (2021.0556 to CR) and Associazione Italiana contro le Leucemie-Linfomi e Mielomi ONLUS (AIL) (Sezione di Cuneo "Paolo Rubino") (MM, ET). The funders were not involved in the study design, collection, analysis, interpretation of data, the writing of this article or the decision to submit it for publication.

Conflict of interest

MM reports advisory boards for AbbVie, Janssen-Cilag, Sanofi, and research funding from Sanofi; MG reports advisory boards for Amgen, Bristol Myers Squibb, and Janssen-Cilag; MDA reports honoraria for lectures and advisory boards for GlaxoSmithKline, and Sanofi; AL reports honoraria and advisory boards for Janssen-Gilag, Bristol Myers Squibb, Amgen, Takeda, Oncopeptides, GlaxoSmithKline, Sanofi, and Karyopharm.

The remaining authors declare that the research was conducted in the absence of any commercial or financial relationships that could be construed as a potential conflict of interest.

Publisher's note

Supplementary material

The Supplementary Material for this article can be found online at: https://www.frontiersin.org/articles/10.3389/fimmu.2022.1073227/full#supplementary-material

References

1. Robert C. A decade of immune-checkpoint inhibitors in cancer therapy. *Nat Commun* (2020) 11:3801. doi: 10.1038/s41467-020-17670-y

2. Ansell SM, Lesokhin AM, Borrello I, Halwani A, Scott EC, Gutierrez M, et al. PD-1 blockade with nivolumab in relapsed or refractory hodgkin's lymphoma. *N Engl J Med* (2015) 372(4):311–9. doi: 10.1056/NEJMoa1411087

3. Eroglu Z, Zaretsky JM, Hu-Lieskovan S, Kim DW, Algazi A, Johnson DB, et al. High response rate to PD-1 blockade in desmoplastic melanomas. *Nature.* (2018) 553(7688):347–50. doi: 10.1038/nature25187

4. Finn RS, Ryoo BY, Merle P, Kudo M, Bouattour M, Lim HY, et al. Pembrolizumab as second-line therapy in patients with advanced hepatocellular carcinoma in KEYNOTE-240: A randomized, double-blind, phase III trial. *J Clin Oncol* (2020) 38(3):193–202. doi: 10.1200/JCO.19.01307

5. Salik B, Smyth MJ, Nakamura K. Targeting immune checkpoints in hematological malignancies. *J Hematol Oncol* (2020) 13(1):111. doi: 10.1186/s13045-020-00947-6

6. García-Ortiz A, Rodríguez-García Y, Encinas J, Maroto-Martín E, Castellano E, Teixidó J, et al. The role of tumor microenvironment in multiple myeloma development and progression. *Cancers.* (2021) 13:1–22. doi: 10.3390/cancers13020217

7. Lomas OC, Tahri S, Ghobrial IM. The microenvironment in myeloma. *Curr Opin Oncol* (2020) 32(2):170–5. doi: 10.1097/CCO.0000000000000615

8. Danziger SA, McConnell M, Gockley J, Young MH, Rosenthal A, Schmitz F, et al. Bone marrow microenvironments that contribute to patient outcomes in newly diagnosed multiple myeloma: A cohort study of patients in the total therapy clinical trials. *PLoS Med* (2020) 17(11):e1003323. doi: 10.1371/journal.pmed.1003323

9. Castella B, Foglietta M, Sciancalepore P, Rigoni M, Coscia M, Griggio V, et al. Anergic bone marrow Vγ9Vδ2 T cells as early and long-lasting markers of PD-1-targetable microenvironment-induced immune suppression in human myeloma. *Oncoimmunology.* (2015) 4(11):e1047580. doi: 10.1080/2162402X.2015.1047580

10. Liu J, Hamrouni A, Wolowiec D, Coiteux V, Kuliczkowski K, Hetuin D, et al. Plasma cells from multiple myeloma patients express B7-H1 (PD-L1) and increase expression after stimulation with IFN-γ and TLR ligands *via* a MyD88-, TRAF6-, and MEK-dependent pathway. *Blood.* (2007) 110(1):296–304. doi: 10.1182/blood-2006-10-051482

11. An G, Acharya C, Feng X, Wen K, Zhong M, Zhang L, et al. Osteoclasts promote immune suppressive microenvironment in multiple myeloma: Therapeutic implication. *Blood.* (2016) 128(12):1590–603. doi: 10.1182/blood-2016-03-707547

12. Sponaas AM, Waage A, Vandsemb EN, Misund K, Børset M, Sundan A, et al. Bystander memory T cells and IMiD/Checkpoint therapy in multiple myeloma: A dangerous tango? *Front Immunol* (2021) 12:636375. doi: 10.3389/fimmu.2021.636375

13. Castella B, Foglietta M, Riganti C, Massaia M. Vγ9Vδ2 T cells in the bone marrow of myeloma patients: A paradigm of microenvironment-induced immune suppression. *Front Immunol* (2018) 9:1492. doi: 10.3389/fimmu.2018.01492

14. Castella B, Vitale C, Coscia M, Massaia M. Vγ9Vδ2 T cell-based immunotherapy in hematological malignancies: From bench to bedside. *Cell Mol Life Sci* (2011) 68:2419–32. doi: 10.1007/s00018-011-0704-8

15. Harly C, Guillaume Y, Nedellec S, Peigné CM, Mönkkönen H, Mönkkönen J, et al. Key implication of CD277/butyrophilin-3 (BTN3A) in cellular stress sensing by a major human γδ T-cell subset. *Blood.* (2012) 120(11):2269–79. doi: 10.1182/blood-2012-05-430470

16. Riganti C, Castella B, Massaia M. ABCA1, apoA-I, and BTN3A1: A legitimate ménage à trois in dendritic cells. *Front Immunol* (2018) 9(JUN):1246. doi: 10.3389/fimmu.2018.01246

17. Rigau M, Ostrouska S, Fulford TS, Johnson DN, Woods K, Ruan Z, et al. Butyrophilin 2A1 is essential for phosphoantigen reactivity by γδ T cells. *Science* (2020) 367(6478):eaay5516. doi: 10.1126/science.aay5516

18. Karunakaran MM, Willcox CR, Salim M, Paletta D, Fichtner AS, Noll A, et al. Butyrophilin-2A1 directly binds germline-encoded regions of the Vγ9Vδ2 TCR and is essential for phosphoantigen sensing. *Immunity.* (2020) 52(3):487–98.e6. doi: 10.1016/j.immuni.2020.02.014

19. Wesch D, Marx S, Kabelitz D. Comparative analysis of αβ and γδ T cell activation by mycobacterium tuberculosis and isopentenyl pyrophosphate. *Eur J Immunol* (1997) 27(4):952–6. doi: 10.1002/eji.1830270422

20. Granier C, Dariane C, Combe P, Verkarre V, Urien S, Badoual C, et al. Tim-3 expression on tumor-infiltrating PD-1+CD8+ T cells correlates with poor clinical outcome in renal cell carcinoma. *Cancer Res* (2017) 77(5):1075–82. doi: 10.1158/0008-5472.CAN-16-0274

21. Thommen DS, Schreiner J, Müller P, Herzig P, Roller A, Belousov A, et al. Progression of lung cancer is associated with increased dysfunction of T cells defined by coexpression of multiple inhibitory receptors. *Cancer Immunol Res* (2015) 3(12):1344–54. doi: 10.1158/2326-6066.CIR-15-0097

22. Datar I, Sanmamed MF, Wang J, Henick BS, Choi J, Badri T, et al. Expression analysis and significance of PD-1, LAG-3, and TIM-3 in human non-small cell lung cancer using spatially resolved and multiparametric single-cell analysis. *Clin Cancer Res* (2019) 25(15):4663–73. doi: 10.1158/1078-0432.CCR-18-4142

23. Giraldo NA, Becht E, Vano Y, Petitprez F, Lacroix L, Validire P, et al. Tumor-infiltrating and peripheral blood T-cell immunophenotypes predict early relapse in localized clear cell renal cell carcinoma. *Clin Cancer Res* (2017) 23(15):4416–28. doi: 10.1158/1078-0432.CCR-16-2848

24. Tan J, Chen S, Yao D, Zhang Y, Yang L, Lai J, et al. Higher Tim-3 expression concurrent with PD-1 in exhausted CD4+ and CD8+T cells in patients with acute myeloid leukemia. *Exp Hematol* (2017) 53:S84–5. doi: 10.1016/j.exphem.2017.06.190

25. Kwon M, Kim CG, Lee H, Cho H, Kim Y, Lee EC, et al. PD-1 blockade reinvigorates bone marrow CD8+ T cells from patients with multiple myeloma in the presence of TGFb inhibitors. *Clin Cancer Res* (2020) 26(7):1644–55. doi: 10.1158/1078-0432.CCR-19-0267

26. Batorov EV, Aristova TA, Sergeevicheva VV, Sizikova SA, Ushakova GY, Pronkina NV, et al. Quantitative and functional characteristics of circulating and bone marrow PD-1- and TIM-3-positive T cells in treated multiple myeloma patients. *Sci Rep* (2020) 10(1):20846. doi: 10.1038/s41598-020-77941-y

27. Tan J, Chen S, Huang J, Chen Y, Yang L, Wang C, et al. Increased exhausted CD8 + T cells with programmed death-1, T-cell immunoglobulin and mucin-domain-containing-3 phenotype in patients with multiple myeloma. *Asia Pac J Clin Oncol* (2018) 14(5):e266–74. doi: 10.1111/ajco.13033

28. Gogoi D, Biswas D, Borkakoty B, Mahanta J. Exposure to plasmodium vivax is associated with the increased expression of exhaustion markers on γδ T lymphocytes. *Parasite Immunol* (2018) 40(12):1–9. doi: 10.1111/pim.12594

29. Girard P, Charles J, Cluzel C, Degeorges E, Manches O, Plumas J, et al. The features of circulating and tumor-infiltrating γδ T cells in melanoma patients display critical perturbations with prognostic impact on clinical outcome. *Oncoimmunology.* (2019) 8(8):1–16. doi: 10.1080/2162402X.2019.1601483

30. Li X, Lu H, Gu Y, Zhang X, Zhang G, Shi T, et al. Tim-3 suppresses the killing effect of Vγ9Vδ2 T cells on colon cancer cells by reducing perforin and granzyme b expression. *Exp Cell Res* (2019) 386:111719. doi: 10.1016/j.yexcr.2019.111719

31. Wu K, Feng J, Xiu Y, Li Z, Lin Z, Zhao H, et al. Vδ2 T cell subsets, defined by PD-1 and TIM-3 expression, present varied cytokine responses in acute myeloid leukemia patients. *Int Immunopharmacol.* (2020) 80:106122. doi: 10.1016/j.intimp.2019.106122

32. Zhao Y, Shao Q, Peng G. Exhaustion and senescence: Two crucial dysfunctional states of T cells in the tumor microenvironment. *Cell Mol Immunol* (2020) 17(1):27–35. doi: 10.1038/s41423-019-0344-8

33. Suen H, Brown R, Yang S, Weatherburn C, Ho PJ, Woodland N, et al. Multiple myeloma causes clonal T-cell immunosenescence: Identification of potential novel targets for promoting tumour immunity and implications for checkpoint blockade. *Leukemia.* (2016) 30(8):1716–24. doi: 10.1038/leu.2016.84

34. Zelle-Rieser C, Thangavadivel S, Biedermann R, Brunner A, Stoitzner P, Willenbacher E, et al. T Cells in multiple myeloma display features of exhaustion and senescence at the tumor site. *J Hematol Oncol* (2016) 9(1):1–12. doi: 10.1186/s13045-016-0345-3

35. Moreira A, Gross S, Kirchberger MC, Erdmann M, Schuler G, Heinzerling L. Senescence markers: Predictive for response to checkpoint inhibitors. *Int J Cancer.* (2019) 144(5):1147–50. doi: 10.1002/ijc.31763

36. Mariani S, Muraro M, Pantaleoni F, Fiore F, Nuschak B, Peola S, et al. Effector gammadelta T cells and tumor cells as immune targets of zoledronic acid in multiple myeloma. *Leukemia* (2005) 19(4):664–70. doi: 10.1038/sj.leu.2403693

37. Fichtner AS, Ravens S, Prinz I. Human γδ TCR repertoires in health and disease. *Cells* (2020) 9(4):800. doi: 10.3390/cells9040800

38. Gober HJ, Kistowska M, Angman L, Jenö P, Mori L, De Libero G. Human T cell receptor gammadelta cells recognize endogenous mevalonate metabolites in tumor cells. *J Exp Med* (2003) 197(2):163–8. doi: 10.1084/jem.20021500

39. Li Y, Li G, Zhang J, Wu X, Chen X. The dual roles of human γδ T cells: Anti-tumor or tumor-promoting. *Front Immunol* (2021) 11. doi: 10.3389/fimmu.2020.619954

40. Barros-Martins J, Bruni E, Fichtner AS, Cornberg M, Prinz I. OMIP-084: 28-color full spectrum flow cytometry panel for the comprehensive analysis of human γδ T cells. *Cytom Part A.* (2022) 101(10):856–61. doi: 10.1002/cyto.a.24564

41. Crespo J, Sun H, Welling TH, Tian Z, Zou W. T Cell anergy, exhaustion, senescence, and stemness in the tumor microenvironment. *Curr Opin Immunol* (2013) 25(2):214–21. doi: 10.1016/j.coi.2012.12.003

42. Dey M, Huff WX, Kwon JH, Henriquez M, Fetcko K. The evolving role of CD8+CD28- immunosenescent T cells in cancer immunology. *Int J Mol Sci* (2019) 20(11):2810. doi: 10.3390/ijms20112810

43. Noren Hooten N, Evans MK. Techniques to induce and quantify cellular senescence. *J Vis Exp* (2017) 123):55533. doi: 10.3791/55533

44. Zhang Y, Pfannenstiel LW, Bolesta E, Montes CL, Zhang X, Chapoval AI, et al. Interleukin-7 inhibits tumor-induced CD27 -CD28 - suppressor T cells: Implications for cancer immunotherapy. *Clin Cancer Res* (2011) 17(15):4975–86. doi: 10.1158/1078-0432.CCR-10-3328

45. Aiello A, Farzaneh F, Candore G, Caruso C, Davinelli S, Gambino CM, et al. Immunosenescence and its hallmarks: How to oppose aging strategically? a review of potential options for therapeutic intervention. *Front Immunol* (2019) 10:1–19. doi: 10.3389/fimmu.2019.02247

46. Zhao Y, Niu C, Cui J. Gamma-delta (γδ) T cells: Friend or foe in cancer development. *J Transl Med* (2018) 16(1):1–13. doi: 10.1186/s12967-017-1378-2

47. Horenstein AL, Quarona V, Toscani D, Costa F, Chillemi A, Pistoia V, et al. Adenosine generated in the bone marrow niche through a CD38-mediated pathway correlates with progression of human myeloma. *Mol Med* (2016) 22 (1):694–704. doi: 10.2119/molmed.2016.00198

48. Lawrence M, Wiesheu R, Coffelt SB. The duplexity of unconventional T cells in cancer. *Int J Biochem Cell Biol* (2022) 146:106213. doi: 10.1016/j.biocel.2022.106213

49. Zuazo M, Gato-Cañas M, Llorente N, Ibañez-Vea M, Arasanz H, Kochan G, et al. Molecular mechanisms of programmed cell death-1 dependent T cell suppression: Relevance for immunotherapy. *Ann Transl Med* (2017) 5(19):1–9. doi: 10.21037/atm.2017.06.11

50. Pereira BI, De Maeyer RPH, Covre LP, Nehar-Belaid D, Lanna A, Ward S, et al. Sestrins induce natural killer function in senescent-like CD8+ T cells. *Nat Immunol* (2020) 21(6):684–94. doi: 10.1038/s41590-020-0643-3

51. Whiteside TL. Down-regulation of ζ-chain expression in T cells: A biomarker of prognosis in cancer? *Cancer Immunol Immunother* (2004) 53 (10):865–78. doi: 10.1007/s00262-004-0521-0

52. Koyama S, Akbay EA, Li YY, Herter-Sprie GS, Buczkowski KA, Richards WG, et al. Adaptive resistance to therapeutic PD-1 blockade is associated with upregulation of alternative immune checkpoints. *Nat Commun* (2016) 7:1–9. doi: 10.1038/ncomms10501

53. Shayan G, Srivastava R, Li J, Schmitt N, Kane LP, Ferris RL. Adaptive resistance to anti-PD1 therapy by tim-3 upregulation is mediated by the PI3k-akt pathway in head and neck cancer. *Oncoimmunology.* (2017) 6(1):1–11. doi: 10.1080/2162402X.2016.1261779

54. Zhu C, Sakuishi K, Xiao S, Sun Z, Zaghouani S, Gu G, et al. An IL-27/NFIL3 signalling axis drives Tim-3 and IL-10 expression and T-cell dysfunction. *Nat Commun* (2015) 6:1–11. doi: 10.1038/ncomms7072

55. Noviello M, Manfredi F, Ruggiero E, Perini T, Oliveira G, Cortesi F, et al. Bone marrow central memory and memory stem T-cell exhaustion in AML patients relapsing after HSCT. *Nat Commun* (2019) 10(1):1065. doi: 10.1038/s41467-019-08871-1

56. Luo YL, Wang S, Fang ZX, Nie YC, Zhang LT, Huang CQ, et al. STAT1 participates in the induction of substance p expression in airway epithelial cells by respiratory syncytial virus. *Exp Lung Res* (2021) 47(2):78–86. doi: 10.1080/01902148.2020.1850922

57. Castella B, Kopecka J, Sciancalepore P, Mandili G, Foglietta M, Mitro N, et al. The ATP-binding cassette transporter A1 regulates phosphoantigen release and Vγ39Vδ2 T cell activation by dendritic cells. *Nat Commun* (2017) 8:1–14. doi: 10.1038/ncomms15663

58. Blank CU, Haining WN, Held W, Hogan PG, Kallies A, Lugli E, et al. Defining 'T cell exhaustion. ' *Nat Rev Immunol* (2019) 19(11):665–74. doi: 10.1038/s41577-019-0221-9

59. Xu W, Monaco G, Wong EH, Tan WLW, Kared H, Simoni Y, et al. Mapping of γ/δ T cells reveals Vδ2+ T cells resistance to senescence. *EBioMedicine.* (2019) 39:44–58. doi: 10.1016/j.ebiom.2018.11.053

60. Rahmanian N, Shokrzadeh M, Eskandani M. Recent advances in γH2AX biomarker-based genotoxicity assays: A marker of DNA damage and repair. *DNA Repair (Amst)* (2021) 108:103243. doi: 10.1016/j.dnarep.2021.103243

61. Biran A, Zada L, Abou Karam P, Vadai E, Roitman L, Ovadya Y, et al. Quantitative identification of senescent cells in aging and disease. *Aging Cell* (2017) 16(4):661–71. doi: 10.1111/acel.12592

62. Daley D, Zambirinis CP, Seifert L, Akkad N, Mohan N, Werba G, et al. γδ T cells support pancreatic oncogenesis by restraining αβ T cell activation. *Cell.* (2016) 166(6):1485–99.e15. doi: 10.1016/j.cell.2016.07.046

63. Schilbach K, Krickeberg N, Kaißer C, Mingram S, Kind J, Siegers GM, et al. Suppressive activity of Vδ2+ γδ T cells on αβ T cells is licensed by TCR signaling and correlates with signal strength. *Cancer Immunol Immunother.* (2020) 69 (4):593–610. doi: 10.1007/s00262-019-02469-8

64. Wu P, Wu D, Ni C, Ye J, Chen W, Hu G, et al. γδT17 cells promote the accumulation and expansion of myeloid-derived suppressor cells in human colorectal cancer. *Immunity.* (2014) 40(5):785–800. doi: 10.1016/j.immuni.2014.03.013

65. Liu X, Mo W, Ye J, Li L, Zhang Y, Hsueh EC, et al. Regulatory T cells trigger effector T cell DNA damage and senescence caused by metabolic competition. *Nat Commun* (2018) 9(1):249. doi: 10.1038/s41467-017-02689-5

66. Chen J, Moore A, Ringshausen I. ZAP-70 shapes the immune microenvironment in b cell malignancies. *Front Oncol* (2020) 10. doi: 10.3389/fonc.2020.595832

67. Saleh R, Toor SM, Khalaf S, Elkord E. Breast cancer cells and PD-1/PD-L1 blockade upregulate the expression of PD-1, CTLA-4, TIM-3 and LAG-3 immune checkpoints in CD4+ T cells. *Vaccines.* (2019) 7(4):1–13. doi: 10.3390/vaccines7040149

68. Kato R, Yamasaki M, Urakawa S, Nishida K, Makino T, Morimoto-Okazawa A, et al. Increased Tim-3+ T cells in PBMCs during nivolumab therapy correlate with responses and prognosis of advanced esophageal squamous cell carcinoma patients. *Cancer Immunol Immunother.* (2018) 67(11):1673–83. doi: 10.1007/s00262-018-2225-x

69. Kalbasi A, Ribas A. Tumour-intrinsic resistance to immune checkpoint blockade. *Nat Rev Immunol* (2020) 20:25–39. doi: 10.1038/s41577-019-0218-4

70. Abdel-Wahab N, Shah M, Suarez-Almazor ME. Adverse events associated with immune checkpoint blockade in patients with cancer: A systematic review of case reports. *PLoS One* (2016) 11(7):1–16. doi: 10.1371/journal.pone.0160221

71. Chen T, Li Q, Liu Z, Chen Y, Feng F, Sun H. Peptide-based and small synthetic molecule inhibitors on PD-1/PD-L1 pathway: A new choice for immunotherapy? *Eur J Medicinal Chem* (2019) 161:378–98. doi: 10.1016/j.ejmech.2018.10.044

72. Ribrag V, Avigan DE, Green DJ, Wise-Draper T, Posada JG, Vij R, et al. Phase 1b trial of pembrolizumab monotherapy for relapsed/refractory multiple myeloma: KEYNOTE-013. *Br J Haematology* (2019) 186:e41–4. doi: 10.1111/bjh.15888

73. Yang M, Du W, Yi L, Wu S, He C, Zhai W, et al. Checkpoint molecules coordinately restrain hyperactivated effector T cells in the tumor microenvironment. *Oncoimmunology*. (2020) 9(1):1–11. doi: 10.1080/2162402X.2019.1708064

74. Jing W, Gershan JA, Weber J, Tlomak D, McOlash L, Sabatos-Peyton C, et al. Combined immune checkpoint protein blockade and low dose whole body irradiation as immunotherapy for myeloma. *J Immunother Cancer*. (2015) 3(1):1–15. doi: 10.1186/s40425-014-0043-z

frontiers | Frontiers in Immunology

TYPE Original Research
PUBLISHED 13 January 2023
DOI 10.3389/fimmu.2022.1065495

OPEN ACCESS

EDITED BY
John-Maher,
King's College London,
United Kingdom

REVIEWED BY
Rene Hoet,
FairJourney Biologics, Portugal
Dieter Kabelitz,
University of Kiel, Germany

*CORRESPONDENCE
Laura A. Ridgley
laura.ridgley@astrazeneca.com

†PRESENT ADDRESS
Laura A. Ridgley,
Early Oncology, R&D, Astrazeneca,
Cambridge, United Kingdom
Jonathan Caron,
Centre de Recherche des Cordeliers,
INSERM, Cell Death and Drug
Resistance in Lymphoproliferative
Disorders Team, Sorbonne Universite,
Universite Sorbonne Paris Cite,
Universite Paris Descartes, Universite
Paris Diderot, Paris, France

SPECIALTY SECTION
This article was submitted to
Cancer Immunity
and Immunotherapy,
a section of the journal
Frontiers in Immunology

RECEIVED 09 October 2022
ACCEPTED 16 December 2022
PUBLISHED 13 January 2023

CITATION
Ridgley LA, Caron J, Dalgleish A and
Bodman-Smith M (2023) Releasing the
restraints of Vγ9Vδ2 T-cells in
cancer immunotherapy.
Front. Immunol. 13:1065495.
doi: 10.3389/fimmu.2022.1065495

Releasing the restraints of Vγ9Vδ2 T-cells in cancer immunotherapy

Laura A. Ridgley*†, Jonathan Caron†, Angus Dalgleish and Mark Bodman-Smith

Institute for Infection and Immunity, St. George's University of London, London, United Kingdom

Objectives: Vγ9Vδ2 T-cells are a subset of T-cells with a crucial role in immunosurveillance which can be activated and expanded by multiple means to stimulate effector responses. Little is known about the expression of checkpoint molecules on this cell population and whether the ligation of these molecules can regulate their activity. The aim of this study was to assess the expression of both activatory and inhibitory receptors on Vγ9Vδ2 T-cells to assess potential avenues of regulation to target with immunotherapy.

Methods: Expression of various activatory and inhibitory receptors was assessed on Vγ9Vδ2 T-cells by flow cytometry following activation and expansion using zoledronic acid (ZA) and Bacillus Calmette-Guérin (BCG). Expression of these markers and production of effector molecules was also examined following co-culture with various tumour cell targets. The effect of immune checkpoint blockade on Vγ9Vδ2 T-cells was also explored.

Results: Vγ9Vδ2 T-cells expressed high levels of activatory markers both at baseline and following stimulation. Vγ9Vδ2 T-cells expressed variable levels of inhibitory checkpoint receptors with many being upregulated following stimulation. Expression of these markers is further modulated upon co-culture with tumour cells with changes reflecting activation and effector functions. Despite their high expression of inhibitory receptors when cultured with tumour cells expressing cognate ligands there was no effect on Vδ2+ T-cell cytotoxic capacity or cytokine production with immune checkpoint blockade.

Conclusions: Our work suggests the expression of checkpoint receptors present on Vγ9Vδ2 T-cells which may provide a mechanism with the potential to be utilised by tumour cells to subvert Vγ9Vδ2 T-cell cytotoxicity. This work suggests important candidates for blockade by ICI therapy in order to increase the successful use of Vγ9Vδ2 T-cells in immunotherapy.

KEYWORDS

Vγ9Vδ2 T-cell, BCG, ZA, immune checkpoint inhibitor, NKG2A

10.3389/fimmu.2022.1065495

Introduction

The γδ T-cell is a unique cell population making up 1-5% of peripheral blood T-cells (1, 2). In contrast to the αβ T-cell the γδ T-cell comprises of a TCR made of a variable (V) γ chain and Vδ chain. There are numerous subsets of γδ T-cell with the main subsets being the Vδ1, Vδ2 and Vδ3 T-cells. The Vδ1 and Vδ3 subsets are most abundant in the intestinal mucosa whereas the most predominant subtype in the blood is the Vγ9Vδ2 T-cell (Vδ2) which is important in immunosurveillance against infection, for example *Mycobacterium tuberculosis*, *Listeria monocytogenes* and *Salmonella enterica* (3–5). This cell population has also been implicated in anti-tumour responses due to their ability to recognise phosphoantigens from dysregulated mevalonate pathways. Full activation occurs *via* the recruitment of butyrophilin 3A1 (BTN3A1), which together with BTN2A1 engages the T-cell receptor (TCR) (6–10). In addition to recognising phosphoantigens, Vγ9Vδ2 T-cells can also recognise upregulated cell stress ligands through expression of various NK associated activatory receptors (11). Confirming their role in immunosurveillance, the presence of γδ T-cells in tumours has been shown to correlate with clinical outcome in different cancer types (12–14). Genetic signatures reveal the γδ T-cell as the most significantly associated with favourable prognosis (15). Furthermore, high levels of circulating γδ T-cells have been associated with reduced cancer risk and improved survival (15–17).

Due to their inherent killing capacity these cells are promising tools for use in cancer immunotherapy. In the initial exploration into the use of these cells for immunotherapy studies utilized the expansion of γδ T-cells with various phosphoantigen derivates and nitrogen containing bisphosphonates, including zoledronic acid (ZA). Multiple trials have been conducted utilising *in vivo* expansion or *in vitro* expansion followed by adoptive transfer, showing varying degrees of success (18–25). Protocols for expansion of Vδ1 cells include IL-15, IL-7 and phytoheamagglutinin (PHA) or antigen presenting cells (APCs) expressing CD86, 41BBL, CD40L and cytomegalovirus (CMV)-antigen-pp65 (26–28). In contrast protocols most commonly used for expansion of Vδ2 cells include ZA, bromohydrin pyrophosphate (BrHPP) and (E)-4-hydroxy-3-methyl-but-2-enyl pyrophosphate (HMBPP) (22, 29). Potential explanations as to their varying efficacy include anergy, reduced migratory capacity and subsequent infiltration into tumours or high degree of polyclonality resulting in a diverse product.

Other candidates for expansion of Vδ2 T-cells include viruses and bacteria such as Bacillus Calmette-Guérin (BCG), the strain of mycobacterium used in the prevention of tuberculosis and in the treatment of bladder cancer (13, 30–32). BCG injection into melanoma lesions has resulted in regression of lesions and infiltration of IFN-γ-producing Vδ2 T-cells (33). Further support for the use of BCG in Vδ2 T-cell expansion comes as this method has been shown *in vitro* to result in altered cytolytic profiles compared to expansion using ZA (34).

In recent years several additional strategies have been utilized in order to improve γδ T-cell therapy (35, 36). These include antibody therapy, for example, agonistic monoclonal antibodies against BTN3A1, such as ICT01 in phase I/II clinical trial (NCT04243499), bispecific antibodies targeting TCR and tumour antigens, such as Vγ9-TCR engagers against HER2, CD1d and PSMA in clinical trials (NCT04887259 and NCT05369000) and bispecific Vγ9 nanobody-based constructs targeting EGFR in pre-clinical development (37–41). Other strategies focusing on cell therapy include chimeric antigen receptor (CAR)-transduced Vδ2 cells or αβ-T-cells transduced with Vγ9Vδ2 TCR, also called T-cells engineered with defined γδ TCR (TEG) (42–47).

Tumours have many mechanisms of evading the immune system, a key mechanism being the expression of ligands to checkpoint receptors expressed on effector immune cells. Tumours can display, amongst others, increased programmed death ligand 1 (PDL1) and HLA class I histocompatibility antigen alpha chain E (HLA-E), which bind programmed cell death protein 1 (PD1) and CD94/NK group 2 member A (NKG2A) to dampen T-cell and natural killer (NK) cell responses respectively (48). Further immune checkpoints include lymphocyte activation gene 3 (LAG3), T-cell immunoglobulin domain and mucin domain 3 (TIM3), T-cell immunoreceptor with Ig and ITIM domains (TIGIT), B and T lymphocyte attenuator (BTLA) which bind to their ligand's major histocompatibility complex (MHC) class II, Galectin 9 (Gal9), poliovirus receptor (PVR) and herpesvirus entry mediator (HVEM) respectively. Understanding of immune checkpoints in relation to Vδ2 T-cells is currently limited. In a clinical setting, treatment with ipilimumab, an antibody targeting CTLA-4, increases Vδ2 T-cell number indicating a role for checkpoints in Vδ2 T-cell function (16). Confirming the importance of checkpoint receptors on Vδ2 T-cells a recent study documents increased proportions of Vδ2 T-cells expressing LAG3 in melanoma patients, a finding which was associated with earlier relapse and shorter overall survival (17). Upregulation of PD1 expression has been documented on Vδ2 T-cells following antigenic stimulation followed by a gradual decline (49). Furthermore, expression of PD1 is high on γδ T-cells from a variety of tumour types (50–52). Blockade of PD1 was able to enhance cytotoxicity and IFN-γ production although other studies have shown no effect of blockade on γδ T-cell function (49, 53, 54) Moreover, TIM3 co-expression with PD1 has been shown to result in lower IFN-γ and TNF production (55). Interaction with Gal9 lowered Vδ2 T-cell cytotoxicity by limiting perforin and Granzyme B (56). Furthermore, anti-TIM3 was able to enhance anti-tumour activity *via* increased cytokine production, this effect was independent of PD1 blockade suggesting a complex interplay of receptors will be important in Vδ2 T-cells activity (55).

The aim of this study was to investigate further the expression of activatory and inhibitory immune receptors on Vδ2 T-cells to determine the hierarchy of importance of these molecules in Vδ2 T-cell function and the importance of stimulation conditions on activation of Vδ2 T-cells. This will provide crucial information on the use of checkpoint inhibitor therapy alongside Vδ2 T-cell therapy.

Materials and methods

Subjects

Donor blood was obtained from healthy volunteers of leukocyte reduction system (LRS) cones from the National Health Service Blood and Transplant Unit (NHSBT) at St. George's Hospital London under ethical approval SGREC16.0009.

PBMC and Vγ9Vδ2 T-cell isolation

Peripheral blood mononuclear cells (PBMC) were isolated from LRS cones using density centrifugation over Histopaque-1077 (Sigma) as per manufacturer's instructions. Erythrocytes were lysed using RBC lysis buffer (BioLegend) and platelets removed by centrifugation at 200g. PBMCs were stored at -80°C in freezing medium (45% RPMI-1640, 45% FBS, 10% DMSO). Following expansion γδ T-cells were resuspended in MACS buffer (PBS containing 0.5% BSA and 2mM EDTA) and isolated by negative enrichment using magnetic γδ T-cell negative selection kit (Miltenyi Biotech), according to manufacturer's instructions. Isolated cells had median purities of >90%.

Expansion and culture of Vγ9Vδ2 T-cells

For expansion of Vγ9Vδ2 T-cells thawed PBMCs were cultured at $5x10^6$ cells/ml in RPMI-1640 + 10% Foetal Bovine Serum (FBS; Sigma) with final concentrations of 10μM ZA (Sigma) or $2x10^4$ CFU BCG (Pasteur strain, gifts of Dr Rajko Reljic St. George's University of London) both with 15ng/ml IL-2 (R&D Systems) in 200μl total volume in 96 well round bottomed plates. BCG was cultured as previously described (34) and in some cases, where indicated, BCG was heat killed by heating to 80°C for 30 minutes. Cells were cultured at 37°C with 5% CO_2 for 14 days with media containing 15ng/ml IL-2 refreshed every 2-3 days.

Tumour cell culture

Burkitt's Lymphoma B-cell lines Daudi and Raji, and acute monocytic leukemia cell line THP-1, all from the European Collections of Authenticated Cell Cultures (ECACC), were cultured in RPMI-1640 + 10% FBS at $1x10^6$ per ml of $75cm^2$ tissue culture flask (Thermo Fisher Scientific). Cells were passaged every 2-4 days to maintain recommended cell densities and cells were used between passage 5-15. In some cases, prior to culture with γδ T-cells tumour cells were cultured with final concentration of 50μM ZA for 24 hours.

Cytotoxicity assay

For cytotoxicity assays tumour cells were labelled with a final concentration of 0.5μM Cell Trace Far Red (Thermo Fisher Scientific) prior to culture. ZA or BCG stimulated γδ T-cells were co-cultured with Daudi, Raji or THP-1 cells, pre-treated with or without 50μM ZA, at an optimised effector:target cell ratio of 1:1. Cells were cultured in a total volume of 200μl in 96 well plates at $0.5x10^6$ cells/ml in RPMI + 10% FBS for 18 hours before being stained with zombie aqua, as described in Multiparameter Flow Cytometry. Specific killing was calculated by subtracting the dead cell frequency of targets cultured alone from the dead cell frequency of those in co-culture.

CD107b mobilisation assay

For CD107b mobilisation assays γδ T-cells were cultured with tumour cells as previously described for cytotoxicity assay. Cells were cultured for 1 hour alone or with 25ng/ml Phorbol 12-myristate 13-acetate (PMA) and 1μg/ml ionomycin used as a positive control, before the addition of 5μg/ml Brefeldin A (BFA) and 2μM monensin (both Sigma Aldrich) and CD107b-FITC (H4B4; BioLegend) for 3 hours. Cells were harvested and stained for flow cytometry.

TNF release assay

For TNF release assays γδ T-cells were cultured with tumour cells as previously described for cytotoxicity assay. Cells were cultured for 15 minutes before the addition of 10μM TAPI-0 (TNF-α protease inhibitor 0; Biotechne) and TNF-PECy7 (MAb11; Biolegend). Cells were cultured for 4 hours before being harvested and stained for flow cytometry.

Immune checkpoint blockade

For the blockade of immune checkpoints in cytotoxicity and CD107b mobilisation assays the following antibodies were used: anti-IgG1, anti-IgG2, anti-PD1, anti-TIGIT, anti-LAG3, anti-TIM3 and anti-BTLA (all BioLegend). Anti-NKG2A antibodies were developed using a plant manufacturing system (57). All antibodies were used at final concentrations of 5μg/ml.

Multiparameter flow cytometry

Cells were stained with Zombie Aqua viability dye (BioLegend) in PBS, according to manufacturer's instructions, prior to antibody staining. Staining was performed in FACS buffer (PBS containing 2.5% BSA, 0.1% sodium azide and 2mM EDTA) for 30 minutes at 4°C. Cells were stained with the following antibodies as indicated CD3-BUV395 (UCHT1), CD56-BUV737 (NCAM16.2; both BD Biosciences) Vδ2-PE, Vδ2-PerCP-Vio700 (both REA771), PD1-VioBrightFITC (PD1.3.1.3), NKG2A-VioFITC (REA110), NKG2C-PE (REA205; all Miltenyi Biotech), CD3-AF700 (OKT3), BTLA-PE (MIH26), TIGIT-BV421 (A15153G), LAG3-BV711 (11C3C65), TIM3-BV605 (F38-2E2), NKG2D-APC (1D11), DNAM1-BV711 (11A8), KLRG1-BV421 (14C2A07), NKp44-PE (P44-8), NKp30-BV711 (P30-15), NKp46-BV421 (9E2; all BioLegend) and VISTA-APC (B7H5DS8; eBioscience). Cells were fixed with cell fix (BD Biosciences) prior to acquisition.

For intracellular staining cells were stained with Zombie Aqua prior to staining with surface antibodies CD3-BUV395 and Vδ2-PerCP-Vio700. Cells were fixed and permeabilised with fixation and permeabilization buffer (BioLegend), according to manufacturer's instructions, and stained with IFN-γ-BV421 (4S.B3), TNF-BV711 (MAb11), Granzyme B-APC (QA16A02), Perforin-PE-Cy7 (B-D48), Granulysin-PE (DH2; all BioLegend).

Data was collected on a Fortessa X20 (BD Biosciences) and analysed using FlowJo (Treestar), using fluorescence-minus-one (FMO) gating. Debris was excluded by SSC-A versus SSC-W and live cells were gated based on exclusion of zombie aqua viability dye. Vγ9Vδ2 cells, T-cells and NK cells were gated as Vδ2+, CD3+ and CD56+ respectively and activatory and inhibitory receptor expression further examined, gating strategy as depicted in Supplementary Figure 1.

Gene expression of Vγ9Vδ2 T-cells

RNA was extracted from Vγ9Vδ2 T-cells using RNeasy Micro Kit (Qiagen) as per manufacturer's instructions. The purity of the isolated mRNA was assessed using a NanoDrop™ 2000 spectrophotometer (Thermo Fisher Scientific) and the quality and integrity using an Agilent 2100 Bioanalyser (Agilent Technologies). mRNA library was then prepared with the NEBNext Ultra II kit (New England Biolabs) and sequenced with a NextSeq 550 system (Illumina). Raw data was processed and analysed using Partek Flow (Partek).

Statistics

Statistical analysis was performed using GraphPad prism 9 (GraphPad Software Inc). Non-parametric analysis of variance with Sidak *post hoc* pairwise analyses, non-parametric mixed effects analysis with Tukey's *post hoc* pairwise analyses or non-parametric analysis of variance (Friedman's) with Dunn's *post hoc* for multiple pairwise comparisons carried out where indicated. P-values of <0.05 were considered statistically significant.

Results

Vγ9Vδ2 T-cells express NK associated activatory receptors and inhibitory checkpoint receptors

First, we aimed to assess the expression of NK associated activatory markers and inhibitory checkpoint receptors in Vδ2+ T-cells in freshly isolated PBMCs, gating strategy in Supplementary Figure 1.

Vδ2+ T-cells express several activatory receptors including NKG2D, DNAM1 and NKp30 (Figure 1A; Supplementary Figure 2A). Vδ2+ T-cells express a high level of inhibitory checkpoint receptors NKG2A, KLRG1 and BTLA, intermediate levels of PD1, TIGIT and VISTA and very little expression of LAG3 and TIM3 (Figure 1B; Supplementary Figure 2B).

The expression profile of Vδ2+ T-cells as seen by flow cytometry was largely confirmed by RNAseq. Expression of activatory marker NKG2D was particularly high with higher expression of DNAM1 and NKp30 also seen (Figure 1C). In terms of inhibitory receptors KLRG1, NKG2A and VISTA were confirmed at having higher expression at the gene level (Figure 1C).

The expression of NK-associated activatory and inhibitory checkpoint receptors on Vδ2+ T-cells in circulation confirms previous descriptions of these cells as a bridge between the innate and adaptive immune systems, therefore we assessed the expression of these molecules in comparison to CD3+ T-cells and CD56+ NK cells. Vδ2+ T-cells express similar levels of activatory receptors NKp30 compared to CD56+ NK cells from PBMC, however unlike NK cells Vδ2+ T-cells lack expression of NKp44 and NKp46 and have significantly higher expression of NKG2D and DNAM1 (Figure 1D). Compared to NK cells Vδ2+ T-cells express significantly higher levels of NKG2A, KLRG1, BTLA and PD1 and significantly lower levels of TIGIT and TIM3 (Figure 1E). In comparison with CD3+ T-cells Vδ2+ T-cells express significantly higher NKG2D, DNAM1 and NKp30 (Figure 1D). In addition, Vδ2+ T-cells express significantly higher NKG2A, KLRG1, BTLA and VISTA but significantly lower PD1 and TIM3 compared to CD3+ T-cells (Figure 1E).

The receptor expression profile of Vδ2+ T-cells is unique, highlighting the role of these cells as a bridge between the innate and adaptive immune response. This receptor profile provides both a mechanism of recognition and a potential method of regulation of Vγ9Vδ2 T-cells therefore, it will be important to know how the expression of these inhibitory markers is altered following activation as these may provide a mechanism of damping Vδ2+ T-cell response.

10.3389/fimmu.2022.1065495

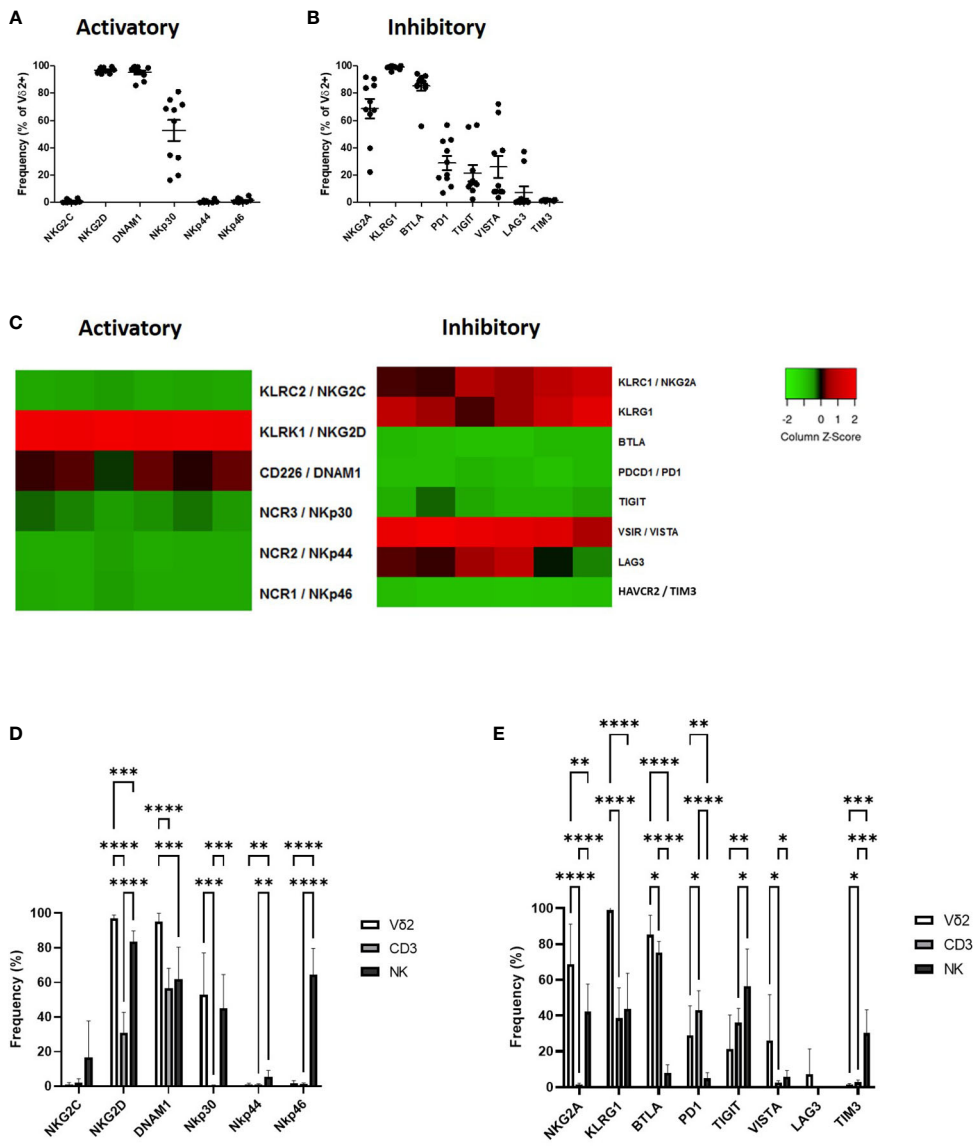

FIGURE 1
Expression of NK associated activatory receptors **(A)** and inhibitory checkpoint receptors **(B)** was determined in Vγ9Vδ2+ cells in PBMCs from healthy donors using flow cytometry. Heat maps showing the expression of NK associated activatory and inhibitory receptors in Vγ9Vδ2+ cells from 6 donors using RNAseq **(C)**. Expression of NK associated activatory receptors **(D)** and inhibitory checkpoint receptors **(E)** in Vγ9Vδ2+ cells was compared to CD3+ T-cells and CD56+ NK cells. N=10. *p<0.05, **p<0.005, ***p<0.0005, ****p<0.0001, non-parametric analysis of variance with Tukey's *post hoc* for multiple pairwise comparisons.

Expression of inhibitory immune checkpoint receptors increases upon Vδ2+ T-cell activation

After showing the expression of a wide range of activatory and inhibitory immune receptors on Vδ2+ T-cells in circulation the next aim was to assess whether Vδ2+ T-cell stimulation resulted in alteration of these molecules. We hypothesised that an upregulation in the expression of inhibitory molecules following stimulation will provide a mechanism by which Vδ2 + T-cells can be restrained, with implications on their efficacy in immunotherapy.

The expression of activatory and inhibitory receptors was explored following 24 hours activation of PBMC. Isolated PBMCs were stimulated with IL-2 with and without previously optimised concentrations of ZA or BCG for 24 hours (34). Expression of activatory and inhibitory markers was assessed by flow cytometry.

The activation of Vδ2+ T-cells by IL-2, ZA and BCG was confirmed by the upregulation of activation marker CD69 (Figure 2A). There was no change in expression of NK-associated activatory receptors from baseline with 24-hour stimulation, with the exception of NKG2D which is significantly reduced with both ZA and BCG (Figure 2B). There was no difference in expression of activatory markers with stimulation method with the exception of NKG2C which was significantly reduced in BCG activated Vδ2+ T-cells compared to ZA activated Vδ2+ T-cells (Figure 2B; Supplementary Figure 2C).

There was no change in the expression of inhibitory immune receptor KLRG1 on Vδ2+ T-cells following ZA stimulation (Figure 2C). In contrast, there was significantly increased expression of NKG2A PD1, TIGIT, VISTA, LAG3 and TIM3 with ZA stimulation. Similarly, TIGIT, LAG3 and TIM3 are significantly increased with BCG stimulation (Figure 2C; Supplementary Figure 2D). However, LAG3 and TIM3 were the only receptors significantly increased compared to IL-2 only control. BTLA is the only inhibitory receptor whose expression decreased upon ZA and BCG stimulation, compared to both baseline and IL-2 stimulation (Figure 2C). There was reduced expression of VISTA and increased expression of TIM3 on BCG activated Vδ2+ T-cells compared to ZA activated Vδ2+ T-cells (Figure 2C).

Furthermore, modulation of activatory and inhibitory receptors following stimulation with ZA and BCG does appear to be specific to Vδ2+ T-cells with minimal changes seen in expression of receptors on CD3+ T-cells and CD56+ NK cells (Supplementary Figure 3). Changes in expression of NKG2D, NKp30, LAG3 and TIM3 do reach statistical significance in CD3+ T-cells (Supplementary Figures 3A, B). For CD56+ cells DNAM1, NKp44, NKG2A, TIGIT, LAG3 and TIM3 also show statistical significance from baseline (Supplementary Figures 3C, D).

Expression of inhibitor immune checkpoint receptors increases upon Vδ2+ T-cell expansion

After documenting changes in the expression of various activatory and inhibitory receptors following 24-hour Vδ2+ T-cell activation the next aim was to assess whether these changes in expression were maintained over longer periods of stimulation, as seen with Vδ2+ T-cell expansion protocols. Therefore, the expression of activatory and inhibitory receptors was next explored following the expansion of Vδ2+ T-cells in PBMC. Isolated PBMCs were stimulated with IL-2 with and without previously optimised concentrations of ZA, BCG or HK-BCG for 14 days. Expression of activatory and inhibitory markers was assessed by flow cytometry.

The expansion of Vδ2+ T-cells was also assessed following 14 days stimulation with ZA, BCG or HK-BCG. There were successful expansions of Vδ2+ T-cells when stimulated with ZA and heat-killed BCG (HKBCG), compared to the control IL-2 alone (Figure 3A).

High expression of NKG2D and DNAM1 was maintained from baseline and 24 hours activation (Figure 3B). NKp44 was increased following 14 days stimulation with ZA (Figure 3B). Furthermore, there was no difference in expression of activatory markers following 14 days stimulation with ZA or BCG (Figure 3C; Supplementary Figure 2E).

There was no change in inhibitory receptors NKG2A, PD1 and VISTA from baseline. However, there was significantly reduced expression of both KLRG1 and BTLA from baseline with both ZA and BCG expansion (Figure 3C). TIGIT, LAG3 and TIM3 were significantly increased following 14-day expansion with ZA whereas only LAG3 and TIM3 were significantly increased following 14-day expansion with BCG (Figure 3C; Supplementary Figure 2F). There was no significant difference in expression of receptors between ZA and BCG-expanded Vδ2+ T-cells suggesting a similar mechanism of activation.

In addition to marker expression as assessed by flow cytometry, corresponding RNAseq analysis of 14 day stimulated Vδ2+ T-cells shows that high expression of NKG2D and DNAM1 is maintained from baseline (Figure 3D). Furthermore, the increase in LAG3 and TIM3 was confirmed from baseline with 14-day stimulation (Figure 3D). In addition, no clear differences were seen in RNA expression of activatory or inhibitory receptors between ZA and BCG expanded Vδ2+ T-cells (Figure 3D).

Following 14-day stimulation there are also differences in expression of activatory and inhibitory receptors on CD3+ T-cells and CD56+ NK cells (Supplementary Figure 4). Expression of BTLA is significantly reduced on CD3+ T-cells following ZA and BCG expansion. Furthermore, TIM3 and LAG3 are significantly increased on CD3+ T-cells following ZA and BCG expansion (Supplementary Figures 4A, B). Similarly, in CD56+ cells LAG3, TIM3 and NKG2A are significantly increased with both ZA and BCG expansion. While KLRG1 is significantly decreased in CD56+ cells with ZA and BCG expansion. Furthermore, DNAM1, NKp30, NKp44 and NKp46 are significantly increased on CD56+ cells with ZA and BCG expansion (Supplementary Figures 4C, D). These changes, largely absent following 24-hour stimulation, suggest an indirect effect of stimulation on other cell populations. High levels of expression of numerous inhibitory receptors may provide a mechanism of immune regulation of Vδ2+ T-cells, important in our understanding when using these cells in immunotherapy.

Expression of checkpoint receptors and cytokine production is modulated upon culture with tumour cells

Many studies have documented the ability of Vδ2+ T-cells to exert strong anti-tumour responses with both direct cytotoxic

10.3389/fimmu.2022.1065495

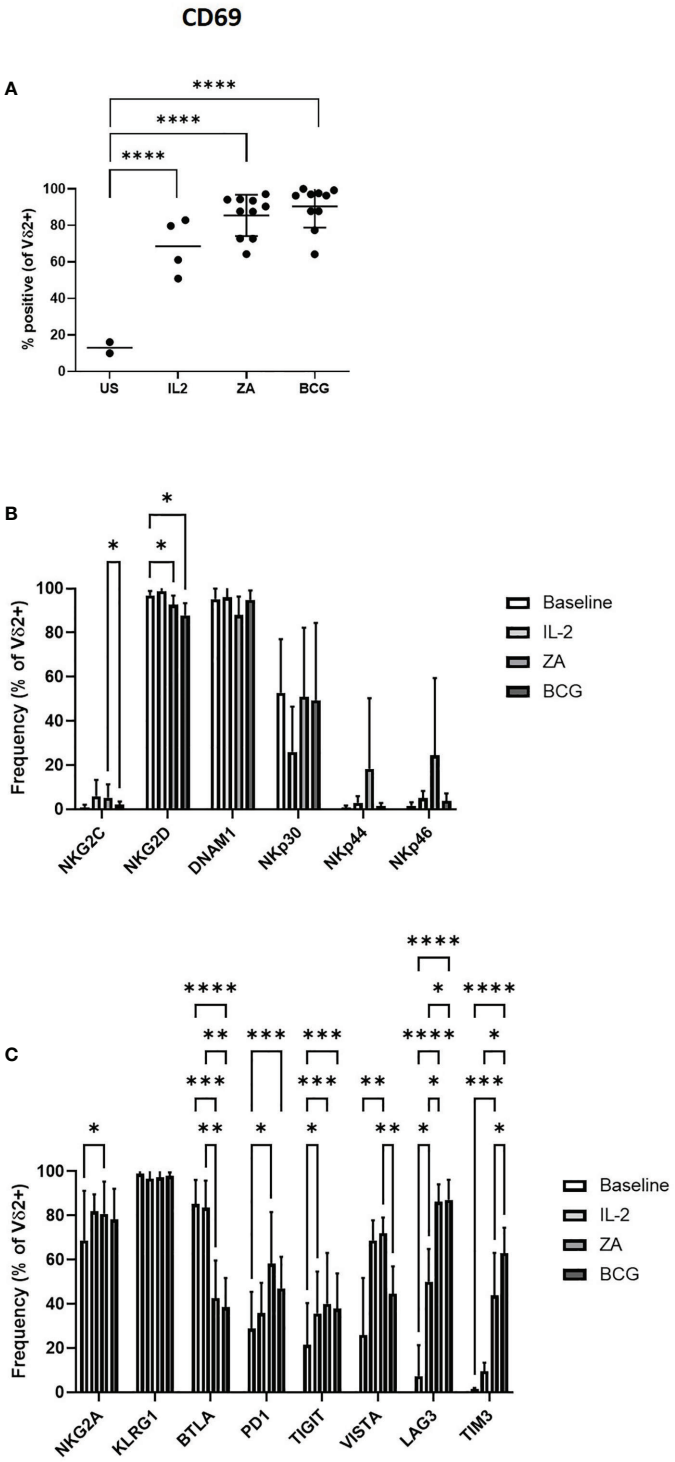

FIGURE 2
Activation of Vδ2 cells was assessed by flow cytometry of CD69 expression following 24 hours stimulation with IL-2, ZA or BCG both with IL-2 **(A)**. Expression of NK associated activatory markers **(B)** and inhibitory checkpoint receptors **(C)** was determined on Vγ9Vδ2 T-cells in PBMC stimulated for 24 hours with IL-2 alone, ZA or BCG, both with IL-2, using flow cytometry. N=10. *p<0.05, **p<0.005, ***p<0.0005, ****p<0.0001, non-parametric mixed effects analysis with Tukey's *post hoc* for multiple pairwise comparisons.

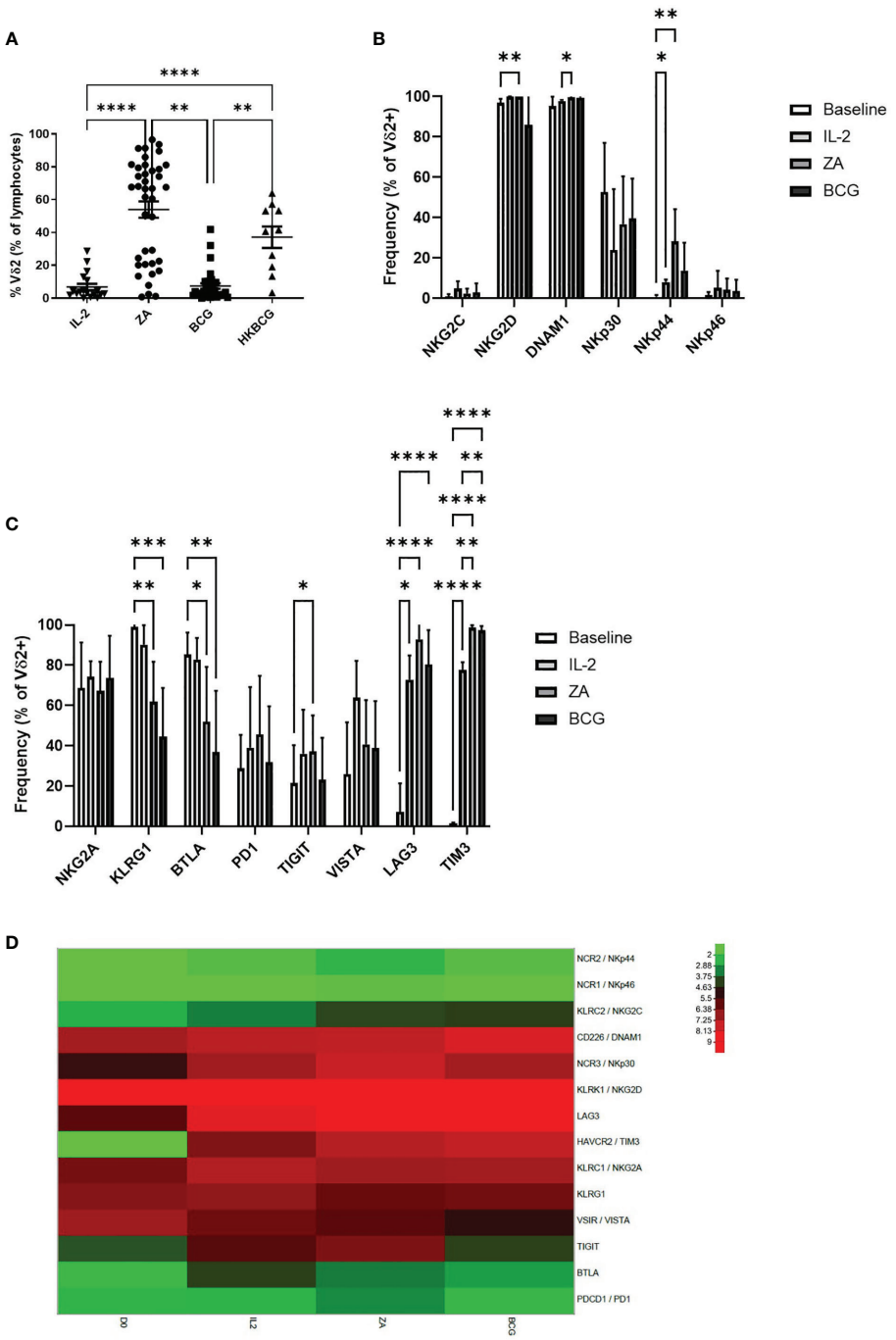

FIGURE 3
Frequency of Vδ2 cells as a percentage of live cells was assessed by flow cytometry following 14 days stimulation with IL-2 alone or IL-2 with ZA, BCG or HK-BCG. N=10-39, **p<0.005, ****p<0.0001, non-parametric analysis of variance with Tukey's *post hoc* for multiple pairwise comparisons **(A)**. Expression of NK associated activatory markers **(B)** and inhibitory checkpoint receptors **(C)** was determined on Vγ9Vδ2 T-cells in PBMC stimulated for 14 days with IL-2 alone, ZA or BCG, both with IL-2, using flow cytometry. N=10, *p<0.05, **p<0.005, ***p<0.0005, ****p<0.0001, non-parametric mixed effects analysis with Tukey's *post hoc* for multiple pairwise comparisons. Expression of activatory and inhibitory receptors was determined in Vγ9Vδ2 T-cells from 6 donors at baseline (D0) and following stimulation for 14 days with IL-2 alone (IL2), ZA (ZA) or BCG (BCG), both with IL-2, using RNAseq **(D)**.

10.3389/fimmu.2022.1065495

function and cytokine production (58, 59). More recently we have shown the ability of BCG to induce a population of Vδ2+ T-cells with superior cytokine and cytolytic mediator production (34). To confirm this, we assessed the ability of Vδ2+ T-cells to lyse various tumour cells and examined the cytokine production of Vδ2+ T-cells in response to stimulation with tumour cells.

Daudi, Raji and Thp1 cells, with and without ZA pre-treatment, were cultured with ZA or HK-BCG expanded Vδ2+ T-cells. As previously shown, there was no significant difference in the killing abilities of Vδ2+ T-cells expanded with ZA or BCG (Figure 4A). Next the cytokine production of Vδ2+ T-cells expanded with ZA or HK-BCG was assessed in response to Thp1 cells. There was no significant increase in cytokine production of Vδ2+ T-cells towards Thp1 cells or Thp1 cells pre-treated with ZA (Figure 4B).

We next assessed the expression of activatory and inhibitory checkpoint receptors on effector Vδ2+ T-cells following culture with tumour cells. The expression of inhibitory receptors PD1 and NKG2A appears to increase according to tumour sensitivity to killing, likely reflecting the activation of Vδ2+ T-cells in response to tumour cells, (Figure 4C). In addition to modulation by activation status/tumour type the expression of inhibitory checkpoint molecules PD1 and NKG2A are also modulated by method of expansion, with significantly decreased expression of PD1 and significantly increased expression of NKG2A on Vδ2+ T-cells expanded with HK-BCG compared to those expanded with ZA (Figure 4C). The difference of stimulation on inhibitory receptor expression suggests a possible mechanism of how these two expansion protocols differ in their cytotoxic abilities and may go some way to explaining the differences in cytokine and cytolytic capabilities of BCG and ZA expanded Vδ2+ T-cells. Moreover, Vδ2+ T-cells expressing the high levels of inhibitory receptors PD1 and NKG2A also produced the highest levels of cytokine TNF (Figure 4D).

Effect of immune checkpoint receptor blockade on anti-tumour responses of Vδ2+ T-cells

A mechanism that tumours employ to evade killing is the engagement of checkpoint receptors *via* the expression of checkpoint ligands hence the next aim was to assess the expression of these markers on tumour cells to provide a system for manipulating the effects of these molecules on Vδ2+ T-cells.

We assessed the expression of ligands towards numerous inhibitory checkpoint receptors by flow cytometry on Thp1 cells at baseline and following pre-treatment with ZA. Thp1 cells express moderate amounts of PDL1, Gal9 and HLA class II and substantial amounts of PVR, HLA-E and HVEM (Figure 5A). The expression of checkpoint ligands was not altered following ZA pre-treatment. Therefore, Thp1 cells were used as a model system to interrogate the role of inhibitory checkpoint receptors on Vδ2+ T-cells.

We next carried out functional studies to investigate whether the effector phenotype of Vδ2+ T-cells could be modulated by culture with immune checkpoint inhibitors. ZA expanded Vδ2+ T-cells were cultured with Thp1 cells, with and without ZA pre-treatment, in the presence of blocking antibodies. The blockade of inhibitory receptors PD1, LAG3, TIM3, and TIGIT had no effect on the cytotoxic abilities of Vδ2+ T-cells against Thp1 cells or Thp1 cells with ZA pre-treatment (Figure 5B). Blockade of BTLA and NKG2A enhanced the cytotoxic effects of Vδ2+ T-cells against Thp1 cells but any effects were lost upon pre-treatment of Thp1 cells with ZA (Figure 5B). Furthermore, there was no influence of blockade of PD1, LAG3, TIM3, TIGIT or BTLA on the production of CD107b and IFN-γ by Vδ2+ T-cells cultured with ZA pre-treated Thp1 cells (Figure 5C). Blockade of NKG2A did however significantly enhance production of CD107b or IFN-γ by Vδ2+ T-cells cultured with both Thp1 cells and Thp1 cells pretreated with ZA (Figure 5C). Despite high expression of inhibitory receptors on expanded Vδ2+ T-cells the blockade of these molecules shows no clear effect on Vδ2+ T-cell function.

Discussion

In this current investigation we have explored the role of activatory and inhibitory receptors on Vδ2+ T-cell function and their potential modulation with different routes of Vδ2+ T-cell activation. We also build on our previous findings which highlights BCG as an important mechanism of Vδ2+ T-cell activation which may provide a more physiologically relevant method of expansion which may bypass the potential exhaustion documented with ZA expansion (34, 60).

Vδ2+ T-cells represent a key cell type in immunosurveillance and therefore a crucial potential target of immunotherapy. A key study has found the γδ T-cell to be the cell type that correlates most closely with favourable clinical outcome in cancer patients (15). Despite this, variable responses have been achieved with clinical trials utilising Vδ2+ T-cells, either *via in vivo* phosphoantigen stimulation or *in vitro* expansion followed by adoptive transfer. Many techniques have been tested for Vδ2 expansion such as pulsing with ZA, use of pro-drugs, use of APC along with various cytokines including IL-15 and IL-2 (61–63). Despite this it is likely there is still a large amount of heterogeneity within the Vδ2 population and a potential for high levels of exhaustion (36).

We explore the use of BCG as a method of Vδ2 expansion as this has been shown to result in regression of melanoma lesions and infiltration of Vδ2 cells when injected into lesions (13). Despite the previously reported differences in cytolytic profile of Vδ2 cells in response to BCG we describe no significant difference in activatory marker or inhibitory marker expression following BCG activation and expansion compared to ZA. We do describe a difference in expression of

10.3389/fimmu.2022.1065495

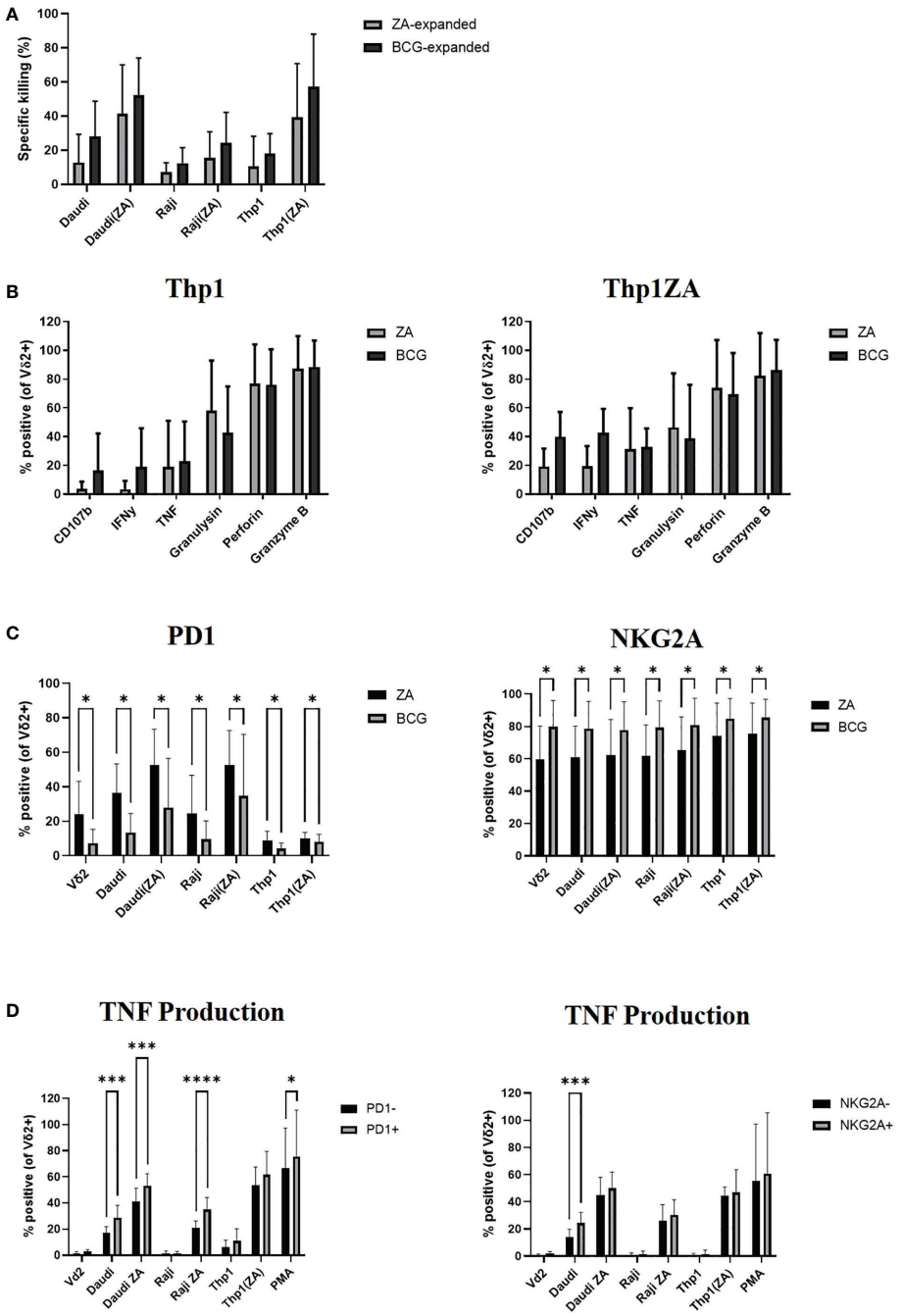

FIGURE 4
Vδ2 cells, expanded with ZA or HK-BCG, were isolated and cultured with CTFR labelled Daudi, Raji or Thp1 cells, cultured with or without 50μM ZA prior to culture with Vδ2 cells, at a 1:1 ratio. Specific killing of tumour cells was calculated after 16 hours co-culture **(A)**. After 4 hours co-culture the production of CD107b, IFNγ, TNF, granulysin, perforin and granzyme B was assessed by flow cytometry **(B)**, expression of PD1 and NKG2A was assessed **(C)** and production of TNF was assessed on receptor positive and receptor negative cells **(D)**. N=6. *p<0.05, ***p<0.0005, ****p<0.0001, non-parametric analysis of variance with Tukey's *post hoc* for multiple pairwise comparisons.

PD1 and NKG2A following culture with tumour cells which suggests these stimuli have different mechanisms of action. Indeed, studies have shown differential roles of accessory cells between ZA, HMBPP and BTN3A1 in Vδ2 activation (64). Therefore, the differences in activation and inhibition warrant further understanding.

Unlike other CD3+ T-cells Vδ2+ T-cell activation can be achieved *via* stimulation through the TCR and BTN3A1/

10.3389/fimmu.2022.1065495

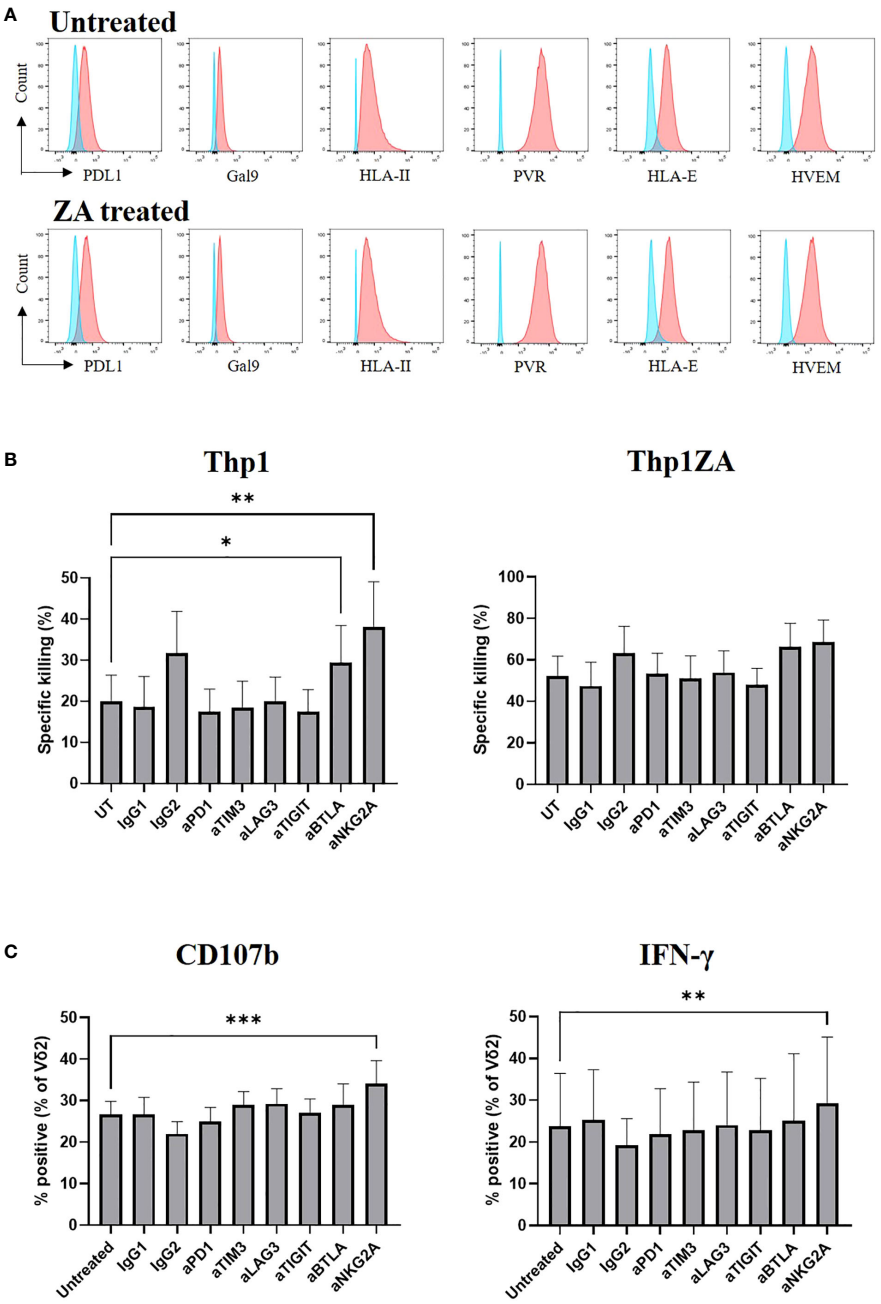

FIGURE 5
Expression of checkpoint receptor ligands (red) was compared to control (blue) on Thp1 cells with and without 50μM ZA pre-treatment **(A)**. ZA expanded Vδ2 cells were isolated and cultured with CTFR labelled Thp1 target cells, with or without 50μM ZA pre-treatment, at a 1:1 ratio in the presence or absence of 5μg anti-PD1, anti-TIM3, anti-LAG3,anti-TIGIT, anti-BTLA and anti-NKG2A. Specific killing of tumour cells was calculated following 16 hours **(B)** and production of CD107b and IFNγ by Vδ2 cells was assessed by ICS and flow cytometry following 4 hours **(C)**. N=7. *<0.05, mixed effects analysis with Dunnett's *post hoc* for multiple pairwise comparisons. **p<0.005, ***p<0.0005.

BTN2A1 or *via* stress ligands recognised by NCR receptors. However, concurrent stimulation through inhibitory checkpoint receptors may block activation and subsequent cytotoxicity. Therefore, it is likely a balance between these activatory and inhibitory receptors may control the outcome upon tumour encounter. First, we have shown that Vδ2+ T-cells in circulation express various activation markers. Vδ2+ T-cell recognition has been widely documented to be due to recognition of phosphoantigens *via* BTN3A1 and the TCR (6–8). Recognition also occurs *via* NKG2D and the recognition of stress ligands

MICA/B and ULBPs (11, 65, 66). The relative contributions of these receptors is debated, with some showing TCR independent recognition with significant reduction in Vδ2+ T-cell mediated killing with NKG2D blockade (11, 65, 67). Others suggest that NKG2D acts as a costimulatory receptor *via* modulating early TCR signals (68, 69). Others highlight roles for both NKG2D and TCR with the perforin granzyme pathway as the main mechanism of cytotoxicity (70).

Further evidence for the costimulatory receptor theory comes from a study showing DNAM1 is constitutively expressed on circulating Vδ2+ T-cells and maintained upon activation, findings which have been recapitulated in our study. Tumour lysis could be inhibited by anti-DNAM1 with NKG2D blockade providing complementary contribution to cytotoxicity (71). The high levels of both NKG2D and DNAM1 on both circulating and activated Vδ2+ T-cells found in this study suggest crucial roles for these receptors in recognition. This can be confirmed as the investigation into the use of Vδ2 cells modified with the addition of NKG2D RNA CAR revealed enhanced cytoltic activity, an effect that was enhanced with the addition of ZA (46).

Expression of NCRs may also play a costimulatory role in Vδ2+ T-cell recognition. In this study we see limited expression of NKp44 and NKp46 on Vδ2+ T-cells but intermediate expression of NKp30. There was no clear upregulation of these markers following stimulation in our study despite expression of these molecules being documented to be upregulated on Vδ1+ T-cells with stimulation with IL-2, IL-15 or TCR (72, 73). NKp30 and NKp46 are enhanced on NK cells exposed my mycobacterium tuberculosis infected monocytes however NKp44 is enhanced on NK cells following BCG stimulation and not by stimulation with mycobacterium tuberculosis infected monocytes (74, 75). This suggests these receptors may play a differential role in recognition of mycobacteria. In this study however, we saw no upregulation of NKp44 on Vδ2+ T-cells expanded with BCG. No differences in NKp44 or NKp46 expression was seen between ZA-expanded and BCG-expanded Vδ2+ T-cells, as previously documented (76).

It is likely that the mechanism of Vδ2+ T-cell recognition involves a complex interplay between a combination of activatory receptors, depending on the ligands present. In this study we did not explore the role of activatory receptors typically found on αβ T-cells such as TNFR-family receptors CD27 and 4-1BB. These molecules have been documented as modulators of Vδ2 activation with roles in proliferation, survival and secretion of inflammatory cytokines and as such these require further investigation into their contribution to Vδ2 activation (77–81). In addition to the expression of stress ligands on tumour cells and recognition by activatory markers, Vδ2 cells may also recognize tumour cells by the downregulation of MHC class I and subsequent activation of KIR and LILR. LILR have been documented to be expressed on Vδ2 cells associated with presence of infection both with CMV and mycobacteria (82, 83). KIR have also been documented to be expressed on Vδ2 cells, particularly more cytolytic CD16+ cells. This expression of KIR likely explains the observation in Figure 4 of increased killing of Daudi cells lacking MHC class I compared to Raji and Thp1 cells which require other mechanisms of recognition (84–87). These additional receptors are important to consider as it is likely that this highly diverse combination of receptors plays a role in the suboptimal use of Vδ2+ T-cells in immunotherapy.

Next, we investigated the expression of inhibitory immune checkpoint receptors on Vδ2+ T-cells. Inhibitory immune checkpoint receptors are well documented on CD4 and CD8 T-cells with roles in suppression of proliferation, activation and cytokine production (88). Less is known about the expression of inhibitory checkpoint receptors on Vδ2+ T-cells and their role in regulation of these cells. Inhibitory receptors PD1, TIM3, LAG3 and BTLA have been documented to be expressed on Vδ2+ T-cells with upregulation upon stimulation (49, 55, 89–92). In contrast we document no change in PD1 expression with mycobacterial or phosphoantigen stimulation. One study documents minimal expression of PD1 on Vδ2+ T-cells which increases following 3 days stimulation with HMBPP followed by a gradual decline (49). This suggests that the time points investigated in this study may have missed any increase in expression of PD1. We document marked decrease in BTLA expression, something which has been documented in the literature, and maximal expression of both TIM3 and LAG3 following stimulation and these molecules, along with PD1, on γδ T-cells have been shown to associate with earlier relapse and shorter overall survival in melanoma patients suggesting these molecules may play a role in Vδ2+ T-cell regulation (17, 93).

NKG2A is a recently emerging checkpoint molecule shown to be expressed on CD8+ T-cells and NK cells with blockade potentiating effector functions (94, 95). We see high levels of expression on Vδ2+ T-cells providing a new cell type which would be targeted by such interventions. In the aforementioned studies blockade of NKG2A increased the frequencies of CD107 and IFN-γ by NK and CD8 T-cells so it will be of interest to study the impact of NKG2A blockade on Vδ2 activation and function.

Finally, we examined the impact of blockade of immune checkpoint receptors on Vδ2+ T-cell function. We saw no difference in Vδ2+ T-cell cytotoxicity nor any difference in cytokine production against Thp1 cells which express intermediate levels of all immune checkpoint ligands. Other studies have demonstrated that blockade of anti-PD1, anti-BTLA and anti-TIM3 result in enhanced proliferation and prevention of apoptosis (53, 89, 93). Any effects of the blockade of immune checkpoints on Vδ2+ T-cells may be limited to proliferation or cell death. Another plausible reason for this difference is the expression of immune checkpoints and corresponding ligands on tumour cells as expression of certain ligands in our model were limited, as in the case of PD1. Despite studies documenting a role of

checkpoint inhibition in Vδ2+ T-cells there is still debate about the significance of this approach in these cells. Some have found no effect of blocking PD1 in cell lines expressing high PDL1 (54). One possibility may be that strong TCR signalling or the additional effect of NKG2D co-signalling may overcome any inhibitory effect of PD1. We also document only low levels of PD1 expression suggesting there is not enough expression for this to be an effective checkpoint. Others have found that a combination of checkpoint blockade has better effect in Vδ2+ T-cells. Blockade of PD1 alone had no effect on cytokine production of Vδ2+ T-cell however when combined with anti-TIM3 elevated cytokine production was observed suggesting PD1 alone is insufficient to correct functional impairment (55).

Due to the high levels of TIM3, LAG3 and NKG2A found upon Vδ2+ T-cells following expansion it is crucial to explore combinations of these checkpoint receptors in Vδ2+ T-cell function. As treatment with ipilimumab has been shown to result in higher proportions of Vδ2 cells and those patients with poor response had lower frequencies of Vδ2 cells the combination of Vδ2 immunotherapy with checkpoint blockade would be envisaged to be beneficial in anti-tumour therapy. As such, trials are ongoing into the combination of Vδ2 activation with anti-BTN3A1 in combination immune checkpoint blockade (NCT04243499) (39). Like ZA, this molecule has been shown to enhance the sensitivity of tumour cells to Vδ2 killing and enhances Vδ2 production of IFN-γ, TNF, granzyme B and perforin.

Overall, we have found a high level of expression of activatory molecules and inhibitory immune checkpoints on Vδ2+ T-cells. Levels of these markers are modulated upon phosphoantigen and mycobacterial activation and provide a crucial target of tumour cells to regulate Vδ2+ T-cell responses. This work suggests crucial combinations of immune checkpoint blockade that would be useful to improve the success of Vδ2+ T-cell in immunotherapy.

Data availability statement

The data discussed in this publication have been deposited in NCBI's Gene Expression Omnibus and are accessible through GEO Series accession number GSE221563 (https://www.ncbi.nlm.nih.gov/geo/query/acc.cgi?&acc=GSE221563).

Ethics statement

The studies involving human participants were reviewed and approved by St George's Research Ethics Committee. The patients/participants provided their written informed consent to participate in this study.

Author contributions

LR conducted the laboratory work, analyses and drafted the manuscript. JC contributed to laboratory work and analysis. MB-S contributed to study conception and design. All authors contributed to the article and approved the submitted version.

Funding

This work was supported by the Institute for Cancer Vaccines and Immunotherapy (Registered Charity Number 1080343).

Acknowledgments

The authors give thanks to Dr Audrey Teh who provided anti-NKG2A antibodies which were used in this study.

Conflict of interest

Author LR is employed by Astrazeneca. The remaining authors declare that the research was conducted in the absence of any commercial or financial relationships that could be construed as a potential conflict of interest.

Publisher's note

Supplementary material

The Supplementary Material for this article can be found online at: https://www.frontiersin.org/articles/10.3389/fimmu.2022.1065495/full#supplementary-material

SUPPLEMENTARY FIGURE 1
Gating strategy for activatory and inhibitory receptor expression. Doublets were excluded by SSC-A versus SSC-W and lymphocytes gated based on SSC-A versus FSC-A. Live cells were gated as negative for viability dye Zombie Aqua. From the live population CD3 was gated against activatory and inhibitory markers including NKG2A, KLRG1, BTLA, PD1, TIGIT, VISTA, LAG3, TIM3, NKG2C, NKG2D, DNAM1, NKp30, NKp44 and NKp46. Positivity was determined by quadrant gates set based on the expression within live cells using a contour plot with level 5%. To identify cell subsets CD3 positive and CD3 negative populations were

gated. From the CD3 positive cells T-cells and Vδ2 cells were gated based on Vδ2 expression. From the CD3 negative population NK cells were gated based on positive expression of CD56. The positive quadrant gates for activatory and inhibitory markers were then copied onto the relevant cell sub-populations.

SUPPLEMENTARY FIGURE 2
Expression of NK associated activatory receptors and inhibitory checkpoint receptors was determined in Vγ9Vδ2+ cells in PBMCs from healthy donors at base line **(A and B)**, following 24 hours stimulation with IL-2 alone, ZA or BCG, both with IL-2 **(C and D)** or following 14 days expansion with IL-2 alone, ZA or BCG, both with IL-2 **(E and F)**. N=10. *p<0.05, **p<0.005, ***p<0.0005, ****p<0.0001, non-parametric analysis of variance with Tukey's *post hoc* for multiple pairwise comparisons.

SUPPLEMENTARY FIGURE 3
Expression of NK associated activatory markers on CD3+ T-cells **(A)** CD56 + NK cells **(B)** and inhibitory checkpoint receptors on CD3+ T-cells **(C)** and CD56+ NK cells **(D)** was determined in PBMC stimulated for 24 hours with IL-2 alone, ZA or BCG, both with IL-2, using flow cytometry. N=10, *p<0.05, **p<0.005, ***p<0.0005, ****p<0.0001, non-parametric mixed effects analysis with Tukey's *post hoc* for multiple pairwise comparisons.

SUPPLEMENTARY FIGURE 4
Expression of NK associated activatory markers on CD3+ T-cells **(A)** CD56 + NK cells **(B)** and inhibitory checkpoint receptors on CD3+ T-cells **(C)** and CD56+ NK cells **(D)** was determined in PBMC stimulated for 14 days with IL-2 alone, ZA or BCG, both with IL-2, using flow cytometry. N=10, *p<0.05, **p<0.005, ***p<0.0005, ****p<0.0001, non-parametric mixed effects analysis with Tukey's *post hoc* for multiple pairwise comparisons.

References

1. Fonseca S, Pereira V, Lau C, Teixeira MDA, Bini-Antunes M, Lima M. Human peripheral blood gamma delta T cells: Report on a series of healthy Caucasian Portuguese adults and comprehensive review of the literature. *Cells* (2020) 9(3):729. doi: 10.3390/cells9030729

2. Cairo C, Armstrong CL, Cummings JS, Deetz CO, Tan M, Lu C, et al. Impact of age, gender, and race on circulating γδ T cells. *Hum Immunol* (2010) 71(10):968–75. doi: 10.1016/j.humimm.2010.06.014

3. Meraviglia S, El Daker S, Dieli F, Martini F, Martino A. γδ T cells cross-link innate and adaptive immunity in mycobacterium tuberculosis infection. *Clinical; Dev Immunol* (2011) 2011:587315. doi: 10.1155/2011/587315

4. Frencher JT, Shen H, Yan L, Wilson JO, Freitag NE, Rizzo AN, et al. HMBPP-deficient listeria mutant immunization alters pulmonary/systemic responses, effector functions, and memory polarization of Vγ2Vδ2 T cells. *J Leukoc Biol* (2014) 96(6):957—967. doi: 10.1189/jlb.6HI1213-632R

5. Workalemahu G, Wang H, Puan KJ, Nada MH, Kuzuyama T, Jones BD, et al. Metabolic engineering of salmonella vaccine bacteria to boost human Vγ2Vδ2 T cell immunity. *J Immunol* (2014) 193(2):708–21. doi: 10.4049/jimmunol.1302746

6. Rigau M, Ostrouska S, Fulford TS, Johnson DN, Woods K, Ruan Z, et al. Butyrophilin 2A1 is essential for phosphoantigen reactivity by γδ T cells. *Science* (2020) 367(6478):eaay5516. doi: 10.1126/science.aay5516

7. Harly C, Guillaume Y, Nedellec S, Peigné CM, Mönkkönen H, Mönkkönen J, et al. Key implication of CD277/butyrophilin-3 (BTN3A) in cellular stress sensing by a major human γδ T-cell subset. *Blood* (2012) 120(11):2269–79. doi: 10.1182/blood-2012-05-430470

8. Vavassori S, Kumar A, Wan GS, Ramanjaneyulu GS, Cavallari M, El Daker S, et al. Butyrophilin 3A1 binds phosphorylated antigens and stimulates human γδ T cells. *Nat Immunol* (2013) 14(9):908–16. doi: 10.1038/ni.2665

9. Karunakaran MM, Willcox CR, Salim M, Paletta D, Fichtner AS, Noll A, et al. Butyrophilin-2A1 directly binds germline-encoded regions of the Vγ9Vδ2 TCR and is essential for phosphoantigen sensing. *Immunity* (2020) 52(3):487–98.e6. doi: 10.1016/j.immuni.2020.02.014

10. Cano CE, Pasero C, de Gassart A, Kerneur C, Gabriac M, Fullana M, et al. BTN2A1, an immune checkpoint targeting Vγ9Vδ2 T cell cytotoxicity against malignant cells. *Cell Rep* (2021) 36(2):109359. doi: 10.1016/j.celrep.2021.109359

11. Rincon-Orozco B, Kunzmann V, Wrobel P, Kabelitz D, Steinle A, Herrmann T. Activation of Vγ9Vδ2 T cells by NKG2D. *J Immunol* (2005) 175 (4):2144 LP – 2151. doi: 10.4049/jimmunol.175.4.2144

12. Raspollini MR, Castiglione F, Rossi Degl'Innocenti D, Amunni G, Villanucci A, Garbini F, et al. Tumour-infiltrating gamma/delta T-lymphocytes are correlated with a brief disease-free interval in advanced ovarian serous carcinoma. *Ann Oncol* (2005) 16(4):590–6. doi: 10.1093/annonc/mdi112

13. Cordova A, Toia F, la Mendola C, Orlando V, Meraviglia S, Rinaldi G, et al. Characterization of human γδ T lymphocytes infiltrating primary malignant melanomas. *PLoS One* (2012) 7(11):e49878–8. doi: 10.1371/journal.pone.0049878

14. Ma C, Zhang Q, Ye J, Wang F, Zhang Y, Wevers E, et al. Tumor-infiltrating γδ T lymphocytes predict clinical outcome in human breast cancer. *J Immunol* (2012) 189(10):5029–36. doi: 10.4049/jimmunol.1201892

15. Gentles AJ, Newman AM, Liu CL, Bratman SV, Feng W, Kim D, et al. The prognostic landscape of genes and infiltrating immune cells across human cancers. *Nat Med* (2015) 21(8):938–45. doi: 10.1038/nm.3909

16. Wistuba-Hamprecht K, Martens A, Haehnel K, Geukes Foppen M, Yuan J, Postow MA, et al. Proportions of blood-borne Vδ1+ and Vδ2+ T-cells are associated with overall survival of melanoma patients treated with ipilimumab. *Eur J Cancer*. (2016) 64:116–26. doi: 10.1016/j.ejca.2016.06.001

17. Girard P, Charles J, Cluzel C, Degeorges E, Manches O, Plumas J, et al. The features of circulating and tumor-infiltrating γδ T cells in melanoma patients display critical perturbations with prognostic impact on clinical outcome. *Oncoimmunology* (2019) 8(8):1601483. doi: 10.1080/2162402X.2019.1601483

18. Abe Y, Muto M, Nieda M, Nakagawa Y, Nicol A, Kaneko T, et al. Clinical and immunological evaluation of zoledronate-activated Vγ9γδ T-cell-based immunotherapy for patients with multiple myeloma. *Exp Hematol* (2009) 37 (8):956–68. doi: 10.1016/j.exphem.2009.04.008

19. Nakajima J, Murakawa T, Fukami T, Goto S, Kaneko T, Yoshida Y, et al. A phase I study of adoptive immunotherapy for recurrent non-small-cell lung cancer patients with autologous gammadelta T cells. *Eur J Cardiothorac Surg* (2010) 37 (5):1191–7. doi: 10.1016/j.ejcts.2009.11.051

20. Nicol AJ, Tokuyama H, Mattarollo SR, Hagi T, Suzuki K, Yokokawa K, et al. Clinical evaluation of autologous gamma delta T cell-based immunotherapy for metastatic solid tumours. *Br J Cancer*. (2011) 105(6):778–86. doi: 10.1038/bjc.2011.293

21. Sakamoto M, Nakajima J, Murakawa T, Fukami T, Yoshida Y, Murayama T, et al. Adoptive immunotherapy for advanced non-small cell lung cancer using zoledronate-expanded γδ T cells: A phase I clinical study. *J Immunother* (2011) 34 (2):202–11. doi: 10.1097/CJI.0b013e318207ecfb

22. Dieli F, Gebbia N, Poccia F, Caccamo N, Montesano C, Fulfaro F, et al. Induction of γδ T-lymphocyte effector functions by bisphosphonate zoledronic acid in cancer patients *in vivo*. *Blood* (2003) 102(6):2310–1. doi: 10.1182/blood-2003-05-1655

23. Dieli F, Vermijlen D, Fulfaro F, Caccamo N, Meraviglia S, Cicero G, et al. Targeting human {gamma}delta} T cells with zoledronate and interleukin-2 for immunotherapy of hormone-refractory prostate cancer. *Cancer Res* (2007) 67 (15):7450–7. doi: 10.1158/0008-5472.CAN-07-0199

24. Lang JM, Kaikobad MR, Wallace M, Staab MJ, Horvath DL, Wilding G, et al. Pilot trial of interleukin-2 and zoledronic acid to augment γδ T cells as treatment for patients with refractory renal cell carcinoma. *Cancer Immunol Immunother*. (2011) 60(10):1447–60. doi: 10.1007/s00262-011-1049-8

25. Meraviglia S, Eberl M, Vermijlen D, Todaro M, Buccheri S, Cicero G, et al. *In vivo* manipulation of Vgamma9Vdelta2 T cells with zoledronate and low-dose interleukin-2 for immunotherapy of advanced breast cancer patients. *Clin Exp Immunol* (2010) 161(2):290–7. doi: 10.1111/j.1365-2249.2010.04167.x

26. Polito VA, Cristantielli R, Weber G, del Bufalo F, Belardinilli T, Arnone CM, et al. Universal ready-to-Use immunotherapeutic approach for the treatment of cancer: Expanded and activated polyclonal γδ memory T cells. *Front Immunol* (2019) 10:2717. doi: 10.3389/fimmu.2019.02717

27. Wu D, Wu P, Wu X, Ye J, Wang Z, Zhao S, et al. Ex vivo expanded human circulating Vδ1 γδT cells exhibit favorable therapeutic potential for colon cancer. *Oncoimmunology* (2015) 4(3):e992749. doi: 10.4161/2162402X.2014.992749

28. Almeida AR, Correia D v, Fernandes-Platzgummer A, da Silva CL, da Silva MG, Anjos DR, et al. Delta one T cells for immunotherapy of chronic lymphocytic leukemia: Clinical-grade Expansion/Differentiation and preclinical proof of concept. *Clin Cancer Res* (2016) 22(23):5795–804. doi: 10.1158/1078-0432.CCR-16-0597

29. Bennouna J, Levy V, Sicard H, Senellart H, Audrain M, Hiret S, et al. Phase I study of bromohydrin pyrophosphate (BrHPP, IPH 1101), a Vγ9Vδ2 T lymphocyte agonist in patients with solid tumors. *Cancer Immunology Immunotherapy* (2010) 59(10):1521–30. doi: 10.1007/s00262-010-0879-0

30. Honda Si, Sakamoto Y, Fujime M, Kitagawa R. Immunohistochemical study of tumor-infiltrating lymphocytes before and after intravesical bacillus calmette-guérin treatment for superficial bladder cancer. *Int J Urology.* (1997) 4(1):68–73. doi: 10.1111/j.1442-2042.1997.tb00143.x

31. Dieli F, Ivanyi J, Marsh P, Williams A, Naylor I, Sireci G, et al. Characterization of lung γδ T cells following intranasal infection with < em<Mycobacterium bovis</em< bacillus calmette-guérin. *J Immunol* (2003) 170(1):463 LP – 469. doi: 10.4049/jimmunol.170.1.463

32. Martino A, Casetti R, Sacchi A, Poccia F. Central memory Vγ9Vδ2 T lymphocytes primed and expanded by bacillus calmette-Guérin-Infected dendritic cells kill mycobacterial-infected monocytes. *J Immunol* (2007) 179(5):3057 LP – 3064. doi: 10.4049/jimmunol.179.5.3057

33. Yang J, Jones MS, Ramos RI, Chan AA, Lee AF, Foshag LJ, et al. Insights into local tumor microenvironment immune factors associated with regression of cutaneous melanoma metastases by mycobacterium bovis bacille calmette-guérin. *Front Oncol* (2017) 7:61. doi: 10.3389/fonc.2017.00061

34. Fenn J, Ridgley LA, White A, Sarfas C, Dennis M, Dalgleish A, et al. Bacillus calmette-guerin (BCG) induces superior anti-tumour responses by Vδ2 + T-cells compared to the aminobisphosphonate drug zoledronic acid. *Clin Exp Immunol* (2022) 208(3):301–15. doi: 10.1093/cei/uxac032

35. Saura-Esteller J, de Jong M, King LA, Ensing E, Winograd B, de Gruijl TD, et al. Gamma delta T-cell based cancer immunotherapy: Past-Present-Future. *Front Immunol* (2022) 13:915837. doi: 10.3389/fimmu.2022.915837

36. Kabelitz D, Serrano R, Kouakanou L, Peters C, Kalyan S. Cancer immunotherapy with γδ T cells: many paths ahead of us. *Cell Mol Immunol* (2020) 17(9):925–39. doi: 10.1038/s41423-020-0504-x

37. de Weerdt I, Lameris R, Ruben JM, de Boer R, Kloosterman J, King LA, et al. A bispecific single-domain antibody boosts autologous Vγ9Vδ2-T cell responses toward CD1d in chronic lymphocytic leukemia. *Clin Cancer Res* (2021) 27 (6):1744–55. doi: 10.1158/1078-0432.CCR-20-4576

38. Oberg HH, Janitschke L, Sulaj V, Weimer J, Gonnermann D, Hedemann N, et al. Bispecific antibodies enhance tumor-infiltrating T cell cytotoxicity against autologous HER-2-expressing high-grade ovarian tumors. *J Leukoc Biol* (2020) 107 (6):1081–95. doi: 10.1002/JLB.5MA1119-265R

39. de Gassart A, Le KS, Brune P, Agaugué S, Sims J, Goubard A, et al. Development of ICT01, a first-in-class, anti-BTN3A antibody for activating Vγ9Vδ2 T cell–mediated antitumor immune response. *Sci Transl Med* (2022) 13 (616):eabj0835. doi: 10.1126/scitranslmed.abj0835

40. Oberg HH, Peipp M, Kellner C, Sebens S, Krause S, Petrick D, et al. Novel bispecific antibodies increase γδ T-cell cytotoxicity against pancreatic cancer cells. *Cancer Res* (2014) 74(5):1349–60. doi: 10.1158/0008-5472.CAN-13-0675

41. de Bruin RCG, Veluchamy JP, Lougheed SM, Schneiders FL, Lopez-Lastra S, Lameris R, et al. A bispecific nanobody approach to leverage the potent and widely applicable tumor cytolytic capacity of Vγ9Vδ2-T cells. *Oncoimmunology* (2018) 7 (1):e1375641. doi: 10.1080/2162402X.2017.1375641

42. Nishimoto KP, Barca T, Azameera A, Makkouk A, Romero JM, Bai L, et al. Allogeneic CD20-targeted γδ T cells exhibit innate and adaptive antitumor activities in preclinical b-cell lymphoma models. *Clin Transl Immunol* (2022) 11 (2):e1373. doi: 10.1002/cti2.1373

43. Makkouk A, Yang X, Barca T, Lucas A, Turkoz M, Wong JTS, et al. Off-the-shelf Vδ1 gamma delta T cells engineered with glypican-3 (GPC-3)-specific chimeric antigen receptor (CAR) and soluble IL-15 display robust antitumor efficacy against hepatocellular carcinoma. *J Immunother Cancer [Internet].* (2021) 9(12):e003441. doi: 10.1136/jitc-2021-003441

44. Straetemans T, Kierkels GJJ, Doorn R, Jansen K, Heijhuurs S, dos Santos JM, et al. GMP-grade manufacturing of T cells engineered to express a defined γδTCR. *Front Immunol* (2018) 9:1062. doi: 10.3389/fimmu.2018.01062

45. Capsomidis A, Benthall G, van Acker HH, Fisher J, Kramer AM, Abeln Z, et al. Chimeric antigen receptor-engineered human gamma delta T cells: Enhanced cytotoxicity with retention of cross presentation. *Mol Ther* (2018) 26(2):354–65. doi: 10.1016/j.ymthe.2017.12.001

46. Ang WX, Ng YY, Xiao L, Chen C, Li Z, Chi Z, et al. Electroporation of NKG2D RNA CAR improves Vγ9Vδ2 T cell responses against human solid tumor xenografts. *Mol Ther Oncolytics* (2020) 17:421–30. doi: 10.1016/j.omto.2020.04.013

47. Barber A, Wang X, Gopisetty A, Mirandola L, Chiriva-Internati M. Abstract LB148: Gamma delta T cells engineered with a chimeric PD-1 receptor effectively control PD-L1 positive tumors in vitro and *in vivo* with minimal toxicities. *Cancer Res* (2021) 81(13_Supplement):LB148–8. doi: 10.1158/1538-7445.AM2021-LB148

48. Marin-Acevedo JA, Kimbrough EO, Lou Y. Next generation of immune checkpoint inhibitors and beyond. *J Hematol Oncol* (2021) 14(1):45. doi: 10.1186/s13045-021-01056-8

49. Iwasaki M, Tanaka Y, Kobayashi H, Murata-Hirai K, Miyabe H, Sugie T, et al. Expression and function of PD-1 in human γδ T cells that recognize phosphoantigens. *Eur J Immunol* (2011) 41(2):345–55. doi: 10.1002/eji.201040959

50. Dondero A, Pastorino F, Della Chiesa M, Corrias MV, Morandi F, Pistoia V, et al. PD-L1 expression in metastatic neuroblastoma as an additional mechanism for limiting immune surveillance. *Oncoimmunology* (2015) 5(1):e1064578–e1064578. doi: 10.1080/2162402X.2015.1064578

51. Hu G, Wu P, Cheng P, Zhang Z, Wang Z, Yu X, et al. Tumor-infiltrating CD39(+)γδTregs are novel immunosuppressive T cells in human colorectal cancer. *Oncoimmunology* (2017) 6(2):e1277305–e1277305. doi: 10.1080/2162402X.2016.1277305

52. Castella B, Foglietta M, Sciancalepore P, Rigoni M, Coscia M, Griggio V, et al. Anergic bone marrow Vγ9Vδ2 T cells as early and long-lasting markers of PD-1-targetable microenvironment-induced immune suppression in human myeloma. *Oncoimmunology* (2015) 4(11):e1047580–e1047580. doi: 10.1080/2162402X.2015.1047580

53. Hwang HJ, Lee JJ, Kang SH, Suh JK, Choi ES, Jang S, et al. The BTLA and PD-1 signaling pathways independently regulate the proliferation and cytotoxicity of human peripheral blood γδ T cells. *Immun Inflammation Dis* (2021) 9(1):274–87. doi: 10.1002/iid3.390

54. Tomogane M, Sano Y, Shimizu D, Shimizu T, Miyashita M, Toda Y, et al. Human Vγ9Vδ2 T cells exert anti-tumor activity independently of PD-L1 expression in tumor cells. *Biochem Biophys Res Commun* (2021) 573:132–9. doi: 10.1016/j.bbrc.2021.08.005

55. Wu K, Feng J, Xiu Y, Li Z, Lin Z, Zhao H, et al. Vδ2 T cell subsets, defined by PD-1 and TIM-3 expression, present varied cytokine responses in acute myeloid leukemia patients. *Int Immunopharmacol.* (2020) 80:106122. doi: 10.1016/j.intimp.2019.106122

56. Li X, Lu H, Gu Y, Zhang X, Zhang G, Shi T, et al. Tim-3 suppresses the killing effect of Vγ9Vδ2 T cells on colon cancer cells by reducing perforin and granzyme b expression. *Exp Cell Res* (2020) 386(1):111719. doi: 10.1016/j.yexcr.2019.111719

57. Ridgley L, Finardi N, Gengenbach B, Opdensteinen P, Croxford Z, Ma J, et al. Killer to healer: Tobacco plant-derived immune checkpoint inhibitors for use in cancer immunotherapy. *Plant Biotechnol J (under review)* (2022).

58. Sparrow EL, Fowler DW, Fenn J, Caron J, Copier J, Dalgleish AG, et al. The cytotoxic molecule granulysin is capable of inducing either chemotaxis or fugetaxis in dendritic cells depending on maturation: a role for Vδ2+ γδ T cells in the modulation of immune response to tumour? *Immunology* (2020) 161:245–58. doi: 10.1111/imm.13248

59. Ryan PL, Sumaria N, Holland CJ, Bradford CM, Izotova N, Grandjean CL, et al. Heterogeneous yet stable Vδ2(+) T-cell profiles define distinct cytotoxic effector potentials in healthy human individuals. *Proc Natl Acad Sci USA* (2016) 113(50):14378—14383. doi: 10.1073/pnas.1611098113

60. Rossini M, Adami S, Viapiana O, Fracassi E, Ortolani R, Vella A, et al. Long-term effects of amino-bisphosphonates on circulating γδ T cells. *Calcif Tissue Int* (2012) 91(6):395–9. doi: 10.1007/s00223-012-9647-9

61. Tanaka Y, Murata-Hirai K, Iwasaki M, Matsumoto K, Hayashi K, Kumagai A, et al. Expansion of human γδ T cells for adoptive immunotherapy using a bisphosphonate prodrug. *Cancer Sci* (2018) 109(3):587–99. doi: 10.1111/cas.13491

62. Nada MH, Wang H, Workalemahu G, Tanaka Y, Morita CT. Enhancing adoptive cancer immunotherapy with Vγ2Vδ2 T cells through pulse zoledronate stimulation. *J Immunother Cancer* (2017) 5(1):9. doi: 10.1186/s40425-017-0209-6

63. Xiao L, Chen C, Li Z, Zhu S, Tay JC, Zhang X, et al. Large-Scale expansion of Vγ9Vδ2 T cells with engineered K562 feeder cells in G-Rex vessels and their use as chimeric antigen receptor–modified effector cells. *Cytotherapy* (2018) 20(3):420–35. doi: 10.1016/j.jcyt.2017.12.014

64. Nerdal PT, Peters C, Oberg HH, Zlatev H, Lettau M, Quabius ES, et al. Butyrophilin 3A/CD277–dependent activation of human γδ T cells: Accessory cell capacity of distinct leukocyte populations. *J Immunol [Internet].* (2016) 197 (8):3059–68. doi: 10.4049/jimmunol.1600913

65. Das H, Groh V, Kuijl C, Sugita M, Morita CT, Spies T, et al. MICA engagement by human Vγ2Vδ2 T cells enhances their antigen-dependent effector function. *Immunity* (2001) 15(1):83–93. doi: 10.1016/S1074-7613(01)00168-6

66. Zingoni A, Molfetta R, Fionda C, Soriani A, Paolini R, Cippitelli M, et al. NKG2D and its ligands: "One for all, all for one". *Front Immunol* (2018) 9:476. doi: 10.3389/fimmu.2018.00476

67. Wrobel P, Shojaei H, Schittek B, Gieseler F, Wollenberg B, Kalthoff H, et al. Lysis of a broad range of epithelial tumour cells by Human ?? T cells: Involvement of NKG2D ligands and T-cell receptor- versus NKG2D-dependent recognition. *Scand J Immunol* (2007) 66(2–3):320–8. doi: 10.1111/j.1365-3083.2007.01963.x

68. Nedellec S, Sabourin C, Bonneville M, Scotet E. NKG2D costimulates human Vγ9Vδ2 T cell antitumor cytotoxicity through protein kinase cθ-dependent modulation of early TCR-induced calcium and transduction signals. *J Immunol* (2010) 185(1):55 LP – 63. doi: 10.4049/jimmunol.1000373

69. Lança T, Correia DV, Moita CF, Raquel H, Neves-Costa A, Ferreira C, et al. The MHC class ib protein ULBP1 is a nonredundant determinant of leukemia/lymphoma susceptibility to γδ T-cell cytotoxicity. *Blood* (2010) 115(12):2407–11. doi: 10.1182/blood-2009-08-237123

70. Alexander AAZ, Maniar A, Cummings JS, Hebbeler AM, Schulze DH, Gastman BR, et al. Isopentenyl pyrophosphate-activated CD56+ {gamma}{delta} T lymphocytes display potent antitumor activity toward human squamous cell carcinoma. *Clin Cancer Res* (2008) 14(13):4232–40. doi: 10.1158/1078-0432.CCR-07-4912

71. Carlsten M, Bjoörkstroöm NK, Norell H, Bryceson Y, van Hall T, Baumann BC, et al. DNAX accessory molecule-1 mediated recognition of freshly isolated ovarian carcinoma by resting natural killer cells. *Cancer Res* (2007) 67(3):1317–25. doi: 10.1158/0008-5472.CAN-06-2264

72. Correia DV, Fogli M, Hudspeth K, da Silva MG, Mavilio D, Silva-Santos B. Differentiation of human peripheral blood Vδ1+ T cells expressing the natural cytotoxicity receptor NKp30 for recognition of lymphoid leukemia cells. *Blood* (2011) 118(4):992–1001. doi: 10.1182/blood-2011-02-339135

73. von Lilienfeld-Toal M, Nattermann J, Feldmann G, Sievers E, Frank S, Strehl J, et al. Activated gammadelta T cells express the natural cytotoxicity receptor natural killer p 44 and show cytotoxic activity against myeloma cells. *Clin Exp Immunol* (2006) 144(3):528–33. doi: 10.1111/j.1365-2249.2006.03078.x

74. Vankayalapati R, Garg A, Porgador A, Griffith DE, Klucar P, Safi H, et al. Role of NK cell-activating receptors and their ligands in the lysis of mononuclear phagocytes infected with an intracellular bacterium. *J Immunol* (2005) 175(7):4611 LP – 4617. doi: 10.4049/jimmunol.175.7.4611

75. Semih E, Giovanna B, Claudio C, Annarita S, Lisa BF, Marisa C, et al. Direct binding of human NK cell natural cytotoxicity receptor NKp44 to the surfaces of mycobacteria and other bacteria. *Infect Immun* (2008) 76(4):1719–27. doi: 10.1128/IAI.00870-07

76. Spencer CT, Abate G, Blazevic A, Hoft DF. Only a subset of phosphoantigen-responsive gamma9delta2 T cells mediate protective tuberculosis immunity. *J Immunol* (2008) 181(7):4471–84. doi: 10.4049/jimmunol.181.7.4471

77. Dieli F, Poccia F, Lipp M, Sireci G, Caccamo N, di Sano C, et al. Differentiation of Effector/Memory Vδ2 T cells and migratory routes in lymph nodes or inflammatory sites. *J Exp Med* (2003) 198(3):391–7. doi: 10.1084/jem.20030235

78. Gioia C, Agrati C, Casetti R, Cairo C, Borsellino G, Battistini L, et al. Lack of CD27–CD45RA–Vγ9Vδ2+ T cell effectors in immunocompromised hosts and during active pulmonary Tuberculosis1. *J Immunol* (2002) 168(3):1484–9. doi: 10.4049/jimmunol.168.3.1484

79. deBarros A, Chaves-Ferreira M, d'Orey F, Ribot JC, Silva-Santos B. CD70–CD27 interactions provide survival and proliferative signals that regulate T cell receptor-driven activation of human γδ peripheral blood lymphocytes. *Eur J Immunol* (2011) 41(1):195–201. doi: 10.1002/eji.201040905

80. Maniar A, Zhang X, Lin W, Gastman BR, Pauza CD, Strome SE, et al. Human γδ T lymphocytes induce robust NK cell–mediated antitumor cytotoxicity through CD137 engagement. *Blood* (2010) 116(10):1726–33. doi: 10.1182/blood-2009-07-234211

81. Lee SJ, Kim YH, Hwang SH, Kim Y, Han IS, Vinay DS, et al. 4–1BB signal stimulates the activation, expansion, and effector functions of γδ T cells in mice and humans. *Eur J Immunol* (2013) 43(7):1839–48. doi: 10.1002/eji.201242842

82. Lee S, Affandi JS, Irish AB, Price P. Cytomegalovirus infection alters phenotypes of different γδ T-cell subsets in renal transplant recipients with long-term stable graft function. *J Med Virol* (2017) 89(8):1442–52. doi: 10.1002/jmv.24784

83. Hogan LE, Jones DC, Allen RL. Expression of the innate immune receptor LILRB5 on monocytes is associated with mycobacteria exposure. *Sci Rep* (2016) 6 (1):21780. doi: 10.1038/srep21780

84. Farrington LA, Callaway PC, Vance HM, Baskevitch K, Lutz E, Warrier L, et al. Opsonized antigen activates Vδ2+ T cells *via* CD16/FCγRIIIa in individuals with chronic malaria exposure. *PLoS Pathog* (2020) 16(10):e1008997. doi: 10.1371/journal.ppat.1008997

85. Trichet V, Benezech C, Dousset C, Gesnel MC, Bonneville M, Breathnach R. Complex interplay of activating and inhibitory signals received by Vγ9Vδ2 T cells revealed by target cell β2-microglobulin Knockdown1. *J Immunol* (2006) 177 (9):6129–36. doi: 10.4049/jimmunol.177.9.6129

86. Halary F, Peyrat MA, Champagne E, Lopez-Botet M, Moretta A, Moretta L, et al. Control of self-reactive cytotoxic T lymphocytes expressing γδ T cell receptors by natural killer inhibitory receptors. *Eur J Immunol* (1997) 27(11):2812–21. doi: 10.1002/eji.1830271111

87. Sebestyen Z, Prinz I, Déchanet-Merville J, Silva-Santos B, Kuball J. Translating gammadelta (γδ) T cells and their receptors into cancer cell therapies. *Nat Rev Drug Discov* (2020) 19(3):169–84. doi: 10.1038/s41573-019-0038-z

88. Pardoll DM. The blockade of immune checkpoints in cancer immunotherapy. *Nat Rev Cancer*. (2012) 12(4):252–64. doi: 10.1038/nrc3239

89. Guo Q, Zhao P, Zhang Z, Zhang J, Zhang Z, Hua Y, et al. TIM-3 blockade combined with bispecific antibody MT110 enhances the anti-tumor effect of γδ T cells. *Cancer Immunology Immunother* (2020) 69(12):2571–87. doi: 10.1007/s00262-020-02638-0

90. Kadekar D, Agerholm R, Viñals MT, Rizk J, Bekiaris V. The immune checkpoint receptor associated phosphatases SHP-1 and SHP-2 are not required for γδT17 cell development, activation, or skin inflammation. *Eur J Immunol* (2020) 50(6):873–9. doi: 10.1002/eji.201948456

91. Bekiaris V, Šedý JR, Macauley MG, Rhode-Kurnow A, Ware CF. The inhibitory receptor BTLA controls γδ T cell homeostasis and inflammatory responses. *Immunity* (2013) 39(6):1082–94. doi: 10.1016/j.immuni.2013.10.017

92. Girard P, Ponsard B, Charles J, Chaperot L, Aspord C. Potent bidirectional cross-talk between plasmacytoid dendritic cells and γδT cells through BTN3A, type I/II IFNs and immune checkpoints. *Front Immunol* (2020) 11:861. doi: 10.3389/fimmu.2020.00861

93. Gertner-Dardenne J, Fauriat C, Orlanducci F, Thibult ML, Pastor S, Fitzgibbon J, et al. The co-receptor BTLA negatively regulates human Vγ9Vδ2 T-cell proliferation: a potential way of immune escape for lymphoma cells. *Blood* (2013) 122(6):922–31. doi: 10.1182/blood-2012-11-464685

94. André P, Denis C, Soulas C, Bourbon-Caillet C, Lopez J, Arnoux T, et al. Anti-NKG2A mAb is a checkpoint inhibitor that promotes anti-tumor immunity by unleashing both T and NK cells. *Cell* (2018) 175(7):1731–43.e13. doi: 10.1016/j.cell.2018.10.014

95. van Montfoort N, Borst L, Korrer MJ, Sluijter M, Marijt KA, Santegoets SJ, et al. NKG2A blockade potentiates CD8 T cell immunity induced by cancer vaccines. *Cell* (2018) 175(7):1744–55.e15. doi: 10.1016/j.cell.2018.10.028

frontiers | Frontiers in Immunology

TYPE Review
PUBLISHED 31 March 2023
DOI 10.3389/fimmu.2023.1140623

OPEN ACCESS

EDITED BY
Trent Spencer,
Emory University, United States

REVIEWED BY
Brian Petrich,
Expression Therapeutics, United States
Claudia De Lalla,
San Raffaele Hospital (IRCCS), Italy

*CORRESPONDENCE
Zishan Zhou
zzs@taiyuanshengwu.com

SPECIALTY SECTION
This article was submitted to Cancer Immunity and Immunotherapy, a section of the journal Frontiers in Immunology

RECEIVED 09 January 2023
ACCEPTED 08 March 2023
PUBLISHED 31 March 2023

CITATION
Ma L, Feng Y and Zhou Z (2023) A close look at current γδ T-cell immunotherapy. *Front. Immunol.* 14:1140623. doi: 10.3389/fimmu.2023.1140623

A close look at current γδ T-cell immunotherapy

Ling Ma[1,2], Yanmin Feng[2] and Zishan Zhou[2*]

[1]Institute of Molecular Medicine, College of Future Technology, Peking University, Beijing, China, [2]Research and Development Department, Beijing Dingchengtaiyuan (DCTY) Biotech Co., Ltd., Beijing, China

Owing to their antitumor and major histocompatibility complex (MHC)-independent capacities, γδ T cells have gained popularity in adoptive T-cell immunotherapy in recent years. However, many unknowns still exist regarding γδ T cells, and few clinical data have been collected. Therefore, this review aims to describe all the main features of the applications of γδ T cells and provide a systematic view of current γδ T-cell immunotherapy. Specifically, this review will focus on how γδ T cells performed in treating cancers in clinics, on the γδ T-cell clinical trials that have been conducted to date, and the role of γδ T cells in the pharmaceutical industry.

KEYWORDS

γδ T cells, adoptive cell transfer (ACT), cancer immunotherapy, clinical trial, immunotherapy

1 Introduction

There are two types of T cells: αβ T cells and γδ T cells. The former expresses a T-cell receptor (TCR) comprising a heterodimer of α and β chains. The latter expresses a TCR comprising a heterodimer of γ and δ chains, which normally do not express the co-receptors CD4 and CD8, and account for, on average, 4% of human peripheral blood T cells (1). γδ T cells as a whole link the innate and adaptive immune responses. However, when referring to γδ T cells, it should be noted that they are not a homogeneous population, but rather a heterogeneous group of cells with diverse properties (Table 1) (2). Based on the TCR δ chain variable gene expression, human γδ T cells are normally divided into Vδ2 T cells and non-Vδ2 T cells, with Vδ1- and Vδ3-expressing γδ T cells accounting for the majority of non-Vδ2 T cells (2, 3). The distribution and frequency of γδ T cell subset differ dramatically in tissues and blood (2). Recently, non-Vγ9Vδ2 T cells have been considered a more appropriate division of γδ T cells and are the dominant γδ T cells in organs and lymphoid tissues, such as the skin, intestine, lungs, liver, lymph nodes, thymus, etc., representing the adaptive-like γδ T cells (2, 4). In human blood, the majority (i.e., approximately 50%–95%) of γδ T cells express a Vδ2 chain paired with a Vγ9 chain (5). This subset (i.e., Vγ9Vδ2 T cells) specifically and universally (*via* semi-invariant polyclonal expansion) recognizes phosphoantigens (PAgs) derived from microbes or transformed cells (6, 7) through butyrophilin (BTN) family members BTN2A1 and BTN3A1 (8–10), representing innate-like γδ T cells.

TABLE 1 Main features of human γδ T cells.

Subset	Distribution	T cells (%)	Ligands	Innate-like receptors	Cytokines
Non-Vγ9Vδ2	Organs and lymphoid tissues (skin, intestine, lung, liver, thymus, lamina propria, decidua, breast, spleen, etc.)	Approximately 0.5–16	BTNL3/BTNL8, CD1a, CD1c, CD1d, MICA, ULBP4, EPCR, HLA-B*5802, β2-microglobulin-free HLA heavy chain, EphA2, MSH2, hsp60, histidyl-tRNA synthetases, PE	NKG2D, TLR, CD16	IFNγ, TNFα, IL-17, IL-4, IL-10, TGFβ
Vγ9Vδ2	Blood	Approximately 2–4	BTN2A1/BTN3A1, F1-ATPase		

BTN, butyrophilin; MICA, MHC class I chain-related protein A; ULBP, UL16-binding protein; EPCR, endothelial protein C receptor; EphA2, ephrin type-A receptor 2; MSH2, MutS homolog 2; hsp60, heat shock protein 60; PE, phycoerythrin.

αβ T cells recognize peptides, lipids, and metabolites presented by the major histocompatibility complex (MHC), CD1, and MHC class I-related protein (MR1), respectively. In contrast, the antigens and ligands recognized by γδ T cells remain largely unknown. Those that have been identified are difficult to classify into clear-cut categories (11–13). Human γδ T cells are MHC independent and have been found to recognize a wide range of ligand molecules, such as BTN family proteins (BTN2A1/BTN3A1 and BTNL3/BTNL8), MHC-related proteins [CD1a, CD1c, CD1d, MHC class I polypeptide-related sequence A (MICA), UL16-binding protein (ULBP4), endothelial protein C receptor (EPCR), HLA-B*5802, and β2-microglobulin-free HLA heavy chain], ephrin type-A receptor 2 (EphA2), and those lacking typical membrane structural proteins [MutS homolog 2 (MSH2), heat shock protein 60 (hsp60), histidyl-tRNA synthetases, phycoerythrin (PE), and mitochondrial F1-ATPase] (12–20). γδ T cells recognize these molecules through their TCRs and also express innate receptors, such as natural killer (NK) receptors (e.g., NKG2D), Toll-like receptors (TLRs), and Fc receptors (e.g., CD16), which recognize ligands such as MICA, MHC class I chain-related (MIC) protein A (MICA), MICB, and UL16-binding protein (ULBP) (21–23).

γδ T cells play a role in fighting infectious and tumorous diseases, as well as a role in homeostasis, wound healing, and aging (4, 19, 24, 25). In mouse studies, γδ T cells also regulate body temperature and shape neurons (2, 26). The immune response of γδ T cells is intrinsically biased toward type I immunity, which exerts strong cytotoxic (mainly through granzyme B and perforin) effects on infected and tumor cells, and results in increased IFNγ production (27). However, the differences in TCR genes between humans and mice (2, 28), especially the absence of Vγ9Vδ2 T cells in common non-primate experimental animals (29, 30), limits the relevance of preclinical *in vivo* studies using mouse models for human Vγ9Vδ2 T cells. Therefore, this review will focus solely on human γδ T cells.

2 γδ T cells in cancer

2.1 Correlation with clinical prognosis

The relationship between γδ T cells and cancer prognosis is influenced by factors such as the pathological type of cancer (31), the γδ T-cell subset (32), the time of sample harvesting (33), and the functioning state of the γδ T cells (34). Clinical prognosis studies typically involve the analysis of either peripheral γδ T cells or tumor-infiltrating γδ T cells, and common methods include flow cytometry (35), immunohistochemistry (31, 36), and gene expression measurement (34, 37). Early studies often measured peripheral γδ T cells without distinguishing subsets (38), whereas later studies began to analyze subsets separately (35).

Overall, γδ T cells are positively correlated with favorable prognosis in cancerous diseases (39). The earliest observations that suggested that γδ T cells play a positive role in cancer prognosis came from a follow-up study of allogeneic stem cell transplantation for treating acute leukemia in the 1990s (40). Long-term follow-up found 5-year disease-free survival (DFS) and overall survival (OS) rates of 54.4% and 70.8%, respectively, among patients with increased levels of peripheral γδ T cells, compared with 19.1% and 19.6%, respectively, among those without increased γδ T cells, with no difference in graft-versus-host disease rate (38). Later studies of acute leukemia in children also supported this finding (41). Children with a higher percentage of CD8+ γδ T cells, even when sampled before treatment, had a better prognosis (33). Further studies indicate that the Vδ8, Vδ4, and Vγ9 subsets are positively correlated with good prognosis in acute leukemia before treatment (42, 43). However, studies carried out in patients with chronic lymphocytic leukemia found that peripheral Vγ9Vδ2 T-cell numbers before treatment were negatively correlated with disease progression and that those γδ T cells were dysfunctional towards zoledronate stimulation (44). This was also true in patients with chronic myeloid leukemia (45).

In the case of solid tumors, peripheral Vγ9Vδ2 T cells have been found to be positively correlated with OS or progression-free survival (PFS) in patients with renal cell carcinoma (46), melanoma (32, 47), and bladder cancer (37), as determined by flow cytometry. However, the presence of the Vδ1 subset in blood was not found to be favorable in melanoma and bladder cancer. As most studies on solid tumors have focused on tumor-infiltrating cells, the majority of correlations between prognosis and γδ T cells have been found in tumor-infiltrating cells. Effector Vδ1 γδ T cells have been found to be beneficial in skin cancers (32, 48), colon cancer (34), and lung cancer (35), based on protein-level analysis. Similarly, using the more commonly used gene expression analysis, tumor-infiltrating γδ T cells were found to be favorable in ovarian cancer (49), head and neck cancer (50), and bladder cancer (37).

However, the roles of γδ T cells have been found to vary in different pathological types of breast cancer and in different studies. In immunohistochemical studies, Ma et al. found that γδ T cells

were negative indicators in non-triple-negative breast cancers (36), whereas Allaoui et al. found the opposite correlation for non-triple-negative cancers, and also found no clear correlations between γδ T-cell infiltration and triple-negative breast cancer (31). It is worth noting that, according to the limited description of their method, Allaoui et al. were comparing the presence and absence of γδ T-cell infiltration, whereas Ma et al. were comparing infiltration with lower and higher numbers of γδ T-cells, which may account for the difference in the findings of the two studies. In other studies, γδ T cells, especially the Vδ1 subset (51), have been more frequently found to predict good outcomes in triple-negative breast cancer that supported by protein-level or gene-level analyses (51, 52). Gene expression analysis, using public databases, indicated that γδ T cells were positively correlated with good outcomes for all types of breast cancer (53, 54). Interestingly, one study found that certain peripheral TCR-γ motifs were positively correlated with OS in breast cancer (55).

In pancreatic cancer, high CD31 levels and low CD73 levels in cancer cells have been found to be associated with increased OS and an increased number of antitumor immune cells, including γδ T cells (56, 57).

2.2 Anti-tumor and pro-tumor effects

The immune responses of γδ T cells toward tumor cells have been well summarized in other reviews (5, 27, 58–61). Generally, human γδ T cells are activated when tumor cells bind to their TCRs and/or innate receptors, such as NK cell receptors, in tumor conditions. They exhibit direct cytotoxicity against different types of cancer cells, modulate antitumor cytokines, and interact with other immune cells to eliminate tumors (27), which is in accordance with the favorable prognosis linked to γδ T cells clinically observed in malignant diseases, as reviewed above. Fighting against tumor growth is among the primary roles of human γδ T cells, whether they are peripheral or tissue-resident. However, clinical investigations have also indicated the importance of the functional state of γδ T cells in cancers (32, 35, 44). In tumor environments, γδ T cells can exhibit protumor effects by producing IL-17, recruiting protumor myeloid immune cells, or suppressing αβ T-cell antitumor activities (62–64). The tumor environment tends to educate γδ T cells to serve it and selects the protumor subsets (65). These "conditioned" protumor findings may contribute to the unfavorable prognosis linked to γδ T cells observed in clinics.

3 γδ T-cell immunotherapy in cancer

The historical development of adoptive T-cell therapy was discovered through hematopoietic stem cell transplantation (HSCT) and the graft-versus-leukemia effect. This effect showed that patients with graft-versus-host disease had a lower relapse rate and that the depletion of T cells led to a higher relapse rate (66). In the case of γδ T cells, their antitumor properties were observed in the late 1980s *in vitro* (67), but it was not until the early 2000s that Hayday's group established their antitumor role in mice (27). Soon after that, γδ T cells began to be tested for treating malignant diseases in humans (68).

Knowing the biological features of immune cells is crucial for using them to help fight diseases. As mentioned above, Vγ9Vδ2 T cells are the dominant and most studied subset in human peripheral blood. Their semi-invariant TCRs recognize small non-peptide pyrophosphate antigens through conformational changes after BTN2A1 and BTN3A1 heterodimers bind PAgs intracellularly (8, 9). Typical natural PAgs include isopentenyl pyrophosphate (IPP) and (E)-4-hydroxy-3-methyl-but-2-enyl pyrophosphate (HMBPP), with the latter being the most potent natural PAg currently known (69). PAgs are crucial metabolites that come from the universally present isoprenoid biosynthesis pathway. IPP exists in all organisms, whereas HMBPP is absent in mammals (69). Studies have shown that the level of IPP is increased in abnormal human cells (7). Other than this direct activating mode, aminobisphosphonates (N-BPs) and certain alkylamines can indirectly activate Vγ9Vδ2 T cells through TCRs. They inhibit the downstream enzyme farnesyl pyrophosphate synthase (FPS, or FPPS), which plays a role in IPP synthesis and leads to endogenous IPP accumulation (2, 70). Once activated, the innate-like Vγ9Vδ2 T cells intrinsically differentiate into cytotoxic and antitumor cytokine-producing effector cells. Compared with other γδ T-cell subsets, Vγ9Vδ2 T cells are relatively harvest and to expand *in vitro*. As more is known about non-Vγ9Vδ2 T cells, and the *in vitro* culturing of Vδ1 γδ T cells on a comparable scale has become possible, Vδ1 γδ T cells have started to attract attention and be introduced to γδ T cell immunotherapy (71).

In this section, we will review the strategies used for applying γδ T cells in patients, the results of completed trials of γδ T-cell therapies, and the results to date of ongoing clinical trials of γδ T-cell therapies.

3.1 Current strategies in practice

Cancer immunotherapy is about how to safely unleash the anticancer power of immune cells. The first and most important step is to efficiently activate immune cells. Until now, most efforts to apply γδ T cells in clinics have focused on boosting the Vγ9Vδ2 subset because its stimulant effect on the immune system is relatively clear. As mentioned earlier, Vγ9Vδ2 T cells can be directly or indirectly activated by PAgs or N-BPs. N-BPs are conveniently well-established drugs in clinics that are used to treat bone diseases such as osteoporosis, metastatic bone disease, multiple myeloma, and hypercalcemia of malignancy (72). N-BP drugs, such as pamidronate and zoledronate, are usually given intravenously, and, therefore, might readily activate the peripherally dominant Vγ9Vδ2 T cells *in vivo*. Early γδ T-cell trials followed this approach (Figure 1A) (68, 73). However, the response rate of patients' Vγ9Vδ2 T cells toward N-BP drugs was not satisfactory and repeated administrations led to a reduction in peripheral Vγ9Vδ2 T cells. All of these shortcomings would greatly hamper the treatment (68, 74).

Activating Vγ9Vδ2 T cells *in vitro* followed by adoptive transfer to patients would largely avoid these problems. Indeed, shortly after the *in vivo* attempt, researchers started to activate (by either direct stimulants, such as IPP and synthetic PAgs, or indirect stimulants such as zoledronate) the patient's own Vγ9Vδ2 T cells *in vitro* and then reinfuse the patient with them (75–77). This

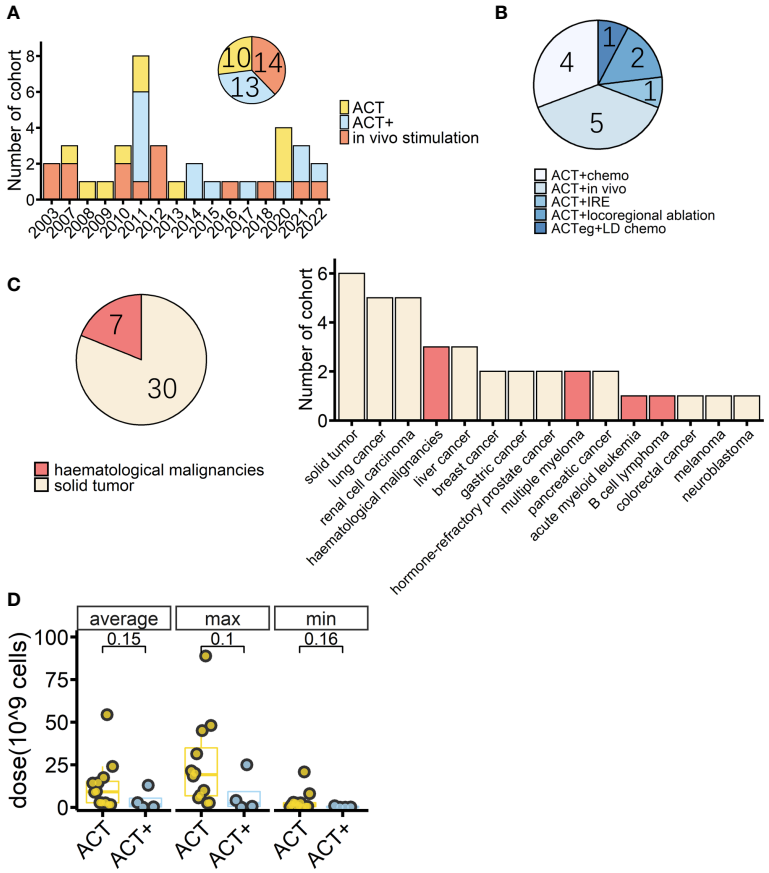

FIGURE 1
Overview of cohorts from completed γδ T-cell immunotherapy trials. **(A)** Timeline of completed γδ T-cell immunotherapy trials in clinics by cohort; colors indicate treatment type (*n* = 37). **(B)** Detailed treatment methods applied in the cohorts treated with adoptive cell transfer (ACT) combined with other treatments except for IL-2 treatment (ACT+) (*n* = 13). Chemo: conventional therapies, mostly chemotherapy. *In vivo*: *in vivo* stimulation of Vγ9Vδ2 T cells using zoledronate. IRE: irreversible electroporation. ACTeg: engineered T cells. LD chemo: lymphodepletion chemotherapy. **(C)** Tumor types (pie chart) and detailed diseases (bar chart) of γδ T-cell immunotherapy cohorts (*n* = 37); colors indicate treated tumor types. **(D)** Average, maximum, and minimum γδ T-cell total infusion doses of cohorts with dosage information (ACT, *n* = 12, ACT+, *n* = 4). The lower and upper hinges of the boxplot show the 25th and 75th percentile, respectively. The medians are indicated inside the box, and *p*-values (Wilcoxon rank-sum test) are also indicated.

approach follows the common practice in adoptive T-cell immunotherapy, which uses autologous cells. However, it also shares flaws with current adoptive T-cell immunotherapy, such as the fact that the immune environment in patients often works against antitumor effects and large differences between patients in γδ T-cell numbers and in their capacity to increase the number of γδ T-cells (32, 47, 78, 79). The unique features of γδ T cells also provide a solution to these problems. By taking advantage of their MHC-independent nature (e.g. they can be used in situations where MHC matching between the donor and recipient is not possible; the innate-like recognition of stress-induced antigens (7) provides a fast reaction; and the more limited repertoire of γδ TCRs (80) means that they are less likely to recognize and attack host tissues), the allogeneic adoptive transfer becomes possible. Early HSCT therapies found that using αβ T-cell depleted method to treat patients caused fewer cases of graft-versus-host disease and, importantly, those who developed graft-versus-host disease but had high levels of γδ T cells were less likely to experience relapse (38, 81). These results are encouraging, supporting the use of the allogeneic adoptive transfer of γδ T cells in cancer immunotherapy.

Repeated infusion of allogeneic Vγ9Vδ2 T cells is safe and has shown promising effects in treating liver and lung cancers (82). In recent years, the use of a humanized anti-BTN3A monoclonal antibody (ICT01) to activate Vγ9Vδ2 T cells has been explored as a potential treatment for multiple cancers (83). Preliminary results showed that the treatment was well tolerated, and disease control rates of 22%–42% were achieved in the completed phase I trial (Imchecktherapeutics.com: Imcheck Therapeutics). In addition to the previously mentioned strategies aimed at utilizing the inherent anticancer capabilities of Vγ9Vδ2 T cells, there have been recent human trials investigating γδ T-cell-related T-cell modifications. These modification techniques include the addition of a chimeric antigen receptor (CAR) to γδ T cells to create CAR-γδ T cells; the transfer of antitumor γδ TCR to αβ T cells (TEG001, GDT002, GDT201); the fusion of an antibody anti-CD19 Fab region and the transmembrane andendo domains of a γδ

TCR, as well as a separate CD19 single-chain variable fragment (scFv) and a 4-1BB costimulatory molecule, to create a novel T cell (ET019003) to treat B-cell lymphoma (84).

As for the new subject of research, Vδ1 γδ T cells, there are currently two phase I clinical trials in progress. Both trials are using allogeneic Vδ1 T cells. The first trial (NCT05001451) is using non-modified Vδ1 T cells (GDX012) to treat acute myeloid leukemia, while the other trial (NCT04735471) is using anti-CD20 CAR-modified Vδ1 T cells (ADI-001) to treat B-cell malignancies.

3.2 Current γδ T-cell immunotherapy clinical results

A PubMed® (National Library of Medicine, Bethesda, MD, USA) search found that, as of October 2022, there were at least 28 studies (37 cohorts) of γδ T-cell immunotherapy in progress in clinics, all of which were using Vγ9Vδ2 T cells. These studies included a total of 559 patients, 396 of whom tumor responses were measurable. As reviewed above, there are different strategies for applying γδ T-cell treatment; thus, in this systematic analysis, *in vivo* stimulation, adoptive cell transfer (ACT, including autologous and allogeneic), and ACT combined with other treatments, except for IL-2 treatment (ACT+), are compared. There were 14 cohorts receiving *in vivo* stimulation and 23 cohorts receiving reinfusion (Figure 1A). Early studies were normally of a single treatment, either *in vivo* stimulation or γδ T-cell infusion, with or without IL-2 treatment and vitamin D supply (68, 73, 75–77, 85–87), while later studies started to combine γδ T-cell therapy with other traditional treatments, typically chemotherapy (Figures 1A, B). A combination of ACT and *in vivo* stimulation produced the first reported complete response in a metastatic renal cell carcinoma cohort of patients (Table 2) (88).

Overall, 81% of the cohorts received γδ T-cell therapy for the treatment of solid cancers (Figure 1C). Patients in these cohorts had a wide range of solid malignancies, with lung cancer and renal cell carcinoma being the most tested tumors (Figure 1C, right). Excluding one study in which the patients' median age was unclear (93), the median age ranged from 13.5 years in those receiving neuroblastoma treatment to 68 years for those receiving treatment for prostate cancer (Table 2). The highest median age, 72 years, was in a cohort with hematological cancer receiving treatment for acute myeloid leukemia (92). In addition, in the case of adoptive transfer treatment, information on the total infusion dose was available for 16 cohorts. The medians of the average total doses for ACT and ACT+ treatment were 9.1×10^9 cells and 1.6×10^9 cells, respectively. There were no differences between ACT and ACT+ in terms of total doses (Figure 1D, Wilcoxon rank-sum test). γδ T-cell therapy was normally applied through multiple infusions, and the range of total infusion dose varied quite widely among patients (from 0.01×10^9 cells to 88.8×10^9 cells).

Of the 307 patients (from 27 cohorts) whose tumor responses could be measured (not including the 89 patients whose outcomes were recorded only in terms of OS and PFS), the overall results, regardless of strategy, were an objective response (OR) rate of 18% [including complete response (CR) and partial response (PR), with a pooled OR rate of 9.7%, 95% confidence interval (CI) 2.7%–19.3%; Figure 2] and a stable disease (SD) rate of 31% (pooled SD rate of 27.6%, 95% CI 20.3%–35.5%; Supplemental Figure 1), based on criteria from RECIST (Response Evaluation Criteria in Solid Tumors) or RECIST v.1.1 (Figures 2, 3A).

The three strategies had statistical differences in outcomes (p = 0.000, Pearson's chi-squared test). According to single-rate meta-analysis, the pooled OR rate for *in vivo* stimulation, ACT, and ACT+ was 8.7% (95% CI 1.1%–20.3%), 0.5% (95% CI 0%–5%), and 35.5% (95% CI 4.8%–73.3%), respectively (Supplemental Figure 2).

When compared separately using the number of patients from each condition, *in vivo* stimulation vs. ACT (p = 0.000, Pearson's chi-squared test; Figure 3A) and ACT vs. ACT+ (p = 0.000, Pearson's chi-squared test; Figure 3A) showed significant differences, while *in vivo* stimulation vs. ACT+ (p = 0.03, Pearson's chi-squared test) were similar at a significance level of 0.017. However, when examining the results in detail, it was found that the best response to *in vivo* stimulation treatments was only PR, with the largest contribution coming from the study that combined *in vivo* stimulation with PD-1 treatment (104). In contrast, 11 out of the 20 OR patients treated with ACT+ achieved CR (Figure 3A, pie chart). Furthermore, as tumor type can have a significant impact on treatment response, the responses of patients with hematological cancers and solid cancers were compared in this group of 307 patients (Figure 3B, Supplemental Figure 4). Of these, 49 patients had hematological cancer, whereas 258 patients had solid cancers. Among hematological cancer patients, 37% (18 patients) achieved OR (pooled OR rate 30.1%, 95% CI 3.2%–65.7%), and among solid tumor patients 14% (36 patients) achieved OR (pooled OR rate 5.6%, 95% CI 0.7%–13.1%).

The two cancer types had significantly different responses to γδ T-cell therapy in general (p = 0.001, Pearson's chi-squared test). However, conclusions should be drawn with caution, as the above analysis shows that the choice of treatment strategy also greatly influences patient response. Among patients with a measurable response, the choice of treatment strategy differed between hematological cancers and solid tumors (p = 0.002, Pearson's chi-squared test), with 32% of solid cancer patients being treated with the lower response rate ACT treatment and 33% of blood cancer patients being treated with ACT+ treatment (Figure 3C, Table 3). It was not possible to compare the responses of different treatments separately in patients with hematological cancers and those with solid tumors, as only the number of patients with solid tumors was sufficient for statistical analysis. In patients with solid tumors, as in patients overall, there were differences in response between treatments (p = 0.003, Pearson's chi-squared test; Table 3), with *in vivo* stimulation and ACT + showing better OR results than ACT alone [OR rates of 19.7% for *in vivo* stimulation and 17.9% for ACT+ vs. 2.4% for ACT alone; pooled OR rates for *in vivo* stimulation, ACT+, and ACT alone of 6.9% (95% CI 0.0%–20.2%), 18.4% (95% CI 0.0%–58.3%), and 0.6% (95% CI 0.0%–5.5%), respectively, Supplemental Figure 6].

Among the 138 patients for whom detailed information, such as age and sex, was recorded alongside treatment responses, no significant differences depending on these characteristics were observed (Table 4, Supplemental Figure 10). Of these 138 patients, 49 and 89 patients suffered from hematological and solid cancers, respectively. Nine hematological malignancies were

TABLE 2 Current γδ T cell therapy clinical results.

Study	Year	Disease	Age (years) (median)	Treatment type	Treatment	Outcome	Reference
Wilhelm et al.	2003	Lymphoma, multiple myeloma	67.5	*In vivo* stimulation	Pamidronate + IL-2 (continuous IV from d3)	1 SD (10%)	(68)
		Lymphoma, multiple myeloma	52	*In vivo* stimulation	Pamidronate + IL-2 (bolus IV from d1)	3 PR (33%), 2 SD (22%)	
Dieli et al.	2007	Prostate cancer	68	*In vivo* stimulation	Zoledronate + Ca/vitamin D	1 SD (11%), 1 PR (11%)	(73)
		Prostate cancer	68	*In vivo* stimulation	Zoledronate + IL-2 + Ca/vitamin D	2 PR (22%), 4 SD (44%)	
Kobayashi et al.	2007	Renal cell carcinoma	51	ACT	Autologous, IPP-expanded Vγ9Vδ2 T cells + IL-2	3 prolonged tumor doubling time (60%)	(75)
Bennouna et al.	2008	Renal cell carcinoma	57	ACT	Innacell $\gamma\delta^{TM}$ + IL-2	6 SD (60%)	(76)
Abe et al.	2009	Multiple myeloma	57.5	ACT	Autologous, zoledronate-expanded Vγ9Vδ2 T cells	4 SD (67%)	(77)
Bennouna et al.	2010	Solid tumor	56	*In vivo* stimulation	BrHPP + IL-2	12 SD (43%)	(85)
Meraviglia et al.	2010	Breast cancer	63	*In vivo* stimulation	Zoledronate + IL-2	1 PR (10%), 2 SD (20%)	(86)
Nakajima et al.	2010	Lung cancer	66	ACT	Autologous zoledronate-expanded Vγ9Vδ2 T cells	3 SD (30%)	(87)
Kobayashi et al.	2011	Renal cell carcinoma	61	ACT+	Autologous IPP-expanded Vγ9Vδ2 T cells + zoledronate + IL-2	1 CR (9%), 5 SD (45%)	(88)
Lang et al.	2011	Renal cell carcinoma	57	*In vivo* stimulation	zoledronate + IL-2	2 SD (17%)	(74)
Nicol et al.	2011	Solid tumor	59.5	ACT+	Autologous zoledronate-expanded Vγ9Vδ2 T cells + zoledronate	2 SD (33%)	(89)
		Solid tumor	61	ACT+	Autologous, zoledronate-expanded Vγ9Vδ2 T cells + zoledronate	1 SD (11%)	
		Solid tumor	44	ACT+	Autologous zoledronate-expanded Vγ9Vδ2 T cells + zoledronate + conventional treatment	1 CR (33%), 2 PR (67%)	
Sakamoto et al.	2011	Lung cancer	67	ACT	Autologous zoledronate-expanded Vγ9Vδ2 T cells	6 SD (40%)	(90)
Noguchi et al.	2011	Solid tumor	60	ACT	Autologous zoledronate-expanded Vγ9Vδ2 T cells	2 SD (50%)	(91)
		Solid tumor	60	ACT+	Autologous zoledronate-expanded Vγ9Vδ2 T cells + zoledronate or conventional therapies	3 PR (30%), 1 SD (10%)	
Kunzmann et al.	2012	Renal cell carcinoma	61	*In vivo* stimulation	Zoledronate + IL-2	3 SD (43%)	(92)
		Melanoma	43.5	*In vivo* stimulation	Zoledronate + IL-2	1 SD (17%)	
		Leukemia	72	*In vivo* stimulation	Zoledronate + IL-2	2 PR (25%), 2 SD (25%)	
Izumi et al.	2013	Colorectal cancer	unclear	ACT	Autologous zoledronate-expanded Vγ9Vδ2 T cells	–	(93)
Wilhelm et al.	2014	Hematological malignancies	67	ACT+	Lymphodepletion + zoledronate + CD4/8 T cell-depleted PBMC	3 CR (75%)	(94)

(Continued)

10.3389/fimmu.2023.1140623

TABLE 2 Continued

Study	Year	Disease	Age (years) (median)	Treatment type	Treatment	Outcome	Reference
Wada et al.	2014	Gastric cancer	58	ACT+	Autologous zoledronate-expanded Vγ9Vδ2 T cells + zoledronate	Tumor cells in ascites reduced	(95)
Cui et al.	2015	Gastric cancer	58.5	ACT+	Autologous NK cells, γδ T cells, and/or cytokine-induced killer cells + chemotherapy	PFS: 14 vs 8.5 months (chemo only) in stage III cancers	(96)
Pressey et al.	2016	Neuroblastoma	13.5	*In vivo* stimulation	Zoledronate + IL-2	1 SD (25%)	(97)
Aoki et al.	2017	Pancreatic cancers	65	ACT+	Autologous zoledronate-expanded Vγ9Vδ2 T cells + chemotherapy	Increased γδ T cell percentage in non-recurrent patients	(98)
Sugie et al.	2018	Breast cancer	65	*In vivo* stimulation	Zoledronate + letrozole	OR rate by MRI: 38.2%; by caliper: 50%; by ultrasound: 51.7%;	(99)
Xu et al.	2020	Lung cancer	59.5	ACT	Allogeneic zoledronate/vitamin C-expanded Vγ9Vδ2 T cells	1 SD (10%)	(82)
		Liver cancer	47.5	ACT	Allogeneic zoledronate/vitamin C-expanded Vγ9Vδ2 T cells	1 CR (12.5%), 1 SD (12.5%)	
Lin et al.	2020	Pancreatic cancer	63	ACT+	Allogeneic zoledronate-expanded Vγ9Vδ2 T cells + irreversible electroporation (IRE)	OS: 14.5 vs. 11 months (IRE only); PFS: 11 vs. 8.5 months (IRE only)	(100)
Kakimi et al.	2020	Lung cancer	66	ACT	Autologous zoledronate-expanded Vγ9Vδ2 T cells + IL-2	Median PFS: 95 days; median OS: 418 days; 1 PR (4%), 16 SD (64%)	(101)
Fazzi et al.	2021	Multiple myeloma	60	*In vivo* stimulation	Zoledronate + IL-2 + Ca/vitamin D	8 CR (18%)	(102)
Zhang et al.	2021	Liver cancer	53	ACT+	Allogeneic zoledronate/vitamin C expanded Vγ9Vδ2 T cells + locoregional therapy (LT)	Median OS: 13 vs. 8 months (LT only); median distant PFS: 8 vs. 4 months (LT only)	(103)
		Intrahepatic cholangiocarcinoma	56	ACT+	Allogeneic zoledronate/vitamin C expanded Vγ9Vδ2 T cells + locoregional therapy	Median OS: 9 vs. 8 months (LT only); median distant PFS: 8 vs. 4 months (LT only)	
Zheng et al.	2022	Lung cancer	59	*In vivo* stimulation	Zoledronate + anti-PD-1	PFS: 5.4 vs. 2.8 months (without zoledronate); OS: 16.7 vs. 12.8 months (without zoledronate); 23 PR (44.2%), 16 SD (30.8%)	(104)
He et al.	2022	Lymphoma	52	ACT engineered	ET019003 T cells	6 CR (50%), 4 PR (33.3%), 1 SD (8.3%)	(84)

SD, stable disease; PR, partial response; CR, complete response; OS, overall survival; PFS, progression-free survival.

treated, with lymphoma being the most tested tumor [including B-cell lymphoma (lymphoma), follicle center lymphoma (FCL), mantle zone lymphoma (MZL), and T-cell non-Hodgkin lymphoma (T-NHL); Figure 4A]. A recent cohort study that used modified γδ T cells to treat B-cell lymphoma had the best response rate (Figure 4A, Table 2) (84). For solid tumors, there were 12 kinds of cancers recorded, with 10 cancers in female patients (n = 38) (Figure 4B, left panels) and seven cancers in male patients (n = 51) (Figure 4B, right panels). The type of cancer found most often in tested patients of both sexes was lung cancer, which was treated in all cases with ACT (Figure 4B, lower panels); however, the outcomes were moderate (Figure 4B, upper panels). Out of 38 female solid cancer patients, three reached OR, all with ACT+ treatment. Although treatment strategy matters, it is interesting to note that, among the ACT+-treated tumors, these positively responding cancers were all female-related (Figure 4B, upper left, pie chart). However, the sample size was too small to draw a conclusion. Among male solid cancer patients, 55% were treated with ACT, two patients reached OR, and the only CR patient received ACT+ treatment (Figure 4B, right panels).

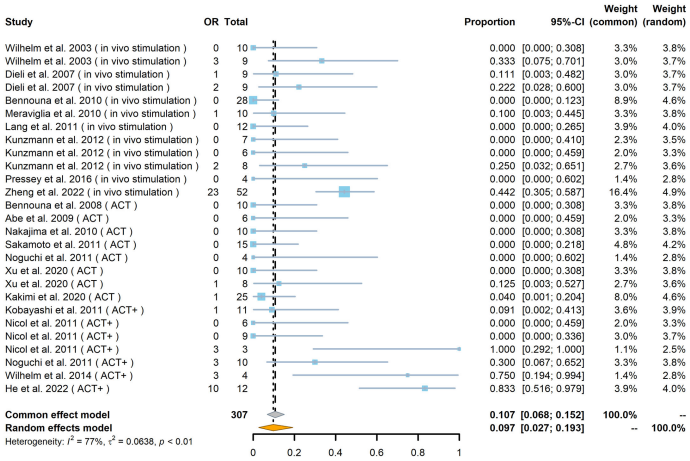

FIGURE 2
Forest plot of objective response (OR) rate (n = 27). The OR indicates the number of patients in each cohort who achieved an objective response. The total indicates the total number of measurable patients in each cohort. The OR rate, 95% confidence interval (CI), and weights of fixed- and random-effects models are indicated for each cohort. Blue squares show the mean OR rate of each cohort, and the size indicates the weight of the cohort; gray lines show the 95% CI, and the diamond shapes show the pooled weighted means of the OR rate using fixed- and random-effects models.

In addition, when investigating if the number of cells reinfused in patients was associated with outcomes, it was found that, among the 94 patients from eight cohorts treated by γδ T-cell reinfusion, dosage information was available for 46 patients (four cohorts). In general, this sample followed the tendency of the above statistical analysis (Table 4, n = 46), except that there were no differences in the frequency of use of each strategy between hematological and solid cancers. Although the sample size was not large enough for statistical analysis, the response rates of blood and solid cancers were quite different (Table 4, n = 46; Figures 5A–C). This was

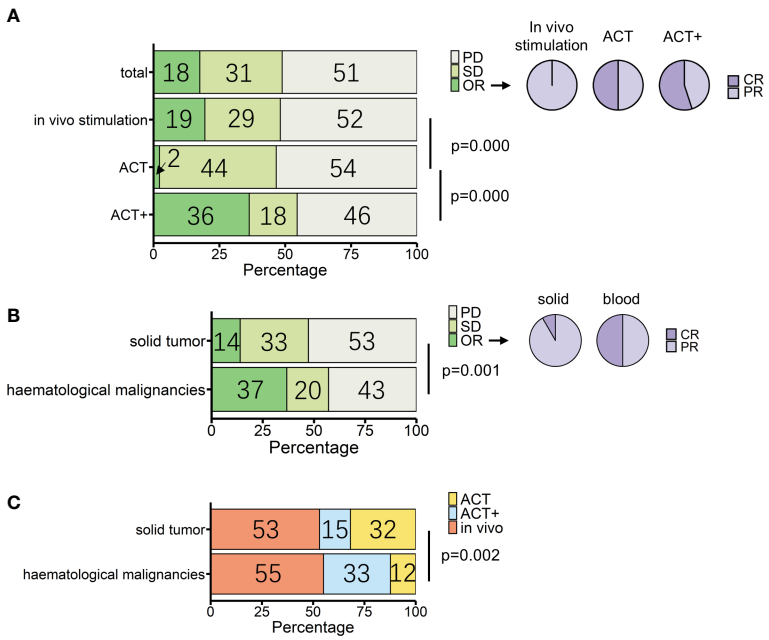

FIGURE 3
Overview of patients treated with γδ T-cell immunotherapy (n = 307). **(A)** Proportions of treatment outcomes in total measurable patients and different treatment types [*in vivo* stimulation, n = 164; adoptive cell transfer (ACT), n = 88; ACT combined with other treatments except for IL-2 treatment (ACT+), n = 55]. Pie charts show the proportions of complete response (CR) and partial response (PR) within objective response (OR) patients for each treatment method (*in vivo* stimulation, n = 32; ACT, n = 2; ACT+, n = 20). **(B)** Proportions of treatment outcomes in different types of tumors (solid, n = 258; hematological, n = 49). Pie charts show the proportions of CR and PR within OR patients for each tumor type (solid, n = 36; hematological, n = 18). **(C)** Proportions of treatment types applied in different types of tumors (solid, n = 258; hematological, n = 49). p-values (Pearson's chi-squared test) are indicated in **(A–C)**. PD, progressive disease; SD, stable disease; OR, objective response; CR, complete response; PR, partial response.

TABLE 3 Treatment strategy influences in γδ T cell immunotherapy (n = 307).

Treatment differences between hematological and solid tumors				Pearson's chi-squared test
	In vivo	ACT	ACT+	p = 0.002
Hematological	27	6	16	
Solid	137	82	39	
Hematological tumors				
	OR	SD	PD	NA
In vivo	5	5	17	
ACT	0	4	2	
ACT+	13	1	2	
Solid tumors				
	OR	SD	PD	p = 0.003
In vivo	27	42	68	
ACT	2	35	45	
ACT+	7	9	23	

NA, not applicable for statistical analysis; OR, objective response; PD, progressed disease; SD, stable disease.

mainly due to the cohort with lymphoma that was treated with modified T cells. This cohort also influenced the difference in responses between age groups (Table 4, n = 46; Figures 5A–D), as 75% of the patients in this cohort were less than 60 years old (84), whereas the other three cohorts had equal numbers of patients above and below 60 years old. Overall, the total cell dose tended to be positively correlated with infusion times (Figure 5) and ranged from 0.1×10^9 cells to 31.4×10^9 cells. Interestingly, those with an OR response were not necessarily reinfused with the highest γδ T-cell numbers, but all received ACT+ treatment (Figures 4A, B, Table 5). This was in accordance with the fact that total infusion doses were generally higher in the case of the less effective ACT treatment than when ACT was combined with other treatments (Figure 5B, Table 5). However, higher doses tended to stabilize disease progression (Figure 5A, Table 5). When considering only unmodified T-cell therapies (n = 34), as the cohort using modified T-cells strongly influence the analysis, the dosages were significantly different when comparing treatment types and sex (Table 4). Male patients tended to be infused with higher doses of Vγ9Vδ2 T cells (Figure 5E, Table 5).

3.3 Currently registered γδ T cell clinical trials

As of 15 November 2022, at least 48 γδ T cell-related clinical trials had been registered on the ClinicalTrials.gov website. Of these trials,

TABLE 4 Sex, age, tumor type, and treatment strategy influences in γδ T cell immunotherapy (n = 138).

Row (R)	Column (C)	Pearson's chi-squared test (n = 138)	Pearson's chi-squared test (n = 46)
Sex	Responses	p = 0.214	p = 0.444
	Treatments	p = 0.619	p = 0.122
	Age	p = 0.018	p = 0.137
	Tumor type	p = 0.789	p = 0.365
Age	Responses	p = 0.087	NA (p = 0.005)
	Treatments	p = 0.351	p = 0.112
	Tumor type	p = 1.000	p = 0.156
Tumor type	Response	p = 0.000	NA (p = 0.001)
	Treatment	p = 0.000	p = 1.000
Treatments	Responses	p = 0.000	NA (p = 0.003)

Comparisons: sex (female vs. male), age (≤ 60 years vs. > 60 years), tumor type (hematological malignancies vs. solid tumor), treatment [in vivo stimulation, adoptive cell transfer (ACT), and ACT combined with other treatments except for IL-2 treatment (ACT+) and responses [objective response (OR), stable disease (SD), and progressed disease (PD)]. The n = 138 sample comprises all the patients with detailed information corresponding to treatment outcomes. The n = 46 sample comprises patients who received γδ T-cell infusions and with indicated infusion cell numbers. NA, not applicable for statistical analysis.

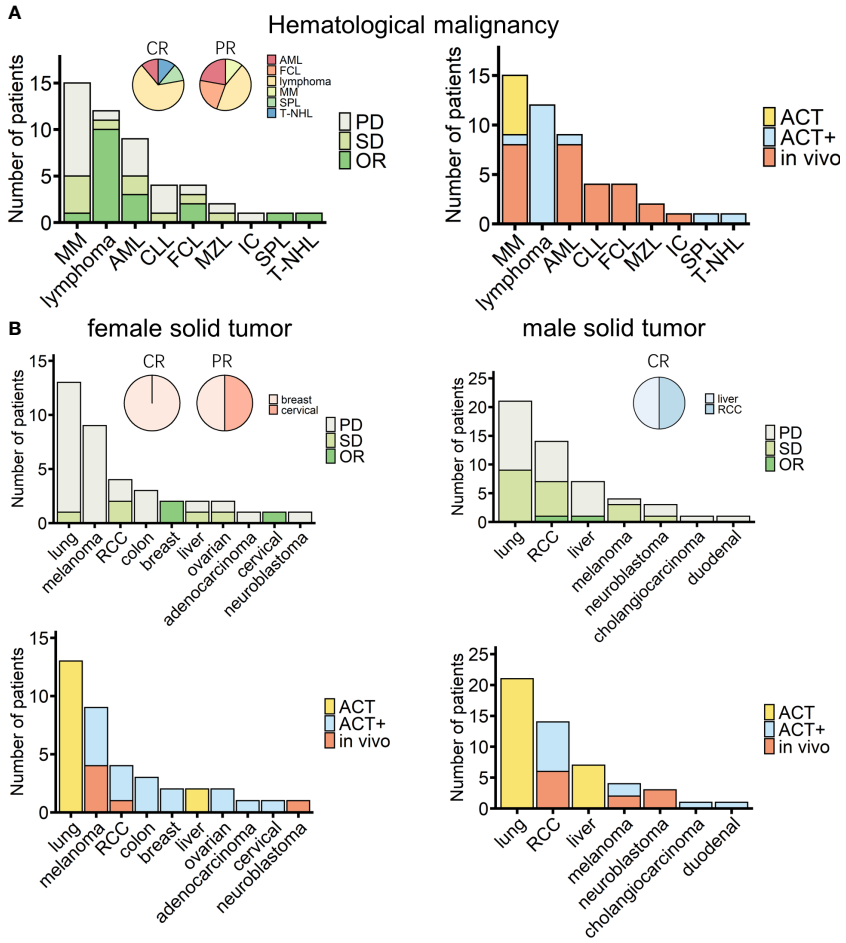

FIGURE 4
Overview of cancer types of patients treated with γδ T-cell immunotherapy (*n* = 138). **(A)** Diseases (left) and chosen treatment strategies (right) of hematological cancer patients (*n* = 49). Pie charts show the proportions of patients who achieved a complete response (CR) or a partial response (PR) after treatment (CR, *n* = 9; PR, *n* = 9). **(B)** Diseases (upper) and chosen treatment strategies (lower) of female (left) and male (right) solid tumor patients (female, *n* = 38; male, *n* = 51). Pie charts show the proportions of patients who achieved a CR or PR after treatment (female CR, *n* = 1; female PR, *n* = 2; male CR, *n* = 2). MM, multiple myeloma; AML, acute myeloid leukemia; CLL, chronic lymphocytic leukemia; FCL, follicle center lymphoma; MZL, mantle zone lymphoma; IC, immunocytoma; SPL, secondary plasma cell leukemia; T-NHL, T-cell non-Hodgkin lymphoma; RCC, renal cell carcinoma.

30 (63%) were ongoing (Figure 6A, left), and most of them were phase I trials aimed at testing the safety and preliminary efficacy of using Vγ9Vδ2 T cells to treat cancers (Figure 6A, middle). China and the United States accounted for 81% of the initiators of all these trials (Figure 6A, right). Compared with the completed trials analyzed above, these registered trials show the dynamic evolution of strategies for applying γδ T cells in clinics (Figure 6B). The earliest γδ T-cell clinical trials registered on ClinicalTrials.gov were started in 2003, the same year that Wilhelm et al. published their study on the use of γδ T cells to treat hematological malignancies (68). More than a decade later, the registration rate was quite stable; from 2003 to 2016, only nine γδ T-cell clinical trials were started.

Interestingly, since 2017, there has been a dramatic increase in the number of γδ T-cell clinical trials (Figures 5B–D). The first clinical trial using modified γδ T cells (CAR-T) was posted in 2016 and started in 2017 in China, the same year that the FDA (US Food and Drug Administration) approved the world's first CAR-T cell immunotherapy (Kymriah) to treat leukemia. Since then, 10 more CAR-modified γδ T-cell therapies, one gene-modified study focused on increasing γδ T cells' chemo drug-resistance (105) (NCT04165941), and one study applying TCR-T cell technology, which transduces tumor cytotoxic γδ TCR to αβ T cells (106, 107) (NCT04688853), have been started. In addition to manipulating T cells directly, the use of Vγ9Vδ2 T-cell-activating antibodies, either humanized anti-BTN3A antibodies (83) (NCT04243499) or engineered tumor-γδ TCR bispecific antibodies (NCT05369000, NCT04887259), has become a new trend in the last 2 years. Antibody drugs have many advantages; for example, they can be obtained "off the shelf", they are easy to produce, it is easy to ensure quality and to operate batch control, and they are relatively low cost. For therapies involving γδ T-cell infusion, 2017 was also a turning point, with healthy donor-derived γδ T cells arriving on the market. Of the 34 adoptive cell transfer trials after 2017, after excluding four trials that did not indicate cell origin, 20 out of 30 clinical trials used allogeneic γδ T cells (Figure 6C). When looking at the treated cancer types, before 2017, γδ T-cell therapy was dedicated to treating solid

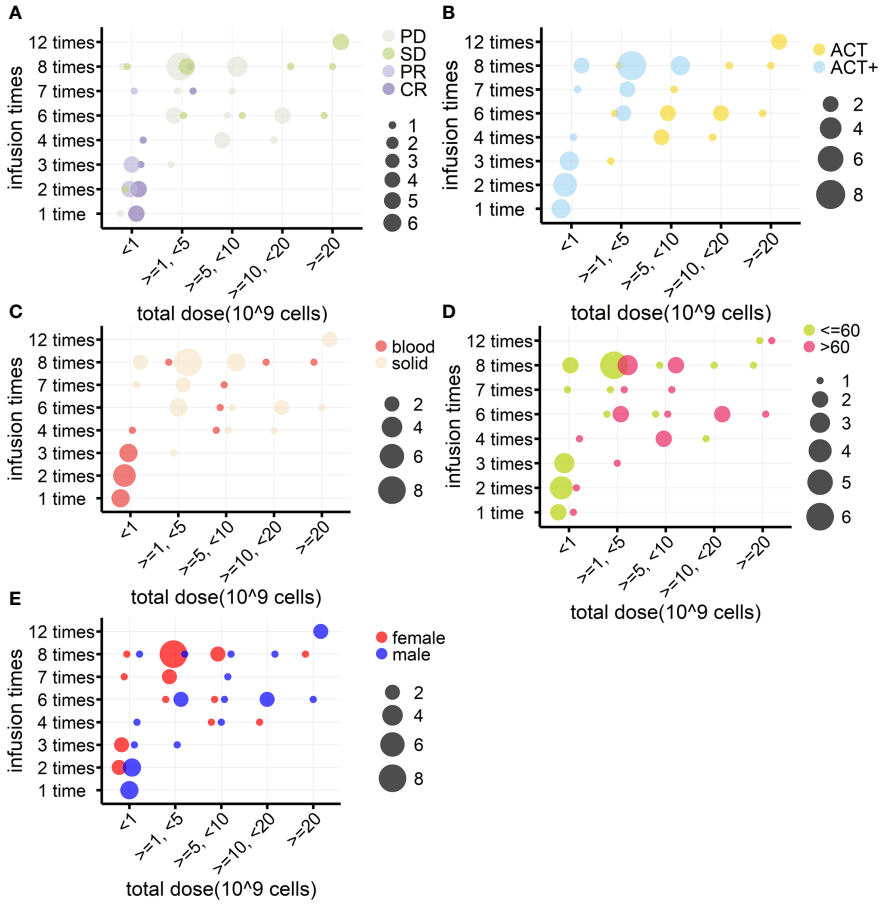

FIGURE 5
Relationships between γδ T cell reinfusion doses and treatment outcome, strategy, tumor type, age, and sex (n = 46). **(A)** Relationship between treatment outcome and dosage. γδ T-cell total infusion cell numbers (10 (9) cells) were divided into five groups and are presented on the x-axis; the y-axis indicates total infusion times. The bubble color indicates the treatment outcome, and the bubble size indicates the number of patients. **(B)** Relationship between treatment strategy and dosage. **(C)** Relationship between tumor type and dosage. **(D)** Relationship between age and dosage. **(E)** Relationship between sex and dosage.

TABLE 5 Cell dosage differences by treatment outcome, strategy, tumor type, age, and sex in γδ T cell immunotherapy (n = 46).

		Median dose (10^9 cells) (n = 46)	p-value (Wilcoxon test) (n = 46)	Median dose (10^9 cells) (n = 34)	p-value (Wilcoxon test) (n = 34)
Responses	OR	0.486	OR vs. SD: 0.003; OR vs. PD: 0.001	3.6	ns
	SD	7.2		9.6	
	PD	4.5		4.6	
Treatments	ACT	10.2	0.000	10.2	0.000
	ACT+	0.95		2.5	
Tumor type	Blood	0.52	0.008	7.8	ns
	Solid	3.8		3.8	
Age (years)	≤60	1.25	ns	3.6	ns
	>60	4.7		5.2	
Sex	Female	3	ns	3.5	0.046
	Male	2.6		7.2	

The n = 46 sample comprises patients who received γδ T cell infusions and with indicated infusion cell numbers. The n = 34 sample comprises patients who were reinfused with unmodified γδ T cells. ns, not significant.

10.3389/fimmu.2023.1140623

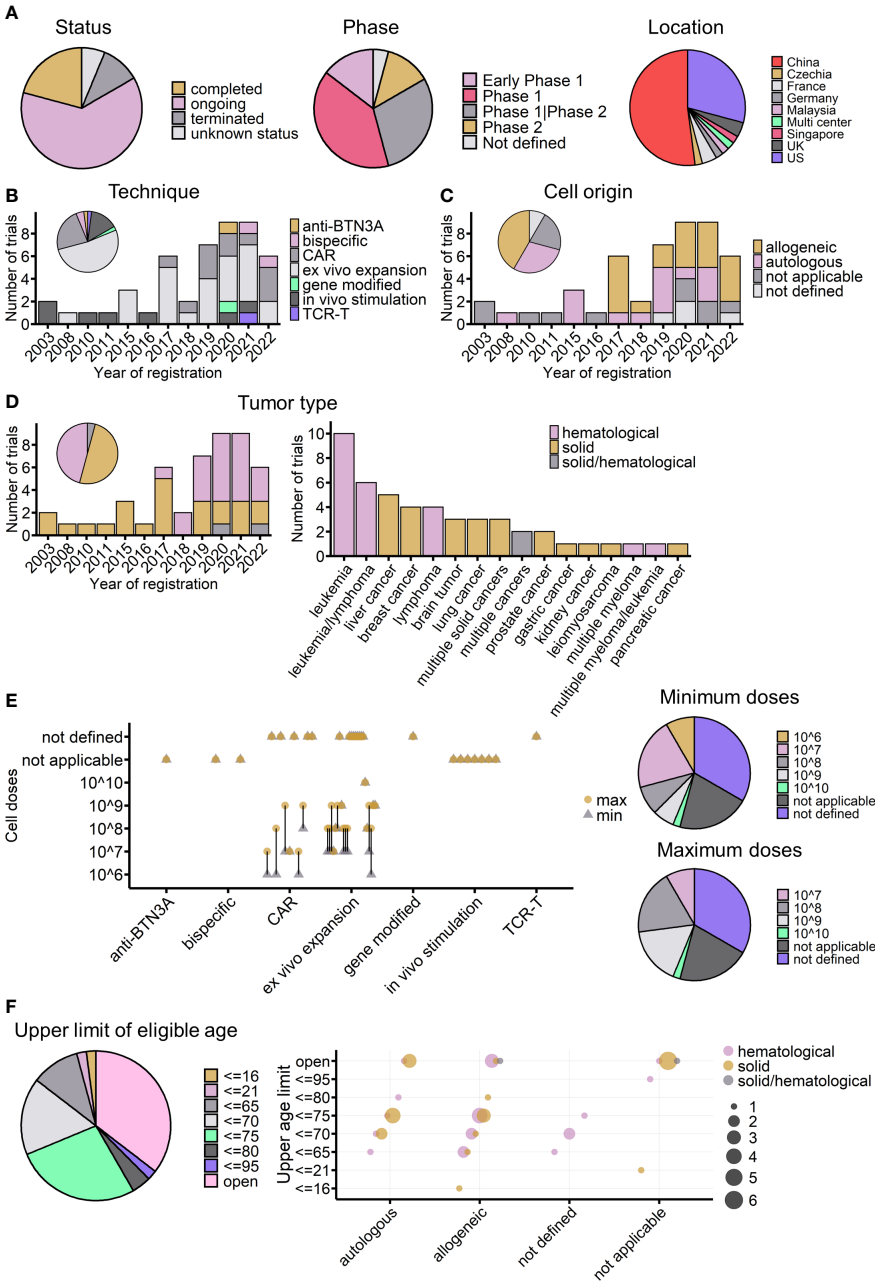

FIGURE 6
Overview of currently registered γδ T-cell immunotherapy clinical trials (*n* = 48). **(A)** Proportions of currently registered γδ T-cell immunotherapy clinical trials according to status, phase, and location. **(B)** Timeline of registered clinical trials by treatment strategy. The pie chart shows the proportion of trials for each strategy. **(C)** Timeline of registered clinical trials by infusion cell origin. **(D)** Timeline of registered clinical trials by tumor type (left) and detailed malignancies involved in registered trials (right). The pie chart indicates the proportions of different tumor types across all registered trials. **(E)** Planned infusion dosage of registered trials. Left: treatment strategies are indicated on the *x*-axis, and planned γδ T-cell infusion cell numbers are indicated on the *y*-axis. The round yellow dot shows the planned maximum infusion dose, and the gray triangle dot shows the planned minimum infusion dose. The bar connects the maximum and minimum number for each trial. Right: the proportions of different planned minimum (upper) and maximum (lower) infusion doses. **(F)** Upper age limit of registered γδ T-cell immunotherapy clinical trials. Left: proportions of different upper age limits. Right: the relationship between upper age limits, treatment strategy usages, and tumor types. The bubble color shows the tumor type of the trial, and the bubble size indicates the number of trials. **(C–F)** Not applicable: strategies not involving cell infusion; not defined: infusion cell origin not defined.

tumors, but this changed after the launch of CAR-γδ T cell therapy (Figure 6D). Currently registered CAR-γδ T-cell therapy trials are mainly testing its use in hematological malignancies, following the successful use of typical CAR-T-cell therapy. Leukemia and liver cancers are the most tested blood and solid cancers, respectively (Figure 6D, right).

In the case of adoptive cell transfer, 22 of the trials provided dosage information. There are two ways of calculating dosage: one

is based on the body weight of patients, giving the infusion cell number per kg, and the other is based on the total cell number per infusion, regardless of body weight. To easily analyze the two systems together and compare the results, as far as possible, with the results of completed trials the cell number was multiplied by 10 for those trials that considered patients' weight for dosage. The expected infusion doses were mainly between 10^7 and 10^8 cells per infusion (Figure 6E). It is important to note that, among the 22 trials, excluding those that did not indicate infusion times, six trials used a single infusion, and eight used multiple infusions (mostly four or six infusions). Thus, when considering body weight and the number of infusions (multiple infusion trials also tended to have a higher dose per infusion), the maximum total planned dose may increase to 10^9 cells for most trials. The planned doses were similar to those administered to the 16 cohorts in completed trials, in which the median of average cell dose (regardless of ACT or ACT+) was 5.85×10^9 cells (Figure 1D), and the medians of the minimum and maximum infusion doses were 0.75×10^9 and 14.15×10^9 cells, respectively.

Furthermore, regarding the T-cell subtype, except for three trials that transferred γδ TCR or part of γδ TCR to αβ T cells, all the other trials used γδ T cells. Currently, only two trials are using allogeneic Vδ1 γδ T cells to treat hematological malignancies (NCT04735471 and NCT05001451); all the other registered clinical trials are focused on the use of Vγ9Vδ2 T cells. As mentioned earlier, the number of Vγ9Vδ2 T cells gradually declines with age (108, 109); this might be considered as a possible influencing factor on treatment outcomes, especially in trials using autologous γδ T cells or trials applying *in vivo* stimulation or activating antibodies. Regarding exclusion criteria, 35% of the registered trials did not set an upper limit on the eligible age of participants (Figure 6F), whereas 27% of the trials used an age below 75 years as an inclusion criterion. Among the 14 trials using autologous γδ T cells, 10 trials included either a lower age limit of 75 years or no age limit in their inclusion criteria. The majority of *in vivo* stimulation and Vγ9Vδ2 T-cell-activating antibodies trials do not have an upper age limit (Figure 6F). Indeed, for early-phase clinical studies, age limitation was not the priority for exclusion criteria. In future, if possible, the effect of age should be carefully tested and compared during these early phases to give better treatment choices for different age groups of patients.

4 Use of γδ T cells in the pharmaceutical industry

Although many features of γδ T cells are still unknown, their practical uses can still be studied and applied. Currently, at least 29 pharmaceutical companies have made progress in developing γδ T-cell-based therapies for fighting cancers. Table 6 lists both the preclinical and clinical stage γδ T-cell-related anticancer products being developed by these companies. Compared with the currently

TABLE 6 Preclinical and clinical stage therapeutic γδ T cells in the pharmaceutical industry.

Company	Drug	Approach	Biological	Condition
Acepodia	ACE1831	Antibody–cell conjugation	Allogeneic, anti-CD20, Vδ2 T cells	Lymphoma
	ACE2016	Antibody–cell conjugation	Allogeneic, anti-EGFR, Vδ2 T cells	EGFR-expressing solid tumors
	ACE1708	Antibody–cell conjugation	Allogeneic, anti-PD-L1, Vδ2 T cells	PD-L1-expressing cancers
	ACE1975	Antibody–cell conjugation	Allogeneic, target undisclosed, Vδ2 T cells	Undisclosed
	ACE2023	Antibody–cell conjugation	Allogeneic, target undisclosed, Vδ2 T cells	Undisclosed
Adicet	ADI-001	CAR	Allogeneic, anti-CD20, Vδ1 T cells	Lymphoma
	ADI-925	Engineered chimeric adapter (CAd)	Allogeneic, tumor stress ligands, Vδ1 T cells	Multiple cancers
	ADI-***	–	Anti-CD70	Multiple cancers
	ADI-***	–	Anti-PSMA	Prostate cancer
	ADI-***	–	Anti-B7-H6	Multiple cancers
	ADI-***	–	Undisclosed	Multiple myeloma
	ADI-***	–	Undisclosed	Solid tumors
	ADI-002	CAR	Allogeneic, anti-GPC3, IL-15 secreting, Vδ1 T cells	Liver cancer
American Gene Technologies	ImmunoTox	Genetic medicine delivered to tumor cells	Up-regulate PAgs in tumor cells to activate Vγ9Vδ2 T cells in situ	Prostate and liver cancer

(Continued)

TABLE 6 Continued

Company	Drug	Approach	Biological	Condition
AVM Biotechnology	AVM0703	High-concentration dexamethasone phosphate drug	–	Lymphoma, leukemia
Beijing Doing Biomedical	NCT02585908s	Unmodified	Autologous, γδ T cells	Gastric cancers
	NCT02656147	CAR	Allogeneic, anti-CD19 CAR γδ T cells	Lymphoma, leukemia
Beijing GD Initiative Cell Therapy Technology	NCT04518774	Unmodified	Allogeneic, γδ T cells	Liver cancer
	NCT04696705	Unmodified	Allogeneic, γδ T cells	Lymphoma
	NCT04028440	Unmodified	Autologous, γδ T cells	Lymphoma, leukemia
Century Therapeutics	CNTY-102	Induced pluripotent stem cells, CAR	Allogeneic, anti-CD19, anti-CD79b, iPSC-derived γδ TCR+, CAR+ T cells CAR-iT)	B-cell malignancies
	CNTY-104	Induced pluripotent stem cells, CAR	Allogeneic, multi-specific, CAR-iT or CAR-iNK	Leukemia
	CNTY-106	Induced pluripotent stem cells, CAR	Allogeneic, multi-specific, CAR-iT or CAR-iNK	Multiple myeloma
	CNTY-***	Induced pluripotent stem cells, CAR	Allogeneic, undisclosed, CAR-iT or CAR-iNK	Solid tumors
CytoMed Therapeutics	CTM-N2D	CAR	Allogeneic, anti-NKG2DL, CAR γδ T cells	Solid tumors
	GDNKT	Induced pluripotent stem cells (iPSC)	Autologous, iPSC-derived γδ NKT cells	Solid tumors
	CTM-GDT	Undisclosed	Allogeneic, γδ T cells	Solid tumors
Eureka(Beijing) Biotechnology	ET190 (ET019003 in NCT04014894, ET019002 in NCT03642496)	Antibody redirected T cells with endogenous modular immune signaling and a co-stimulatory molecule (ARTEMIS®)	Autologous, αβ T cells expressing anti-CD19 Fab-γδ TCR intracellular domain and co-stimulatory molecule	Hematological malignancies
Expression Therapeutics	ET206	Undisclosed	γδ T cells	Neuroblastoma
	ET356, ET406	mRNA and novel CAR	CAR γδ T cells	Lymphoma, leukemia
Gadeta	GDT002	Modified CAR or TCR-T	Autologous, Vγ9Vδ2 TCR-expressing αβ T cells	Multiple myeloma, ovarian cancer
	GDT201	Modified CAR or TCR-T	Autologous, non-Vδ2 γδ TCR-expressing αβ T cells	Colorectal cancer
	GDT3nn	Undisclosed	Undisclosed	Solid tumors
GammaDelta Therapeutics Ltd. (Takeda)	GDX012	Unmodified	Allogeneic, non-modified Vδ1 γδ T cells	Leukemia
Adaptate Biotherapeutics (Takeda)	–	Engager antibody	Anti-Vδ1	Undisclosed
Guangdong GD Kongming Biotech	Undisclosed	Undisclosed	Allogeneic, Vγ9Vδ2 T cells	Multiple cancers
Hebei Senlang Biotechnology	Senl_uγδT-123	CAR	Allogeneic, CAR γδ T cells	Undisclosed (possibly AML NCT04796441, NCT05388305)
ImCheck	ICT01	Monoclonal antibody	Anti-BTN3A	Multiple cancers
	ICT03	Monoclonal antibody	Anti-BTN2A	Multiple cancers
	ICT04–08	Monoclonal antibody	Anti-5 BTNs	Multiple cancers
Immatics (with Editas medicine)	ACTallo®	CAR or TCR-T, CRISPR gene editing	Allogeneic, CAR, or TCR-T engineered Vγ9Vδ2 T cells	Undisclosed

(Continued)

TABLE 6 Continued

Company	Drug	Approach	Biological	Condition
IN8bio	INB-200	Gene modification	Autologous, gene-modified chemo drug-resistant γδ T cells	Brain tumor
	INB-100	Unmodified	Allogeneic, γδ T cells	Leukemia
	INB-400	Gene modification	Allogeneic, gene-modified chemo drug-resistant γδ T cells	Glioblastoma
	INB-300	Gene modification, CAR	Gene-modified chemo drug-resistant anti chlorotoxin CAR-expressing γδ T cells	Solid tumors
Kiromic BioPharma	Deltacel™	Unmodified	Allogeneic, γδ T cells	Undisclosed
	Procel™	CAR	Allogeneic, anti-PD-L1 CAR γδ T cells	Undisclosed
	ALEXIS-PRO-1 Procel™	CAR	Allogeneic, anti-PD-L1 CAR γδ T cells	Undisclosed
	Isocel™	CAR	Allogeneic, anti-mesothelin CAR γδ T cells	Undisclosed
	ALEXIS- ISO-1 Isocel™	CAR	Allogeneic, anti-mesothelin CAR γδ T cells	Undisclosed
LAVA Therapeutics	LAVA-051	Bispecific γδ T-cell engaging antibody	Anti-CD1d, anti-γδ TCR	Multiple myeloma, leukemia
	LAVA-1207	Bispecific γδ T-cell engaging antibody	Anti-PSMA, anti-γδ TCR	Prostate cancer
	LAVA-1223	Bispecific γδ T-cell engaging antibody	Anti-EGFR, anti-γδ TCR	Solid tumors
	LAVA-1266	Bispecific γδ T-cell engaging antibody	Anti-CD123, anti-γδ TCR	Hematological malignancies
	LAVA-1278	Bispecific γδ T-cell engaging antibody	Anti-CD40, anti-γδ TCR	Hematological malignancies
Legend Biotech	Undisclosed	Enhance the persistence of CAR-γδ T cells *in vivo*	Undisclosed	Undisclosed
Leucid bio	T2	CAR	Allogeneic, CAR γδ T cells	Undisclosed
One Chain Immunotherapeutics	OC-3	Unmodified	Allogeneic, Vδ1 T cells	Undisclosed
PersonGen BioTherapeutics (Suzhou)	UCAR-γδ T	CAR	Target undisclosed (anti-CD7 in NCT04702841, anti CD19/CD20 in NCT04700319), CAR γδ T cells	Multiple cancers
PhosphoGam	Undisclosed	Unmodified, purification step free	Allogeneic, Vδ2 T cells	Undisclosed
PureTech	LYT-210	Blocking antibody	Anti-Vδ1	Solid tumors
Shattuck	GADLEN	Bispecific engager antibody	BTN3A1/BTN2A1 extracellular domain heterodimer, anti-tumor specific antigen (e.g., CD19)	Undisclosed
TC BioPharm	OmnImmune®	Unmodified	Allogeneic, unmodified γδ T cells	Leukemia
	Undisclosed	CAR	Allogeneic, CAR γδ T cells	Multiple cancers
UNICET biotech	Undisclosed	Antibody, cell therapy, CAR	Undisclosed	Undisclosed

EGFR, epidermal growth factor receptor; iT, immunotherapy; PSMA, prostate-specific membrane antigen; GPC3, glypican-3.
All the information can be found on each company's website under pipeline web pages or scientific introduction web pages. Those with clinical trial register numbers can also be found on the ClinicalTrials.gov website.
*** means product number not indicated.

registered clinical trials, the approaches designed by the pharmaceutical industry are more diverse.

There are four broad types of strategies being employed in the pharmaceutical industry. The first is the unmodified strategy, in which researchers focus on harnessing the natural capacity of effector γδ T cells and exploiting their MHC-independent nature to take advantage of "off-the-shelf", safe-to-use, and easy-to-produce benefits. This approach involves utilizing both Vδ2 and Vδ1 γδ T cells, focusing on optimizing the expansion steps, such as the products of GammaDelta Therapeutics Ltd. and PhosphoGam.

Second is the modified strategy. Introducing the classical CAR structure to γδ T cells is the starting point for this strategy, with at least nine companies using the typical CAR T-cell technique. The targets of CAR γδ T cells can be classified into two types: one is antigens highly expressed in tumors, such as GPC3 and mesothelin, and the other is receptors, such as NKG2DL and PD-L1 (Table 6). One study targeting the former found that PD-L1-targeting CAR (αβ) T cells had increased cytotoxicity toward high-PD-L1-expressing tumor cells (110). In addition, many companies have designed modified CARs. One strategy, similar to TCR-T-cell techniques, is transplanting the selected antitumor γδ TCR into αβ T cells, such as Gadeta, or using γδ TCR domains to modify CARs, which has been developed by companies such as Eureka Biotechnology (Beijing). The other strategy combines induced pluripotent stem cells (iPSCs) and CAR techniques to produce off-the-shelf CAR γδ T cells, such as those produced by Century Therapeutics and CytoMed Therapeutics. Studies of the former type have shown the feasibility of generating iPSC-derived antitumor CAR γδ T cells (111, 112). In addition to modifying γδ T cells by CAR, gene editing by CRISPR has also been commonly used in recent years by companies such as IN8bio and Immatics.

Third is the antibody-based strategy. ImCheck has used anti-BTN antibodies to stimulate Vγ9Vδ2 T cells *in vivo*; in an early analysis from their phase I/II clinical trial, ICT01 (anti-BTN3A) demonstrated a 36% disease control rate in a 22-patient cohort (Imchecktherapeutics.com: Imcheck Therapeutics). Several companies, such as LAVA Therapeutics and Shattuck, have used bispecific antibodies to activate and endow specificity on γδ T cells. PureTech has used an anti-Vδ1 antibody to block protumor Vδ1 γδ T cells (Table 6). Acepodia has combined the antibody-based approach with adoptive cell transfer, in which γδ T cells are chemically modified by tumor-specific antibodies.

Last is the use of chemical drugs and the modification of tumors. American Gene Technologies aims to genetically modify tumor cells to increase their PAgs level and activate Vγ9Vδ2 T cells *in situ*. AVM Biotechnology's preclinical results show that the antitumor effects of high concentrations of the drug dexamethasone phosphate involve the activation of γδ TCR^+ NKT cells. This drug can be given alone or as a preconditioning agent before CAR-T-cell treatment (113, 114).

5 Discussion

The applications of γδ T cells in cancerous diseases have been carefully reviewed here, but several limitations should be taken into consideration. First, we used PubMed and ClinicalTrials.gov only as the primary search databases. For ongoing trials, clinical trial registration websites in the EU, Japan, China, Australia, and New Zealand were not cross-checked. However, the analyzed trials should provide a proper overview of current developments in γδ T-cell immunotherapy. Second, in the review of current γδ T-cell treatment outcomes, the aim was to obtain a general idea of whether or not the use of different treatment strategies could influence outcomes based on the limited sample numbers and diverse conditions of different studies. For instance, we roughly divided the treatment strategies into three categories (i.e., *in vivo* stimulation, ACT, and ACT+), but recent studies have tried to combine *in vivo* stimulation with other treatments, such as checkpoint inhibiter treatment (Table 2) (104). In addition, the modification of T cells was included in the ACT+ group so that the ACT group, as far as possible, included only conventional γδ T-cell infusion. Such comparisons will become more accurate as the use of γδ T-cell therapies increases in clinics in the future.

Despite these limitations, several conclusions can be drawn from reviewing past γδ T-cell immunotherapies. First, although not covered in this review, γδ T-cell immunotherapy is a safe approach in clinics, whether it involves *in vivo* stimulation, reinfusion, or autologous or allogeneic reinfusion. In general, adverse events more severe than grade 2 were not directly related to γδ T-cell treatment and could be adequately controlled. Second, the treatment method appears to have a significant impact on the outcomes. Reinfusion of γδ T cells tended to have a greater potential for complete responses than *in vivo* stimulation (Figure 3A). Even for the less effective treatment of ACT alone, one of the two patients who achieved OR had a complete response (Figure 3A), and ACT treatment had the highest pooled SD rate (Supplemental Figures 3 and 7). This may be related to the patient's response to zoledronate treatment. Many *in vivo* stimulation studies involved a zoledronate sensitivity test when selecting patients (76, 85, 92). Although patients were considered to be responsive to zoledronate, multiple treatments reduced the reaction (74, 90). This would not happen with multi-reinfusion of active γδ T cells, especially with cells of allogeneic origin. In addition, for reinfusion, allogeneic γδ T cells from healthy donors may be more resilient to the tumor environment.

Furthermore, combining γδ T-cell therapy with other conventional therapies or *in vivo* stimulation showed promising results. Studies have shown the stimulatory immunomodulating effects of radiotherapy (115). The activated tumor microenvironment resulting from such combined therapy may help the reinfused effector γδ T cells to operate effectively inside the tumor. Unlike CAR-T-cell treatment, γδ T-cell therapy often involves multiple infusions. Infusion times and dosages were not necessarily positively related to treatment responses (Figure 5A). It is interesting to note that male patients tended to receive higher reinfusion dosages than female patients (Figure 5E). In addition, it is interesting to note the regional difference (Supplemental Figures 8, 9). This was probably mainly due to when the γδ T-cell therapy was applied, as early studies tended to use the direct stimulation strategy. Thus, most *in vivo* stimulation results came from European countries, whereas reinfusion studies were more often carried out in Asian countries. In the future, it would be interesting to investigate if different treatments perform the same in different countries.

From the findings of prognosis studies, it is evident that the functional state of γδ T cells plays a critical role in cancer treatment. The difference in prognoses based on the role γδ T cells play in acute and chronic hematological cancers highlights the importance of manipulating the functioning state of γδ T cells in future immunotherapy design. Long-term disease settings seem to culture dysfunctional γδ T cells and select the protumor subset (65). Therefore, reinfusing fully functioning γδ T cells that are resistant to the tumor microenvironment (TME) could efficiently control cancer progression. In addition, in contrast to CAR-T-cell or TCR-T-cell immunotherapies, conventional γδ T-cell immunotherapy protocols usually do not include the lymphodepletion step. However, one study found that certain

chemotherapy drugs could activate tumor macrophages and help create an antitumor TME (116), suggesting that optimizing treatment protocols could also help to improve γδ T-cell immunotherapy outcomes. Furthermore, in solid tumor treatments in women, the three (8%) instances of OR were in breast and cervical cancer patients. Future studies could focus on investigating if these cancers are more sensitive than other types of cancer to γδ T-cell therapy. This is especially important as breast and gynecological cancers have the highest incidence and mortality rates among female cancers according to the Global Cancer Observatory [Global Cancer Observatory (iarc.fr)]. Moreover, in addition to the "quality" of γδ T cells, multiple reinfusion of large numbers of natural γδ T cells tended to stabilize disease progression (Figure 5A, Supplemental Figure 3). With their MHC-independent advantages, unmodified allogeneic γδ T cells could serve as a good treatment option for providing late-stage cancer patients with more time before undergoing further tumor-eliminating treatments. In addition, understanding the distinctions between responding and non-responding patients is crucial for enhancing the effectiveness of γδ T-cell immunotherapy. Whether the differences lie in genetics or microenvironments, this knowledge should enhance the understanding of γδ T cells as well as enable researchers to make informed decisions regarding precision treatment.

Author contributions

LM collected and analyzed the data, made the figures and tables, and wrote the manuscript. ZZ and YF helped to correct the manuscript and gave valuable advice. All authors contributed to the article and approved the submitted version.

Conflict of interest

LM, YF, and ZZ are employed by Beijing DCTY Biotech Co., Ltd. LM is also employed as a postdoctoral researcher at Peking University.

Publisher's note

Supplementary material

The Supplementary Material for this article can be found online at: https://www.frontiersin.org/articles/10.3389/fimmu.2023.1140623/full#supplementary-material

SUPPLEMENTARY FIGURE 1
Forest plot of stable disease (SD) rate (n = 27). SD indicates the number of patients in each cohort who achieved stable disease. The total indicates the total number of measurable patients in each cohort. The SD rate, 95% confidence interval (CI), and weights of fixed- and random-effects models are indicated for each cohort. Blue squares show the mean SD rate of each cohort, and the size indicates the weight of the cohort; gray lines show the 95% CI, and the diamond shapes show the pooled weighted means of the SD rate using fixed- and random-effects models.

SUPPLEMENTARY FIGURE 2
Forest plot of objective response (OR) rate sub-grouped by treatment strategy (n = 27). The OR indicates the number of patients in each cohort who achieved an objective response. The total indicates the total number of measurable patients in each cohort. The OR rate, 95% confidence interval (CI), and weights of fixed- and random-effects models are indicated for each cohort. Blue squares show the mean OR rate of each cohort, and the size indicates the weight of the cohort; gray lines show the 95% CI, and the diamond shapes indicate the pooled weighted means of OR rates for each treatment subgroup and for all cohorts using fixed- and random-effects models.

SUPPLEMENTARY FIGURE 3
Forest plot of stable disease (SD) rate subgrouped by treatment strategy (n = 27).

SUPPLEMENTARY FIGURE 4
Forest plot of objective response (OR) rate subgrouped by tumor type (n = 27).

SUPPLEMENTARY FIGURE 5
Forest plot of stable disease (SD) rate subgrouped by tumor type (n = 27).

SUPPLEMENTARY FIGURE 6
Forest plot of objective response (OR) rate in solid tumor cohorts subgrouped by treatment (n = 21).

SUPPLEMENTARY FIGURE 7
Forest plot of stable disease (SD) rate in solid tumor cohorts subgrouped by treatment (n = 21).

SUPPLEMENTARY FIGURE 8
Forest plot of objective response (OR) rate subgrouped by research location (n = 27).

SUPPLEMENTARY FIGURE 9
Forest plot of stable disease (SD) rate subgrouped by research location (n = 27).

SUPPLEMENTARY FIGURE 10
Overview of the effects of sex and age influence on outcomes for patients treated with γδ T-cell immunotherapy (n = 138). **(A)** Proportions of treatment outcomes in male and female patients (male, n = 81; female, n = 57). Pie charts show the proportions of complete response (CR) and partial response (PR) within objective response (OR) patients of each sex (male, n = 14; female, n = 9). **(B)** Proportions of treatment outcomes in different age groups (≤ 60 years, n = 67; > 60 years, n = 71). Pie charts show the proportions of CR and PR within the OR patients of each age group (≤ 60 years, n = 16; > 60 years, n = 7). p-values (Pearson's chi-squared test) are indicated in **(A, B)**. To take full advantage of these previous human studies, there were 138 patients for whom detailed information, such as age and sex, was available alongside treatment responses. The overall treatment responses were different among the three strategies (p = 0.000, Pearson's chi-squared test, n = 138; Table 3), but, in this smaller sample, adoptive cell transfer (ACT) combined with other treatments except for IL-2 treatment (ACT+) had the best response rate [38% OR rate vs. 11% of *in vivo* stimulation patients (p = 0.013) and 2% of ACT patients (p = 0.000)]. Of these 138 patients, 57 were female and 81 were male. The responses [OR, SD, and progressive disease (PD)] to different treatments were similar when compared between sexes (p = 0.214, Pearson's chi-squared test, n = 138; Table 3), whereas the age distribution was different between female and male patients (p = 0.008, Wilcoxon rank-sum test), with 61% and 40% of female and male patients less than 60 years old, respectively (median age: 57 years for females and 63 years for males). In addition, previous studies indicated that the percentage of

Vγ9Vδ2 T cells was lower in elderly people and showed defects in functioning (92, 104); for this reason, the patients here were divided into age groups of ≤ 60 years and > 60 years (in order to have similar sample sizes in each group) to give a general idea of the effect of age on treatment response. There were no response, treatment type, or tumor type differences between these age groups (n = 138; Table 3). In addition, when comparing tumor types (hematological vs. solid), this smaller sample followed the same trend as the n = 307 sample presented above (Figure 2B; Table 2), in which both responses and treatment types were different between blood and solid tumors (Table 3; n = 138). This may emphasize the importance of different γδ T-cell therapy strategies on treatment outcomes.

References

1. Chien Y-h, Meyer C, Bonneville M. γδ T cells: first line of defense and beyond. *Annu Rev Immunol* (2014) 32:121–55. doi: 10.1146/annurev-immunol-032713-120216

2. Papadopoulou M, Sanchez Sanchez G, Vermijlen D. Innate and adaptive γδ T cells: How, when, and why. *Immunol Rev* (2020) 298(1):99–116. doi: 10.1111/imr.12926

3. Saura-Esteller J, de Jong M, King LA, Ensing E, Winograd B, de Gruijl TD, et al. Gamma delta T-cell based cancer immunotherapy: Past-Present-Future. *Front Immunol* (2022) 13:915837. doi: 10.3389/fimmu.2022.915837

4. Nielsen MM, Witherden DA, Havran WL. γδ T cells in homeostasis and host defence of epithelial barrier tissues. *Nat Rev Immunol* (2017) 17(12):733–45. doi: 10.1038/nri.2017.101

5. Silva-Santos B, Serre K, Norell H. γδ T cells in cancer. *Nat Rev Immunol* (2015) 15 (11):683–91. doi: 10.1038/nri3904

6. Laplagne C, Ligat L, Foote J, Lopez F, Fournié FJ, Laurent C, et al. Self-activation of Vγ9Vδ2 T cells by exogenous phosphoantigens involves TCR and butyrophilins. *Cell Mol Immunol* (2021) 18(8):1861–70. doi: 10.1038/s41423-021-00720-w

7. Gober H-J, Kistowska M, Angman L, Jenö P, Mori L, De Libero G. Human T cell receptor gammadelta cells recognize endogenous mevalonate metabolites in tumor cells. *J Exp Med* (2003) 197(2):163–8. doi: 10.1084/jem.20021500

8. Rigau M, Ostrouska S, Fulford TS, Johnson DN, Woods K, Ruan Z, et al. Butyrophilin 2A1 is essential for phosphoantigen reactivity by γδ T cells. *Science*. (2020) 367(6478):eaay5516. doi: 10.1126/science.aay5516

9. Karunakaran MM, Willcox CR, Salim M, Paletta D, Fichtner AS, Noll A, et al. Butyrophilin-2A1 directly binds germline-encoded regions of the Vγ9Vδ2 TCR and is essential for phosphoantigen sensing. *Immunity*. (2020) 52(3):487–498.e6. doi: 10.1016/j.immuni.2020.02.014

10. Cano CE, Pasero C, de Gassart A, Kerneur C, Gabriac M, Fullana M, et al. BTN2A1, an immune checkpoint targeting Vγ9Vδ2 T cell cytotoxicity against malignant cells. *Cell Rep* (2021) 36(2):109359. doi: 10.1016/j.celrep.2021.109359

11. Hayday AC. γδ T cell update: Adaptate orchestrators of immune surveillance. *J Immunol* (2019) 203(2):311–20. doi: 10.4049/jimmunol.1800934

12. Vermijlen D, Gatti D, Kouzeli A, Rus T, Eberl M. γδ T cell responses: How many ligands will it take till we know? *Semin Cell Dev Biol* (2018) 84:75–86. doi: 10.1016/j.semcdb.2017.10.009

13. Willcox BE, Willcox CR. γδ TCR ligands: the quest to solve a 500-million-year-old mystery. *Nat Immunol* (2019) 20(2):121–8. doi: 10.1038/s41590-018-0304-y

14. Willcox CR, Vantourout P, Salim M, Zlatareva I, Melandri D, Zanardo L, et al. Butyrophilin-like 3 directly binds a human Vγ4+ T cell receptor using a modality distinct from clonally-restricted antigen. *Immunity*. (2019) 51(5):813–825.e4. doi: 10.1016/j.immuni.2019.09.006

15. Herrmann T, Karunakaran MM, Fichtner AS. A glance over the fence: Using phylogeny and species comparison for a better understanding of antigen recognition by human γδ T-cells. *Immunol Rev* (2020) 298(1):218–36. doi: 10.1111/imr.12919

16. Wegrecki M, Ocampo TA, Gunasinghe SD, von Borstel A, Tin SY, Reijneveld JF, et al. Atypical sideways recognition of CD1a by autoreactive γδ T cell receptors. *Nat Commun* (2022) 13(1):3872. doi: 10.1038/s41467-022-31443-9

17. Willcox CR, Pitard V, Netzer S, Couzi L, Salim M, Silberzahn T, et al. Cytomegalovirus and tumor stress surveillance by binding of a human γδ T cell antigen receptor to endothelial protein c receptor. *Nat Immunol* (2012) 13(9):872–9. doi: 10.1038/ni.2394

18. Bruder J, Siewert K, Obermeier B, Malotka J, Scheinert P, Kellermann J, et al. Target specificity of an autoreactive pathogenic human γδ-T cell receptor in myositis. *J Biol Chem* (2012) 287(25):20986–95. doi: 10.1074/jbc.M112.356709

19. Vantourout P, Hayday A. Six-of-the-best: unique contributions of γδ T cells to immunology. *Nat Rev Immunol* (2013) 13(2):88–100. doi: 10.1038/nri3384

20. Gavlovsky P-J, Tonnerre P, Guitton C, Charreau B. Expression of MHC class I-related molecules MICA, HLA-e and EPCR shape endothelial cells with unique functions in innate and adaptive immunity. *Hum Immunol* (2016) 77(11):1084–91. doi: 10.1016/j.humimm.2016.02.007

21. Pistoia V, Tumino N, Vacca P, Veneziani I, Moretta A, Locatelli F, et al. Human γδ T-cells: From surface receptors to the therapy of high-risk leukemias. *Front Immunol* (2018) 9:984. doi: 10.3389/fimmu.2018.00984

22. Pietschmann K, Beetz S, Welte S, Martens I, Gruen J, Oberg HH, et al. Toll-like receptor expression and function in subsets of human gammadelta T lymphocytes. *Scand J Immunol* (2009) 70(3):245–55. doi: 10.1111/j.1365-3083.2009.02290.x

23. Angelini DF, Borsellino G, Poupot M, Diamantini A, Poupot R, Bernardi G, et al. FcgammaRIII discriminates between 2 subsets of Vgamma9Vdelta2 effector cells with different responses and activation pathways. *Blood*. (2004) 104(6):1801–7. doi: 10.1182/blood-2004-01-0331

24. Hu W, Shang R, Yang J, Chen C, Liu Z, Liang G, et al. Skin γδ T cells and their function in wound healing. *Front Immunol* (2022) 13:875076. doi: 10.3389/fimmu.2022.875076

25. Xu W, Lau ZWX, Fulop T, Larbi A. The aging of γδ T cells. *Cells*. (2020) 9 (5):1181. doi: 10.3390/cells9051181

26. Ribot JC, Lopes N, Silva-Santos B. γδ T cells in tissue physiology and surveillance. *Nat Rev Immunol* (2021) 21(4):221–32. doi: 10.1038/s41577-020-00452-4

27. Silva-Santos B, Mensurado S, Coffelt SB. γδ T cells: pleiotropic immune effectors with therapeutic potential in cancer. *Nat Rev Cancer* (2019) 19(7):392–404. doi: 10.1038/s41568-019-0153-5

28. Adams EJ, Gu S, Luoma AM. Human gamma delta T cells: Evolution and ligand recognition. *Cell Immunol* (2015) 296(1):31–40. doi: 10.1016/j.cellimm.2015.04.008

29. Fichtner AS, Karunakaran MM, Starick L, Truman RW, Herrmann T. The armadillo (Dasypus novemcinctus): A witness but not a functional example for the emergence of the butyrophilin 3/Vγ9Vδ2 system in placental mammals. *Front Immunol* (2018) 9:265. doi: 10.3389/fimmu.2018.00265

30. Karunakaran MM, Göbel TW, Starick L, Walter L, Herrmann T. Vγ9 and Vδ2 T cell antigen receptor genes and butyrophilin 3 (BTN3) emerged with placental mammals and are concomitantly preserved in selected species like alpaca (Vicugna pacos). *Immunogenetics*. (2014) 66(4):243–54. doi: 10.1007/s00251-014-0763-8

31. Allaoui R, Hagerling C, Desmond E, Warfvinge C-F, Jirström K, Leandersson K. Infiltration of γδ T cells, IL-17+ T cells and FoxP3+ T cells in human breast cancer. *Cancer biomark* (2017) 20(4):395–409. doi: 10.3233/CBM-170026

32. Girard P, Charles J, Cluzel C, Degeorges E, Manches O, Plumas J, et al. The features of circulating and tumor-infiltrating γδ T cells in melanoma patients display critical perturbations with prognostic impact on clinical outcome. *Oncoimmunology*. (2019) 8(8):1601483. doi: 10.1080/2162402X.2019.1601483

33. Pawlik-Gwozdecka D, Zieliński M, Sakowska J, Adamkiewicz-Drożyńska E, Trzonkowski P, Niedźwiecki M. CD8+ γδ T cells correlate with favorable prognostic factors in childhood acute lymphoblastic leukemia. *Arch Med Sci* (2021) 17(2):561–3. doi: 10.5114/aoms/132316

34. Bruni E, Cimino MM, Donadon M, Carriero R, Terzoli S, Piazza R, et al. Intrahepatic CD69+Vδ1 T cells re-circulate in the blood of patients with metastatic colorectal cancer and limit tumor progression. *J Immunother Cancer* (2022) 10(7): e004579. doi: 10.1136/jitc-2022-004579

35. Wu Y, Biswas D, Usaite I, Angelova M, Boeing S, Karasaki T, et al. A local human Vδ1 T cell population is associated with survival in nonsmall-cell lung cancer. *Nat Cancer* (2022) 3(6):696–709. doi: 10.1038/s43018-022-00376-z

36. Ma C, Zhang Q, Ye J, Wang F, Zhang Y, Wevers E, et al. Tumor-infiltrating γδ T lymphocytes predict clinical outcome in human breast cancer. *J Immunol* (2012) 189 (10):5029–36. doi: 10.4049/jimmunol.1201892

37. Nguyen S, Chevalier MF, Benmerzoug S, Cesson V, Schneider AK, Rodrigues-Dias S, et al. Vδ2 T cells are associated with favorable clinical outcomes in patients with bladder cancer and their tumor reactivity can be boosted by BCG and zoledronate treatments. *J Immunother Cancer* (2022) 10(8):e004880. doi: 10.1136/jitc-2022-004880

38. Godder KT, Henslee-Downey PJ, Mehta J, Park BS, Chiang KY, Abhyankar S, et al. Long term disease-free survival in acute leukemia patients recovering with increased gammadelta T cells after partially mismatched related donor bone marrow transplantation. *Bone Marrow Transplant* (2007) 39(12):751–7. doi: 10.1038/sj.bmt.1705650

39. Gentles AJ, Newman AM, Liu CL, Bratman SV, Feng W, Kim D, et al. The prognostic landscape of genes and infiltrating immune cells across human cancers. *Nat Med* (2015) 21(8):938–45. doi: 10.1038/nm.3909

40. Lamb LS, Henslee-Downey PJ, Parrish RS, Godder K, Thompson J, Lee C, et al. Increased frequency of TCR gamma delta + T cells in disease-free survivors following T cell-depleted, partially mismatched, related donor bone marrow transplantation for leukemia. *J Hematother* (1996) 5(5):503–9. doi: 10.1089/scd.1.1996.5.503

41. Perko R, Kang G, Sunkara A, Leung W, Thomas PG, Dallas MH. Gamma delta T cell reconstitution is associated with fewer infections and improved event-free survival

after hematopoietic stem cell transplantation for pediatric leukemia. *Biol Blood Marrow Transplant* (2015) 21(1):130–6. doi: 10.1016/j.bbmt.2014.09.027

42. Jin Z, Luo Q, Lu S, Wang X, He Z, Lai J, et al. Oligoclonal expansion of TCR vδ T cells may be a potential immune biomarker for clinical outcome of acute myeloid leukemia. *J Hematol Oncol* (2016) 9(1):126. doi: 10.1186/s13045-016-0353-3

43. Kong X, Zheng J, Liu X, Wang W, Jiang X, Chen J, et al. High TRGV 9 subfamily expression marks an improved overall survival in patients with acute myeloid leukemia. *Front Immunol* (2022) 13:823352. doi: 10.3389/fimmu.2022.823352

44. Coscia M, Vitale C, Peola S, Foglietta M, Rigoni M, Griggio V, et al. Dysfunctional Vγ9Vδ2 T cells are negative prognosticators and markers of dysregulated mevalonate pathway activity in chronic lymphocytic leukemia cells. *Blood.* (2012) 120(16):3271–9. doi: 10.1182/blood-2012-03-417519

45. Molina-Aguilar R, Montiel-Cervantes LA, Anguiano-Peñaloza SV, Lezama R, Vela-Ojeda J, Reyes-Maldonado E. γδ T cells number, CD200, and Flt3 expression is associated with higher progression free survival in patients with chronic myeloid leukemia. *Arch Med Res* (2020) 51(3):194–203. doi: 10.1016/j.arcmed.2020.01.013

46. Kobayashi H, Tanaka Y, Nakazawa H, Yagi J, Minato N, Tanabe K. A new indicator of favorable prognosis in locally advanced renal cell carcinomas: gamma delta T-cells in peripheral blood. *Anticancer Res* (2011) 31(3):1027–31.

47. Wistuba-Hamprecht K, Martens A, Haehnel K, Foppen MG, Yuan J, Postow MA, et al. Proportions of blood-borne Vδ1+ and Vδ2+ T-cells are associated with overall survival of melanoma patients treated with ipilimumab. *Eur J Cancer* (2016) 64:116–26. doi: 10.1016/j.ejca.2016.06.001

48. Gherardin NA, Waldeck K, Caneborg A, Martelotto LG, Balachander S, Zethoven M, et al. γδ T cells in merkel cell carcinomas have a proinflammatory profile prognostic of patient survival. *Cancer Immunol Res* (2021) 9(6):612–23. doi: 10.1158/2326-6066.CIR-20-0817

49. Raspollini MR, Castiglione F, Rossi Degl'innocenti D, Amunni G, Villanucci A, Garbini F, et al. Tumour-infiltrating gamma/delta T-lymphocytes are correlated with a brief disease-free interval in advanced ovarian serous carcinoma. *Ann Oncol* (2005) 16 (4):590–6. doi: 10.1093/annonc/mdi112

50. Lu H, Dai W, Guo J, Wang D, Wen S, Yang L, et al. High abundance of intratumoral γδ T cells favors a better prognosis in head and neck squamous cell carcinoma: A bioinformatic analysis. *Front Immunol* (2020) 11:573920. doi: 10.3389/fimmu.2020.573920

51. Wu Y, Kyle-Cezar F, Woolf RT, Naceur-Lombardelli C, Owen J, Biswas D, et al. An innate-like Vδ1+ γδ T cell compartment in the human breast is associated with remission in triple-negative breast cancer. *Sci Transl Med* (2019) 11(513):eaax9364. doi: 10.1126/scitranslmed.aax9364

52. Boissière-Michot F, Chabab G, Mollevi C, Guiu S, Lopez-Crapez E, Ramos J, et al. Clinicopathological correlates of γδ T cell infiltration in triple-negative breast cancer. *Cancers (Basel)* (2021) 13(4):765. doi: 10.3390/cancers13040765

53. Bense RD, Sotiriou C, Piccart-Gebhart MJ, Haanen JBAG, van Vugt MATM, de Vries EGE, et al. Relevance of tumor-infiltrating immune cell composition and functionality for disease outcome in breast cancer. *J Natl Cancer Inst* (2017) 109(1): djw192. doi: 10.1093/jnci/djw192

54. Zheng S, Zou Y, Xie X, Liang J, Yang A, Yu K, et al. Development and validation of a stromal immune phenotype classifier for predicting immune activity and prognosis in triple-negative breast cancer. *Int J Cancer* (2020) 147(2):542–53. doi: 10.1002/ijc.33009

55. Chobrutskiy A, Chobrutskiy BI, Zaman S, Hsiang M, Blanck G. Chemical features of blood-borne TRG CDR3s associated with an increased overall survival in breast cancer. *Breast Cancer Res Treat* (2021) 185(3):591–600. doi: 10.1007/s10549-020-05996-6

56. Katsuta E, Qi Q, Peng X, Hochwald SN, Yan L, Takabe K. Pancreatic adenocarcinomas with mature blood vessels have better overall survival. *Sci Rep* (2019) 9(1):1310. doi: 10.1038/s41598-018-37909-5

57. Chen Q, Pu N, Yin H, Zhang J, Zhao G, Lou W, et al. CD73 acts as a prognostic biomarker and promotes progression and immune escape in pancreatic cancer. *J Cell Mol Med* (2020) 24(15):8674–86. doi: 10.1111/jcmm.15500

58. Chitadze G, Oberg H-H, Wesch D, Kabelitz D. The ambiguous role of γδ T lymphocytes in antitumor immunity. *Trends Immunol* (2017) 38(9):668–78. doi: 10.1016/j.it.2017.06.004

59. Raverdeau M, Cunningham SP, Harmon C, Lynch L. γδ T cells in cancer: a small population of lymphocytes with big implications. *Clin Transl Immunol* (2019) 8(10): e01080. doi: 10.1002/cti2.1080

60. Li Y, Li G, Zhang J, Wu X, Chen X. The dual roles of human γδ T cells: Anti-tumor or tumor-promoting. *Front Immunol* (2020) 11:619954. doi: 10.3389/fimmu.2020.619954

61. Chabab G, Barjon C, Bonnefoy N, Lafont V. Pro-tumor γδ T cells in human cancer: Polarization, mechanisms of action, and implications for therapy. *Front Immunol* (2020) 11:2186. doi: 10.3389/fimmu.2020.02186

62. Wu P, Wu D, Ni C, Ye J, Chen W, Hu G, et al. γδT17 cells promote the accumulation and expansion of myeloid-derived suppressor cells in human colorectal cancer. *Immunity.* (2014) 40(5):785–800. doi: 10.1016/j.immuni.2014.03.013

63. Jin C, Lagoudas GK, Zhao C, Bullman S, Bhutkar A, Hu B, et al. Commensal microbiota promote lung cancer development *via* γδ T cells. *Cell.* (2019) 176(5):998–1013.e16. doi: 10.1016/j.cell.2018.12.040

64. Daley D, Zambirinis CP, Seifert L, Akkad N, Mohan N, Werba G, et al. γδ T cells support pancreatic oncogenesis by restraining αβ T cell activation. *Cell.* (2016) 166 (6):1485–1499.e15. doi: 10.1016/j.cell.2016.07.046

65. Reis BS, Darcy PW, Khan IZ, Moon CS, Kornberg AE, Schneider VS, et al. TCR-vγδ usage distinguishes protumor from antitumor intestinal γδ T cell subsets. *Science.* (2022) 377(6603):276–84. doi: 10.1126/science.abj8695

66. Singh AK, McGuirk JP. CAR T cells: continuation in a revolution of immunotherapy. *Lancet Oncol* (2020) 21(3):e168–78. doi: 10.1016/S1470-2045(19)30823-X

67. Mingari MC, Varese P, Bottino C, Melioli G, Moretta A, Moretta L. Clonal analysis of CD4-CD8- human thymocytes expressing a T cell receptor gamma/delta chain. direct evidence for the *de novo* expression of CD8 surface antigen and of cytolytic activity against tumor targets. *Eur J Immunol* (1988) 18(11):1831–4. doi: 10.1002/eji.1830181127

68. Wilhelm M, Kunzmann V, Eckstein S, Reimer P, Weissinger F, Ruediger T, et al. Gammadelta T cells for immune therapy of patients with lymphoid malignancies. *Blood.* (2003) 102(1):200–6. doi: 10.1182/blood-2002-12-3665

69. Morita CT, Jin C, Sarikonda G, Wang H. Nonpeptide antigens, presentation mechanisms, and immunological memory of human Vgamma2Vdelta2 T cells: discriminating friend from foe through the recognition of prenyl pyrophosphate antigens. *Immunol Rev* (2007) 215:59–76. doi: 10.1111/j.1600-065X.2006.00479.x

70. Kunzmann V, Bauer E, Feurle J, Weissinger F, Tony HP, Wilhelm M. Stimulation of gammadelta T cells by aminobisphosphonates and induction of antiplasma cell activity in multiple myeloma. *Blood* (2000) 96(2):384–92. doi: 10.1182/blood.V96.2.384

71. Almeida AR, Correia DV, Fernandes-Platzgummer A, da Silva CL, da Silva MG, Anjos DR, et al. Delta one T cells for immunotherapy of chronic lymphocytic leukemia: Clinical-grade Expansion/Differentiation and preclinical proof of concept. *Clin Cancer Res* (2016) 22(23):5795–804. doi: 10.1158/1078-0432.CCR-16-0597

72. Papapetrou PD. Bisphosphonate-associated adverse events. *Hormones (Athens)* (2009) 8(2):96–110. doi: 10.14310/horm.2002.1226

73. Dieli F, Vermijlen D, Fulfaro F, Caccamo N, Meraviglia S, Cicero G, et al. Targeting human {gamma}delta} T cells with zoledronate and interleukin-2 for immunotherapy of hormone-refractory prostate cancer. *Cancer Res* (2007) 67 (15):7450–7. doi: 10.1158/0008-5472.CAN-07-0199

74. Lang JM, Kaikobad MR, Wallace M, Staab MJ, Horvath DL, Wilding G, et al. Pilot trial of interleukin-2 and zoledronic acid to augment γδ T cells as treatment for patients with refractory renal cell carcinoma. *Cancer Immunol Immunother* (2011) 60 (10):1447–60. doi: 10.1007/s00262-011-1049-8

75. Kobayashi H, Tanaka Y, Yagi J, Osaka Y, Nakazawa H, Uchiyama T, et al. Safety profile and anti-tumor effects of adoptive immunotherapy using gamma-delta T cells against advanced renal cell carcinoma: a pilot study. *Cancer Immunol Immunother* (2007) 56(4):469–76. doi: 10.1007/s00262-006-0199-6

76. Bennouna J, Bompas E, Neidhardt EM, Rolland F, Philip I, Galéa C, et al. Phase-I study of innacell gammadelta, an autologous cell-therapy product highly enriched in gamma9delta2 T lymphocytes, in combination with IL-2, in patients with metastatic renal cell carcinoma. *Cancer Immunol Immunother* (2008) 57(11):1599–609. doi: 10.1007/s00262-008-0491-8

77. Abe Y, Muto M, Nieda M, Nakagawa Y, Nicol A, Kaneko T, et al. Clinical and immunological evaluation of zoledronate-activated Vgamma9gammadelta T-cell-based immunotherapy for patients with multiple myeloma. *Exp Hematol* (2009) 37(8):956–68. doi: 10.1016/j.exphem.2009.04.008

78. Andreu-Ballester JC, Galindo-Regal L, Hidalgo-Coloma J, Cuéllar C, García-Ballesteros C, Hurtado C, et al. Differences in circulating γδ T cells in patients with primary colon cancer and relation with prognostic factors. *PloS One* (2020) 15(12): e0243545. doi: 10.1371/journal.pone.0243545

79. Burnham RE, Zoine JT, Story JY, Garimalla SN, Gibson G, Rae A, et al. Characterization of donor variability for γδ T cell ex vivo expansion and development of an allogeneic γδ T cell immunotherapy. *Front Med (Lausanne)* (2020) 7:588453. doi: 10.3389/fmed.2020.588453

80. Fichtner AS, Ravens S, Prinz I. Human γδ TCR repertoires in health and disease. *Cells.* (2020) 9(4):800. doi: 10.3390/cells9040800

81. Lamb LS, Gee AP, Hazlett LJ, Musk P, Parrish RS, O'Hanlon TP, et al. Influence of T cell depletion method on circulating gammadelta T cell reconstitution and potential role in the graft-versus-leukemia effect. *Cytotherapy.* (1999) 1(1):7–19. doi: 10.1080/0032472031000141295

82. Xu Y, Xiang Z, Alnaggar M, Kouakanou L, Li J, He J, et al. Allogeneic Vγ9Vδ2 T-cell immunotherapy exhibits promising clinical safety and prolongs the survival of patients with late-stage lung or liver cancer. *Cell Mol Immunol* (2021) 18(2):427–39. doi: 10.1038/s41423-020-0515-7

83. Gassart A, Le K-S, Brune P, Agaugué S, Sims J, Goubard A, et al. Development of ICT01, a first-in-class, anti-BTN3A antibody for activating Vγ9Vδ2 T cell-mediated antitumor immune response. *Sci Transl Med* (2021) 13(616):eabj0835. doi: 10.1126/scitranslmed.abj0835

84. He P, Liu H, Zimdahl B, Wang J, Luo M, Chang Q, et al. A novel antibody-TCR (AbTCR) T-cell therapy is safe and effective against CD19-positive relapsed/refractory b-cell lymphoma. *J Cancer Res Clin Oncol* (2022). doi: 10.1007/s00432-022-04132-9

85. Bennouna J, Levy V, Sicard H, Senellart H, Audrain M, Hiret S, et al. Phase I study of bromohydrin pyrophosphate (BrHPP, IPH 1101), a Vgamma9Vdelta2 T

lymphocyte agonist in patients with solid tumors. *Cancer Immunol Immunother* (2010) 59(10):1521–30. doi: 10.1007/s00262-010-0879-0

86. Meraviglia S, Eberl M, Vermijlen D, Todaro M, Buccheri S, Cicero G, et al. *In vivo* manipulation of Vgamma9Vdelta2 T cells with zoledronate and low-dose interleukin-2 for immunotherapy of advanced breast cancer patients. *Clin Exp Immunol* (2010) 161(2):290–7. doi: 10.1111/j.1365-2249.2010.04167.x

87. Nakajima J, Murakawa T, Fukami T, Goto S, Kaneko T, Yoshida Y, et al. A phase I study of adoptive immunotherapy for recurrent non-small-cell lung cancer patients with autologous gammadelta T cells. *Eur J Cardiothorac Surg* (2010) 37(5):1191–7. doi: 10.1016/j.ejcts.2009.11.051

88. Kobayashi H, Tanaka Y, Yagi J, Minato N, Tanabe K. Phase I/II study of adoptive transfer of γδ T cells in combination with zoledronic acid and IL-2 to patients with advanced renal cell carcinoma. *Cancer Immunol Immunother* (2011) 60(8):1075–84. doi: 10.1007/s00262-011-1021-7

89. Nicol AJ, Tokuyama H, Mattarollo SR, Hagi T, Suzuki K, Yokokawa K, et al. Clinical evaluation of autologous gamma delta T cell-based immunotherapy for metastatic solid tumours. *Br J Cancer* (2011) 105(6):778–86. doi: 10.1038/bjc.2011.293

90. Sakamoto M, Nakajima J, Murakawa T, Fukami T, Yoshida Y, Murayama T, et al. Adoptive immunotherapy for advanced non-small cell lung cancer using zoledronate-expanded γδTcells: a phase I clinical study. *J Immunother* (2011) 34 (2):202–11. doi: 10.1097/CJI.0b013e318207ecfb

91. Noguchi A, Kaneko T, Kamigaki T, Fujimoto K, Ozawa M, Saito M, et al. Zoledronate-activated Vγ9γδ T cell-based immunotherapy is feasible and restores the impairment of γδ T cells in patients with solid tumors. *Cytotherapy.* (2011) 13(1):92–7. doi: 10.3109/14653249.2010.515581

92. Kunzmann V, Smetak M, Kimmel B, Weigang-Koehler K, Goebeler M, Birkmann J, et al. Tumor-promoting versus tumor-antagonizing roles of γδ T cells in cancer immunotherapy: results from a prospective phase I/II trial. *J Immunother* (2012) 35(2):205–13. doi: 10.1097/CJI.0b013e318245bb1e

93. Izumi T, Kondo M, Takahashi T, Fujieda N, Kondo A, Tamura N, et al. Ex vivo characterization of γδ T-cell repertoire in patients after adoptive transfer of Vγ9Vδ2 T cells expressing the interleukin-2 receptor β-chain and the common γ-chain. *Cytotherapy.* (2013) 15(4):481–91. doi: 10.1016/j.jcyt.2012.12.004

94. Wilhelm M, Smetak M, Schaefer-Eckart K, Kimmel B, Birkmann J, Einsele H, et al. Successful adoptive transfer and *in vivo* expansion of haploidentical γδ T cells. *J Transl Med* (2014) 12:45. doi: 10.1186/1479-5876-12-45

95. Wada I, Matsushita H, Noji S, Mori K, Yamashita H, Nomura S, et al. Intraperitoneal injection of *in vitro* expanded Vγ9Vδ2 T cells together with zoledronate for the treatment of malignant ascites due to gastric cancer. *Cancer Med* (2014) 3(2):362–75. doi: 10.1002/cam4.196

96. Cui J, Li L, Wang C, Jin H, Yao C, Wang Y, et al. Combined cellular immunotherapy and chemotherapy improves clinical outcome in patients with gastric carcinoma. *Cytotherapy.* (2015) 17(7):979–88. doi: 10.1016/j.jcyt.2015.03.605

97. Pressey JG, Adams J, Harkins L, Kelly D, You Z, Lamb LS. *In vivo* expansion and activation of γδ T cells as immunotherapy for refractory neuroblastoma: A phase 1 study. *Med (Baltimore)* (2016) 95(39):e4909. doi: 10.1097/MD.0000000000004909

98. Aoki T, Matsushita H, Hoshikawa M, Hasegawa K, Kokudo N, Kakimi K. Adjuvant combination therapy with gemcitabine and autologous γδ T-cell transfer in patients with curatively resected pancreatic cancer. *Cytotherapy.* (2017) 19(4):473–85. doi: 10.1016/j.jcyt.2017.01.002

99. Sugie T, Suzuki E, Yamauchi A, Yamagami K, Masuda N, Gondo N, et al. Combined effects of neoadjuvant letrozole and zoledronic acid on γδT cells in postmenopausal women with early-stage breast cancer. *Breast.* (2018) 38:114–9. doi: 10.1016/j.breast.2017.12.017

100. Lin M, Zhang X, Liang S, Luo H, Alnaggar M, Liu A, et al. Irreversible electroporation plus allogenic Vγ9Vδ2 T cells enhances antitumor effect for locally advanced pancreatic cancer patients. *Signal Transduct Target Ther* (2020) 5(1):215. doi: 10.1038/s41392-020-00260-1

101. Kakimi K, Matsushita H, Masuzawa K, Karasaki T, Kobayashi Y, Nagaoka K, et al. Adoptive transfer of zoledronate-expanded autologous Vγ9Vδ2 T-cells in patients with treatment-refractory non-small-cell lung cancer: a multicenter, open-label, single-arm, phase 2 study. *J Immunother Cancer* (2020) 8(2):e001185. doi: 10.1136/jitc-2020-001185

102. Fazzi R, Petrini I, Giuliani N, Morganti R, Carulli G, Palma BD, et al. Phase II trial of maintenance treatment with IL2 and zoledronate in multiple myeloma after bone marrow transplantation: Biological and clinical results. *Front Immunol* (2020) 11:573156. doi: 10.3389/fimmu.2020.573156

103. Zhang T, Chen J, Niu L, Liu Y, Ye G, Jiang M, et al. Clinical safety and efficacy of locoregional therapy combined with adoptive transfer of allogeneic γδ T cells for advanced hepatocellular carcinoma and intrahepatic cholangiocarcinoma. *J Vasc Interv Radiol* (2022) 33(1):19–27.e3. doi: 10.1016/j.jvir.2021.09.012

104. Zheng Y, Wang P-P, Fu Y, Chen Y-Y, Ding Z-Y. Zoledronic acid enhances the efficacy of immunotherapy in non-small cell lung cancer. *Int Immunopharmacol* (2022) 110:109030. doi: 10.1016/j.intimp.2022.109030

105. Lamb LS, Bowersock J, Dasgupta A, Gillespie GY, Su Y, Johnson A , et al. Engineered drug resistant γδ T cells kill glioblastoma cell lines during a chemotherapy challenge: a strategy for combining chemo- and immunotherapy. *PloS One* (2013) 8(1): e51805. doi: 10.1371/journal.pone.0051805

106. Strijker JGM, Pscheid R, Drent E, van der Hoek JJF, Koopmans B, Ober K, et al. αβ-T cells engineered to express γδ-T cell receptors can kill neuroblastoma organoids independent of MHC-I expression. *J Pers Med* (2021) 11(9):923. doi: 10.3390/jpm11090923

107. Straetemans T, Kierkels GJJ, Doorn R, Jansen K, Heijhuurs S, Santos JMD, et al. GMP-grade manufacturing of T cells engineered to express a defined γδTCR. *Front Immunol* (2018) 9:1062. doi: 10.3389/fimmu.2018.01062

108. Michishita Y, Hirokawa M, Guo Y-M, Abe Y, Liu J, Ubukawa K, et al. Age-associated alteration of γδ T-cell repertoire and different profiles of activation-induced death of Vδ1 and Vδ2 T cells. *Int J Hematol* (2011) 94(3):230–40. doi: 10.1007/s12185-011-0907-7

109. Kallemeijn MJ, Boots AMH, van der Klift MY, Brouwer E, Abdulahad WH, Verhaar JAN, et al. Ageing and latent CMV infection impact on maturation, differentiation and exhaustion profiles of T-cell receptor gammadelta T-cells. *Sci Rep* (2017) 7(1):5509. doi: 10.1038/s41598-017-05849-1

110. Liu M, Wang X, Li W, Yu X, Flores-Villanueva P, Xu-Monette ZY, et al. Targeting PD-L1 in non-small cell lung cancer using CAR T cells. *Oncogenesis.* (2020) 9 (8):72. doi: 10.1038/s41389-020-00257-z

111. Themeli M, Kloss CC, Ciriello G, Fedorov VD, Perna F, Gonen M, et al. Generation of tumor-targeted human T lymphocytes from induced pluripotent stem cells for cancer therapy. *Nat Biotechnol* (2013) 31(10):928–33. doi: 10.1038/nbt.2678

112. Zeng J, Tang SY, Wang S. Derivation of mimetic γδ T cells endowed with cancer recognition receptors from reprogrammed γδ T cell. *PloS One* (2019) 14(5): e0216815. doi: 10.1371/journal.pone.0216815

113. Deisher T, Taylor M, Ashok A, Jarzyna P, Zahid Y, Lee-Diaz S, et al. AVM0703, a new treatment option for lymphoma patients. *Blood.* (2019) 134 (Supplement_1):5308. doi: 10.1182/blood-2019-128812

114. Deisher T, Sawas S, Suwito K, Rylatt C, Jarzyna PA, Zahid Y, et al. AVM0703 tumor debulking enhances Cy/Flu efficacy. *Blood.* (2021) 138(Supplement 1):4498. doi: 10.1182/blood-2021-153990

115. Formenti SC, Rudqvist N-P, Golden E, Cooper B, Wennerberg E, Lhuillier C, et al. Radiotherapy induces responses of lung cancer to CTLA-4 blockade. *Nat Med* (2018) 24(12):1845–51. doi: 10.1038/s41591-018-0232-2

116. Srivastava S, Furlan SN, Jaeger-Ruckstuhl CA, Sarvothama M, Berger C, Smythe KS, et al. Immunogenic chemotherapy enhances recruitment of CAR-T cells to lung tumors and improves antitumor efficacy when combined with checkpoint blockade. *Cancer Cell* (2021) 39(2):193–208.e10. doi: 10.1016/j.ccell.2020.11.005

frontiers | Frontiers in Immunology

TYPE Original Research
PUBLISHED 19 July 2023
DOI 10.3389/fimmu.2023.1185564

OPEN ACCESS

EDITED BY
Girdhari Lal,
National Centre for Cell Science, India

REVIEWED BY
Mary Poupot-Marsan,
INSERM U1037 Centre de Recherche en Cancérologie de Toulouse, France
Trent Spencer,
Emory University, United States

*CORRESPONDENCE
Anna Bold
anna.bold@klinikum-nuernberg.de

†These authors have contributed equally to this work and share last authorship

RECEIVED 13 March 2023
ACCEPTED 30 June 2023
PUBLISHED 19 July 2023

CITATION
Bold A, Gross H, Holzmann E, Knop S, Hoeres T and Wilhelm M (2023) An optimized cultivation method for future *in vivo* application of γδ T cells. *Front. Immunol.* 14:1185564. doi: 10.3389/fimmu.2023.1185564

An optimized cultivation method for future *in vivo* application of γδ T cells

Anna Bold[1]*, Heike Gross[1], Elisabeth Holzmann[1], Stefan Knop[1], Timm Hoeres[1,2†] and Martin Wilhelm[1†]

[1]Department of Hematology and Medical Oncology, Paracelsus Medical University, Nuremberg, Germany, [2]Fraunhofer-Institute for Translational Medicine & Pharmacology (ITMP), Clinical Research, Frankfurt, Germany

γδ T cells, with their properties of both the innate and acquired immune systems, are suitable candidates for cellular immunotherapy in cancer. Because of their non-major histocompatibility complex (MHC) binding T cell receptor, allogenic transfer is feasible without relevant graft versus host reactions. In recent years, much experience has been gained with *ex vivo* expansion and stimulation of γδ T cells using bisphosphonates and Interleukin 2. Unfortunately, many current stimulation protocols are based on the use of xenogenic materials and other potentially hazardous supplements, which conflicts with basic principles of Good Manufacturing Practice (GMP). Adherence to the concept and current guidelines of GMP is state of the art for production of Advanced Therapy Medicinal Products (ATMP) like cell therapeutics and a necessity for clinical use under a regulatory perspective. In this study, we developed a new stimulation protocol that induces a marked increase of γδ T cell counts and allows for an easier transition from research to clinical applications with minimized regulatory workload. It reliably leads to a cell product with a purity of more than 90% γδ T cells and improved *in vitro* anti-tumor activity compared to our previous standard procedure. Furthermore, by investigating correlations between properties of unstimulated γδ T cells and proliferation rate as well as degranulation ability of stimulated γδ T cells, we can draw conclusions about suitable donors. Finally, we examined if expansion can be improved by pulsing zoledronate and/or using Interleukin 15 with or without Interleukin 2. Significant improvements can be achieved with respect to intrinsic and antibody-dependent cell-mediated cytotoxicity. Our results demonstrate that the stimulation protocol presented here leads to an improved γδ T cell product for future clinical applications.

KEYWORDS

γδ T cells, Vγ9Vδ2 T cells, cellular immunotherapy, zoledronate, interleukin 2, interleukin 15, ADCC, cell culture

Introduction

Cellular immunotherapy is becoming increasingly important in the treatment of cancer. One of the novel approaches for immunotherapy are γδ T cells. In contrast to αβ T cells, their T cell receptor (TCR) is not restricted to bind antigens in the context of a major histocompatibility complex (MHC) molecule. Part of the TCR are the variable Vγ and Vδ chains, with the Vγ9Vδ2 T cells being the dominant subpopulation and accounting for approximately 5% of T cells in peripheral blood (1). The anti-tumor effects of γδ T cells mediated by different mechanisms including cytokine production, perforin and interferon γ (IFNγ) release and antibody-dependent cell-mediated cytotoxicity (ADCC) have been demonstrated in detail *in vitro* and *in vivo* (2–5). Because of the MHC-independent recognition of target cells, no graft versus host reaction is to be expected with allogenic transfer of γδ T cells as has already been shown in several clinical studies (6–8).

Strategies to use γδ T cells as cellular therapy include activation of either the patient's own γδ T cells or transferred allogenic γδ T cells *in vivo* or expansion and stimulation of autologous as well as allogenic γδ T cells *ex vivo* with subsequent adoptive transfer (6, 7, 9). The expansion and stimulation of Vγ9Vδ2 T cells both *in vivo* and *ex vivo* is usually achieved via aminobisphosphonates or natural or synthetic phosphoantigens and addition of co-stimulators, mostly cytokines, like Interleukin 2 (IL-2) (10, 11). The aminobisphosphonate zoledronate (Zol) inhibits the farnesyl pyrophosphate synthase enzyme in the mevalonate pathway of antigen presenting cells like monocytes, which consequently leads to accumulation of isopentenyl pyrophosphate (IPP). As natural phosphoantigens, IPP and its metabolites bind to butyrophilin 3A (BTN3A) molecules, which interact with BTN2A1 and are recognized by the TCR of Vγ9Vδ2 T cells with subsequent proliferation (12–14). A disadvantage of *in vivo* activation is the toxic effect of IL-2 at higher doses and of zoledronate when used at short intervals (10). Additionally, the *in vivo* stimulability of γδ T cells decreases with repeated administrations of the activators (15). However, the need of repetitive treatment is supported by our own clinical data. Indeed, the *in vivo* stimulation of haploidentical γδ T cells induced remission in most patients, but all of them relapsed within one year (6, 16). The number and functionality of the patient's own γδ T cells is often limited (especially in cancer patients), so expansion and stimulation of these cells is usually unsuccessful both *in vivo* and *ex vivo* (10). For these reasons, we believe that *ex vivo* stimulation of healthy donor γδ T cells followed by adoptive transfer is the way forward.

In recent years, numerous cultivation methods have been published to stimulate γδ T cells *ex vivo*, but many of them use cell culture medium supplemented with fetal bovine serum (FBS). Using xenogeneic products bears the risk of contamination with known and even unknown pathogens and transmission of zoonotic diseases. In addition, such protocols often require culturing in plates and manual splitting, which is not compatible with a closed, sterile cultivation system advantageous for implementation of a GMP-compliant process. Thus, we developed a new stimulation protocol using a cell culture medium free of xenogenic products and serum and culturing in bottles without splitting. This can later be more easily expanded to the closed system of a cell growth device for clinical use without the need of fundamental adjustments.

The aim of this work was to evaluate and improve this newly developed protocol called "Ko-Op" with regard to the quantity and quality of the generated cell product. In addition to cell number and purity, we therefore investigated the cytoplasmic perforin and IFNγ in γδ T cells. Both proteins are produced in stimulated immune cells and have immunostimulatory and anti-tumor effects. We also determined CD107a on the surface of γδ T cells as a marker for degranulation and thus activation either as a result of sole stimulation or additionally in response to incubation with tumor cells. Furthermore, we measured the cytotoxicity of the stimulated γδ T cells against lymphoma cell line Daudi with or without monoclonal antibodies which induce ADCC (17, 18).

Despite a highly standardized cultivation procedure, stimulated γδ T cells from various donors differ in yield and anti-tumor activity when expanded *in vitro*. Therefore, we investigated if certain parameters prior to stimulation can indicate whether the cells are highly stimulable and activatable.

Finally, we examined if the cultivation procedure Ko-Op could be further improved. Nada et al. showed that improved proliferation rate and anti-tumor activity can be achieved by pulsed, high-dose zoledronate administration (19). Furthermore, some studies suggest that the addition of Interleukin 15 (IL-15) also leads to an improved proliferation rate and anti-tumor cytotoxicity of γδ T cells (20, 21). We therefore modified the cultivation protocol in several steps by using a zoledronate pulse instead of zoledronate standard and adding IL-15 instead of or additional to IL-2 and compared it with the standard procedure.

Materials and methods

Cell culture, cell isolation and *ex vivo* stimulation of γδ T cells

Our investigations were performed with peripheral blood obtained from healthy adult donors. The studies involving human participants were reviewed and approved by the Institutional Review Board of the Paracelsus Medical University Nuremberg. Written informed consent to participate in this study was provided by the participants. All donors signed an agreement according to General Data Protection Regulation.

Peripheral blood mononuclear cells (MNC) were isolated by density gradient centrifugation with Biocoll (Biochrom, Darmstadt, Germany/Bio&SELL, Feucht, Germany) and divided in several fractions in order to expand them using different cultivation methods.

To expand and stimulate γδ T cells we used our previously established protocol "R10F" and a new developed "Ko-Op". MNC were incubated up to 17 days at 37°C and 5% CO_2 in both protocols.

R10F

For cultivation according to the R10F protocol MNC at a concentration of 5.0E+05/ml were cultured in 96 U-bottom plates

(Greiner bio-one, Frickenhausen, Germany) using standard medium consisting of RPMI 1640 supplemented with 10% fetal bovine serum (FCS), 1% 200mM L-glutamine and 1% penicilline/streptomycin (all from Biochrom, Darmstadt, Germany/Bio&SELL, Feucht, Germany). On day 0, 1 µM Zoledronate (Zol) (Sigma-Aldrich, St. Louis, USA) and 100 U/ml Interleukin 2 (IL-2) (Burton-on-Trent, Great Britain, United Kingdom) were added. From day 7, the cells were harvested twice a week, washed and reseeded at a concentration of 6.0E+05/ml in 96 well plates with fresh medium and 100 U/ml IL-2.

Ko-Op

For cultivation according to the Ko-Op protocol MNC at a concentration of 5.0E+05/ml were cultured in 50 ml cell culture flasks (Sarstedt, Nuembrecht, Germany) using medium consisting of OpTmizer™ CTS™ T-Cell Expansion Basal Medium, OpTmizer™ CTS™ T-Cell Expansion Supplement (Gibco/Thermo Fisher, Waltham, USA) and 1% 200 mM L-Glutamin. On day 0, 10 µM Zol were added and 1000 U/ml IL-2 were added on day 2. On day 4, 7, 9, 11 and 14 half of the medium was removed and replaced by fresh medium containing 2x 1000 U/ml IL-2 for a final concentration of 1000 U/ml. In some experiments we added 10 ng/ml Interleukin 15 (IL-15) (Peprotech, Cranbury, USA) instead of or in addition to 1000 U/ml IL-2. Cells were not split at any time. From day 4 on, cell culture flasks were shaken at 250 rpm. For pulsing zoledronate, 100 µM Zol were added on day 0. After 4 hours incubating at 37°C and 5% CO_2 MNC were harvested, washed twice and reseeded at a concentration of 5.0E+05/ml in cell culture flasks with fresh medium. The addition of IL-2 and/or IL-15 from day 2 and further cultivation was done as described above.

The lymphoma cell line Daudi was obtained from the German collection of microorganisms and cell culture (DSMZ, Braunschweig, Germany) and cultured in our standard medium R10F.

Cell counts and cell viability were established using a hemocytometer and the trypan blue exclusion method. Cell count and proliferation rate of γδ T cells was calculated on the basis of the cell number of the MNC and the percentage of γδ T cells on the MNC determined by flow cytometry.

Flow cytometry and antibodies

A FC500 and a Navios flow cytometer (both Beckman Coulter, Brea, USA) were used for multicolor immunofluorescence and functional tests.

Cells were stained in appropriate combinations according to use with following antibodies: anti-T-cell receptor (TCR) γδ-FITC [clone IMMU510], anti-CD3-r-Phycoerythrin-Texas Red (ECD) [clone UCHT1], anti-CD56-phycoerythrin-cyanine 5 (PC5) [clone N901], anti-CD27-phycoerythrin-cyanine 5 (PC5) [clone 1A4CD27], anti-CD56-phycoerythrin-cyanine 7 (PC7) [clone N901] (all Beckman Coulter, Brea, USA); anti-T-cell receptor (TCR) γδ-FITC [clone 11F2], anti-CD107a-PE [clone H4A3], anti-IFNγ–PE [clone 45-15], anti-CD45RA-PE [clone REA 562] (all Miltenyi Biotec, Bergisch Gladbach, Germany); and anti-perforin-PE [clone B-D48] (Biolegend, San Diego, USA).

As negative control, anti-IgG-PE [clone IS5-32F5] (Miltenyi Biotec, Bergisch Gladbach, Germany) was used.

γδ cells were defined as $CD3^+$ TCR $\gamma\delta^+$ MNC, NK cells as $CD3^-$ $CD56^+$ MNC and αβ T cells as $CD3^+$ TCR $\gamma\delta^-$ MNC.

For functional assay, the therapy grade monoclonal antibodies rituximab and obinutuzumab (both Roche, Grenzach-Wyhlen, Germany) as well as the IgG1-kappa control antibody (Sigma-Aldrich, St. Louis, USA) were used.

Cytoplasmic staining

After staining the surface antigens with anti-TCR γδ-FITC and anti-CD3-ECD, intracellular IFNγ or intracellular perforin were stained with anti-IFNγ-PE or anti-perforin-PE or anti-IgG-PE as control using the inside stain kit (Miltenyi Biotec, Bergisch Gladbach, Germany) according to manufacturer's instructions. Afterwards, the cells were analyzed by flow cytometry. To define $perforin^+$ or $IFN\gamma^+$ γδ T cells, cells were stained with an isotype control and the gate was adjusted so that 2% of the cells in the isotype control were defined as positive. ΔMFI was calculated as MFI (IFNγ or perforin) minus MFI (isotype control).

Degranulation assay

The surface antigen CD107a as marker for degranulation was determined in our degranulation assay. For this, stimulated MNC were co-cultured with Daudi in a 1:2 ratio or with the respective medium with the addition of the anti-CD107a-PE or anti-IgG-PE as control in 96 well V-bottom plates (Greiner bio-one, Frickenhausen, Germany) for 3h. Subsequently, the cells were washed, the surface antigens were stained with anti-TCR γδ-FITC and anti-CD3-ECD and the cells were analyzed by flow cytometry. The definition of $CD107a^+$ γδ T cells as well as the determination of the ΔMFI of CD107a was performed analogously to the procedure for perforin and IFNγ.

Immuno-magnetic depletion

MNC stimulated with R10F and Ko-Op consist mainly of γδ T cells, but especially after stimulation with R10F also of αβ T cells and NK cells. To compare the cytotoxicity of γδ T cells when cultured with R10F or Ko-Op, αβ T cells and $NKp46^+$ cells were depleted from stimulated MNC after 10 days of cultivation using the MidiMACS system and anti-TCRαβ and anti-NKp46 MicroBeads (all from Miltenyi Biotec, Bergisch Gladbach, Germany) according to manufacturer's instructions except using HSA (CSL Behring GmbH, Marburg, Germany) instead of BSA as part of the washing buffer. In order to proof the success of depletion, the cells were stained before and after depletion with anti-TCR γδ-FITC, anti-CD3-ECD and anti-CD56-PC5 to diversify the different cell populations. Cell counts and cell viability were determined using a hemocytometer and the trypan blue exclusion method.

Cytotoxicity assay

Cytotoxicity experiments were conducted in 96 well V-bottom plates (Greiner bio-one, Frickenhausen, Germany) as co-cultures at different effector to target cell ratios with 1 µg/ml rituximab, 1 µg/ml obinutuzumab or 1 µg/ml isotype control antibody. Daudi were used as target cells and previously labeled with carboxyfluorescein succinimidyl ester (CFSE) (BioLegend, San Diego, USA) and taken up into the respective culture medium (R10F or OpTmizer™ CTS™ T-Cell Expansion Medium). Effector cells, which differed in regard to stimulation protocol, were used in this assay. If indicated, TCRαβ$^+$ and NKp46$^+$ cells were depleted as described above before performing the assay. Following co-culture of effector and target cells for 4 h, cells were harvested, technical replicates were pooled, treated with 7-AAD (Beckman Coulter, Brea, USA) and analyzed by flow cytometry. Specific cell mediated cytotoxicity is expressed as "specific lysis %" and calculated by the formula: specific lysis % = [% 7-AAD$^+$ target cells in the respective effector to target ratio – % 7-AAD$^+$ target cells in target cell only culture] *100/ [100 – % 7-AAD$^+$ target cells in target cell only culture]. The lytic units per 10^6 effector cells were calculated according to Bryant et al. with the following formula: *lytic units per* 10^6 *effector cells* = $10^6 \cdot exp(\frac{\overline{Y^\star} - Y_p^\star}{C})/(T \cdot \overline{X_G})$ (22). Y is the specific lysis measured in a defined effector to target ratio. Y is logistically transformed ($Y^\star$) by following formula: $Y^\star = LN(\frac{Y}{100-Y})$. We defined a reference lysis p of 60%, which is also logistically transformed ($Y_p^\star$). $\overline{Y^\star}$ is the arithmetic mean of the logistically transformed specific lyses measured in each effector to target ratio, C is a constant with relation to the slope of the curve (defined as 1), T is the number of target cells (10^4), and $\overline{X_G}$ is the geometric mean of the effector to target ratios used in the assay.

Data and statistical analysis

Data were analyzed with the software Kaluza analysis V2.1 (Beckman Coulter, Brea, USA), Excel 2016 (Microsoft, Redmond, USA) and SPSS Statistics 22 (IBM, Armonk, USA). Data are presented as mean ± standard deviation (SD). The normal distribution of the data was verified using the Shapiro test. Levels of significance were calculated using the paired t-test or the Wilcoxon test. Correlation coefficient R was calculated according to Spearman. $p<0.05$ is considered statistically significant.

Results

Proliferation, purity and anti-tumor efficiency of γδ T cells by using Ko-Op for *ex vivo* stimulation

To establish a GMP-compliant and effective cultivation of γδ T cells, we developed a new protocol called "Ko-Op". For this, we replaced our previous cultivation media "R10F", which contains FBS, with the xeno-free OpTmizer™ CTS™ T cell expansion medium. In order to achieve an optimal result in terms of yield, we further increased the concentrations of zoledronate and IL-2 and did not administer the first IL-2 addition until day 2 as it is already done successfully (23). Furthermore, we used flasks instead of 96 well plates to facilitate upscalability. Assuming that the nutrient supply to the cells is limited by diffusion due to sedimentation of cells in standing flasks, we placed them on an orbital shaker from day 4 of cultivation, but not earlier because of the need of the cell-cell contact between monocytes and γδ T cells for stimulation. Table 1 shows the relevant differences to our established protocol R10F (17, 24).

MNC of twelve healthy donors were isolated and stimulated with Zol/IL-2 using the protocols R10F and Ko-Op over 17 days. Every three to four days, the number of MNC was counted and the percentage of γδ T cells, αβ T cells and NK cells was determined by flow cytometry as exemplary shown in Figures 1A, S1A. In terms of γδ T cells, an average proliferation rate of more than 400-fold of the baseline can be achieved (Figure 1B). The percentage of γδ T cells is significantly higher when Ko-Op was used for cultivation (Figure 1C). Very strikingly, there was clearly less inter-donor variability when using Ko-Op compared to R10F. Additionally, the percentage of αβ T cells and NK cells is significantly lower when stimulated with Ko-Op also with low inter-donor variability (Figures 1C, S1B). The question arises if the higher doses of zoledronate and IL-2 within the Ko-Op protocol leads to reduced viability. Therefore, the vitality of MNC was determined by trypan blue exclusion test showing no statistical difference between the two different cultivation protocols (Figure S1C). A detailed viability analysis using annexin/7AAD staining performed on a part of the experiments also did not reveal an increased rate of apoptosis or dead cells when stimulated with Ko-Op compared to R10F (data not shown).

To evaluate the activity of stimulated γδ T cells, cytoplasmic perforin and IFNγ were stained every three to four days and the percentage of perforin$^+$ and IFNγ$^+$ γδ T cells as well as the ΔMFI was determined by flow cytometry. γδ T cells produced significantly more perforin when cultured according to the Ko-Op protocol (Figures 1D, S1D). With regard to IFNγ, the ΔMFI was only significantly increased on day 7 and the percentage of IFNγ$^+$ γδ T

TABLE 1 Relevant differences of the protocols R10F and Ko-Op for *ex vivo* stimulation of γδ T cells.

	R10F	Ko-Op
Media	RPMI 1640 Media	OpTmizer™ T-Cell Expansion SFM
Supplements	Fetal bovine serum, Glutamine, Penicillin/Streptomycin	Glutamine
Culture plate	96-well U-plate (200 µl/well)	50 ml flask (10 ml/flask)
Stimulants	1 µM Zol d0 100 U/ml IL-2 d0, d7, d10, d14	10 µM Zol d0 1000 U/ml IL-2 d2, d4, d7, d9, d11, d14
Others		shaker from d4

10.3389/fimmu.2023.1185564

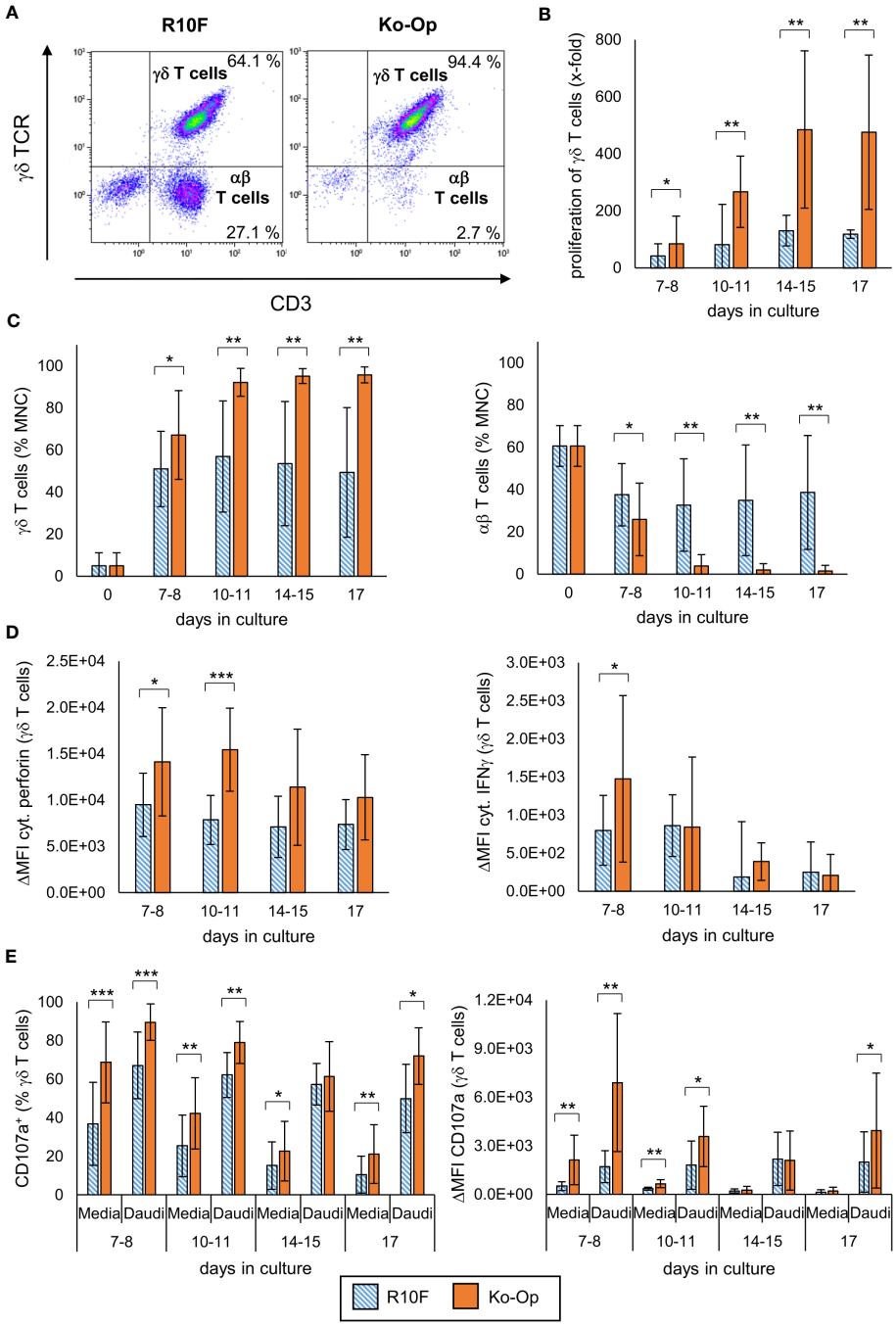

FIGURE 1
Proliferation, purity and anti-tumor efficiency of γδ T cells by using Ko-Op for *ex vivo* stimulation. MNC of healthy donors were isolated and stimulated with Zol/IL-2 according to the protocols R10F (blue hatched bars) and Ko-Op (orange bars) up to 17 days. **(A)** Representative FACS analysis of MNC cultured according to the protocols R10F or Ko-Op for ten days. γδ T cells and αβ T cells were defined by using anti-γδ TCR-FITC and anti-CD3-ECD. **(B)** Proliferation rate of γδ T cells calculated on the basis of the cell number of the MNC and the percentage of γδ T cells on the MNC determined by flow cytometry. **(C)** Percentage of γδ T cells and αβ T cells at different days of cultivation measured by flow cytometry. **(D)** Cytoplasmic perforin and IFNγ in γδ T cells were stained at different days of cultivation and measured by flow cytometry. ΔMFI is calculated as MFI (perforin or IFNγ) minus MFI (isotype control). **(E)** MNC were incubated with media control or Daudi at different days of cultivation in order to perform the degranulation assay. After 3h CD107a$^+$ γδ T cells and ΔMFI of CD107a on γδ T cells were detected by flow cytometry. The data are presented as mean ± SD of 12 **(B, C)** or 9 **(D, E)** independent experiments. *p<0.05, **p<0.01 and ***p<0.001 comparing the two different stimulation protocols.

cells did not differ between the two cultivation protocols (Figures 1D, S1D).

For investigation of the anti-tumor efficiency of stimulated γδ T cells, degranulation of γδ T cells after 3h incubation with the tumor cell line Daudi or media only was determined by measuring the surface molecule CD107a by flow cytometry from day 7 onwards every three to four days. With and without tumor cells, stimulation with Ko-Op increased both the percentage of CD107a$^+$ γδ T cells

and the amount of CD107a on the surface of γδ T cells as determined by ΔMFI compared to stimulation with R10F (Figure 1E). To directly determine the anti-tumor activity of γδ T cells against the tumor cell line Daudi, we performed cytotoxicity assays on day 10 of cultivation. For this, αβ T cells and NKp46$^+$ cells were paramagnetically depleted from the cell suspension in order to isolate the γδ T cells on day 10. The cell composition before and after depletion is shown Figure 2A. By cultivation using the Ko-Op protocol compared to R10F, a significant increase in the cytotoxicity of γδ T cells against Daudi could be achieved with both the monoclonal antibodies rituximab and obinutuzumab and their non-specific isotype control (Figure 2B). The specific lysis of Daudi cells under addition of IgG corresponds to the intrinsic cytotoxicity of γδ T cells as the unspecific isotype control does not mediate ADCC. To confirm this, we tested if there is a difference in specific lysis of Daudi between addition of IgG or no isotype control and could not find a significant difference both when stimulated with R10F or Ko-Op (data not shown). In summary, cultivation with Ko-Op enhances the proliferation rate, the purity, the anti-tumor activity and the cytotoxicity of stimulated γδ T cells.

Since we did not see a clear improvement in IFNγ production by stimulation with Ko-Op compared with R10F, we wondered whether all tested parameters could be equally optimized by stimulation. We therefore tested the proliferation rate of MNC, the percentage of γδ T cells, the CD107a expression and the cytoplasmic IFNγ on day 10 for correlations. While, as expected,

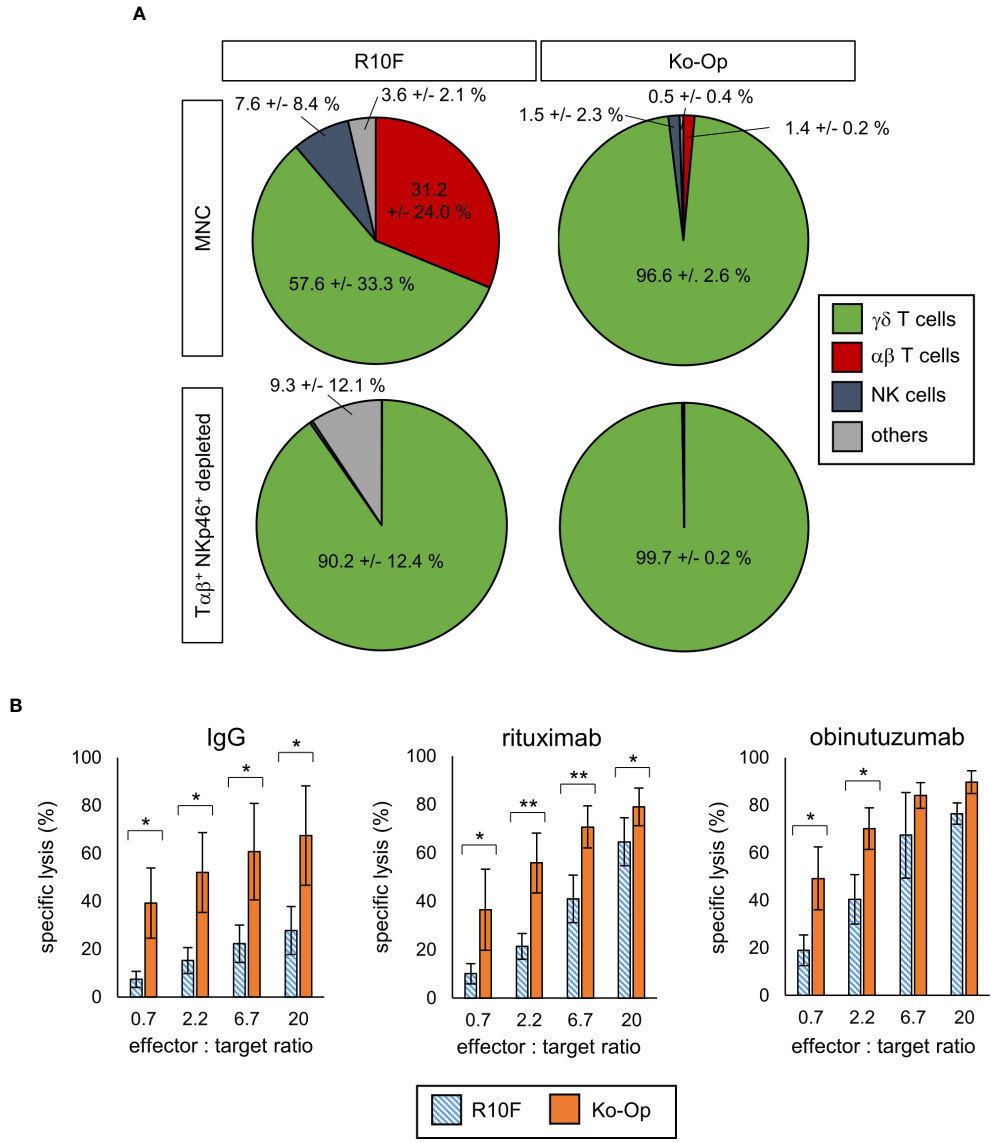

FIGURE 2
Cytotoxicity of γδ T cells by using Ko-Op for *ex vivo* stimulation. MNC of healthy donors were isolated and stimulated with Zol/IL-2 according to the protocols R10F and Ko-Op. On day 10 of cultivation, the paramagnetic depletion of Tαβ$^+$ and NKp46$^+$ cells was performed. **(A)** Composition of undepleted and Tαβ$^+$ and NKp46$^+$ depleted MNC on day 10. **(B)** Depleted MNC were incubated with Daudi and the monoclonal antibodies rituximab, obinutuzumab or their unspecific isotype control (IgG) for 4h in different effector to target ratios. Specific target cell lysis was measured by flow cytometry. The data are presented as mean ± SD of 4 **(A)** or 3-4 **(B)** independent experiments. *p<0.05 and **p<0.01 comparing the two different stimulation protocols.

the proliferation rate and purity as well as IFNγ production and CD107a expression were significantly related (data not shown), there was a negative correlation between cell concentration of γδ T cells and IFNγ production (Figure 3). Since we did not split the cell cultures during the cultivation with Ko-Op, the cell concentration is a direct indicator of cell count of γδ T cells. Thus, not all target parameters can be equally enhanced with our cultivation method.

Correlation of donor characteristics with the proliferation and anti-tumor activity of their stimulated γδ T cells

Especially when multiple donors are available, it would be helpful to be able to deduce from the demographic or clinical characteristics of the donors or their unstimulated γδ T cells whether their stimulated γδ T cells have the potential for high yield and high anti-tumor activity. We could not find a significant correlation between the donors' sex and the cell concentration of γδ T cells on day 10 of stimulation (data not shown). There was also no significant correlation between cell concentration at day 10 and the donors' age, although the significance level for the negative correlation between age and cell concentration of γδ T cells was just not reached with a p value of 0.052 (Figure 4A). However, we observed a positive correlation between the cell concentration of γδ T cells on day 10 of stimulation and the percentage of γδ T cells of unstimulated MNC, which in turn correlated negatively with age (Figures 4B, C). Additionally, we found a negative correlation between age of donors and the ΔMFI of CD107a in the degranulation assay without incubation with Daudi cells (Figure 4D). In conclusion, higher age seems to be associated with lower percentage of γδ T cells in MNC and therefore with lower proliferation when stimulated by using Ko-Op. Additionally, the stimulated γδ T cells of older donors probably bear less anti-tumor activity compared to them of younger donors. Thus, the percentage of γδ T cells as well as the age of the donors can be used as a decision-making aid in the selection of donors.

Modification of proliferation, purity and anti-tumor activity of γδ T cells by altering the stimulants within the Ko-Op protocol

We next investigated whether the Ko-Op protocol could be improved by a zoledronate pulse or by applying IL-15 in addition to or in place of IL-2, or by the combination of both. For this, MNC of healthy donors were isolated and stimulated using the Ko-Op standard protocol or according to different alterations concerning the zoledronate addition and the composition of the interleukins up to ten days. For zoledronate pulse, 100 µM zoledronate was added to the isolated MNC and washed out again after 4 hours of incubation. When IL-15 was used, this was at a concentration of 10 ng/ml, with the concentration of IL-2 remaining unchanged at 1000 U/ml.

Pulsing the cells with high-dose zoledronate led to a significant lower proliferation rate of γδ T cells on day 7 of cultivation (Figure 5A). While compared to the standard protocol, the combined application of IL-2 and IL-15 led to no significant change in proliferation rate of γδ T cells, the proliferation was significantly lower when IL-15 was used alone (Figure 5B). The combination of zoledronate pulse and adding IL-2 and IL-15 also did not lead to any improvement (Figure 5C). The proportion of γδ T cells and thus the purity of the cell product was significantly reduced by pulsing zoledronate, by using IL-15 instead of IL-2 and by combining both modifications (Figures 5D–F).

Regarding cytoplasmic perforin, the use of IL-15 instead of IL-2 led to a significant reduction both without and with zoledronate pulse (Figures 6B, C). The zoledronate pulse alone and the use of IL-15 in addition to IL-2 did not lead to any significant change (Figures 6A–C). The modifications of the Ko-Op protocol had no significant effect on cytoplasmic IFNγ and CD107a expression in the degranulation assay (data not shown). We next performed cytotoxicity assays with the different cultivated MNC. To be able to compare the methods more accurately, we calculated the lytic units per 10^6 effector cells according to Bryant et al. (22). A lytic unit is the number of effector cells, which is required to lyse a specific percentage of target cells. A significant

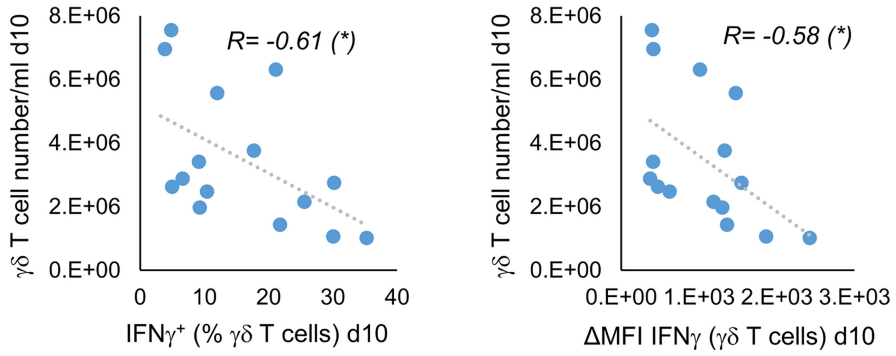

FIGURE 3
Indirect correlation of cell concentration and IFNγ production of stimulated γδ T cells. MNC of healthy donors were isolated and stimulated with Zol/IL-2 according to the protocol Ko-Op. On day 10, the γδ T cell number/ml was calculated on the basis of cell number/ml of MNC and percentage of γδ T cells on the MNC. The cytoplasmic IFNγ in γδ T cells was determined by flow cytometry. The results were tested for correlation. The data are presented as correlation chart of 15 independent experiments. Correlation coefficient R is calculated according to Spearman. *p<0.05 correlating the indicated variables.

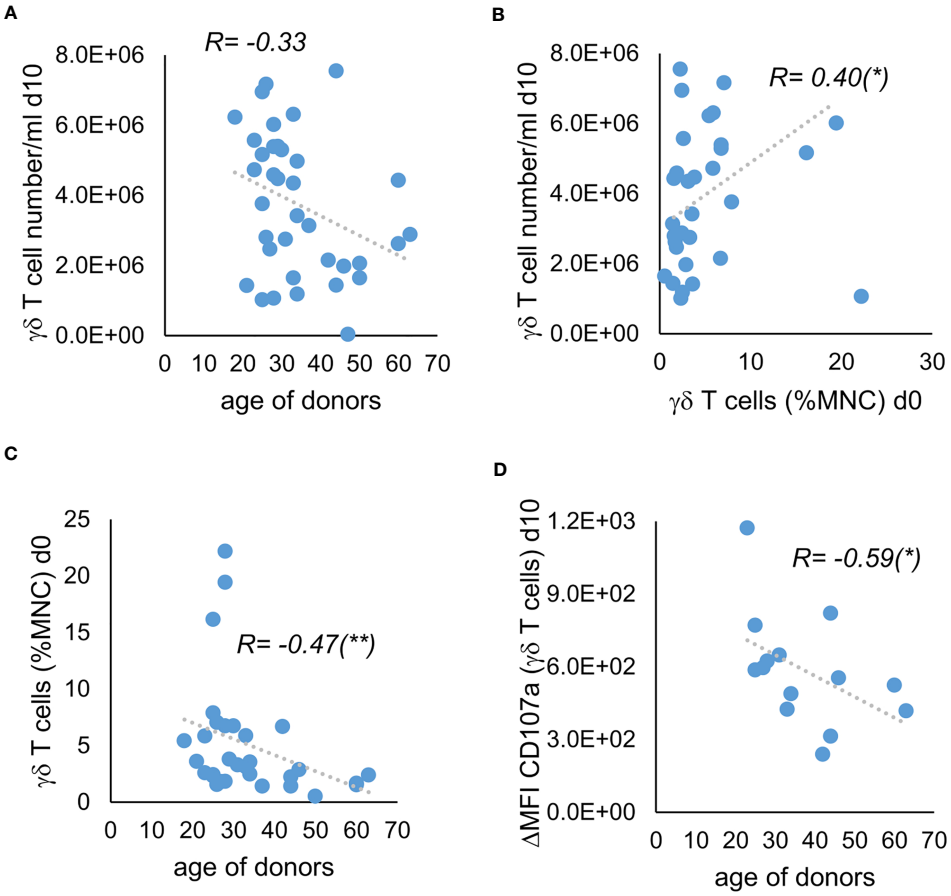

FIGURE 4
Correlation of donor characteristics with the proliferation and anti-tumor activity of their stimulated γδ T cells. MNC of healthy donors were isolated and stimulated with Zol/IL-2 according to the protocol Ko-Op. The percentage of γδ T cells was determined by flow cytometry. On day 10 of cultivation, the degranulation assay was performed. **(A)** Correlation between the age of donors and the γδ T cell number/ml on day 10 of stimulation. **(B)** Correlation between the percentage of γδ T cells when unstimulated and the γδ T cell number/ml on day 10 of stimulation. **(C)** Correlation between the age of the healthy donors and the percentage of γδ T cells when unstimulated. **(D)** Correlation between the age of the healthy donors and the ΔMFI of CD107a on γδ T cells on day 10 of stimulation. The data are presented as correlation chart of 36 **(A–C)** or 14 **(D)** independent experiments. Correlation coefficient R is calculated according to Spearman. *p<0.05 and **p<0.01 correlating the indicated variables.

increase in lytic units could be achieved with the zoledronate pulse compared to the standard protocol when no therapeutic antibodies are added (Figure 6D). The combination of IL-15 and IL-2 led to no change in lytic units both with and without antibodies compared to the standard protocol, but to significant higher lytic units compared to IL-15 alone (Figure 6E). Interestingly, when the modifications were combined, an increase in lytic units could be achieved without antibody when IL-15 alone or IL-15 and IL-2 were added, and with antibody when IL-15 and IL-2 were added, compared to the zoledronate pulse without modification of the interleukins (Figure 6F).

As IL-15 is known to promote the stimulation of central memory T cells, we analyzed certain subclasses of stimulated γδ T cells. γδ T cells were classified into naive, central memory, effector memory and terminally differentiated γδ T cells based on the expression of CD45RA and CD27 (20, 25). As expected, the stimulation with IL-15 instead of IL-2 led to an elevated percentage of central memory γδ T cells (TCM) and to a reduced percentage of effector γδ T cells (TEM), also if combined with pulsing zoledronate (Figures 6H, I). Pulsing zoledronate and addition of IL-2 as stimulant also resulted in more TCM (Figure 6G). Interestingly, combining IL-2 with IL-15 significantly reduced the percentage of TCM, but the difference was marginal (Figure 6H).

In conclusion, pulsing zoledronate and co-stimulation by the combination of IL-2 and IL-15 lead to significant changes in *in vitro* anti-tumor activity and in the subclasses of stimulated γδ T cells.

Discussion

Improvement of immunotherapeutic cell products by a newly developed cultivation method

The aim of this work was to lay the groundwork for a GMP-compliant cultivation process for γδ T cells that would reliably produce a cell product with high proliferation rate, purity and anti-tumor activity. By combining known and partly new process steps like shaking, we established the xenogen-free cultivation protocol

10.3389/fimmu.2023.1185564

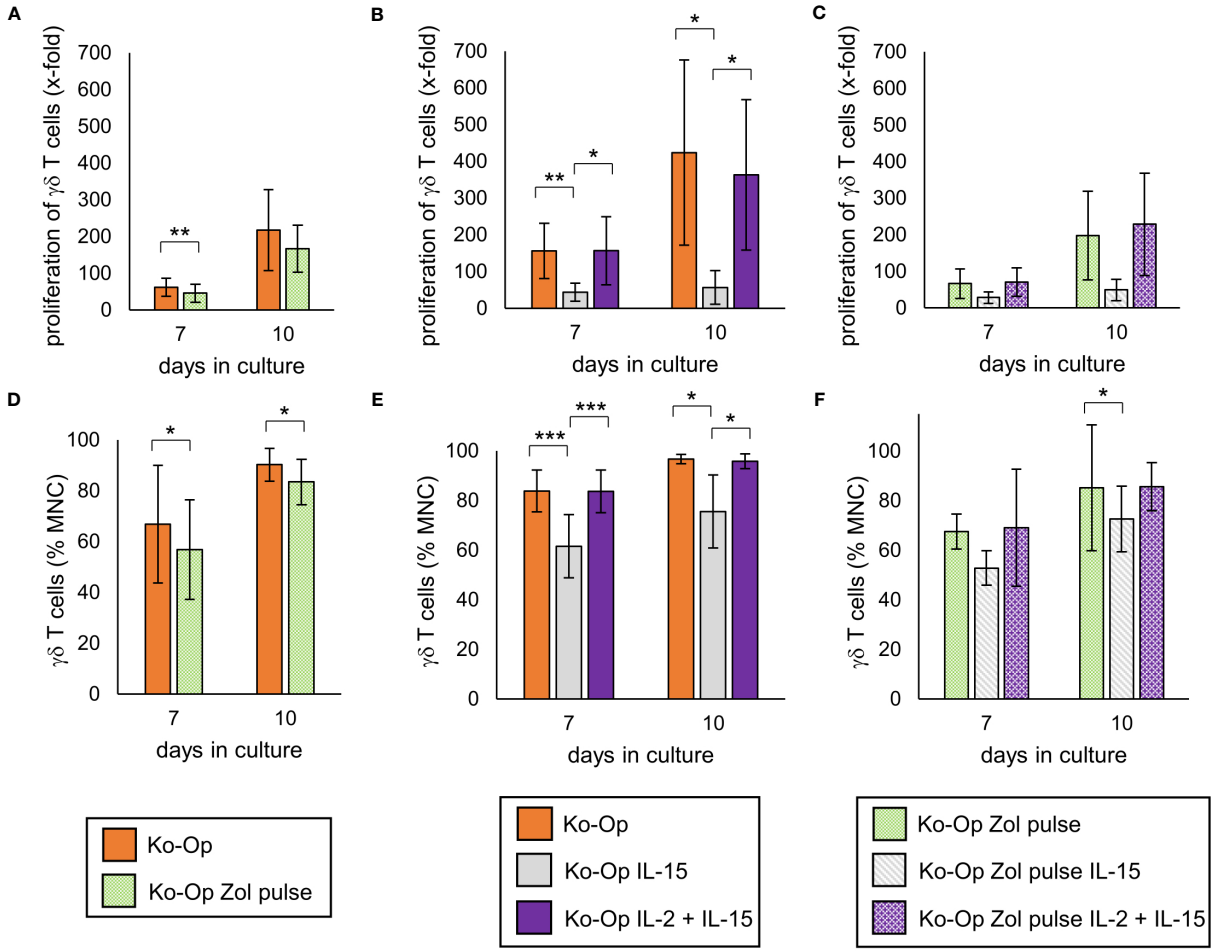

FIGURE 5
Modification of proliferation, purity and anti-tumor activity of γδ T cells by altering the stimulants within the Ko-Op protocol. MNC of healthy donors were isolated and stimulated according to the Ko-Op standard protocol (orange bars) or to different alterations concerning the zoledronate addition (Zol pulse) and the composition of the interleukins (IL-15, IL-2 + IL-15) up to ten days. **(A–C)** Proliferation rate of γδ T cells at day 7 and 10 of cultivation. **(D–F)** Percentage of γδ T cells at day 7 and 10 of cultivation measured by flow cytometry. The data are presented as mean ± SD of 7 **(A, D)**, 6 **(B, E)** or 4 **(C, F)** independent experiments. *p<0.05, **p<0.01 and ***p<0.001 comparing the different cultivation protocols.

"Ko-Op". When stimulating MNC with this cultivation method, γδ T cell counts increased more than 400-fold on average and the cell product consisted of over 90% γδ T cells. Compared to our previous standard procedure, cultivation with Ko-Op led to higher production of cytoplasmic perforin, to higher degranulation and to stronger cytotoxicity with and without monoclonal antibodies directed against target cells. However, stimulation with Ko-Op increased cytoplasmic IFNγ only on day 7 of cultivation compared with our previous standard protocol "R10F". IFNγ is a pro-inflammatory cytokine and its production is a typical hallmark of activated Vγ9Vδ2 T cells associated with their effector functions in cancer (26, 27). Interestingly, for γδ T cells stimulated with Ko-Op in our study, we observed a negative correlation between the proliferation rate at day 10 and both the proportion of cytoplasmic IFNγ expressing γδ T cells and the ΔMFI of cytoplasmic IFNγ in γδ T cells. Possibly, the IFNγ producing γδ T cells are distinctively differentiated and proliferate less upon stimulation by IL-2. Consistent with this, $CD27^+$ γδ T cells were found to proliferate, but to have a reduced capacity to secrete IFNγ (28).

That OpTmizer is a suitable medium for serum-free expansion of γδ T cells has also been shown by Sutton et al. (29). Interestingly, the purity of γδ T cells after stimulation with Ko-Op in our study is notably higher than the described percentage of γδ T cells in their study. This could be due to the fact that we use a higher dose of zoledronate, do not split and shake the cells from day 4 onwards. However, we know that shaking is not the main reason for the higher purity as stimulation with Ko-Op without shaking leads to comparable purity but reduced vitality of MNC compared to Ko-Op standard stimulation (data not shown). We do not add IL-2 before d2. This could explain why the percentage of NK cells, which are known to proliferate upon IL-2 stimulation, is comparatively low after stimulation with Ko-Op. While the presence of NK cells might not negatively influence the anti-tumor activity of the final cell product and even be beneficial in some indications (30), the αβ T cells cause graft versus host reaction and must be depleted prior to adoptive transfer with resulting losses in cell count. We therefore prefer a process that results in a cell product of high purity, as is achieved by stimulation with Ko-Op. That no depletion step would

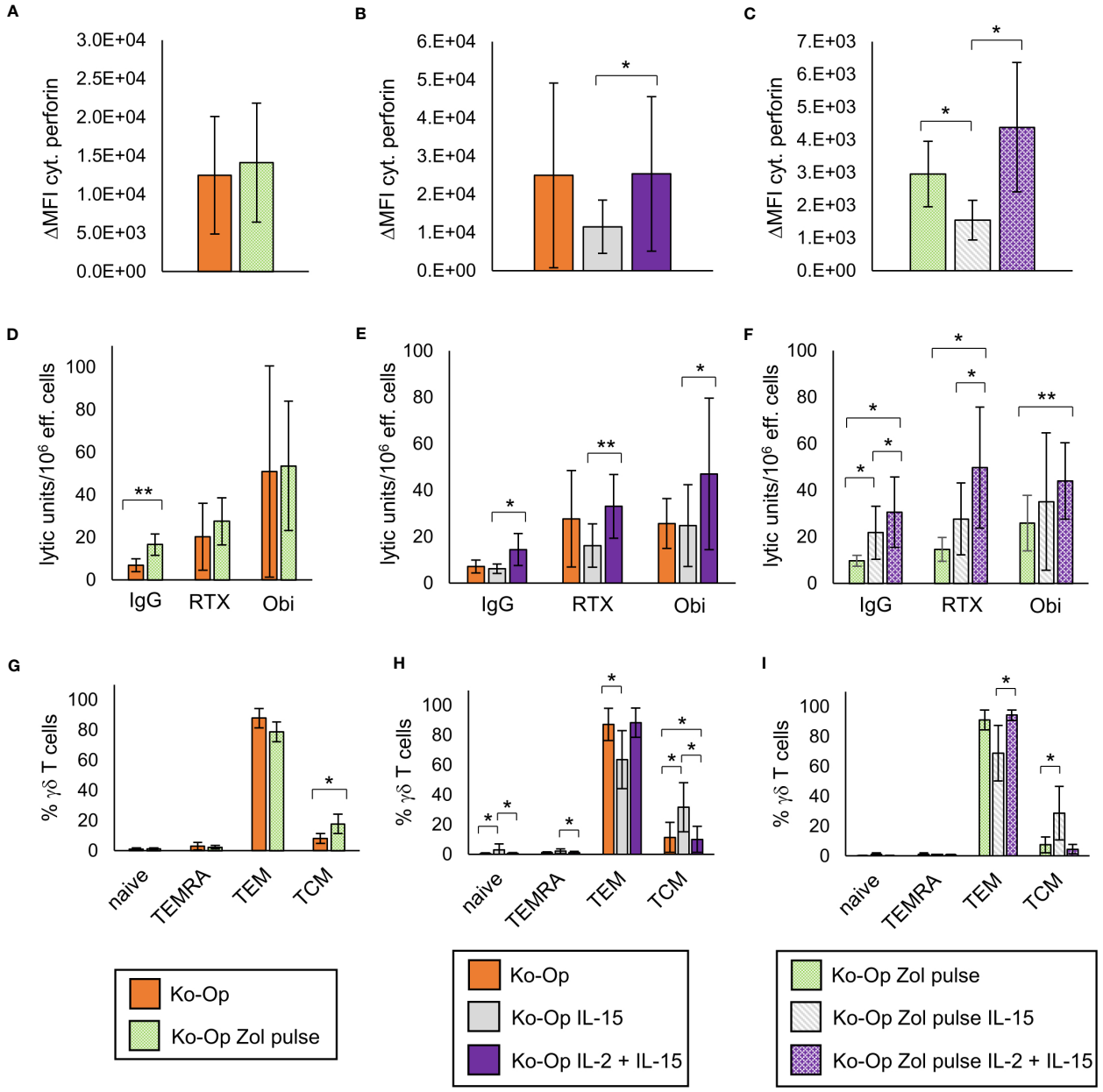

FIGURE 6
Modification of anti-tumor activity and differentiation of γδ T cells by altering the stimulants within the Ko-Op protocol. MNC of healthy donors were isolated and stimulated according to the Ko-Op standard protocol (orange bars) or to different alterations concerning the zoledronate additon (Zol pulse) and the composition of the interleukins (IL-15, IL-2 + IL-15) up to ten days. **(A–C)** Cytoplasmic perforin of γδ T cells was stained at day 10 of cultivation. ΔMFI was measured by flow cytometry. **(D–F)** MNC were incubated with Daudi with the monoclonal antibodies rituximab, obinutuzumab or their unspecific isotype control for 4h in order to perform the cytotoxicity assay at day 10 of cultivation. Lytic units per 10^6 effector cells were calculated based on the specific target cells lysis obtained with different effector to target ratios from 0.7:1 to 20:1. **(G–I)** Percentage of the γδ T cells differentiated in naive ($CD45RA^+CD27^+$), TCM ($CD45RA^-CD27^+$), TEM ($CD45RA^-CD27^-$) and TEMRA ($CD45RA^+CD27^-$). The data are presented as mean ± SD of 5 **(A, F, G)**, 6 **(B, E, H)** or 4 **(C, D, I)** independent experiments. *p<0.05 and **p<0.01 comparing the different cultivation protocols.

be necessary after stimulation with Ko-Op is demonstrated by the following calculation example using the percentage data from the 12 donors of Figure 1C. Assuming that $3.0x10^6$ stimulated MNC per kilogram body weight are to be transplanted, we would administer an average of $2.77x10^6$ γδ T cells per kilogram body weight (equivalent to 92.19% γδ T cells of MNC) on day 10/11 of cultivation, which in our experience would be an appropriate cell number (6, 16). The number of αβ T cells thereby administered would be $1.14x10^5$ αβ T cells per kilogram body weight (equivalent to 3.81% αβ T cells of MNC). On day 14/15, we would even administer only $5.97x10^4$ αβ T cells per kilogram body weight (equivalent to 1.99% αβ T cells of MNC). We know from *in vivo* studies with NK cells that αβ T cell numbers lower than $5x10^5$ per kilogram body weight are tolerable (31, 32). In only one of the 12 donors was the percentage of αβ T cells too high on day 10 of stimulation, but by day 14 the percentage would have been

within the acceptable range. Therefore, MNC stimulated with Ko-Op should be usable without the need for an additional purification step.

Beside bisphosphonate-based protocols, K562 feeder cell-based methods with or without zoledronate, have been developed to expand γδ T cells for cellular therapy in recent years (33, 34). Since this provides sustained stimulation over several weeks, expansion rates are very high and in a direct comparison also higher than with a bisphosphonate-based protocol (33). However, the use of feeder cells increases the complexity of the process and may reduce the chance of regulatory approval. In addition, the K562-based protocol is under patent protection. In conclusion, our newly developed protocol can be more rapidly implemented in the clinic and is more easily applicable for broader use in academia or industry.

The optimal donor and time schedule for *ex vivo* expansion of γδ T cells with Ko-Op

Adoptive transfer of haploidentical γδ T cells is feasible without limiting side effects (6, 8). Therefore, if several donors are available the question of selecting the most suitable donor arises. Despite our promising results presented here, we see differences between the various donors in terms of yield and anti-tumor activity when we stimulate their MNC *in vitro* using the new cultivation procedure Ko-Op. We found a weak but significant inverse relationship between age and degranulation and a positive correlation between percentage of γδ T cells of unstimulated MNC and proliferation rate of γδ T cells. This is consistent with the finding that γδ T cells from older people do not respond well to IPP (35). Our results also fit the finding of Sutton et al. that the initial γδ T cell number correlates with the final γδ T cell number (29). As consequence, we would choose the youngest adult donor with the highest percentage of γδ T cells of unstimulated MNC to achieve the best possible yield and anti-tumor activity of cells.

The question remains as to the optimal culture duration and timing for adoptive cell transfer. Yield and purity as well as anti-tumor activity should be as high as possible. In view of all the findings, we consider the resulting cell product on day 10 to be the most suitable of the tested days for *in vivo* application and thus also for our further *in vitro* investigations. This is in line with others who also see an optimal outcome at day 10 of *ex vivo* stimulation also in terms of a lower proportion of terminally differentiated cells. However, their stimulation protocol differs from ours as they used K562 artificial antigen presenting cells in combination with zoledronate to expand γδ T cells (36).

Modulating Ko-Op by pulsing zoledronate and addition of IL-15

The benefits of pulsing zoledronate or addition of IL-15 for expansion and stimulation of γδ T cells have been demonstrated several times (8, 19–21). The rationale for washing out zoledronate after 4h is to reduce cellular toxicity by the aminobisphosphonate (19, 37). But in contrast to others, we saw no benefit regarding the proliferation and the purity when adjusting the Ko-Op protocol by pulsing of zoledronate. The purity was even reduced. However, we already achieved an excellent purity with Ko-Op standard, which could explain the missing benefit of pulsing zoledronate. Additionally, the toxicity of remaining zoledronate does obviously not prevail the possible benefit of not washing out. Indeed, by pulsing, both the culture medium of the first four hours with possibly already released cytokines contributing to the stimulation and the stimulant zoledronic acid itself are lost. However, an increase of intrinsic cytotoxicity of γδ T cells can be achieved by pulsing zoledronate. Furthermore, pulsing zoledronate leads to a higher proportion of TCM, which is associated with a more effective tumor control *in vivo*, at least in αβ T cells studies (38, 39).

The impact of combining IL-2 with IL-15 for γδ T cell stimulation on the proliferation rate is controversial. Van Acker et al. described enhancing effects on proliferation (20). Xu et al. also observed a higher proliferation rate, but they additionally stimulated with vitamin C (8). Like us, Aehnlich et al. and Burnham et al. did not find a benefit (21, 40). Regarding the intrinsic and antibody-dependent cell-mediated cytotoxicity, we unexpectedly only saw benefits of combining IL-2 and IL-15 when zoledronate was pulsed. With respect to the current literature, we would have expected also an enhancing effect if IL-2 and IL-15 is combined with our Ko-Op standard protocol. However, for the intrinsic and the obinutuzumab-mediated cytotoxicity, we could observe higher lytic units when IL-2 was combined with IL-15. Here, because of the high variability of the results of single experiments, a significance level was not reached. IL-15 has already been safely administered in clinical trials, facilitating GMP-compliant use (41).

We also tested the use of IL-15 instead of IL-2 for expansion and found significantly reduced proliferation, purity, cytoplasmic perforin and cytotoxicity. Interestingly, we observed an increased intrinsic cytotoxicity when pulsing zoledronate was combined with IL-15 instead of IL-2. However, because of the small recovery, we do not consider it practical for clinical use to stimulate with IL-15 only.

In summary, pulsing zoledronate and additional administration of IL-15 modifies the anti-tumor activity and the differentiation of stimulated γδ T cells. While enhanced cytotoxicity and a higher percentage of TCM can be considered as improvements, the question arises whether the lower purity by pulsing zoledronate is acceptable for clinical-scale application. This might possibly require an additional depletion step, with corresponding cell loss, before their adoptive transfer. Still, the cultivation procedure for the γδ T cell product can be adjusted to the actual requirements of the clinical application.

Conclusions and outlook

With this study, we have achieved our goal of establishing an expansion protocol for γδ T cells that is easy to scale up and convert to a GMP-compliant process. We also demonstrated that it is

superior to our previous standard procedure with respect to almost all target parameters considered. Furthermore, we examined our results for correlations with donor characteristics in order to draw conclusions about a suitable donor for *ex vivo* expansion followed by haploidentical transplantation. Finally, we demonstrated that the expansion protocol Ko-Op can be further modified by pulsing zoledronate and combining IL-15 and IL-2 as co-stimulators. Further tests with frozen and thawed stimulated cells and *in vivo* studies remain necessary to verify whether the results obtained in this study are reflected by the anti-tumor activity *in vivo*.

Data availability statement

The raw data supporting the conclusions of this article will be made available by the authors, without undue reservation.

Ethics statement

The studies involving human participants were reviewed and approved by the Institutional Review Board of the Paracelsus Medical University Nuremberg. Written informed consent to participate in this study was provided by the participants. All donors signed an agreement according to General Data Protection Regulation.

Author contributions

AB designed the experiments, performed research, analyzed and interpreted data and wrote the paper. HG performed research, interpreted data and edited the paper. EH performed research. SK edited the paper. TH contributed to conception and design, interpreted data and edited the paper. MW contributed to conception and design, interpreted data and edited the paper. These authors contributed equally to this work and share last authorship: TH and MW.

Funding

AB, HG and this study were supported by “Verein Hilfe für Krebskranke e.V.” and a scholarship from the “W. Lutz Stiftung”.

Conflict of interest

The authors declare that the research was conducted in the absence of any commercial or financial relationships that could be construed as a potential conflict of interest.

Publisher’s note

Supplementary material

The Supplementary Material for this article can be found online at: https://www.frontiersin.org/articles/10.3389/fimmu.2023.1185564/full#supplementary-material

SUPPLEMENTARY FIGURE 1
Percentage of NK cells, vitality of MNC and percentage of perforin$^+$ and IFNγ$^+$ γδ T cells after *ex vivo* stimulation. MNC of healthy donors were isolated and stimulated with Zol/IL-2 according to the protocols R10F (blue hatched bars) and Ko-Op (orange bars) up to 17 days. **(A)** Representative FACS analysis of MNC cultured according to the protocols R10F or Ko-Op for ten days. NK cells were defined by using anti-CD56-PC5 and anti-CD3-ECD. **(B)** Percentage of NK cells at different days of cultivation measured by flow cytometry. **(C)** Vitality of MNC at different days of cultivation determined by trypan blue exclusion. **(D)** Cytoplasmic perforin and IFNγ in γδ T cells were stained at different days of cultivation and measured by flow cytometry. The data are presented as mean ± SD of 12 **(B, C)** or 9 **(D)** independent experiments. *p<0.05 and **p<0.01 comparing the two different stimulation protocols.

References

1. Morita CT, Mariuzza RA, Brenner MB. Antigen recognition by human gamma delta T cells: pattern recognition by the adaptive immune system. *Springer Semin Immunopathol* (2000) 22(3):191–217. doi: 10.1007/s002810000042

2. Silva-Santos B, Serre K, Norell H. γδ T cells in cancer. *Nat Rev Immunol* (2015) 15 (11):683–91. doi: 10.1038/nri3904

3. D'Asaro M, La Mendola C, Di Liberto D, Orlando V, Todaro M, Spina M, et al. V Gamma 9V delta 2 T lymphocytes efficiently recognize and kill zoledronate-sensitized, imatinib-sensitive, and imatinib-resistant chronic myelogenous leukemia cells. *J Immunol* (2010) 184(6):3260–8. doi: 10.4049/jimmunol.0903454

4. Todaro M, D'Asaro M, Caccamo N, Iovino F, Francipane MG, Meraviglia S, et al. Efficient killing of human colon cancer stem cells by gammadelta T lymphocytes. *J Immunol* (2009) 182(11):7287–96. doi: 10.4049/jimmunol.0804288

5. Girardi M, Oppenheim DE, Steele CR, Lewis JM, Glusac E, Filler R, et al. Regulation of cutaneous malignancy by gammadelta T cells. *Science* (2001) 294 (5542):605–9. doi: 10.1126/science.1063916

6. Wilhelm M, Smetak M, Schaefer-Eckart K, Kimmel B, Birkmann J, Einsele H, et al. Successful adoptive transfer and *in vivo* expansion of haploidentical γδ T cells. *J Transl Med* (2014) 12:45. doi: 10.1186/1479-5876-12-45

7. Alnaggar M, Xu Y, Li J, He J, Chen J, Li M, et al. Allogenic Vγ9Vδ2 T cell as new potential immunotherapy drug for solid tumor: a case study for cholangiocarcinoma. *J Immunother Cancer* (2019) 7(1):36. doi: 10.1186/s40425-019-0501-8

8. Xu Y, Xiang Z, Alnaggar M, Kouakanou L, Li J, He J, et al. Allogeneic Vγ9Vδ2 T-cell immunotherapy exhibits promising clinical safety and prolongs the survival of patients with late-stage lung or liver cancer. *Cell Mol Immunol* (2021) 18(2):427–39. doi: 10.1038/s41423-020-0515-7

9. Yazdanifar M, Barbarito G, Bertaina A, Airoldi I. γδ T cells: the ideal tool for cancer immunotherapy. *Cells* (2020) 9(5):1305. doi: 10.3390/cells9051305

10. Hoeres T, Smetak M, Pretscher D, Wilhelm M. Improving the efficiency of Vγ9Vδ2 T-cell immunotherapy in cancer. *Front Immunol* (2018) 9:800. doi: 10.3389/fimmu.2018.00800

11. Wang RN, Wen Q, He WT, Yang JH, Zhou CY, Xiong WJ, et al. Optimized protocols for γδ T cell expansion and lentiviral transduction. *Mol Med Rep* (2019) 19 (3):1471–80. doi: 10.3892/mmr.2019.9831

12. Vavassori S, Kumar A, Wan GS, Ramanjaneyulu GS, Cavallari M, El Daker S, et al. Butyrophilin 3A1 binds phosphorylated antigens and stimulates human γδ T cells. *Nat Immunol* (2013) 14(9):908–16. doi: 10.1038/ni.2665

13. Willcox CR, Salim M, Begley CR, Karunakaran MM, Easton EJ, von Klopotek C, et al. Phosphoantigen sensing combines TCR-dependent recognition of the BTN3A IgV domain and germline interaction with BTN2A1. *Cell Rep.* (2023) 42(4):112321. doi: 10.1016/j.celrep.2023.112321

14. Sandstrom A, Peigné CM, Léger A, Crooks JE, Konczak F, Gesnel MC, et al. The intracellular B30.2 domain of butyrophilin 3A1 binds phosphoantigens to mediate activation of human Vγ9Vδ2 T cells. *Immunity* (2014) 40(4):490–500. doi: 10.1016/j.immuni.2014.03.003

15. Sicard H, Ingoure S, Luciani B, Serraz C, Fournié JJ, Bonneville M, et al. *In vivo* immunomanipulation of V gamma 9V delta 2 T cells with a synthetic phosphoantigen in a preclinical nonhuman primate model. *J Immunol* (2005) 175(8):5471–80. doi: 10.4049/jimmunol.175.8.5471

16. Bold A, Gaertner J, Bott A, Mordstein V, Schaefer-Eckart K, Wilhelm M. Haploidentical γδ T cells induce complete remission in chemorefractory b-cell non-Hodgkin lymphoma. *J Immunother* (2023) 46(2):56–8. doi: 10.1097/CJI.0000000000000450

17. Hoeres T, Pretscher D, Holzmann E, Smetak M, Birkmann J, Triebel J, et al. Improving immunotherapy against b-cell malignancies using γδ T-cell-specific stimulation and therapeutic monoclonal antibodies. *J Immunother* (2019) 42(9):331–44. doi: 10.1097/CJI.0000000000000289

18. Tokuyama H, Hagi T, Mattarollo SR, Morley J, Wang Q, So HF, et al. V Gamma 9 V delta 2 T cell cytotoxicity against tumor cells is enhanced by monoclonal antibody drugs–rituximab and trastuzumab. *Int J Cancer* (2008) 122(11):2526–34. doi: 10.1002/ijc.23365

19. Nada MH, Wang H, Workalemahu G, Tanaka Y, Morita CT. Enhancing adoptive cancer immunotherapy with Vγ2Vδ2 T cells through pulse zoledronate stimulation. *J Immunother Cancer* (2017) 5:9. doi: 10.1186/s40425-017-0209-6

20. Van Acker HH, Anguille S, Willemen Y, Van den Bergh JM, Berneman ZN, Lion E, et al. Interleukin-15 enhances the proliferation, stimulatory phenotype, and antitumor effector functions of human gamma delta T cells. *J Hematol Oncol* (2016) 9(1):101. doi: 10.1186/s13045-016-0329-3

21. Aehnlich P, Carnaz Simões AM, Skadborg SK, Holmen Olofsson G, Thor Straten P. Expansion with IL-15 increases cytotoxicity of Vγ9Vδ2 T cells and is associated with higher levels of cytotoxic molecules and T-bet. *Front Immunol* (2020) 11:1868. doi: 10.3389/fimmu.2020.01868

22. Bryant J, Day R, Whiteside TL, Herberman RB. Calculation of lytic units for the expression of cell-mediated cytotoxicity. *J Immunol Methods* (1992) 146(1):91–103. doi: 10.1016/0022-1759(92)90052-U

23. Holmen Olofsson G, Idorn M, Carnaz Simões AM, Aehnlich P, Skadborg SK, Noessner E, et al. Vγ9Vδ2 T cells concurrently kill cancer cells and cross-present tumor antigens. *Front Immunol* (2021) 12:645131. doi: 10.3389/fimmu.2021.645131

24. Hoeres T, Holzmann E, Smetak M, Birkmann J, Wilhelm M. PD-1 signaling modulates interferon-γ production by gamma delta (γδ) T-cells in response to leukemia. *Oncoimmunology* (2019) 8(3):1550618. doi: 10.1080/2162402X.2018.1550618

25. Dieli F, Poccia F, Lipp M, Sireci G, Caccamo N, Di Sano C, et al. Differentiation of effector/memory Vdelta2 T cells and migratory routes in lymph nodes or inflammatory sites. *J Exp Med* (2003) 198(3):391–7. doi: 10.1084/jem.20030235

26. Gao Y, Yang W, Pan M, Scully E, Girardi M, Augenlicht LH, et al. Gamma delta T cells provide an early source of interferon gamma in tumor immunity. *J Exp Med* (2003) 198(3):433–42. doi: 10.1084/jem.20030584

27. Lawand M, Déchanet-Merville J, Dieu-Nosjean MC. Key features of gamma-delta T-cell subsets in human diseases and their immunotherapeutic implications. *Front Immunol* (2017) 8:761. doi: 10.3389/fimmu.2017.00761

28. Gioia C, Agrati C, Casetti R, Cairo C, Borsellino G, Battistini L, et al. Lack of CD27-CD45RA-V gamma 9V delta 2+ T cell effectors in immunocompromised hosts and during active pulmonary tuberculosis. *J Immunol* (2002) 168(3):1484–9. doi: 10.4049/jimmunol.168.3.1484

29. Sutton KS, Dasgupta A, McCarty D, Doering CB, Spencer HT. Bioengineering and serum free expansion of blood-derived γδ T cells. *Cytotherapy* (2016) 18(7):881–92. doi: 10.1016/j.jcyt.2016.04.001

30. Jonus HC, Burnham RE, Ho A, Pilgrim AA, Shim J, Doering CB, et al. Dissecting the cellular components of *ex vivo* γδ T cell expansions to optimize selection of potent cell therapy donors for neuroblastoma immunotherapy trials. *Oncoimmunology* (2022) 11(1):2057012. doi: 10.1080/2162402X.2022.2057012

31. Geller MA, Cooley S, Judson PL, Ghebre R, Carson LF, Argenta PA, et al. A phase II study of allogeneic natural killer cell therapy to treat patients with recurrent ovarian and breast cancer. *Cytotherapy* (2011) 13(1):98–107. doi: 10.3109/14653249.2010.515582

32. Miller JS, Soignier Y, Panoskaltsis-Mortari A, McNearney SA, Yun GH, Fautsch SK, et al. Successful adoptive transfer and *in vivo* expansion of human haploidentical NK cells in patients with cancer. *Blood* (2005) 105(8):3051–7. doi: 10.1182/blood-2004-07-2974

33. Choi H, Lee Y, Hur G, Lee SE, Cho HI, Sohn HJ, et al. γδ T cells cultured with artificial antigen-presenting cells and IL-2 show long-term proliferation and enhanced effector functions compared with γδ T cells cultured with only IL-2 after stimulation with zoledronic acid. *Cytotherapy* (2021) 23(10):908–17. doi: 10.1016/j.jcyt.2021.06.002

34. Xiao L, Chen C, Li Z, Zhu S, Tay JC, Zhang X, et al. Large-Scale expansion of Vγ9Vδ2 T cells with engineered K562 feeder cells in G-Rex vessels and their use as chimeric antigen receptor-modified effector cells. *Cytotherapy* (2018) 20(3):420–35. doi: 10.1016/j.jcyt.2017.12.014

35. Colonna-Romano G, Potestio M, Aquino A, Candore G, Lio D, Caruso C. Gamma/delta T lymphocytes are affected in the elderly. *Exp Gerontol* (2002) 37(2-3):205–11. doi: 10.1016/S0531-5565(01)00185-1

36. Boucher JC, Yu B, Li G, Shrestha B, Sallman D, Landin AM, et al. Large Scale *ex vivo* expansion of γδ T cells using artificial antigen-presenting cells. *J Immunother* (2023) 46(1):5–13. doi: 10.1097/CJI.0000000000000445

37. Wang H, Sarikonda G, Puan KJ, Tanaka Y, Feng J, Giner JL, et al. Indirect stimulation of human Vγ2Vδ2 T cells through alterations in isoprenoid metabolism. *J Immunol* (2011) 187(10):5099–113. doi: 10.4049/jimmunol.1002697

38. Klebanoff CA, Gattinoni L, Torabi-Parizi P, Kerstann K, Cardones AR, Finkelstein SE, et al. Central memory self/tumor-reactive CD8+ T cells confer superior antitumor immunity compared with effector memory T cells. *Proc Natl Acad Sci USA* (2005) 102(27):9571–6. doi: 10.1073/pnas.0503726102

39. Gattinoni L, Klebanoff CA, Palmer DC, Wrzesinski C, Kerstann K, Yu Z, et al. Acquisition of full effector function *in vitro* paradoxically impairs the *in vivo* antitumor efficacy of adoptively transferred CD8+ T cells. *J Clin Invest* (2005) 115(6):1616–26. doi: 10.1172/JCI24480

40. Burnham RE, Zoine JT, Story JY, Garimalla SN, Gibson G, Rae A, et al. Characterization of donor variability for γδ T cell. *Front Med (Lausanne)* (2020) 7:588453. doi: 10.3389/fmed.2020.588453

41. Conlon KC, Lugli E, Welles HC, Rosenberg SA, Fojo AT, Morris JC, et al. Redistribution, hyperproliferation, activation of natural killer cells and CD8 T cells, and cytokine production during first-in-human clinical trial of recombinant human interleukin-15 in patients with cancer. *J Clin Oncol* (2015) 33(1):74–82. doi: 10.1200/JCO.2014.57.3329

frontiers | Frontiers in Immunology

TYPE Review
PUBLISHED 24 July 2023
DOI 10.3389/fimmu.2023.1199145

OPEN ACCESS

EDITED BY
Maurizio Chiriva-Internati,
University of Texas MD Anderson Cancer Center, United States

REVIEWED BY
Tamara Laskowski,
Lonza, United States
Meisam Naeimi Kararoudi,
Nationwide Children's Hospital, United States

*CORRESPONDENCE
Feifei Luo
feifeiluo@fudan.edu.cn
Yiwei Chu
yiweichu@fudan.edu.cn

RECEIVED 03 April 2023
ACCEPTED 05 July 2023
PUBLISHED 24 July 2023

CITATION
Lv Z, Luo F and Chu Y (2023) Strategies for overcoming bottlenecks in allogeneic CAR-T cell therapy. *Front. Immunol.* 14:1199145. doi: 10.3389/fimmu.2023.1199145

Strategies for overcoming bottlenecks in allogeneic CAR-T cell therapy

Zixin Lv[1,2], Feifei Luo[2,3]* and Yiwei Chu[1,2]*

[1]Department of Immunology, School of Basic Medical Sciences, and Institutes of Biomedical Sciences, Fudan University, Shanghai, China, [2]Biotherapy Research Center, Fudan University, Shanghai, China, [3]Department of Digestive Diseases, Huashan Hospital, Fudan University, Shanghai, China

Patient-derived autologous chimeric antigen receptor (CAR)-T cell therapy is a revolutionary breakthrough in immunotherapy and has made impressive progress in both preclinical and clinical studies. However, autologous CAR-T cells still have notable drawbacks in clinical manufacture, such as long production time, variable cell potency and possible manufacturing failures. Allogeneic CAR-T cell therapy is significantly superior to autologous CAR-T cell therapy in these aspects. The use of allogeneic CAR-T cell therapy may provide simplified manufacturing process and allow the creation of 'off-the-shelf' products, facilitating the treatments of various types of tumors at less delivery time. Nevertheless, severe graft-versus-host disease (GvHD) or host-mediated allorejection may occur in the allogeneic setting, implying that addressing these two critical issues is urgent for the clinical application of allogeneic CAR-T cell therapy. In this review, we summarize the current approaches to overcome GvHD and host rejection, which empower allogeneic CAR-T cell therapy with a broader future.

KEYWORDS

allogeneic CAR-T cell, gene-editing technology, non-gene editing technology, T cell subsets, pluripotent stem cell

1 Introduction

Chimeric antigen receptor (CAR)-T cell therapy is an innovative approach in cancer treatment, which has achieved great success in hematological malignancies and emerged as a promising treatment modality against solid tumors (1, 2). With the sixth CAR-T product approved by FDA and likely more to come (3), autologous CAR-T cell therapy, in which a patient's own T cells are genetically engineered *in vitro* and then infused back into the patient, has demonstrated its importance in clinical applications. However, autologous CAR-T products inevitably raise challenging issues due to the customized and complex process flows. Since the clinical manufacture of CAR-T cells takes 1 to 3 weeks from collecting the patient's blood to the final harvest of qualified cell products (4), patients with rapidly progressive tumors may lose access to CAR-T administration. Besides, the

personalized pattern of autologous products means that CAR-T products may derive from different batches even for the same patient, which represents complicated processes and excessive costs (5). Moreover, T cell dysfunction caused by the healthy level and previous treatment of patients, as well as flawed processes in clinic manufacture, can contribute to the possibility of manufacturing failure (6, 7). Allogeneic CAR-T cells, which are also known as 'off-the-shelf' CAR-T cells, is an alternative to potentially overcome all these issues. For example, allogeneic CAR-T cells with starting materials sourced from healthy donors have the potential to increase predictable efficacy and treat all eligible patients. Compared with autologous CAR-T cells, a large number of allogeneic CAR-T cells can be produced in a single manufacturing run, meeting the needs of treatment for multiple patients and the requirements for cost reduction due to scale-up production. In addition, elimination the delay of treatment through reviving pre-frozen allogeneic cells in time whenever patients need may improve the clinical outcomes (Figure 1) (8, 9).

Although allogeneic CAR-T cell therapy has such advantages, it still remains hurdles to hamper its practical application. From an immunological perspective, donor CAR-T cells may attack host tissues to induce graft-versus-host disease (GvHD), and may be recognized by host immune system to cause host-mediated allorejection (8, 10). In this review, we describe the present strategies to address these risks through technology approaches in αβ T cells or using different cell types. We also discuss clinical transformation of universal allogeneic CAR-T cells based on the current strategies.

2 Modifying αβ T cells

Human leukocyte antigen (HLA) mismatch between donor and recipient is the major cause of GvHD and host immune rejection. The HLA system is a cluster of gene complex located on chromosome 6 in humans, which encodes cell-surface proteins responsible for presenting peptides to the αβ T-cell receptor (TCR) on T cells (11). HLA is known to be the most polymorphic gene region mainly caused by multiple alleles and codominance, and thus leads to high possibility of HLA mismatch in populations. The αβ TCR from donor CAR-T cells, which is composed of α- and β-chains, is able to recognize foreign HLA molecules with peptides restrictively, hence inducing acute or chronic GvHD. In turn, host αβ T cells may attack allogeneic CAR-T cells in an HLA-restricted way and trigger host rejection. Natural killer (NK) cells also participate in the rejection of donor CAR-T cells through tilting the dynamic balance between signals from cell surface activating and inhibitory receptors. Upon the unique recognition of inhibitory receptors and their ligands HLA class I (HLA-I) molecules, NK cells acquire immune tolerance to self, which means that mismatch between donor HLA-I and inhibitory receptors of recipient NK cells will weaken the transmitted inhibitory signal and then activate NK cells (12). In addition to cellular rejection, antibody-mediated rejection driven by donor-specific antibodies (DSAs) is also associated with graft damage after transplantation. DSAs contain antibodies against recipient's HLA antigens and non-HLA antigens like minor histocompatibility antigens and autoantigens. In clinical trials of allogeneic cell therapy, DSAs were reported to induce cell killing through antibody-mediated cellular cytotoxicity (ADCC) and complement-dependent cytotoxicity (CDC) (13). Therefore, efforts are necessarily needed to solve these two problems in allogeneic CAR-T cell therapy.

2.1 Using gene editing technology

Modification of allogeneic CAR-T cells via gene editing technology is one of the major strategies to avoid GvHD and host-mediated allorejection. Gene editing technology is based on two mechanisms: double-strand breaks can be repaired to mediate

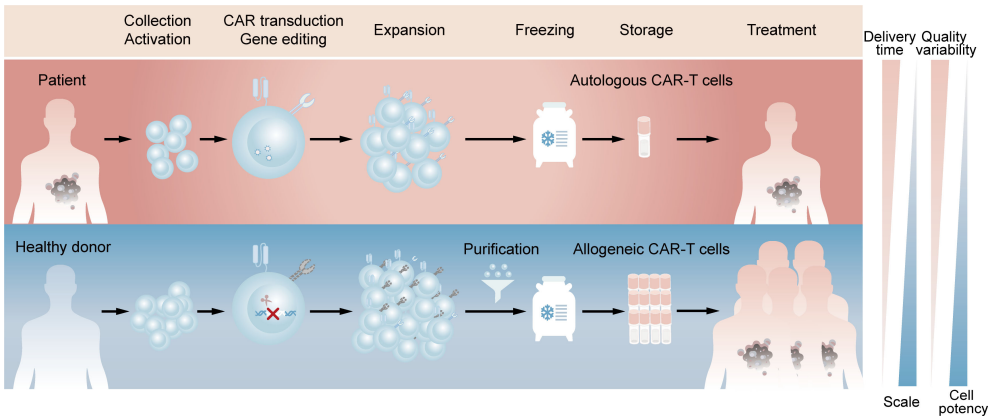

FIGURE 1
Comparison of clinic manufacturing process between autologous and allogeneic CAR-T cells. The above (red) represents the process flows of patient-derived autologous CAR-T cells. T lymphocytes are firstly enriched and activated from peripheral blood mononuclear cells. Afterwards, CARs are introduced by viral transduction and the obtained CAR-T cells are expanded and frozen, which are available for the patient's own use after reviving. The below (blue) represents the process flows of healthy donor-derived allogeneic CAR-T cells. T lymphocytes are same enriched and activated, followed by elimination of TCR at the time of CAR introduction. The TCR-negative CAR-T cells are then purified from expanded cell population and the final frozen cells are available for different patients.

gene knock-in through homologous recombination or gene knockout through non-homologous end joining when template strand is introduced or not, respectively (14). Currently, a series of powerful gene editing tools, such as zinc-finger nucleases (ZFNs), transcription activator-like effector nucleases (TALENs), and clustered regularly interspaced short palindromic repeats-CRISPR-associated protein 9 (CRISPR-Cas9), have played a role in preclinical and clinical studies of allogeneic CAR-T cells (15–17).

Genetically editing donor CAR-T cells to eliminate endogenous αβ TCR may effectively prevent TCR-mediated alloreactivity without compromising CAR-dependent function. Torikai et al. (15) first proposed that TCR-negative allogeneic anti-CD19 CAR-T cells, in which αβ TCR was deleted through ZFN-driven gene editing, showed the expected cytotoxicity of CD19 redirection without responding to TCR stimulation. This pioneering work introduced gene editing technology into allogeneic CAR-T cells, paving the way for its further use by utilizing different editing tools. More recently, a two-in-one strategy that inserting CAR gene into TCR α constant region (TRAC) through CRISPR system was designed (Figure 2A) (18). The produced allogeneic CAR-T cells lacked the unwanted graft-versus-host response, and were protected from the side effects of CAR transduction, such as virus usage and random integration. This two-in-one strategy further suggested that integrating CAR gene into targeted gene locus through gene editing may be a promising approach to both avoid the defects of CAR transduction and achieve the desired goal of targeted gene knockout. For example, CAR insertion in PDCD1 locus may resist exhaustion of CAR-T cells (19, 20).

Several strategies have also been developed to escape host rejection. One of the most commonly used in clinical settings is disrupting CD52 in donor CAR-T cells combined with lymphodepletion through Alemtuzumab, a humanized anti-CD52 monoclonal antibody (Figure 2B) (21, 22). CD52 is widely distributed on the surface of lymphocytes and many other hematopoietic cells, so pretreatment with Alemtuzumab can prevent host rejection and facilitate the expansion and survival of infused CD52-decifient CAR-T cells, which are resistant to Alemtuzumab. Since HLA-I molecules are expressed on the surface of most nucleated cells, abrogating their expression in CAR-T cells is another feasible strategy to evade the recognition by the recipient T cells. Disruption of β2-microglobulin (B2M) gene was reported to efficiently eliminate the expression of HLA-I molecules, as B2M is a highly-conserved component of HLA-I heterodimer. Nevertheless, the removal of HLA-I may lead to the activation and killing of NK cells, suggesting the limitations of direct deletion. Therefore, different modification methods were proposed to guarantee no 'missing-self' response by host NK cells. One is to express a single-chain HLA-E with minimal polymorphism fused to the B2M locus, which can effectively prevents killing of NKG2A^{+} NK cells (Figure 2D) (23, 24). Another is to construct an inventory containing HLA-C-retained cells that disrupts both HLA-A and HLA-B alleles. An induced pluripotent stem cell bank containing 12 lines of HLA-C-retained cells was found to be immunocompatible with >90% of the world population (25), demonstrating the construction of a cell inventory is potentially viable (Figure 2E). While not expressed in naive T

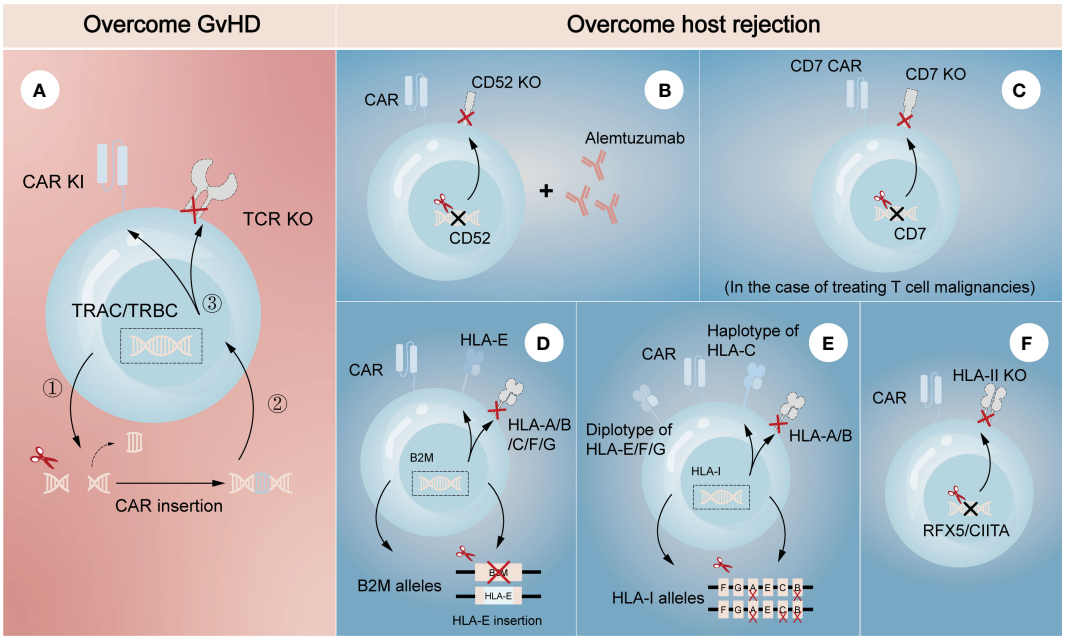

FIGURE 2
Gene editing technologies for overcoming GvHD and host-mediated allorejection. The left **(A)** represents the strategy to overcome GvHD that inserting CAR gene into the TRAC/TRBC loci. The right **(B–F)** represents the strategies to overcome host rejection, showing a combination strategy by removing CD52 in CAR-T cells with lymphodepletion through Alemtuzumab **(B)**, knockout of CD7 in CAR-T cells when treating CD7-positive T cell malignancies **(C)**, HLA-E insertion in one allele of B2M while another allele is knocked out **(D)**, construction of HLA-C-retained cells that disrupts both HLA-A and HLA-B alleles **(E)**, and knockout of transcription factors like RFX5/CIITA to achieve elimination of HLA-II **(F)**. TRAC, TCR α constant region; TRBC, TCR β constant region.

cells, HLA class II (HLA-II) molecules are upregulated in activated T cells under the control of several trans-acting regulatory factors such as RFX5 and CIITA (26–28). Previous studies found that mutations in these regulatory genes led to lack of HLA-II antigen expression and $CD4^+$ T cell-dependent immune response (29), indicating depletion of them would be a strategy to overcome host rejection caused by HLA-II-restricted recognition (Figure 2F). In the case of treating T cell malignancies, CD7-targeting allogeneic CAR-T cells with genetic modifications of CD7 depletion are also an encouraging approach to resist fratricide in addition to T cell-mediated rejection (Figure 2C) (30). As CD5 is also a pan-T marker acting as an inhibitory regulator of TCR signaling and regularly expresses on ~85% of T cell malignancies (31), it can also be an attractive target against T cell malignancies in allogeneic CAR-T therapy.

Combination of these strategies to overcome both host-mediated allorejection and GvHD has been intensively studied in the field of allogeneic CAR-T therapy (16, 19, 32). For instance, a recent study successfully generated CAR-T cells with immune-evasive properties by inserting CAR and HLA-E gene into TCR and B2M loci, respectively (33). These engineered cells were proved to evade the attack of T cells and NK cells, as well as extend their antitumor activity and persistence both *in vitro* and *in vivo*. The success of combination strategy in preclinical models enables the use of allogeneic T cells for adoptive T cell therapy, supporting the translation of research into clinical practice. To date, a number of clinical trials using gene-edited allogeneic T cells as the source of effector cells for CAR-T cell therapy are underway worldwide, most of which target hematological malignancies (34–36). UCART19 is the first-in-class allogeneic CAR-T product developed for the treatment of CD19-positive hematological malignancies, which is engineered to eliminate the expression of TCR and CD52 through TALEN system. A clinical trial (NCT02746952) based on UCART19 showed great expansion and antitumor activity of CAR-T cells in patients with relapsed or refractory B-cell acute lymphoblastic leukemia, in which only 2 patients developed grade 1 acute cutaneous GvHD (37). Many other clinical trials have also shown no or minimal GvHD and host rejection in gene-edited allogeneic CAR-T products, indicating the safety in clinical applications.

2.2 Using non-gene editing technology

Although gene editing technology is an excellent tool to modify allogeneic T cells, it actually carries various potential risks associated with carcinogenicity and chromosomal abnormalities. CRISPR-Cas9 editing was reported to potentially trigger p53-mediated programmed cell death, while downregulation of p53 made the cells more likely to be edited (38, 39). The findings suggest that p53-mutant cells are easier to be edited, therefore raising the risk of cell carcinogenesis. Moreover, cells with mutations in other cancer driver genes, such as the KRAS gene, have a competitive advantage after CRISPR-Cas9 editing (40). Numerical or structural chromosomal abnormalities are also hidden dangers of CRISPR-Cas9 editing (41, 42). CRISPR-Cas9 cleavage may cause chromosomal aberrations in human T cells, including chromosomal truncations, translocations and frequent aneuploidy (43, 44). All the reports point that global detection is needed to eliminate potential risks if CRISPR-Cas9 gene-edited cells are used for treatment. As an alternative, non-gene editing technologies have been explored to mitigate the risk of GvHD and host immune rejection.

Unlike gene editing technology that performs precise genetic manipulation in TCR locus to avoid alloreactivity of donor CAR-T cells, non-gene editing technology prefers to disrupt the downstream mechanisms of action. Since the formation of the TCR/CD3 complex is required for antigen recognition and downstream signal generation (45), inhibition of its assembly or cell surface expression may effectively prevent endogenous TCR-driven T cell activation. From the mRNA level, knocking down any subunit of TCR/CD3 complex through specific short hairpin RNA (shRNA) is one of the effective strategies to inhibit this complex formation (Figure 3A). On this basis, CYAD-211, a non-gene edited allogeneic CAR-T product that co-expresses CD3ζ shRNA with BCMA CAR via a single viral vector, was subsequently explored. A phase 1 trial (NCT04613557) evaluating CYAD-211 in adult patients with relapsed or refractory multiple myeloma showed an encouraging antitumor effect with a favorable safety profile (46), suggesting that knockdown of components in the complex is feasible. Several means of affecting the formation of TCR/CD3 complex on cell surface at the protein level have also been proposed. As the complex is assembled in the endoplasmic reticulum (ER), a specific protein expression blocker (PEBL) that consists of anti-CD3ε scFv and peptide predicted to anchor to ER was designed, thereby retaining the complex intracellularly (Figure 3B) (47, 48). Besides, expression of a TCR inhibitory molecule (TIM) that consists of a truncated CD3ζ peptide can result in dominant suppressive effects in TCR downstream signal through competitively form TCR/TIM complex (Figure 3C). By co-expressing a NKG2D CAR and a TIM, the CAR-T product CYAD-101 was proved to have antitumor activity without GvHD in mouse models and clinical trials (NCT03692429) (49, 50).

Resistance of allogeneic CAR-T cells to the recipient's immune system requires eliminating alloreactive response mediated by T cells, NK cells and DSAs (Figure 3D). Activated lymphocytes temporarily upregulate the expression of several surface markers to provide additional costimulatory signals (51, 52), which can be targeted to eliminate host T cells and NK cells activated by allogeneic T cells, thereby preventing allogeneic T cells from being rejected. Based on the proof of principles, an alloimmune defense receptor (ADR) that consisted of an extracellular 4-1BB ligand-derived recognizing fragment fused to an intracellular CD3ζ chain was proposed to apply to allogeneic CAR-T cell therapy (53). The expression of ADR was shown to effectively resist host rejection and fratricide as the expression of ADR could downregulate or mask their own 4-1BB. As NK cells can be activated by 'missing self' recognition, Hu et al. (30) generated an NK cell inhibitory receptor (NKi), which was composed of the EC1-EC2 extracellular domain of E-cadherin and the CD28 intracellular domain. Due to the fact that E-cadherin negatively regulates NK cell function through KLRG1 binding and that CD28 intracellular domain enhances the inhibitory effect of NKi (54), the incorporation of NKi into CAR-T

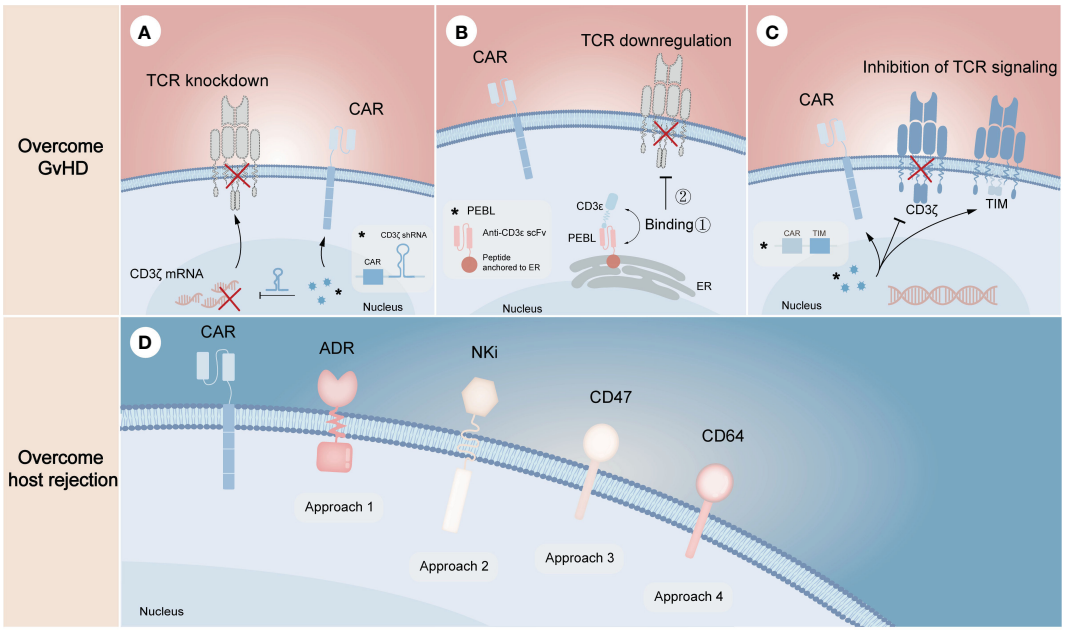

FIGURE 3
Non-gene editing technologies for overcoming GvHD and host-mediated allorejection. The above **(A–C)** represents the strategies to overcome GvHD, illustrating the knockdown of TCR complex through CD3ζ mRNA silencing **(A)**, the downregulation of TCR complex through expressing a CD3ε-specific PEBL that retaining the complex in cytoplasm **(B)**, and the inhibition of TCR signaling by expressing TIM molecules that can competitively replace CD3ζ when binding αβ TCR **(C)**. The below **(D)** represents the strategies to overcome host rejection, in which approach 1-4 show the expression of ADR for evading the killing of host T and NK cells, the expression of NKi to inhibit the activation of host NK cells and thus to reduce NK cell-mediated cytotoxicity, the overexpression of CD47 to escape host NK cell-mediated rejection, the overexpression of CD64 to escape antibody-mediated rejection, respectively. The symbol "*" represents the general schematic of a molecule (e.g., labeled virus particles (blue) in **A**) and its specific structure or composition (e.g., labeled white box in **A**).

cells resulted in a reduction in NK cell-mediated cytotoxicity. Besides, previous studies showed that upregulation of CD47 expression specifically prevented NK cells from killing allogeneic stem cells and cells with HLA-I deletion, illustrating that ectopic expression of CD47 in CAR-T cells may be a novel strategy to solve NK cell-mediated rejection (55, 56). However, it still needs to be further evaluated in preclinical models. More recently, overexpression of CD64 was found to protect CAR-T cells from HLA and non-HLA antibody killing (13). Since CD64 is a high-affinity receptor for the fragment crystallizable (F_c) region of IgG, CAR-T cells that overexpress CD64 can capture IgG F_c and make DSAs inaccessible to effector cells and complement, thus allowing CAR-T cells to evade ADCC and CDC.

3 Using different T cell subpopulations

Despite the fact that αβ T cells are the dominant source of effector cells in CAR-T cell therapy, their use in allogeneic settings still needs significant efforts. In addition to the manufacturing process required for traditional autologous CAR-T cells, allogeneic CAR-αβ T cells, whether modified via gene-editing or non-gene editing technologies, requires additional process to achieve the clearance of GvHD and host-mediated allorejection, as well as to ensure the clinical safety of the modified cells (9). Therefore, a number of studies attempt to broaden the source of effector cells to achieve a final product with less process and higher safety. Here we describe the advantages of novel T cell subsets available for CAR-T therapy over traditional αβ T cells (Table 1), and summarize the clinical progress of CAR-T therapy based on them (Table 2).

3.1 CAR-invariant natural killer T cells

Invariant NKT (iNKT) cells are a CD1d-restricted, TCR semi-invariant T cell subpopulation with TCR containing an invariant Vα24-Jα18 chain. The monomorphism of CD1d gives iNKT cells the ability to overcome HLA-restricted GvHD in the allogeneic settings without inactivating their endogenous TCR, thus providing a safer source of effector cells for the 'off-the-shelf' CAR-T platform (63). Preclinical models showed that CAR-NKT cells had better localization ability to tumor tissues than conventional CAR-T cells and played a dual killing effect by targeting CAR-positive tumor cells and CD1d-positive M2 or tumor cells to reduce the immune escape of tumor cells (64–66). Moreover, they were able to facilitate maturation of DC through CD40L/CD40 and TCR/CD1d signaling and thus indirectly activate $CD8^+$ T cells (67). The first clinical trial based on autologous CAR-NKT cells was conducted previously (NCT03294954) (68). NKT cells were engineered to co-express a CAR that could specifically recognize GD2-expressing neuroblastoma and IL-15 that could support the survival of NKT cells. The GD2.CAR.15 NKT cells showed enhanced persistence, better tumor localization and improved tumor control without

TABLE 1 Summary of allogeneic CAR-T products from different T cell sources.

CAR-T product	Target antigen	T cell source	Conditions	Phase	Reference
KUR-502	CD19	iNKT	Relapsed or refractory B-cell malignancies	Phase 1 (NCT00840853)	(57)
CD123CAR-DOTs	CD123	γδT	acute myeloid leukemia	Preclinical	(58)
ADI-002	GPC3	γδT	Hepatocellular carcinoma	Preclinical	(59)
ADI-001	CD20	γδT	B cell malignancies	Phase 1 (NCT04735471)	(60)
CTM-N2D	NKG2DL	γδT	Advanced solid tumors or hematological malignancies	Phase1 (NCT05302037)	
CD19-CAR-DNT	CD19	DNT	B-cell non-Hodgkin's lymphoma	Phase1 (NCT05453669)	(61)
FT819	CD19	iPSC-derived TCRαβ-deficient T	Relapsed or refractory B-cell malignancies	Phase1 (NCT04629729)	(62)
CNTY-102	CD19 and CD22	iPSC-derived γδT	Relapsed or refractory B-cell malignancies	Preclinical	

significant toxicity, which suggests the great potential of CAR-NKT cells over conventional CAR-T cells. In addition, donor-derived iNKT cells were proved to exert antitumor function without exacerbating GvHD after allogeneic hematopoietic cell transplantation, indicating the possibility for 'off-the-shelf' production and use (69).

Because of the relative rarity that iNKT cells account for only 0.01%-1% of peripheral blood T cells (70), expansion of them from donor peripheral blood mononuclear cells (PBMC) to therapeutic level is crucial for clinical use. Rotolo et al. (66) built a system in which TCRVα24Jα18$^+$ lymphocytes were activated by CD3/CD28 beads and cultured with an aliquot of irradiated autologous mononuclear cells at a 1:1 ratio in the presence of IL-15, resulting in an average 750-fold expansion of 3rd CAR19-iNKT cells after 3 weeks. Ngai et al. (71) also found that co-culture of iNKT cells with an aliquot of αGalCer-pulsed irradiated autologous PBMC in the presence of IL2 and IL-21 led to an average 600-fold expansion and increased CD62L$^+$ frequency in 10-12 days. Currently, a clinical study of allogeneic CD19 CAR-NKT cells for relapsed or refractory B-cell malignancies is underway (NCT00840853) (57). The NKT cells were modified to express a CD19-targeting CAR, IL-15, and shRNA targeting B2M and CD74 to downregulate HLA-I and HLA-II molecules, respectively. The initial results indicated that these allogeneic cells were well-tolerated and could mediate antitumor responses in patients.

3.2 CAR-γδ T cells

γδ T cells, whose TCR consists of γ- and δ-chain, are a subpopulation of T cells appearing in peripheral blood and barriers like intestine (72). Different from αβ T cells that recognize the MHC-peptide complex, γδ T cells play an important role in both innate and adaptive immune responses through multiple receptor-ligand interactions. In antitumor immunity, γδ T cells function in an MHC-independent manner of antigen recognition and tumor killing, as well as play an indirect role by activating B cells, αβ T cells and NK cells (73, 74). Multiple preclinical trials have found that the presence of γδ T cells after allogeneic stem cell transplantation do not induce GvHD (75, 76), a feature that makes them an attractive pool for allogeneic CAR-T therapy. A previous γδ T-based GD2 CAR-T study showed that CAR-γδ T cells could better migrate and infiltrate into tumor site, exert antitumor effects and cross-present antigens to tumor-infiltrating αβ T cells through uptake of released tumor-associated antigens (77). Other studies of CAR-γδ T cells also

TABLE 2 Comparation among different T cell sources.

T cell subset	Frequency in human peripheral blood T cells	MHC restriction	Advantages	Disadvantages
αβT	90%-95%	YES	Highly abundance; well-established system for clinical application	GvHD and host rejection; the need for multiple manipulations
iNKT	0.01%-1%	NO	Double killing effects; lack of GvHD; better tumor localization	Low frequency; host rejection
γδT	5%-10%	NO	Multiple mechanisms of action; lack of GvHD; better migration and infiltration; antigen cross-presentation	Low frequency; host rejection
DNT	1%-3%	NO	Multiple targeting; lack of GvHD and host rejection	Low frequency
MAIT	1%-10%	NO	Multiple mechanisms of action; lack of GvHD; effector memory-like phenotype	Low frequency; host rejection; immature expansion system

described several established production process of high-purity CAR-γδ T from PBMC (58, 59, 78). These harvested CAR-γδ T cells were shown to kill antigen-negative tumor cells without evidence of GvHD, indicating the ability to eliminate tumors even after antigen loss. All these characteristics mark their potential advantages over conventional CAR-αβ T cells. Currently, several allogeneic CAR-T cell therapies based on γδ T cells (NCT04735471, NCT05302037) are in phase 1 clinical trials for the treatment of hematological malignancies or solid tumors (60).

3.3 CAR-double negative T cells

Double negative T (DNT) cells are a small subset of mature T cells that comprise approximately 1%-3% of T lymphocytes in human peripheral blood (79). Distinguished from conventional T cells and NKT cells, DNT cells lack both CD4 and CD8 in addition to not binding CD1d tetramers. DNT cells can recognize tumor cells through NKG2D or DNAM-1 and exert antitumor functions through cytokines or Fas/FasL signaling pathway (80). This MHC-independent and multi-targeted mechanism of action allows DNT cells to not cause GvHD and to kill tumor cells that do not express MHC molecules. Various preclinical models demonstrate that allogeneic DNT cells can target a range of tumor types and mediate significant cytotoxicity without triggering GvHD and host rejection (81–84). For example, healthy donor-derived DNT cells significantly inhibited the growth of late-stage lung cancer xenografts in mouse models (85). A Phase 1 clinical trial (NCT03027102) using healthy donor-derived DNT cells also validated objective responses without observed toxicity to normal tissues in patients with acute myeloid leukemia (86). These studies all suggest that DNT cells, which do not induce alloreactivity without modification, have the properties to be used in allogeneic settings.

Although the frequency of DNT cells in peripheral blood is relatively low, large-scale expansion to therapeutic levels can be reached under GMP conditions. Briefly, CD4- and CD8-negative PBMC are sorted and cultured in the presence of IL-2 and CD3 mAbs for 17 days, which allows the harvested DNT cells to reach an average fold and purity of 1558 and 91.9%, respectively (82, 83). As IL-33 has recently been reported to promote the proliferation and survival of DNT cells *in vitro* (87), adding IL-33 may be an optimized strategy to improve the current clinical expansion system for DNT cells. However, an optimal dosage-frequency regimen for IL-33 requires further exploration. More recently, Vasic et al. (88) generated CAR19-DNT cells by transducing CD19-specific CAR into DNT cells. These modified cells efficiently inhibited tumor growth with no off-tumor toxicity in mouse models, while they were able to evade the alloreactivity of mouse-derived T cells. Therefore, DNT cells have met several requirements for clinical application of allogeneic CAR-T products, including the efficacy, lack of alloreactivity and large-scale production.

3.4 CAR-mucosal-associated invariant T cells

Mucosal-associated invariant T (MAIT) cells are an evolutionarily conserved, unconventional T cell subpopulation, of which approximately 90% are phenotypically $CD161^{+}CD8^{+}$. MAIT cells have the unique semi-constant TCR that consists of TRAV1 combined with three kinds of TRAJ (TRAJ33, TRAJ12, TRAJ20) and a limited repertoire of β chains in human (89). The TCR can recognize modified derivatives from vitamin B2 synthesis pathway presented by MHC class I-related molecule MR1 on APCs, promoting the proliferation and secretion of cytokines, cytotoxic molecules and chemokines of MAIT in the face of most microorganisms. Moreover, they express several NK activating receptors, which act as a second pathway to initiate response. In antitumor immunity, MAIT cells can kill tumor cells via TCR or NK activating receptors, meanwhile boosting DC through upregulating CD40L and inhibiting TAM and MDSC through binding MR1 and NK ligand (90). MAIT cells are distributed in peripheral blood, liver, lung and intestinal lamina propria (91). Previous studies have showed that $CD161^{+}CD8^{+}$ MAIT cells upregulate tissue-specific chemokine receptors like CXCL6, CCR6 and CCR9 (92), the reason that they are highly enriched in non-lymphoid organs through tissue homing. Besides, MAIT cells present an effector memory-like phenotype and can produce IFN-γ and granzyme B upon stimulation. Since MR1 is a conserved molecule, MAIT cells are devoid of alloreactive potential, as confirmed by their failure to proliferate in response to alloantigen stimulation *in vitro* and to expand or participate in tissue damage during GvHD *in vivo* (93). This potential has also been proved by clinical data showing that the number of engrafted allogeneic MAIT cells is positively correlated with improved survival and less allogeneic adverse events (94). All the intrinsic characteristics of MAIT cells, including multiple targeting, memory phenotype and lack of alloreactivity, make them candidates for allogeneic cell therapy against cancer.

As engineering immune cells with CAR is an effective measure to enhance antitumor function, Dogan et al. (95) constructed anti-CD19 and anti-HER2 CAR-MAIT cells to evaluate their efficacy while compared with conventional CAR-T cells. They found CAR-MAIT cells showed similar or even higher cytotoxicity but lower proinflammatory cytokine secretion compared with conventional CAR-T cells *in vitro* assays, indicating MAIT cells may represent safer and more effective effector cells for CAR-T cell therapy. However, the efficacy and safety evaluation of CAR-MAIT cells *in vivo* and in allogeneic settings have not been studied yet, which means more efforts are needed to explore the allogeneic CAR-MAIT therapy. In order to apply allogeneic CAR-MAIT cells in clinical conditions, a key issue is to achieve efficient expansion of MAIT cells. There are two expansion protocols for MAIT cells. The first is co-culture MAIT cells with artificial APCs generated by immobilizing antigen-loaded MR1 tetramers and CD28 mAbs on cell-size latex beads (96). The protocol leads to a 60-fold expansion of pure MAIT cells in 3 weeks. Another is co-culture MAIT cells with autologous PBMC at a ratio of 1:10 in a serum replacement-supplemented medium in the presence of IL-2, which results in a 200-fold expansion of high-purity MAIT cells in 3 weeks (97). For better clinical application, it is worthwhile to optimize the amplification system of MAIT cells.

4 Using pluripotent stem cells

Although the 'off-the-shelf' CAR-T cells have been a window of opportunity for the generalization and productization of CAR-T

cell therapy, there are still inevitable drawbacks in process flows. Given the nature of T cells themselves, CAR-T cells undergo limited expansion and gradual transition to exhausted phenotypes in manufacturing (4), which creates the need for repeated collection of T cells from different donors as source materials and thus leads to heterogeneity of CAR-T products. In addition, CAR gene insertion or gene editing at the T cell level is technically challenging and requires complex safety assessments to prevent adverse events such as chromosomal abnormalities and oncogenic mutations (5).

Pluripotent stem cells (PSCs) such as induced pluripotent stem cells (iPSCs) and embryonic stem cells (ESCs) may be a better choice of source materials to solve the problems in clinic manufacture. In contrast to T cells that require large-scale quality control to avoid adverse events, the successfully engineered PSCs with security can be select easily to create a master cell bank for downstream use (98). Besides, gene editing and CAR transduction do not affect the properties of PSCs to proliferate indefinitely. A qualified master CAR-PSC cell bank can provide an inexhaustible source of starting cells, ensuring the generation of numerous homogeneous CAR-T cell products for a large number of patients (99). However, *in vitro* generation of mature T cells from PSCs that are phenotypically and functionally similar to classical TCR$\alpha\beta^+$ T cells is a challenge to overcome.

To address this problem, Schmitt et al. (100) first proposed a simple system of co-culture ESCs with OP9-DL1, a mouse bone marrow stromal cell line expressing Notch ligand delta-like 1 (DL1). Since it was previously reported that culture of ESCs on OP9 promoted the development of hematopoietic lineage and that DL1 signaling induced differentiation of hematopoietic stem cells into T cells (101, 102), ESCs were effectively differentiated into functional single-positive T cells in this system. Nevertheless, the hematopoietic progenitor cells obtained in the process were proved to have low engraftment levels and hematopoietic chimerism in transplantation (103, 104), reflecting that the conditions for hematopoietic differentiation still need refining. Therefore, several methods were used to improve conditions for definitive hematopoietic specification (105). For example, transcription factor respecification, optimized procedures for co-culture with stromal cells, and direct differentiation in a serum-free condition with cytokines or in a cytokine-free condition were all shown to facilitate definitive hematopoiesis (104, 106–108). Although these improved approaches partially yield mature T cells, there still remain a large number of T cells in precursor stage or with innate phenotype. Two novel methods were then designed to increase the quality of T cells in final harvests (Figure 4). One is to culture PSCs with MS5 cells expressing Delta-like-4 (DL4) in a 3D organoid culture system, a method that is readily deployable and technically advanced (109). The system successfully differentiated PSCs into high proportions of mature αβ T cells, which were transcriptionally similar to naive CD8$^+$ T cells and produced cytokines in response to antigens. Besides, the system also permitted the generation of highly functional CAR-T cells from CAR-iPSCs (110), providing a platform for 'off-the-shelf' CAR-T therapy. Since co-culture with stromal cells is difficult in clinical manufacture, another method aims to generate T cells in a totally serum-free and stroma-free system that is clinically applicable and scalable. The approach replaced DL4-expressing stromal cells with DL4-Fc recombinant protein, eliminating the role of stromal cells in the culture system. More recently, some improvements to this system have also been reported. The first is to replace plate-bound DL4-Fc recombinant protein with mobile DL4-μbeads (111), providing a cell suspension culture applicable for scale up production. The second is coupling the system with histone methyltransferase EZH1 repression (112). The final harvested EZ-T cells showed similar molecular features to peripheral blood αβ T cells, and displayed effector and memory-like phenotypes after

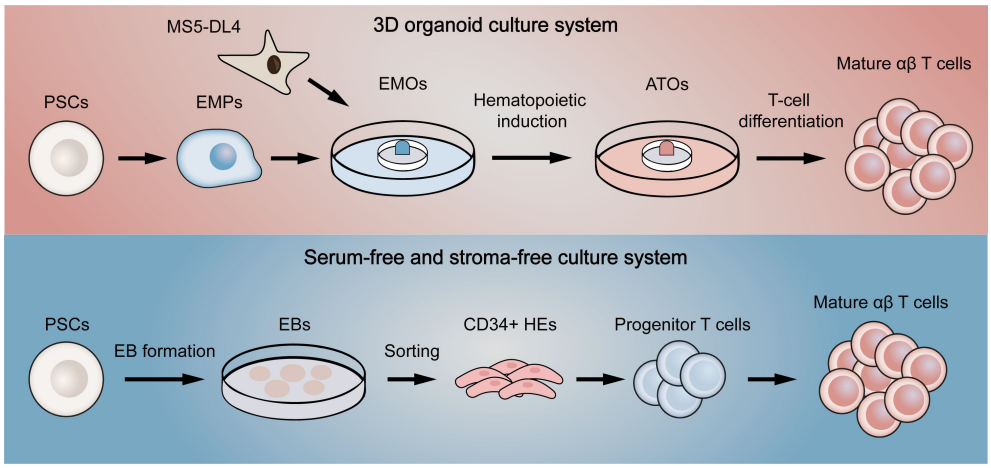

FIGURE 4
Two novel differentiation systems for generation T cells from pluripotent stem cells. The above (red) briefly summarizes the flow of the 3D organoid culture system. EMPs differentiated by PSCs are first co-cultured with DL4-expressing MS5 cells to form EMOs. After hematopoietic induction, ATOs are then formed. Finally, T-cell differentiation is fulfilled to generate single-positive T cells. The below (blue) represents the serum-free and stroma-free culture system. PSCs are first differentiated into EBs. CD34-positive HEs are then obtained by dissociating EBs, which later gradually differentiate into progenitor T cells, double-positive T cells and finally mature as single-positive T cells. EMPs, embryonic mesodermal progenitor cells; EMOs, embryonic mesodermal organoids; ATOs, artificial thymus organoids; EBs, embryoid bodies; HEs, hemogenic endothelial cells.

activation. Besides, CAR-T cells based on EZ-T exhibited robust antitumor activity in mouse models. In summary, mature CAR-T cells can be efficiently generated from PSCs nowadays, greatly facilitating the path to 'off-the-shelf' allogeneic CAR-T cell therapy.

5 Conclusion and perspectives

Although the elimination of GvHD and host-mediated rejection has enabled the clinical application of allogeneic CAR-T cell therapy, other challenges will also affect the safety and efficacy of the treatment. The clinical applications of allogeneic CAR-αβT products are made possible by a series of technologies inhibiting the occurrence of GvHD and host rejection, which prevent the damage to normal tissues and rapid clearance of allogeneic CAR-T cells in patients. However, neither gene knockout nor mRNA silencing can achieve complete removal of TCR from cell population (113). Additional depletion of remaining TCR^+ cells is inevitable in clinic manufacture, which largely determines efficacy and toxicity. These complicated and time-consuming profiles limit the function of T cells, suggesting the importance to shorten *in vitro* manufacturing workflows by improving T cell culture technology or optimizing the processes. For other T cell subsets with low frequency and PSC-derived T cells, optimal strategies for expansion or differentiation systems are needed to explore. For example, further investigations of how gene networks manipulate key events in T cell development, such as T-cell lineage specification and commitment, β selection and positive selection, may help understand what shapes T cell fate. By promoting or inhibiting functions of some important genes in differentiation system, the number, phenotype and function in final products may be profoundly affected. In addition, previous research confirmed the importance of signals from TCR to maintain T cell homeostasis and long-term survival *in vivo* (114). A clinical study also showed limited efficiency and persistence of allogeneic CAR-T cells relative to autologous CAR-T cells (115). This deficiency not only affects the antitumor efficacy, but also implies the possibility of repeated dosing and consequent lymphodepletion, putting additional burdens on patients. Taken together, maintaining the long-term survival of allogeneic CAR-T cells *in vivo* will inevitably require the introduction of new modification strategies, such as modifying the CAR structure to attenuate CAR signaling or modulating the metabolic profiles to improve the persistence of allogeneic CAR-T cells.

Allogeneic CAR-T platform has facilitated the shift from customization to generalization of CAR-T cell therapy in cell source, meeting the urgent need of patients both in cell quality and delivery time. While many hurdles remain along the way, 'off-the-shelf' allogeneic CAR-T cell therapy has yielded promising results so far and has great possibilities waiting to be discovered due to their properties in addressing the pain points of autologous CAR-T therapy.

Author contributions

ZL, FL, and YC wrote, critically reviewed, and edited the manuscript. All authors contributed to the article and approved the submitted version.

Funding

This work was supported by the National Natural Science Foundation of China (82130050, 82121002).

Conflict of interest

The authors declare that the research was conducted in the absence of any commercial or financial relationships that could be construed as a potential conflict of interest.

Publisher's note

References

1. Lu J, Jiang G. The journey of CAR-T therapy in hematological malignancies. *Mol Canc* (2022) 21(1):194. doi: 10.1186/s12943-022-01663-0

2. Young RM, Engel NW, Uslu U, Wellhausen N, June CH. Next-generation CAR T-cell therapies. *Cancer Discov* (2022) 12(7):1625–33. doi: 10.1158/2159-8290.CD-21-1683

3. Mullard A. FDA approves second BCMA-targeted CAR-T cell therapy. *Nat Rev Drug Discov* (2022) 21(4):249. doi: 10.1038/d41573-022-00048-8

4. Roddie C, O'Reilly M, Dias Alves Pinto J, Vispute K, Lowdell M. Manufacturing chimeric antigen receptor T cells: issues and challenges. *Cytotherapy* (2019) 21(3):327–40. doi: 10.1016/j.jcyt.2018.11.009

5. Dai X, Mei Y, Cai D, Han W. Standardizing CAR-T therapy: Getting it scaled up. *Biotechnol Adv* (2019) 37(1):239–45. doi: 10.1016/j.biotechadv.2018.12.002

6. Shah NN, Fry TJ. Mechanisms of resistance to CAR T cell therapy. *Nat Rev Clin Oncol* (2019) 16(6):372–85. doi: 10.1038/s41571-019-0184-6

7. Philip M, Schietinger A. CD8(+) T cell differentiation and dysfunction in cancer. *Nat Rev Immunol* (2022) 22(4):209–23. doi: 10.1038/s41577-021-00574-3

8. Graham C, Jozwik A, Pepper A, Benjamin R. Allogeneic CAR-T cells: more than ease of access? *Cells* (2018) 7(10):155. doi: 10.3390/cells7100155

9. Depil S, Duchateau P, Grupp SA, Mufti G, Poirot L. 'Off-the-shelf' allogeneic CAR T cells: development and challenges. *Nat Rev Drug Discov* (2020) 19(3):185–99.

10. Ferrara JL, Deeg HJ. Graft-versus-host disease. *N Engl J Med* (1991) 324 (10):667–74. doi: 10.1056/NEJM199103073241005

11. Shiina T, Hosomichi K, Inoko H, Kulski JK. The HLA genomic loci map: expression, interaction, diversity and disease. *J Hum Genet* (2009) 54(1):15–39. doi: 10.1038/jhg.2008.5

12. Vivier E, Tomasello E, Baratin M, Walzer T, Ugolini S. Functions of natural killer cells. *Nat Immunol* (2008) 9(5):503–10. doi: 10.1038/ni1582

13. Gravina A, Tediashvili G, Rajalingam R, Quandt Z, Deisenroth C, Schrepfer S, et al. Protection of cell therapeutics from antibody-mediated killing by CD64 overexpression. *Nat Biotechnol* (2023) 41(5):717–27. doi: 10.1038/s41587-022-01540-7

14. Kim S, Hupperetz C, Lim S, Kim CH. Genome editing of immune cells using CRISPR/Cas9. *BMB Rep* (2021) 54(1):59–69. doi: 10.5483/BMBRep.2021.54.1.245

15. Torikai H, Reik A, Liu PQ, Zhou Y, Zhang L, Maiti S, et al. A foundation for universal T-cell based immunotherapy: T cells engineered to express a CD19-specific chimeric-antigen-receptor and eliminate expression of endogenous TCR. *Blood* (2012) 119(24):5697–705. doi: 10.1182/blood-2012-01-405365

16. Kagoya Y, Guo T, Yeung B, Saso K, Anczurowski M, Wang CH, et al. Genetic ablation of HLA class I, class II, and the T-cell receptor enables allogeneic T cells to be used for adoptive T-cell therapy. *Cancer Immunol Res* (2020) 8(7):926–36. doi: 10.1158/2326-6066.CIR-18-0508

17. Dimitri A, Herbst F, Fraietta JA. Engineering the next-generation of CAR T-cells with CRISPR-Cas9 gene editing. *Mol Canc* (2022) 21(1):78. doi: 10.1186/s12943-022-01559-z

18. Eyquem J, Mansilla-Soto J, Giavridis T, van der Stegen SJ, Hamieh M, Cunanan KM, et al. Targeting a CAR to the TRAC locus with CRISPR/Cas9 enhances tumour rejection. *Nature* (2017) 543(7643):113–7. doi: 10.1038/nature21405

19. Liu X, Zhang Y, Cheng C, Cheng AW, Zhang X, Li N, et al. CRISPR-Cas9-mediated multiplex gene editing in CAR-T cells. *Cell Res* (2017) 27(1):154–7. doi: 10.1038/cr.2016.142

20. Ren J, Liu X, Fang C, Jiang S, June CH, Zhao Y. Multiplex genome editing to generate universal CAR T cells resistant to PD1 inhibition. *Clin Cancer Res* (2017) 23(9):2255–66. doi: 10.1158/1078-0432.CCR-16-1300

21. Poirot L, Philip B, Schiffer-Mannioui C, Le Clerre D, Chion-Sotinel I, Derniame S, et al. Multiplex genome-edited T-cell manufacturing platform for "Off-the-shelf" Adoptive T-cell immunotherapies. *Cancer Res* (2015) 75(18):3853–64. doi: 10.1158/0008-5472.CAN-14-3321

22. Mailankody S, Matous JV, Chhabra S, Liedtke M, Sidana S, Oluwole OO, et al. Allogeneic BCMA-targeting CAR T cells in relapsed/refractory multiple myeloma: phase 1 UNIVERSAL trial interim results. *Nat Med* (2023) 29(2):422–9. doi: 10.1038/s41591-023-02306-7

23. Gornalusse GG, Hirata RK, Funk SE, Riolobos L, Lopes VS, Manske G, et al. HLA-E-expressing pluripotent stem cells escape allogeneic responses and lysis by NK cells. *Nat Biotechnol* (2017) 35(8):765–72. doi: 10.1038/nbt.3860

24. Guo Y, Xu B, Wu Z, Bo J, Tong C, Chen D, et al. Mutant B2M-HLA-E and B2M-HLA-G fusion proteins protects universal chimeric antigen receptor-modified T cells from allogeneic NK cell-mediated lysis. *Eur J Immunol* (2021) 51(10):2513–21. doi: 10.1002/eji.202049107

25. Xu H, Wang B, Ono M, Kagita A, Fujii K, Sasakawa N, et al. Targeted Disruption of HLA Genes via CRISPR-Cas9 Generates iPSCs with Enhanced Immune Compatibility. *Cell Stem Cell* (2019) 24(4):566–78.e7. doi: 10.1016/j.stem.2019.02.005

26. Mach B, Steimle V, Martinez-Soria E, Reith W. Regulation of MHC class II genes: lessons from a disease. *Annu Rev Immunol* (1996) 14:301–31. doi: 10.1146/annurev.immunol.14.1.301

27. Holling TM, van der Stoep N, Quinten E, van den Elsen PJ. Activated human T cells accomplish MHC class II expression through T cell-specific occupation of class II transactivator promoter III. *J Immunol* (2002) 168(2):763–70. doi: 10.4049/jimmunol.168.2.763

28. Wright KL, Ting JP. Epigenetic regulation of MHC-II and CIITA genes. *Trends Immunol* (2006) 27(9):405–12. doi: 10.1016/j.it.2006.07.007

29. Surmann EM, Voigt AY, Michel S, Bauer K, Reuschenbach M, Ferrone S, et al. Association of high CD4-positive T cell infiltration with mutations in HLA class II-regulatory genes in microsatellite-unstable colorectal cancer. *Cancer Immunol Immunother* (2015) 64(3):357–66. doi: 10.1007/s00262-014-1638-4

30. Hu Y, Zhou Y, Zhang M, Zhao H, Wei G, Ge W, et al. Genetically modified CD7-targeting allogeneic CAR-T cell therapy with enhanced efficacy for relapsed/refractory CD7-positive hematological malignancies: a phase I clinical study. *Cell Res* (2022) 32(11):995–1007. doi: 10.1038/s41422-022-00721-y

31. Dai Z, Mu W, Zhao Y, Cheng J, Lin H, Ouyang K, et al. T cells expressing CD5/CD7 bispecific chimeric antigen receptors with fully human heavy-chain-only domains mitigate tumor antigen escape. *Signal Transduct Target Ther* (2022) 7(1):85. doi: 10.1038/s41392-022-00898-z

32. Sugita M, Galetto R, Zong H, Ewing-Crystal N, Trujillo-Alonso V, Mencia-Trinchant N, et al. Allogeneic TCRalphabeta deficient CAR T-cells targeting CD123 in acute myeloid leukemia. *Nat Commun* (2022) 13(1):2227.

33. Jo S, Das S, Williams A, Chretien AS, Pagliardini T, Le Roy A, et al. Endowing universal CAR T-cell with immune-evasive properties using TALEN-gene editing. *Nat Commun* (2022) 13(1):3453. doi: 10.1038/s41467-022-30896-2

34. Ottaviano G, Georgiadis C, Gkazi SA, Syed F, Zhan H, Etuk A, et al. Phase 1 clinical trial of CRISPR-engineered CAR19 universal T cells for treatment of children with refractory B cell leukemia. *Sci Transl Med* (2022) 14(668):eabq3010. doi: 10.1126/scitranslmed.abq3010

35. Hu Y, Zhou Y, Zhang M, Ge W, Li Y, Yang L, et al. CRISPR/cas9-engineered universal CD19/CD22 dual-targeted CAR-T cell therapy for relapsed/refractory B-cell acute lymphoblastic leukemia. *Clin Cancer Res* (2021) 27(10):2764–72. doi: 10.1158/1078-0432.CCR-20-3863

36. Li S, Wang X, Yuan Z, Liu L, Luo L, Li Y, et al. Eradication of T-ALL cells by CD7-targeted universal CAR-T cells and initial test of ruxolitinib-based CRS management. *Clin Cancer Res* (2021) 27(5):1242–6. doi: 10.1158/1078-0432.CCR-20-1271

37. Benjamin R, Jain N, Maus MV, Boissel N, Graham C, Jozwik A, et al. UCART19, a first-in-class allogeneic anti-CD19 chimeric antigen receptor T-cell therapy for adults with relapsed or refractory B-cell acute lymphoblastic leukaemia (CALM): a phase 1, dose-escalation trial. *Lancet Haematol* (2022) 9(11):e833–43. doi: 10.1016/S2352-3026(22)00245-9

38. Haapaniemi E, Botla S, Persson J, Schmierer B, Taipale J. CRISPR-Cas9 genome editing induces a p53-mediated DNA damage response. *Nat Med* (2018) 24(7):927–30. doi: 10.1038/s41591-018-0049-z

39. Ihry RJ, Worringer KA, Salick MR, Frias E, Ho D, Theriault K, et al. p53 inhibits CRISPR-Cas9 engineering in human pluripotent stem cells. *Nat Med* (2018) 24(7):939–46. doi: 10.1038/s41591-018-0050-6

40. Sinha S, Barbosa K, Cheng K, Leiserson MDM, Jain P, Deshpande A, et al. A systematic genome-wide mapping of oncogenic mutation selection during CRISPR-Cas9 genome editing. *Nat Commun* (2021) 12(1):6512. doi: 10.1038/s41467-021-26788-6

41. Leibowitz ML, Papathanasiou S, Doerfler PA, Blaine LJ, Sun L, Yao Y, et al. Chromothripsis as an on-target consequence of CRISPR-Cas9 genome editing. *Nat Genet* (2021) 53(6):895–905. doi: 10.1038/s41588-021-00838-7

42. Kosicki M, Tomberg K, Bradley A. Repair of double-strand breaks induced by CRISPR-Cas9 leads to large deletions and complex rearrangements. *Nat Biotechnol* (2018) 36(8):765–71. doi: 10.1038/nbt.4192

43. Nahmad AD, Reuveni E, Goldschmidt E, Tenne T, Liberman M, Horovitz-Fried M, et al. Frequent aneuploidy in primary human T cells after CRISPR-Cas9 cleavage. *Nat Biotechnol* (2022) 40(12):1807–13. doi: 10.1038/s41587-022-01377-0

44. Stadtmauer EA, Fraietta JA, Davis MM, Cohen AD, Weber KL, Lancaster E, et al. CRISPR-engineered T cells in patients with refractory cancer. *Science* (2020) 367(6481):eaba7365. doi: 10.1126/science.aba7365

45. Alcover A, Alarcon B, Di Bartolo V. Cell biology of T cell receptor expression and regulation. *Annu Rev Immunol* (2018) 36:103–25. doi: 10.1146/annurev-immunol-042617-053429

46. Al-Homsi A-S, Anguille S, Deeren D, Nishihori T, Meuleman N, Abdul-Hay M, et al. Immunicy-1: targeting BCMA with cyad-211 to establish proof of concept of an shRNA-based allogeneic CAR T cell therapy platform. *Blood* (2021) 138(Supplement 1):2817. doi: 10.1182/blood-2021-147738

47. Alarcon B, Berkhout B, Breitmeyer J, Terhorst C. Assembly of the human T cell receptor-CD3 complex takes place in the endoplasmic reticulum and involves intermediary complexes between the CD3-gamma.delta.epsilon core and single T cell receptor alpha or beta chains. *J Biol Chem* (1988) 263(6):2953–61.

48. Kamiya T, Wong D, Png YT, Campana D. A novel method to generate T-cell receptor-deficient chimeric antigen receptor T cells. *Blood Adv* (2018) 2(5):517–28. doi: 10.1182/bloodadvances.2017012823

49. Prenen H, Dekervel J, Anguille S, Hendlisz A, Michaux A, Sotiropoulou PA, et al. CYAD-101: An innovative non-gene edited allogeneic CAR-T for solid tumor cancer therapy. *J Clin Oncol* (2020) 38(15_suppl):3032. doi: 10.1200/JCO.2020.38.15_suppl.3032

50. Michaux A, Mauën S, Breman E, Dheur MS, Twyffels L, Saerens L, et al. Clinical grade manufacture of CYAD-101, a NKG2D-based, first in class, non-gene-edited allogeneic CAR T-cell therapy. *J Immunother Canc* (2022) 45(3):150–61. doi: 10.1097/CJI.0000000000000413

51. Watts TH. TNF/TNFR family members in costimulation of T cell responses. *Annu Rev Immunol* (2005) 23(1):23–68. doi: 10.1146/annurev.immunol.23.021704.115839

52. Chester C, Sanmamed MF, Wang J, Melero I. Immunotherapy targeting 4-1BB: mechanistic rationale, clinical results, and future strategies. *Blood* (2018) 131(1):49–57. doi: 10.1182/blood-2017-06-741041

53. Mo F, Watanabe N, McKenna MK, Hicks MJ, Srinivasan M, Gomes-Silva D, et al. Engineered off-the-shelf therapeutic T cells resist host immune rejection. *Nat Biotechnol* (2021) 39(1):56–63. doi: 10.1038/s41587-020-0601-5

54. Rosshart S, Hofmann M, Schweier O, Pfaff AK, Yoshimoto K, Takeuchi T, et al. Interaction of KLRG1 with E-cadherin: new functional and structural insights. *Eur J Immunol* (2008) 38(12):3354–64. doi: 10.1002/eji.200838690

55. Deuse T, Hu X, Gravina A, Wang D, Tediashvili G, De C, et al. Hypoimmunogenic derivatives of induced pluripotent stem cells evade immune rejection in fully immunocompetent allogeneic recipients. *Nat Biotechnol* (2019) 37(3):252–8. doi: 10.1038/s41587-019-0016-3

56. Deuse T, Hu X, Agbor-Enoh S, Jang MK, Alawi M, Saygi C, et al. The SIRPα-CD47 immune checkpoint in NK cells. *J Exp Med* (2021) 218(3):e20200839. doi: 10.1084/jem.20200839

57. Ramos CA, Courtney AN, Robinson SN, Dakhova O, Lulla PD, Kamble R, et al. Allogeneic NKT cells expressing a CD19-specific CAR in patients with relapsed or refractory B-cell malignancies: an interim analysis. *Blood* (2021) 138(Supplement 1):2819–. doi: 10.1182/blood-2021-149712

58. Sánchez Martínez D, Tirado N, Mensurado S, Martínez-Moreno A, Romecín P, Gutiérrez Agüera F, et al. Generation and proof-of-concept for allogeneic CD123 CAR-

Delta One T (DOT) cells in acute myeloid leukemia. *J ImmunoTherapy Cancer* (2022) 10(9):e005400. doi: 10.1136/jitc-2022-005400

59. Makkouk A, Yang X, Barca T, Lucas A, Turkoz M, Wong JTS, et al. Off-the-shelf Vδ1 gamma delta T cells engineered with glypican-3 (GPC-3)-specific chimeric antigen receptor (CAR) and soluble IL-15 display robust antitumor efficacy against hepatocellular carcinoma. *J ImmunoTherapy Cancer* (2021) 9(12):e003441. doi: 10.1136/jitc-2021-003441

60. Nishimoto KP, Barca T, Azameera A, Makkouk A, Romero JM, Bai L, et al. Allogeneic CD20-targeted γδ T cells exhibit innate and adaptive antitumor activities in preclinical B-cell lymphoma models. *Clin Trans Immunol* (2022) 11(2):e1373. doi: 10.1002/cti2.1373

61. Yang L, Wang D, Xu S, Wang L, Tong J, Zhu H, et al. Abstract 5510: Preclinical study of allogeneic CD19-CAR-DNT cells as an off-the-shelf immunotherapy drug for NHL. *Cancer Res* (2022) 82(12_Supplement):5510–. doi: 10.1158/1538-7445.AM2022-5510

62. Mehta A, Farooq U, Chen A, McGuirk JP, Ly T, Wong L, et al. Interim phase I clinical data of FT819-101, a study of the first-ever, off-the-shelf, iPSC-derived TCR-less CD19 CAR T-cell therapy for patients with relapsed/refractory B-cell malignancies. *Blood* (2022) 140(Supplement 1):4577–8. doi: 10.1182/blood-2022-167194

63. Zhang Y, Springfield R, Chen S, Li X, Feng X, Moshirian R, et al. α-GalCer and iNKT cell-based cancer immunotherapy: realizing the therapeutic potentials. *Front Immunol* (2019) 10:1126. doi: 10.3389/fimmu.2019.01126

64. Heczey A, Liu D, Tian G, Courtney AN, Wei J, Marinova E, et al. Invariant NKT cells with chimeric antigen receptor provide a novel platform for safe and effective cancer immunotherapy. *Blood* (2014) 124(18):2824–33. doi: 10.1182/blood-2013-11-541235

65. Xu X, Huang W, Heczey A, Liu D, Guo L, Wood M, et al. NKT cells coexpressing a GD2-specific chimeric antigen receptor and IL15 show enhanced *in vivo* persistence and antitumor activity against neuroblastoma. *Clin Cancer Res* (2019) 25(23):7126–38. doi: 10.1158/1078-0432.CCR-19-0421

66. Rotolo A, Caputo VS, Holubova M, Baxan N, Dubois O, Chaudhry MS, et al. Enhanced anti-lymphoma activity of CAR19-iNKT cells underpinned by dual CD19 and CD1d targeting. *Cancer Cell* (2018) 34(4):596–610.e11. doi: 10.1016/j.ccell.2018.08.017

67. Look A, Burns D, Tews I, Roghanian A, Mansour S. Towards a better understanding of human iNKT cell subpopulations for improved clinical outcomes. *Front Immunol* (2023) 14:1176724. doi: 10.3389/fimmu.2023.1176724

68. Heczey A, Courtney AN, Montalbano A, Robinson S, Liu K, Li M, et al. Anti-GD2 CAR-NKT cells in patients with relapsed or refractory neuroblastoma: an interim analysis. *Nat Med* (2020) 26(11):1686–90. doi: 10.1038/s41591-020-1074-2

69. Jahnke S, Schmid H, Secker KA, Einhaus J, Duerr-Stoerzer S, Keppeler H, et al. Invariant NKT Cells From Donor Lymphocyte Infusions (DLI-iNKTs) Promote *ex vivo* Lysis of Leukemic Blasts in a CD1d-Dependent Manner. *Front Immunol* (2019) 10:1542. doi: 10.3389/fimmu.2019.01542

70. Montoya CJ, Pollard D, Martinson J, Kumari K, Wasserfall C, Mulder CB, et al. Characterization of human invariant natural killer T subsets in health and disease using a novel invariant natural killer T cell-clonotypic monoclonal antibody, 6B11. *Immunology* (2007) 122(1):1–14. doi: 10.1111/j.1365-2567.2007.02647.x

71. Ngai H, Tian G, Courtney AN, Ravari SB, Guo L, Liu B, et al. IL-21 selectively protects CD62L(+) NKT cells and enhances their effector functions for adoptive immunotherapy. *J Immunol* (2018) 201(7):2141–53. doi: 10.4049/jimmunol.1800429

72. Kabelitz D, Serrano R, Kouakanou L, Peters C, Kalyan S. Cancer immunotherapy with γδ T cells: many paths ahead of us. *Cell Mol Immunol* (2020) 17(9):925–39. doi: 10.1038/s41423-020-0504-x

73. Dong R, Zhang Y, Xiao H, Zeng X. Engineering γδ T cells: recognizing and activating on their own way. *Front Immunol* (2022) 13.

74. Mensurado S, Blanco-Domínguez R, Silva-Santos B. The emerging roles of γδ T cells in cancer immunotherapy. *Nat Rev Clin Oncol* (2023) 20(3):178–91. doi: 10.1038/s41571-022-00722-1

75. Handgretinger R, Schilbach K. The potential role of γδ T cells after allogeneic HCT for leukemia. *Blood* (2018) 131(10):1063–72. doi: 10.1182/blood-2017-08-752162

76. Andrlová H, Miltiadous O, Kousa AI, Dai A, DeWolf S, Violante S, et al. MAIT and Vδ2 unconventional T cells are supported by a diverse intestinal microbiome and correlate with favorable patient outcome after allogeneic HCT. *Sci Trans Med* (2022) 14(646):eabj2829. doi: 10.1126/scitranslmed.abj2829

77. Capsomidis A, Benthall G, Van Acker HH, Fisher J, Kramer AM, Abeln Z, et al. Chimeric antigen receptor-engineered human gamma delta T cells: enhanced cytotoxicity with retention of cross presentation. *Mol Ther* (2018) 26(2):354–65. doi: 10.1016/j.ymthe.2017.12.001

78. Rozenbaum M, Meir A, Aharony Y, Itzhaki O, Schachter J, Bank I, et al. Gamma-delta CAR-T cells show CAR-directed and independent activity against leukemia. *Front Immunol* (2020) 11. doi: 10.3389/fimmu.2020.01347

79. Merims S, Li X, Joe B, Dokouhaki P, Han M, Childs RW, et al. Anti-leukemia effect of *ex vivo* expanded DNT cells from AML patients: a potential novel autologous T-cell adoptive immunotherapy. *Leukemia* (2011) 25(9):1415–22. doi: 10.1038/leu.2011.99

80. Wu Z, Zheng Y, Sheng J, Han Y, Yang Y, Pan H, et al. CD3+CD4-CD8- (Double-negative) T cells in inflammation, immune disorders and cancer. *Front Immunol* (2022) 13. doi: 10.3389/fimmu.2022.816005

81. Young KJ, Kay LS, Phillips MJ, Zhang L. Antitumor activity mediated by double-negative T cells. *Cancer Res* (2003) 63(22):8014–21.

82. Lee J, Minden MD, Chen WC, Streck E, Chen B, Kang H, et al. Allogeneic human double negative T cells as a novel immunotherapy for acute myeloid leukemia and its underlying mechanisms. *Clin Cancer Res* (2018) 24(2):370–82. doi: 10.1158/1078-0432.CCR-17-2228

83. Lee JB, Kang H, Fang L, D'Souza C, Adeyi O, Zhang L. Developing allogeneic double-negative T cells as a novel off-the-shelf adoptive cellular therapy for cancer. *Clin Cancer Res* (2019) 25(7):2241–53. doi: 10.1158/1078-0432.CCR-18-2291

84. Yao J, Ly D, Dervovic D, Fang L, Lee JB, Kang H, et al. Human double negative T cells target lung cancer via ligand-dependent mechanisms that can be enhanced by IL-15. *J ImmunoTherapy Cancer* (2019) 7(1):17. doi: 10.1186/s40425-019-0507-2

85. Fang L, Ly D, Wang S-S, JB L, Kang H, Xu H, et al. Targeting late-stage non-small cell lung cancer with a combination of DNT cellular therapy and PD-1 checkpoint blockade. *J Exp Clin Cancer Res* (2019) 38(1):123. doi: 10.1186/s13046-019-1126-y

86. Baolin T, Lee J, Cheng S, Yao W, Wang D, Tu M, et al. Safety and Efficacy of Ex Vivo Expanded Healthy Donor-Derived Double Negative T Cells for the Treatment of AML Relapsed after Allogeneic Stem Cell Transplantation: A First in-Human Phase I/IIa Clinical Trial. *Blood* (2020) 136(Supplement 1):1–2. doi: 10.1182/blood-2020-141505

87. Sun X, Zhang C, Sun F, Li S, Wang Y, Wang T, et al. IL-33 promotes double negative T cell survival via the NF-kappaB pathway. *Cell Death Dis* (2023) 14(4):242.

88. Vasic D, Lee JB, Leung Y, Khatri I, Na Y, Abate-Daga D, et al. Allogeneic double-negative CAR-T cells inhibit tumor growth without off-tumor toxicities. *Sci Immunol* (2022) 7(70):eabl3642. doi: 10.1126/sciimmunol.abl3642

89. Chen Z, Wang H, D'Souza C, Sun S, Kostenko L, Eckle SB, et al. Mucosal-associated invariant T-cell activation and accumulation after in *vivo* infection depends on microbial riboflavin synthesis and co-stimulatory signals. *Mucosal Immunol* (2017) 10(1):58–68. doi: 10.1038/mi.2016.39

90. Li YR, Wilson M, Yang L. Target tumor microenvironment by innate T cells. *Front Immunol* (2022) 13:999549. doi: 10.3389/fimmu.2022.999549

91. Legoux F, Salou M, Lantz O. MAIT cell development and functions: the microbial connection. *Immunity* (2020) 53(4):710–23. doi: 10.1016/j.immuni.2020.09.009

92. Dusseaux M, Martin E, Serriari N, Peguillet I, Premel V, Louis D, et al. Human MAIT cells are xenobiotic-resistant, tissue-targeted, CD161hi IL-17-secreting T cells. *Blood* (2011) 117(4):1250–9. doi: 10.1182/blood-2010-08-303339

93. Tourret M, Talvard-Balland N, Lambert M, Ben Youssef G, Chevalier MF, Bohineust A, et al. Human MAIT cells are devoid of alloreactive potential: prompting their use as universal cells for adoptive immune therapy. *J Immunother Cancer* (2021) 9(10):e003123. doi: 10.1136/jitc-2021-003123

94. Li YR, Zhou K, Wilson M, Kramer A, Zhu Y, Dawson N, et al. Mucosal-associated invariant T cells for cancer immunotherapy. *Mol Ther* (2023) 31(3):631–46. doi: 10.1016/j.ymthe.2022.11.019

95. Dogan M, Karhan E, Kozhaya L, Placek L, Chen X, Yigit M, et al. Engineering human MAIT cells with chimeric antigen receptors for cancer immunotherapy. *J Immunol* (2022) 209(8):1523–31. doi: 10.4049/jimmunol.2100856

96. Priya R, Brutkiewicz RR. MR1 tetramer-based artificial APCs expand MAIT cells from human peripheral blood that effectively kill glioblastoma cells. *Immunohorizons* (2021) 5(6):500–11. doi: 10.4049/immunohorizons.2100003

97. Parrot T, Healy K, Boulouis C, Sobkowiak MJ, Leeansyah E, Aleman S, et al. Expansion of donor-unrestricted MAIT cells with enhanced cytolytic function suitable for TCR redirection. *JCI Insight* (2021) 6(5):e140074. doi: 10.1172/jci.insight.140074

98. Wang B, Iriguchi S, Waseda M, Ueda N, Ueda T, Xu H, et al. Generation of hypoimmunogenic T cells from genetically engineered allogeneic human induced pluripotent stem cells. *Nat BioMed Eng* (2021) 5(5):429–40. doi: 10.1038/s41551-021-00730-z

99. Themeli M, Rivière I, Sadelain M. New cell sources for T cell engineering and adoptive immunotherapy. *Cell Stem Cell* (2015) 16(4):357–66. doi: 10.1016/j.stem.2015.03.011

100. Schmitt TM, de Pooter RF, Gronski MA, Cho SK, Ohashi PS, Zúñiga-Pflücker JC. Induction of T cell development and establishment of T cell competence from embryonic stem cells differentiated *in vitro*. *Nat Immunol* (2004) 5(4):410–7. doi: 10.1038/ni1055

101. Nakano T, Kodama H, Honjo T. Generation of lymphohematopoietic cells from embryonic stem cells in culture. *Science* (1994) 265(5175):1098–101. doi: 10.1126/science.8066449

102. Schmitt TM, Zúñiga-Pflücker JC. Induction of T cell development from hematopoietic progenitor cells by delta-like-1 *in vitro*. *Immunity* (2002) 17(6):749–56. doi: 10.1016/S1074-7613(02)00474-0

103. Tian X, Woll PS, Morris JK, Linehan JL, Kaufman DS. Hematopoietic engraftment of human embryonic stem cell-derived cells is regulated by recipient innate immunity. *Stem Cells* (2006) 24(5):1370–80. doi: 10.1634/stemcells.2005-0340

104. Kennedy M, Awong G, Sturgeon CM, Ditadi A, LaMotte-Mohs R, Zuniga-Pflucker JC, et al. T lymphocyte potential marks the emergence of definitive hematopoietic progenitors in human pluripotent stem cell differentiation cultures. *Cell Rep* (2012) 2(6):1722–35. doi: 10.1016/j.celrep.2012.11.003

105. Iriguchi S, Yasui Y, Kawai Y, Arima S, Kunitomo M, Sato T, et al. A clinically applicable and scalable method to regenerate T-cells from iPSCs for off-the-shelf T-cell immunotherapy. *Nat Commun* (2021) 12(1):430. doi: 10.1038/s41467-020-20658-3

106. Galat Y, Dambaeva S, Elcheva I, Khanolkar A, Beaman K, Iannaccone PM, et al. Cytokine-free directed differentiation of human pluripotent stem cells efficiently produces hemogenic endothelium with lymphoid potential. *Stem Cell Res Ther* (2017) 8 (1):67. doi: 10.1186/s13287-017-0519-0

107. Elcheva I, Brok-Volchanskaya V, Kumar A, Liu P, Lee JH, Tong L, et al. Direct induction of haematoendothelial programs in human pluripotent stem cells by transcriptional regulators. *Nat Commun* (2014) 5:4372. doi: 10.1038/ncomms5372

108. Timmermans F, Velghe I, Vanwalleghem L, De Smedt M, Van Coppernolle S, Taghon T, et al. Generation of T cells from human embryonic stem cell-derived hematopoietic zones. *J Immunol* (2009) 182(11):6879–88. doi: 10.4049/jimmunol.0803670

109. Montel-Hagen A, Seet CS, Li S, Chick B, Zhu Y, Chang P, et al. Organoid-induced differentiation of conventional T cells from human pluripotent stem cells. *Cell Stem Cell* (2019) 24(3):376–89.e8. doi: 10.1016/j.stem.2018.12.011

110. Wang Z, McWilliams-Koeppen HP, Reza H, Ostberg JR, Chen W, Wang X, et al. 3D-organoid culture supports differentiation of human CAR+ iPSCs into highly functional CAR T cells. *Cell Stem Cell* (2022) 29(4):515–27.e8. doi: 10.1016/j.stem.2022.02.009

111. Trotman-Grant AC, Mohtashami M, De Sousa Casal J, Martinez EC, Lee D, Teichman S, et al. DL4-μbeads induce T cell lineage differentiation from stem cells in a stromal cell-free system. *Nat Commun* (2021) 12(1):5023.

112. Jing R, Scarfo I, Najia MA, Lummertz da Rocha E, Han A, Sanborn M, et al. EZH1 repression generates mature iPSC-derived CAR T cells with enhanced antitumor activity. *Cell Stem Cell* (2022) 29(8):1181–96e6. doi: 10.1016/j.stem.2022.06.014

113. Qasim W, Zhan H, Samarasinghe S, Adams S, Amrolia P, Stafford S, et al. Molecular remission of infant B-ALL after infusion of universal TALEN gene-edited CAR T cells. *Sci Transl Med* (2017) 9(374). doi: 10.1126/scitranslmed.aaj2013

114. Stenger D, Stief TA, Kaeuferle T, Willier S, Rataj F, Schober K, et al. Endogenous TCR promotes in *vivo* persistence of CD19-CAR-T cells compared to a CRISPR/Cas9-mediated TCR knockout CAR. *Blood* (2020) 136(12):1407–18. doi: 10.1182/blood.2020005185

115. DiNofia AM, Grupp SA. Will allogeneic CAR T cells for CD19(+) malignancies take autologous CAR T cells 'off the shelf'? *Nat Rev Clin Oncol* (2021) 18(4):195–6. doi: 10.1038/s41571-021-00485-1

frontiers | Frontiers in Immunology

TYPE Original Research
PUBLISHED 13 November 2023
DOI 10.3389/fimmu.2023.1294555

OPEN ACCESS

EDITED BY
Daniel Abate-Daga,
Moffitt Cancer Center, United States

REVIEWED BY
Nelli Bejanyan,
Moffitt Cancer Center, United States
Jeffrey A. Medin,
Medical College of Wisconsin,
United States

*CORRESPONDENCE
H. Trent Spencer
hspence@emory.edu

RECEIVED 14 September 2023
ACCEPTED 26 October 2023
PUBLISHED 13 November 2023

CITATION
Branella GM, Lee JY, Okalova J, Parwani KK, Alexander JS, Arthuzo RF, Fedanov A, Yu B, McCarty D, Brown HC, Chandrakasan S, Petrich BG, Doering CB and Spencer HT (2023) Ligand-based targeting of c-kit using engineered γδ T cells as a strategy for treating acute myeloid leukemia. *Front. Immunol.* 14:1294555. doi: 10.3389/fimmu.2023.1294555

Ligand-based targeting of c-kit using engineered γδ T cells as a strategy for treating acute myeloid leukemia

Gianna M. Branella[1,2,3], Jasmine Y. Lee[1,2,3], Jennifer Okalova[1,3,4], Kiran K. Parwani[1,2,3], Jordan S. Alexander[1,3], Raquel F. Arthuzo[1,2,3], Andrew Fedanov[1,3], Bing Yu[5], David McCarty[5], Harrison C. Brown[5], Shanmuganathan Chandrakasan[1,3], Brian G. Petrich[5], Christopher B. Doering[1,3,4] and H. Trent Spencer[1,3,4]*

[1]Department of Pediatrics, Emory University School of Medicine, Atlanta, GA, United States, [2]Graduate Division of Biological and Biomedical Sciences, Laney Graduate School, Emory University, Atlanta, GA, United States, [3]Aflac Cancer and Blood Disorders Center, Children's Healthcare of Atlanta, Atlanta, GA, United States, [4]Molecular Systems Pharmacology Program, Graduate Division of Biological and Biomedical Sciences, Laney Graduate School, Emory University, Atlanta, GA, United States, [5]Expression Therapeutics, Inc., Tucker, GA, United States

The application of immunotherapies such as chimeric antigen receptor (CAR) T therapy or bi-specific T cell engager (BiTE) therapy to manage myeloid malignancies has proven more challenging than for B-cell malignancies. This is attributed to a shortage of leukemia-specific cell-surface antigens that distinguish healthy from malignant myeloid populations, and the inability to manage myeloid depletion unlike B-cell aplasia. Therefore, the development of targeted therapeutics for myeloid malignancies, such as acute myeloid leukemia (AML), requires new approaches. Herein, we developed a ligand-based CAR and secreted bi-specific T cell engager (sBite) to target c-kit using its cognate ligand, stem cell factor (SCF). c-kit is highly expressed on AML blasts and correlates with resistance to chemotherapy and poor prognosis, making it an ideal candidate for which to develop targeted therapeutics. We utilize γδ T cells as a cytotoxic alternative to αβ T cells and a transient transfection system as both a safety precaution and switch to remove alloreactive modified cells that may hinder successful transplant. Additionally, the use of γδ T cells permits its use as an allogeneic, off-the-shelf therapeutic. To this end, we show mSCF CAR- and hSCF sBite-modified γδ T cells are proficient in killing c-kit$^+$ AML cell lines and sca-1$^+$ murine bone marrow cells *in vitro*. *In vivo*, hSCF sBite-modified γδ T cells moderately extend survival of NSG mice engrafted with disseminated AML, but therapeutic efficacy is limited by lack of γδ T-cell homing to murine bone marrow. Together, these data demonstrate preclinical efficacy and support further investigation of SCF-based γδ T-cell therapeutics for the treatment of myeloid malignancies.

KEYWORDS

acute myeloid leukemia (AML), gamma delta (γδ) T cells, ligand-based therapeutics, chimeric antigen receptor (CAR), secreted bispecific T cell engager, stem cell factor (SCF), c-kit (CD117)

1 Introduction

Adoptive cell therapy (ACT), such as chimeric antigen receptor (CAR) T therapy, has significantly advanced the treatment of B cell malignancies, leading to the FDA approval of multiple cellular products (1–6). However, ACT for other leukemias, like acute myeloid leukemia (AML), do not share the same success. Current treatment regimens for AML consist of genotoxic chemotherapeutics (7) that have severe toxicities in the bone marrow (8), with approximately 30% of children relapsing (9–12). This leads to a drop in survival from 70% to a mere 20% (9, 13), highlighting the need for new treatment options.

Unfortunately, there are a lack of known leukemia-specific, cell-surface antigens that distinguish healthy from malignant myeloid cells (14). This makes the translation of traditional cell-based immunotherapies with long-term persistence challenging in this setting, as myeloid depletion cannot be managed like B-cell aplasia. However, as hematopoietic stem cell transplantation (HSCT) is considered curative for AML, it may be important to take advantage of novel therapeutics that display off-tumor toxicities in the hematopoietic compartment that can be corrected with HSCT. In fact, toxicity within the bone marrow may prove advantageous to dually prepare the patient for transplant and target residual disease congruently.

We have developed receptor-directed, ligand-based ACT to target malignant myeloid tissue through interaction with c-kit using its cognate ligand, stem cell factor (SCF). Up to 90% of AML patients have c-kit expression correlating with poor prognosis and resistance to chemotherapy (15, 16), making this receptor an attractive target for malignant myeloid cell and leukemic stem cell (LSC) ablation. In fact, we (17) and others (18–22) have shown the continued use of c-kit as a target for non-genotoxic conditioning due to its expression on hematopoietic stem cells (HSCs). These therapies have proven safe for use in preclinical murine models with toxicities only observed within the hematopoietic compartment (17) despite limited c-kit expression on some organs outside of the hematopoietic compartment, like the cerebellum, female reproductive organs, and lungs. Clinically, c-kit is the target of monoclonal antibody briquilimab, which has shown promise in treating patients with AML and myelodysplastic syndromes (MDS) in a Phase 1 clinical trial (NCT04429191), Fanconi anemia in a Phase 1/2 clinical trial (NCT04784052), severe combined immunodeficiency (SCID) in a Phase 1/2 clinical trial (NCT02963064), and sickle cell disease in a Phase 1/2 clinical trial (NCT05357482) with no treatment-related adverse events in 130 dosed subjects as of late September 2023 (23, 24).

Herein, we utilize ligand-based, c-kit-directed, CAR- and secreted bispecific T-cell engager (sBite)-modified T cells as a therapeutic for the treatment of AML. Traditionally, CARs and bispecific antibodies are designed with single chain variable fragments (scFvs) as their antigen-binding domains that specifically redirect T cells to kill cancer cells without the need for antigen processing and presentation by the human leukocyte antigen (HLA) (25). However, these designs are not without flaws. Primarily, scFv molecules are prone to aggregation and produce higher order complexes through intermolecular variable heavy (V_H) and variable light (V_L) association, resulting in tonic signaling and thereby lower therapeutic efficacy (26–28). Our proposed ligand-based design circumvents these issues.

Furthermore, we employ CAR- and sBite-modified γδ T cells as a cytotoxic alternative to αβ T cells. γδ T cells contribute to graft-versus-leukemia (GvL) reactions to enhance cancer eradication through the recognition of stress antigens expressed by leukemia cells (29–31). Additionally, as γδ T cells recognize antigen independent of HLA, they can be transplanted across HLA barriers in the presence of immunosuppression, thus creating opportunity for an off-the-shelf therapeutic. Importantly, we (31–36) and others (37) have optimized the use of γδ T cells and can expand these cells *ex vivo* using a novel serum-free protocol resulting in a cellular product of highly purified Vγ9Vδ2 T cells with low percentages of NK cells and negligible αβ T cell contamination. The chemokine receptor expression and exhaustion profiles of these cells have been reported (35, 38)., in addition to the phenotype of the contaminating NK cells within our cellular product (38).

These studies establish a ligand-based cell therapy strategy using engineered γδ T cells as a cytotoxic alternative to traditional ACT for the treatment of AML. Non-modified allogeneic γδ T cells expanded under our Good Manufacturing Practice (GMP)-compliant serum-free protocol are currently under clinical investigation in a Phase 1 trial for the treatment of relapsed/refractory neuroblastoma (NCT05400603). In the context of myeloid malignancies, we have previously demonstrated non-modified γδ T cells have enhanced cytotoxicity against AML cell lines in combination with chemotherapeutic agents that upregulate stress antigens expressed by AML cells (31). More recently, we showed our efforts in optimizing and utilizing expanded γδ T cells transiently transfected with mRNA encoding a CD19 CAR for the treatment of B-cell malignancies (39). Here, we expand our repertoire by investigating the transient modification of γδ T cells using a ligand-based CAR and sBite. These studies provide the basis for further investigation into the use of ligand-based γδ T cell therapies.

2 Materials and methods

2.1 c-kit and NKG2D ligand expression on healthy donor and patient samples

The St. Jude Cloud (pecan.stjude.cloud) was queried for c-kit expression using transcriptomic data from 2,480 pediatric patients (40, 41). The Human Protein Atlas (v22.proteinatlas.org) was queried for c-kit expression in healthy tissues and cell lines by RNA sequencing (42). The R2 Genomics Analysis and Visualization Platform (https://r2.amc.nl) was used to query multiple datasets using the Megasampler R2 module for expression of c-kit, ULBP1, ULBP2, and MICA/MICB by RNA sequencing. The u133a chip with MAS5.0 normalization was used exclusively. Datasets utilized in this study were as follows: PBMC (Novershtern, 211 samples), HSC (OGIC, 21 samples), and AML (Bohlander, 422 samples and Delwel, 293 samples).

2.2 Cell lines

The NOMO-1, Kasumi-1, KG-1, and MOLM-13 cell lines were kindly gifted by the laboratory of Dr. Douglas Graham (Emory University, Atlanta, GA, USA). The CMK cell line was kindly provided by the laboratory of Dr. Brian Petrich (Emory University, Atlanta, GA, USA). The Jurkat, K562, and 697 cell lines were obtained from the American Type Culture Collection (Manassas, VA, USA). NOMO-1, K562, 697, KG-1, and Jurkat cells were cultured in RPMI-1640 with L-glutamine (Corning CellGro, Manassas, VA, USA) supplemented with 10% fetal bovine serum (FBS; R&D Systems, Minneapolis, MN, USA) and 1% Penicillin-Streptomycin (Cytiva, Marlborough, MA, USA). The CMK, Kasumi-1, and MOLM-13 cell lines were cultured under the same conditions using 20% FBS.

2.3 Design and cloning of mSCF CAR and hSCF sBite

mSCF CAR and hSCF sBite DNA sequences were cloned into vectors containing the necessary components for mRNA or lentiviral production as follows:

To clone the mSCF CAR, the full-length DNA sequence for secreted murine SCF obtained from UniProt (uniprot.org) (43) was ordered as a gene fragment product flanked by AscI and NheI restriction enzyme sites or BamHI and NotI restriction enzyme sites (Integrated DNA Technologies, Coralville, IA, USA). The gene fragment product was cloned into a recipient plasmid with paired AscI and NheI or BamHI and NotI sites upstream of the CD8α, CD28, and CD3ζ CAR components using corresponding restriction enzymes AscI and NheI or BamHI and NotI (New England BioLabs, Ipswich, MA, USA) behind a UBC or T7 promoter. The DNA construct was codon optimized for expression in T cells by Expression Therapeutics (Tucker, GA, USA) using Expression Cassette Optimization (eCO) technology and confirmed by Sanger sequencing (Genewiz, Burlington, MA, USA).

To clone the hSCF sBite, the coding sequence of secreted isoform of human SCF was obtained from GenBank (M59964.1). The sequence of the SCF signal peptide through mature core fragment was identified as bases 1- 426 of the native cDNA sequence. To generate the sBite, this fragment was combined with a G4S linker and CD3 scFv derived from clone OKT3. The sequence was then codon optimized for expression in γδ T cells by Expression Therapeutics (Tucker, GA, USA) using Expression Cassette Optimization (eCO) technology. The optimized sequence was then synthesized and cloned into a pcDNA3.1-based plasmid using seamless ligation technology by Genscript (Piscataway, NJ, USA) behind a T7 promoter.

2.4 Production of mSCF CAR and hSCF sBite mRNA

The mMessage mMachine T7 Transcription kit (Thermo Fisher Scientific, Waltham, MA, USA) was used to produce mSCF CAR mRNA after linearization with restriction enzyme XhoI, whose restriction site cuts directly after the CD3ζ sequence.

The HiScribe T7 mRNA kit with CleanCap Reagent AG Plasmid (New England BioLabs, Ipswich, MA, USA) was used to produce hSCF sBite Cap-1 mRNA after linearization with NotI. Poly(a) tailing was subsequently performed using E. coli poly(a) polymerase (New England BioLabs, Ipswich, MA, USA).

RNA gel electrophoresis was used to confirm efficient poly-A tail extension and quality of mRNA products.

2.5 Production of mSCF CAR and CD19 CAR lentiviral vectors

High-titer, recombinant, self-inactivating HIV lentiviral vectors were produced and titered as previously described (44–46). Briefly, HEK-293T cells were transiently transfected with packaging plasmids encoding Gag-Pol, Rev, VSVG envelope, and the CAR transgene plasmid using calcium phosphate (Sigma Aldrich, St. Loius, MO, USA). Cells were cultured in DMEM (Thermo Fisher Scientific, Waltham, MA, USA) supplemented with 10% FBS and supernatant was collected for 3 days beginning 48 hours after transfection. Supernatants were passed through a 0.45-μm filter, pooled, and concentrated by overnight centrifugation at 10,000 × *g* at 4°C. The following morning, viral particles were passed through a 0.22-μm filter and stored at -80°C. Titers were determined using quantitative real-time PCR analysis on HEK-293T cell genomic DNA.

2.6 Expansion and modification of primary αβ T cells

Peripheral blood from healthy adult volunteers were obtained under an IRB approved protocol (IRB00101797) through the Emory University Children's Clinical and Translational Discovery Core (CCTDC), after which peripheral blood mononuclear cells (PBMCs) were isolated using a Ficoll-Plaque PLUS density gradient (GE HealthCare, Chicago, IL, USA) and cryopreserved. Alternatively, cryopreserved PBMCs were procured from AllCells (Alameda, CA, USA). T cells were negatively selected from thawed PBMCs using the EasySep Human T cell Isolation Kit (Stemcell Technologies, Vancouver, BC, CA) and stimulated with anti-CD3/CD28 Human T-Activator Dynabeads (Thermo Fisher Scientific, Waltham, MA, USA) at a 1:1 bead-to-cell ratio in X-VIVO 15 (Lonza, Basel, Switzerland) supplemented with 10% FBS, 1% penicillin-streptomycin, 100 IU/mL human IL-2 (PeproTech, Rocky Hill, NJ, USA), and 5 ng/mL human IL-7 (PeproTech, Rocky Hill, NJ, USA) at 2 × 10^6 cells/mL. After 48 hours of stimulation, beads were removed and 1 × 10^6 cells were transduced at MOI 20 with 10 μg/mL polybrene (EMD Millipore, Billerica, MA, USA) for 18 hours. MOI was determined using the following calculation:

$$\mathbf{MOI} = \frac{titer \times volume\ (mL)}{\#\ of\ cells}$$

After 18 hours, cells were resuspended in fresh media and underwent an early cell dilution of ~100,000 cells/mL, then left to expand for 96 hours before CAR expression was determined and used in cytotoxicity assays or animal studies.

2.7 Expansion and transfection of primary γδ T cells

Peripheral blood from healthy consenting volunteers (30-40 mL) was obtained as previously mentioned (under the Expansion and modification of primary αβ T cells section) through the CCTDC or fresh leukopaks were procured from the American Red Cross. From either source, PBMCs were isolated using a Ficoll-Plaque PLUS density gradient and cultured in OpTmizer serum-free media (Thermo Fisher Scientific, Waltham, MA, USA) supplemented with 2 mM L-glutamine, 1% penicillin-streptomycin, 500-1000 IU/mL human IL-2, and 5 μM zoledronic acid (Sigma-Aldrich, St. Louis, MO, USA) using our previously published Good Manufacturing Practice-compliant 12-day expansion protocol (31, 33, 35). Expanded γδ T cells were cryopreserved in 5% human serum albumin (HSA; Grifols, Barcelona, Spain) and 10% dimethylsulfoxide (DMSO; Sigma-Aldrich, St. Louis, MO, USA) diluted in PlasmaLyte A (Baxter International Inc. Deerfield, IL, USA) in 1×10^7 – 1×10^8 cell aliquots.

Cryopreserved γδ T cells were thawed in three volumes of 5% HSA diluted in PlasmaLyte A and centrifuged at 250 × *g* for 10 minutes. Cells were resuspended in OpTmizer serum-free media supplemented with 2 mM L-glutamine, 1% penicillin-streptomycin, and 1000 IU/mL of human IL-2 and rested for 2 hours at 37°C, 5% CO_2. Rested γδ T cells (5-25 × 10^6 cells) were then transiently transfected to express an mSCF CAR or hSCF sBite through mRNA electroporation by first washing the cells three times with PBS and spinning at 250 × g for 10 minutes, then resuspending in Opti-MEM (ThermoFisher Scientific, Waltham, MA, USA) with 15 μg of purified mRNA or equal volume vehicle control for mock transfection. Cells were then electroporated using a square wave function at 500 V for 5 ms in a 4 mm electroporation cuvette (Fisher Scientific, Hampton, NH, USA) using the GenePulser Xcell Electroporation System (Bio-Rad Laboratories, Hercules, CA, USA). Modified γδ T cells were used 24 hours after electroporation for *in vitro* studies and 1-4 hours after electroporation for *in vivo* studies.

2.8 Measuring CAR expression by western blotting

mSCF CAR-modified cells were lysed with RIPA buffer (Sigma-Aldrich, St. Louis, MO, USA) supplemented with Protease Inhibitor Cocktail diluted 1:100 (Sigma-Aldrich, St. Louis, MO, USA) and PMSF protease inhibitor diluted 1:100 (ThermoFisher Scientific, Waltham, MA, USA) for 30 minutes on ice, after which cell lysates were clarified by centrifugation at 14,000 × *g* at 4°C for 10 minutes. The supernatant was collected as a whole cell lysate. Protein concentrate was quantified using a Bradford Assay (Bio-Rad Laboratories, Hercules, CA, USA). 20-40 μg of protein was first heated at 100°C for 10 minutes, then loaded into a 4-15% pre-cast gel (Bio-Rad Laboratories, Hercules, CA, USA) with Precision Plus Protein Dual Color Standards (Bio-Rad Laboratories, Hercules, CA, USA) and separated by SDS-PAGE. Protein was transferred to a nitrocellulose membrane (Bio-Rad Laboratories, Hercules, CA, USA) at 250 constant Amps for 60 minutes and then washed in TBS containing 0.1% Tween-20 prior to incubation with a mouse anti-human CD3ζ primary antibody diluted 1:1000 (BioLegend, San Diego, CA, USA) and goat anti-mouse HRP secondary antibody diluted 1:500 (BioLegend, San Diego, CA, USA). Blots were then imaged by chemiluminescence with a Bio-Rad ChemiDoc XR+ Molecular Imager.

2.9 Measuring CAR expression by flow cytometry

Jurkat or primary CAR T cells were stained with 20 ng of Recombinant Mouse c-kit Fc Chimera Protein (R&D Systems, Minneapolis, MN, USA) or 20 ng of Recombinant Human c-kit Fc Chimera Protein (R&D Systems, Minneapolis, MN, USA) and incubated on ice for 30 minutes. Cells were washed once with FACS buffer (PBS + 2.5% FBS), then stained with 2 μL R-Phycoerythrin F (ab')2 secondary antibody (Jackson ImmunoResearch, West Grove, PA, USA) and eBioscience Fixable Viability Dye eFluor 780 (Thermo Fisher Scientific, Waltham, MA, USA) to exclude dead cells and incubated on ice for 15 minutes. Cells were then washed once with FACS buffer, then subjected to flow cytometry (Cytek Aurora) and analyzed with FlowJo software (v10).

2.10 *In vitro* cytotoxicity assays

To assess the cytotoxicity of mSCF CAR- or hSCF sBite-T cells against AML cell lines, unmodified or modified primary T cells were co-cultured with 50,000 target cells (CMK or Kasumi-1) stained with VPD450 (BD, Franklin Lakes, NJ, USA) at indicated effector-to-target ratios for 4-24 hours at 37°C, 5% CO_2. Co-cultures were then washed once with Annexin V Binding Buffer (0.025 mM calcium chloride + 1.4 mM sodium chloride + 0.1 mM HEPES) and stained with 3 μL Annexin V-APC (BioLegend, San Diego, CA, USA) for 20 minutes at room temperature. Cells were then washed once with Annexin V Binding Buffer. 7-AAD Viability Dye (BioLegend, San Diego, CA, USA) was added 2 minutes before the sample was subjected to flow cytometric analysis (Cytek Aurora). Samples were analyzed with FlowJo software (v10), where percent cytotoxicity was measured by the sum of Annexin V^+, 7-AAD^+, and Annexin-V^+/7-AAD^+ target cells.

2.11 *In vitro* activation assays

Jurkat or primary CAR T cells were co-cultured with VPD450 (BD, Franklin Lakes, NJ, USA) stained target cells (CMK, Kasumi-1,

Nomo-1, or 697) at indicated effector-to-target ratios for 4 hours at 37°C, 5% CO_2. Co-cultures were then washed once with FACS buffer and stained with 3 µL anti-CD69-APC-Cy7 antibody (BD, Franklin Lakes, NJ, USA) for 20 minutes at 4°C. After staining, cells were washed once with FACS buffer, then subjected to flow cytometry (Cytek Aurora) and analyzed with FlowJo software (v10). Dead cells were excluded from the analysis using 3 µL of 7-AAD Viability Dye added 2 minutes before analysis on the cytometer.

2.12 Colony forming unit assay

For each bone marrow sample, 0.8-8 × 10^4 cells isolated from mouse femurs by flushing were first resuspended in RPMI 1640 supplemented with 10% FBS and 1% penicillin-streptomycin. Resuspended cells were then added to 4 mL Methocult GF M3434 (Stemcell Technologies, Vancouver, BC, CA) and plated on sterile 35 mm plates in triplicate. Plates were incubated at 37°C 5% CO_2 for 7 days, then colonies were counted under a microscope.

2.13 Animal studies

NOD.Cg-Prkdc^{scid}Il2rg^{tw1Wjl}/SzJ (NSG) mice were purchased from Jackson Laboratories (Bar Harbor, ME, USA) and maintained in a pathogen-free environment at an Emory University Division of Animal Resources facility. All animal studies were conducted in accordance with established policies set forth by the Emory University Institutional Animal Care and Use Committee (IACUC) under an approved animal use protocol (PROTO201800202). Equal numbers of male and female mice were used for all studies.

To determine the toxicity of mSCF CAR-modified αβ T cells, 8-week-old NSG mice were first preconditioned with 100 rads of x-ray irradiation (Rad Source Technologies, RS 2000 Small Animal Irradiator, Buford, GA, USA) then administered 5 × 10^6 luciferase-modified CMK cells by intravenous injection into the lateral tail-vein the following morning. The following day, mice were either treated with 5 × 10^6 mock-transduced αβ T cells (n = 6) or mSCF CAR-modified αβ T cells (n = 6, transduction efficiency:<8%) via tail-vein injection, with PBS administered as an untreated control (n = 3). Peripheral blood was collected at 3 weeks to assess for tumor burden and CAR T-cell engraftment. Mice were euthanized when end-point criteria were met, which includes changes in weight, scruff, movement, and hunched state.

To examine the persistence of γδ T cells in mice, 7-13-week-old NSG mice were administered 1 × 10^7 non-modified γδ T cells via retro-orbital injection. In an effort to enhance persistence, mice were either treated with vehicle control (n = 6), 13,000 IU IL-2 twice a week via intraperitoneal injection (n = 6), or a combination of 13,000 IU IL-2 twice a week via intraperitoneal injection and 70 µg/kg zoledronic acid (NorthStar Rx, Memphis, TN, USA) via subcutaneous injection (n = 6). Once a day for 4 days, peripheral blood was collected, and leukocytes were assessed for the presence of human CD45$^+$ cells by flow cytometric analysis (Cytek Aurora) and analyzed with FlowJo software (v10). On day 4, mice were euthanized, and spleens and bone marrow were harvested to assess for the presence of human CD45$^+$ cells as before.

To examine the toxicity of mSCF CAR-modified γδ T cells in mice, 8-12-week-old NSG mice were anesthetized and administered 2-8 × 10^6 mock transfected γδ T cells (n = 4) or mSCF CAR-modified γδ T cells (n = 4), with PBS as an untreated control (n = 3) via intraosseous injection in the left femur. Mice were given 5 mg/kg meloxicam (Baudax Bio, Malvern, PA, USA) via subcutaneous injection immediately after the intraosseous injection as an analgesic. After 2 days, mice were euthanized and peripheral blood, spleens, and bone marrow from both the left and the right femur were harvested to assess for the presence of human CD3$^+$ human γδTCR$^+$ cells and murine c-kit$^+$ cells by flow cytometry (Cytek Aurora). Data was analyzed using the FlowJo software (v10). At this time, a CFU assay was performed to assess for multipotent progenitor cells. The left and the right femurs from each mouse were kept as separate samples in the flow and CFU assays in this experiment.

To assess the cytotoxicity of mSCF CAR- and hSCF sBite-modified γδ T cells in an AML model, 5–9-week-old NSG mice were first preconditioned with 20 mg/kg busulfan (DSM Pharmaceuticals, Inc., Greenville, NC, USA) via intraperitoneal injection, then administered 5 × 10^6 luciferase-modified CMK cells via tail-vein injection the following morning. Beginning in the afternoon on the same day and then once daily for the following 3 days for a total of 4 doses, mice were treated with 1 × 10^7 mock transfected γδ T cells (n = 6), mSCF CAR-modified γδ T cells (n = 3), or hSCF sBite-modified γδ T cells (n = 6) by intravenous injection into the lateral tail-vein, with PBS to serve as an untreated control (n = 8). Tumor growth and overall health of the mice were monitored two times per week IVIS (*In vivo* Imaging System, Perkin Elmer, Waltham, MA, USA) imaging and weighing, respectively. Freshly made D-luciferin (PerkinElmer, Waltham, MA, USA) was injected at 150 mg/kg via intraperitoneal injection 10 minutes prior to imaging. Bioluminescence was quantified using Living Image Software (PerkinElmer, Waltham, MA, USA) or Aura Software (Spectral Instruments Imaging, Tucson, AZ, USA). Peripheral blood was collected at 3 weeks to assess for c-kit expression on CD33$^+$ AML cells and to perform complete blood counts. Mice were euthanized when end-point criteria were met, which includes changes in weight, scruff, movement, and hunched state.

2.14 Statistical analysis

All statistical analyses were performed using Prism 8 software (GraphPad Software Inc). Results are presented as mean ± standard deviation of the mean and were considered statistically significant at $P< 0.05$. Unpaired or paired two-tailed Student's *t*-test, one-way ANOVA, or log-rank (Mantel-Cox) test were used to determine statistical significance as appropriate.

3 Results

3.1 c-kit is highly expressed on pediatric AML and healthy HSCs

We first sought to determine c-kit expression on healthy tissues. The Human Protein Atlas (proteinatlas.org) demonstrates

undetectable c-kit expression in most adult human organs by immunohistochemistry (IHC). Exceptions to this include high protein expression in the cerebellum, medium protein expression in the female reproductive organs (breast, fallopian tubes, and ovary), lung, skin, and testis, and low protein expression in the kidney, colon, and rectum. Data from the St. Jude Cloud (pecan.stjude.cloud) show many pediatric malignancies have high c-kit expression, with AML as the highest (Figure 1A). High expression of c-kit is corroborated in adult AML samples taken at time of diagnosis, with expression significantly higher than normal PBMCs yet comparable to HSCs (Figure 1B). To validate these findings, we confirmed c-kit expression on eight specific leukemia cell lines (proteinatlas.org) (Figure 1C) and by flow cytometry (Figure 1D). Four of five AML cell lines tested (AML cell lines denoted by arrows in Figure 1C) demonstrate high c-kit expression compared to three healthy donor PBMCs (Figure 1D).

3.2 mSCF CAR αβ T cells induce AML cell death *in vitro*

To this end, we generated a ligand-based c-kit directed CAR (mSCF CAR) by lentiviral gene delivery. The CAR construct includes full-length murine SCF followed by a CD8α hinge, CD28 co-stimulatory domain, and CD3ζ signaling domain (Figure 2A). We chose to use the murine sequence for SCF as it binds both the human and murine c-kit receptor (47), making it possible to evaluate both cancer eradication and off-tumor toxicities in a murine model.

The first transgene tested included a bicistronic lentiviral vector encoding for dual expression of eGFP by a P2A ribosomal skipping sequence as a transduction marker (Figure 2A). Binding of the murine c-kit receptor to the mSCF CAR can be determined using a murine c-kit receptor conjugated to a constant fragment (Fc; c-kit-Fc) (Figure S1A). Jurkat T cells were used to evaluate CAR protein expression, ability to bind the human c-kit receptor, and AML specificity, with antigen-irrelevant CD19 CAR as a control. Jurkat T cells transduced with mSCF CAR at multiplicities of infection (MOIs) 0.5 and 2.5 resulted in 18% ± 0.4% and 49% ± 0.3% GFP^+ cells respectively, while cells transduced with the control CD19 CAR resulted in 57% ± 0.2% and 92% ± 0.1% GFP^+ cells, respectively (Figure 2B). Importantly, binding of the c-kit-Fc to mSCF CAR-modified Jurkat T cells results in CD69 upregulation and subsequent activation increasing with increasing MOIs, but not in CD19 CAR-modified Jurkat T cells (Figure 2C). Interestingly,

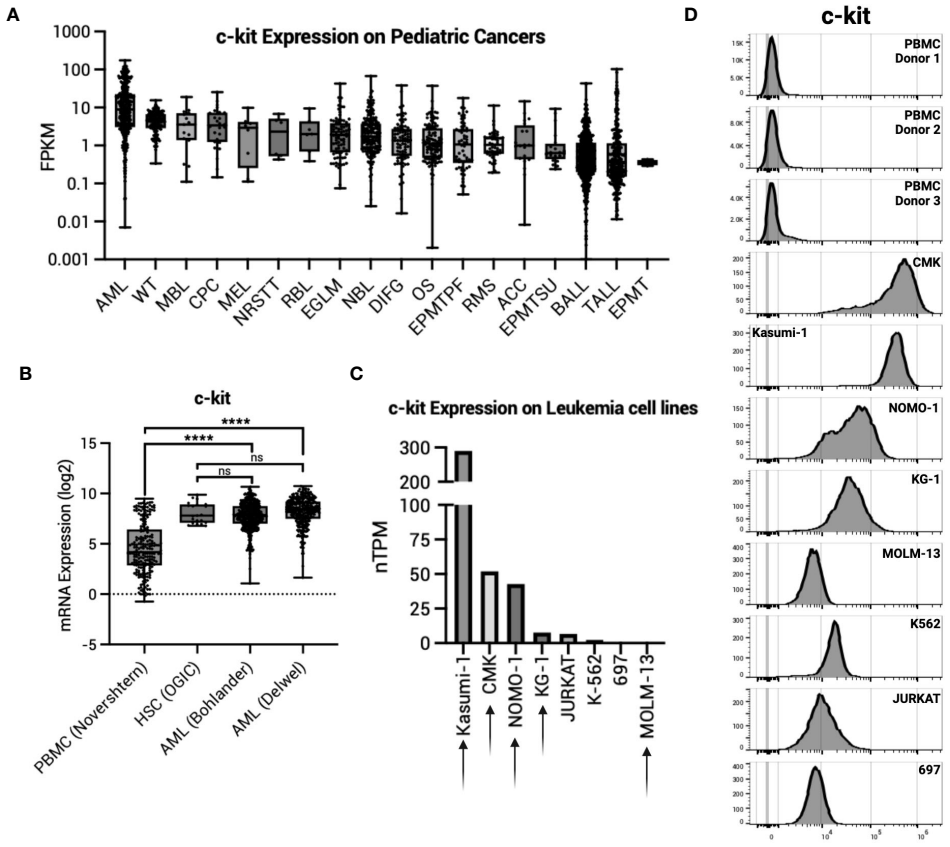

FIGURE 1
c-kit expression on AML. **(A)** c-kit expression as fragments per kilobase per million (FPKM) on pediatric cancers from the St. Jude Cloud (pecan.stjude.cloud). Error bars represent SD. **(B)** c-kit mRNA expression across one normal PBMC dataset, one normal HSC dataset, and two AML datasets from R2: Genomics Analysis and Visualization Platform (https://r2.amc.nl). Error bars represent SD. Statistical analysis represents One-Way ANOVA (****p< 0.0001; ns, p > 0.05). **(C)** c-kit expression as nTPM on select leukemia cell lines from the Human Protein Atlas (v22.proteinatlas.org). Arrow denotes AML cell line. **(D)** Histograms depicting c-kit expression in healthy donor PBMCs (n = 3) and select leukemia cell lines in **(C)**.

10.3389/fimmu.2023.1294555

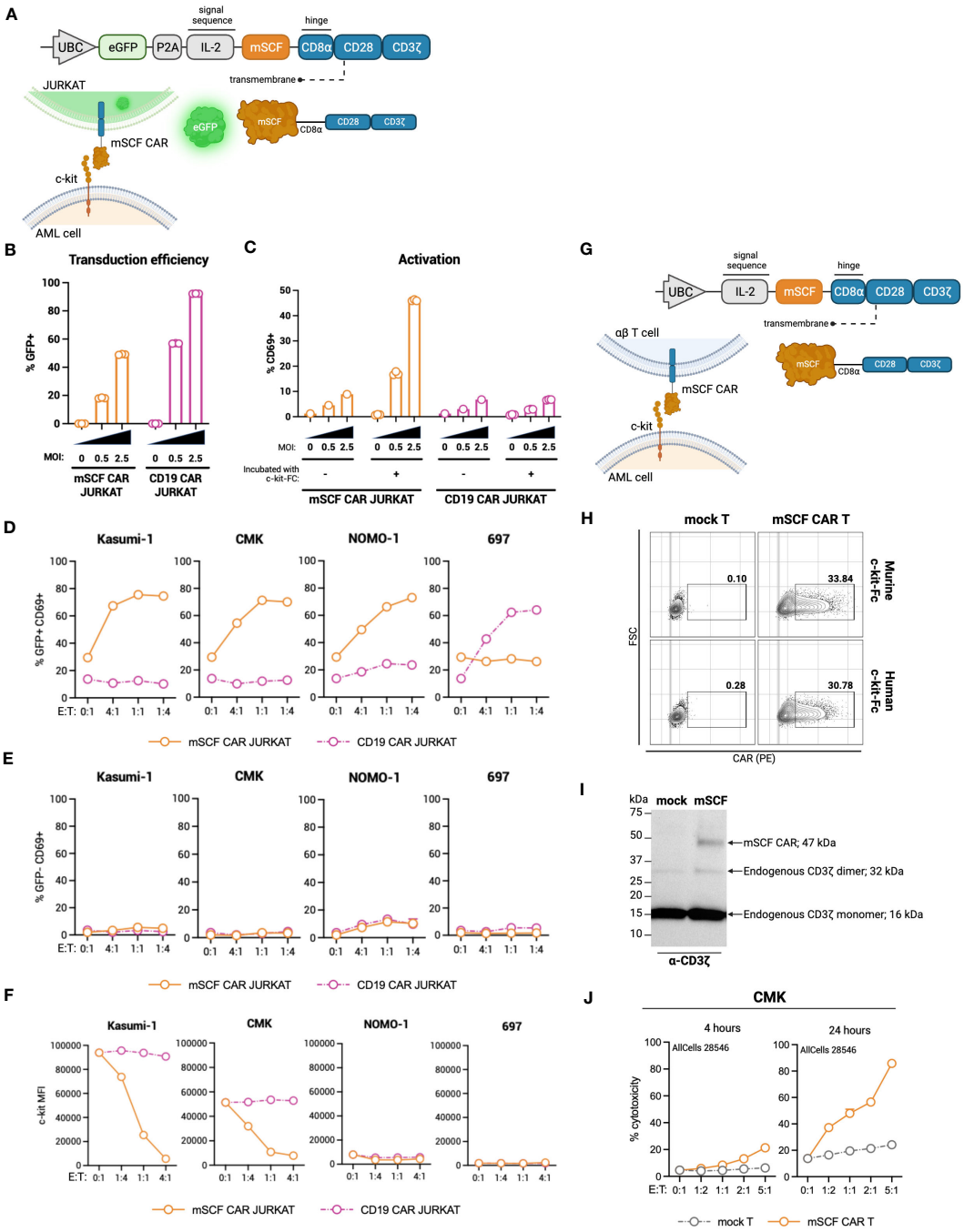

FIGURE 2
Design of novel ligand-based mSCF CAR and modification of αβ T cells. **(A)** Schematic of lentiviral GFP mSCF CAR DNA construct. **(B)** Transduction efficiency as depicted by %GFP$^+$ live Jurkat T cells. Error bars represent SD. n = 3 experimental replicates. **(C)** Activation of live mSCF CAR- or CD19 CAR-modified Jurkat T cells as depicted by %CD69$^+$ when stained with 20 ng murine c-kit-Fc chimera. Error bars represent SD. n = 1-3 experimental replicates. **(D)** %CD69 activation of live mSCF CAR- or CD19 CAR-modified GFP$^+$ Jurkat T cells when co-cultured with 4 different leukemia cell lines at 4 different effector-to-target (E:T) ratios. Error bars represent SD. n = 2 experimental replicates. **(E)** %CD69 activation of live un-modified GFP- Jurkat T cells under the same conditions as **(D)**. Error bars represent SD. n = 2 experimental replicates. **(F)** c-kit MFI of 4 leukemia cell lines when co-cultured with mSCF CAR- or CD19 CAR-modified Jurkat T cells under the same conditions as **(D)**. Error bars represent SD. n = 2 experimental replicates. **(G)** Schematic of lentiviral mSCF CAR DNA construct without GFP marker. **(H)** Representative flow plots depicting mSCF CAR expression on primary T cells transduced at MOI 20 when stained with 20 ng of murine or human c-kit-Fc chimera. **(I)** Western blot depicting CAR expression from whole cell lysates of primary T cells transduced with mSCF CAR at MOI 20. Western blot antibody against human CD3ζ. **(J)** Four- and 24-hour flow cytometry cytotoxicity assays of mSCF CAR-modified primary T cells against c-kit expressing AML cell line CMK compared to mock T cell controls. Percent cytotoxicity is the sum of 7AAD$^+$, Annexin V$^+$, and 7AAD$^+$ Annexin V$^+$ cells when gated on VPD450-stained target cells only. Error bars represent SD. n = 2 experimental replicates with 1 donor.

this increase in activation is only seen when both c-kit-Fc and secondary F(ab')2 are used (Figure S2B), suggesting multiple binding domains of the secondary F(ab')2 may potentially induce CD3ζ cross-linking among CAR molecules (Figure S1C), though further evidence is required.

To assess interaction of the mSCF CAR with human c-kit and the ability to activate Jurkat T cells, mSCF CAR Jurkat T cells were co-cultured with c-kit$^+$ human cell lines Kasumi-1, CMK, and Nomo-1 at various effector-to-target (E:T) ratios, with the B-cell leukemia cell line 697 as an antigen-negative control, as it does not express c-kit. CD19 CAR Jurkat T cells were used as an antigen-irrelevant control for co-cultures with c-kit$^+$ cell lines, as they do not express CD19, and a positive control when co-cultured with 697 cells, as 697 cells do express CD19. Indeed, transduced (GFP$^+$) Jurkat T cells resulted in increased CD69$^+$ activation when co-cultured with their antigen-matched target cells (Figure 2D), while un-transduced (GFP$^-$) Jurkat T cells do not exhibit increased CD69$^+$ activation (Figure 2E). Furthermore, it is known that interaction of SCF with the c-kit receptor causes receptor internalization (48). Indeed, co-culture of mSCF CAR Jurkat T cells with c-kit$^+$ cell lines resulted in decreased c-kit MFI, while MFI remain unchanged when target cells were co-cultured with CD19 CAR Jurkat T cells (Figure 2F).

As a ligand-based therapeutic, it is important to consider the consequences of CAR shedding, as additional SCF in circulation may promote cancer cell proliferation (48). To assess CAR shedding, c-kit$^+$ AML cell lines CMK and Kasumi-1 were incubated with media from mSCF CAR αβ T cells or CD19 CAR αβ T cells, with mock αβ T cells as a control. As a positive control, cell lines were incubated with T cell media supplemented with recombinant murine SCF to induce receptor internalization. After a 15-minute incubation, there is no evidence of receptor internalization when cells were incubated with mSCF CAR media, suggesting the mSCF CAR is not shed from the surface of the cell at levels sufficient to influence surface c-kit levels (Figure S2).

To investigate the mSCF CAR in a more clinically relevant setting, we tested a second lentiviral mSCF CAR transgene cassette that had eGFP removed in primary αβ T cells (Figure 2G). Primary αβ T cells were transduced at MOI 20, after which binding of mSCF CAR αβ T cells to both murine and human c-kit-Fc was confirmed by flow cytometry (Figure 2H) and overall protein expression was confirmed by western blotting against CD3ζ (Figure 2I). To assess cytotoxicity, mSCF CAR αβ T cells were co-cultured with c-kit$^+$ CMK cells at increasing E:T ratios for 4- or 24-hours and showed increased cytotoxicity compared to mock αβ T controls (Figure 2J). Specifically, after 24-hours of co-culture, mSCF CAR αβ T cells induced cytotoxicity to an average of 37% at a 1:2, 48% at a 1:1, 57% at a 2:1, and 86% at a 5:1 E:T ratio. Together, these data show mSCF CAR T cells induce efficient and c-kit-specific killing of c-kit$^+$ AML cell lines *in vitro*.

3.3 mSCF CAR αβ T cells expand *in vivo* in the absence of AML

To identify possible toxicities of mSCF CAR αβ T cells *in vivo*, NOD.Cg-Prkdc^{scid}Il2rg^{tm1Wjl}/SzJ (NSG) mice were administered 5×10^6 total mSCF CAR-modified αβ T cells by tail-vein injection. To assess clonal expansion of the CAR$^+$ population *in vivo*, αβ T cells were transduced at low MOIs, providing approximately 8% CAR$^+$ cells (Figure 3A). Six weeks after administration of T cells, mice were sacrificed to assess clonal expansion of CAR$^+$ cells in the peripheral blood, spleen, and bone marrow compartments by flow cytometry. Significantly more CAR$^+$ αβ T cells were found in the bone marrow (26% ± 6%) than in the peripheral blood (5% ± 1%) (Figure 3B), with the percentage of CAR$^+$ cells found in the peripheral blood closely resembling percent CAR$^+$ cells injected at the beginning of the study.

To test clonal expansion in the presence of AML cells, NSG mice were first subjected to 100 rads of x-ray irradiation, then inoculated with 5×10^6 luciferase-modified CMK cells by tail-vein injection. The following day, mice were intravenously injected with one dose of 5×10^6 total mock or mSCF CAR αβ T cells (8% CAR$^+$). Three weeks later, circulating human CD3$^+$ T cells were significantly higher in mSCF CAR αβ T-cell treated mice (48% ± 26%) compared to mock αβ T-cell treated mice (18% ± 18%) (Figure 3C). No expansion of CAR$^+$ cells was observed in the periphery, as only 7% ± 3% CAR$^+$ cells were found in circulation three-weeks after injection, resembling the percentage of CAR$^+$ cells in the injected product (Figure 3D).

CD33$^+$ AML burden in the periphery was significantly decreased in mSCF CAR-treated mice (0.2% ± 0.2%) compared to untreated controls (2% ± 0.5%) three-weeks after treatment, though not significantly different than mock αβ T-cell treated mice (0.2% ± 0.2%) (Figure 3E). However, despite a lack of difference in AML burden in the periphery between treatment groups, mSCF CAR αβ T cell treated mice met endpoint criteria significantly sooner than untreated or mock αβ T treated mice, suggesting greater toxicity *in vivo* despite low CAR transduction (Figure S3).

Though we did not observe clonal expansion of CAR$^+$ αβ T cells in the periphery of AML bearing mice, we hypothesized there could be clonal expansion in other hematopoietic organs with high c-kit expression, such as the bone marrow. Despite promising *in vitro* data, we determined that mSCF CAR-modified αβ T cells induced excessive toxicity *in vivo* even at low modification efficiency. Thus, we sought additional safety modifications in our design.

3.4 c-kit-targeting γδ T cells induce AML cell death *in vitro*

γδ T cells have an innate ability to recognize stress antigens through NKG2D expression (49). NKG2D ligands—MICA/MICB and ULBP1-6—interact with NKG2D on γδ T cells and activate innate killing mechanisms (50). Primary AML samples taken at time of diagnosis from two different datasets express significantly higher transcript levels of NKG2D ligands MICA/MICB, ULBP1, and ULBP2 compared to healthy PBMC control (Figures 4A–C). These results were corroborated with cell surface expression on AML cell lines as measured by flow cytometry (Figures 4D–F).

To test c-kit-directed ligand-based therapeutics in γδ T cells, we developed a transgene to express the mSCF CAR under a T7 promoter for mRNA production (Figure 5A). Similarly, we also

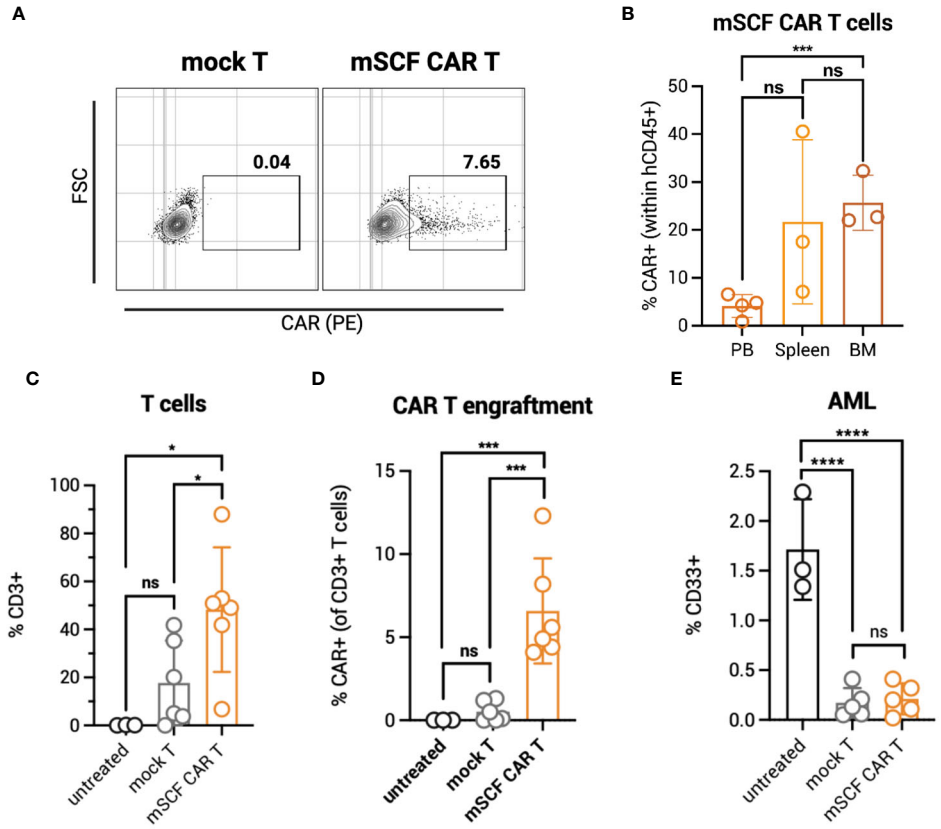

FIGURE 3
mSCF CAR αβ T cells expand in vivo in the absence of AML. **(A)** Representative flow plots depict mSCF CAR expression of injected αβ T cells in the naive context and in the context of AML. **(B)** Briefly, NSG mice were injected with 5 x 10^6 mSCF CAR-modified αβ T cells intraveneously in the absence of AML. %CAR+ αβ T cells (gated on live human CD45+ cells) within the peripheral blood (PB), spleen, and bone marrow (BM) compartments. Error bars represent SD. Statistical analysis represents Student's t test (***p<0.001; ns, p > 0.05). **(C)** Briefly, NSG mice recieved 100 rads of x-ray irradiation in the morning followed by IV injection of 5 x 10^6 CMK cells in the afternoon on day -1. The following day, mice were treated with 5 x 10^6 mock αβ T cells or mSCF CAR-modified αβ T cells (<8% CAR+) intraveneously. Peripheral blood leukocytes were collected 3 weeks after treatment to assess for leukemia engraftment. n = 3 untreated, n = 6 mock T, n = 6 mSCF CAR T. %CD3 live αβ T cells circulating within the periphery 3 weeks after treatment. Error bars represent SD. Statistical analysis represents Student's t test (*p<0.05; ns, p > 0.05). **(D)** %CAR+ αβ T cells (gated on live human CD3+ cells) circulating within the periphery 3 weeks after treatment. Error bars represent SD. Statistical analysis represents Student's t test (***p<0.001; ns, p > 0.05). **(E)** %CD33+ live AML cells circulating within the periphery 3 weeks after treatment. Error bars represent SD. Statistical analysis represents Student's t test (****p < 0.0001; ns, p > 0.05).

developed a ligand-based secreted bispecific T-cell engager (sBite) using the human sequence for SCF and an anti-CD3 scFv (clone: OKT3) (Figure 5B). When expressed in a γδ T cell, the hSCF sBite is secreted and dually binds to the γδ T-cell receptor (TCR) and c-kit, which is expressed on the target cell, and induces cytotoxicity. As γδ T cells have innate cytotoxicity against cancer cells, we posited that expressing these targeted transgenes transiently would provide potent tumor clearance without long-term off-target toxicities within the c-kit compartment. Flow cytometric analysis confirms CAR surface expression using mouse and human c-kit-Fc (Figure 5C). Interestingly, γδ T cells modified with the hSCF sBite shift positively when incubated with the human c-kit-Fc, suggesting sBite secretion, binding to surface CD3ϵ and ability to bind to human c-kit. Importantly, this also confirms that the human sequence for SCF is unable to bind to murine c-kit (Figure 5C). Overall, mSCF CAR transfection efficiency averages to 63% ± 18% from samples across eight healthy donors (Figure 5D).

To assess cytotoxicity of mSCF CAR and hSCF sBite-modified γδ T cells, human AML cell lines CMK and Kasumi-1 were co-cultured for 4-hours with mock γδ T cells, mSCF CAR γδ T cells, or hSCF sBite γδ T cells at increasing E:T ratios (Figure 5E). As expected, the degree of toxicity of non-modified γδ T cells against some AML cell lines is donor dependent (35). Cytotoxicity increased as E:T ratios increased across the three donors to variable degrees and importantly, CAR and sBite modification enhanced cytotoxicity in all donors (Figure 5E). To further confirm secretion of the hSCF sBite from modified γδ T cells, c-kit$^+$ CMK cells were co-cultured with mock γδ T cells, mock γδ T cells supplemented with hSCF sBite conditioned media, or hSCF sBite-modified γδ T cells at increasing E:T ratios. Mock γδ T cells supplemented with hSCF sBite conditioned media induced the same degree of cytotoxicity as hSCF sBite-modified γδ T cells, indicating the hSCF sBite is secreted into the media and can act on both modified and non-modified cells (Figure 5F).

10.3389/fimmu.2023.1294555

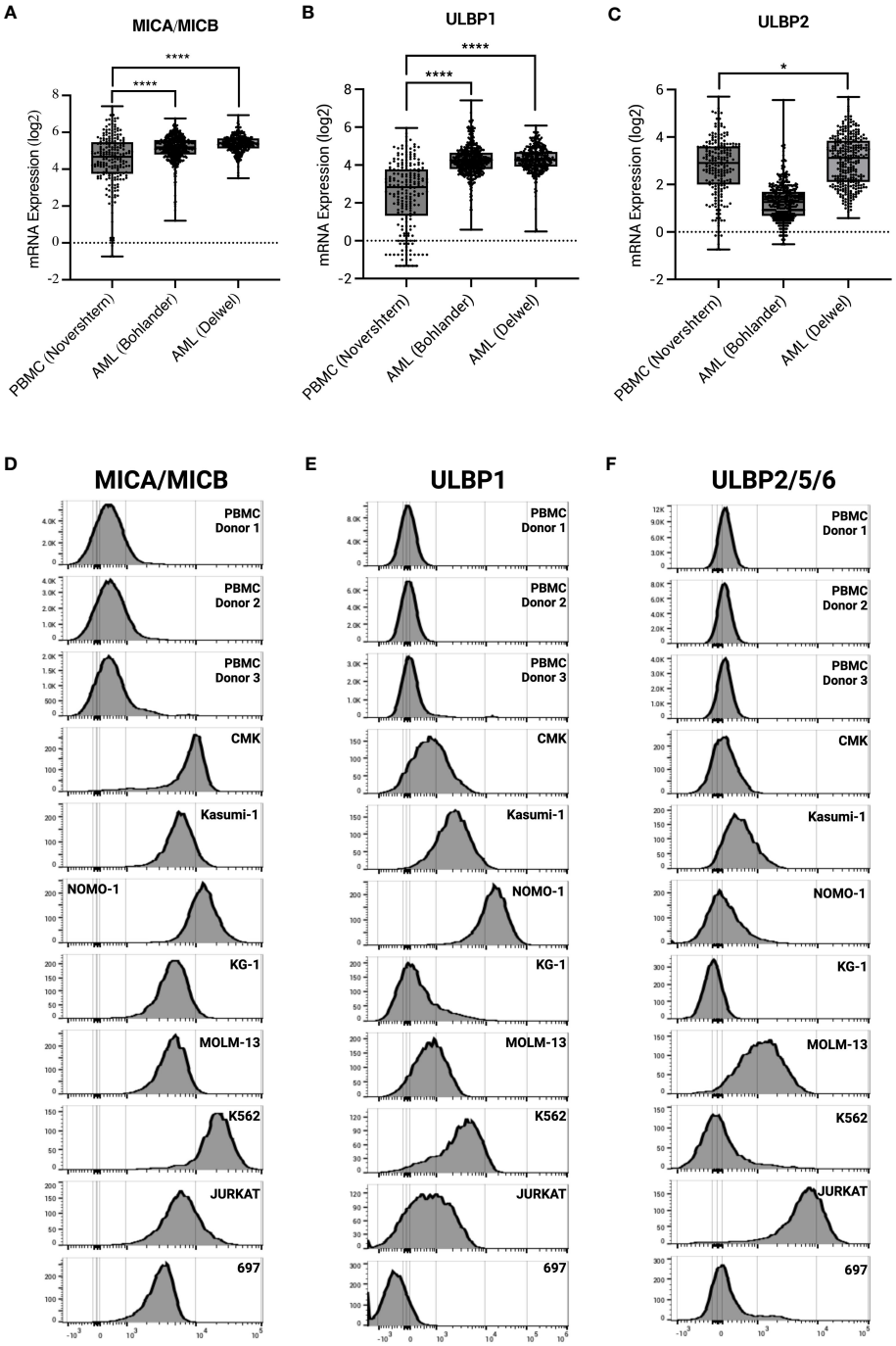

FIGURE 4
AML and leukemia cell lines express sress antigens MICA/MICB, ULBP1, and ULBP2/5/6. mRNA expression of stress antigens MICA/MICB **(A)**, ULBP1 **(B)**, and ULBP2 **(C)** on normal PBMC and two AML datasets queried using R2: Genomics Analysis and Visualization Platform (https://r2.amc.nl). Error bars represent SD. Statistical analysis represents One-Way ANOVA (****p < 0.0001; *p < 0.05). Histograms depict stress antigen expression of MICA/MICB **(D)**, ULBP1 **(E)**, and ULBP2/5/6 **(F)** in healthy donor PBMC (n = 3) and leukemia cell lines by flow cytometry.

3.5 c-kit-targeting mSCF CAR γδ T cells induce sca-1$^+$ cell death *ex vivo*

While hSCF sBite-modified γδ T cells should not induce toxicity against murine c-kit$^+$ cells in the bone marrow, as human SCF does not bind to murine c-kit, it is still important to consider the toxicity of mSCF CAR-modified γδ T cells against murine c-kit$^+$ cells in the bone marrow. To accomplish this, mSCF CAR γδ T cells and hSCF sBite γδ T cells were co-cultured for 24-hours with sca-1$^+$ isolated murine bone marrow at an E:T ratio of 1:2. Importantly, cells were co-cultured in both the absence and presence of supraphysiological levels of recombinant murine SCF

10.3389/fimmu.2023.1294555

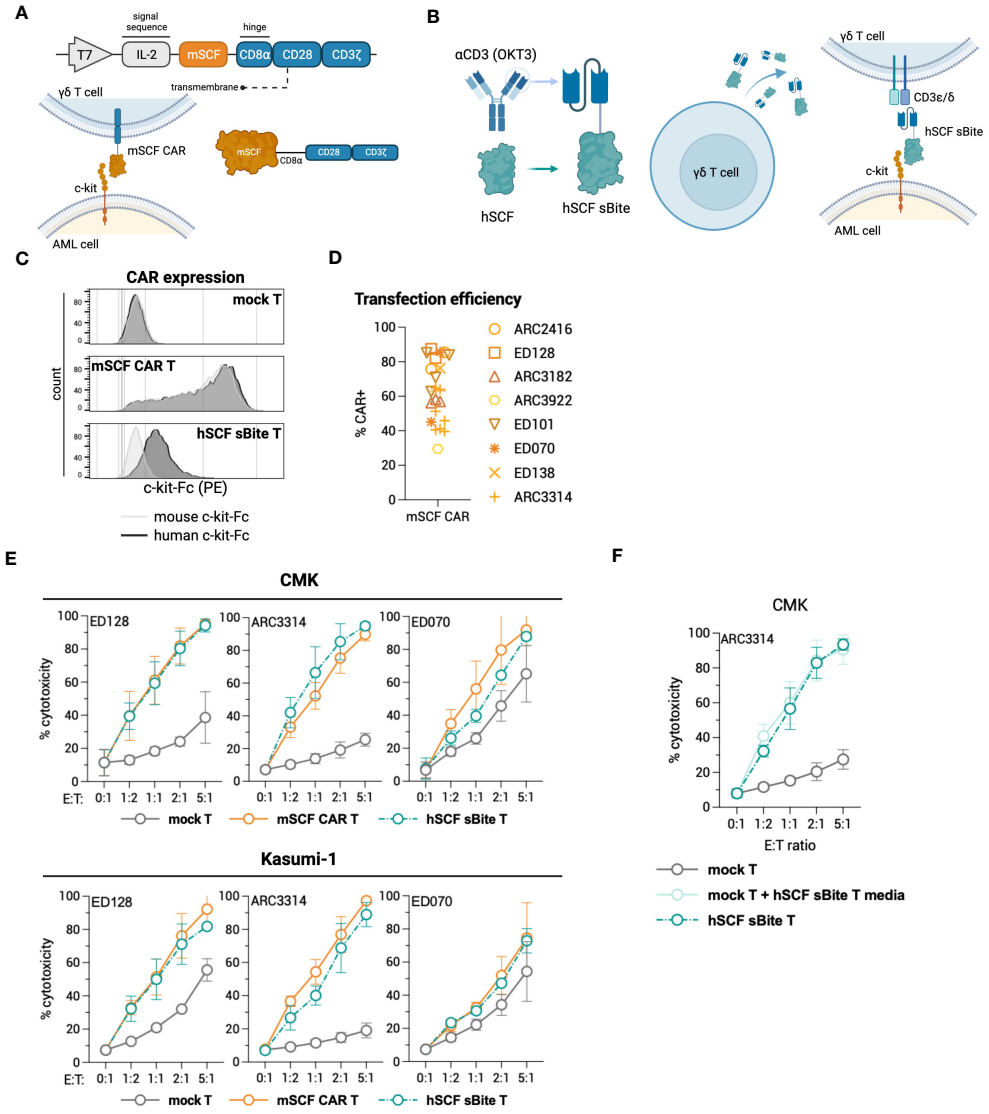

FIGURE 5
Design of novel ligand-based therapeutics and transient modification of γδ T cells. **(A)** Schematic of mSCF CAR construct for mRNA generation. **(B)** Diagram of hSCF sBite construct for mRNA generation. **(C)** Representative flow plots depicting mSCF CAR expression on primary γδ T cells transfected with 15 μg mRNA encoding denoted construct when stained with 20 ng of murine or human c-kit-Fc chimera. **(D)** Pooled transfection efficiency of primary γδ T cells modified with the mSCF CAR. n = 8 donors with n = 1-7 biological replicates. **(E)** Four-hour flow cytometry cytotoxicity assays of mSCF CAR- and hSCF sBite-modified primary γδ T cells against c-kit expressing AML cell lines compared to mock γδ T cell controls. Percent cytotoxicity is the sum of 7AAD$^+$, Annexin V$^+$, and 7AAD$^+$ Annexin V$^+$ cells when gated on VPD450-stained target cells only. Error bars represent SD. n = 3 donors with n = 2-7 biological replicates each. **(F)** Four-hour flow cytometry cytotoxicity assay of hSCF sBite γδ T cells against c-kit$^+$ CMK cells compared to mock γδ T cell control. Mock γδ T cells were co-cultured with media from hSCF sBite-modified cells and c-kit$^+$ CMK cells to measure sBite secretion. Error bars represent SD. n = 1 donor with n = 4 biological replicates.

to assess the functionality of a ligand-based therapy in a ligand competing environment.

After 24-hours, mSCF CAR γδ T cells, but not hSCF sBite or mock γδ T cells, reduced the c-kit$^+$ and Lineage$^-$ sca-1$^+$ c-kit$^+$ (LSK) compartments of murine bone marrow (Figures 6A, B). A colony forming unit (CFU) assay cultured at a 1:2 E:T ratio confirms a depletion of progenitor cells in only the cells co-cultured with mSCF CAR γδ T cells (Figure 6C). Importantly, this depletion can be seen in both the presence and absence of recombinant murine SCF, suggesting ligand competition inhibiting functionality is minimal.

3.6 γδ T cells have limited persistence in NSG mice

Given enhanced toxicity of mSCF CAR γδ T cells *ex vivo*, and the *in vivo* expansion of αβ T cells in murine bone marrow, we next determined γδ T-cell kinetics *in vivo* to evaluate possible bone marrow toxicity. To this end, NSG mice were injected with 10^7 γδ T cells by intravenous, retro-orbital injection and peripheral blood leukocytes were collected once daily for 4 days (Figure 7A). To determine if IL-2 or zoledronic acid enhanced *in vivo* persistence, a treatment regimen of two doses of 13,000 IU recombinant human

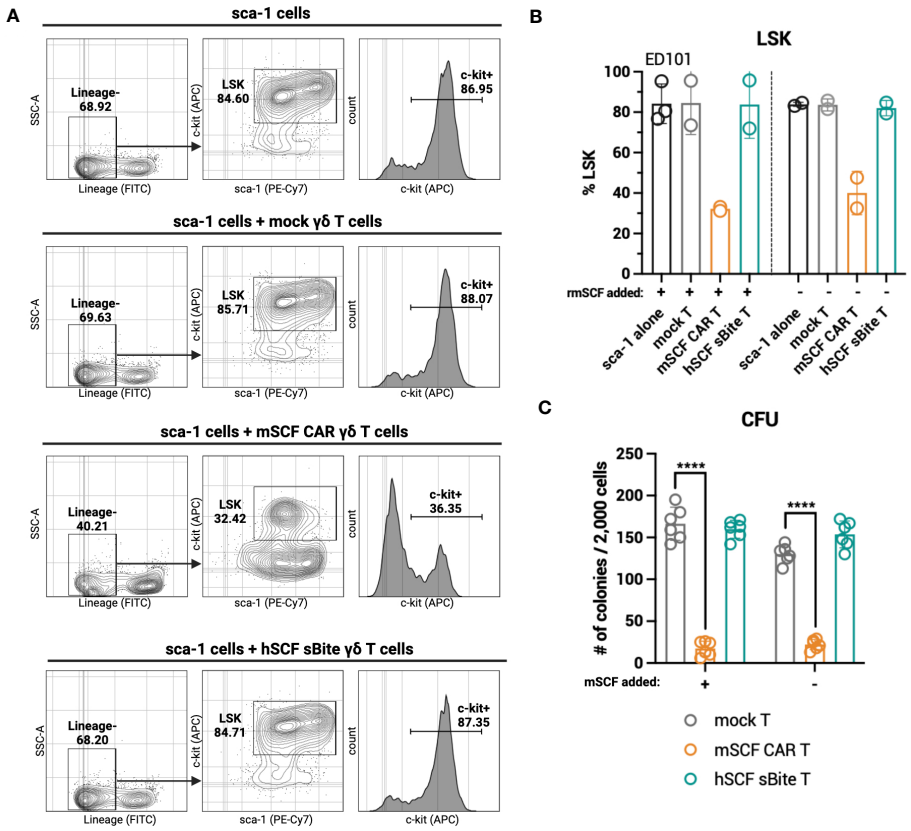

FIGURE 6
mSCF CAR-modified γδ T cells, but not hSCF sBite-modified γδ T cells, are cytotoxic against murine bone marrow *ex vivo*. **(A-C)** Briefly, murine sca-1$^+$ cells were harvested from bone marrow of C57BL/6 mice, rested for 1 day in media supplemented with mIL-3 (20 ng/mL), hIL-11 (100 ng/mL), and hFlt3 (100 ng/mL) and with or without mSCF (100 ng/mL), then co-cultured with γδ T cells for 24-hours at a 1:2 E:T ratio. Co-cultures were subject to flow cytometry analysis to assess LSK and c-kit$^+$ compartments. **(A)** Representative flow plots depict LSK and c-kit$^+$ compartments of murine sca-1$^+$ cells in a 24-hour *ex vivo* co-culture of mock γδ T cells, mSCF CAR γδ T cells, or hSCF sBite γδ T cells supplemented with all cytokine excluding mSCF. **(B)** %LSK (gated on live hCD3$^-$ hγδTCR$^-$ cells). Error bars represent SD. n = 2-3 biological replicates. **(C)** Number of colonies counted from colony forming unit (CFU) assay after 24-hour co-culture. Error bars represent SD. n = 3 technical replicates. n = 2 biological replicates.

IL-2 by intraperitoneal injection and one dose of 70 μg/kg zoledronic acid by subcutaneous injection or two doses of IL-2 alone were given. Percent γδ T cells were highest in circulation 48 hours after injection, with a steady decline in persistence up to 4 days after injection (Figure 7B). γδ T cells were found in the spleen (Figure 7C) and bone marrow 4 days after injection, though very low levels were found in the bone marrow (Figure 7D). Neither treatment with IL-2 or combination IL-2 and zoledronic acid treatment enhanced γδ T-cell persistence.

The lack of γδ T cells infiltrating the extravascular bone marrow space of NSG mice may prove advantageous to control on-target off-tumor toxicity in the bone marrow compartment. To investigate this further, we directly injected mSCF CAR γδ T cells into the left femur of NSG mice, with mock γδ T cells as a control, and assessed for bone marrow clearance two days later, when γδ T cells have previously been shown to be at their highest in circulation. Indeed, human CD3$^+$ human γδTCR$^+$ γδ T cells were found in the peripheral blood and spleen two days after injection (Figures 7E–G). However, only a small number γδ T cells remained in the injected left femur (Figure 7G). Additionally, changes in the c-kit$^+$ compartment of the peripheral blood, spleen, and bone marrow of the left and right femur were not observed between groups (Figures 7H–J). A CFU assay confirmed no changes in progenitor cell populations between the left (injected) and right (control) femur (Figure 7K).

Together, these data show γδ T cells do not persist beyond four days in NSG mice and do not efficiently infiltrate the extravascular bone marrow compartment. This, in addition to transient transgene expression, can serve as a safety mechanism to limit toxicity.

3.7 hSCF sBite-modified γδ T cells moderately improve survival *in vivo*

To assess efficacy against AML *in vivo*, NSG mice were first pre-conditioned with busulfan, then 5 × 10^6 luciferase-expressing CMK cells were established by intravenous injection the following morning. Beginning that afternoon, and for the next 3 days for a total of 4 doses, 1 × 10^7 total mSCF CAR γδ T cells or hSCF sBite γδ T cells were injected intravenously, with mock γδ T cells as a control (Figure 8A). Bioluminescence was assessed regularly throughout the study (Figure 8B).

10.3389/fimmu.2023.1294555

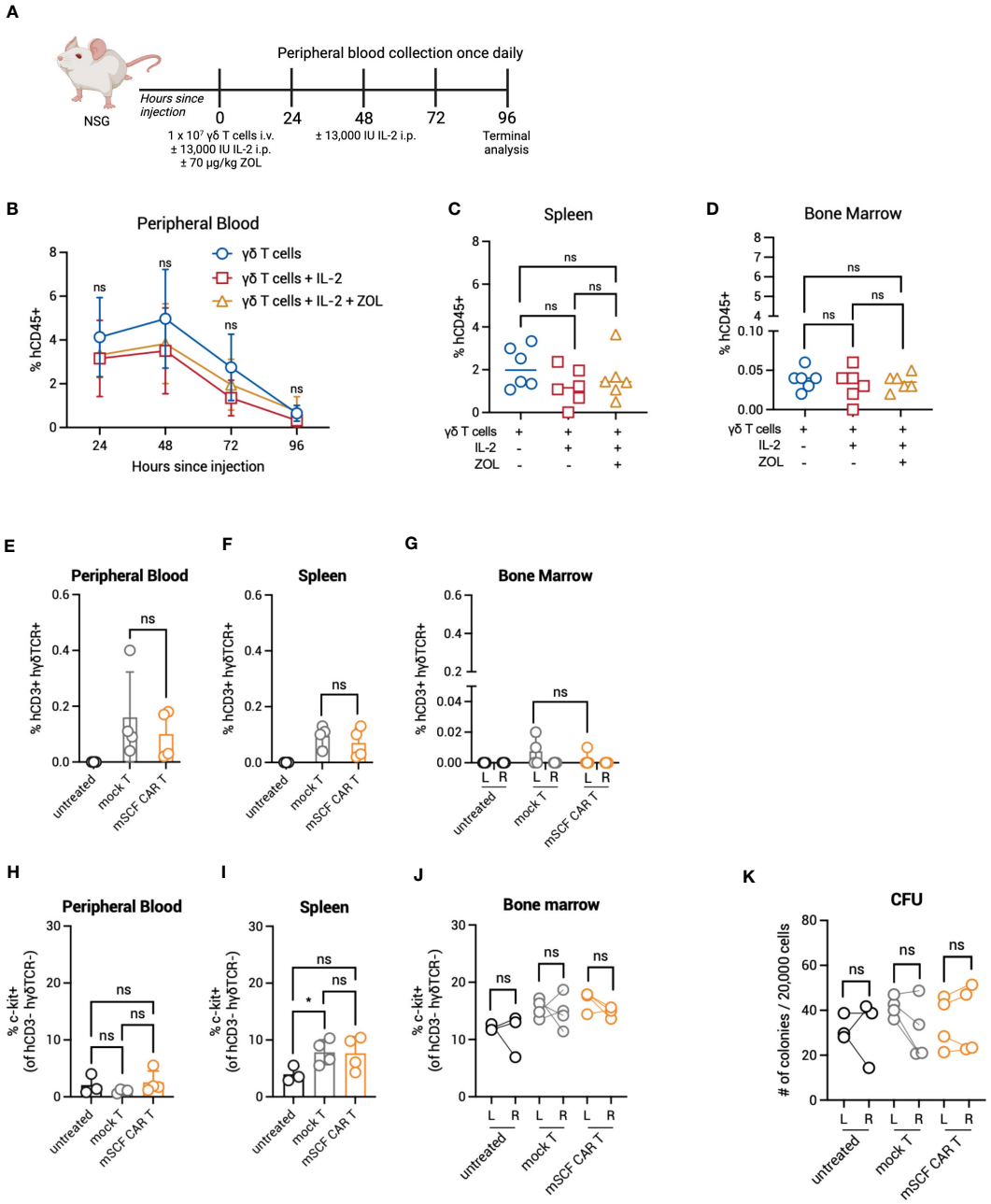

FIGURE 7
Persistence and toxicity of mSCF CAR γδ T cells in immunocompromised mice. **(A)** Schematic. NSG mice were injected with 1 x 10^7 γδ T cells IV alone on day 0 (n = 6), 1 x 10^7 γδ T cells IV on day 0 and two doses of 13,000 IU IL-2 IP on day 0 and day 2 (n = 6), or 1 x 10^7 γδ T cells IV on day 0, two doses of 13,000 IU IL-2 IP on day 0 and day 2, and one dose of 70 µg/mg zoledronic acid SC on day 0 (n = 6). Peripheral blood leukocytes were collected daily beginning 24-hours after the start of treatment and assessed for the presence of human γδ T cells. Four days later, mice were sacrificed to assess for human γδ T cells within the spleen and bone marrow. **(B)** %hCD45+ (gated on live cells) within the peripheral blood at each timepoint. Error bars represent SD. Statistical analysis represents Student's t test (ns, $p > 0.05$). **(C–D)** %hCD45+ (gated on live cells) within the spleen **(C)** and bone marrow **(D)** at end point. Statistical analysis represents Student's t test (ns, $p > 0.05$). **(E–G)** %hCD3+ hγδTCR+ (gated on live cells) within the peripheral blood **(E)**, spleen **(F)**, and the left and right femurs **(G)**. Error bars represent SD. Statistical analysis represents Student's t test (ns, $p > 0.05$). **(H–J)** %c-kit+ (gated on hCD3- hγδTCR- live cells) within the peripheral blood **(H)**, spleen **(I)**, and left and right femurs **(J)**. Error bars represent SD. Statistical analysis represents unpaired **(H, I)** or paired **(J)** Student's t test (*$p < 0.05$; ns, $p > 0.05$). **(K)** Number of colonies counted from a CFU assay on the left and right femurs. Statistical analysis represents paired Student's t test (ns, $p > 0.05$). Data point graphed is averaged from n = 3 technical replicates per mouse.

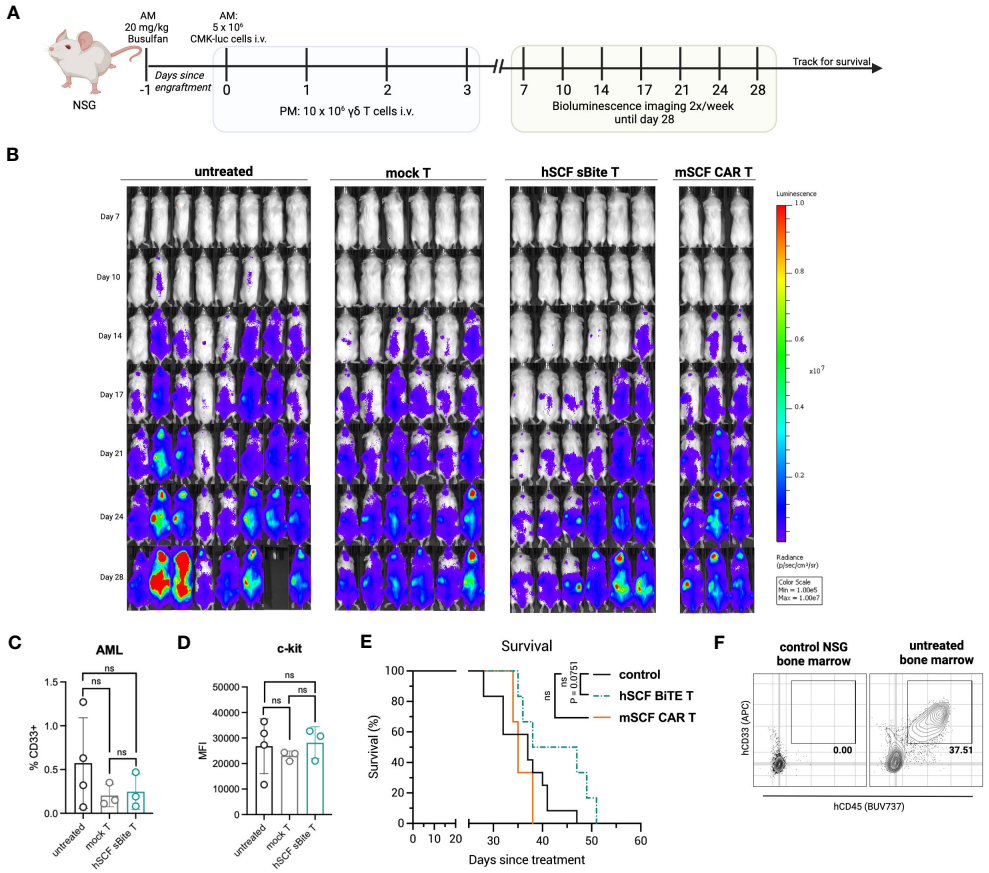

FIGURE 8
Treatment of hSCF sBite-modified γδ T cells only moderately prolongs survival *in vivo*, despite aggressive treatment regimen. **(A)** Experimental design. Briefly, NSG mice were pre-conditioned with 20 mg/kg busulfan IP on day -1, then injected with 5 x 10^6 CMK cells via tail-vein injection in the morning on day 0. Beginning in the afternoon on day 0, and then once daily for the next 3 days for a total of 4 doses, 1 x 10^7 γδ T cells were injected via tail-vein injection. Mice were subjected to bioluminescence imaging for the following 3 weeks, then followed for survival until they met endpoint. n = 8 untreated, n = 6 mock T treated, n = 6 hSCF sBite treated, n = 3 mSCF CAR treated. **(B)** Bioluminescence images. **(C)** Peripheral blood leukocytes were collected 3 weeks after the start of treatment and assessed for presence of $CD33^+$ CMK cells. Error bars represent SD. Statistical analysis represents Student's t test (ns, $p > 0.05$). **(D)** MFI of c-kit on CMK cells within the periphery. Statistical analysis represents Student's t test (ns, $p > 0.05$). **(E)** Kaplan-Meier survival analysis. Untreated and mock γδ T treated groups were combined as a control group. Statistical analysis represents log rank (Mantel-Cox) test (ns > 0.05). P-value is shown. **(F)** Representative flow plots of $hCD33^+$ $hCD45^+$ CMK cells in the bone marrow of an untreated mouse sacrificed near end-point.

There was a clear delay in cancer development in hSCF sBite γδ T cell-treated mice that was not observed in mSCF CAR γδ T cell-treated mice (Figure 8B). We postulate this suppression of growth despite similar *in vitro* results can be attributed to the secretion of the hSCF sBite and its ability to engage all γδ T cells, whereas the mSCF CAR can only function through transfected cells as it is a surface-bound protein.

Three weeks after the establishment of AML, peripheral blood leukocytes were collected and subject to flow cytometry analysis for the presence of $CD33^+$ CMK cells. At this time, there were few CMK cells in the peripheral blood, especially in mSCF CAR and hSCF sBite treated mice (Figure 8C). The mean percentage of CMK cells was lower in CAR and sBite treated mice compared to untreated mice (0.3% vs 0.6%), however the differences did not approach significance (Figure 8C). The surface expression of c-kit, as measured by MFI, on circulating CMK cells did not differ among groups, suggesting antigen escape is not a mechanism of immune evasion (Figure 8D). Complete blood counts (CBCs) did not show significant differences among groups, though all mice experienced thrombocytopenia, which was likely due to cancer progression affecting hematopoiesis (Figures S4A–H).

Treatment with mSCF CAR did not result in a significant survival benefit under the conditions tested, whereas hSCF sBite γδ T cells showed a trend towards survival enhancement (Figure 8E, $p = 0.075$). One possibility as a mechanistic explanation for the discrepancy between the efficient *in vitro* cytotoxicity and *in vivo* tumor clearance is the observation that surviving CMK cells were primarily observed in the extravascular bone marrow compartment (Figure 8F). We have previously shown that γδ T cells do not readily migrate to murine bone marrow (39), possibly due to minimal CXCR4 expression (Figure S5), an important chemokine receptor that helps leukocytes migrate from the periphery to the bone marrow (51). Taken together, these data suggest CMK cell growth is inhibited at early time points when injected into peripheral circulation up until they leave circulation and populate the bone marrow, where even high doses of γδ T cells cannot control disease burden in the extravascular bone marrow compartment.

4 Discussion

AML proves more difficult to manage with targeted therapeutics, such as CAR T therapy, than B-cell malignancies due to a scarcity of cancer-specific target receptors. Despite this, preclinical efforts to develop CAR T therapies for AML are ongoing and include targets such as CD33 (14), CD123 (52, 53), and CD70 (54). Most notably, therapeutics targeting CD33 (NCT03971799) and CD123 (NCT04678336) have advanced to clinical trials and show some clinical promise. However, critical measures are needed to mitigate off-target toxicities of these therapies within the bone marrow niche, as HSCs express both CD33 and CD123. As HSCT is curative for patients with AML and toxicities associated with pre-transplantation conditioning are severe (8), it has been observed that these toxicities may be advantageous and can even replace pre-transplantation conditioning.

C-kit, or CD117, has also been explored as a potential target for the development of CAR T therapy in the context of AML (22, 55). As c-kit is expressed on HSCs, current therapeutics targeting c-kit have been designed as a bridge-to-transplant by eradicating HSCs and leukemia simultaneously. Indeed, preclinical studies targeting c-kit as a means of pre-transplantation conditioning alone using antibody-immunotoxin conjugates by our lab (17) and others (18) and using CAR T cells (21) are ongoing. Clinically, briquilimab has shown promise in a Phase 1/2 dose-escalation trial of patients undergoing HSCT for severe combined immunodeficiency (SCID; NCT02963064) and a Phase 1 trial of patients undergoing HSCT for MDS/AML (NCT04429191).

Herein, we designed a ligand-based CAR and sBite to target c-kit using its cognate ligand SCF for the treatment of AML. The reasons for choosing a ligand-based design over a traditional scFv are many. Primarily, the elimination of stabilizing interactions that exist in the original antibody structure and simultaneous introduction of a non-native linker sequence between the variable heavy and light domains can result in thermal instability, partial scFv unfolding, domain swapping, and uncontrolled heterodimerization between two scFv molecules (27, 56). Therefore, to ensure stability of the antigen-binding domain and prevent scFv aggregation leading to tonic signaling of the CAR or inefficiency of the sBite, we tested a ligand-based design. It is true that some ligands, such as SCF, have dimerization potential; however, this does not interfere with receptor binding (and, in turn, therapeutic efficacy), as ligand dimers may still bind their receptors, though it may lead to enhanced tonic signaling. In fact, this design may prove advantageous over a traditional scFv-based design due to differences in affinity of the binding domain to the receptor. While the binding affinity for human SCF to human c-kit is strong and falls within the nanomolar range (57), it is still weaker than that of an antibody-antigen interaction, which can fall as low as picomolar range (58). Recent studies suggest that low-affinity CAR T cells have a lower risk of antigen escape through decreased trogocytosis (59), increased tumor selectivity (60), reduced exhaustion (61), and a reduced risk of cytokine release syndrome (CRS) due to decreased cytokine secretion (61). Together, these benefits may promote an enhanced safety profile of the therapeutic and allow for the potential combination with other therapeutics. That said, ligand-based therapeutics have been tested preclinically (62), with some advancing to clinical testing. For example, ligand-based IL-13Rα2-targeting CAR T cells whose binding domain utilizes a modified IL-13 ligand have shown promise for the treatment of childhood glioblastoma multiforme (GBM), resulting in tumor regression with enhanced IFN-γ signaling to activate the host immune system (63, 64).

The strategy of expressing CAR or sBite transgenes transiently in γδ T cells (rather than traditional αβ T cells) can serve as a safety modification and as a potential off-the-shelf therapeutic. γδ T cells do not cause graft-versus-host-disease (GvHD) reactions when transplanted across HLA barriers, as γδ T cells recognize antigen independent of HLA, while also contributing to graft-versus-leukemia (GvL) effect partially through the recognition of stress antigens (29–31). Importantly, pediatric patients with higher numbers of γδ T cells after HSCT have significantly higher event-free survival, a lower probability of infection, and a lower risk of relapse, with the survival advantage lasting as long as 7 years after HSCT (65, 66). Additionally, γδ T-cell infiltration into tumors has been identified as the most favorable prognostic factor in a pan-cancer analysis (67), further solidifying their clinical benefit.

We have been able to expand γδ T cells *ex vivo* from healthy donors using a serum-free Good Manufacturing Practice (GMP) compliant expansion protocol (33, 35) and have shown preclinical efficacy in B-cell leukemia (39) and neuroblastoma models (32, 38). In fact, this manufacturing strategy is under clinical investigation in a Phase 1 trial in the context of childhood neuroblastoma (NCT05400603). With respect to AML, it is known that difficulties in manufacturing multiple doses and a lack of persistence of mRNA-based αβ CAR T cells led to limited outcomes in clinical trials for anti-CD123 mRNA αβ CAR T cells in patients with r/r AML (NCT02623582) (68). Concerns about manufacturing can be reduced by instead employing γδ T cells as opposed to αβ T cells, which can be manufactured from healthy donors and serve as an off-the-shelf therapeutic. Furthermore, transient expression of a c-kit-directed therapeutic may limit off-target toxicity in the bone marrow niche, and un-modified γδ T cells can provide additional cancer surveillance through interaction with stress antigens, which we have shown are up regulated on AML cells.

In this study, c-kit-directed, ligand-based, mSCF CAR and hSCF sBite γδ T cells were generated by mRNA electroporation, achieving >60% CAR modification on average. *In vitro*, we show mSCF CAR- and hSCF sBite-modified γδ T cells are cytotoxic against c-kit$^+$ AML cell lines, ablating >90% of AML cell lines during a short-term cytotoxicity assay at a low effector-to-target ratio. Furthermore, a significant decrease in the LSK compartment of murine bone marrow during a 24-hour *ex vivo* co-culture was shown with mSCF CAR-modified γδ T cells, confirming the possibility of toxicity within the bone marrow compartment. Interestingly, this decrease in the LSK compartment was observed in both the absence and presence of supraphysiological levels of murine SCF and was confirmed by CFU assay, suggesting mSCF CAR γδ T cells affected LSK pluripotency. One possible explanation for this surprising result is that while the addition of SCF to the co-culture may have initially protected LSK cells from γδ T-cell

induced cell death by c-kit receptor internalization, subsequent re-expression of c-kit on the cell surface 12-14 hours later (69) may render them susceptible again, though more experiments are needed to test this hypothesis.

However, despite this toxicity *ex vivo*, it was not observed *in vivo*, likely due to limited trafficking of γδ T cells to the bone marrow niche. As such, treatment of AML-bearing mice with hSCF sBite-modified γδ T cells only slightly prolonged survival. This, in combination with previously published (38, 39, 70) and ongoing studies within our group, now defines an important limitation of studying human IL-2/zoledronic acid-expanded γδ T cells in the murine setting, as these cells do not migrate to the bone marrow, which is the site of later stage CMK cell growth in this AML mouse model. Alternatively, it is also possible that the inefficient migration of human γδ T cells into the murine extravascular bone marrow compartment may simply be due to specific-specific chemokine-receptor incompatibility. Despite this limitation, our data suggest that the hSCF sBite provides better control of tumor growth than the mSCF CAR, which can be attributed to the activation of both modified and non-modified cells, as the sBite is secreted and can interact with all $CD3^+$ cells.

As many myeloid malignancies include bone marrow involvement, a lack of trafficking of γδ T cells to the bone marrow niche proves challenging for clinical translation. Indeed, others have shown difficulty in trafficking of leukocytes to the bone marrow and have proposed the overexpression of CXCR4 by retroviral transduction as a means of enhancing trafficking (21). Another strategy may instead aim to enhance CXCR4 expression through modification of our expansion protocol, as it has been shown that the addition of TGF-β to expansion media upregulates CXCR4 on γδ T cells (70, 71). However, to date, we have not been successful in repeating this finding, possibly due to our unique serum-free method of expansion. Further studies aim to enhance γδ T-cell persistence in the bone marrow by similar modifications, and are currently underway. Despite these limitations, these data demonstrate ligand-based γδ T-cell therapies targeting c-kit for the treatment of AML is fundamentally possible. Future investigation will focus on efforts to enhance γδ T cell migration and infiltration into the bone marrow, and specifically address toxicities associated with hSCF sBite expression within the bone marrow compartment.

Data availability statement

The raw data supporting the conclusions of this article will be made available by the authors, without undue reservation.

Ethics statement

The studies involving humans were approved by the Institutional Review Board (IRB), Emory University, Atlanta, GA. The studies were conducted in accordance with the local legislation and institutional requirements. The participants provided their written informed consent to participate in this study. The animal study was approved by the Institutional Animal Care and Use Committee (IACUC), Emory University, Atlanta, GA. The study was conducted in accordance with the local legislation and institutional requirements.

Author contributions

GB: Conceptualization, Data curation, Formal Analysis, Funding acquisition, Investigation, Methodology, Visualization, Writing – original draft, Writing – review & editing. JL: Investigation, Writing – review & editing. JO: Investigation, Writing – review & editing. KP: Investigation, Writing – review & editing. JA: Investigation, Writing – review & editing. RA: Investigation, Writing – review & editing. AF: Resources, Writing – review & editing. BY: Resources, Writing – review & editing. DM: Resources, Writing – review & editing. HB: Resources, Writing – review & editing. SC: Conceptualization, Methodology, Writing – review & editing. BP: Conceptualization, Methodology, Writing – review & editing. CD: Conceptualization, Data curation, Formal Analysis, Funding acquisition, Methodology, Supervision, Writing – review & editing. HS: Conceptualization, Data curation, Formal Analysis, Funding acquisition, Methodology, Supervision, Writing – review & editing.

Funding

The author(s) declare financial support was received for the research, authorship, and/or publication of this article. This work was supported by grants from Curing Kids Cancer and the National Institutes of Health under an R21 grant (5R21CA223300 to HS) and an F31 grant awarded to Emory University (5F31CA265249-02 to GB).

Acknowledgments

The NOMO-1, Kasumi-1, KG-1, and MOLM-13 cell lines were generously donated by the laboratory of Dr. Douglas Graham at Emory University. The CMK cell line was kindly gifted by the laboratory of Dr. Brian Petrich when he was at Emory University. All healthy donor blood samples were obtained through the Emory Children's Clinical and Translational Discovery Core (CCTDC). Flow cytometers were maintained by the Pediatrics/Winship Flow Cytometry Core of Winship Cancer Institute of Emory University, who is supported by Children's Healthcare of Atlanta, Winship Cancer Institute, Emory University and NIH/NCI under award number P30CA138292. All figures were created using BioRender.com.

Conflict of interest

BY, HB, DM, and BP are employees of Expression Therapeutics, which develops cancer immunotherapies using

engineered γδ T cells. GB, CD, and HS are inventors on a patent application describing ligand-based cell and gene therapies for hematopoietic cancers owned by Emory University and licensed to Expression Therapeutics, Inc. HS and CD are cofounders of Expression Therapeutics and own equity in the company. The terms of these arrangements have been reviewed and approved by Emory University in accordance with its conflict-of-interest policies.

The remaining authors declare that the research was conducted in the absence of any commercial or financial relationships that could be construed as a potential conflict of interest.

The author(s) declared that they were an editorial board member of Frontiers, at the time of submission. This had no impact on the peer review process and the final decision.

Publisher's note

Supplementary material

The Supplementary Material for this article can be found online at: https://www.frontiersin.org/articles/10.3389/fimmu.2023.1294555/full#supplementary-material

References

1. Maude SL, Frey N, Shaw PA, Aplenc R, Barrett DM, Bunin NJ, et al. Chimeric antigen receptor T cells for sustained remissions in leukemia. *New Engl J Med* (2014) 371(16):1507–17. doi: 10.1056/NEJMoa1407222

2. Davila ML, Riviere I, Wang X, Bartido S, Park J, Curran K, et al. Efficacy and toxicity management of 19-28z Car T cell therapy in B cell acute lymphoblastic leukemia. *Sci Trans Med* (2014) 6(224):224ra25–ra25. doi: 10.1126/scitranslmed.3008226

3. Turtle CJ, Hanafi LA, Berger C, Gooley TA, Cherian S, Hudecek M, et al. Cd19 Car-T cells of defined Cd4+:Cd8+ Composition in adult B cell all patients. *J Clin Invest* (2016) 126(6):2123–38. doi: 10.1172/jci85309

4. Abramson JS, Palomba ML, Gordon LI, Lunning MA, Wang M, Arnason J, et al. Lisocabtagene maraleucel for patients with relapsed or refractory large B-cell lymphomas (Transcend nhl 001): A multicentre seamless design study. *Lancet* (2020) 396(10254):839–52. doi: 10.1016/s0140-6736(20)31366-0

5. Munshi NC, Anderson LD, Shah N, Madduri D, Berdeja J, Lonial S, et al. Idecabtagene vicleucel in relapsed and refractory multiple myeloma. *New Engl J Med* (2021) 384(8):705–16. doi: 10.1056/nejmoa2024850

6. Wang M, Munoz J, Goy A, Locke FL, Jacobson CA, Hill BT, et al. Kte-X19 car T-cell therapy in relapsed or refractory mantle-cell lymphoma. *New Engl J Med* (2020) 382(14):1331–42. doi: 10.1056/nejmoa1914347

7. Lichtman MA. A historical perspective on the development of the cytarabine (7 days) and daunorubicin (3 days) treatment regimen for acute myelogenous leukemia: 2013 the 40th anniversary of 7 + 3. *Blood Cells Mol Dis* (2013) 50(2):119–30. doi: 10.1016/j.bcmd.2012.10.005

8. Briot T, Roger E, Thépot S, Lagarce F. Advances in treatment formulations for acute myeloid leukemia. *Drug Discovery Today* (2018) 23(12):1936–49. doi: 10.1016/j.drudis.2018.05.040

9. Rubnitz JE, Razzouk BI, Lensing S, Pounds S, Pui CH, Ribeiro RC. Prognostic factors and outcome of recurrence in childhood acute myeloid leukemia. *Cancer* (2007) 109(1):157–63. doi: 10.1002/cncr.22385

10. de Rooij JD, Zwaan CM, van den Heuvel-Eibrink M. Pediatric Aml: from biology to clinical management. *J Clin Med* (2015) 4(1):127–49. doi: 10.3390/jcm4010127

11. Lie SO, Abrahamsson J, Clausen N, Forestier E, Hasle H, Hovi L, et al. Long-term results in children with Aml: Nopho-Aml study group–report of three consecutive trials. *Leukemia* (2005) 19(12):2090–100. doi: 10.1038/sj.leu.2403962

12. Smith FO, Alonzo TA, Gerbing RB, Woods WG, Arceci RJ, Children's Cancer G. Long-term results of children with acute myeloid leukemia: A report of three consecutive phase iii trials by the children's cancer group: Ccg 251, Ccg 213 and Ccg 2891. *Leukemia* (2005) 19(12):2054–62. doi: 10.1038/sj.leu.2403925

13. Sander A, Zimmermann M, Dworzak M, Fleischhack G, von Neuhoff C, Reinhardt D, et al. Consequent and intensified relapse therapy improved survival in pediatric Aml: results of relapse treatment in 379 patients of three consecutive Aml-Bfm trials. *Leukemia* (2010) 24(8):1422–8. doi: 10.1038/leu.2010.127

14. Kim MY, Yu K-R, Kenderian SS, Ruella M, Chen S, Shin T-H, et al. Genetic inactivation of Cd33 in hematopoietic stem cells to enable car T cell immunotherapy for acute myeloid leukemia. *Cell* (2018) 173(6):1439–53.e19. doi: 10.1016/j.cell.2018.05.013

15. Heo SK, Noh EK, Kim JY, Jeong YK, Jo JC, Choi Y, et al. Targeting C-kit (Cd117) by dasatinib and radotinib promotes acute myeloid leukemia cell death. *Sci Rep* (2017) 7(1):15278. doi: 10.1038/s41598-017-15492-5

16. Hassan HT. C-kit expression in human normal and Malignant stem cells prognostic and therapeutic implications. *Leuk Res* (2009) 33(1):5–10. doi: 10.1016/j.leukres.2008.06.011

17. Russell AL, Prince C, Lundgren TS, Knight KA, Denning G, Alexander JS, et al. Non-genotoxic conditioning facilitates hematopoietic stem cell gene therapy for hemophilia a using bioengineered factor viii. *Mol Ther Methods Clin Dev* (2021) 21:710–27. doi: 10.1016/j.omtm.2021.04.016

18. Czechowicz A, Palchaudhuri R, Scheck A, Hu Y, Hoggatt J, Saez B, et al. Selective hematopoietic stem cell ablation using cd117-antibody-drug-conjugates enables safe and effective transplantation with immunity preservation. *Nat Commun* (2019) 10(1):1–12. doi: 10.1038/s41467-018-08201-x

19. Czechowicz A, Kraft D, Weissman IL, Bhattacharya D. Efficient transplantation via antibody-based clearance of hematopoietic stem cell niches. *Science* (2007) 318(5854):1296–9. doi: 10.1126/science.1149726

20. Palchaudhuri R, Saez B, Hoggatt J, Schajnovitz A, Sykes DB, Tate TA, et al. Non-genotoxic conditioning for hematopoietic stem cell transplantation using a hematopoietic-cell-specific internalizing immunotoxin. *Nat Biotechnol* (2016) 34(7):738–45. doi: 10.1038/nbt.3584

21. Arai Y, Choi U, Corsino CI, Koontz SM, Tajima M, Sweeney CL, et al. Myeloid conditioning with C-kit-targeted car-T cells enables donor stem cell engraftment. *Mol Ther* (2018) 26(5):1181–97. doi: 10.1016/j.ymthe.2018.03.003

22. Myburgh R, Kiefer JD, Russkamp NF, Magnani CF, Nuñez N, Simonis A, et al. Anti-human Cd117 car T-cells efficiently eliminate healthy and Malignant Cd117-expressing hematopoietic cells. *Leukemia* (2020) 34(10):2688–703. doi: 10.1038/s41375-020-0818-9

23. Muffly LS, Chin M, Kwon H-S, Lieber C, Smith S, Sikorski R, et al. Early results of phase 1 study of Jsp191, an anti-Cd117 monoclonal antibody, with non-myeloablative conditioning in older adults with Mrd-positive Mds/Aml undergoing allogeneic hematopoietic cell transplantation. *J Clin Oncol* (2021) 39(15_suppl):7035. doi: 10.1200/JCO.2021.39.15_suppl.7035

24. Jasper Therapeutics I. *Jasper Therapeutics to Present New Positive Data on Briquilimab Conditioning in Patients with Fanconi Anemia at the 2023 Fanconi Anemia Research Fund Scientific Symposium [Press Release]* . Available at: https://irjaspertherapeuticscom/news-releases/news-release-details/jasper-therapeutics-present-new-positive-data-briquilimab.

25. Gill S, Maus MV, Porter DL. Chimeric antigen receptor T cell therapy: 25years in the making. *Blood Rev* (2016) 30(3):157–67. doi: 10.1016/j.blre.2015.10.003

26. Long AH, Haso WM, Shern JF, Wanhainen KM, Murgai M, Ingaramo M, et al. 4-1bb costimulation ameliorates T cell exhaustion induced by tonic signaling of chimeric antigen receptors. *Nat Med* (2015) 21(6):581–90. doi: 10.1038/nm.3838

27. Zajc CU, Salzer B, Taft JM, Reddy ST, Lehner M, Traxlmayr MW. Driving cars with alternative navigation tools – the potential of engineered binding scaffolds. *FEBS J* (2021) 288(7):2103–18. doi: 10.1111/febs.15523

28. Butler SE, Brog RA, Chang CH, Sentman CL, Huang YH, Ackerman ME. Engineering a natural ligand-based car: directed evolution of the stress-receptor Nkp30. *Cancer Immunol Immunothe* (2021) 71:165–76. doi: 10.1007/s00262-021-02971-y

29. Pistoia V, Tumino N, Vacca P, Veneziani I, Moretta A, Locatelli F, et al. Human Γδ T-cells: from surface receptors to the therapy of high-risk leukemias. *Front Immunol* (2018) 9:984. doi: 10.3389/fimmu.2018.00984

30. Blazar BR, Hill GR, Murphy WJ. Dissecting the biology of allogeneic Hsct to enhance the Gvt effect whilst minimizing Gvhd. *Nat Rev Clin Oncol* (2020) 17:475–92. doi: 10.1038/s41571-020-0356-4

31. Story JY, Zoine JT, Burnham RE, Hamilton JAG, Spencer HT, Doering CB, et al. Bortezomib enhances cytotoxicity of ex vivo-expanded gamma delta T cells against

acute myeloid leukemia and T-cell acute lymphoblastic leukemia. *Cytotherapy* (2021) 23(1):12–24. doi: 10.1016/j.jcyt.2020.09.010

32. Zoine JT, Knight KA, Fleischer LC, Sutton KS, Goldsmith KC, Doering CB, et al. Ex vivo expanded patient-derived gammadelta T-cell immunotherapy enhances neuroblastoma tumor regression in a murine model. *Oncoimmunology* (2019) 8 (8):1593804. doi: 10.1080/2162402X.2019.1593804

33. Sutton KS, Dasgupta A, McCarty D, Doering CB, Spencer HT. Bioengineering and serum free expansion of blood-derived Γδ T cells. *Cytotherapy* (2016) 18(7):881–92. doi: 10.1016/j.jcyt.2016.04.001

34. Burnham RE, Tope D, Branella G, Williams E, Doering CB, Spencer HT. Human serum albumin and chromatin condensation rescue ex vivo expanded Γδ T cells from the effects of cryopreservation. *Cryobiology* (2021) 99:78–87. doi: 10.1016/j.cryobiol.2021.01.011

35. Burnham RE, Zoine JT, Story JY, Garimalla SN, Gibson G, Rae A, et al. Characterization of donor variability for Γδ T cell ex vivo expansion and development of an allogeneic Γδ T cell immunotherapy. *Front Med* (2020) 7:588453. doi: 10.3389/fmed.2020.588453

36. Fleischer LC, Becker SA, Ryan RE, Fedanov A, Doering CB, Spencer HT. Non-signaling chimeric antigen receptors enhance antigen-directed killing by Γδ T cells in contrast to Aβ T cells. *Mol Ther Oncol* (2020) 18:149–60. doi: 10.1016/j.omto.2020.06.003

37. Boucher JC, Yu B, Li G, Shrestha B, Sallman D, Landin AM, et al. Large scale ex vivo expansion of Γδ T cells using artificial antigen-presenting cells. *J Immunothe (Hagerstown Md: 1997)* (2023) 46(1):5. doi: 10.1097/CJI.0000000000000445

38. Jonus HC, Burnham RE, Ho A, Pilgrim AA, Shim J, Doering CB, et al. Dissecting the cellular components of<I>Ex vivo</I> Γδ T cell expansions to optimize selection of potent cell therapy donors for neuroblastoma immunotherapy trials. *OncoImmunology* (2022) 11(1). doi: 10.1080/2162402x.2022.2057012

39. Becker SA, Petrich BG, Yu B, Knight KA, Brown HC, Raikar SS, et al. Enhancing the effectiveness of Γδ T cells by mrna transfection of chimeric antigen receptors or bispecific T cell engagers. *Mol Ther Oncol* (2023) 29:145–57. doi: 10.1016/j.omto.2023.05.007

40. McLeod C, Gout AM, Zhou X, Thrasher A, Rahbarinia D, Brady SW, et al. St. Jude cloud: A pediatric cancer genomic data-sharing ecosystem. *Cancer Discovery* (2021) 11(5):1082–99. doi: 10.1158/2159-8290.CD-20-1230

41. Zhou X, Edmonson MN, Wilkinson MR, Patel A, Wu G, Liu Y, et al. Exploring genomic alteration in pediatric cancer using proteinpaint. *Nat Genet* (2016) 48(1):4–6. doi: 10.1038/ng.3466

42. Uhlén M, Fagerberg L, Hallström BM, Lindskog C, Oksvold P, Mardinoglu A, et al. Proteomics. Tissue-based map of the human proteome. *Science* (2015) 347 (6220):1260419. doi: 10.1126/science.1260419

43. Consortium TU. Uniprot: the universal protein knowledgebase in 2023. *Nucleic Acids Res* (2022) 51(D1):D523–D31. doi: 10.1093/nar/gkac1052

44. Raikar SS, Fleischer LC, Moot R, Fedanov A, Paik NY, Knight KA, et al. Development of chimeric antigen receptors targeting T-cell Malignancies using two structurally different anti-Cd5 antigen binding domains in Nk and Crispr-edited T cell lines. *Oncoimmunology* (2018) 7(3):e1407898. doi: 10.1080/2162402X.2017.1407898

45. Zoine JT, Prince C, Story JY, Branella GM, Lytle AM, Fedanov A, et al. Thrombopoietin-based car-T cells demonstrate in vitro and in vivo cytotoxicity to Mpl positive acute myelogenous leukemia and hematopoietic stem cells. *Gene Ther* (2021) 29:1–12. doi: 10.1038/s41434-021-00283-5

46. Lee JY, Jonus HC, Sadanand A, Branella GM, Maximov V, Suttapitugsakul S, et al. Identification and targeting of protein tyrosine kinase 7 (Ptk7) as an immunotherapy candidate for neuroblastoma. *Cell Rep Med* (2023) 4(6):101091. doi: 10.1016/j.xcrm.2023.101091

47. Smith KA, Zsebo KM. Measurement of human and murine stem cell factor (C-*kit* ligand). *Curr Protoc Immunol* (1992) 4(1):6.17.1–6.17.11. doi: 10.1002/0471142735.im0617s04

48. Lennartsson J, Rönnstrand L. Stem cell factor receptor/C-kit: from basic science to clinical implications. *Physiol Rev* (2012) 92(4):1619–49. doi: 10.1152/physrev.00046.2011

49. Rigau M, Ostrouska S, Fulford TS, Johnson DN, Woods K, Ruan Z, et al. Butyrophilin 2a1 is essential for phosphoantigen reactivity by Γδ T cells. *Science* (2020) 367(6478):eaay5516. doi: 10.1126/science.aay5516

50. Wrobel P, Shojaei H, Schittek B, Gieseler F, Wollenberg B, Kalthoff H, et al. Lysis of a broad range of epithelial tumour cells by human?? T cells: involvement of Nkg2d ligands and T-cell receptor- versus Nkg2d-dependent recognition. *Scand J Immunol* (2007) 66(2-3):320–8. doi: 10.1111/j.1365-3083.2007.01963.x

51. Brenner S, Whiting-Theobald N, Kawai T, Linton GF, Rudikoff AG, Choi U, et al. Cxcr4-transgene expression significantly improves marrow engraftment of cultured hematopoietic stem cells. *Stem Cells* (2004) 22(7):1128–33. doi: 10.1634/stemcells.2003-0196

52. Gill S, Tasian SK, Ruella M, Shestova O, Li Y, Porter DL, et al. Preclinical targeting of human acute myeloid leukemia and myeloablation using chimeric antigen receptor–modified T cells. *Blood* (2014) 123(15):2343–54. doi: 10.1182/blood-2013-09-529537

53. Mardiros A, Dos Santos C, McDonald T, Brown CE, Wang X, Budde LE, et al. T cells expressing Cd123-specific chimeric antigen receptors exhibit specific cytolytic effector functions and antitumor effects against human acute myeloid leukemia. *Blood J Am Soc Hematol* (2013) 122(18):3138–48. doi: 10.1182/blood-2012-12-474056

54. Sauer T, Parikh K, Sharma S, Omer B, Sedloev D, Chen Q, et al. Cd70-specific car t-cells have potent activity against acute myeloid leukemia (aml) without hsc toxicity. *Blood* (2021) 138(4):318–30. doi: 10.1182/blood.2020008221

55. Magnani CF, Myburgh R, Brunn S, Chambovey M, Ponzo M, Volta L, et al. Anti-cd117 car T cells incorporating a safety switch eradicate human acute myeloid leukemia and hematopoietic stem cells. *Mol Ther Oncol* (2023) 30:56–71. doi: 10.1016/j.omto.2023.07.003

56. Willuda J, Honegger A, Waibel R, Schubiger PA, Stahel R, Zangemeister-Wittke U, et al. High thermal stability is essential for tumor targeting of antibody fragments: engineering of a humanized anti-epithelial glycoprotein-2 (Epithelial cell adhesion molecule) single-chain Fv fragment. *Cancer Res* (1999) 59(22):5758–67.

57. Tilayov T, Hingaly T, Greenshpan Y, Cohen S, Akabayov B, Gazit R, et al. Engineering stem cell factor ligands with different C-kit agonistic potencies. *Molecules* (2020) 25(20):4850. doi: 10.3390/molecules25204850

58. Landry JP, Ke Y, Yu G-L, Zhu XD. Measuring affinity constants of 1450 monoclonal antibodies to peptide targets with a microarray-based label-free assay platform. *J Immunol Methods* (2015) 417:86–96. doi: 10.1016/j.jim.2014.12.011

59. Nicholson RI, Gee JMW, Harper ME. Egfr and cancer prognosis. *Eur J Cancer* (2001) 37:9–15. doi: 10.1016/s0959-8049(01)00231-3

60. Arcangeli S, Rotiroti MC, Bardelli M, Simonelli L, Magnani CF, Biondi A, et al. Balance of anti-Cd123 chimeric antigen receptor binding affinity and density for the targeting of acute myeloid leukemia. *Mol Ther* (2017) 25(8):1933–45. doi: 10.1016/j.ymthe.2017.04.017

61. Singh AP, Zheng X, Lin-Schmidt X, Chen W, Carpenter TJ, Zong A, et al. Development of a quantitative relationship between car-affinity, antigen abundance, tumor cell depletion and car-T cell expansion using a multiscale systems Pk-Pd model. *mAbs* (2020) 12(1):1688616. doi: 10.1080/19420862.2019.1688616

62. Branella GM, Spencer HT. Natural receptor- and ligand-based chimeric antigen receptors: strategies using natural ligands and receptors for targeted cell killing. *Cells* (2021) 11(1):21. doi: 10.3390/cells11010021

63. Brown CE, Alizadeh D, Starr R, Weng L, Wagner JR, Naranjo A, et al. Regression of glioblastoma after chimeric antigen receptor T-cell therapy. *New Engl J Med* (2016) 375(26):2561–9. doi: 10.1056/nejmoa1610497

64. Alizadeh D, Wong RA, Gholamin S, Maker M, Aftabizadeh M, Yang X, et al. Ifnγ Is critical for car T cell–mediated myeloid activation and induction of endogenous immunity. *Cancer Discovery* (2021) 11(9):2248–65. doi: 10.1158/2159-8290.cd-20-1661

65. Perko R, Kang G, Sunkara A, Leung W, Thomas PG, Dallas MH. Gamma delta T cell reconstitution is associated with fewer infections and improved event-free survival after hematopoietic stem cell transplantation for pediatric leukemia. *Biol Blood Marrow Transplant* (2015) 21(1):130–6. doi: 10.1016/j.bbmt.2014.09.027

66. Minculescu L, Marquart HV, Ryder LP, Andersen NS, Schjoedt I, Friis LS, et al. Improved overall survival, relapse-free-survival, and less graft-vs.-host-disease in patients with high immune reconstitution of Tcr gamma delta cells 2 months after allogeneic stem cell transplantation. *Front Immunol* (2019) 10:1997. doi: 10.3389/fimmu.2019.01997

67. Gentles AJ, Newman AM, Liu CL, Bratman SV, Feng W, Kim D, et al. The prognostic landscape of genes and infiltrating immune cells across human cancers. *Nat Med* (2015) 21(8):938–45. doi: 10.1038/nm.3909

68. Cummins KD, Frey N, Nelson AM, Schmidt A, Luger S, Isaacs RE, et al. Treating relapsed/refractory (Rr) Aml with biodegradable anti-Cd123 car modified T cells. *Blood* (2017) 130:1359.

69. Chen C-L, Faltusova K, Molik M, Savvulidi F, Chang K-T, Necas E. Low C-kit expression level induced by stem cell factor does not compromise transplantation of hematopoietic stem cells. *Biol Blood Marrow Transplant* (2016) 22(7):1167–72. doi: 10.1016/j.bbmt.2016.03.017

70. Beatson RE, Parente-Pereira AC, Halim L, Cozzetto D, Hull C, Whilding LM, et al. Tgf-B1 potentiates Vγ9vδ2 T cell adoptive immunotherapy of cancer. *Cell Rep Med* (2021) 2(12). doi: 10.1016/j.xcrm.2021.100473

71. Peters C, Meyer A, Kouakanou L, Feder J, Schricker T, Lettau M, et al. Tgf-B Enhances the cytotoxic activity of Vδ2 T cells. *Oncoimmunology* (2019) 8(1):e1522471. doi: 10.1080/2162402X.2018.1522471

frontiers | Frontiers in Immunology

TYPE Original Research
PUBLISHED 23 November 2023
DOI 10.3389/fimmu.2023.1282710

OPEN ACCESS

EDITED BY
Jonathan Fisher,
University College London,
United Kingdom

REVIEWED BY
Alok Kumar Singh,
Johns Hopkins Medicine, United States
Mary Poupot-Marsan,
INSERM U1037 Centre de Recherche en Cancérologie de Toulouse, France

*CORRESPONDENCE
Allen Ka Loon Cheung
akcheung@hkbu.edu.hk

RECEIVED 24 August 2023
ACCEPTED 03 November 2023
PUBLISHED 23 November 2023

CITATION
Lui KS, Ye Z, Chan HC, Tanaka Y and Cheung AKL (2023) Anti-PD1 does not improve pyroptosis induced by γδ T cells but promotes tumor regression in a pleural mesothelioma mouse model.
Front. Immunol. 14:1282710.
doi: 10.3389/fimmu.2023.1282710

Anti-PD1 does not improve pyroptosis induced by γδ T cells but promotes tumor regression in a pleural mesothelioma mouse model

Ka Sin Lui[1], Zuodong Ye[1], Hoi Ching Chan[1], Yoshimasa Tanaka[2] and Allen Ka Loon Cheung[1]*

[1]Department of Biology, Faculty of Science, Hong Kong Baptist University, Hong Kong, Hong Kong, SAR, China, [2]Center for Medical Innovation, Nagasaki University, Nagasaki, Japan

Introduction: Mesothelioma is an aggressive tumor in the pleural cavity that is difficult to treat. Diagnosis is usually late with minimal treatment options available for the patients and with unfavorable outcomes. However, recent advances in immunotherapy using γδ T cells may have potential against mesothelioma, given its ample tumoricidal and tumor-migratory properties could allow its infiltration to the widespread tumor mass. Thus, we hypothesize that Vδ2 T cells can perform cytotoxic activities against mesothelioma especially when combined with immune checkpoint blocker against PD-1.

Methods: Human Vδ2 T cells were expanded from peripheral blood mononuclear cells using Tetrakis-pivaloyloxymethyl 2-(thiazole-2-ylamino) ethylidene-1,1-bisphosphonate (PTA) plus IL-2 for 13 days, before used to test for cytotoxicity against mesothelioma cell lines. Mesothelioma-bearing mice was established by Intrapleural administration of mesothelioma cell lines to test for the efficacy of Vδ2 T cells plus anti-PD-1 antibody combination treatment. Pyroptosis was evaluated by cell morphology, western blot analysis, and ELISA experiments. Flow cytometry was used to examine expression of BTN2A1, BTN3A1, PD-L1, PD-L2 on mesothelioma cell lines. Immunofluorescence staining was performed to detect Vδ2 T cells post adoptive transfer and characteristics of pyroptosis in *ex vivo* mesothelioma tissue sections.

Results: Indeed, our data demonstrated that Vδ2 T cells killing mesothelioma can be enhanced by anti-PD-1 antibody *in vitro*, especially for high PD-1 expressing cells, and in vivo in the intrapleural mesothelioma mice model established by us. Adoptive transfer of Vδ2 T cells into these mice leads to tumor regression by 30-40% compared to control. Immunofluorescence of the tumor section confirmed infiltration of Vδ2 T cells into the tumor, especially to cells with BTN2A1 expression (a Vδ2 T cell activating molecule) despite PD-L1 co-localization. Interestingly, these cells co-expressed cleaved gasdermin D, suggesting that pyroptosis was induced by Vδ2 T cells. This was verified by Vδ2 T/mesothelioma co-culture experiments demonstrating membrane ballooning morphology, increased cleaved caspase-3 and gasdermin E, and upregulated IL-1β and IL-18.

10.3389/fimmu.2023.1282710

Discussion: Vδ2 T cells plus anti-PD1 exhibited cytotoxicity against mesothelioma in vivo. However, we found no advantage for anti-PD-1 against PD-1 high expressing Vδ2 T cells in promoting pyroptosis. Taken together, our work demonstrated that Vδ2 T cells combined with anti-PD-1 antibody can be developed as a potential combination immunotherapy for mesothelioma.

KEYWORDS

gamma-delta T cells, mesothelioma, pyroptosis, anti-PD1, pleural mesothelioma

Introduction

Mesothelioma is an aggressive cancer that occurs in the mesothelial lining of the pleura, pericardium, and peritoneum (1). It is primarily caused by exposure to asbestos in construction materials during the 1950s, leading to the transformation of mesothelium cells into tumor cells with a latency period of over 30 years (1–3). In 2020, at least 26,000 mesothelioma-related deaths were reported globally (4), and the incidence and mortality rates are expected to rise, especially in undeveloped countries or cities where asbestos is still used. Unfortunately, the survival rate for mesothelioma patients remains low, and the available treatment options, including chemotherapy, surgical resection, and certain immunotherapies, only provide limited improvements in patient lifespan (5). Moreover, traditional therapies often result in unsatisfactory outcomes, with serious complications such as empyema leading to death (6, 7). Additionally, the lack of accurate and reliable biomarkers for mesothelioma detection hinders the widespread use of advanced immunotherapies like CAR $CD8^+$ T cells, which require high antigen specificity (8). In light of these challenges, alternative natural immune cells with tumoricidal properties that do not rely on antigen recognition may hold potential against mesothelioma.

Pyroptosis is a form of programmed cell death mediated by inflammatory caspases like Caspase 1, 3, 4, 5, 11, which enables an inflammatory response and the release of active IL-1β and IL-18 (7, 9). Pyroptosis is characterized by membrane blebbing, where cleaved gasdermin D and E proteins form membrane pores that induce cell swelling, rupture, and the release of cytokines (10–12) The cleavage of gasdermin D is mediated by the non-canonical activation of caspase 4, 5 or 11, while gasdermin E is cleaved by canonical pathway activated caspase 1 or 3 (10, 12–16). Pyroptotic cell death activates anti-tumor immune responses, making it a focus of cancer treatment research. Recent studies have shown upregulated pyroptosis-related genes in mesothelioma compared to other cancers, correlating with the susceptibility of mesothelioma cells to pyroptosis induction (15, 17). Therefore, utilizing Vδ2 T cells in our model may hold therapeutic potential for inducing pyroptosis and improving clinical outcomes for mesothelioma patients.

The Vδ2 subset of gamma-delta T cells (γδ T cells) possesses ample cytotoxicity against various cancers, including cholangiocarcinoma, pancreatic cancer, and lung cancer (18–20). We recently shown in a nasopharyngeal carcinoma mice model that Vδ2 T cells can infiltrate into tumor mass, particularly to areas of cells that express BTN2A1/BTN3A1 (21). These molecules facilitate the presentation of phosphoantigen (pAg) and subsequent activation of Vδ2 T cells, with increased pAg found in tumor cells. Importantly, Vδ2 T cells can be robustly expanded *in vitro* using a prodrug called tetrakis-pivaloxloxymethyl 2-(thiazole-2-ylamino) ethylidene-1,1-bisphosphonate (PTA), which exhibits cytotoxicity against mesothelioma through three distinct mechanisms (21–23).

Despite the advantages of Vδ2 T cells, they can become "exhausted" in the tumor microenvironment due to immune checkpoint molecules such as PD-1 and the ligands PD-L1 and PD-L2. Immune checkpoint inhibitors like nivolumab (anti-PD-1 antibody) or durvalumab (anti-PD-L1 antibody) are used clinically to restore the cytotoxic function of immune cells by blocking the PD-1/PD-L1 interaction (9, 24). These inhibitors have shown to extend the lifespan of mesothelioma patients by at least 10 months (25–30). Thus, we hypothesized that combining anti-PD-1 antibody with Vδ2 T cells can enhance the efficacy against mesothelioma.

Our data shows that anti-PD-1 antibody (nivolumab) can enhance the anti-tumor ability of Vδ2 T cells against mesothelioma *in vitro* in a pleural mesothelioma mice model, especially those cells with high PD-1 expression. Immunofluorescence staining of tissue sections revealed an increased number of tumor infiltrating Vδ2 T cells. Interestingly, live-imaging of Vδ2 T cells co-cultured with mesothelioma showed the induction of pyroptosis in the cells, which was confirmed by the detection of the active Caspase 3 and gasdermin E protein expressoion, as well as increased IL-1β and IL-18. However, the pyroptotic effect was not enhanced by anti-PD-1 antibody.

Materials and methods

Cell lines

Human mesothelioma cell lines MSTO-211H (hereafter referred to as MSTO) and NCI-H2052 cells (hereafter referred to as H2052) were purchased from ATCC, were cultured with RPMI 1640 medium (ATCC modification) (Cat. no. A1049101, GIBCO) supplemented with 10% fetal bovine serum (FBS) (Cat. no. 10270106, GIBCO). Cells were incubated at 37°C in 5% CO_2. MSTO

and H2052 cells are derived from the lung of male patients who suffered from biphasic and stage 4 mesothelioma, respectively.

Construction of luciferase reporter mesothelioma cell lines

pLV-Fluc-mCherry-Puro plasmid encoding luciferase reporter gene and mCherry gene (provided by Yue Jianbo, City University of Hong Kong) and the two packaging plasmids, pMD2.G (Cat. no. 12259, Addgene) and psPAX2 (Cat. no. 12260, Addgene) were co-transfected into 293T cells to generate lentiviruses. After 48 h post-transfection, the supernatant containing lentiviruses was collected and used to transduce the luciferase gene into MSTO or H2052 cells. Polybrene (10 μg/ml) was added to the cells to improve the lentiviral infection efficiency. After overnight incubation, MSTO or H2052 cells that tested positive for mCherry were selected by replacing culture medium supplemented with puromycin (2 μg/ml) after 2 days post-infection. Single-cell clones were further obtained by limiting dilution methods, and the luciferase activity was verified by Perkin Elmer EnSight Microplate Reader. The stable luciferase reporter mesothelioma cell lines – MSTO-luc and H2052-luc were then established.

Expansion and purification of γδ T cells *in vitro*

Peripheral blood mononuclear cells (PBMC) were isolated from human whole blood (Hong Kong Red Cross) using density gradient medium (Lymphoprep, Cat. no. 07861, STEMCELL Technologies). Tetrakis-pivaloyloxymethyl 2-(thiazole-2-ylamino) ethylidene-1,1-bisphosphonate (PTA) (PTA; 1 μM/ml; kindly provided by Prof Yoshimasa Tanaka, Nagasaki University) were used to stimulate the expansion of PBMC (4 x 10^6 cell/ml) in recombinant human IL-2 protein (rhIL-2; 100 IU/ml; Cat. no. 202-IL-500, R&D systems) containing RPMI 1640 medium (Gibco) supplemented with 10% FBS (GIBCO) at 37°C in 5% CO_2 incubator for 13 days with 50% media change every 2-3 days. After 13 days in culture, γδ T cells were purified by human TCR γ/$δ^+$ T Cell Isolation Kit (Cat. no. 130-092-892, Miltenyi Biotec). The purity of $CD3^+Vδ2^+$ cells were achieved to >95% before used for subsequent experiments.

Western blotting

MSTO-luc and H2052-luc were co-cultured with pre-treated γδ T cells using nivolumab (anti-PD-1 antibody) (Cat. no. HY-P9903, MedChemExpress) for 6 hours. 10 μM raptinal (Cat. no. HY-121320, MedChemExpress) and 20 μM terfenadine (Cat. no. HY-B1193, MedChemExpress) served as positive controls, mesothelioma cells alone served as negative control. Protein extraction from the cells was performed using denaturing lysis buffer (31). Protein concentrations were measured using Pierce BCA Protein Assay Kit (Cat. no. 23227, Thermo Scientific), 20 μg protein lysates were loaded into 10% SDS-PAGE gel for electrophoresis, followed by wet-transfer onto Immobilon PVDF membrane (Cat. no. ISEQ00005, Sigma-Aldrich) in Trans-Blot Electrophoretic Transfer Cell (Bio-Rad). Membranes were blotted with 5% skimmed milk (Blotting-grade Blocker, Cat. no. 1706404, Biorad) and 0.5% BSA (Cat. no. A3983, Sigma-Aldrich) in TBS-T (1x Tris-buffered saline with 0.1% Tween-20) at room temperature for 1 h. Unconjugated primary antibodies and HRP conjugated secondary antibodies used are shown in Supplementary Table 1. The protein bands were detected by ChemiDoc (Bio-Rad) using SuperSignal™ West Pico PLUS Chemiluminescent Substrate (Cat. no. 34580, Thermo Scientific). ImageJ software (http://imagej.nih.gov/ij/) was used to analyze the band intensities.

Flow cytometry

Cells were collected and washed with FACS buffer (1% FBS in PBS). The cells were then incubated with the appropriate conjugated antibodies, as indicated in Supplementary Table 1 in 100 μl FACS buffer at 4°C for 30 min for surface protein staining. Cells were analyzed using BD FACSCanto™ II or BD FACSymphony™ A1 flow cytometer.

Cytotoxicity assay

Mesothelioma cells were pre-labelled with 2 μM Calcein AM (Cat. No. C3100MP, Invitrogen). Luciferase reporter mesothelioma cells were co-cultured with Vδ2 T cells with or without pre-treatment of nivolumab (Anti-PD-1 antibody). Different ratios between Vδ2 T (effector): mesothelioma cells (target) (E:T) were performed in U-round bottom 96 well plate (Cat. No. 168136, Thermo Fischer Scientific) at 37°C in 5% CO_2 incubator for 4 h. 1% Triton X-100 was used as the positive control to induce maximum cell death. After centrifuging the plate at 400 xg for 5 minutes, the supernatant was transferred to a black 96-well plate, followed by measuring the released Calcein fluorescence signal at excitation wavelengths 495 nm and emission 515 nm wavelengths. Cell lysis percentage was calculated by $\frac{(\text{calcein of sample release} - \text{spontaneous release})}{(\text{maximum release} - \text{spontaneous release})} \times 100\,\%$. Maximum release refers to the positive control. Spontaneous release refers to Calcein-labelled target cells only.

Live cell imaging using Incucyte S3

To monitor total live and dead mesothelioma cells, mesothelioma cells were pre-labelled with 2 μM Calcein AM. Reporter mesothelioma cells were co-cultured with Vδ2 T cells with or without nivolumab pre-treatment at different E:T ratios in a 96-well flat bottom culture plate (Cat. No. CS016 – 0096, ExCell Bio) and incubated at 37°C in 5% CO_2 incubator. To track cell death, 250 nM Cytotox Red Reagent (Cat. No. 4632, Sartorius) was added to the culture medium, and the cells were monitored over a 4-hour period. Images were captured at regular intervals of 20-30 minutes using the IncuCyte S3 Live-Cell Analysis System (Sartorius) and analyzed using the Incucyte software (Sartorius).

Enzyme-linked immunosorbent assay

Different ratios of Vδ2 T cells to MSTO-luc and H2052-luc cells were co-cultured. Vδ2 T cells were pre-treated (or not) with nivolumab for 6 hours in a 96-well plate at various ratios. Controls include tumor cells only, raptinal or terfenadine treatment. After co-culture, the plate was centrifuge at 400 xg for 5 min before collecting the supernatants. Supernatants were stored at -80°C until they were used for the IL-1β ELISA kit, following the manufacturer's instructions (Cat. No. HSLB00D, R&D Systems). Optical density was measured at 450 nm with the wavelength correction at 540 nm using the microplate reader (BioTek Absorbance Microplate Reader), and the concentration of IL-1β in the samples was calculated.

Mice experiments

NOD.Cg-*Prkdc*^{scid}*Il2rg*^{tm1Wjl}/SzJ (NSG) mice were obtained from the City University of Hong Kong Laboratory Animal Research Unit. All animal experiment were approved by Hong Kong Baptist University Research Ethics Committee (#REC/20-21/0217 and #REC/21-22/0217, #REC/22-23/0438). To establish the xenograft pleural mesothelioma-bearing mice, 5 x 10^6 MSTO-luc or H2052-luc were injected into NSG mice intrapleurally (i.pl). On day 2, when luciferase signals became detectable, 1 x 10^7 Vδ2 T cells were adoptive transferred into the mice intravenously (i.v.) in 100 µl PBS. Nivolumab was administered intraperitoneally (i.p.) on day 3 and 6 post-tumor injection. PBS injection served as control. Mesothelioma luciferase activities were measured every 3-4 days by NightOWL II LB 983 *In Vivo* Imaging System (Berthold Technologies).

Immunofluorescence staining of tumor tissue sections

Tumor were fixed with 10% formalin solution (Cat. no. HT501128, Sigma-Aldrich) followed by dehydration of a series of 70%, 80%, 95%, 100% ethanol and xylene (Cat. no. 1330-20-7, RCI labscan), as well as paraffin (Cat. no. P3808, Sigma-Aldrich) for embedding. 5 µm tumor sections made using the microtome (Shandon Finesse 325 Rotary Microtome, Thermo Fisher Scientific), placed onto adhesive microscope glass slides (Cat. No. 0810501, Marienfeld) and kept at room temperature and in the dark until used. Tumor tissue sections were dewaxed, and antigen retrieval was performed using citrate-based antigen unmasking solution (Cat. No. H-3300, Vector Laboratories). Following blocking with 10% normal goat serum, the tumor sections were stained with unconjugated primary antibodies and conjugated secondary antibodies shown as Supplementary Table 1. Images were acquired by Stellaris confocal microscope (Leica). Counting of nucleated cells was based on Hoechst 33258 staining, with combinations three independent experiments.

Statistical analysis

Statistical analyses were performed using Student's *t*-test, one-way or two-way analysis of variance (ANOVA), unless otherwise indicated. $P< 0.05$ is considered statistically significant.

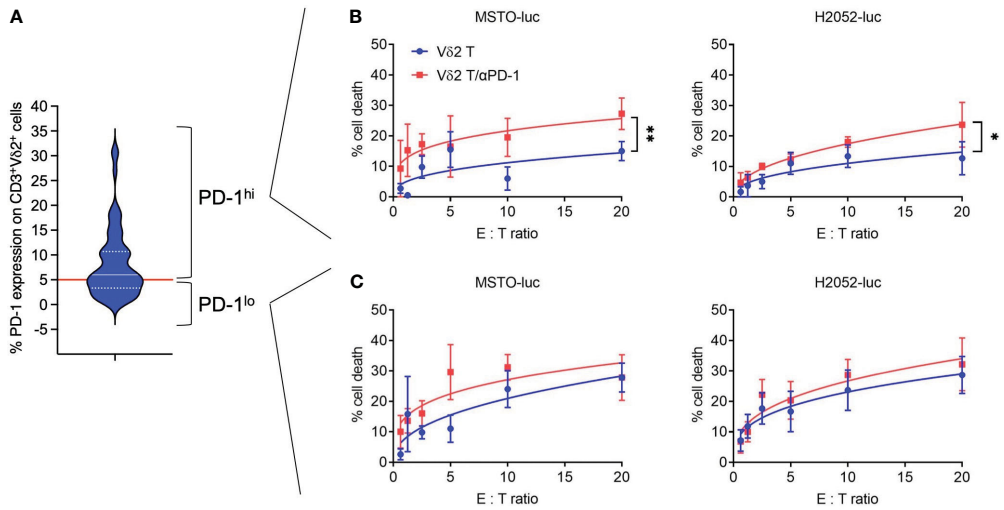

FIGURE 1
Anti-PD-1 enhances PD-1^{hi} Vδ2 T cells cytotoxicity towards mesothelioma cell lines. **(A)** PD-1 expression on CD3$^+$Vδ2$^+$ cells analyzed by flow cytometry shown as a violin plot. Red line indicates a cut-off of 5.99% as the median. **(B)** PD-1^{hi} Vδ2 T cells and **(C)** PD-1^{lo} Vδ2 T cells were co-cultured with luciferase reporter-transduced mesothelioma cell lines (MSTO-luc and H2052-luc) at different effector: target (E:T) ratios in a cytotoxicity assay. Data represents mean ± SEM from ≥ 3 independent experiments. Student's *t*-test was performed. *$P< 0.05$, **$P< 0.01$.

Results

Human Vδ2 T cells exerts cytotoxicity against mesothelioma cell lines

Freshly isolated human PBMCs were used to expand Vδ2 T cells for 13 days using PTA and IL-2 following the previously described protocol (21), where cell clusters are formed and expanded (Supplementary Figure 1A), with cell numbers that can be increased by 100-1000 fold (Supplementary Figure 1B). The purity of the $CD3^+V\delta2^+$ cells reached approximately 80% after expansion and was further enriched to >95% using microbeads (Supplementary Figures 1C–F). These cells were then used for cytotoxicity assays against two human mesothelioma cell lines with transduced luciferase expression (MSTO-luc and H2052-luc) (Supplementary Figure 2). Considering that PD-1 serves as an indicator of "exhausted" function in Vδ2 T cells, we first analyzed its expression by flow cytometry (Figure 1A). The median expression of PD-1 was found to be ~5.99%, which was used as the cut-off to distinguish PD-1^{lo} and PD-1^{hi} Vδ2 T cells. As shown in (Figures 1B, C), PD-1^{lo} Vδ2 T cells exhibited cytotoxic responses up to ~25% against MSTO-luc and H2052-luc. In contrast, PD-1^{hi} Vδ2 T cells resulted in ~12% and ~10% of cytotoxicity against MSTO-luc and H2052-luc, respectively. Thus, we tested the effect of pre-treating the cells with αPD-1 (nivolumab) to improve the cytotoxic functions. Indeed, αPD-1 could boost the cytotoxic effect of PD-1^{hi} Vδ2 T cells against MSTO-luc and H2052-luc by ~2-fold significantly (Figure 1B). However, the antibody only modestly enhanced cytotoxicity without statistical significance (Figure 1C). Therefore, determining the level of PD-1 expression on Vδ2 T cells is crucial in justifying the use of anti-PD-1 immune checkpoint inhibitors as immunotherapy for mesothelioma.

Vδ2 T cells plus αPD-1 retarded mesothelioma tumor growth *in vivo*

To test whether the combination of Vδ2 T cells and αPD-1 could be effective *in vivo*, we first established a mouse model of pleural mesothelioma. We injected NOD.Cg-*Prkdc*^{scid}*Il2rg*^{tm1Wjl}/SzJ (NSG) immunodeficient mice, aged 4-6 weeks, with 5 x 10^6 MSTO-luc or H2052-luc cells intrapleurally (i.pl). *In vivo* imaging showed xenograft detection in the upper body as early as two days post-injection, with signals increasing over time (Figures 2A–C, Supplementary Figures 3A, 4A). Tumor masses were observed in the pleural cavity, mesothelium, pleural lining, and pericardial lining (Supplementary Figures 3C, 4C).

Having established this model, we aimed to test the effectiveness of Vδ2 T cells combined with or without αPD-1 in these MSTO-luc and H2052-luc bearing mice. To validate the *in vitro* cytotoxicity data, we injected PD-1^{lo} and PD-1^{hi} Vδ2 T cells into the MSTO-luc bearing mice on day 3 and/or day 6 post-tumor injection (Figure 2A). One dose of intravenous (i.v.) injection of PD-1^{lo} or PD-1^{hi} Vδ2 T cells reduced tumor growth by ~48% and ~36%, respectively, as measured by tumor luciferase activity (Figures 2B, C). However, two doses of PD-1^{lo} Vδ2 T cells further reduced tumor by another ~10%, whilst PD-1^{hi} Vδ2 T cells improved it by ~12% (Figure 2C). Next, we sought to determine the effect of intraperitoneal (i.p.) αPD-1 treatment in combination with a 2-dose Vδ2 T cell adoptive immunotherapy in MSTO-luc mice in a separate experiment (Figure 2A). As shown in Figure 2D, two doses of PD-1^{hi} Vδ2 T cells with αPD-1 resulted in ~58% reduction in tumor growth compared to PBS control. Two doses of PD-1^{lo} Vδ2 T cells with αPD-1 resulted in ~67% reduction in tumor growth significantly. Control mice with tumor survived for 17 days, but those that received the PD-1^{lo} or PD-1^{hi} Vδ2 T cells with αPD-1 treatments survived for up to 21 days (Figure 2E), despite the significant tumor regression.

In the H2052-luc tumor-bearing mice, we tested the effectiveness of αPD-1 treatment in improving PD-1^{hi} Vδ2 T cells adoptive immunotherapy (Figure 2F). Two doses of PD-1^{hi} Vδ2 T cells showed an advantage over one dose in reducing tumor growth, by ~37% and ~19%, respectively. Further, one and two doses of PD-1^{hi} Vδ2 T cells/αPD-1 were able to decrease tumor growth by ~28% and ~49%, respectively. These data suggest that immune checkpoint blockade for Vδ2 T cells with high PD-1 expression confers a better prognosis for decreasing mesothelioma tumor mass. However, survival was only prolonged for one day with two doses of combined treatment in 33% of mice compared to control (Figure 2G). For the mice experiments, no significant weight loss was detected (Supplementary Figures 3B, 4B).

Expression of Vδ2 T cell activating and inhibitory molecules in mesothelioma

BTN2A1/BTN3A1 are essential molecules for the activation of Vδ2 T cells (32), as we have previously shown their detection in solid tumors (21). As the results suggest that Vδ2 T cells have certain effectiveness against mesothelioma, we next examined the expression of BTN2A1, BTN3A1, and PD-L1 in mesothelioma tumor tissue sections obtained from the mice experiments described earlier, at the time of death between 17-21 days.

As shown in Supplementary Figure 5A, BTN2A1, BTN3A1, and PD-L1 appears to express differentially on cells and in different regions by immunofluorescence and tile scan from confocal microscopy. Vδ2-TCR^+ cells were observed to have infiltrated into the tumor, with the cells present in 14% of the tumor area for the two-dose treatment, compared to 9% for the one-dose treatment (Figure 3A). Moreover, Vδ2-TCR^+ cells seemed to be located in regions where tumor cells expressed BTN2A1 (Figure 3A) and were found to coincide with cells that co-expressed PD-L1 (Supplementary Figure 5A). However, there are also regions in the tumor that only expressed BTN2A1, BTN3A1/PD-L1 or BTN2A1/BTN3A1/PD-L1 (Supplementary Figure 5A). In the tumors of mice that also received αPD-1 treatment along with Vδ2 T cells, Vδ2 T cells tended to localize to $BTN2A1^+$ cells, similar to those mice that received Vδ2 T cells only (Figure 3A). To further illustrate the characteristics of the tumor cells in the microenvironment, we quantified the cells expressing combinations of BTN2A1, PD-L1, and/or PD-L2 in the tile scan of the tumor section from the two-dose treatment

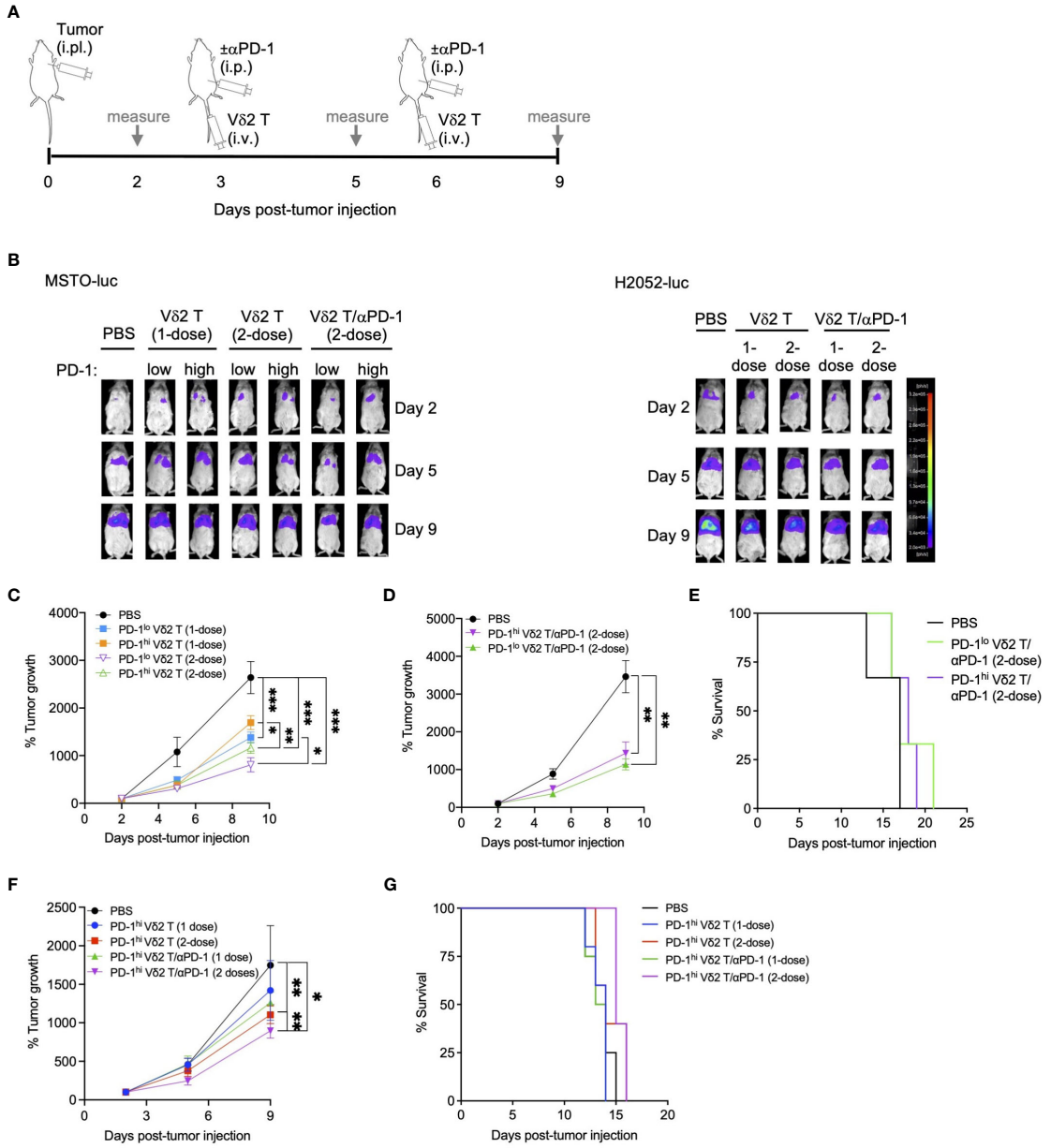

FIGURE 2
Vδ2 T cells and anti-PD-1 retard mesothelioma tumor growth *in vivo*. **(A)** Timeline of both MSTO-luc and H2052-luc mice experiment indicating the day for cell or αPD-1 injection, or measuring tumor size based on luciferase activity in tumor bearing mice. **(B)** Representative images of luciferase activities of MSTO-luc and H2052-luc bearing mice receiving PD-1^{lo} Vδ2 T with or without αPD-1 at 1-dose or 2-dose regimen. PBS injection served as control. **(C, D)** Tumor growth measured by luciferase activities over time compared to day 2 post MSTO-luc tumor injection for different treatment groups. Each group contains 3 to 6 mice. **(E)** Kaplan-Meier plot for MSTO-luc mice receiving 2-dose of PD-1^{lo} or PD-1^{hi} Vδ2 T with αPD-1 over time. **(F)** Tumor growth of H2052-luc mice receiving one or two doses of PD-1^{hi} Vδ2 T with or without αPD-1 over time, with survival as Kaplan-Meier plot **(G)**. Each group contains 4-5 mice. Data represents mean ± SEM. Two-way ANOVA statistical test was used for analyzing tumor growth curves. *P< 0.05, **P< 0.01, ***P< 0.001.

(Supplementary 5B). Out of the 24,636 nucleated cells counted, 29.7% did not express these markers, while 26.8% expressed all three markers. Interestingly, cells expressing BTN2A1 or BTN3A1 alone accounted for 27.5% and 2.0% of cells, respectively. 5.9% of cells co-expressed BTN2A1/BTN3A1, suggesting that Vδ2 T cells with full functional capacity could potentially target 32.7% of cells in the tumor if unhindered by the presence of PD-L1 or blocked by αPD-1. By flow cytometry, we analyzed MSTO-luc and H2052-luc cell lines for the expression of BTN2A1, BTN3A1, PD-L1 and PD-L2 (Figure 3B), BTN2A1 expression accounted for ~6.2% of MSTO-luc and ~4.6% of H2052-luc cells (Figure 3C). However, only<1% of cells co-expressed surface BTN2A1 and BTN3A1 (Figure 3D). A higher frequency of cells with PD-L1 expression was found in BTN2A1$^-$ (MSTO-luc: ~20%, H2052-luc: ~20%) compared to BTN2A1$^+$ (MSTO-luc: ~0.91%, H2052-luc: ~0.79%) sub-populations (Figure 3E). PD-L2 expression was found on ~2.1% of BTN2A1$^+$ and ~3.4% of BTN2A1$^-$ cells for MSTO-luc, and ~1.5% of BTN2A1$^+$ and ~8.0% of BTN2A1$^-$ cells for H2052-luc (Figure 3F).

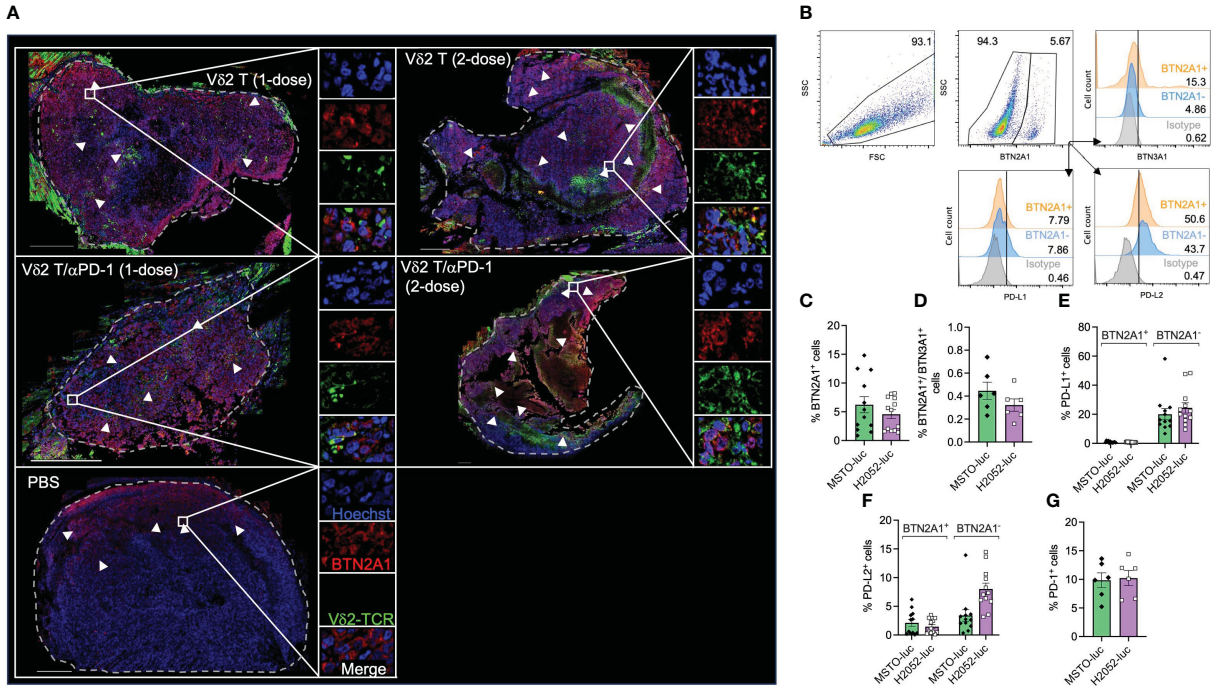

FIGURE 3
Analysis of Vδ2 T cell infiltration to BTN2A1$^+$ mesothelioma cells, and expression of BTN2A1, BTN3A1, PD-L1 and PD-L2. **(A)** H2052-luc tumor tissue sections from PBS, Vδ2 T (1-dose), Vδ2 T (2-dose), Vδ2 T/αPD-1 (1-dose), and Vδ2 T/αPD-1 (2-dose) mice were immunostained for Vδ2-TCR$^+$ (green), BTN2A1 (red), and nucleus (blue) with Hoechst 33258. Scale bar represents 500 µm. Representative tile scan images acquired by confocal microscopy are shown. Insets are expanded views of the rectangular regions. Dashed lines indicate the perimeter of the tumor. White arrows indicate regions of BTN2A1-expressing cells. **(B–G)** Flow cytometric analysis of the expression of BTN2A1, BTN3A1, PD-1, PD-L1, PD-L2 on MSTO-luc and H2052-luc cells. Gating strategy is shown in **(B)** with analysis for the expression (numbers are percentages) shown as column graphs for **(C)** BTN2A1$^+$, **(D)** BTN2A1$^+$/BTN3A1$^+$, **(E)** PD-L1$^+$, **(F)** PD-L2$^+$ and **(G)** PD-1$^+$ on MSTO-luc and H2052-luc cells. Data represents mean SEM from ≥ 6 independent experiments.

The expression of these molecules may explain the difference in the susceptibility of the cell lines towards Vδ2 T cell cytotoxicity (Figure 1). Moreover, we considered the expression of PD-1 on the mesothelioma cells (33), but it was found in only ~10% of cells (Figure 3G), and the expanded Vδ2 T cells exhibited an average 1.7 ±2.2% PD-L1 expression. Therefore, our analysis reveals that the expression of BTN2A1/BTN3A1 is low on the tumor cells in mesothelioma, where a high percentage of cells express PD-L1/PD-L2, which could hinder the effectiveness of Vδ2 T cells for immunotherapy. This suggests the necessity of αPD-1 co-treatment.

Vδ2 T cells induce pyroptotic cell death in mesothelioma cells

By performing live-imaging of the co-culture between Vδ2 T cells and mesothelioma cells, we observed the membrane blebbing (or "ballooning") phenotype while the tumor cells were undergoing cell death (Supplementary Video 1 and Supplementary Figure 6), which is indicative of pyroptosis. To confirm whether Vδ2 T cells are capable of inducing pyroptosis, western blot was used to determine whether the cleavage forms of gasdermin D (GasD), gasdermin E (GasE), caspase 3, 4 could be induced by co-culture of Vδ2 T cells with MSTO-luc cells. Tumor cells only served as negative control. Raptinal and terfenadine treatments served as positive controls for caspase 3 and caspase 4 activation, respectively. After 6 h of co-culture, there was increased level of cleaved caspase 3, particularly at the 10:1 E:T ratio (Figure 4A). αPD-1 treatment resulted in higher level of cleaved caspase 3 for the 10:1 ratio, but to a lesser extent with 5:1 and 2.5:1 ratios (Figure 4A). While cleavage of GasE (which can be mediated by caspase 3) seems to have a corresponding effect at 10:1 (Figure 4A). Band intensity values and the ratio of cleaved GasE over full-length GasE, and other proteins, are shown in Supplementary Figure 7. There was a small increase in cleaved GasD compared to control, particularly at the 5:1 ratios for Vδ2 T and/or αPD-1 (Figure 4A). However, cleaved caspase 4, and full-length forms of caspase 3, caspase 4, GasD and GasE were similar between the treatments (Figure 4A), suggesting that co-culture of Vδ2 T and MSTO-luc induced the active form of GasE likely due to caspase 3, and active form of GasD not due to caspase 4. While raptinal induced clear caspase 3 and GasE activation, terfenadine was not successful for caspase 4 and GasD in the mesothelioma cell lines (Figure 4A). In contrast, the effect on the active form of IL-18 was more obvious at 10:1 ratio co-culture, with a coupled decrease of pro-IL-18 (Figure 4B). However, αPD-1 did not increase the level of active IL-18 detected even at the 10:1 ratio. In concordance, there was an increased level of IL-1β released at 10:1 ratio compared to target cells alone, but addition of αPD-1 treatment had no improvement (Figure 4C). For H2052-luc co-cultured with Vδ2, cleavage of caspase 3, GasE and IL-18 can be

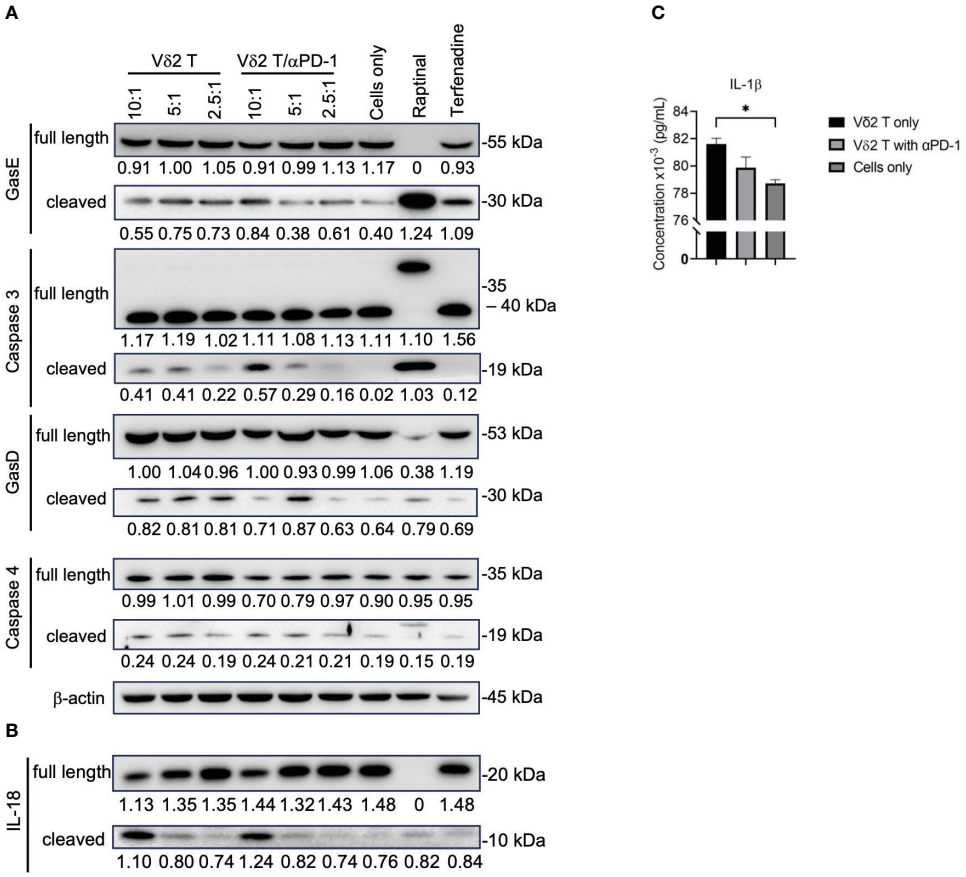

FIGURE 4
Vδ2 T cells induce pyroptosis in mesothelioma cells. **(A)** Analysis of protein expression level of gasdermin (Gas)E, caspase 3, GasD, caspase 4, and **(B)** IL-18, following 6 h of co-culture between Vδ2 T cells and MSTO-luc. Controls include raptinal and terfenadine, or cells only. Arrows indicate expected band size of the full-length or cleaved proteins. Numbers under the bands represent band intensity normalized to β-actin. Representative immunoblots are shown. **(C)** ELISA analysis of IL-1β release following 6 h of co-culture between Vδ2 T cells and MSTO-luc at 10:1 ratio. plotted as a column graph of mean ± SEM. Data from three independent experiments are shown. One-way ANOVA statistical test was used. *$P< 0.05$.

found only at the 10:1 ratio but not for GasD, caspase 4 or IL-1β (Supplementary Figures 8A, B). Interestingly, Vδ2 T cells did not induce cleaved form of caspase 3 in nasopharyngeal carcinoma (NPC) cell lines (Supplementary Figure 9). Taken together, Vδ2 T cells can induce pyroptosis in mesothelioma cells via the canonical pathway but only induce active IL-18 and IL-1β in MSTO-luc but not H2052-luc cells, which may suggest the higher resistance of H2052-luc cells towards Vδ2 T cell killing.

To verify this *in vivo*, we examined H2052-luc tumor tissue sections from control mice or mice that received one or two doses of PD-1^{hi} Vδ2 T cell and/or αPD-1 treatment, for the expression of Vδ2-TCR and cleaved GasD from different treatment groups. Indeed, higher frequency of cleaved GasD was found adjacent to Vδ2-TCR^{+} cells in those that received two-dose treatment (19%) compared to one-dose treatment (8%) (Figure 5). However, we did not find noticeable difference for one or two doses of Vδ2 T cell treatment with αPD-1 to without αPD-1 (Figure 5). These data may suggest that the greater effect of tumor regression could be related to the level of pyroptosis induced by Vδ2 T cells.

Discussion

Mesothelioma, which commonly affects the pleural cavity, poses a challenge for treatment due to its widespread nature and late-stage diagnosis. While immune checkpoint inhibitors have shown limited efficacy in treating this cancer (25, 26, 34), another promising approach is the use of chimeric antigen receptor (CAR)-T cell therapy, which has demonstrated high effectiveness against leukemia and certain solid tumors like neuroblastoma (35, 36). However, the lack of well-defined antigens specific to mesothelioma poses a significant obstacle in successfully implementing CAR-T cell therapy for this cancer. Nevertheless, clinical trials combining αPD-1 antibodies with CAR-T cells have shown promise, with median overall survival of mesothelioma patients potentially extended to around 20 months (37).

Alternatively, gamma-delta T cells have garnered attention as a non-MHC-restricted cell therapy for cancer due to their inherent tumor-killing and tumor-migratory properties (38). In the context of mesothelioma, a recent study demonstrated that Vδ2 T cells, when

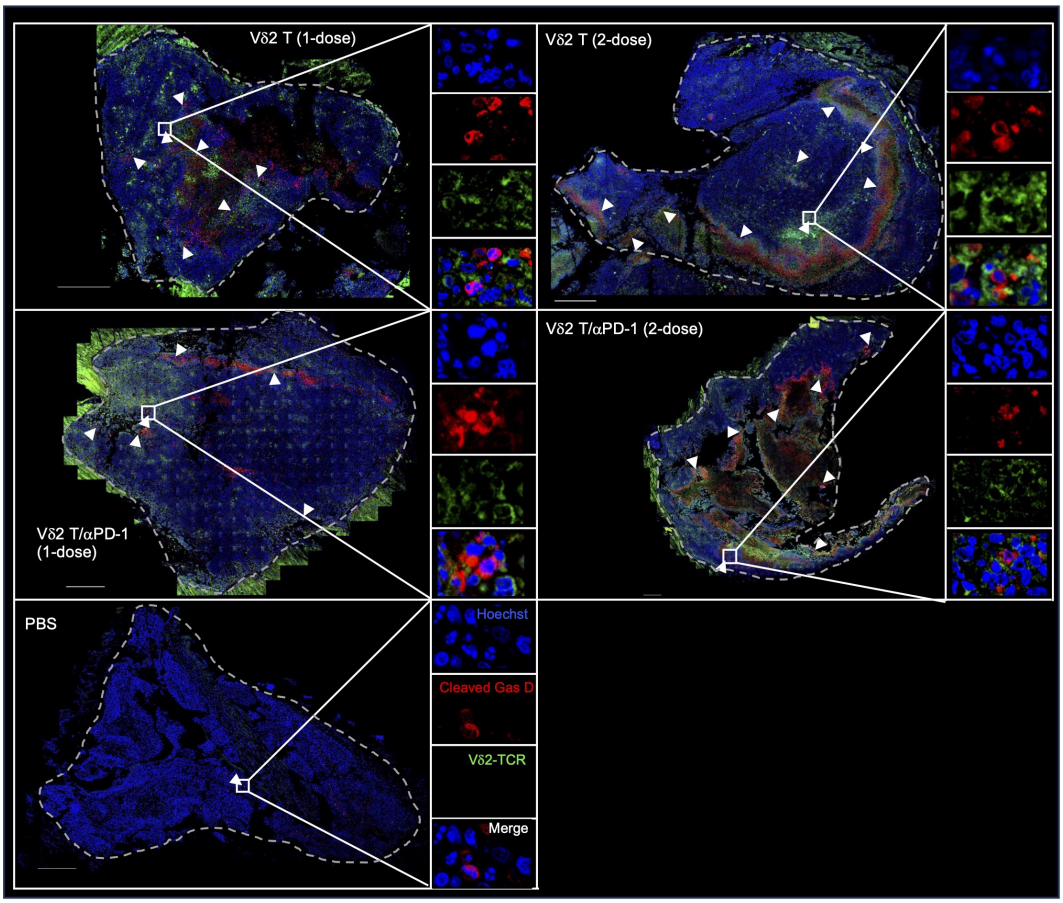

FIGURE 5
Vδ2 T cells induce pyroptosis in mesothelioma bearing mice. H2052-luc tumour tissue sections from PBS, Vδ2 T (1-dose), Vδ2 T (2-dose), Vδ2 T/αPD-1 (1-dose), and Vδ2 T/αPD-1 (2-dose) mice were immunostained for Vδ2-TCR (green), cleaved GasD (red), and nucleus (blue) with Hoechst 33258. Scale bar represents 500 µm. Representative tile scan images are shown. Insets are expanded views of the rectangular regions. Arrows indicate regions of cells with cleaved GasD expression.

stimulated by PTA, exhibit high cytotoxicity against tumor cells, particularly at a ratio of 200:1 (23). Although this high ratio may raise clinical concerns, it provides valuable insight into the potential of Vδ2 T cells for combating this type of cancer. The study further revealed that these cells can engage three different killing mechanisms: NKG2D, T cell receptor (TCR), and CD16/antibody-dependent cell cytotoxicity (ADCC) (23). The practicality of testing the possible *in vivo* effects is realized in this study, where we utilized an immunodeficient NSG mouse model of pleural mesothelioma, enabling the adoptive transfer of human Vδ2 T cells. To the best of our knowledge, this is the first study to employ such a model for studying mesothelioma and evaluating human immune cell therapy. Indeed, using this model, we found that Vδ2 T cells can retard tumor growth. However, complete tumor elimination may require a larger number of Vδ2 T cells, which needs to be carefully considered due to the potential physiological burden associated with transferring up to nearly 200 times more cells than the tumor itself.

One may consider achieving high efficacy for mesothelioma by combining Vδ2 T cells with immune checkpoint inhibitor, such as anti-PD-1 antibody, to maintain the tumoricidal functions. Our work here demonstrated that PTA-expanded Vδ2 T cells from different donors exhibited varying levels of PD-1 expression, ranging from 0.5% to 30.9% of the cells. Notably, we found that anti-PD-1 treatment enhanced PD-1^{hi} Vδ2 T cells by at least ~10-20%, based on data from tumor size and cytotoxicity assay. This suggests that further refinement and development of this combination therapy are warranted, and would be necessary to conduct profiling of different clinical mesothelioma to better understand the tumor immune landscape. In this consideration, besides anti-PD-1, other immune checkpoint inhibitors such as anti-BTLA, anti-CTLA-4, anti-Siglec-10, anti-TIGIT, anti-TIM-3, anti-LAG-3 could be tested in combination to investigate their suitability for enhancing Vδ2 T cell efficacy in this mesothelioma model. Previous studies have identified that BTLA can suppress the proliferation of Vδ2 T cells (39), while blocking the PD-1 and CTLA-4 pathways can restore T cell function and improve survival in melanoma, colon carcinoma, and ovarian carcinoma (40, 41). Inhibition of Siglec-10 has been shown to decrease the expression of immune inhibitory molecules within the tumor microenvironment and enhance the anti-tumor activity of cytotoxic T lymphocytes in hepatocellular carcinoma (42). Simultaneous blockade of TIGIT and PD-L1 has elicited tumor rejection and antigen-specific

protection in CT-26 tumor-bearing mice (43), and TIM-3 has been implicated in inhibiting the cytotoxic function of Vδ2 T cells by suppressing the release of granzyme B and perforin (44). Moreover, LAG-3 and PD-1 have been found to synergistically promote tumoral immune escape in melanoma and colon adenocarcinoma (45). Therefore, targeting these immune checkpoint molecules could help ensure the optimal function of Vδ2 T cells *in vivo*.

The induction of pyroptosis in mesothelioma cells by Vδ2 T cells is surprising. Pyroptosis is a type of inflammatory cell death that is characterized by the onset of inflammasome leading to the activation of caspase 3. Subsequently, cleaved caspase 3 activates GasE proteins, which migrate to the cell membrane, forming pores that allow osmosis and the formation of membrane blebbing due to cell swelling, ultimately resulting in cell rupture (10, 12). Simultaneously, the activated inflammasome caspase 1 cleaves pro-IL-18 and pro-IL-1β, releasing their active forms outside the cell through the GasE pore (10, 12, 14, 16). Alternatively, the non-canonical pathway can also lead to the formation of membrane pores through the activation of caspase 4, 5, or 11, which cleave GasD. In our study, we observed that co-culture of Vδ2 T cells with MSTO cells induced pyroptosis, as evidenced by the expression of caspase 3, GasE, GasD, IL-18, and IL-1β, which was confirmed through live-imaging. However, we did not observe stimulation of caspase 4 cleavage by Vδ2 T cells, suggesting that the cleaved GasD in MSTO cells may be mediated by caspase 5, caspase 8, or other mechanisms. While activation of pyroptosis has been demonstrated using various small molecules, chemotherapy drugs, or cell death inducers, this is the first instance where cell-cell interaction leading to pyroptosis has been shown for innate immune cells, particularly Vδ2 T cells. It would be worthwhile to investigate the cell surface proteins responsible for activating pyroptosis, as this knowledge could provide insights into enhancing the effectiveness of immune cell therapy by incorporating such proteins into the arsenal for combating cancer cells.

Data availability statement

The original contributions presented in the study are included in the article/Supplementary Material. Further inquiries can be directed to the corresponding author.

Ethics statement

The animal study was approved by (REC/22-23/0438) Animal Ethics Committee Hong Kong Baptist University. The study was conducted in accordance with the local legislation and institutional requirements.

Author contributions

KL: Data curation, Formal Analysis, Investigation, Methodology, Writing – original draft, Writing – review & editing. ZY: Investigation, Methodology, Resources. HC: Investigation, Methodology. YT: Writing – review & editing, Resources. AC: Conceptualization, Data curation, Funding acquisition, Investigation, Methodology, Project administration, Supervision, Visualization, Writing – original draft, Writing – review & editing.

Funding

The author(s) declare financial support was received for the research, authorship, and/or publication of this article. This work was supported by the Health and Medical Research Fund (HMRF) (18170032), Research Grant Council (RGC) Theme-based Research Scheme (TBRS, T12-712/21-R) and General Research Fund (GRF, 1120222), Pneumoconiosis Compensation Fund Board Research Grant (2022), Interdisciplinary Research Matching Scheme (RC-IRCs-1718-03), Faculty Research Grant (FRG2/17-18/066), Faculty Start-up Fund (SCI-17-18-01),Tier2 Start-up Grant (RC-SGT2/18-19/SCI/007), Incentive Award for External Competitive Research Grants, and Research Council Start-up Grant of Hong Kong Baptist University (to AC).

Acknowledgments

The authors thank Ms Yee Man Lee for laboratory and experimental support and contribution to this work. We thank Dr Tianfeng Tan and Mr Wai Shing Chung for technical support for confocal microscopy. We thank Miss Lap Yu Kung and Miss Tsz Man Yau for assistance in the counting the cells in the tumor tile scans.

Conflict of interest

The authors declare that the research was conducted in the absence of any commercial or financial relationships that could be construed as a potential conflict of interest.

The author(s) declared that they were an editorial board member of Frontiers, at the time of submission. This had no impact on the peer review process and the final decision.

Publisher's note

Supplementary material

The Supplementary Material for this article can be found online at: https://www.frontiersin.org/articles/10.3389/fimmu.2023.1282710/full#supplementary-material

References

1. Fels Elliott DR, Jones KD. Diagnosis of mesothelioma. *Surg Pathol Clin* (2020) 13 (1):73–89. doi: 10.1016/j.path.2019.10.001

2. Wong CK, Wan SH, Yu IT. History of asbestos ban in Hong Kong. *Int J Environ Res Public Health* (2017) 14(11):1327. doi: 10.3390/ijerph14111327

3. Tse LA, Yu IT, Goggins W, Clements M, Wang XR, Au JS, et al. Are current or future mesothelioma epidemics in Hong Kong the tragic legacy of uncontrolled use of asbestos in the past? *Environ Health Perspect* (2010) 118(3):382–6. doi: 10.1289/ehp.0900868

4. Board CNE. *Mesothelioma: Statistics.* (2023). Available at: https://www.cancer.net/cancer-types/mesothelioma/statistics.

5. Huang J, Chan SC, Pang WS, Chow SH, Lok V, Zhang L, et al. Global incidence, risk factors, and temporal trends of mesothelioma: A population-based study. *J Thorac Oncol* (2023) 18(6):792–802. doi: 10.1016/j.jtho.2023.01.095

6. Bueno R, Opitz I, Taskforce IM. Surgery in Malignant pleural mesothelioma. *J Thorac Oncol* (2018) 13(11):1638–54. doi: 10.1016/j.jtho.2018.08.001

7. Berzenji L, Van Schil P. Multimodality treatment of Malignant pleural mesothelioma. *F1000Res* (2018) 7:F1000 Faculty Rev-1681. doi: 10.12688/f1000research.15796.1

8. Guazzelli A, Meysami P, Bakker E, Bonanni E, Demonacos C, Krstic-Demonacos M, et al. What can independent research for mesothelioma achieve to treat this orphan disease? *Expert Opin Investig Drugs* (2019) 28(8):719–32. doi: 10.1080/13543784.2019.1638363

9. Zitvogel L, Kroemer G. Targeting PD-1/PD-L1 interactions for cancer immunotherapy. *Oncoimmunology* (2012) 1(8):1223–5. doi: 10.4161/onci.21335

10. Kovacs SB, Miao EA. Gasdermins: effectors of pyroptosis. *Trends Cell Biol* (2017) 27(9):673–84. doi: 10.1016/j.tcb.2017.05.005

11. Zhang X, Zhang P, An L, Sun N, Peng L, Tang W, et al. Miltirone induces cell death in hepatocellular carcinoma cell through GSDME-dependent pyroptosis. *Acta Pharm Sin B* (2020) 10(8):1397–413. doi: 10.1016/j.apsb.2020.06.015

12. Li KP, Shanmuganad S, Carroll K, Katz JD, Jordan MB, Hildeman DA. Dying to protect: cell death and the control of T-cell homeostasis. *Immunol Rev* (2017) 277 (1):21–43. doi: 10.1111/imr.12538

13. Shi H, Gao Y, Dong Z, Yang J, Gao R, Li X, et al. GSDMD-mediated cardiomyocyte pyroptosis promotes myocardial I/R injury. *Circ Res* (2021) 129 (3):383–96. doi: 10.1161/CIRCRESAHA.120.318629

14. He WT, Wan H, Hu L, Chen P, Wang X, Huang Z, et al. Gasdermin D is an executor of pyroptosis and required for interleukin-1beta secretion. *Cell Res* (2015) 25 (12):1285–98. doi: 10.1038/cr.2015.139

15. Zhang Z, Zhang Y, Xia S, Kong Q, Li S, Liu X, et al. Gasdermin E suppresses tumour growth by activating anti-tumour immunity. *Nature* (2020) 579(7799):415–20. doi: 10.1038/s41586-020-2071-9

16. Tsuchiya K, Nakajima S, Hosojima S, Thi Nguyen D, Hattori T, Manh Le T, et al. Caspase-1 initiates apoptosis in the absence of gasdermin D. *Nat Commun* (2019) 10 (1):2091. doi: 10.1038/s41467-019-09753-2

17. Khan M, Ai M, Du K, Song J, Wang B, Lin J, et al. Pyroptosis relates to tumor microenvironment remodeling and prognosis: A pan-cancer perspective. *Front Immunol* (2022) 13:1062225. doi: 10.3389/fimmu.2022.1062225

18. Alnaggar M, Xu Y, Li J, He J, Chen J, Li M, et al. Allogenic Vγ9Vδ2 T cell as new potential immunotherapy drug for solid tumor: a case study for cholangiocarcinoma. *J Immunother Cancer* (2019) 7(1):36. doi: 10.1186/s40425-019-0501-8

19. Lin M, Zhang X, Liang S, Luo H, Alnaggar M, Liu A, et al. Irreversible electroporation plus allogenic Vγ9Vδ2 T cells enhances antitumor effect for locally advanced pancreatic cancer patients. *Signal Transduct Target Ther* (2020) 5(1):215. doi: 10.1038/s41392-020-00260-1

20. Kakimi K, Matsushita H, Murakawa T, Nakajima J. γδ T cell therapy for the treatment of non-small cell lung cancer. *Transl Lung Cancer Res* (2014) 3(1):23–33. doi: 10.3978/j.issn.2218-6751.2013.11.01

21. Liu Y, Lui KS, Ye Z, Fung TY, Chen L, Sit PY, et al. EBV latent membrane protein 1 augments γδ T cell cytotoxicity against nasopharyngeal carcinoma by induction of butyrophilin molecules. *Theranostics* (2023) 13(2):458–71. doi: 10.7150/thno.78395

22. Tanaka Y, Murata-Hirai K, Iwasaki M, Matsumoto K, Hayashi K, Kumagai A, et al. Expansion of human γδ T cells for adoptive immunotherapy using a bisphosphonate prodrug. *Cancer Sci* (2018) 109(3):587–99. doi: 10.1111/cas.13491

23. Umeyama Y, Taniguchi H, Gyotoku H, Senju H, Tomono H, Takemoto S, et al. Three distinct mechanisms underlying human γδ T cell-mediated cytotoxicity against Malignant pleural mesothelioma. *Front Immunol* (2023) 14:1058838. doi: 10.3389/fimmu.2023.1058838

24. Jiang X, Wang J, Deng X, Xiong F, Ge J, Xiang B, et al. Role of the tumor microenvironment in PD-L1/PD-1-mediated tumor immune escape. *Mol Cancer* (2019) 18(1):10. doi: 10.1186/s12943-018-0928-4

25. Quispel-Janssen J, van der Noort V, de Vries JF, Zimmerman M, Lalezari F, Thunnissen E, et al. Programmed death 1 blockade with nivolumab in patients with recurrent Malignant pleural mesothelioma. *J Thorac Oncol* (2018) 13(10):1569–76. doi: 10.1016/j.jtho.2018.05.038

26. Okada M, Kijima T, Aoe K, Kato T, Fujimoto N, Nakagawa K, et al. Clinical efficacy and safety of nivolumab: results of a multicenter, open-label, single-arm, Japanese phase II study in Malignant pleural mesothelioma (MERIT). *Clin Cancer Res* (2019) 25(18):5485–92. doi: 10.1158/1078-0432.CCR-19-0103

27. Alley EW, Lopez J, Santoro A, Morosky A, Saraf S, Piperdi B, et al. Clinical safety and activity of pembrolizumab in patients with Malignant pleural mesothelioma (KEYNOTE-028): preliminary results from a non-randomised, open-label, phase 1b trial. *Lancet Oncol* (2017) 18(5):623–30. doi: 10.1016/S1470-2045(17)30169-9

28. Desai A, Karrison T, Rose B, Tan Y, Hill B, Pemberton E, et al. OA08. 03 phase II trial of pembrolizumab (NCT02399371) in previously-treated Malignant mesothelioma (MM): final analysis. *J Thorac Oncol* (2018) 13(10):S339. doi: 10.1016/j.jtho.2018.08.277

29. Kindler H, Karrison T, Tan YHC, Rose B, Ahmad M, Straus C, et al. OA13. 02 phase II trial of pembrolizumab in patients with Malignant Mesothelioma (MM): interim analysis. *J Thorac Oncol* (2017) 12(1):S293–4. doi: 10.1016/j.jtho.2016.11.301

30. Hassan R, Thomas A, Nemunaitis JJ, Patel MR, Bennouna J, Chen FL, et al. Efficacy and safety of avelumab treatment in patients with advanced unresectable mesothelioma: phase 1b results from the JAVELIN solid tumor trial. *JAMA Oncol* (2019) 5(3):351–7. doi: 10.1001/jamaoncol.2018.5428

31. Cheung AKL, Kwok HY, Huang Y, Chen M, Mo Y, Wu X, et al. Gut-homing Δ42PD1+Vδ2 T cells promote innate mucosal damage via TLR4 during acute HIV type 1 infection. *Nat Microbiol* (2017) 2(10):1389–402. doi: 10.1038/s41564-017-0006-5

32. Rigau M, Ostrouska S, Fulford TS, Johnson DN, Woods K, Ruan Z, et al. Butyrophilin 2A1 is essential for phosphoantigen reactivity by γδ T cells. *Science* (2020) 367(6478):eaay5516. doi: 10.1126/science.aay5516

33. Patsoukis N, Wang Q, Strauss L, Boussiotis VA. Revisiting the PD-1 pathway. *Sci Adv* (2020) 6(38):eabd2712. doi: 10.1126/sciadv.abd2712

34. Peters S, Scherpereel A, Cornelissen R, Oulkhouir Y, Greillier L, Kaplan MA, et al. First-line nivolumab plus ipilimumab versus chemotherapy in patients with unresectable Malignant pleural mesothelioma: 3-year outcomes from CheckMate 743. *Ann Oncol* (2022) 33(5):488–99. doi: 10.1016/j.annonc.2022.01.074

35. Todorovic Z, Todorovic D, Markovic V, Ladjevac N, Zdravkovic N, Djurdjevic P, et al. CAR T cell therapy for chronic lymphocytic leukemia: successes and shortcomings. *Curr Oncol* (2022) 29(5):3647–57. doi: 10.3390/curroncol29050293

36. CAR-T cells for solid tumors. *Nat Biotechnol* (2023) 41(5):588. doi: 10.1038/s41587-023-01803-x

37. Otsuka K, Mitsuhashi A, Goto H, Hanibuchi M, Koyama K, Ogawa H, et al. Anti-PD-1 antibody combined with chemotherapy suppresses the growth of mesothelioma by reducing myeloid-derived suppressor cells. *Lung Cancer* (2020) 146:86–96. doi: 10.1016/j.lungcan.2020.05.023

38. Willcox CR, Mohammed F, Willcox BE. The distinct MHC-unrestricted immunobiology of innate-like and adaptive-like human γδ T cell subsets-Nature's CAR-T cells. *Immunol Rev* (2020) 298(1):25–46. doi: 10.1111/imr.12928

39. Gertner-Dardenne J, Fauriat C, Orlanducci F, Thibult ML, Pastor S, Fitzgibbon J, et al. The co-receptor BTLA negatively regulates human Vγ9Vδ2 T-cell proliferation: a potential way of immune escape for lymphoma cells. *Blood* (2013) 122(6):922–31. doi: 10.1182/blood-2012-11-464685

40. Duraiswamy J, Kaluza KM, Freeman GJ, Coukos G. Dual blockade of PD-1 and CTLA-4 combined with tumor vaccine effectively restores T-cell rejection function in tumors. *Cancer Res* (2013) 73(12):3591–603. doi: 10.1158/0008-5472.CAN-12-4100

41. Gide TN, Quek C, Menzies AM, Tasker AT, Shang P, Holst J, et al. Distinct immune cell populations define response to anti-PD-1 monotherapy and anti-PD-1/anti-CTLA-4 combined therapy. *Cancer Cell* (2019) 35(2):238–255.e6. doi: 10.1016/j.ccell.2019.01.003

42. Xiao N, Zhu X, Li K, Chen Y, Liu X, Xu B, et al. Blocking siglec-10hi tumor-associated macrophages improves anti-tumor immunity and enhances immunotherapy for hepatocellular carcinoma. *Exp Hematol Oncol* (2021) 10(1):36. doi: 10.1186/s40164-021-00230-5

43. Johnston RJ, Comps-Agrar L, Hackney J, Yu X, Huseni M, Yang Y, et al. The immunoreceptor TIGIT regulates antitumor and antiviral CD8(+) T cell effector function. *Cancer Cell* (2014) 26(6):923–37. doi: 10.1016/j.ccell.2014.10.018

44. Li X, Lu H, Gu Y, Zhang X, Zhang G, Shi T, et al. Tim-3 suppresses the killing effect of Vγ9Vδ2 T cells on colon cancer cells by reducing perforin and granzyme B expression. *Exp Cell Res* (2020) 386(1):111719. doi: 10.1016/j.yexcr.2019.111719

45. Woo SR, Turnis ME, Goldberg MV, Bankoti J, Selby M, Nirschl CJ, et al. Immune inhibitory molecules LAG-3 and PD-1 synergistically regulate T-cell function to promote tumoral immune escape. *Cancer Res* (2012) 72(4):917–27. doi: 10.1158/0008-5472.CAN-11-1620

frontiers | Frontiers in Immunology

TYPE Original Research
PUBLISHED 29 February 2024
DOI 10.3389/fimmu.2024.1331322

OPEN ACCESS

EDITED BY
Daniel Abate-Daga,
Moffitt Cancer Center, United States

REVIEWED BY
Pawel Muranski,
Columbia University, United States
Miroslav Malkovsky,
University of Wisconsin-Madison,
United States

*CORRESPONDENCE
H. Trent Spencer
hspence@emory.edu

RECEIVED 31 October 2023
ACCEPTED 07 February 2024
PUBLISHED 29 February 2024

CITATION
Parwani KK, Branella GM, Burnham RE, Burnham AJ, Bustamante AYS, Foppiani EM, Knight KA, Petrich BG, Horwitz EM, Doering CB and Spencer HT (2024) Directing the migration of serum-free, *ex vivo*-expanded Vγ9Vδ2 T cells. *Front. Immunol.* 15:1331322. doi: 10.3389/fimmu.2024.1331322

Directing the migration of serum-free, *ex vivo*-expanded Vγ9Vδ2 T cells

Kiran K. Parwani[1,2], Gianna M. Branella[1,2], Rebecca E. Burnham[2], Andre J. Burnham[2], Austre Y. Schiaffino Bustamante[1,2], Elisabetta Manuela Foppiani[2], Kristopher A. Knight[2], Brian G. Petrich[3], Edwin M. Horwitz[2], Christopher B. Doering[2] and H. Trent Spencer[2]*

[1]Cancer Biology Program, Graduate Division of Biological and Biomedical Sciences, Emory University, Atlanta, GA, United States, [2]Aflac Cancer and Blood Disorders Center, Department of Pediatrics, Emory University School of Medicine and Children's Healthcare of Atlanta, Atlanta, GA, United States, [3]Expression Therapeutics LLC, Tucker, GA, United States

Vγ9Vδ2 T cells represent a promising cancer therapy platform because the implementation of allogenic, off-the-shelf product candidates is possible. However, intravenous administration of human Vγ9Vδ2 T cells manufactured under good manufacturing practice (GMP)-compliant, serum-free conditions are not tested easily in most mouse models, mainly because they lack the ability to migrate from the blood to tissues or tumors. We demonstrate that these T cells do not migrate from the circulation to the mouse bone marrow (BM), the site of many malignancies. Thus, there is a need to better characterize human γδ T-cell migration *in vivo* and develop strategies to direct these cells to *in vivo* sites of therapeutic interest. To better understand the migration of these cells and possibly influence their migration, NSG mice were conditioned with agents to clear BM cellular compartments, i.e., busulfan or total body irradiation (TBI), or promote T-cell migration to inflamed BM, i.e., incomplete Freund's adjuvant (IFA), prior to administering γδ T cells. Conditioning with TBI, unlike busulfan or IFA, increases the percentage and number of γδ T cells accumulating in the mouse BM, and cells in the peripheral blood (PB) and BM display identical surface protein profiles. To better understand the mechanism by which cells migrate to the BM, mice were conditioned with TBI and administered γδ T cells or tracker-stained red blood cells. The mechanism by which γδ T cells enter the BM after radiation is passive migration from the circulation, not homing. We tested if these *ex vivo*-expanded cells can migrate based on chemokine expression patterns and showed that it is possible to initiate homing by utilizing highly expressed chemokine receptors on the expanded γδ T cells. γδ T cells highly express CCR2, which provides chemokine attraction to C-C motif chemokine ligand 2 (CCL2)-expressing cells. IFNγ-primed mesenchymal stromal cells (MSCs) (γMSCs) express CCL2, and we developed *in vitro* and *in vivo* models to test γδ T-cell homing to CCL2-expressing cells. Using an established neuroblastoma NSG mouse model, we show that intratumorally-

injected γMSCs increase the homing of γδ T cells to this tumor. These studies provide insight into the migration of serum-free, *ex vivo*-expanded Vγ9Vδ2 T cells in NSG mice, which is critical to understanding the fundamental properties of these cells.

KEYWORDS

gamma delta T cells, gamma delta T cell migration, bone marrow, blood–bone marrow barrier, cancer immunotherapy

1 Introduction

Human γδ T cells represent 1%–5% of all T lymphocytes (1). γδ T cells, which diverge from their αβ T-cell counterpart that comprises 65%–70% of T cells, were discovered by their variant (V) γ chain of the T-cell receptor (TCR) (2). Variations of the γ and δ chains generate different subsets of γδ T cells (3, 4) with Vδ1, Vδ2, and Vδ3 as the main subsets of γδ T cells. Vδ1 and Vδ3 are abundant in the gut mucosa, whereas Vδ2 makes up the Vγ9Vδ2 subset and is the most prominent in circulation (5). Within the peripheral blood (PB), Vγ9Vδ2 T cells represent 60%–95% of the γδ T cells (6) and are considered part of both the innate and adaptive immune systems (7). They possess potent antitumor activity, which includes the inhibition of cancer cell proliferation and angiogenesis and the promotion of cancer cell apoptosis (8). An important feature of these cells is their TCR recognition of phospho-antigens (pAg) that accumulate in cancer cells through the dysregulation of the mevalonate pathway. Additionally, γδ T cells are not restricted to major histocompatibility complex (MHC)-mediated antigen presentation and thus do not require priming to recognize and kill targeted cells (9–11).

It has been demonstrated that γδ T cells can migrate *via* their chemoattractant properties (9, 12). Activated $V\delta2^+$ T cells upregulate C-C chemokine receptors CCR1 and CCR2 and C-X-C chemokine receptor CXCR3, among others, and migrate to their respective, secreted chemokine ligands (13, 14). Many cells including epithelial cells (15), mesenchymal stromal cells (MSCs) (16), T cells (17), and tumor cells (18) have been shown to secrete the chemokine for CCR2, C-C motif chemokine ligand 2 (CCL2). Importantly, the CCR2/CCL2 axis has also been implicated in mobilizing cells to and from the bone marrow (BM) and to sites of inflammation (19). Chemokine analysis in melanoma samples prior to treatment identified elevated CCL2, which corresponded with increased T-cell migration and positive response to treatment (20). Another chemokine receptor, CXCR4, is highly expressed in $CD4^+$ and $CD8^+$ T cells (21), and CXCR4 mRNA is moderately expressed in γδ T cells (22). The ligand for CXCR4, CXC motif ligand 12 (CXCL12), is expressed by various types of stromal cells such as the skin, lymph nodes, and the BM (23). BM inflammation increases the secretion of CXCL12, which augments T-cell co-stimulation, proliferation, cytokine production, and migration (24). $CD4^+$ and $CD8^+$ T cells have been shown to home to inflamed BM based on the strength of the CXCR4/CXCL12 axis (21). However, the migration of γδ T cells is not as well understood.

Ex vivo-expanded γδ T cells are manufactured by stimulating peripheral blood mononuclear cells (PBMCs) with various agents including cytokines and aminobisphosphonates (ABPs) (25–27). γδ T cells require growth factors to expand, and the cytokines interleukin-2 (IL-2) and 15 (IL-15) are frequently added to culture conditions to promote γδ T-cell growth and enhance their antitumor properties (9, 28). Culturing with IL-15 significantly increases the expression of cytotoxic factors such as perforin and granzyme B, and IL-2 acts as a growth factor to increase γδ T-cell yield during expansion (29, 30). These cytokines are combined with ABP agents to further stimulate Vγ9Vδ2 T cells. ABP drugs inhibit the mevalonate pathway to produce the pAgs that activate butyrophilin in PBMCs, which stimulate the TCR of Vγ9Vδ2 T cells (31, 32). Zoledronate (zol) is a well-characterized ABP drug used alone or with IL-2 to activate Vγ9Vδ2 cells. Alternatively, synthetic ABPs, such as isopentenyl pyrophosphate (IPP) and IL-2, have been employed to expand Vγ9Vδ2 T cells (27, 33, 34). In addition, *ex vivo*-expanded Vγ9Vδ2 T cells can be engineered to express chimeric antigen receptors (CARs), which do not interfere with cellular innate killing or antigen-presenting capabilities (35), or bispecific T-cell engagers, for example, targeting CD19, a marker of B-cell malignancies, and have shown effective killing of $CD19^+$ cell lines *in vitro* and *in vivo* (36, 37). In addition, non-signaling CARs were generated that activate alternate killing mechanisms of the engineered cells, such as through the receptor CD314 (NKG2D) (38).

We developed and optimized a good manufacturing practice (GMP)-compliant method of expanding and transducing or transfecting Vγ9Vδ2 T cells *ex vivo* (39, 40), which have been tested against glioblastoma, neuroblastoma, and T- and B-cell leukemias (22, 36, 41–43). The GMP-compliant expansion protocol is being tested in ongoing preclinical and clinical trials for several cancers. For example, a Phase I clinical trial is testing the combination of allogeneic Vγ9Vδ2 T cells with chemotherapy and the anti-GD2 antibody, dinutuximab, in relapsed or refractory neuroblastoma (NCT05400603). Although the preclinical data for these trials are extensive, they are confounded by the possible differences in partitioning of these cells within *in vivo* models, for example, mice, compared to the clinical setting. Several groups have shown that modified and non-modified cells are extremely effective

in vitro; however, we routinely identify homing to the sites of malignancy as a limiting factor for *in vivo* therapeutic efficacy.

Despite their multi-faceted attributes, the Vγ9Vδ2 T-cell migratory phenotype *in vivo* has not been well defined, especially the migration pattern of serum-free expanded cells in NSG mice. Thus, the goal of this study was to better understand how *ex vivo*, serum-free-expanded Vγ9Vδ2 T cells function in NSG mouse models, particularly their migration and homing to the mouse BM, where systemically administered leukemias and lymphomas develop. Here, we employed various pharmacological agents, expansion protocols, and chemokine relationships to further elucidate the *in vivo* migration properties of Vγ9Vδ2 T cells and to induce cell migration to predetermined sites.

2 Materials and methods

2.1 Animal studies

All animal studies were conducted in accordance with the Emory University Institutional Animal Care and Use Committee (IACUC) regulations [protocol: PROTO201800202]. NOD.Cg-Prkdc^{scid}IL2rg^{tm1Wjl}/SzJ (NSG) mice (5–7 weeks old) were purchased from Jackson Laboratory (Bar Harbor, ME, USA) and housed in a pathogen-free facility. Where possible, equal numbers of male and female mice were used for all studies. γδ T cells were administered using retro-orbital injections, as this route has been well-characterized and shown to be as effective as tail vein injections (44, 45).

2.2 γδ T cells

γδ T-cell expansions were performed based on our previously published GMP-compliant protocol, which has been well-described and utilized in several publications from our group (22, 36, 39, 46). Whole blood was obtained from healthy donors through the Children's Clinical Translational Discovery Core at Emory University, under approved Emory University Institutional Review Board (IRB) protocol, or from Expression Therapeutics LLC (Atlanta, GA, USA). PBMCs were isolated from fresh blood using Ficoll-Paque Plus (GE Healthcare Life Sciences, Milwaukee, WI, USA) density centrifugation. To preferentially select and expand γδ T cells, PBMCs were cultured in OpTmizer (Life Technologies, Carlsbad, CA, USA) containing OpTmizer supplement (Gibco, Grand Island, NY, USA), 1% penicillin/streptomycin (HyClone, Logan, UT, USA), and 2 mM L-glutamine (HyClone). Cells were then counted and resuspended at a concentration of 2e6 cells/mL in fresh culture media every 3 days. On days 0 and 3 of expansion, 5 μM zoledronate (Sigma-Aldrich, St. Louis, MO, USA) and 500 IU/mL IL-2 (PeproTech, Cranbury, NJ, USA) were added to the media. On day 6 of expansion, an αβ depletion was performed, described as previously published (47). Additionally, on days 6 and 9, 1,000 IU/mL IL-2 was added to the media. Expansion was ceased on day 12, and γδ T cells were used either fresh for experiments or frozen in PlasmaLyte A (Baxter International, Deerfield, IL, USA) containing 5% human serum albumin (Grifols, Barcelona, Spain) and 10% dimethyl sulfoxide (DMSO) (Sigma-Aldrich). Flow cytometry was performed on days 0, 6, and 12 to confirm successful expansion. Successful expansions resulted in cultures containing about 90% γδ T cells and less than 4% natural killer (NK) cells. The number of γδ T cells was determined by live cell counts multiplied by the percent of γδ T cells derived from flow cytometry (live CD3$^+$ γδTCR$^+$ cells). γδ T-cell fold expansion was determined by dividing the number of γδ T cells by the number on day 0 of expansion. Expansion results were analyzed on FlowJo software (v10).

2.3 Cell lines

Nalm6 and Nalm6-luciferase cells were a gift from the Porter Laboratory (Emory University). IMR5 cells were kindly provided by the Goldsmith Laboratory (Emory University). Nalm6 and IMR5 cells were cultured in RPMI 1640 (Corning, New York, NY, USA), 10% fetal bovine serum (FBS) (Bio-Techne, Minneapolis, MN, USA), and 1% penicillin/streptomycin (HyClone). CMK-luciferase cells were kindly provided by the Petrich Laboratory (Emory University) and were cultured with RPMI 1640, 20% FBS, and 1% penicillin/streptomycin.

2.4 Human MSCs

MSCs were isolated from BM in the residua (waste) of BM harvest collection bags obtained from healthy donors undergoing marrow harvest for clinical indications (Children's Hospital Atlanta, Emory University). Where possible, equal numbers of male and female donors were used for each study. The protocol was classified as exempt from oversight by the Emory University IRB. MSCs were isolated by adherence to plastic cell culture plates (Corning), a method that has been well-documented and a standard for isolating MSCs (48). Cells were then expanded in culture with Dulbecco's modified Eagle medium (DMEM) supplemented with 10% FBS, 1% penicillin/streptomycin, and 2 mM L-glutamine. In passage 2, our MSCs met the criteria proposed by the International Society for Cellular Therapy, and cells were maintained in culture at ~60% confluence in media. Media were also supplemented with 1 ng/mL IFNγ (PeproTech) for 48 hours to create IFNγ-primed human MSCs (γMSCs). The resulting media were used for conditioned medium experiments.

2.5 Tissue collection and analysis

Mouse tissue collection was performed at the endpoint of each experiment. Mouse PB was collected using capillary tubes and deposited in tubes containing 10% ethylenediaminetetraacetic acid (EDTA) (Invitrogen, Carlsbad, CA, USA). Samples were centrifuged at 2,400 ×*g* for 15 minutes at 4°C. The plasma layer was discarded, and the remaining pellet was resuspended in 100 μL phosphate-buffered saline (PBS). Three red blood cell (RBC) lysis steps were performed by adding 3 mL RBC lysis buffer (Sigma), vortexing, and incubating at room temperature for 10 minutes.

Samples were centrifuged at 300 ×*g* for 10 minutes, and the supernatant was discarded. After the last lysis, blood samples were resuspended in 100 µL PBS and stained for flow cytometry. Mouse BM was collected by harvesting femurs and tibias and cutting off the distal bone tips. A 23G needle (BD Horizon, Franklin Lakes, NJ, USA) was used to flush 1 mL PBS through the bone, and the marrow was collected. Samples were centrifuged at 300 ×*g* for 10 minutes. The supernatant was discarded, and the pellet was resuspended in 200 µL PBS. Samples were transferred to 0.35-µM cell strainers (Chemglass Life Sciences, Vineland, NJ, USA) on flow tubes. Tubes were centrifuged at 300 ×*g* for 10 minutes. The supernatant was discarded, and one RBC lysis was performed. After centrifugation at 300 ×*g* for 10 minutes, samples were stained for flow cytometry analysis.

2.6 Flow cytometry staining

When cells were ready for staining for flow cytometry, all samples were washed in flow tubes with 2 mL fluorescence-activated cell sorting (FACS) buffer. FACS buffer contains 2.5% fetal bovine serum (Bio-Techne) in PBS (Cytiva, Marlborough, MA, USA). Samples were centrifuged at 320 ×*g* for 3 minutes and decanted. Half the volume of "live/dead" control was removed and added to the "dead" tube, which was placed at 100°C for 2 minutes and then on ice for 2 minutes. Dead cells were added back to "live/dead" control. An antibody cocktail (all flow cytometry antibodies used in this study are listed in Table 1) was generated according to manufacturers' dilution recommendations, along with BV buffer (BD Horizon), and 100 µL was added to each sample. One drop of UltraComp eBeads (Invitrogen), 1 µL antibody, and 100 µL FACS buffer were used as compensation controls. All tubes were covered and incubated for 20 minutes on ice and vortexed at 10 minutes. Then, 2 mL FACS buffer was added, and samples were centrifuged at 320 ×*g* for 3 minutes. The supernatant was decanted post-centrifugation, and flow cytometry was performed. Samples were run on the Cytek Aurora (Cytek Biosciences, Fremont, CA, USA) and analyzed using FlowJo. Mean fluorescence intensity (MFI) was calculated on FlowJo software (v10) and graphed on GraphPad Prism software (v10).

2.7 *In vivo* conditioning experiment

NSG mice were conditioned with 25 mg/kg busulfan (Busulfex, DSM Pharmaceuticals, Durham, NC, USA) intraperitoneal injection, 300 µL incomplete Freund's adjuvant (Millipore Sigma, Burlington, MA, USA) 1:1 with sterile PBS *via* intraperitoneal injection, or 1.5-Gy total body X-ray radiation (Rad Source RS 2000 Biological Research Irradiator). Twenty-four hours after conditioning, each mouse was retro-orbitally injected with 8e6 γδ T cells. PB and BM were collected after 24 hours and stained for flow cytometry with γδ TCR (BD Biosciences, San Jose, CA, USA), CD3 (BioLegend, San Diego, CA, USA), mCD45 (BioLegend), hCD45 (BD Horizon), and CXCR4 (BD OptiBuild). Results were analyzed on FlowJo software (v10).

TABLE 1 All flow cytometry antibodies used in this study.

Marker (all human unless denoted otherwise)	Stain	Company	Catalog number	Clone/ lot number
***CXCR4 #1**	BV480	BD OptiBuild	746621	12G5/ 3009131
CXCR4 #2	APC	R&D Systems	FAB173A-025	44717
CXCR4 #3	AF 647	R&D Systems	FAB172R-100UG	44716
CXCR4 #4	APC-Vio 770	Miltenyi	130-116-667	REA649
CCR2 #1	BV711	BioLegend	357232	K036C2
CCR2 #2	BV786	BD OptiBuild	747855	LS132.1D9
***CD3**	Spark Blue 550	BioLegend	344851	SK7/ B311325
***CD45**	BUV395	BD Horizon	563792	HI30/ 2017963
***mCD45**	BV510	BioLegend	103138	30-F11/ B360620
***γδTCR**	PE	BD Biosciences	347907	11F2/ 2292377
***CD69**	APC	BioLegend	310910	FN50/ B268175
***CD335 (NKp46)**	BV711	BD Horizon	563043	9E2/ 0321062
***TIGIT**	APC-Fire750	BioLegend	372707	A15153G/ B327004
***CD226 (DNAM-1)**	BV605	BioLegend	338323	11A8/ B310112
***CD56**	APC-R700	BD Horizon	565139	NCAM16.2/ 1105545
***CD27**	BV650	BD Horizon	564894	M-T271/ 9217315
***CD94**	BV421	BD OptiBuild	743948	HP-3D9/ 1174031
***CD62L**	PE-Cy7	BioLegend	304821	DREG-56/B288473
***CD314 (NKG2D)**	PerCP-Cy5.5	BioLegend	320818	1D11/ B308592

Antibodies denoted with an asterisk were used in the γδ T *in vivo* phenotype experiment.

2.8 *In vivo* radiation dosage experiment

NSG mice were conditioned with irradiation of 1.5 Gy or a split dose of 6 Gy (3 Gy at 4 hours apart). The protocol was then followed identically as the *in vivo* conditioning experiment described above.

2.9 *In vivo* cell tracking

BALB/cJ mice were bled, and blood was collected in tubes containing 10% EDTA. Cell Trace CFSE Cell Proliferation Kit (Thermo Fisher Scientific, Waltham, MA, USA) stock solution was prepared according to the manufacturer's protocol by combining 18 µL DMSO to one vial of carboxyfluorescein succinimidyl ester (CFSE). This DMSO/CFSE solution was transferred to 20 mL of sterile PBS (CFSE/PBS solution). Blood samples were centrifuged at 250 ×*g* for 5 minutes, and the plasma layer was discarded. Cells were then resuspended in PBS, and 10e6 cells per mouse were counted. Cells were centrifuged at 250 ×*g* for 5 minutes. After centrifugation, cells were resuspended in the CFSE/PBS solution at a ratio of 10e6 cells to 5 mL CFSE/PBS. Then, cells and solution were incubated at 37°C shaking at 150 RPM for 20 minutes. Samples were then centrifuged at 250 ×*g* for 5 minutes. The supernatant was decanted, and cells were washed with 5 mL PBS and centrifuged again. After the last spin, the supernatant was decanted, and cells were resuspended at a concentration of 10e6 cells/100 µL PBS. CFSE-stained blood was loaded into insulin syringes and injected into NSG mice retro-orbitally 24 hours after mice were conditioned with a split dose of 6-Gy radiation, 3 Gy at 4 hours apart. Twenty-four hours after CFSE-blood transfusion, NSG mice were bled, and PB was collected into tubes containing 10% EDTA. Mice were euthanized, and femurs were collected; BM was harvested. PB samples and BM were prepared for flow cytometry according to the tissue collection protocol and stained with mCD45.1 (BD Biosciences), mCD45.2 (BioLegend), and TER119 (BioLegend). Flow cytometry was then performed, and results were analyzed on FlowJo software (v10).

2.10 γδ T-cell *in vivo* phenotype

NSG mice were conditioned with a split dose of 6-Gy radiation and observed for 48 hours. After conditioning for 24 hours, 8.2e6 γδ T cells were injected retro-orbitally. Twenty-four hours after T-cell injection, 100 µL PB and BM from both femurs and tibias were obtained from all mice. All cells from each condition were combined and stained for various T-cell markers for flow cytometry. Flow cytometry antibodies used in this experiment are denoted with an asterisk in Table 1. Flow cytometry was then performed, and results were analyzed on FlowJo software (v10).

2.11 Leukemia study

NSG mice were injected with 5e6 CMK-luciferase cells or 2e6 Nalm6-luciferase cells *via* the tail vein. Fifteen days post-inoculation, bioluminescent imaging was performed by injecting D-luciferin (PerkinElmer, Waltham, MA, USA) at a dose of 150 mg/kg *via* intraperitoneal injection 10 minutes prior to imaging. Images were then quantified using the IVIS Spectrum imaging system (PerkinElmer) for confirmation of cancer engraftment. On day 16, mice were then retro-orbitally injected with 1e6 γδ T cells. Twenty-four hours after the T-cell injection, the spleen and both femurs were harvested from mice. Cells were stained with markers for CMK, $CD3^{-}/CD33^{+}$ (BD Horizon), and Nalm6, CD19 (BD Horizon), as well as γδ T-cell markers. Flow cytometry was performed, and the results were analyzed on FlowJo software (v10).

2.12 Intraosseous MSC/γMSC study

MSCs were primed with 1 ng/mL IFNγ, and NSG mice were irradiated with 1.5-Gy total body irradiation (TBI) on the same day. Twenty-four hours later, 1.6e5 MSC or γMSCs were injected *via* intraosseous injection into the left femur of all mice. After 24 hours, 4e6 cells were injected retro-orbitally into all mice. Twenty-four hours post-γδ T-cell injection, femurs were harvested and stained for MSCs or γMSCs ($CD90^{+}/CD105^{+}$ both from BD Horizon) and γδ T cells. Flow cytometry was performed, and the results were analyzed on FlowJo software (v10).

2.13 Transwell migration

Polycarbonate 6.5-mm Transwell plates with a 3.0-µM pore (Corning Life Sciences) were used for transwell migration assays. In the lower chamber, 600 µL media and 500,000 γMSCs or non-primed MSCs were placed, and 500,000 γδ T cells were placed in the top chamber. Four hours after incubation, a Cellometer (Nexcelom, Lawrence, MA, USA) was used to count the number of γδ T cells that migrated to the bottom chamber. Then, the specific migration of cells to the bottom chamber was calculated using the equation below.

$$\text{Specific migration} = \frac{\text{number of cells migrated to experimental media} - \text{number of migrated to control media}}{\text{total number cells added to top chamber}}.$$

To confirm that CCL2 induced γδ T-cell migration to γMSCs, a transwell migration assay was performed using a CCL2 antibody (R&D Systems, Minneapolis, MN, USA; MAB679-500) blockade. In the bottom chamber, 600 µL media and 500,000 γMSCs were placed along with 5 µg or 10 µg CCL2 antibody. In the top chamber, 500,000 γδ T cells were placed. Four hours after incubation, the Cellometer was used to count the total number of γδ T cells that migrated to the bottom chamber.

2.14 CCL2 chemokine assay

Using the Proteome Profiler Human Chemokine Kit reagents (R&D Systems), IFNγ-primed and non-primed human MSC-conditioned media (24-hour incubation) were analyzed for the presence of secreted chemokines. To compare chemokine relative expression levels between activated and non-activated media, membrane blots were developed and imaged on Blue Devil X-ray autoradiography film (Genesee Scientific, El Cajon, CA, USA) on an X-ray film developer (MXR Imaging, San Diego CA, USA; SRX-101A) according to profiler kit manufacturer's instructions.

2.15 γδ T-cell neuroblastoma model

This human neuroblastoma NSG mouse model has been previously published by our group as a bona fide model in which to study γδ T-cell characteristics in targeting cancer (41, 46). NSG mice were administered IMR5-luciferase cells subcutaneously. Tumors were measured using a caliper, and when they reached approximately 125 mm^3 in volume, either 5e5 MSCs or γMSCs were injected intratumorally. Twelve hours after, γδ T cells labeled with 2.5e6 XenoLight DiR Fluorescent Dye (PerkinElmer) were infused *via* the tail vein, and migration throughout the animals was determined using the IVIS Spectrum imaging system (PerkinElmer). Isoflurane anesthesia (Piramal, Bethlehem, PA, USA) was used during imaging. Living Image software was used to acquire and analyze fluorescence and bioluminescence data and then to scale for analysis. Whole-body images were captured to determine the distribution of fluorescence throughout the body. To quantify the fluorescence at the site of the tumor, the lungs, head, and tail were physically covered to only capture images of the tumor, which were used to quantify tumor-specific fluorescence. Twenty-four hours post-γδ T-cell administration, tumors were harvested and stained for the presence of γδ T cells. Stained cells were processed *via* flow cytometry, and results were analyzed on FlowJo software (v10).

2.16 RNA sequencing

Two biological replicates of two different healthy donor PBMC samples were collected. γδ T cells were isolated from donor PBMC samples and expanded in serum free, *ex vivo* media. RNA was extracted from γδ T cells using the commercially available RNeasy Micro Kit (Qiagen, Valencia, CA, USA; 74004). Sequencing libraries were prepared using Illumina platforms. Samples were run on Illumina NovaSeq 6000 (instrument identifier number: HWI-ST1276) with a minimum of 20 million paired-end reads. Fastq files were mapped and aligned to GrCh38p13 and GenCode36 using Illumina Dragen v3.10.4a on Amazon Web Services. Quantification of aligned samples was achieved using salmon through Illumina Dragen v3.10.4a. Quantification files were imported into R using tximport, low counts were filtered out, and differential expression analysis was performed using DESeq2. Counts were averaged and normalized, and log2 of normalized counts was ascertained and plotted in a scatter plot using GraphPad Prism software (v10).

2.17 CCL2 ELISA

Using the Human MCP-1/CCL2 ELISA Kit (Millipore Sigma), IFNγ-primed and non-primed human MSCs were analyzed for the presence of secreted CCL2 24, 48, and 72 hours after priming. This assay was performed according to the manufacturer's protocol. The quantitative γMSC CCL2 readout (pg/mL) was compared to the manufacturer's standard curve and recorded at OD 450 nm using a spectrometer (Molecular Devices, San Jose, CA, USA; SpectraMax). CCL2 concentration was calculated and analyzed using GraphPad Prism.

2.18 Rigor of data/statistical analysis

All animal experiments were performed with a minimum of three biological replicates and in accordance with the Animal Use Alternatives (3Rs— reduction, refinement, and replacement). All *in vitro* studies were performed with a minimum of three biological replicates with the exception of the RNA-sequencing data and the chemokine blots of MSCs and γMSCs. However, these two pieces of data i) served as confirmation of previously published findings and ii) were supplemented by additional experiments, which are included in the manuscript. All statistical analyses were performed on GraphPad Prism, and each analysis method is provided in the figure legends. Results are presented as the mean ± standard deviation of the mean. Statistical significance is denoted by asterisks if $p < 0.05$.

3 Results

3.1 TBI enhances human γδ T-cell migration to murine bone marrow

We previously demonstrated that *ex vivo*, serum-free-expanded human Vγ9Vδ2 T cells, denoted herein as γδ T cells, do not persist in, or migrate to, murine BM (36). This is a concern because the NSG mouse is often used in preclinical testing of cell-based immunotherapies. Because γδ T cells migrate to sites of inflammation and tissue damage (49), in an attempt to enhance migration of human γδ T cells to murine BM, we conditioned NSG mice with low-dose TBI (1.5 Gy), incomplete Freund's adjuvant (IFA), or 25 mg/kg busulfan, and we surveyed γδ T-cell percentages in the PB and BM. Radiation and busulfan are often used as conditioning agents to clear the BM compartment and initiate immune suppression in preparation for BM or mobilized hematopoietic stem cell transplants (50–52). IFA has been utilized in a prior study to boost the effectiveness of αβ T-cell migration to inflamed BM (21). Twenty-four hours after conditioning with these agents, we intravenously infused γδ T cells. Radiation significantly increased the relative percentage of human γδ T cells in the BM compared to the PB; IFA and busulfan did not show a significant difference in the relative percentages of γδ T cells in each compartment (Figure 1A). To further confirm that TBI increases the percentage of human γδ T cells in the BM, we conditioned mice with 1.5 Gy or 6 Gy and administered human γδ T cells. Conditioning mice with 1.5 Gy resulted in a minor increase in the percentage of γδ T cells, and 6 Gy significantly and dramatically increased this percentage (Figure 1B). Based on these findings, we used 6-Gy radiation for subsequent experiments.

We then evaluated if the γδ T cells entering the BM were phenotypically different than those remaining in circulation. We surveyed cell surface proteins using markers of γδ T-cell activation, inhibition, or enhancement of other specific properties: CD27, CD56, CD62L, CD69, CD94, CD226, CD314, CD335, CXCR4, and TIGIT. The expression of these markers was similar whether the cells were in circulation or the BM, with the exception of CD69, an activation marker of γδ T cells, which was elevated in cells in the BM (53) (Figure 1C). Importantly, the trend remained the same

10.3389/fimmu.2024.1331322

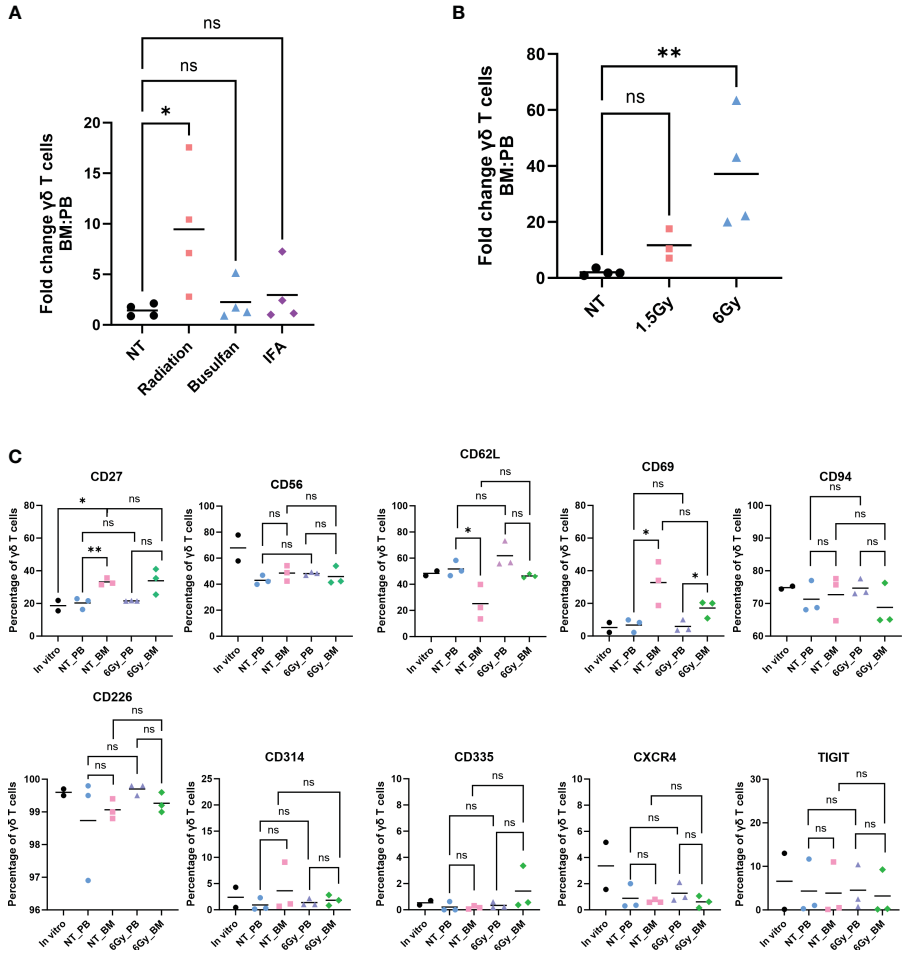

FIGURE 1
Human γδ T cells migrate to mouse bone marrow after radiation, and their phenotype is identical to that in the *in vitro*-expanded cells and circulation. Mice were conditioned with **(A)** 1.5-Gy radiation, 25 mg/kg busulfan, or 300 µL IFA (1:1 with PBS) or **(B)** 1.5 Gy or 6-Gy radiation; then, γδ T cells were administered, and 24 hours later, the percentage of γδ T cells was assessed by flow cytometry (gated on $CD3^+$ γδTCR^+ cells). **(A, B)** Statistics analyzed by non-parametric one-way ANOVA with *post hoc* ($p < 0.05$ = *); the sample mean is denoted with a black line; n = 3–4 mice per condition. **(C)** Mice were conditioned with 6-Gy radiation and 24 hours later injected with γδ T cells, and phenotype markers of live γδ T cells were assessed by flow cytometry. Each combination of samples was statistically analyzed by Student's t-test ($p > 0.05$ = ns; $p < 0.05$ = *; $p < 0.01$ = **). ns, not significant. The *in vitro* combinations were all non-significant except for CD27. The sample mean is denoted with a black line. *In vitro* data represent two biological replicates; *in vivo* studies represent n = 3 mice for each condition. IFA, incomplete Freund's adjuvant; PBS, phosphate-buffered saline.

between the PB and BM of non-treated mice and irradiated mice. Furthermore, the γδ T-cell phenotype remained unchanged when comparing *in vitro* cultured cells to *in vivo* circulating cells obtained from the PB or BM, with the one exception of CD27. In addition, the distribution of cells with regard to each marker in the γδ T-cell population was similar when comparing cells in the PB to cells with those in the BM (Supplementary Figure 1). Therefore, of the conditions tested, TBI, busulfan, or IFA, TBI is an effective conditioning treatment to enhance migration of human γδ T cells into mouse BM, and the γδ T cells entering the BM are phenotypically unchanged from those cultured *in vitro*, in the PB, or in non-treated mice.

We next determined if human leukemia cells could provide a driving force to induce γδ T-cell migration into the BM. Prior studies from our lab using leukemia models demonstrated that γδ T cells, administered shortly after cancer inoculation in a mouse, do not traffic to the leukemic BM (36, 54). Therefore, the administered T cells do not target the BM-residing cancer, even if the T cells are engineered to express CARs against leukemia antigens. We employed a modified experimental design wherein we allowed time for two different luciferase-tagged, human leukemia cell lines (CMK, acute megakaryoblastic leukemia, and Nalm6, B-cell precursor leukemia) to completely engraft in the BM (Supplementary Figure 2A) before systemically infusing γδ T cells. Even under high leukemic stress, γδ T cells do not enter the BM despite the presence of human hematopoietic leukemia cells (Supplementary Figure 2B). Furthermore, we also did not observe an overall greater percentage of γδ T cells in the spleen (Supplementary Figure 2C). Therefore, *ex vivo*, serum-free-expanded γδ T cells do not traffic to the BM of mice even under a high leukemic burden.

10.3389/fimmu.2024.1331322

3.2 Homing is not the mechanism of radiation-induced migration of γδ T cells into the bone marrow

Although increased percentages of γδ T cells were observed in the BM of TBI-treated mice, we next determined if the γδ T cells were entering the BM due to a homing/trafficking axis or passively through the circulation. As shown in Figure 1, the phenotype of γδ T cells was similar in the BM and PB, which led us to hypothesize that these T cells do not home to the BM but instead passively flow into the BM from the circulation. To test this, we stained RBCs from BALB/cJ mice with CellTrace CFSE proliferation dye and systemically injected them into irradiated or non-irradiated NSG mice. We found that 6-Gy radiation did not significantly affect the total number of cells in the PB, BM, or spleen (Figure 2A), and radiation did not alter the percentage of $CFSE^+$ RBCs or γδ T cells in the circulation (Figure 2B). Consistent with our previous results, we observed radiation significantly increased the percentage of γδ T

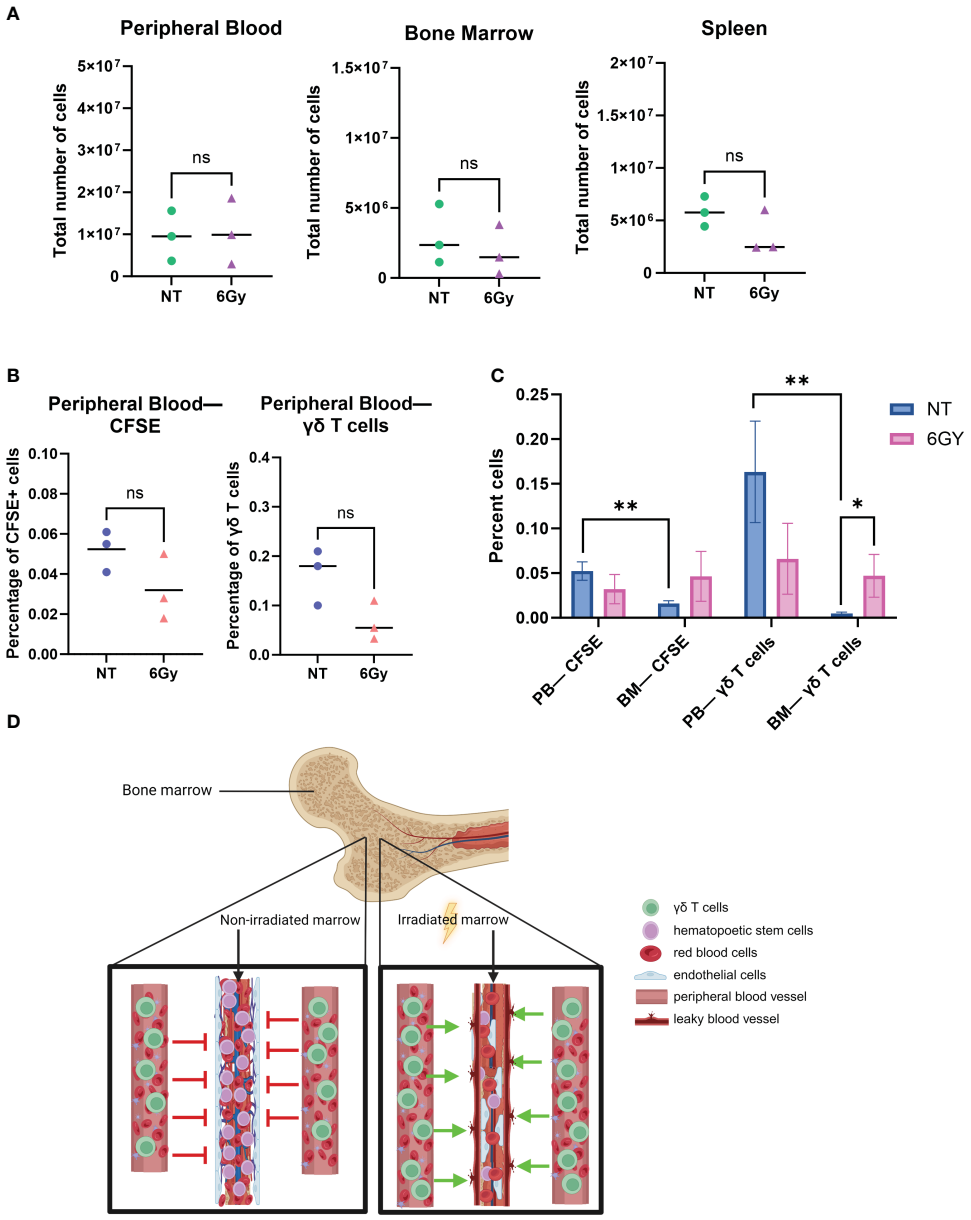

FIGURE 2
Radiation breaks down the blood–bone marrow barrier, allowing circulating γδ T cells to filter into and through the bone marrow space. **(A)** Mice were conditioned with 6-Gy radiation 24 hours prior to the injection of γδ T cells; 24 hours after administration of γδ T cells, blood, marrow, and spleen were harvested, and cells were counted with trypan blue. **(B)** Mice were conditioned with 6-Gy radiation, and then 24 hours later, they were injected with 10e6 γδ T cells or CellTrace CFSE-stained red blood cells from BALB/cJ mice; blood was collected and assessed for percentage of live CFSE-tagged cells (gated on $CFSE^+$ $TER119^+$ cells) or γδ T cells *via* flow cytometry. **(C)** Comparison of percentage CFSE+ cells and γδ T cells in non-treated or irradiated mouse blood and marrow. All experiments in this figure were performed with n = 3 mice per condition. All statistics analyzed by Student's t-test ($p< 0.05$ = *; $p< 0.01$ = **), and the sample mean is denoted with a black line. **(D)** Graphical depiction of passive migration of circulating cells entering the bone marrow due to radiation-induced mechanical breakdown of blood–bone marrow barrier. CFSE, carboxyfluorescein succinimidyl ester. ns, not significant.

cells in the BM (Figure 2C). In addition, when comparing CFSE$^+$ RBCs or γδ T cells in non-treated mouse PB versus BM, we again observed a lower percentage of γδ T cells in the BM compared to PB. However, after radiation, the percentage of CFSE-marked RBCs was higher compared to that in non-treated mice and was similar to the percentage of marked cells in PB. Therefore, radiation allows CFSE$^+$ RBCs to migrate freely through the BM, as the barrier that limits movement into the BM appears to be eliminated.

To demonstrate that TBI effects on the BM are quantitatively different than the effects of other agents, mice were conditioned with 25 mg/kg busulfan and then systematically injected with CFSE$^+$ RBCs 24 hours later, and CFSE$^+$ RBCs were surveyed in the PB and BM. The difference in the percentage of CFSE$^+$ RBCs in the PB of non-treated mice compared to busulfan-treated mice was insignificant (Supplementary Figure 3A), and there was no significant difference in the percentage of CFSE$^+$ RBCs in the BM of non-treated or busulfan-treated mice (Supplementary Figure 3B), a result different from that observed with radiation, as TBI significantly increased the percentage of γδ T cells in the BM (Figure 2C).

These data show that i) the γδ T-cell phenotype is the same when comparing cells harvested from PB or BM after *ex vivo*-expanded cells are administered to NSG mice; ii) the phenotype of the cells in circulation and in the BM is similar to that of cultured γδ T cells; iii) TBI, but not busulfan, resulted in an increase in the absolute number and percentage of γδ T cells in the BM; iv) similar to γδ T cells, there are fewer CFSE$^+$ RBCs in BM compared to the PB, unless the mice are irradiated; and v) there was no difference in the percentage of CFSE$^+$ RBCs or γδ T cells in the PB or BM when mice are conditioned with TBI. Therefore, because it is known that radiation induces the breakdown of the blood–BM barrier (55, 56), it is reasonable to conclude that TBI allows γδ T cells to passively flow through the marrow niche, as depicted in Figure 2D.

3.3 The lack of γδ T-cell homing to the BM is, in part, due to the absence of CXCR4 expression

When inflammation is induced in the BM, BM stromal cells release the chemokine CXCL12, or stromal-cell derived factor-1α (SDF-1α) (57, 58). BM-infiltrating αβ T cells highly express CXCR4, the G-protein-coupled receptor (GPCR) for CXCL12, and migrate to the BM based on CXCR4-CXCL12 chemoattraction (21). We show by RNA sequencing (RNA-seq) analysis that *CXCR4* mRNA was highly expressed in γδ T cells (top 6% of all RNA sequenced, Figure 3A), indicating that these cells should also migrate *via* the CXCR4/CXCL12 axis. Surprisingly, the percentage of CXCR4$^+$ γδ T cells in the BM was very low regardless of conditioning regimen (Figure 3B), and there was a slightly higher percentage of circulating CXCR4$^+$ γδ T cells (Figure 3C). Therefore, although the *CXCR4* mRNA was high in these γδ T cells, CXCR4 protein expression was low, which is consistent with previous studies (59, 60). To further characterize CXCR4 expression and determine if the lack of expression can be a consequence of serum-free expansion, γδ T cells were expanded from four donor PBMCs in either FBS media (SM) or serum-free media (SFM). The difference in the number of γδ T cells in each donor was non-significant in expanding in SM versus SFM, although there was the expected donor variability where some donors expanded better in one medium compared to the other (Figure 4A). Additionally, there was no change in the overall fold expansion (Figure 4B). The percentage of γδ T cells was higher in three out of the four donors expanded in SM on day 6 of expansion, but there was no significant difference in this percentage by the end of the expansion on day 12 (Figure 4C). Overall, we did not observe significant changes in major cell characteristics within the cellular product with the addition of serum to our expansion protocol.

To determine whether CXCR4 expression changes in γδ T cells expanded in SM or SFM, we evaluated the CXCR4 expression in γδ T cells expanded in zol from PBMCs from three different donors and cultured in either SM or SFM. All samples had low CXCR4 expression regardless of culturing media, but we noted a slight, non-significant increase in CXCR4$^+$ γδ T cells from PBMCs expanded in SFM (Figure 4D). We confirmed these data using four different CXCR4 flow cytometry-confirmed antibody clones, with Nalm6 cells as a positive control (Supplementary Figure 4A). Furthermore, to determine if zol impacts CXCR4 expression, we measured CXCR4 by flow cytometry on γδ T cells from PBMCs and compared it to zol-expanded γδ T cells from four different donors. CXCR4 expression was similar in all samples, indicating that zol did not alter CXCR4 expression (Figure 4E).

Within these SF- or SFM-expanded cells, we also determined the percentage of NK cells, CD56$^+$ γδ T cells, and CD16$^+$ cells, which can be markers for enhanced cytotoxicity and improved antibody-dependent cellular cytotoxicity (61–63). The percentage of NK cells decreased in three of the four donor samples during expansion regardless of SM or SFM (Supplementary Figure 4B), and CD16 showed a minor increase at the end of expansion (Supplementary Figure 4C). Lastly, the percentage of CD56$^+$ γδ T cells increased slightly or remained the same over the course of expansion, similar in SF or SFM (Supplementary Figure 4D). Therefore, SM does not appear to dramatically alter the phenotype of *ex vivo*-expanded γδ T cells.

Taken together, these data show that despite varying culturing and manufacturing conditions, γδ T cells express low levels of surface CXCR4, the level of which is likely insufficient to induce trafficking to the BM *via* the CXCR4/CXCL12 axis.

3.4 γδ T-cell homing can be directed by controlling chemokine expression

We showed that the chemokine receptor CXCR4 is not highly expressed on the surface of Vγ9Vδ2 cells, which we infer may be a mechanism for their poor migration to murine BM. This raised the concern as to whether or not these cells can migrate *via* other chemokine/chemokine receptor relationships. To determine if these *ex vivo*-expanded cells can migrate *via* receptor/ligand interactions and if these receptors can be leveraged to direct migration of γδ T cells to predetermined sites, we developed a model that conditionally expresses CCL2. We previously demonstrated that of the chemokine receptors expressed on the surface of serum-free-expanded γδ T cells, CCR2 showed the greatest expression (22). To confirm these results, we measured CCR2 expression with two

10.3389/fimmu.2024.1331322

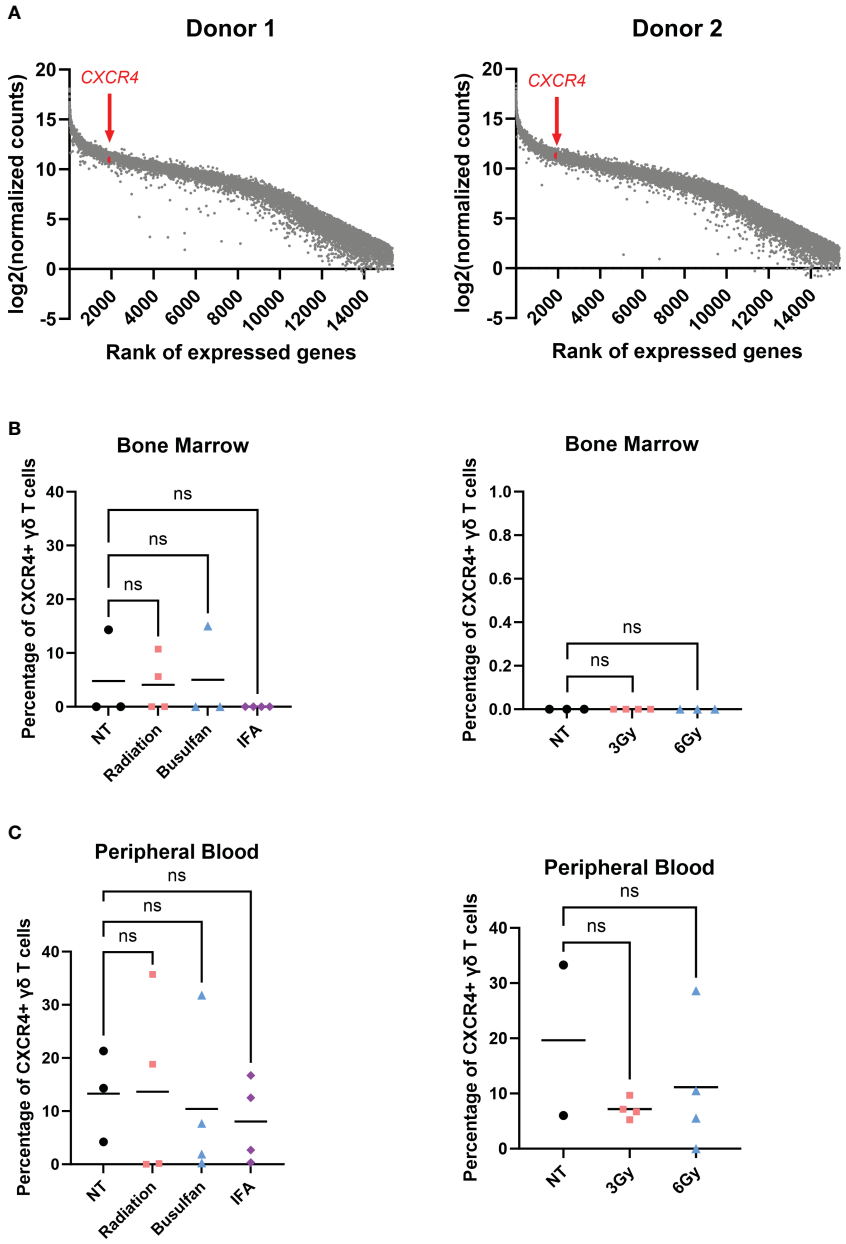

FIGURE 3
γδ T cells do not migrate to the bone marrow *via* the CXCR4/CXCL12 axis. **(A)** RNA-seq performed on two individual biological replicates of γδ T cells isolated from two different PBMC donors; genes were ranked, and log2(normalized counts) was calculated; *CXCR4* highlighted in red. **(B)** Mice were conditioned with 1.5-Gy radiation, 25 mg/kg busulfan, or 300 µL IFA (1:1 with PBS) or 3-Gy or 6-Gy radiation and then systemically infused with γδ T cells; 24 hours later, bone marrow and **(C)** blood were harvested and assessed for live CXCR4$^+$ γδ T cells *via* flow cytometry using the CXCR4 BV480 antibody. For NT, n = 2–3 mice, and n = 4 for conditioned mice **(B, C)**. **(B, C)** Statistics analyzed by non-parametric one-way ANOVA with *post hoc* ($p > 0.05$ = ns), ns, not significant, and the sample mean is denoted with a black line. RNA-seq, RNA sequencing; PBMC, peripheral blood mononuclear cell; IFA, incomplete Freund's adjuvant; PBS, phosphate-buffered saline.

different flow cytometry antibody clones (Figure 5A). Additionally, RNA-seq results using RNA isolated from γδ T cells from two different PBMC donors showed high *CCR2* expression, which was in the top 17% of RNA sequenced (Supplementary Figure 5A). Therefore, CCR2 had high protein expression correlating with high mRNA expression, unlike CXCR4.

It is well-established that CCR2 ligands include CCL2, CCL7, CCL8, and CCL13 with CCL2 considered to be the major ligand (64, 65). We developed a model to conditionally express CCL2, which takes advantage of chemokine expression differences when *ex vivo*-expanded MSCs are treated with interferon γ (IFNγ) to produce γMSCs. *Ex vivo*-expanded MSCs typically do not robustly express chemokines, but a human chemokine array demonstrated that γMSCs highly secrete CXCL9, CXCL10, CCL7, and CCL2 compared to non-primed MSCs (Figure 5B). CCL2 secretion was specifically monitored by enzyme-linked immunosorbent assay (ELISA), which showed that CCL2

10.3389/fimmu.2024.1331322

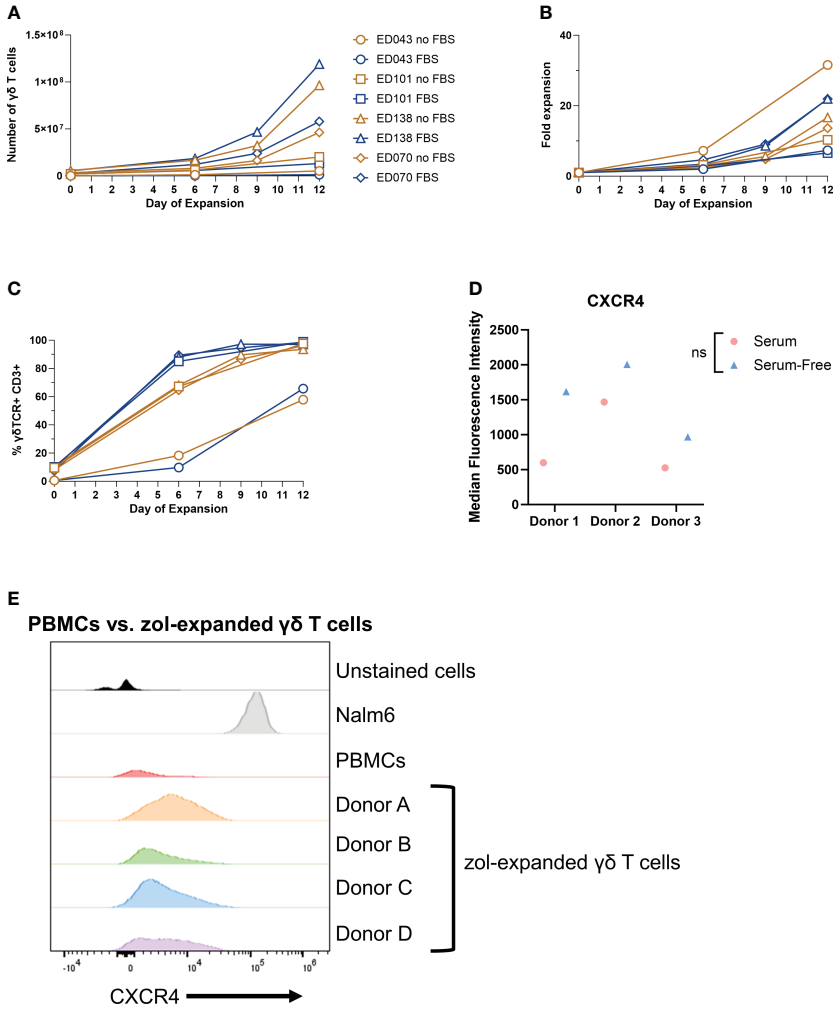

FIGURE 4
Low γδ T-cell CXCR4 expression is not due to serum-free expansion. Peripheral blood mononuclear cell samples from four individual healthy donors (n = 4 biological replicates) were selected for γδ T cells expanded in serum- or serum-free media. The following parameters were determined: **(A)** number of γδ T cells (live cell counts multiplied by percent γδ T cells derived from flow, $CD3^+$ $γδTCR^+$), **(B)** fold expansion (number γδ T cells divided by number on day 0), and **(C)** the percentage of γδ T cells by flow cytometry gated on $γδTCR^+$ $CD3^+$ cells. **(D)** CXCR4 mean fluorescence intensity (MFI) of γδ T cells expanded in serum- or serum-free media from three healthy peripheral blood mononuclear cells (n = 3 biological replicates) calculated in FlowJo software. Statistics analyzed by paired t-test ($p > 0.05$ = ns). ns, not significant. **(E)** Histogram of $CXCR4^+$ γδ T cells in unstained γδ T cells, Nalm6 cells as a positive control, peripheral blood mononuclear cells, and four different zoledronate-expanded γδ T cells (n = 4 biological replicates).

significantly increased as early as 24 hours after priming and continued to increase for at least 72 hours (Supplementary Figure 5B). Therefore, γMSCs can be used to test the chemokine-induced migration ability of *ex vivo*, serum-free-expanded γδ T cells by capitalizing on the high CCL2 secretion after MSC priming.

To evaluate the migration of γδ T cells to γMSCs, a transwell migration assay was used with γδ T cells in the upper chamber and MSCs or γMSCs below (Figure 5C). Analysis of this assay showed significantly greater migration of the γδ T cells to the γMSCs than to the un-primed MSCs (Figure 5D). To further confirm that the trafficking is due to the CCR2/CCL2 axis, a transwell migration assay was performed, but a CCL2 blocking antibody was included to suppress CCL2 interaction with CCR2. Blocking CCL2 secretion significantly decreased γδ T-cell migration to γMSCs (Supplementary Figure 5C), indicating that these cells, indeed, show specific migration along this chemokine/receptor axis. To determine whether γδ T cells can significantly migrate to γMSCs *in vivo* as they do *in vitro*, MSCs or γMSCs were injected intrafemorally, and γδ T cells were administered systemically *via* retro-orbital infusion 24 hours later. γδ T cells were found to indeed migrate to γMSC BM significantly more than to MSC BM (Figure 6A).

To further investigate the chemoattraction properties of γδ T-cell migration, a neuroblastoma NSG mouse model was developed using IMR5-luciferase cells (Figure 6B), as we previously published (41, 46). IMR5 tumors were established in NSG mice, and MSCs or γMSCs were administered intratumorally. Then, DiR-labeled γδ T cells were administered intravenously 12 hours later. Tumor infiltration of γδ T cells was measured 24 hours later. Increased presence of γδ T cells was consistently observed in the tumors that harbor γMSCs (Figure 6C). In addition, there was no difference between the percentage of γδ T cells that infiltrated the tumor when no MSCs or non-primed MSCs were administered; however, there was a significant increase in the

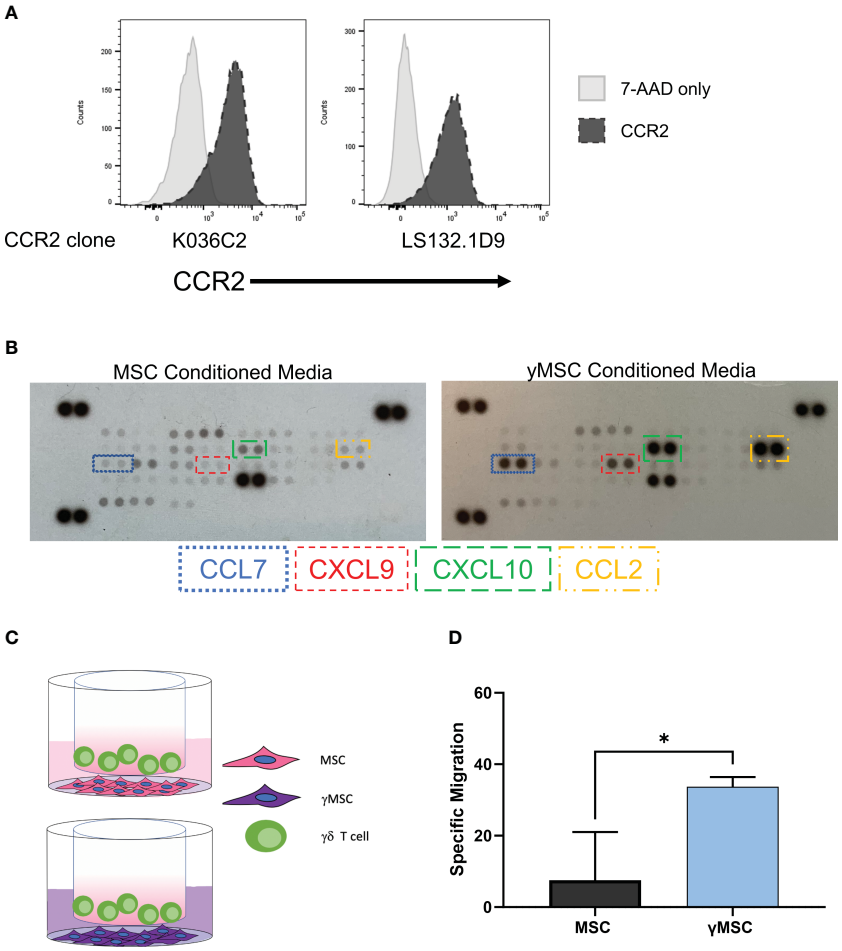

FIGURE 5
γδ T-cell homing can be influenced by leveraging the CCR2/CCL2 axis. **(A)** Flow cytometry histograms depicting CCR2 expression on γδ T cells with two different CCR2 antibody clones; 7-AAD was used as a live/dead control. **(B)** Representative human chemokine array membrane blot surveying secretion by MSCs from MSC- or γMSC-conditioned media. **(C)** Graphical depiction of the transwell migration assay with γδ T cells migrating to either MSCs or γMSCs with the respective conditioned media. **(D)** Specific migration of γδ T cells to MSCs or γMSCs in the transwell assay; n = 3 biological replicates, statistics analyzed by Student's t-test ($p < 0.05$ = *), and error bars represent standard deviation. MSCs, mesenchymal stromal cells.

percentage of γδ T cells in the tumor when the tumors harbored γMSCs (Figure 6D). Taken together, these data demonstrate that *ex vivo*, serum-free-expanded γδ T cells can migrate along chemoattractant pathways, using chemokine receptors that, *a priori*, have been shown to be upregulated at the mRNA and protein levels.

4 Discussion

There is an unmet need in the field of γδ T-cell therapeutic development to better understand the fundamental properties of these cells, such as migration and trafficking, especially in diverse models of cancer. In this study, we characterized various aspects of serum-free, *ex vivo*-expanded human Vγ9Vδ2 T-cell migration in mice and explored the use of varying methods of directing the migration of these cells. Overall, we demonstrated that γδ T-cell migration can be influenced either through physical means, such as the use of TBI, or by utilizing chemokine expression profiling.

γδ T cells share many effector characteristics with αβ T cells such as cytokine production, cytotoxicity, and antigen presentation (49). Unlike αβ T cells, γδ T cells are not dependent on peptide/class II presentation and therefore can be used as an allogeneic treatment without causing graft-versus-host disease (GvHD) (66, 67). γδ T cells can also be significantly expanded and stimulated by different methods without compromising their antitumor properties (68). Indeed, we and others have documented the therapeutic potential of γδ T cells, and there are now several methods for expanding these cells under GMP conditions (22, 36, 38–43, 46). The foundation on which these cells can be employed as anti-cancer therapeutics has been well-documented. For example, a study surveying 18,000 tumors across 39 malignancies reported γδ T cells as the most prognostically favorable subset of tumor-infiltrating lymphocytes (TILs) (69). Additionally, a correlation was uncovered between the relative abundance of γδ TILs and favorable response to immune-checkpoint therapy in many cancers, highlighting an important combination therapeutic approach (6).

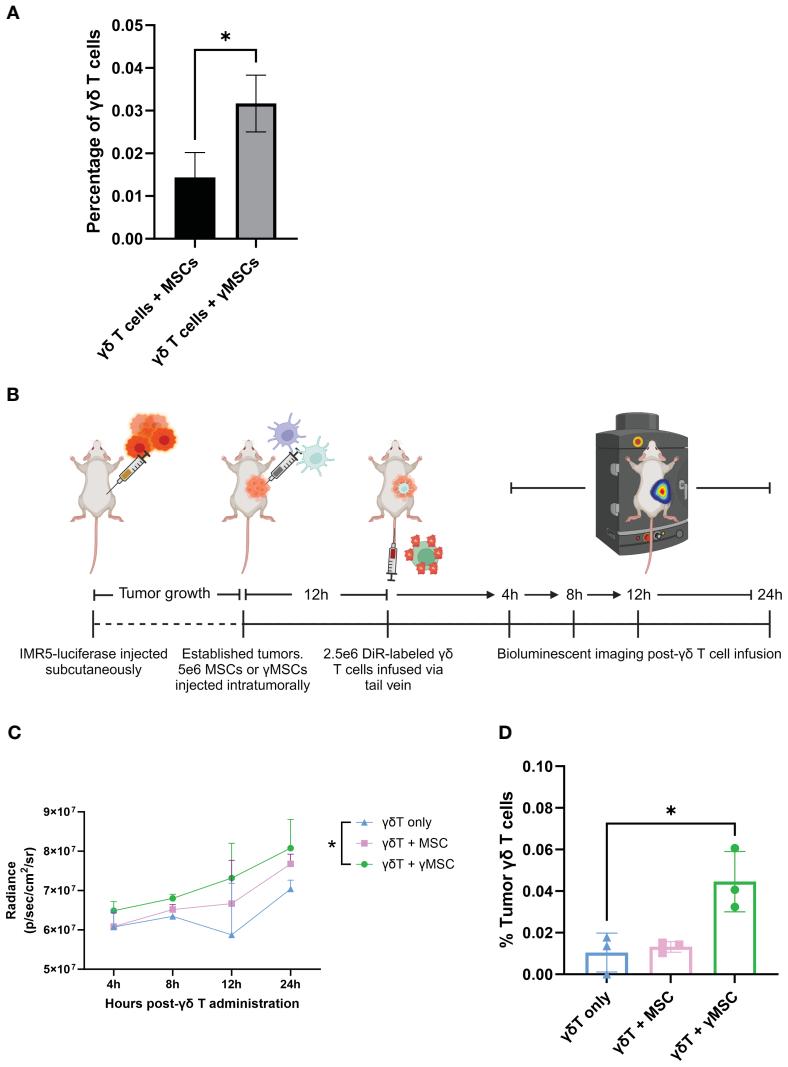

FIGURE 6
γδ T cells can be recruited to bone marrow and tumors through chemoattractant relationships. **(A)** NSG mice (n = 3 per condition) were conditioned with 1.5-Gy TBI 24 hours prior to intraosseous injection of 1.6e5 MSCs or γMSCs. After 24 hours, γδ T cells were injected retro-orbitally. Twenty-four hours later, femurs were harvested and stained for flow cytometry. The percentage of γδ T cells was then calculated. Error bars represent standard deviation. Statistical significance was analyzed by Student's t-test ($p < 0.05$ = *). **(B)** Schematic of experiment. Mice were injected with IMR5-luciferase cells; tumors were established, and MSCs or γMSCs were injected intratumorally. n = 3 mice per condition. Twelve hours later, DiR-labeled γδ T cells were injected *via* the tail vein, and migration *in vivo* was monitored over 24 hours through relative bioluminescence. **(C)** Bioluminescent quantitative analysis of γδ T-cell trafficking to tumor over 24 hours. Statistics analyzed by paired t-test with Bonferroni correction ($p < 0.05$ = *). **(D)** Flow cytometry analysis of the percentage of γδ T cells per tumor 24 hours post-infusion. Statistics analyzed by paired t-test with Bonferroni correction ($p < 0.05$ = *), and error bars represent standard deviation. TBI, total body irradiation; MSCs, mesenchymal stromal cells.

Although we and others demonstrated the cytotoxic potential of γδ T cells and an enhancement of target cell killing when engineered to express CARs targeting human cancers (36, 70, 71), a limiting aspect of using these cells is the lack of migration to the sites of tumors, such as the BM (36, 59). We surveyed varying agents that are known to affect the BM compartment. TBI and busulfan are experimentally and clinically used to clear the BM in preparation for BM transplants (51), and IFA is an adjuvant described to promote immune stimulation of αβ T cells (21). We demonstrated a significant increase in the percentage of γδ T cells entering the BM when mice are treated with TBI compared to other conditioning agents. Furthermore, our findings indicate that the increased migration of γδ T cells to the BM is the result of increased blood flow through the BM, which we postulate is caused by a TBI-induced breakdown of the blood–BM barrier. This phenomenon is important, as it has been shown that BM inflammation and breakdown enhance T-cell trafficking to the BM (72, 73); nevertheless, we show that mechanical breakdown of the blood–BM barrier causes passive migration from circulation and is the likely mechanism for the increased cellular accumulation.

Kuksin et al. found human CXCR4$^+$ αβ T cells home to mouse BM *via* the chemoattractant relationship between CXCR4 and the highly secreted CXCL12 by the BM stromal cells caused by increased BM inflammation (21). We hypothesized that this relationship should apply to γδ T cells as well. However, despite RNA-seq showing high *CXCR4* mRNA expression, we found our *ex*

vivo, SFM-expanded γδ T cells do not highly express CXCR4 protein on the cell surface. Our data are consistent with previous findings (59), and we can conclude that the lack of CXCR4 is at least one reason that these *ex vivo*, SFM-expanded γδ T cells do not traffic to the BM *via* the CXCR4/CXCL12 axis.

We also determined the low CXCR4 surface expression contrasted with its high mRNA expression. CXCR4 has been described in non-γδ T cells to undergo ligand-induced endocytosis, like other GPCRs, upon CXCL12 binding (74, 75). CXCR4 endocytosis is then followed by ubiquitination and degradation of the protein (76). Although this event has not been studied in γδ T cells, we initially thought that degradation of CXCR4 also occurs in γδ T cells after binding to CXCL12, which would explain why mRNA is high and surface protein is low. However, since these cells do not traffic to the BM and interact with the CXCL12 axis, this event cannot account for low CXCR4 levels in our γδ T cells. Nevertheless, this phenomenon is important for future studies to i) elucidate the mRNA–protein discrepancy and ii) engineer methods by which to increase extracellular CXCR4 and cause γδ T-cell trafficking to CXCL12. For example, recent studies have utilized γδ T-cell SFM containing the regulatory cytokine transforming growth factor (TGF) β to stimulate T cells and increase cytotoxicity and upregulation of chemokines (59, 77). TGF-β was shown to increase CXCR4 on some γδ T-cell expansions and promote migration to transformed cells. Beatson et al. demonstrated an increase in TGF-β-exposed γδ T-cell cytotoxicity of cell lines and significant clearing of cancer *in vivo* compared to cells expanded in ABP and IL-2 alone (59). Additionally, culturing γδ T cells in TGF-β instead of with IL-2 alone significantly increases the γδ T-cell migration to the BM (59).

Although the use of TGF-β has been documented for enhancing the cytotoxic activity and chemokine receptor expression of γδ T cells, it has also been well-characterized as a promoter of cancer cell epithelial-to-mesenchymal transition (EMT), cell proliferation, and evasion of immune surveillance and is not uniformly effective in γδ T-cell expansions (78–81). Moreover, TGF-β can negatively regulate the adaptive and innate immune systems by inhibiting important immune cells such as NK cells, effector T cells, and antigen-presenting dendritic cells (82). Studies have also shown that TGF-β strongly decreases key antitumor cytolytic contributors such as NKG2D and perforin/granzyme A and B on γδ T cells while upregulating the inhibitory molecule NKG2A (59, 77, 83). Finally, Beatson et al. observed that cells expanded with TGF-β are cytotoxic against immortalized and non-cancerous cells, posing a possible risk of autoimmunity and toxicity (59). Thus, culturing γδ T cells with TGF-β can possibly enhance γδ T-cell trafficking, but additional studies are needed to understand the possible limitations of this manufacturing strategy.

One of our concerns was whether our SFM-expanded cells retain any migratory properties. To determine whether γδ T-cell trafficking *in vivo* can be manipulated by inducing chemokine expression and taking advantage of corresponding receptors expressed on γδ T cells, we demonstrated that γδ T cells express high *CCR2* mRNA and CCR2 protein. MSCs cultured with IFNγ have increased secretion of the chemokines CCL2 and CCL7, compared to secretion from non-primed MSCs. CCL2 and CCL7 are two chemokine ligands for the CCR2 chemokine receptor (64, 65). Therefore, we sought to examine whether $CCR2^+$ γδ T cells can migrate to CCL2-secreting cells *in vivo*. Using intraosseous injections and a human neuroblastoma *in vivo* model, which we previously established (41, 46), it was shown that γMSCs significantly recruit γδ T cells compared to MSCs or a placebo, illustrating that migration of *ex vivo*, SFM-expanded cells can, indeed, be manipulated based on their chemokine receptor profile.

Though a limitation of this study and other murine studies employing human γδ T cells is the lack of long-term *in vivo* persistence, this can be countered using strategies of multiple cell infusions, which have already been clinically tested and well-tolerated (84, 85). However, if the cells do not migrate to the malignant site, increasing the number of cells per dose or the frequency of dosing will not be useful. Therefore, understanding the mechanisms of migration and basic properties of these cells remains a critical aspect of study and is needed, as these cells are being employed clinically in numerous cancer settings. We and others have consistently i) demonstrated the effectiveness of γδ T cells against various types of cancer, ii) illustrated how well these cells expand *ex vivo*, iii) determined their chemokine receptor expression can be manipulated, and iv) showed that the cells retain high cytotoxic potentials independent of HLA class II presentation. Still, we have a fundamental lack of understanding of human γδ T-cell migration *in vivo*, particularly in standard animal models of cancer. We identified important features of γδ T-cell migration *in vivo*, which we think can be useful for future studies. Based on these findings, it is expected that other chemokine relationships of importance can be leveraged to direct γδ T-cell migration *in vivo*, providing additional therapeutic targets, including malignant and non-malignant diseases.

Data availability statement

The datasets presented in this study can be found in online repositories. The names of the repository/repositories and accession number(s) can be found below: NCBI Sequence Read Archive (SRA) [BioProject ID PRJNA1014486].

Ethics statement

The studies involving humans were approved by The Emory University Institutional Review Board (IRB). The studies were conducted in accordance with the local legislation and institutional requirements. The participants provided their written informed consent to participate in this study. The animal study was approved by Emory University Institutional Animal Care and Use Committee. The study was conducted in accordance with the local legislation and institutional requirements.

Author contributions

KP: Conceptualization, Formal analysis, Investigation, Software, Validation, Visualization, Writing – original draft, Writing – review & editing. GB: Conceptualization, Investigation, Validation,

Visualization, Writing – review & editing. RB: Conceptualization, Formal analysis, Investigation, Validation, Visualization, Writing – review & editing. AB: Conceptualization, Investigation, Validation, Visualization, Writing – review & editing. AS: Conceptualization, Investigation, Software, Validation, Writing – review & editing. EF: Writing – review & editing, Data curation, Formal analysis. KK: Writing – review & editing, Data curation, Formal analysis. BP: Resources, Writing – review & editing, Conceptualization, Investigation, Validation. EH: Funding acquisition, Project administration, Resources, Supervision, Writing – review & editing. CD: Funding acquisition, Project administration, Resources, Supervision, Writing – review & editing. HTS: Conceptualization, Funding acquisition, Project administration, Resources, Supervision, Visualization, Writing – review & editing.

Funding

The author(s) declare financial support was received for the research, authorship, and/or publication of this article. This work was supported by grants from Curing Kids Cancer Inc. and the National Institute of Health under R21 Grant [5R21CA223300 awarded to HTS].

Acknowledgments

The Nalm6 cell line was generously donated by Dr. Christopher Porter's laboratory at Emory University. MSCs and IFNγ were kindly gifted by Dr. Edwin Horwitz's laboratory at Emory University. We also thank the Emory Pediatrics/Winship Flow Cytometry Core for their data consultation. Lastly, we would like to thank Katie Skinner from Dr. Andrew Hong's laboratory at Emory University for her expertise in RNA sequencing. Figures 2D, 5C, 6A were created using BioRender.com.

Conflict of interest

HTS and CD have equity in Expression Therapeutics, which is developing cancer treatments based on engineered γδ T cells. BP is an employee of Expression Therapeutics.

The remaining authors declare that the research was conducted in the absence of any commercial or financial relationships that could be construed as a potential conflict of interest.

The author(s) declared that they were an editorial board member of Frontiers, at the time of submission. This had no impact on the peer review process and the final decision.

Publisher's note

Supplementary material

The Supplementary Material for this article can be found online at: https://www.frontiersin.org/articles/10.3389/fimmu.2024.1331322/full#supplementary-material

SUPPLEMENTARY FIGURE 1
γδ T cell phenotype remains unchanged from peripheral blood to bone marrow. Mice were conditioned with 6Gy radiation, 24 hours later injected with γδ T cells, and phenotype markers of live γδ T cells were assessed by flow cytometry. Representative tSNE plots from one of the three biological replicates show protein distribution in each cell population.

SUPPLEMENTARY FIGURE 2
Human γδ T cells do not migrate to mouse bone marrow despite the presence of human hematopoietic-derived cell lines. NSG mice were inoculated via tail vein with 5e6 CMK-luciferase cells (n = 3) or 2e6 Nalm6-luciferase cells (n = 3). In addition to these mice, appropriate control mice were added: no leukemia or γδ T cell control (n = 1) and γδ T cell only (n = 2). **(A)** After 15 days, mice were surveyed via bioluminescent imaging to track cancer engraftment in the bone marrow. Sixteen days post-leukemia inoculation, 1e6 γδ T cells were systemically infused via retro-orbital injection. Twenty-four hours after, **(B)** bone marrow and **(C)** spleen were harvested and flow cytometry was performed to confirm presence of cancer and percentage of γδ T cells. All statistical combinations were not significant via Student's t test ($p > 0.05$ = ns). ns, not significant.

SUPPLEMENTARY FIGURE 3
Busulfan does not cause γδ T cells to enter the bone marrow. Mice were conditioned with 25mg/kg busulfan and 24 hours later were administered with 10e6 CellTrace CFSE-stained blood from BALB/cJ mice; **(A)** blood and **(B)** bone marrow were harvested and assessed for percentage of CFSE-tagged cells (gated on $CFSE^+$ $TER119^+$ cells) via flow cytometry, n = 4 mice per condition. Statistics analyzed by Student's t test, and the sample mean is denoted with a black line.

SUPPLEMENTARY FIGURE 4
γδ T cells do not express CXCR4 despite differences in expansion methods. **(A)** Histogram of four different CXCR4 flow cytometry antibody clones tested with serum-free-expanded γδ T cells; the Nalm6 cell line was used as a positive control. Peripheral blood mononuclear cell samples from four individual healthy donors were selected for γδ T cells expanded in serum- or serum-free media. The following parameters were analyzed via flow cytometry: **(B)** percentage natural killer cells ($CD3^-$ $CD56^+$ cells), **(C)** percentage $CD16^+$ γδ T cells (gated on $CD3^+$ γδTCR^+), **(D)** percentage $CD56^+$ γδ T cells (gated on $CD3^+$ γδTCR^+).

SUPPLEMENTARY FIGURE 5
γδ T cells express CCR2, and γMSCs secrete CCL2. **(A)** RNA-seq performed on two biological replicates of γδ T cells isolated from two different PBMC donors; genes were ranked, log2(normalized counts) were calculated, and *CCR2* highlighted in red. **(B)** Graph of ELISA of CCL2 secretion by MSCs or γMSCs every 24 hours for 72 hours, n = 3 biological replicates, and each biological replicate is an average of two technical replicates. Statistics analyzed by one-way ANOVA with *post hoc* ($p < 0.05$ = *, $p < 0.01$ = **, $p < 0.001$ = ***). The sample mean is denoted with a black line. **(C)** Graph of transwell migration assay of γδ T cell migration to γMSCs treated with CCL2 antibody, n = 3 biological replicates, and each biological replicate is an average of two technical replicates. Statistics analyzed by one-way ANOVA with *post hoc* ($p<0.05$ = *); the sample mean is denoted with a black line.

References

1. Ridgley LA, Caron J, Dalgleish A, Bodman-Smith M. Releasing the restraints of Vγ9Vδ2 T-cells in cancer immunotherapy. *Front Immunol.* (2022) 13:1065495. doi: 10.3389/fimmu.2022.1065495

2. Zhao Y, Niu C, Cui J. Gamma-delta (γδ) T cells: friend or foe in cancer development? *J Trans Med.* (2018) 16:3. doi: 10.1186/s12967-017-1378-2.

3. Wu D, Wu P, Qiu F, Wei Q, Huang J. Human γδT-cell subsets and their involvement in tumor immunity. *Cell Mol Immunol.* (2017) 14:245–53. doi: 10.1038/cmi.2016.55.

4. Lawand M, Déchanet-Merville J, Dieu-Nosjean M-C. Key features of gamma-delta T-cell subsets in human diseases and their immunotherapeutic implications. *Front Immunol.* (2017) 8. doi: 10.3389/fimmu.2017.00761.

5. Lee D, Rosenthal CJ, Penn NE, Dunn ZS, Zhou Y, Yang L. Human γδ T cell subsets and their clinical applications for cancer immunotherapy. *Cancers (Basel).* (2022) 14. doi: 10.3390/cancers14123005.

6. Künkele K-P, Wesch D, Oberg H-H, Aichinger M, Supper V, Baumann C. Vγ9Vδ2 T cells: can we re-purpose a potent anti-infection mechanism for cancer therapy? *Cells.* (2020) 9:829. doi: 10.3390/cells9040829

7. Hoeres T, Smetak M, Pretscher D, Wilhelm M. Improving the efficiency of Vγ9Vδ2 T-cell immunotherapy in cancer. *Front Immunol.* (2018) 9. doi: 10.3389/fimmu.2018.00800.

8. Di Carlo E, Bocca P, Emionite L, Cilli M, Cipollone G, Morandi F, et al. Mechanisms of the antitumor activity of human Vγ9Vδ2 T cells in combination with zoledronic acid in a preclinical model of neuroblastoma. *Mol Ther.* (2013) 21:1034–43. doi: 10.1038/mt.2013.38.

9. Park JH, Lee HK. Function of γδ T cells in tumor immunology and their application to cancer therapy. *Exp Mol Med.* (2021) 53:318–27. doi: 10.1038/s12276-021-00576-0.

10. Yazdanifar M, Barbarito G, Bertaina A, Airoldi I. γδ T cells: the ideal tool for cancer immunotherapy. *Cells.* (2020) 9. doi: 10.3390/cells9051305.

11. Paul S, Lal G. Regulatory and effector functions of gamma-delta (γδ) T cells and their therapeutic potential in adoptive cellular therapy for cancer. *Int J Cancer.* (2016) 139:976–85. doi: 10.1002/ijc.30109.

12. O'Brien RL, Born WK. Dermal γδ T cells–What have we learned? *Cell Immunol.* (2015) 296:62–9. doi: 10.1016/j.cellimm.2015.01.011

13. Chan KF, Duarte JDG, Ostrouska S, Behren A. γδ T cells in the tumor microenvironment-interactions with other immune cells. *Front Immunol.* (2022) 13:894315. doi: 10.3389/fimmu.2022.894315.

14. Lança T, Costa MF, Gonçalves-Sousa N, Rei M, Grosso AR, Penido C, et al. Protective role of the inflammatory CCR2/CCL2 chemokine pathway through recruitment of type 1 cytotoxic γδ T lymphocytes to tumor beds. *J Immunol.* (2013) 190:6673–80. doi: 10.4049/jimmunol.1300434

15. Standiford TJ, Kunkel SL, Phan SH, Rollins BJ, Strieter RM. Alveolar macrophage-derived cytokines induce monocyte chemoattractant protein-1 expression from human pulmonary type II-like epithelial cells. *J Biol Chem.* (1991) 266:9912–8. doi: 10.1016/S0021-9258(18)92905-4.

16. Whelan DS, Caplice NM, Clover AJP. Mesenchymal stromal cell derived CCL2 is required for accelerated wound healing. *Sci Rep.* (2020) 10:2642. doi: 10.1038/s41598-020-59174-1.

17. Owen JL, Torroella-Kouri M, Handel-Fernandez ME, Iragavarapu-Charyulu V. GM-CSF up-regulates the expression of CCL2 by T lymphocytes in mammary tumor-bearing mice. *Int J Mol Med.* (2007) 20:129–36. doi: 10.3892/ijmm.

18. Jin J, Lin J, Xu A, Lou J, Qian C, Li X, et al. CCL2: an important mediator between tumor cells and host cells in tumor microenvironment. *Front Oncol.* (2021) 11. doi: 10.3389/fonc.2021.722916.

19. Gschwandtner M, Derler R, Midwood KS. More than just attractive: how CCL2 influences myeloid cell behavior beyond chemotaxis. *Front Immunol.* (2019) 10. doi: 10.3389/fimmu.2019.02759.

20. Shields BD, Mahmoud F, Taylor EM, Byrum SD, Sengupta D, Koss B, et al. Indicators of responsiveness to immune checkpoint inhibitors. *Sci Rep.* (2017) 7:807. doi: 10.1038/s41598-017-01000-2.

21. Arieta Kuksin C, Gonzalez-Perez G, Minter LM. CXCR4 expression on pathogenic T cells facilitates their bone marrow infiltration in a mouse model of aplastic anemia. *Blood.* (2015) 125:2087–94. doi: 10.1182/blood-2014-08-594796.

22. Burnham RE, Zoine JT, Story JY, Garimalla SN, Gibson G, Rae A, et al. Characterization of donor variability for γδ T cell *ex vivo* expansion and development of an allogeneic γδ T cell immunotherapy. *Front Med (Lausanne).* (2020) 7:588453. doi: 10.3389/fmed.2020.588453.

23. Sánchez-Martín L, Estecha A, Samaniego R, Sánchez-Ramón S, Vega MÁ, Sánchez-Mateos P. The chemokine CXCL12 regulates monocyte-macrophage differentiation and RUNX3 expression. *Blood.* (2011) 117:88–97. doi: 10.1182/blood-2009-12-258186.

24. Shi Y, Riese DJ, Shen J. The role of the CXCL12/CXCR4/CXCR7 chemokine axis in cancer. *Front Pharmacol.* (2020) 11. doi: 10.3389/fphar.2020.574667.

25. Kunzmann V, Bauer E, Feurle J, Tony HP, Weissinger F, Wilhelm M. Stimulation of γδ T cells by aminobisphosphonates and induction of antiplasma cell activity in multiple myeloma. *Blood.* (2000) 96:384–92. doi: 10.1182/blood.V96.2.384.

26. Nicol AJ, Tokuyama H, Mattarollo SR, Hagi T, Suzuki K, Yokokawa K, et al. Clinical evaluation of autologous gamma delta T cell-based immunotherapy for metastatic solid tumours. *Br J Cancer.* (2011) 105:778–86. doi: 10.1038/bjc.2011.293.

27. Wang RN, Wen Q, He WT, Yang JH, Zhou CY, Xiong WJ, et al. Optimized protocols for γδ T cell expansion and lentiviral transduction. *Mol Med Rep.* (2019) 19:1471–80. doi: 10.3892/mmr.

28. Ribot JC, Ribeiro ST, Correia DV, Sousa AE, Silva-Santos B. Human γδ thymocytes are functionally immature and differentiate into cytotoxic type 1 effector T cells upon IL-2/IL-15 signaling. *J Immunol.* (2014) 192:2237–43. doi: 10.4049/jimmunol.1303119.

29. Song Y, Liu Y, Teo HY, Liu H. Targeting cytokine signals to enhance γδT cell-based cancer immunotherapy. *Front Immunol.* (2022) 13:914839. doi: 10.3389/fimmu.2022.914839.

30. Ghaffari S, Torabi-Rahvar M, Aghayan S, Jabbarpour Z, Moradzadeh K, Omidkhoda A, et al. Optimizing interleukin-2 concentration, seeding density and bead-to-cell ratio of T-cell expansion for adoptive immunotherapy. *BMC Immunol.* (2021) 22:43. doi: 10.1186/s12865-021-00435-7.

31. Chen Z, Cordero J, Alqarni AM, Slack C, Zeidler MP, Bellantuono I. Zoledronate extends health span and survival via the mevalonate pathway in a FOXO-dependent manner. *Journals Gerontology: Ser A.* (2021) 77:1494–502. doi: 10.1093/gerona/glab172.

32. Göbel A, Thiele S, Browne AJ, Rauner M, Zinna VM, Hofbauer LC, et al. Combined inhibition of the mevalonate pathway with statins and zoledronic acid potentiates their anti-tumor effects in human breast cancer cells. *Cancer Lett.* (2016) 375:162–71. doi: 10.1016/j.canlet.2016.03.004.

33. Kabelitz D, Serrano R, Kouakanou L, Peters C, Kalyan S. Cancer immunotherapy with γδ T cells: many paths ahead of us. *Cell Mol Immunol.* (2020) 17:925–39. doi: 10.1038/s41423-020-0504-x.

34. Salim M, Knowles TJ, Baker AT, Davey MS, Jeeves M, Sridhar P, et al. BTN3A1 discriminates γδ T cell phosphoantigens from nonantigenic small molecules via a conformational sensor in its B30.2 domain. *ACS Chem Biol.* (2017) 12:2631–43. doi: 10.1021/acschembio.7b00694.

35. Capsomidis A, Benthall G, Van Acker HH, Fisher J, Kramer AM, Abeln Z, et al. Chimeric antigen receptor-engineered human gamma delta T cells: enhanced cytotoxicity with retention of cross presentation. *Mol Ther.* (2018) 26:354–65. doi: 10.1016/j.ymthe.2017.12.001.

36. Becker SA, Petrich BG, Yu B, Knight KA, Brown HC, Raikar SS, et al. Enhancing the effectiveness of γδ T cells by mRNA transfection of chimeric antigen receptors or bispecific T cell engagers. *Mol Ther Oncolytics.* (2023) 29:145–57. doi: 10.1016/j.omto.2023.05.007.

37. Rozenbaum M, Meir A, Aharony Y, Itzhaki O, Schachter J, Bank I, et al. Gamma-delta CAR-T cells show CAR-directed and independent activity against leukemia. *Front Immunol.* (2020) 11. doi: 10.3389/fimmu.2020.01347.

38. Fleischer LC, Becker SA, Ryan RE, Fedanov A, Doering CB, Spencer HT. Non-signaling chimeric antigen receptors enhance antigen-directed killing by γδ T cells in contrast to αβ T cells. *Mol Ther Oncolytics.* (2020) 18:149–60. doi: 10.1016/j.omto.2020.06.003.

39. Sutton KS, Dasgupta A, McCarty D, Doering CB, Spencer HT. Bioengineering and serum free expansion of blood-derived γδ T cells. *Cytotherapy.* (2016) 18:881–92. doi: 10.1016/j.jcyt.2016.04.001.

40. Burnham RE, Tope D, Branella G, Williams E, Doering CB, Spencer HT. Human serum albumin and chromatin condensation rescue *ex vivo* expanded γδ T cells from the effects of cryopreservation. *Cryobiology.* (2021) 99:78–87. doi: 10.1016/j.cryobiol.2021.01.011.

41. Jonus HC, Burnham RE, Ho A, Pilgrim AA, Shim J, Doering CB, et al. Dissecting the cellular components of *ex vivo* γδ T cell expansions to optimize selection of potent cell therapy donors for neuroblastoma immunotherapy trials. *Oncoimmunology.* (2022) 11:2057012. doi: 10.1080/2162402X.2022.2057012.

42. Lamb LS Jr., Bowersock J, Dasgupta A, Gillespie GY, Su Y, Johnson A, et al. Engineered drug resistant γδ T cells kill glioblastoma cell lines during a chemotherapy challenge: a strategy for combining chemo- and immunotherapy. *PloS One.* (2013) 8:e51805. doi: 10.1371/journal.pone.0051805.

43. Lamb LS, Pereboeva L, Youngblood S, Gillespie GY, Nabors LB, Markert JM, et al. A combined treatment regimen of MGMT-modified γδ T cells and temozolomide chemotherapy is effective against primary high grade gliomas. *Sci Rep.* (2021) 11:21133. doi: 10.1038/s41598-021-00536-8.

44. Steel CD, Stephens AL, Hahto SM, Singletary SJ, Ciavarra RP. Comparison of the lateral tail vein and the retro-orbital venous sinus as routes of intravenous drug delivery in a transgenic mouse model. *Lab Anim (NY).* (2008) 37:26–32. doi: 10.1038/laban0108-26.

45. Schoch A, Thorey IS, Engert J, Winter G, Emrich T. Comparison of the lateral tail vein and the retro-orbital venous sinus routes of antibody administration in pharmacokinetic studies. *Lab Anim (NY).* (2014) 43:95–9. doi: 10.1038/laban.481.

46. Zoine JT, Knight KA, Fleischer LC, Sutton KS, Goldsmith KC, Doering CB, et al. *Ex vivo* expanded patient-derived γδ T-cell immunotherapy enhances neuroblastoma tumor regression in a murine model. *Oncoimmunology*. (2019) 8:1593804. doi: 10.1080/2162402X.2019.1593804.

47. Capietto AH, Martinet L, Fournié JJ. Stimulated γδ T cells increase the *in vivo* efficacy of trastuzumab in HER-2+ breast cancer. *J Immunol*. (2011) 187:1031–8. doi: 10.4049/jimmunol.1100681.

48. Baghaei K, Hashemi SM, Tokhanbigli S, Asadi Rad A, Assadzadeh-Aghdaei H, Sharifian A, et al. Isolation, differentiation, and characterization of mesenchymal stem cells from human bone marrow. *Gastroenterol Hepatol Bed Bench*. (2017) 10:208–13.

49. Wo J, Zhang F, Li Z, Sun C, Zhang W, Sun G. The role of gamma-delta T cells in diseases of the central nervous system. *Front Immunol*. (2020) 11. doi: 10.3389/fimmu.2020.580304.

50. Montecino-Rodriguez E, Kong Y, Casero D, Rouault A, Dorshkind K, Pioli PD. Lymphoid-biased hematopoietic stem cells are maintained with age and efficiently generate lymphoid progeny. *Stem Cell Rep*. (2019) 12:584–96. doi: 10.1016/j.stemcr.2019.01.016.

51. Ciurea SO, Andersson BS. Busulfan in hematopoietic stem cell transplantation. *Biol Blood Marrow Transplant*. (2009) 15:523–36. doi: 10.1016/j.bbmt.2008.12.489.

52. Sabloff M, Tisseverasinghe S, Babadagli ME, Samant R. Total body irradiation for hematopoietic stem cell transplantation: what can we agree on? *Curr Oncol*. (2021) 28:903–17. doi: 10.3390/curroncol28010089.

53. Cibrián D, Sánchez-Madrid F. CD69: from activation marker to metabolic gatekeeper. *Eur J Immunol*. (2017) 47:946–53. doi: 10.1002/eji.201646837.

54. Branella GM, Lee JY, Okalova J, Parwani KK, Alexander JS, Arthuzo RF, et al. Ligand-based targeting of c-kit using engineered γδ T cells as a strategy for treating acute myeloid leukemia. *Front Immunol*. (2023) 14. doi: 10.3389/fimmu.2023.1294555.

55. Kopp HG, Avecilla ST, Hooper AT, Rafii S. The bone marrow vascular niche: home of HSC differentiation and mobilization. *Physiol (Bethesda)*. (2005) 20:349–56. doi: 10.1152/physiol.00025.2005.

56. Green DE, Rubin CT. Consequences of irradiation on bone and marrow phenotypes, and its relation to disruption of hematopoietic precursors. *Bone*. (2014) 63:87–94. doi: 10.1016/j.bone.2014.02.018.

57. Janssens R, Struyf S, Proost P. The unique structural and functional features of CXCL12. *Cell Mol Immunol*. (2018) 15:299–311. doi: 10.1038/cmi.2017.107.

58. Gilbert W, Bragg R, Elmansi AM, McGee-Lawrence ME, Isales CM, Hamrick MW, et al. Stromal cell-derived factor-1 (CXCL12) and its role in bone and muscle biology. *Cytokine*. (2019) 123:154783. doi: 10.1016/j.cyto.2019.154783.

59. Beatson RE, Parente-Pereira AC, Halim L, Cozzetto D, Hull C, Whilding LM, et al. TGF-β1 potentiates Vγ9Vδ2 T cell adoptive immunotherapy of cancer. *Cell Rep Med*. (2021) 2:100473. doi: 10.1016/j.xcrm.2021.100473.

60. Barros M, de Araújo ND, Magalhães-Gama F, Pereira Ribeiro TL, Alves Hanna FS, Tarragô AM, et al. γδ T cells for leukemia immunotherapy: new and expanding trends. *Front Immunol*. (2021) 12. doi: 10.3389/fimmu.2021.729085.

61. Nörenberg J, Jaksó P, Barakonyi A. Gamma/delta T cells in the course of healthy human pregnancy: cytotoxic potential and the tendency of CD8 expression make CD56 + γδT cells a unique lymphocyte subset. *Front Immunol*. (2021) 11. doi: 10.3389/fimmu.2020.596489

62. Poznanski SM, Ashkar AA. Shining light on the significance of NK cell CD56 brightness. *Cell Mol Immunol*. (2018) 15:1071–3. doi: 10.1038/s41423-018-0163-3.

63. Wang W, Erbe AK, Hank JA, Morris ZS, Sondel PM. NK cell-mediated antibody-dependent cellular cytotoxicity in cancer immunotherapy. *Front Immunol*. (2015) 6. doi: 10.3389/fimmu.2015.00368.

64. Shao Z, Tan Y, Shen Q, Hou L, Yao B, Qin J, et al. Molecular insights into ligand recognition and activation of chemokine receptors CCR2 and CCR3. *Cell Discovery*. (2022) 8:44. doi: 10.1038/s41421-022-00403-4.

65. She S, Ren L, Chen P, Wang M, Chen D, Wang Y, et al. Functional roles of chemokine receptor CCR2 and its ligands in liver disease. *Front Immunol*. (2022) 13:812431. doi: 10.3389/fimmu.2022.812431.

66. Drobyski WR, Majewski D, Hanson G. Graft-facilitating doses of *ex vivo* activated gammadelta T cells do not cause lethal murine graft-vs. *-host disease. Biol Blood Marrow Transplant*. (1999) 5:222–30. doi: 10.1053/bbmt.1999.v5.pm10465102.

67. Handgretinger R, Schilbach K. The potential role of γδ T cells after allogeneic HCT for leukemia. *Blood*. (2018) 131:1063–72. doi: 10.1182/blood-2017-08-752162.

68. Chabab G, Boissière-Michot F, Mollevi C, Ramos J, Lopez-Crapez E, Colombo PE, et al. Diversity of tumor-infiltrating, γδ T-cell abundance in solid cancers. *Cells*. (2020) 9. doi: 10.3390/cells9061537.

69. Gentles AJ, Newman AM, Liu CL, Bratman SV, Feng W, Kim D, et al. The prognostic landscape of genes and infiltrating immune cells across human cancers. *Nat Med*. (2015) 21:938–45. doi: 10.1038/nm.3909.

70. Saura-Esteller J, de Jong M, King LA, Ensing E, Winograd B, de Gruijl TD, et al. Gamma delta T-cell based cancer immunotherapy: past-present-future. *Front Immunol*. (2022) 13. doi: 10.3389/fimmu.2022.915837.

71. Ganapathy T, Radhakrishnan R, Sakshi S, Martin S. CAR γδ T cells for cancer immunotherapy. Is the field more yellow than green? *Cancer Immunol Immunother*. (2023) 72:277–86. doi: 10.1007/s00262-022-03260-y.

72. Fu H, Ward EJ, Marelli-Berg FM. Mechanisms of T cell organotropism. *Cell Mol Life Sci*. (2016) 73:3009–33. doi: 10.1007/s00018-016-2211-4.

73. Di Rosa F, Gebhardt T. Bone marrow T cells and the integrated functions of recirculating and tissue-resident memory T cells. *Front Immunol*. (2016) 7. doi: 10.3389/fimmu.2016.00051.

74. van Buul JD, Voermans C, van Gelderen J, Anthony EC, van der Schoot CE, Hordijk PL. Leukocyte-endothelium interaction promotes SDF-1-dependent polarization of CXCR4. *J Biol Chem*. (2003) 278:30302–10. doi: 10.1074/jbc.M304764200.

75. Rose JJ, Foley JF, Murphy PM, Venkatesan S. On the mechanism and significance of ligand-induced internalization of human neutrophil chemokine receptors CXCR1 and CXCR2. *J Biol Chem*. (2004) 279:24372–86. doi: 10.1074/jbc.M401364200.

76. Marchese A, Benovic JL. Agonist-promoted ubiquitination of the G protein-coupled receptor CXCR4 mediates lysosomal sorting. *J Biol Chem*. (2001) 276:45509–12. doi: 10.1074/jbc.C100527200.

77. Peters C, Meyer A, Kouakanou L, Feder J, Schricker T, Lettau M, et al. TGF-β enhances the cytotoxic activity of Vδ2 T cells. *Oncoimmunology*. (2019) 8:e1522471. doi: 10.1080/2162402X.2018.1522471.

78. Melzer C, Hass R, von der Ohe J, Lehnert H, Ungefroren H. The role of TGF-β and its crosstalk with RAC1/RAC1b signaling in breast and pancreas carcinoma. *Cell Communication Signaling*. (2017) 15:19. doi: 10.1186/s12964-017-0175-0.

79. Parvani JG, Schiemann WP. Sox4, EMT programs, and the metastatic progression of breast cancers: mastering the masters of EMT. *Breast Cancer Res*. (2013) 15:R72. doi: 10.1186/bcr3466.

80. Baba AB, Rah B, Bhat GR, Mushtaq I, Parveen S, Hassan R, et al. Transforming growth factor-beta (TGF-β) signaling in cancer-A betrayal within. *Front Pharmacol*. (2022) 13. doi: 10.3389/fphar.2022.791272.

81. Bagati A, Kumar S, Jiang P, Pyrdol J, Zou AE, Godicelj A, et al. Integrin αvβ6–TGFβ–SOX4 pathway drives immune evasion in triple-negative breast cancer. *Cancer Cell*. (2021) 39:54–67. e9. doi: 10.1016/j.ccell.2020.12.001.

82. Batlle E, Massagué J. Transforming growth factor-β Signaling in immunity and cancer. *Immunity*. (2019) 50:924–40. doi: 10.1016/j.immuni.2019.03.024.

83. Rafia C, Loizeau C, Renoult O, Harly C, Pecqueur C, Joalland N, et al. The antitumor activity of human Vγ9Vδ2 T cells is impaired by TGF-β through significant phenotype, transcriptomic and metabolic changes. *Front Immunol*. (2022) 13:1066336. doi: 10.3389/fimmu.2022.1066336

84. Abe Y, Muto M, Nieda M, Nakagawa Y, Nicol A, Kaneko T, et al. Clinical and immunological evaluation of zoledronate-activated Vgamma9gammadelta T-cell-based immunotherapy for patients with multiple myeloma. *Exp Hematol*. (2009) 37:956–68. doi: 10.1016/j.exphem.2009.04.008.

85. Jhita N, Raikar SS. Allogeneic gamma delta T cells as adoptive cellular therapy for hematologic Malignancies. *Explor Immunol*. (2022) 2:334–50. doi: 10.37349/ei.

frontiers | Frontiers in Immunology

TYPE Review
PUBLISHED 21 March 2024
DOI 10.3389/fimmu.2024.1360237

OPEN ACCESS

EDITED BY
Jonathan Fisher,
University College London, United Kingdom

REVIEWED BY
Prashant Sharma,
University of Arizona, United States
Brian Petrich,
Expression Therapeutics, United States
Martin Wilhelm,
Nürnberg Hospital, Germany

*CORRESPONDENCE
Wenjun Wang
wenjun27@stanford.edu
Alice Bertaina
aliceb1@stanford.edu

†These authors have contributed equally to this work

RECEIVED 22 December 2023
ACCEPTED 07 March 2024
PUBLISHED 21 March 2024

CITATION
Yuan M, Wang W, Hawes I, Han J, Yao Z and Bertaina A (2024) Advancements in γδT cell engineering: paving the way for enhanced cancer immunotherapy.
Front. Immunol. 15:1360237.
doi: 10.3389/fimmu.2024.1360237

Advancements in γδT cell engineering: paving the way for enhanced cancer immunotherapy

Megan Yuan†, Wenjun Wang*†, Isobel Hawes, Junwen Han, Zhenyu Yao and Alice Bertaina*

Division of Hematology, Oncology, Stem Cell Transplantation and Regenerative Medicine, Department of Pediatrics, Stanford University, School of Medicine, Stanford, CA, United States

Comprising only 1-10% of the circulating T cell population, γδT cells play a pivotal role in cancer immunotherapy due to their unique amalgamation of innate and adaptive immune features. These cells can secrete cytokines, including interferon-γ (IFN-γ) and tumor necrosis factor-α (TNF-α), and can directly eliminate tumor cells through mechanisms like Fas/FasL and antibody-dependent cell-mediated cytotoxicity (ADCC). Unlike conventional αβT cells, γδT cells can target a wide variety of cancer cells independently of major histocompatibility complex (MHC) presentation and function as antigen-presenting cells (APCs). Their ability of recognizing antigens in a non-MHC restricted manner makes them an ideal candidate for allogeneic immunotherapy. Additionally, γδT cells exhibit specific tissue tropism, and rapid responsiveness upon reaching cellular targets, indicating a high level of cellular precision and adaptability. Despite these capabilities, the therapeutic potential of γδT cells has been hindered by some limitations, including their restricted abundance, unsatisfactory expansion, limited persistence, and complex biology and plasticity. To address these issues, gene-engineering strategies like the use of chimeric antigen receptor (CAR) T therapy, T cell receptor (TCR) gene transfer, and the combination with γδT cell engagers are being explored. This review will outline the progress in various engineering strategies, discuss their implications and challenges that lie ahead, and the future directions for engineered γδT cells in both monotherapy and combination immunotherapy.

KEYWORDS

γδT cells, immunotherapy, engineering, cellular therapy, cancer, CAR-T

1 Introduction

Immunotherapy has revolutionized cancer treatment, effectively integrating with established medical practices such as surgery and chemotherapy (1, 2). This approach boosts the immune system's capability to target and eliminate malignant cells, thereby increasing antitumor efficacy and minimizing off-target effects (3). Within the realm of

immunotherapy, various strategies have been developed, including the use of immune cells, checkpoint inhibitors, and cytokines. Notably, T cell-based therapies, particularly Chimeric Antigen Receptor (CAR) T cell therapy, have demonstrated significant success against blood cancers (4). In parallel, therapies utilizing NK cells, macrophages, and B cells are emerging as novel treatments for solid tumors and other malignancies (5–7).

Immune cells play crucial roles in the body's defense mechanisms, including T cells, which are central to cell-mediated immune responses; B cells, which produce antibodies and mediate humoral immunity; and NK cells, which can induce apoptosis in infected or malignant cells as part of the innate immune response (3). Among these immune cells, γδT cells stand out for their unique role in bridging innate and adaptive immunity (8–10). They target and kill cancer cells without the restriction of major histocompatibility complex (MHC) molecules, thus having a broader recognition on cancer cells, including those deficient in MHC class I. γδT cells are adept at secreting cytokines like interferon-γ (IFN-γ) and tumor necrosis factor-α (TNF-α), and they can directly eliminate tumor cells through mechanisms such as Fas/FasL and antibody-dependent cell-mediated cytotoxicity (ADCC) (11). Their ability to migrate to peripheral tissues and respond rapidly to target cells (12), coupled with their lack of involvement in graft-versus-host disease (GvHD) (13, 14), makes them ideal candidates for off-the-shelf cell therapy solutions.

Furthermore, γδT cells are crucial in orchestrating anti-tumor immune responses. They can act as professional antigen-presenting cells (APCs) or influence other APCs like dendritic cells, thereby enhancing the activation of αβT cells and the overall immune response against tumors (15, 16). Theproduction of cytokines, including IL-17 and IL-22, by γδT cells plays a vital role in shaping the tumor microenvironment (TME), thereby influencing tumor growth in various contexts (16–23). This dual role highlights the complexity and importance of γδT cells in tumor immunology and fuels ongoing research into leveraging their therapeutic potential in novel cancer immunotherapies, such as adoptive cell therapy (ACT) (9, 24–27).

Despite their significant therapeutic promise, the clinical application of γδT cells faces challenges. As a minor subset of T cells, they often struggle with *in vivo* survival and proliferation (28), limited persistence, and potential functional suppression upon infiltrating the complex TME (29, 30). To overcome these obstacles, recent advancements in gene-engineering technologies are paving the way for optimizing the therapeutic potential of γδT cells in cancer treatment (8, 9, 15, 28, 31, 32). By genetically modifying these cells to express CARs or enhancing their native T cell receptors (TCRs), their specificity and cytotoxicity against tumor cells can be significantly bolstered. The use of genetic editing tools like CRISPR/Cas9 to knock out inhibitory receptors or to insert cytokine genes further enhances their proliferative and cytotoxic capacities. Concurrently, combination therapies are being explored to enhance the anti-tumor activity of γδT cells, including the use of bispecific antibodies, checkpoint blockade, and cytokine co-administration.

This review aims to deliver a comprehensive overview of cutting-edge approaches to augment γδT cell immunotherapy. It delves into the biological underpinnings and inherent advantages of γδT cells pertinent to their role in immunotherapeutic applications, as well as scrutinizes the forefront of gene-engineering methods being crafted to surmount existing barriers within γδT cell treatment modalities. Additionally, the synergy of gene-modified γδT cells with other treatment modalities is explored, informed by recent clinical research findings. These studies will shed light on the prospective trajectory of γδT cell immunotherapy, underscoring its potential to significantly enhance treatment outcomes for cancer patients.

2 Properties and functions of γδT cells

2.1 γδT cells ontogeny and γδTCRs diversity

γδT cells are the first T cell lineage to develop in the thymus and can be observed in humans as early as 12.5 weeks of gestational age. However, once generated, these cells will expand and mature extrathymically, and their gene repertoire changes in response to age (33). γδT cells derive their name from their TCRs, which are made up of gamma and delta chains. Like αβT cells, γδT cells undergo somatic V(D)J rearrangement, a process that generates diverse TCRs to respond to a wide range of antigens (34). However, in contrast to αβTCRs, γδTCRs allow cross-reactivity with multiple ligands and each combination is associated with different functional avidities (35). Despite the fact that V(D)J rearrangement of γδT cells generates less diversity than αβT cells, TCR δ chains have a higher potential of diversity at the complementarity-determining region 3 (CDR3) junction and can provide information on a person's unique history of infection (33, 36, 37).

2.2 Tumor targeting mechanisms

γδT cells target real and perceived immunological insults through the production and release of soluble factors. One example of this is when γδT cells recognize pathogen specific antibodies and stress-induced antigens. In response, γδT cells will produce Th1 cytokines including IFN-γ and TNF-α. Subsequently, γδT cells also release cytotoxic granules containing perforin and granzyme, further promoting pathogen degradation (38). Additionally, there is evidence in literature suggesting that Vγ9Vδ2 cells–a subset of γδT cells (discussed in the next section) can act as sensors of a dysregulated isoprenoid metabolism that target specifically cancer cells (39). Moreover, several recent studies have indicated that different subsets of γδT cells may have remarkably different functions in targeting tumor cells (40–43). Therefore, it is important to understand the structure and subsets of γδT cells, which we describe in the next section.

2.3 γδT cell subsets

This section will focus on two main subsets of γδT cells: Vδ1 and Vγ9Vδ2.

2.3.1 Vδ1 γδT cells

Vδ1 T cells are primarily localized in various human tissues, particularly abundant in the intestine, skin, spleen, and liver (44) (Figure 1). Their properties, particularly their inherent tissue-specific adaptations, have attracted growing interest in the context of cancer immunosurveillance and immunotherapy applications. Phenotypically, these tissue-resident Vδ1 T cells express homing chemokine receptors (e.g., CXCR3, CXCR6) as well as tissue-retention markers (e.g., CD69, CD103, and CD49a) (45–47). Intratumoral Vδ1 T cells have been detected in several solid tumors, exhibiting features of tissue-resident memory T cells (T_{RM}) (46, 47). There are also peripheral Vδ1 cells that preferentially express CCR5, CCR6, and CXCR3 (48).

Additionally, Vδ1 T cells have private TCR repertoires and significant TCR diversity that mainly originate from *TRD* repertoires (49). They also manifest features of adaptive immunity, including long-lasting functional memory in γδT cells and adaptive clonal expansion, particularly in response to viral infections (49–51). Studies demonstrate that Vδ1 T cells recognize tumor antigens or cell stress signals through γδTCR and various activating receptors shared with NK cells. These include NK group 2 member D (NKG2D), natural cytotoxicity receptors (NCR, such as NKp30, NKp44, NKp46), and coactivating/adhesion DNAX-activating molecule (DNAM-1) (52–56). Their ligands are frequently expressed on stressed neoplastic cells, for instance, MHC class I chain-related protein A and B (MICA/B), UL16-binding proteins (ULBP) 1-4 are common ligands for NKG2D. Vδ1+ T cells can be directly activated through NKG2D upon the expression of its ligand (e.g., MICA) on tumors, without the need for overt TCR stimulation as seen in αβT cells (55, 57). Moreover, the expression of NCRs on Vδ1 T cells is correlated with increased granzyme B and enhanced cytotoxicity against lymphoid leukemia cells (55). Evidence in the literature suggests that Vδ1 T cells can recognize stress-induced antigens including non-classical MHC class I-like molecules, such as CD1 family (including CD1c, CD1d), MICA/B, ULBP molecules (including ULBP3), and annexin A2 (52–54, 58–62). Interestingly, Vδ1+ T cells are less susceptible to activation-induced cell death (AICD) compared to Vδ2+ T cells. Despite variations in their antigen recognition, both Vδ2 and Vδ1 T cells share similar cytotoxic mechanisms via the perforin/granzyme-B mediated secretory pathway and death receptor pathways such as TRAIL/TRAIL-R, Fas/FasL (38).

Recognition of CD1d is dependent on the presence of lipid and glycolipid on foreign antigens, suggesting that Vδ1 T cells could recognize these antigens in a lipid-dependent manner (63). Bai et al.'s study directly demonstrates this principle of antigen presentation of MHC and lipid recognition by Vδ1 T cells (64). However, the exact mechanism of CD1d recognition in Vδ1 T cells is still unclear and remains an area of continued investigation.

Furthermore, MICA, a stress-induced antigen, triggers activation and expansion of Vδ1 subset via NKG2D when it is expressed on the surface of tumor cells (52–54). These cells have also been shown to recognize ULBP3, a "kill me" signal, expressed on leukemic B cells, suggesting an additional mechanism through

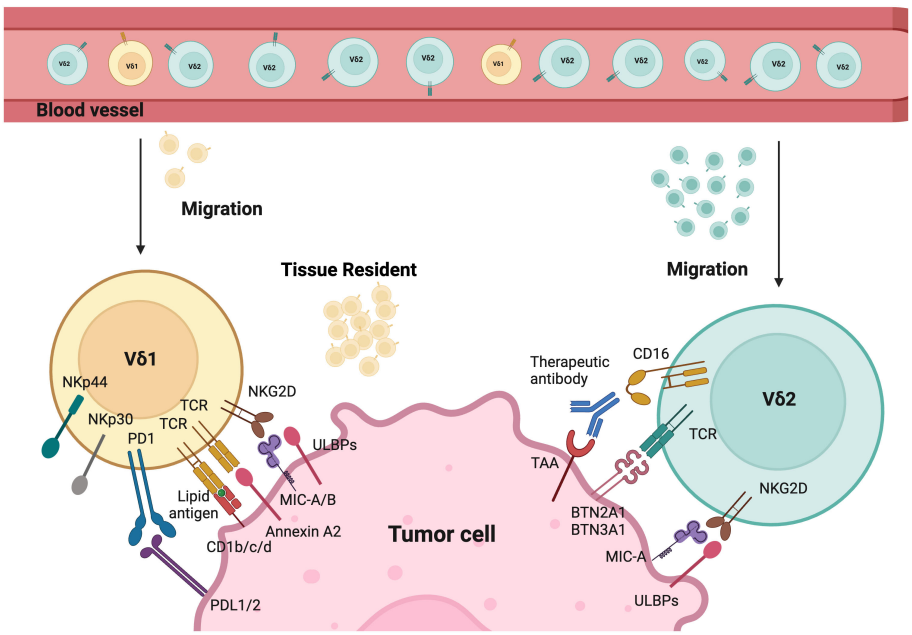

FIGURE 1
Tumor targeting mechanisms of Vδ1 and Vδ2. Different γδT cells activation modes by tumor cells. The tissue resident Vδ1 T cells recognize cancer cells via their specific Vδ1 T cell receptors (TCRs), which bind Annexin A2 and lipid antigens presented by CD1. Besides, Vδ1 T cells also use NKG2D and natural cytotoxicity receptors (NCRs) such as NKp30, NKp44, and NKp46 for tumor cell recognition. Vδ2 T cells are predominant in the peripheral blood and can migrate into tumor tissues. Their specific Vδ2 TCRs recognize BTN3A1 and BTN2A1 after the isopentenyl pyrophosphate (IPP) accumulation. CD16 expressed by Vδ2 T cells can bind therapeutic antibodies to trigger Vδ2-mediated antibody-dependent cell-mediated cytotoxicity (ADCC). In addition, both Vδ1 and Vδ2 T cells express natural killer receptors (NKRs), which recognize tumor cells by binding to MHC class I chain-related protein A and B (MICA/B), and UL16-binding proteins (ULBPs). Created with BioRender.com.

which these cells can participate in anti-tumor immune regulation (60).

With advances in innovative isolation techniques and deepening comprehension of Vδ1 T cells, these cells hold high promise as a potential candidate for cancer immunotherapy, particularly as tissue-associated or tumor-infiltrating lymphocytes. Their manipulation using well-designed cell engagers or immune checkpoint inhibitors *in situ* represents an accessible and cost-effective approach. In the future, the use of single cell sequencing/proteomics techniques will be essential to dissect the heterogeneity and functional plasticity of Vδ1 T cells shaped by the TME, thereby aiding their clinical implementation.

2.3.2 Vγ9Vδ2 γδT cells

Vγ9Vδ2 (Vδ2) T cells are among the most studied subsets of γδT cells, partially because these cells represent the most abundant subset in peripheral blood (Figure 1). Vγ9Vδ2 cells are generally considered as the first line of defense, forming an essential part of the innate immunity. All Vγ9Vδ2 T cells consist of a public Vγ9 chain and private Vδ2 chain. However, Vδ2 T cells can be further divided into two subclasses (Vγ9+Vδ2+ and Vγ9-Vδ2+) that exhibit distinct properties. Vγ9+Vδ2+ T cells exhibit innate characteristics, while Vγ9-Vδ2+ T cells show adaptive features and undergo pathogen-driven differentiation similar to conventional CD8+ T cells (44, 65, 66).

Similarly, the recognition of Vδ2 cells is mediated by γδTCR or NK cell-activating receptors such as NKG2D and DNAM1. These cells are unique due to their semi-invariant property that allows recognition of specific antigens. Vδ2+ TCRs are capable to recognize phosphoantigens (P-Ag), non-peptide antigens that accumulated in tumor cells due to their dysregulated mevalonate pathway (67). The activation of γδ T cells is intricately linked to the recognition of P-Ag. This process heavily involves the proteins butyrophilin 2A1 (BTN2A1) and butyrophilin 3A1 (BTN3A1). BTN2A1 binds to Vγ9+ γδTCRs. BTN3A1 acts as a critical mediator by presenting P-Ag to γδ T cells through its intracellular B30.2 domain (68). This interaction is pivotal for initiating the downstream signaling pathways that lead to γδ T cell activation and immune responses. Furthermore, Vγ9Vδ2 T cells have distinct patterns of development in fetus and adults. Fetal Vγ9Vδ2T cells are generated in the fetal thymus, while adult Vγ9Vδ2 T cells are developed after birth in response to environmental stimuli and expanded polyclonally by microbial P-Ag exposure (37, 69). The CD16+ Vδ2 T cells can also mediate ADCC upon binding to tumor-specific antibodies, which is absent in Vδ1 T cells (70). Additionally, these cells can function like professional APCs by phagocytosing and processing target antigens, then presenting them with MHC molecules. This process, in turn, induces CD4+ and CD8+ responses in αβT cells (16, 71–73).

Recent studies suggest both subclasses of Vγ9Vδ2 T cells play key roles in the immune defense against pathogens and tumor cells. The number of Vγ9Vδ2 T cells increases dramatically during some infections and these cells display potent cytotoxic activity. During stimulation with non-peptidic antigens, Vγ9Vδ2 T cells can be activated via a dual mechanism involving the recognition of FcγRIIIa (CD16a) following the TCR-CD3 complex, which are cell surface antigens for T lymphocytes and NK cells (74). This activation schema belies a keystone role for Vγ9Vδ2 T cells in the defense of pathological infection as well as tumorigenesis.

3 Sources of γδT cells and their expansion strategies

3.1 Sources of γδT cells

The successful clinical application of γδT cell-based immunotherapy must address several challenges, starting with the selection of appropriate sources (Figure 2). Inconsistent effects of autologous γδT cells have prompted investigators to design standardized cell products. Because HLA-matching is not required, fully allogeneic mismatched or haplo-identical γδT cells sourced from healthy donors have emerged as an appealing approach with a commendable safety profile (75, 76). A thorough investigation into the donor's infection history can also benefit patient outcomes when used as a screening criterion. For instance, the reactivation of cytomegalovirus (CMV) in patients receiving HSCT can potentially induce the expansion of $V\delta2^{neg}$ γδT cell clones, which exhibit dual reactivity to CMV and acute myeloid leukemia (AML) (77–79). Another challenge lies in determining which γδT cell subset will be more effective for a specific tumor considering their differing characteristics, particularly their chemotaxis ability and tumor cytotoxicity. Up to now, the main sources of γδT cells include cord blood, peripheral blood, skin, and inducible pluripotent stem cells (iPSCs).

The developmental trajectory of γδT cells reveals that Vδ1+ cells constitute the predominant population (approximately 50%) of γδT cells in cord blood at birth, while Vδ2+ cells typically represent 25% (80). Over time, Vγ9Vδ2 T cells emerge as the predominant subset (over 75%) of the γδT cell population in peripheral blood by adulthood, with less than 10% being Vδ1+ (80). Therefore, cord blood has been explored for its predominant expansion of Vδ1+ cells, or occasional viable expansion of Vδ2+ cells (81–83). However, there are several challenges associated with the *in vitro* expansion of γδT cells from cord blood, including a low number of γδT cells (less than 1% of cord blood lymphocytes), phenotypically and functionally immature γδT cells, and a poor response to IL-2 and phosphoantigen stimulation (80). In contrast, γδT cells isolated from peripheral blood mononuclear cells (PBMCs) are predominantly Vγ9Vδ2 (84). Due to their relative convenience and availability, PBMCs provide easy and stable access for expanding Vγ9Vδ2 T cells and viable Vδ1+ cells such as Delta One T (DOT) cells. Additionally, owing to natural tissue tropism of Vδ1+ cells, human tissues such as skin also provide an alternative source of Vδ1+ cells through enzymatic digestion or other methods (85, 86). Despite the roles of skin γδT cells in the cutaneous malignances such as melanoma, complex skin γδT cell subsets necessitate a thorough investigation for therapeutic strategies (87).

In addition to γδT cells derived from donors, these cells can also be generated from iPSCs (88, 89). Two companies, Century

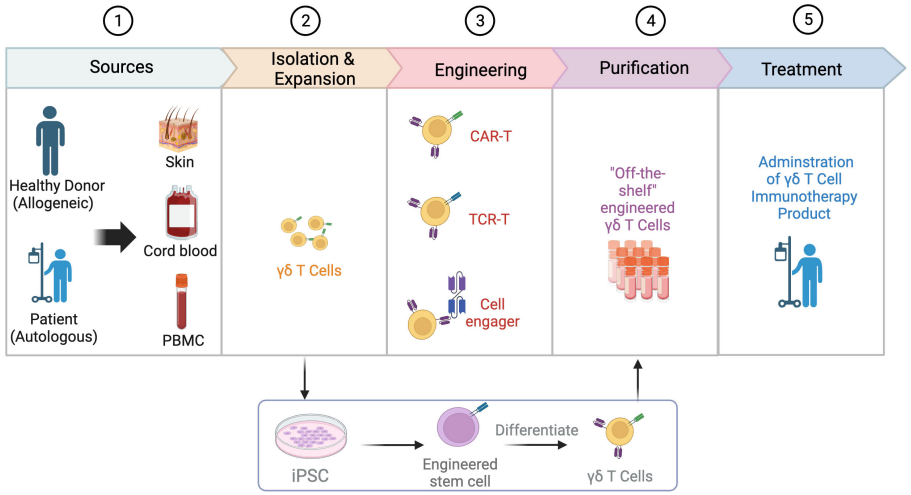

FIGURE 2
Process of engineering γδT cells. The process of engineering γδT cells involves several key steps. Common sources of γδT cells include the skin, cord blood, and peripheral blood mononuclear cells (PBMCs), with the allogeneic pathway involving isolation from a healthy donor and the autologous pathway involving isolation from the patient's own cells. After isolation, γδT cells are expanded and engineered through various strategies such as the use of chimeric antigen receptors (CARs), T cell receptor (TCR) transfer, and cell engager. Engineered γδT cells can also be derived from induced pluripotent stem cells (iPSCs). In the next step, γδT cells go through purification to develop "off-the-shelf" engineered γδT cells. Finally, the engineered γδT cell product is administered to patients as a form of immunotherapy. Created with BioRender.com.

Therapeutics and CytoMed Therapeutics, have developed platforms that enrich γδT cells from healthy donor leukapheresis and then reprogram them into T cell-derived iPSCs (TiPSCs). TiPSCs are engineered with CAR expression, followed by directed differentiation into γδ CAR-T cells (Figure 2) (90). During this process, the genome characterization of a single CAR-TiPSC clone enables the production of a highly uniform clonal γδ CAR-T cell bank (> 95% CAR expression) and minimal DNA mutation caused by engineering (90, 91). This off-the-shelf platform provides an appealing source of γδT cells with several benefits: overcoming quantitative limitations of γδT, reducing the wait time for *ex vivo* expansion of γδT cells, and not relying on the *ex vivo* expansion efficiency of PBMC-derived γδT cells (92). Importantly, TiPSC-derived γδT cells retain cytotoxicity to solid and blood tumor through both γδTCR and NKG2D (92). However, this complex manufacturing process is time-consuming and needs more evaluation on potential risks.

Overall, most of the research is adopting PBMC and cord blood as the primary source of γδT cells. In contrast, investigations into skin-derived and iPSC-derived γδT cells are still in the preclinical stages. Our current understanding of the migration and colonization of γδT cells in peripheral tissues primarily relies on research conducted in mice. Further studies involving humans will significantly advance our comprehension of tissue-specific γδT cells, potentially expanding the applications of Vδ1+ cells in immunotherapy.

3.2 Strategies to expand γδT cells: prerequisite for therapeutic infusion

The clinical-scale manufacturing of γδT cells requires robust and highly reproducible expansion methods that meet good manufacturing practice (GMP) standards. Current approaches mainly include cytokine only, synthetic p-Ag and bisphosphonate (BP) stimulation, antibody-based expansion, and feeder cell-based strategies as summarized in Table 1. Undoubtably, cytokine combinations strategies simplify the manufacturing process but often produce insufficient expansion.

p-Ag or BPs have been recognized as the most established approaches to selectively expand Vδ2+ γδT cells (9). Zoledronic acid (ZOL), a BP, has been widely used to numerically expand Vγ9Vδ2 T cells *in vivo* and *ex vivo*. ZOL can be used alone or in combination with IL-2 to achieve these effects (115). ZOL (5 uM) and IL-2 (1000IU/ml) administration over 14 days has been reported to initiate an over 4000-fold proliferation and expansion of γδT cells (mainly Vγ9Vδ2) from PBMCs of both healthy donors and patients with advanced non-small cell lung cancer (116). However, the expansion folds and purities of γδT cells vary in different published results.

Current protocols for expanding Vδ1+ T cells *in vitro* primarily rely on mitogenic plant lectins such as phytohemagglutinin (PHA) or concanavalin-A (ConA), which induce AICD in Vγ9Vδ2 T cells (93, 117). To transition from the laboratory to the clinic, more efforts have been made to avoid potentially hazardous components. Almeida et al. first developed a clinical-grade two-step method through combination of cytokines (IL-1β, IL-4, IL-21, and IFN-γ) and anti-CD3 mAb (clone: OKT-3) to achieve the expansion of Vδ1+ T cells (94). This method enables large-scale expansion (up to 2,000-fold) of Vδ1+ T cells known as DOT cells (94). GDX012, based on DOT cells, has been granted orphan drug designation by FDA for AML treatment and is currently undergoing evaluation in a phase I trial (NCT05001451). Recently, Ferry et al. also apply only anti-CD3 mAb and IL-15 to stimulate αβTCR- and CD56-depleted PBMC, resulting in robust Vδ1 cell expansion (97).

TABLE 1 Comparison of different methods for γδ-T cell expansion.

Source	Expansion strategy	Expand subsets	ref
Tumor specimens	Anti-MICA antibodies	Vδ1	(54)
Healthy donor PBMCs and patient derived	PHA and IL-7	Vδ1	(93)
Healthy donor PBMCs	DOT	Vδ1	(94)
Healthy donor PBMCs	4–1BB	Vδ1	(95)
Healthy donor PBMCs	Mitogen Con A	Vδ1	(96)
Healthy donor PBMCs	anti-CD3 mAb (clone: OKT-3) and IL-15	Vδ1	(97)
Patient-derived	ZOL and BrHPP	Vγ9Vδ2	(98)
Healthy donor and lung cancer patient PBMCs	PTA	Vγ2Vδ2	(99, 100)
PBMCs	IPP and IL-2	Vγ9Vδ2	(101)
Healthy donor PBMCs	Aminobisphosphonates	Vγ9Vδ2	(102)
Healthy donor PBMCs	IL-2 and IL-15	Vγ9Vδ2	(84)
Healthy donor PBMCs	IL-2 or IL-15 combined with TGF-β	Vγ9Vδ2	(103)
Healthy donor PBMCs	Costimulation of ZA and IL-2 in addition to aAPC	Vγ9Vδ2	(104, 105)
Healthy donor PBMCs	Vitamin C with IL-2, ZOL, and HMBPP	Vγ9Vδ2	(106)
Healthy donor PBMCs	CD40L/pp65 and pp65 aAPCs	Polyclonal with predominant Vδ1 phenotype	(107)
Healthy donor PBMCs	K562 feeder cells	Polyclonal γδ	(108, 109)
Healthy donor PBMCs	OKT3	Polyclonal γδ	(110)
Healthy donor PBMCs	anti-TCRγδ antibody	Both	(111, 112)
PBMCs	ZOL	Not specified	(113)
Healthy donor PBMCs	ZOL, IL-2, and IL-18	Not specified	(114)

aAPCs, artificial antigen-presenting cells; BrHPP, bromohydrin pyrophosphate; Con A, concanavalin A; DOT, Delta One T; HMBPP, (E)-4-hydroxy-3-methyl-but-2-enyl pyrophosphate; MICA, MHC class I chain-related protein A; NB, neuroblastoma; OKT3, anti-CD3 antibody; PHA, phytohemagglutinin; PTA, tetrakis-pivaloyloxymethyl 2-(thiazole-2-ylamino) ethylidene-1,1-bisphosphonate; ZOL, zoledronate.

The feeder cell-based method utilizing artificial antigen-presenting cells (aAPCs) has been explored to provide γδT cells with a sustained activation and costimulation signal. K562, a human chronic erythroleukemic cell line lacking MHC expression, is primarily used as aAPCs. These cells are engineered with costimulatory molecules (like CD80, CD86, CD137) and antigens (e.g., CMV antigen-pp65), allowing for the targeted expansion of specific γδT cell subsets (108, 118). Deniger et al. first activated and propagated polyclonal γδT cells utilizing K562-based aAPCs as irradiated feeders (108, 118). This method requires the additional labor-intensive manufacturing process of culturing feeder cells, yet it mitigates the AICD effects in γδT cells associated with prolonged antigen exposure. Additionally, methods of removing all residual feeder cells before infusion remains a hurdle to clinical implementation of this approach. To address this, several solutions have been proposed, such as gamma-irradiation of aAPCs and the transduction of aAPCs with an inducible suicide gene (107). The *ex vivo* aAPC expanded donor-derived γδT cells are under evaluation of safety and cell dose in a phase I/II trial (NCT05015426) in patients with high-risk acute leukemia (104).

In the future, efforts should focus more on eliminating the use of xenogeneic serum and feeder cells and integrating GMP/pharmaceutical-grade reagents into the expansion process. An example of such a method is the protocol proposed by Bold et al. in a recently published article, which has shown better outcomes in terms of expansion and purity (119). Further efforts can be directed towards enhancing the rate of γδT cell expansion, optimizing the procedure, and lowering manufacturing costs. Besides assessing quantity, evaluating the quality of expanded γδT cells–such as memory and exhaustion phenotypes, is crucial for maximizing therapeutic efficacy and requires further investigations.

4 Engineering strategies: the advances and advantages of γδT cell-based immunotherapy

To date, the pharmaceutical industry has explored three primary categories of strategies for γδT cell engineering, which encompass: (1) CAR-T therapy; (2) antibody-based approaches, such as cell engagers or bispecific antibodies; and (3) engineering or transfer of TCRs. CAR-T therapy remains the predominant approach, while antibody-based strategies are gaining prominence due to several advantages. Research is ongoing to investigate combination of therapies aimed at maximizing the unique capabilities of γδT cells. Lists of engineering strategies and ongoing clinical trials are presented in Tables 2, 3, respectively.

4.1 γδ CAR-T cell therapy: extend from but exceed the conventional αβ CAR-T therapy

CAR-T therapy, with its potential for HLA-independent tumor antigen recognition, has found its place as a key player in cancer immunotherapy. Traditionally, αβT cells have been the main candidates for CAR development (150). However, despite their effectiveness, these cells present several limitations. They are susceptible to GvHD, can cause severe and potentially lethal toxicities, contribute to the development of cytokine release syndrome (CRS), and pose issues related to antigen escape (150).

TABLE 2 Different strategies for engineering γδT cells.

Product	γδT Source	Subsets	Disease	Transduction methods	Ref
CAR-T					
ADI-002 (Allogeneic GPC3-CAR-γδT Cell)	Healthy donor PBMCs	Vδ1	Solid tumors	γ-retrovirus	Adicet Bio, Inc (120)
ADI-925 (Enhanced intracellular DAP10 chimeric adaptor protein)	Donor PBMCs	Vδ1	Hematologic and solid tumor	–	Adicet Bio, Inc (121)
ADI-270 (CD27-derived CAR-γδT)	Healthy donor PBMCs	Vδ1	CD70+ cancers	–	Adicet Bio, Inc
NKG2DL-targeting CAR Vγ9Vδ2T	Autologous/ Allogeneic PBMC	Vγ9Vδ2	Solid tumors	mRNA electroporation	(122)
ns19CAR γδT	Healthy donor PBMCs	Vγ9Vδ2	B cell leukemias	Lentivirus	IN8bio (123)
TMZ and MGMT-modified γδT cells	Healthy donor PBMCs	Vγ9Vδ2	Glioblastoma	Lentivirus	(124)
γδCAR-T cells	Healthy donor PBMCs	Not specified	Leukemia	Retrovirus	(125)
BCMA—Specific CAR	Healthy donor PBMCs	Vγ9Vδ2	MM	mRNA electroporation	(126)
ACTallo®	Healthy donor PBMCs	Vγ9Vδ2	N/A	CRISPR gene editing	Immatics
MUC1-Tn-targeting CAR-Vγ9Vδ2T cells	Healthy donor PBMCs	Vγ9Vδ2	Solid tumors	Lentivirus	(127)
Vδ1 T cells engineered with a GPC-3 CAR and sIL-15	Healthy donor PBMCs	Vδ1	HCC	Retrovirus	(128)
CD5-NSCAR- and CD19-NSCAR-γδT cells	Healthy donor PBMCs	Vγ9Vδ2	T-ALL and B-ALL	Lentivirus	(129)
iPSC-derived γδ CAR-T (γδ CAR-iT)	Allogeneic γδT cell-derived iPSCs	Vγ9Vδ2	Hematological and solid tumors	CRISPR gene editing	Century Therapeutics (90)
CNTY-102 (iPSC-derived γδ anti-CD19 and CD22 CAR-T)		Not specified	relapsed, refractory B-cell lymphoma and other B-cell malignancies	CRISPR gene editing	Century Therapeutics
CNTY-107 (iPSC-derived γδ anti-Nectin-4 CAR-T)		Not specified	Solid tumor	CRISPR gene editing	
Anti-GD2 Co-stimulation-Only CAR	Healthy donor PBMCs	Vγ9Vδ2	Neuroblastoma	Retrovirus	(130)
CD123-specific CAR	Healthy donor PBMCs	Vγ9Vδ2	AML	mRNA electroporation	(131)
CD5 -non-signaling CAR (NSCAR), CD19-NSCAR	Healthy donor PBMCs	Vγ9Vδ2	T-ALL and B-ALL	Lentivirus	(129)
T cell engager and bispecific Abs					
CD40-bispecific γδT cell engager	N/A	Vγ9Vδ2	B-cell malignancies	N/A	(132)
CD1d-specific Vγ9Vδ2-T cell engager	N/A	Vγ9Vδ2	CLL	N/A	(133)
Bispecific Antibody Targeting Both the Vγ2 TCR and PD-L1	N/A	Vγ9Vδ2	Solid tumors	N/A	(134), Wuhan YZY Biopharma Co., Ltd
GADLEN (bispecific γδ T cell engagers containing heterodimeric BTN2A1/3A1 extracellular domains)	N/A	Vγ9Vδ2	B-cell lymphoma	N/A	Shattuck
Her2/Vγ9 antibody	N/A	Vγ9Vδ2	Pancreatic cancer	N/A	(135)

(Continued)

TABLE 2 Continued

Product	γδT Source	Subsets	Disease	Transduction methods	Ref
T cell engager and bispecific Abs					
Anti-TRGV9/anti-CD123 bispecific antibody	N/A	Vγ9Vδ2	AML	N/A	(136)
EGFR-Vδ2 bispecific T cell engager	N/A	Vγ9Vδ2	EGFR-Expressing Tumors	N/A	(137)
TCRs engineering or transfer					
γδT cells transduced with the αβTCR and CD8 αβ genes	Healthy donor PBMCs	Vγ9Vδ2	MAGE-A4-expressing tumor	Retrovirus	(138)
αβTCRs engineered γδT cells	Healthy donor PBMCs	Not specified	Leukemia	Retrovirus	(139, 140)
TCR transfer combined with genome editing	Healthy donor PBMCs	Vγ9Vδ2	B cell leukemias	CRISPR/Cas9 Lentivirus	(141)
KK-LC-1-specific TCR-transduced γδT cells	Healthy donor PBMCs	Not specified	Lung cancer	Retrovirus	(142)
NKT cell TCR-transfected γδT cells	Healthy donor PBMCs	Vγ9Vδ2	Not specified	Electroporation	(143)

AML, acute myeloid leukemia; CLL, chronic lymphocytic leukemia; EGFR, epidermal growth factor receptor; HCC, hepatocellular carcinoma; MAGE-A4, melanoma antigen-A4; MM, multiple myeloma; T-All and B-All, T and B cell acute lymphoblastic leukemia. N/A, not applicable.

These challenges have spurred an interest in alternative solutions, with γδT cells showing potential to offset these limitations.

Given the wealth of limitations associated with αβT cells, γδT cells are garnering interest as an alternative for CAR-T therapy. These cells do not instigate GvHD, curb antigen escape resulting in decreased relapse rates, and retain beneficial traits such as a less differentiated phenotype with enhanced antigen presentation capacity (125, 151). With these advantages, γδ CAR-T cells may have the potential to overcome the obstacles that have historically troubled conventional αβ CAR-T therapy.

The primary goal of CAR design is producing extracellular domains capable of targeting unique tumor cell antigens while sparing healthy tissues (150, 152). Owing to the deficit of tumor-specific antigens, lineage-specific antigens have been a key focus in CAR T cell development. Under investigation are promising candidates like CD19 (153, 154), GD2 (130, 155), GPC-3 (128), CD123 (131, 156), CD5, CEA, CD20 (10), B7H3 B7H3 (157), and PSCA (151) (Table 2). While CD19-targeting CAR-T products have earned FDA approval for treating B-cell lymphoma and leukemia, they carry risks, like CRS, neurotoxicity, and B-cell aplasia, primarily due to on-target off-tumor toxicities (152, 153). Interestingly, γδ anti-CD19 CAR-T cells have been reported to produce fewer inflammatory cytokines compared to their αβ counterparts, suggesting a potential decrease in cytokine-mediated side effects (90).

However, the optimization of CAR for highly specific antigen recognition remains vital. Recent studies have investigated the incorporation of ligands like NKG2DL and inhibitory receptor programmed cell death ligand 1 (PD-L1) into CAR constructs to improve safety or efficacy (158). Some attempts have even added T cell antigen coupling (TAC) components to γδT cells, thereby redirecting them to target tumors with reduced off-tumor toxicity compared to conventional CAR-T cells (159, 160) (Figure 3D). Adicet Bio is working on CAR designs that target tumor intracellular antigens using their TCR-Like monoclonal antibodies (TCRLs) technology (91).

Clinical trials are in progress for CAR-γδT cells targeting various antigens such as CD19 (NCT02656147, NCT05554939), CD20, NKG2DL, CD7, CD33, CD28, and CD123 (Table 3). While many of these trials have yet to disclose their results, some promising preliminary findings have been reported. For instance, Adicet Bio, Inc. is testing an allogeneic CD20 CAR+ Vδ1 γδT cell

TABLE 3 Summary of ongoing clinical trials of engineered γδT products.

Product	Source & subset	Disease	Clinical Trial ref	Phase	Outcome	Company
CAR-T therapy						
ADI-001 (Anti-CD20 Allogeneic Gamma Delta CAR-T)	Leukapheresis from healthy donor (Vδ1)	B cell malignancies	NCT04735471	I	No GvHD; 3/6 patients had AESIs	Adicet Bio, Inc (10, 144)
ADI-001	Allogeneic	Lymphoma	NCT04911478	N/A	N/A	Adicet Bio, Inc

(Continued)

TABLE 3 Continued

Product	Source & subset	Disease	Clinical Trial ref	Phase	Outcome	Company
CAR-T therapy						
CD19-CAR-γδT cells	Allogeneic	B Cell Malignancies	NCT02656147	I	N/A	Beijing Doing Biomedical Co., Ltd.
CD19-CAR-γδT cells	Allogeneic	NHL	NCT05554939	I/II	N/A	Chinese PLA General Hospital
Allogeneic NKG2DL-targeting CAR γδT Cells (CTM-N2D)	PBMC from healthy donor	Advanced Solid Tumors or Hematological Malignancies	NCT05302037	I	N/A	CytoMed Therapeutics Pte Ltd
NKG2DL-targeting CAR-grafted γδT Cells	Haploidentical/ Allogeneic	Solid Tumor	NCT04107142	I	N/A	
Universal Dual-target NKG2D-NKp44 CAR-T Cells	N/A	Advanced Solid Tumors	NCT05976906	I	N/A	Zhejiang University
CD7-CAR – γδT Cells	Unknown	$CD7^+$ T cell-derived malignant tumors	NCT04702841	Early Phase 1	N/A	PersonGen BioTherapeutics (Suzhou) Co., Ltd.
Generation of CD33-CD28 γδT Cells	Vδ2 from peripheral blood and bone marrow	AML	NCT03885076	N/A	N/A	TC Biopharm
Universal CAR-γδT Cell Injection targeting CD123	Allogeneic	AML	NCT05388305	N/A	N/A	Hebei Senlang Biotechnology Inc., Ltd.
Universal CAR-γδT cell	Allogeneic	AML	NCT04796441	N/A	N/A	Hebei Senlang Biotechnology Inc., Ltd.
Cell engager and bispecific antibodies						
LAVA-051 (Vγ9Vδ2-T cell engaging bispecific antibody)	N/A	CLL, MM, AML	NCT04887259	I/IIa	Dose level of 45μg without CRS or DLTs	LAVA Therapeutics (145)
LAVA-1207 (bispecific Vγ9Vδ2-T cell engager)	N/A	Prostate Cancer	NCT05369000	I/IIa	Dose level of 40μg without DLTs; 3/8 patients SD at 8 weeks	LAVA Therapeutics (146)
ET019003 (anti-CD19 Fab - TCR-γδT cells)	N/A	CD19+ Leukemia and Lymphoma	NCT04014894	I	50% (6/12) complete response and 33% (4/12) partial response	Wuhan Union Hospital, China (147)
ACE1831 (allogeneic αCD20-conjugated Vδ2 T cells)	PBMC from healthy donor	Relapsed/ Refractory CD20-expressing B-cell Malignancies	NCT05653271	I	N/A	Acepodia Biotech, Inc. (148)
ICT01 (anti-BTN3A antibody)	N/A	Advanced solid or hematologic tumors	NCT04243499	N/A	Dose level of 700μg without CRS or DLTs in 6/6 patients	ImCheck Therapeutics
TCRs engineering or transfer						
GDT002 (Vγ9Vδ2TCR-bearing αβT cells)	PBMC from healthy donor	Multiple myeloma	NCT04688853	I/II	N/A	GADETA
Combination therapy						
INB-200 (MGMT modified γδT +TMZ	Autologous	Glioblastoma	NCT04165941	I	No CRS, DLTs, or ICANS in 15/15 patients	In8bio Inc. (149)
INB-400 (MGMT modified γδT +TMZ)	Autologous/ allogeneic	Glioblastoma	NCT05664243	Ib/II	N/A	In8bio Inc.

AESIs, adverse events of special interest; AML, acute myeloid leukemia; CLL, chronic lymphocytic leukemia; CRS, cytokine release syndrome; DLBCL, diffuse large B cell lymphoma; DLTs, dose limiting toxicities; ICANS, immune effector cell-associated neurotoxicity syndrome; MM, multiple myeloma; NHL, non-Hodgkin lymphomas. N/A: not applicable.

called ADI-001, designed for patients with refractory B cell malignancies (NCT04735471). Their early report shows a 71% overall response rate and 63% complete response rate among patients with aggressive B-Cell non-Hodgkin lymphoma, all without the presentation of GvHD (91).

One challenge with CAR-T therapy is its potential ineffectiveness in tumors exhibiting heterogeneity or low antigen expression. Dual-specific CARs, which target two antigens concurrently, are proposed as a potential solution, although this requires further investigation (161). Other research focuses on fine-tuning other CAR components, including the intracellular signaling and transmembrane domain, with construction of Boolean logic gates for combinatorial antigen sensing. Balancing the DNA length of dual-CAR plasmids and transduction efficiency necessitates further study.

Recent innovative extracellular designs aimed at enhancing safety also include the development of ON/OFF switches like the masked CAR. Here, the antigen-binding site of CAR is coupled with a masking peptide through a protease-sensitive linker. Activation of masked CAR-T cells occurs when tumor microenvironment proteases cleave this linker, causing the masking peptide to detach, and revealing the antigen-binding site (162) (Figure 3C). In essence, this provides a level of control, reducing risks associated with unregulated CAR-T activation (162).

To sum up, while there are promising advancements in the development of γδT cell-based CAR-T therapies, it is critical to continue fine-tuning these interventions for increasing specificity and safety. A combination of innovative design strategies and rigorous clinical trials may bring forth the next generation of cancer immunotherapies. The hope is for these novel treatments to cure more patients, more reliably, with fewer side effects, revolutionizing the approach to cancer treatment.

4.1.1 Co-stimulatory domain design and combinatorial strategies: emphasize the unique characteristics of γδT cells

Over the years, CARs have progressed through several generations, differentiated by the quantity and nature of their co-stimulatory domains, like CD28 and 4-1BB, which play a pivotal role in γδT cell activation and cytotoxic function (163) (Figure 3A). Initial designs of CAR γδT cells were largely based on pre-existing CAR-αβT designs, failing to capitalize on the unique benefits of γδT cells due to a dearth of knowledge on the fundamental CAR signaling mechanisms in γδT cells. CAR-αβT cells recognize tumor cells through the CAR pathway while completely bypassing the αβTCR. Meanwhile, in CAR-γδT cells, the inherent γδTCR signal can synergize with logic-gated CARs, providing MHC-independent cytotoxicity and downstream CD3ζ signals. Besides, CAR-γδT cells retain multiple activating NK receptors alongside CAR and TCRγδ, potentially enhancing recognition and activation. In the tumor immunoescape setting, CAR-γδT cells have been proved the ability to recognize antigen-negative tumor cells in CAR-independent manner (125). CARs designed for γδT cells can also incorporate γδT cell-specific signaling domains, such as NKG2D-DAP10, as an intracellular costimulatory domain for activation. Despite this development, contemporary research on CAR γδT cells predominantly employs second or third-generation designs. It has been observed, though, that single antigen recognition in these CARs leads to poor discrimination between tumor and healthy cells, contributing to on-target off-tumor toxicity. Furthermore, CAR-T cells exhibit strong limitations in treating T cell malignancies due to difficulties like lethal T cell aplasia and CAR-T cell fratricide stemming from shared target antigens (129). Even extending CAR T cell therapies to T cell acute lymphoblastic leukemia (T-ALL) has proven challenging, despite shared molecular commonalities with B cell acute lymphoblastic leukemia (B-ALL).

Moreover, CARs providing both CD3ζ stimulus and CD28 co-stimulation are prone to tonic signaling, leading to functional exhaustion and impaired CAR-T cell function. A unique construct called ADI-925 has been developed by Adicet Bio to help tackle this. It incorporates an enhanced intracellular DAP10 chimeric adaptor (CAd), 4–1BB, and a modified CD3ζ co-stimulation, designed to enhance tumor targeting through endogenous NKG2D receptors (121, 164) (Figure 3B).

Novel strategies are also emerging, employing Boolean logic gates (like AND, OR, AND NOT) enabling CAR-T cells to detect multiple antigens, reducing off-tumor toxicity and minimizing potential antigen escape (Figures 3E, F). Dual-targeting CAR γδT cells, like those targeting GD2 and PTK7 in preclinical studies for neuroblastoma, were developed to help avoid antigen escape through an OR-gate strategy) (165). Though promising, tandem bispecific OR-gate CAR-T cells may induce excessive CD3ζ signaling during co-stimulation, necessitating alternative strategies (165).

Bi-specific CARs with split co-stimulatory signals and a shared CD3ζ domain have emerged as another strategy, allowing for optimal CAR-T cell activation only when both antigens are simultaneously present (161, 166). Furthermore, ideas like chimeric costimulatory receptors (CCRs), also known as recognition-based logic-gated CAR, and non-signaling CARs (NSCARs) have been proposed to mitigate on-target off-tumor toxicity (123, 129). CCRs, traditional CARs without CD3ζ signaling domain, provide co-stimulation whilst avoiding tonic CD3ζ signaling of γδT cells. Thus, these reduce on-target off-tumor toxicity by separating co-stimulatory input from the primary TCR signal (129). Moreover, CCRs have the potential to target malignant cells while sparing healthy tissues in scenarios where the target antigen is broadly expressed (123, 129). Fisher et al. developed a co-stimulation-only CAR, wherein the CAR is fit only to provide co-stimulation, thereby restricting tonic signaling but still facilitating rapid downstream response upon activation (164). Concurrently, CAR-γδT cytotoxicity can be selectively triggered by both the CAR signal and the inherent γδTCR signal when encountering cancer cells (130). CCR can also function as a switch chimeric receptor combined with a second-generation CAR (Figure 3B). The switch receptor typically includes an inhibitory receptor (e.g. PD-1 or TIGIT) and an intracellular costimulatory signal (167). For instance, the PD-1-CD28 construct as anti-PD-L1 CCR can potentially convert the inhibitory signal into an activating one (167). Such a design can accelerate activation of CAR-T cells and improve their survival in the immunosuppressive tumor microenvironment (167, 168). On

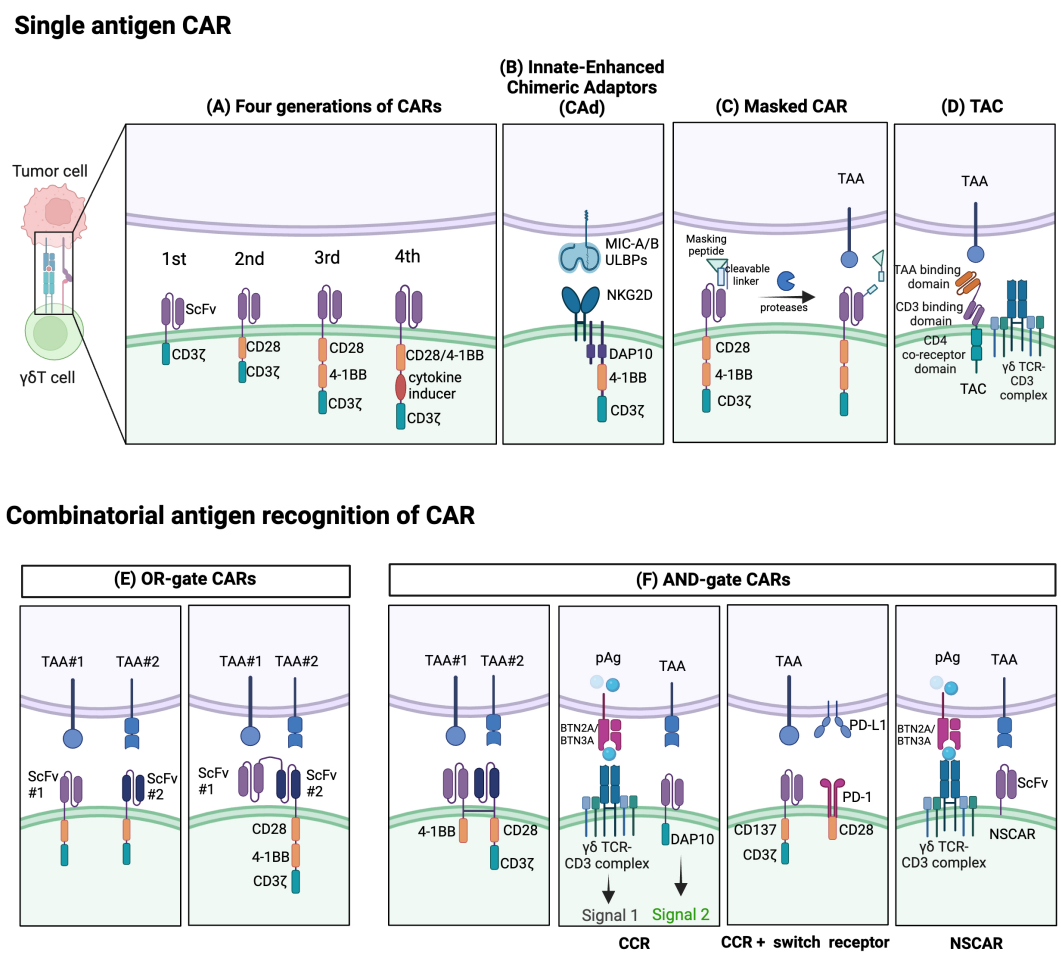

FIGURE 3
Established strategies for CAR- γδT cells. Single-antigen CAR recognition: **(A)** Conventional CARs are classified as first-, second-, third-, or fourth generation depending on their number of costimulatory domains. **(B)** Innate enhanced DAP10 chimeric adaptor (CAd), combined with 4–1BB and modified CD3ζ co-stimulation, enhances tumor targeting through endogenous NKG2D receptors. **(C)** The masked CAR (mCAR) incorporates a masking peptide. When proteases are present in the tumor microenvironment (TME), the linker is cleaved, releasing the masking peptide, and activating the CAR. This mechanism helps reduce on-target off-tumor toxicity. **(D)** A T cell antigen coupler (TAC) is also designed to reduce toxicity and promote more efficient anti-tumor response. It is comprised of a tumor-associated antigen (TAA) binding domain, CD3 binding domain, and CD4 co-receptor domain. Combinatorial antigen CAR recognition: **(E)** OR-gate CARs enable dual-targeting of antigens with separate single-chain variable fragment (scFv) domains. To prevent antigen escape, they can be designed to have two consecutive scFv domains connected to the standard CAR chassis. **(F)** AND-gate CARs are only activated when both antigens are present simultaneously, employing two separate receptors comprising the CD3ζ and costimulatory domains. A chimeric costimulatory receptors (CCR)-based AND-gate has its CD3ζ signaling domain from a γδTCR and can target multiple antigens which can enhance cytotoxicity and prevent tonic CD3ζ signaling. CCR can also be paired with a switch receptor which can be an inhibitor receptor such as programmed death-1 (PD-1) along with a costimulatory domain like CD28. Non-signaling CARs (NSCARs) do not possess signaling domains and utilize an antigen-specific tumor targeting mechanism. Created with BioRender.com.

the other hand, NSCARs capitalize on γδT cells' MHC-independent cytotoxic capacity while eliminating all CAR signaling domains (129). This results in antigen-specific tumor cell-targeting capability without influencing T cell activation, as demonstrated by Fleischer et al. with CD5-NSCAR- and CD19-NSCAR-engineered γδT cells, designed specifically for T-ALL and B-ALL relief (129).

Despite the promise of these technologies, factors like NSCAR shedding on γδT cells and antigen downregulation in target cells have somewhat limited their translational application in clinical therapies. Additionally, the necessity of intracellular signaling domains in CAR design is being reconsidered when applied to γδT cells. Deletion of these domains can potentially allow for the transduction of multiple NSCARs, due to a decrease in overall CAR size.

In conclusion, recent years have seen significant expansion in the approaches to T cell engineering, including innovations such as synNotch receptors, iCAR, and several others (158, 169). However, the design and development of CARs for γδT cells haven't kept pace. A deeper understanding of γδT cell cytotoxicity mechanisms and further research into these novel CAR structures will be critical in achieving maximum safety and efficacy, thereby unlocking the full potential of CAR γδT cell therapies.

4.1.2 CAR transduction methods

The primary methodologies for CAR-T therapy involve permanent DNA-based transfection methods that include viral transduction (using lentiviruses or retroviruses) and non-viral

transfection, typically utilizing transposon systems like Sleeping Beauty and Piggy Bac (170) (Table 2). While lentiviruses and retroviruses are commonly used, concerns about their safety, predominantly due to their immunogenic properties, and their complex and costly manufacturing processes may limit their utility. Despite these concerns, retrovirally-modified CAR-T cells have proven tolerable safety profiles in extensive clinical trials (171). However, the transduction of γδT cells has been challenged due to their relatively limited proliferation and susceptibility to AICD compared to that of αβT cells (172). Gammaretroviruses necessitate active cell proliferation for the penetration of viral nucleic acids into the nucleus. This poses a challenge for the transduction of γδT cells compared to αβT cells, demanding necessary specific proliferative stimuli for effective γδT cell transduction (172).

Simultaneously, advancements are being made in non-viral technologies to address some drawbacks associated with viral transductions, such as potential oncogenesis, immunogenicity, and high cost (170). Non-viral transposon vectors possess simpler manufacturing processes, cost efficiency, enhanced safety, stable integration of large sequence (>10 kb), but often face efficiency challenges (173). These non-viral integrative vectors rely on temporary cell pore formation or endocytosis, accomplished via various chemical or physical techniques, including electroporation and liposomes (174).

More recently, non-permanent gene transfer methods that utilize non-integrating gene delivery like mRNA-based CAR expression have started to gain traction (154). The utilization of mRNA in CAR-T cells allows for a "biodegradable" approach, in which the cell's potency is short-term. The use of mRNA electroporation was first applied in early stages of αβ CAR-T development, but initial clinical trials indicated a lack of efficacy, potentially due to the poor quality and quantity of patient-derived autologous αβT cells (NCT02623582). This led researchers to explore the use of allogeneic Vγ9Vδ2 T cells from healthy donors. Investigations revealed that after mRNA electroporation, CAR expression persisted for up to 120 hours, with peak expression at the 24-hour mark (175). Enhanced anti-AML activity of mRNA-based anti-CD123 γδ CAR-T was observed both *in vivo* and *in vitro* (131). Despite these promising results, the transient nature of receptor expression means that further applications may need to employ strategies such as repeated or intratumoral injections to ensure therapeutic efficacy. Future advancements in CAR γδT cell therapy may favor non-viral integrating and lipid nanoparticles technological platforms (170).

In the domain of hematological malignancies, CAR γδT cell therapy holds formidable promise. However, the development of universal CAR γδT cells capable of effectively treating solid tumors remains a pressing need, necessitating ongoing research to overcome the physical and immunological challenges associated with solid tumor immunity. Given the unique stimulatory signals and recognition mechanisms of γδT cells, it is evident that the design of CARs for these cells needs to undergo revisions and refinements as our understanding of their biological mechanisms deepens. In essence, while there has been substantial progress in the field of CAR γδT cell therapy, future work that ensures the safety, efficacy, and broad applicability of this promising therapy modality, especially in the context of solid tumors, remains a critical need in the field.

4.2 Cell engagers or bispecific antibodies: easier ways to enhance γδT cells recognition

Cell engagers and bispecific antibodies have become an increasingly attractive immunotherapeutic method for enhancing the anti-cancer activity of γδT cells. Bispecific T cell engagers (bsTCEs) are specially designed antibodies, each having two separate binding areas aimed at individual components like tumor-associated antigens (TAAs) and the TCR complex (Vδ2 or Vγ9) (176). The flexibility of bsTCEs allows for varied applications, such as MHC-independent targeting of TAAs by γδT cells, immune checkpoint modulation, and controlling inflammatory and other signaling pathways (176). These functionalities provide several unique advantages, including their small molecular size and high versatility, eliminating the need for additional co-stimulatory signals for T cell activation, low picomolar range for the half-maximal effective concentration (EC50), effectiveness against both blood-borne and solid tumors, excellent safety profile, and efficient and cost-effective production (177). Most frequently, cell engagers incorporate a fragment-based design or IgG/IgG-like formats (136, 137). Fragment-based designs principally modify constructs such as scFv (178), Fab (135), or single-domain antibodies (sdAbs, also known as V_{HH}) (176) into their binding regions (Figures 4A-C). sdAbs, originating from the variable domain of heavy-chain-only antibodies, have attracted attention because of their unique features, including small size, target specificity, and minor immunogenicity (179). Currently, cell engagers can be applied both as stand-alone therapies and in partnership with allogeneic γδT cells to generate readily available products.

The first CD3-targeting bsTCEs, exemplified by blinatumomab and Tebentafusp, yielded significant positive outcomes in B-cell malignancy and melanoma patients during clinical trials (NCT03070392) (180). However, adverse effects like CRS and immune effector cell-associated neurotoxicity syndrome (ICANS) constrained their clinical usage (177). Further, CD3-targeting bsTCEs may unintentionally activate other CD3+ T cell subsets, which could depress tumor-specific immune responses (137). As a category of innate T cells, γδT cells present a logical choice for engagement to reduce CRS and off-tumor toxicity.

The successful usage of bsTCEs in LAVA Therapeutics' Gammabody platform, employing tandem single-domain antibodies (V_{HH}s) (Figure 4D), exemplifies their potential. These include EGFR-Vδ2, CD1d-Vδ2, CD40-Vδ2, and PSMA-Vδ2 bsTCEs (Table 3). EGFR-Vδ2 bsTCEs have displayed compelling activation of Vγ9Vδ2 T cells which induce cytotoxicity against EGFR+ tumor cells (137, 154). The CD1d-Vδ2 bsTCE, or LAVA-051, has shown anti-tumor potential against hematological malignancies expressing CD1d in preclinical models (176). Its specificity for NKT and Vγ9Vδ2-T cells, alongside low-nanomolar range EC50 values *in vitro*, further demonstrates its potential (176).

Bispecific antibodies (bsAbs) comprise a class of engineered antibodies with two distinct binding sites, setting them apart from

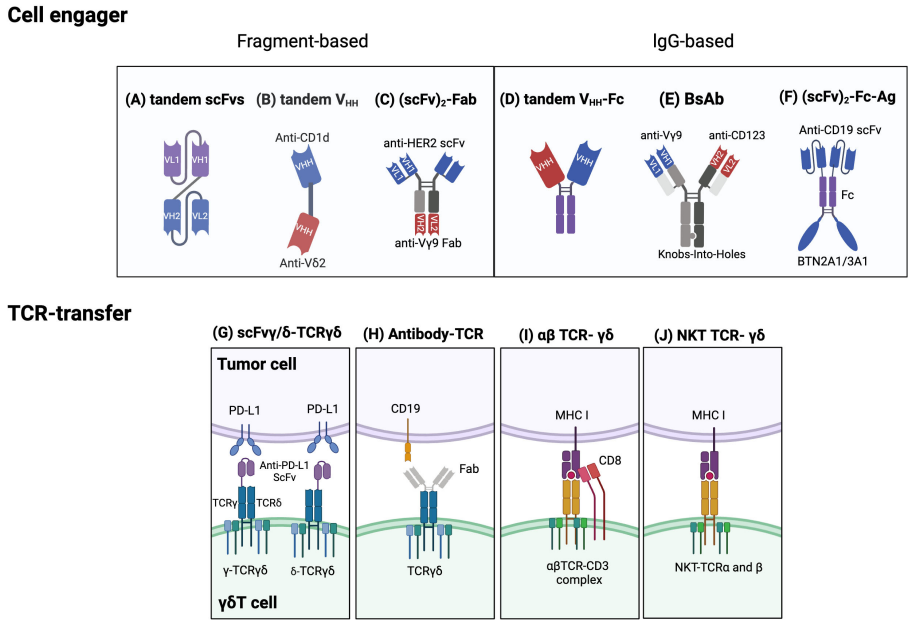

FIGURE 4
Established strategies for engineering γδT cells. Cell engager designs: Fragment based cell engagers include tandem single-chain variable fragment (scFv), tandem variable heavy chain (VHH), and (scFv)2-Fab. **(A)** A tandem scFv antibody comprises two different scFvs joined by a linker. **(B)** Tandem VHH is depicted as a bispecific T cell engager (bsTCE) with an anti-CD1d VHH linked to an anti-Vδ2 VHH. **(C)** An example of (scFv)2-Fab antibody, Her2/Vγ9, is composed of an anti-Vγ9 Fab domain and two anti-Her2 scFvs. This design selectively recruits γδ T cells and enhances cytotoxicity. IgG based cell engagers encompass tandem VHH-Fc, bispecific antibodies (BsAb), and (scFv)2-Fc-Ag. **(D)** Tandem VHH-Fc antibodies involve two VHHs linked to a Fc domain. **(E)** One type of BsAb connects an anti-Vγ9 domain and an anti-CD123 domain via Knobs-into-holes heterodimerization technology. **(F)** (scFv)2-Fc-Ag is shown as an anti-CD19 scFv connected to a BTN2A1/3A1 domain via an Fc linker. Engineering γδTCRs and transferring specific αβT-TCR or NKT-TCRs into γδT cells: **(G)** One approach to engineering γδTCRs is to fuse an anti- programmed cell death ligand 1 (PD-L1) scFv to either the γ or δ chain of γδTCR to limit T cell exhaustion. **(H)** Another approach is an antibody-TCR, such as an anti-CD19 Fab domain linked to a γδTCR. **(I)** αβTCRs and CD8 αβ genes can be transferred to γδT cells to enable targeting specific tumor cells and avoid TCR mispairing. **(J)** Natural killer T (NKT) cell-derived αβTCRs can also be transferred into γδT cells to enhance proliferation, IFN-γ production, and antitumor effects. Created with BioRender.com.

traditional antibodies (181) (Figures 4D-F). These antibodies, as exemplified by anti-Vγ9/CD123 bsAbs, selectively rally Vγ9+ γδT cells, promoting cell conjugate formation between γδT cells and AML cells (136). As such, these cell engagers can enhance Vγ9Vδ2+ T cell cytotoxicity against B-cell lymphoma, particularly when accompanied by a co-stimulatory signal pair (178). ImCheck Therapeutics' humanized anti-BTN3A antibody, ICT01, serves as another example. It operates by recognizing three distinct BTN3A forms and prompting their activated conformation, thereby selectively activating Vγ9Vδ2 T cells in an antigen-independent manner (182).

In a phase I/II clinical trial, ICT01 showed tolerable safety profile and increased infiltration of Vγ9Vδ2 T cells into tumor tissue in patients with advanced solid tumors (NCT04243499). (Table 3) Besides, LAVA-1207 (PSMA-Vδ2 bsTCEs) has shown a favorable safety profile and clinical symptom improvement (decreased PSA level) in a Phase 1/2a clinical trial involving metastatic castration-resistant prostate cancer (mCRPC) patients (N=20, NCT05369000) (137).

Notably, as cell engagers depend on the activation and migration of the patient's inherent γδT cell pool, initial Vγ9δ2T cell counts could be a useful predictor for clinical outcomes. Take, for instance, a melanoma patient with a high baseline count of circulating Vγ9Vδ2 T cells who showed considerable tumor infiltration of Vγ9+ T cells post ICT01 administration (182). Cell engagers can also be combined with γδT cell-based therapies to develop easily available TAA-targeting γδT cell products (148).

Acepodia's technology, for instance, conjugates antibodies to cells to create products like ACE1831, which is the CD20-targeting γδT cells (148). This product is currently under phase I trial for patients with relapsed/refractory B-cell lymphomas (NCT05653271). Other products, ACE2016 (EGFR-targeting γδT) and ACE1708 (PD-L1-targeting γδT), are in the preclinical exploratory stage (183).

In conclusion, while cell engagers and bispecific antibodies present significant potential compared to CAR-T therapy, their definitive superiority is yet to be determined. Like CAR-T therapy, cell engagers also encounter hurdles such as immune escape owing to loss of target antigen expression and an immunosuppressive tumor microenvironment. Further research is needed to modify cell engagers specifically for γδT cells, paving the way for effective treatments in the future.

4.3 TCRs engineering or transfer: a highly specific and reproducible manner

Harnessing natural receptors through the engineering or transfer of T cell receptors (TCRs) serves as an alternative approach to the use of synthetic ones. The transduction of

cancer-specific TCRs is an appealing strategy for generating large volumes of readily available, antigen-specific T cells. Transferring cancer-specific αβTCR engenders T cell specificity, simplifying procedures compared to isolating specific T cell subsets. However, the transgenic transfer of αβTCRs to other αβT cells runs the risk of triggering TCR competition and mispairing. Recognizing these limitations, γδT cells are appreciated as safe and ideal carriers for antigen-specific effector cells because TCR-α and -β chains can't pair with TCR-γ and -δ chains (138, 184). To produce cytotoxic γδT cells capable of attacking tumor cells and secreting cytokines via αβ and γδTCR-dependent activity, one can isolate tumor antigen-specific αβ CD8+ cytotoxic T lymphocytes and clone their TCR αβ genes (138) (Figure 4I). However, a notable reduction in γδTCR expression post αβTCR transduction was observed, likely due to competition for limited CD3 molecules (138).

Van der Veken et al. demonstrated that αβTCR -transduced γδT cells display sustained *in vivo* endurance and can elicit a recall response (139, 184). More so, infusing αβTCRs from invariant natural killer T (iNKT) cells into γδT cells can create bi-potential T cells with NKT cell functionality (143) (Figure 4J). Other research endeavors are concentrated on transferring γδTCR to αβT cells to leverage the superior understanding of their effects and memory function mechanisms (185). One product, GDT002, which contains Vγ9Vδ2TCR-expressing αβT cells, allows αβT cells to detect augmented phosphoantigens in stressed or malignant cells (185). An ongoing phase 1/2 study is investigating GDT002's safety and tolerability in patients with multiple myeloma. Furthermore, strategies for engineering TCRγδ involve fusing with single-chain variable fragments (scFv) or Fab fragments from antibodies. For example, one study used CRISPR/Cas9 to fuse an anti-PD-L1 scFv to the TCRγ or δ chain in activated γδT cells, creating scFv-γ/δ-TCRγδ cells that showcased anti-tumor capacity akin to traditional CAR-T cells (186) (Figure 4G). Alternatively, the Fab domain of an antibody can be connected to the C-terminal signaling domain of the γ and δ chains of the TCR, creating an antibody-TCR construct (187) (Figure 4H). The use of the TCR alongside endogenous costimulatory molecules can lower co-stimulation input compared to CAR constructs, thus diminishing cytokine release and mitigating the exhaustion phenotype (187). Anti-CD19 Fab – TCR-γδT cells or ET019003, for instance, have displayed similar anti-tumor actions against B-cell lymphoma as CAR-T cells *in vivo* (187).

Promisingly, a phase I clinical trial (NCT04014894) indicates that, aside from showing agreeable safety profiles, ET019003 has achieved an impressive clinical response rate (87.5%) among patients with relapsed or refractory diffuse large B-cell lymphoma (188). However, TCR gene transduction or engineering research has somewhat stagnated in recent years, possibly due to complex manufacturing processes involved. In summary, the exploration of novel therapeutic approaches incorporating γδT cells continues to expand, with significant potential for future cancer treatment innovations.

4.4 Combination therapy

CAR-T cell therapy has proven extremely promising for treating hematologic malignancies. However, distinct issues related to the immunosuppressive microenvironment of solid tumors require further refinement and personalization of this approach. A potential solution could be combination therapies that adequately address the complexity of solid malignancies.

The concurrent usage of CAR-T/bsTCE therapies and immune checkpoint inhibitors is recognized as a potentially effective strategy to overcome immune system suppression. Exhaustion status, marked by the upregulation of inhibitory receptors, can potentially compromise the therapeutic efficacy of CAR-T cells (189). In a murine model of bone metastatic prostate cancer, γδ CAR-T cells persisted in the tumor-bearing tibia for approximately 21 days post-infusion. However, these cells exhibited an upregulation of PD-1 expression while simultaneously losing expression of activation markers (151). Consequently, the combination of therapies such as ICT01 and pembrolizumab, an anti-PD1 antibody, exhibited favorable safety profiles in a phase I clinical trial (NCT04243499). This suggests that the co-administration of CAR-T/bsTCE therapy with anti-PD-1/PD-L1 antibodies could potentially boost treatment benefits (151).

Chemotherapy and radiotherapy, owing to their immune-sensitizing attributes, are plausible options for combination therapy with immunotherapy (190). Temozolomide (TMZ), a chemotherapy mainstay for glioblastoma (GBM), transiently heightens the expression of stress-associated antigens such as NKG2DL on tumor cells. Engineering γδT cells to express the methylguanine DNA methyltransferase (MGMT) can thus potentially confer TMZ resistance, enabling the engineered cells to operate efficiently despite the presence of therapeutic concentrations of chemotherapy. The amalgamation of TMZ and MGMT-modified autologous γδT cells, or drug resistant immunotherapy (DRI), showed improved survival outcomes in a model of high-grade gliomas compared to monotherapy (124).

In a phase I clinical trial, INB-200 (an example of DRI) displayed a favorable safety profile, extended progression-free survival (PFS), and presented no dose-limiting toxicities, CRS, or neurotoxicity in glioblastoma multiforme patients (NCT04165941). As a result, autologous DRI- γδT cells (INB-400) have proceeded to a phase II clinical trial, and MGMT-modified allogeneic γδT cells (INB-410) are currently undergoing a phase Ib clinical trial (NCT05664243). The product INB-400/410, developed by IN8bio, has been granted FDA Orphan Drug Designation for the Treatment of Newly Diagnosed Glioblastoma.

As it stands, most approved combination immunotherapies largely rely on a combination of immune checkpoint inhibitors (ICIs) and have emerged as first-line treatments for several major cancer types (191). The future of combination immunotherapies with γδT cells likely extends beyond ICI-based approaches, aiming for control and eradication of established tumors. Further research in this area will be instrumental in harnessing the full therapeutic potential of γδT cells.

5 Challenges and limitations

Tapping into the potential of genetically engineered γδT cells holds the promises of breakthroughs in cancer immunotherapy,

albeit with scientific and technical hurdles. The multifaceted nature of γδT cell biology coupled with the complexities of genetic manipulation throws inevitable challenges in the way of optimizing therapeutic potential.

The extensive heterogeneity of γδT cells, which includes various subsets with distinct antigen recognition patterns, homing properties, and effector functionalities, presents a significant challenge in standardizing genetic engineering strategies (192). Additionally, our understanding of the γδTCR repertoire lags behind that of αβTCRs (141). Although cell engagers and bispecific antibodies have shown potential to robustly activate γδT cells, effective signal optimization is still underway (178). Certain constraints of gene-engineering, such as the need for CD8 or other co-stimulators which γδT cells lack, and the intricate manufacturing processes involved, serve as significant obstacles (138). Although gene-transduction techniques, such as mRNA electroporation and lentiviral transduction, have seen noticeable advancements over the past years, the efficiency of integrating genes into γδT cells using either viral or non-viral vectors is yet to reach optimal levels. mRNA electroporation allows for rapid expression and poses fewer risks of insertional mutations, while also being associated with lower cellular toxicity. However, this method only provides transient expression of CARs, requiring multiple infusions of CAR T-cells and an extension of their cytotoxic lifespans from a therapeutic perspective (154). On the other hand, lentiviral transduction, often considered time-consuming, also carries the risk of damaging essential genes or regulatory sequences during the period required for expression (193–195)..

In comparison to αβ CAR-T cells, γδ CAR-T cells often present less complete clearance of tumor cells *in vivo*. This characteristic could be attributed to reduced persistence of γδ CAR-T in the immunosuppressive microenvironment (125, 196), necessitating multiple infusions and a large supply of γδ CAR-T cells. Furthermore, CAR-T cells could potentially contribute to antigen loss in target cells, resulting in diminished antigen density (197).

While the introduction of bispecific T cell engagers has propelled cancer immunotherapy, especially against hematological malignancies by offering an easy and cost-effective treatment option, their efficacy remains undermined by co-triggering of immunosuppressive T cell populations, such as regulatory T cells (Tregs) (137). Even though the combination of CAR and bispecific γδT cell engagers has shown promising results towards improving anti-tumor efficacy and reducing cytotoxicity, the tumor cells' ability to evade the immune system strengthened by γδT cells is still under investigation (198).

Interestingly, γδT cells, under certain conditions, may also promote tumor growth (199, 200). This trait might be influenced by the TME or interactions with other immune cells. γδT cells have been known to promote tumor growth by producing IL-17, a process influenced by factors such as TME-related metabolism, microbial products, and inflammatory cells (201, 202). Considering the association of γδT cells with autoimmune diseases, a thorough investigation of their long-term clinical outcomes is essential when their activation or suppression is incorporated into treatments (203).

Implementing engineered γδT cell immunotherapy in a clinical setting presents its own set of challenges. Identifying suitable patients and healthy donors and creating standardized monitoring guidelines are crucial. Determining the correct dosage—whether based on body weight or the number of cells per infusion—and understanding its relation to treatment success is a significant hurdle. There is also a pressing need to address the risk of disease recurrence post-treatment, bolster the therapy's durability, and decide whether to opt for monotherapy (with a single or several doses) or a combination approach (204). In addition, as production is resource-intensive and coupled with strict regulatory, ethical, and safety considerations, and high costs. Thus, widespread access to this form of therapy is limited. To fully employ the potential of γδT cell therapies, extensive research and collaboration are necessary.

6 Conclusions and future perspectives

γδT cell-based immunotherapies represent a promising frontier in cancer treatment, introducing innovative approaches to overcome the limitations of traditional therapies. The development of gene-engineering strategies, such as CAR T therapy, bispecific antibodies and cell engagers, and TCR gene transfer, has significantly advanced the efficacy of γδT cells, addressing their challenges in abundance, expansion, and targeting efficiency. Despite these strides, hurdles such as the nuanced understanding of γδT cell behaviors, targeting solid tumors effectively, and preventing post-treatment relapse persist.

The remarkable potential of γδT cell therapies lies in their ability to offer a paradigm shift in cancer treatment, utilizing their unique properties for more precise, potent, and personalized interventions. Their versatility in recognizing cancer cells without MHC restriction provides a substantial advantage in reducing the risk of immune escape and addressing tumor heterogeneity.

Looking ahead, research must focus on understanding γδT cells' metabolic needs and cytokine profiles within the tumor microenvironment to enhance their antitumor activity. Additionally, it is critical to develop strategies that improve the persistence of CAR γδT cells and maintain target antigen visibility, ensuring long-term therapeutic success. The exploration of Vδ1 subsets and the creation of iPSC-derived γδT cells hold promise for developing universally applicable CAR γδT cell therapies. Furthermore, optimizing the engineering of γδT cells for safer and more efficient delivery, coupled with the strategic combination of these therapies with other treatments, will enhance efficacy and durability.

Emphasis should also be placed on designing therapies that reduce the risk of relapse and increase sustainability. Regulatory, manufacturing, and logistical challenges will need to be addressed to facilitate the clinical translation of these therapies. The ultimate goal is to harness the full therapeutic potential of γδT cells, offering new hope to patients with various types of cancer.

The future of γδT cell immunotherapy lies in the convergence of molecular biology, genetic engineering, and clinical research. As our understanding evolves, so will the potential of γδT cells as a powerful tool in the arsenal against cancer, paving the way for more effective, tailored, and sustainable cancer treatments.

Author contributions

MY: Writing – original draft, Writing – review & editing. WW: Writing – original draft, Writing – review & editing. IH: Writing – review & editing. JH: Writing – review & editing. ZY: Writing – review & editing. AB: Writing – review & editing.

Funding

The author(s) declare that financial support was received for the research, authorship, and/or publication of this article. This research was funded by Lorry Lokey Faculty Scholar.

Conflict of interest

The authors declare that the research was conducted in the absence of any commercial or financial relationships that could be construed as a potential conflict of interest.

Publisher's note

References

1. Mizukoshi E, Kaneko S. Immune cell therapy for hepatocellular carcinoma. *J Hematol Oncol.* (2019) 12:52. doi: 10.1186/s13045-019-0742-5

2. Riley RS, June CH, Langer R, Mitchell MJ. Delivery technologies for cancer immunotherapy. *Nat Rev Drug Discovery.* (2019) 18:175–96. doi: 10.1038/s41573-018-0006-z

3. Zhang Y, Zhang Z. The history and advances in cancer immunotherapy: understanding the characteristics of tumor-infiltrating immune cells and their therapeutic implications. *Cell Mol Immunol.* (2020) 17:807–21. doi: 10.1038/s41423-020-0488-6

4. Labanieh L, Mackall CL. Car immune cells: design principles, resistance and the next generation. *Nature.* (2023) 614:635–48. doi: 10.1038/s41586-023-05707-3

5. Myers JA, Miller JS. Exploring the nk cell platform for cancer immunotherapy. *Nat Rev Clin Oncol.* (2021) 18:85–100. doi: 10.1038/s41571-020-0426-7

6. Burger JA, Wiestner A. Targeting B cell receptor signalling in cancer: preclinical and clinical advances. *Nat Rev Cancer.* (2018) 18:148–67. doi: 10.1038/nrc.2017.121

7. Mantovani A, Allavena P, Marchesi F, Garlanda C. Macrophages as tools and targets in cancer therapy. *Nat Rev Drug Discovery.* (2022) 21:799–820. doi: 10.1038/s41573-022-00520-5

8. Mensurado S, Blanco-Domínguez R, Silva-Santos B. The emerging roles of Γδ T cells in cancer immunotherapy. *Nat Rev Clin Oncol.* (2023) 20:178–91. doi: 10.1038/s41571-022-00722-1

9. Yazdanifar M, Barbarito G, Bertaina A, Airoldi I. Γδ T cells: the ideal tool for cancer immunotherapy. *Cells.* (2020) 9:1305. doi: 10.3390/cells9051305

10. Nishimoto KP, Barca T, Azameera A, Makkouk A, Romero JM, Bai L, et al. Allogeneic cd20-targeted Γδ T cells exhibit innate and adaptive antitumor activities in preclinical B-cell lymphoma models. *Clin Trans Immunol.* (2022) 11:e1373. doi: 10.1002/cti2.1373

11. Lopes N, Silva-Santos B. Functional and metabolic dichotomy of murine Γδ T cell subsets in cancer immunity. *Eur J Immunol.* (2021) 51:17–26. doi: 10.1002/eji.201948402

12. Khairallah C, Chu TH, Sheridan BS. Tissue adaptations of memory and tissue-resident gamma delta T cells. *Front Immunol.* (2018) 9:2636. doi: 10.3389/fimmu.2018.02636

13. Wiebking V, Lee CM, Mostrel N, Lahiri P, Bak R, Bao G, et al. Genome editing of donor-derived T-cells to generate allogenic chimeric antigen receptor-modified T cells: optimizing αβ T cell-depleted haploidentical hematopoietic stem cell transplantation. *Haematologica.* (2021) 106:847–58. doi: 10.3324/haematol.2019.233882

14. Ye W, Kong X, Zhang W, Weng Z, Wu X. The roles of Γδ T cells in hematopoietic stem cell transplantation. *Cell Transplant.* (2020) 29:963689720966980. doi: 10.1177/0963689720966980

15. Lee D, Rosenthal CJ, Penn NE, Dunn ZS, Zhou Y, Yang L. Human Γδ T cell subsets and their clinical applications for cancer immunotherapy. *Cancers (Basel).* (2022) 14:3005. doi: 10.3390/cancers14123005

16. Brandes M, Willimann K, Moser B. Professional antigen-presentation function by human Γδ T cells. *Science.* (2005) 309:264–8. doi: 10.1126/science.1110267

17. Imbert C, Olive D. Γδ T cells in tumor microenvironment. *Adv Exp Med Biol.* (2020) 1273:91–104. doi: 10.1007/978-3-030-49270-0_5

18. Agerholm R, Bekiaris V. Evolved to protect, designed to destroy: il-17-producing Γδ T cells in infection, inflammation, and cancer. *Eur J Immunol.* (2021) 51:2164–77. doi: 10.1002/eji.202049119

19. Zhang H, Chai W, Yang W, Han W, Mou W, Xi Y, et al. The increased il-17-producing Γδt cells promote tumor cell proliferation and migration in neuroblastoma. *Clin Immunol.* (2020) 211:108343. doi: 10.1016/j.clim.2020.108343

20. Mensurado S, Rei M, Lança T, Ioannou M, Gonçalves-Sousa N, Kubo H, et al. Tumor-associated neutrophils suppress pro-tumoral il-17+ Γδ T cells through induction of oxidative stress. *PloS Biol.* (2018) 16:e2004990. doi: 10.1371/journal.pbio.2004990

21. Chen X, Morrissey S, Chen F, Yan J. Novel insight into the molecular and metabolic mechanisms orchestrating il-17 production in Γδ T cells. *Front Immunol.* (2019) 10:2828. doi: 10.3389/fimmu.2019.02828

22. Ma Y, Aymeric L, Locher C, Mattarollo SR, Delahaye NF, Pereira P, et al. Contribution of il-17-producing gamma delta T cells to the efficacy of anticancer chemotherapy. *J Exp Med.* (2011) 208:491–503. doi: 10.1084/jem.20100269

23. Wakita D, Sumida K, Iwakura Y, Nishikawa H, Ohkuri T, Chamoto K, et al. Tumor-infiltrating il-17-producing gammadelta T cells support the progression of tumor by promoting angiogenesis. *Eur J Immunol.* (2010) 40:1927–37. doi: 10.1002/eji.200940157

24. Jhita N, Raikar SS. Allogeneic gamma delta T cells as adoptive cellular therapy for hematologic Malignancies. *Explor Immunol.* (2022) 2:334–50. doi: 10.37349/ei.2022.00054

25. Bertaina A, Roncarolo MG. Graft engineering and adoptive immunotherapy: new approaches to promote immune tolerance after hematopoietic stem cell transplantation. *Front Immunol.* (2019) 10:1342. doi: 10.3389/fimmu.2019.01342

26. Xu Y, Xiang Z, Alnaggar M, Kouakanou L, Li J, He J, et al. Allogeneic Vγ9vδ2 T-cell immunotherapy exhibits promising clinical safety and prolongs the survival of patients with late-stage lung or liver cancer. *Cell Mol Immunol.* (2021) 18:427–39. doi: 10.1038/s41423-020-0515-7

27. Vydra J, Cosimo E, Lesný P, Wanless RS, Anderson J, Clark AG, et al. A phase I trial of allogeneic Γδ T lymphocytes from haploidentical donors in patients with refractory or relapsed acute myeloid leukemia. *Clin Lymphoma Myeloma Leuk.* (2023) 23:e232–e9. doi: 10.1016/j.clml.2023.02.003

28. Saura-Esteller J, de Jong M, King LA, Ensing E, Winograd B, de Gruijl TD, et al. Gamma delta T-cell based cancer immunotherapy: past-present-future. *Front Immunol.* (2022) 13:915837. doi: 10.3389/fimmu.2022.915837

29. Godfrey DI, Le Nours J, Andrews DM, Uldrich AP, Rossjohn J. Unconventional T cell targets for cancer immunotherapy. *Immunity.* (2018) 48:453–73. doi: 10.1016/j.immuni.2018.03.009

30. Chen D, Guo Y, Jiang J, Wu P, Zhang T, Wei Q, et al. Gammadelta T cell exhaustion: opportunities for intervention. *J Leukoc Biol.* (2022) 112:1669–76. doi: 10.1002/JLB.5MR0722-777R

31. Deng J, Yin H. Gamma delta (Γδ) T cells in cancer immunotherapy; where it comes from, where it will go? *Eur J Pharmacol.* (2022) 919:174803. doi: 10.1016/j.ejphar.2022.174803

32. Hu Y, Hu Q, Li Y, Lu L, Xiang Z, Yin Z, et al. Γδ T cells: origin and fate, subsets, diseases and immunotherapy. *Signal Transduction Targeted Ther.* (2023) 8:434. doi: 10.1038/s41392-023-01653-8

33. Parker CM, Groh V, Band H, Porcelli SA, Morita C, Fabbi M, et al. Evidence for extrathymic changes in the T cell receptor gamma/delta repertoire. *J Exp Med.* (1990) 171:1597–612. doi: 10.1084/jem.171.5.1597

34. Saito H, Kranz DM, Takagaki Y, Hayday AC, Eisen HN, Tonegawa S. Complete primary structure of a heterodimeric T-cell receptor deduced from cdna sequences. *Nature.* (1984) 309:757–62. doi: 10.1038/309757a0

35. Gründer C, van Dorp S, Hol S, Drent E, Straetemans T, Heijhuurs S, et al. Γ9 and Δ2cdr3 domains regulate functional avidity of T cells harboring Γ9δ2tcrs. *Blood*. (2012) 120:5153–62. doi: 10.1182/blood-2012-05-432427

36. Chien Y-h, Konigshofer Y. Antigen recognition by Γδ T cells. *Immunol Rev*. (2007) 215:46–58. doi: 10.1111/j.1600-065X.2006.00470.x

37. Ravens S, Fichtner AS, Willers M, Torkornoo D, Pirr S, Schöning J, et al. Microbial exposure drives polyclonal expansion of innate Γδ T cells immediately after birth. *Proc Natl Acad Sci U.S.A*. (2020) 117:18649–60. doi: 10.1073/pnas.1922588117

38. Ramstead AG, Jutila MA. Complex role of Γδ T-cell-derived cytokines and growth factors in cancer. *J Interferon Cytokine Res*. (2012) 32:563–9. doi: 10.1089/jir.2012.0073

39. Li J, Herold MJ, Kimmel B, Müller I, Rincon-Orozco B, Kunzmann V, et al. Reduced expression of the mevalonate pathway enzyme farnesyl pyrophosphate synthase unveils recognition of tumor cells by Vγ9vδ2 T cells1. *J Immunol*. (2009) 182:8118–24. doi: 10.4049/jimmunol.0900101

40. Christopoulos P, Bukatz D, Kock S, Malkovsky M, Finke J, Fisch P. Improved analysis of tcrγδ Variable region expression in humans. *J Immunol Methods*. (2016) 434:66–72. doi: 10.1016/j.jim.2016.04.009

41. Chabab G, Boissière-Michot F, Mollevi C, Ramos J, Lopez-Crapez E, Colombo P-E, et al. Diversity of tumor-infiltrating, Γδ T-cell abundance in solid cancers. *Cells*. (2020) 9:1537.

42. Nguyen S, Chevalier MF, Benmerzoug S, Cesson V, Schneider AK, Rodrigues-Dias SC, et al. Vδ2 T cells are associated with favorable clinical outcomes in patients with bladder cancer and their tumor reactivity can be boosted by bcg and zoledronate treatments. *J Immunother Cancer*. (2022) 10:e004880. doi: 10.1136/jitc-2022-004880

43. Bruni E, Cimino MM, Donadon M, Carriero R, Terzoli S, Piazza R, et al. Intrahepatic cd69(+)Vδ1 T cells re-circulate in the blood of patients with metastatic colorectal cancer and limit tumor progression. *J Immunother Cancer*. (2022) 10:e004579. doi: 10.1136/jitc-2022-004579

44. Bukowski JF, Morita CT, Band H, Brenner MB. Crucial role of tcrγ Chain junctional region in prenyl pyrophosphate antigen recognition by Γδ T cells1. *J Immunol*. (1998) 161:286–93. doi: 10.4049/jimmunol.161.1.286

45. Hunter S, Willcox CR, Davey MS, Kasatskaya SA, Jeffery HC, Chudakov DM, et al. Human liver infiltrating Γδ T cells are composed of clonally expanded circulating and tissue-resident populations. *J Hepatol*. (2018) 69:654–65. doi: 10.1016/j.jhep.2018.05.007

46. Wu Y, Biswas D, Usaite I, Angelova M, Boeing S, Karasaki T, et al. A local human Vδ1 T cell population is associated with survival in nonsmall-cell lung cancer. *Nat Cancer*. (2022) 3:696–709. doi: 10.1038/s43018-022-00376-z

47. Zakeri N, Hall A, Swadling L, Pallett LJ, Schmidt NM, Diniz MO, et al. Characterisation and induction of tissue-resident gamma delta T-cells to target hepatocellular carcinoma. *Nat Commun*. (2022) 13:1372. doi: 10.1038/s41467-022-29012-1

48. Glatzel A, Wesch D, Schiemann F, Brandt E, Janssen O, Kabelitz D. Patterns of chemokine receptor expression on peripheral blood Γδ T lymphocytes: strong expression of ccr5 is a selective feature of Vδ2/Vγ9 Γδ T cells1. *J Immunol*. (2002) 168:4920–9. doi: 10.4049/jimmunol.168.10.4920

49. Davey MS, Willcox CR, Joyce SP, Ladell K, Kasatskaya SA, McLaren JE, et al. Clonal selection in the human Vδ1 T cell repertoire indicates Γδ Tcr-dependent adaptive immune surveillance. *Nat Commun*. (2017) 8:14760. doi: 10.1038/ncomms14760

50. Di Lorenzo B, Ravens S, Silva-Santos B. High-throughput analysis of the human thymic Vδ1+ T cell receptor repertoire. *Sci Data*. (2019) 6:115. doi: 10.1038/s41597-019-0118-2

51. Ravens S, Schultze-Florey C, Raha S, Sandrock I, Drenker M, Oberdörfer L, et al. Human Γδ T cells are quickly reconstituted after stem-cell transplantation and show adaptive clonal expansion in response to viral infection. *Nat Immunol*. (2017) 18:393–401. doi: 10.1038/ni.3686

52. Bauer S, Groh V, Wu J, Steinle A, Phillips JH, Lanier LL, et al. Activation of nk cells and T cells by nkg2d, a receptor for stress-inducible mica. *Science*. (1999) 285:727–9. doi: 10.1126/science.285.5428.727

53. Groh V, Rhinehart R, Secrist H, Bauer S, Grabstein KH, Spies T. Broad tumor-associated expression and recognition by tumor-derived gamma delta T cells of mica and micb. *Proc Natl Acad Sci U.S.A*. (1999) 96:6879–84. doi: 10.1073/pnas.96.12.6879

54. Qi J, Zhang J, Zhang S, Cui L, He W. Immobilized mica could expand human Vδ1 Γδ T cells in vitro that displayed major histocompatibility complex class I chain-related a-dependent cytotoxicity to human epithelial carcinomas. *Scandinavian J Immunol*. (2003) 58:211–20. doi: 10.1046/j.1365-3083.2003.01288.x

55. Correia DV, Fogli M, Hudspeth K, da Silva MG, Mavilio D, Silva-Santos B. Differentiation of human peripheral blood Vδ1+ T cells expressing the natural cytotoxicity receptor nkp30 for recognition of lymphoid leukemia cells. *Blood*. (2011) 118:992–1001. doi: 10.1182/blood-2011-02-339135

56. Mikulak J, Oriolo F, Bruni E, Roberto A, Colombo FS, Villa A, et al. Nkp46-expressing human gut-resident intraepithelial Vδ1 T cell subpopulation exhibits high antitumor activity against colorectal cancer. *JCI Insight*. (2019) 4:e125884. doi: 10.1172/jci.insight.125884

57. Wu Y, Kyle-Cezar F, Woolf RT, Naceur-Lombardelli C, Owen J, Biswas D, et al. An innate-like Vδ1(+) Γδ T cell compartment in the human breast is associated with remission in triple-negative breast cancer. *Sci Transl Med*. (2019) 11:eaax9364. doi: 10.1126/scitranslmed.aax9364

58. Luoma Adrienne M, Castro Caitlin D, Mayassi T, Bembinster Leslie A, Bai L, Picard D, et al. Crystal structure of Vδ1 t cell receptor in complex with cd1d-sulfatide shows mhc-like recognition of a self-lipid by human Γδ T cells. *Immunity*. (2013) 39:1032–42. doi: 10.1016/j.immuni.2013.11.001

59. Uldrich AP, Le Nours J, Pellicci DG, Gherardin NA, McPherson KG, Lim RT, et al. Cd1d-lipid antigen recognition by the Γδ Tcr. *Nat Immunol*. (2013) 14:1137–45. doi: 10.1038/ni.2713

60. Poggi A, Venturino C, Catellani S, Clavio M, Miglino M, Gobbi M, et al. Vdelta1 T lymphocytes from B-cll patients recognize ulbp3 expressed on leukemic B cells and up-regulated by trans-retinoic acid. *Cancer Res*. (2004) 64:9172–9. doi: 10.1158/0008-5472.Can-04-2417

61. Marlin R, Pappalardo A, Kaminski H, Willcox CR, Pitard V, Netzer S, et al. Sensing of cell stress by human Γδ Tcr-dependent recognition of annexin A2. *Proc Natl Acad Sci U.S.A*. (2017) 114:3163–8. doi: 10.1073/pnas.1621052114

62. Groh V, Steinle A, Bauer S, Spies T. Recognition of stress-induced mhc molecules by intestinal epithelial gammadelta T cells. *Science*. (1998) 279:1737–40. doi: 10.1126/science.279.5357.1737

63. Spada FM, Grant EP, Peters PJ, Sugita M, Melián A, Leslie DS, et al. Self-recognition of cd1 by Γ/Δ T cells: implications for innate immunity. *J Exp Med*. (2000) 191:937–48. doi: 10.1084/jem.191.6.937

64. Bai L, Picard D, Anderson B, Chaudhary V, Luoma A, Jabri B, et al. The majority of cd1d-sulfatide-specific T cells in human blood use a semiinvariant Vδ1 tcr. *Eur J Immunol*. (2012) 42:2505–10. doi: 10.1002/eji.201242531

65. Davey MS, Willcox CR, Hunter S, Kasatskaya SA, Remmerswaal EBM, Salim M, et al. The human Vδ2+ T-cell compartment comprises distinct innate-like Vγ9+ and adaptive Vγ9- subsets. *Nat Commun*. (2018) 9:1760. doi: 10.1038/s41467-018-04076-0

66. McMurray JL, von Borstel A, Taher TE, Syrimi E, Taylor GS, Sharif M, et al. Transcriptional profiling of human Vδ1 T cells reveals a pathogen-driven adaptive differentiation program. *Cell Rep*. (2022) 39:110858. doi: 10.1016/j.celrep.2022.110858

67. Benzaïd I, Mönkkönen H, Stresing V, Bonnelye E, Green J, Mönkkönen J, et al. High phosphoantigen levels in bisphosphonate-treated human breast tumors promote vgamma9vdelta2 T-cell chemotaxis and cytotoxicity in vivo. *Cancer Res*. (2011) 71:4562–72. doi: 10.1158/0008-5472.Can-10-3862

68. Rigau M, Ostrouska S, Fulford TS, Johnson DN, Woods K, Ruan Z, et al. Butyrophilin 2a1 is essential for phosphoantigen reactivity by Γδ T cells. *Science*. (2020) 367:eaay5516. doi: 10.1126/science.aay5516

69. Papadopoulou M, Tieppo P, McGovern N, Gosselin F, Chan JKY, Goetgeluk G, et al. Tcr sequencing reveals the distinct development of fetal and adult human Vγ9vδ2 T cells. *J Immunol*. (2019) 203:1468–79. doi: 10.4049/jimmunol.1900592

70. Fisher JP, Yan M, Heuijerjans J, Carter L, Abolhassani A, Frosch J, et al. Neuroblastoma killing properties of Vδ2 and Vδ2-negative Γδt cells following expansion by artificial antigen-presenting cells. *Clin Cancer Res*. (2014) 20:5720–32. doi: 10.1158/1078-0432.Ccr-13-3464

71. Brandes M, Willimann K, Bioley G, Lévy N, Eberl M, Luo M, et al. Cross-presenting human gammadelta T cells induce robust cd8+ Alphabeta T cell responses. *Proc Natl Acad Sci U.S.A*. (2009) 106:2307–12. doi: 10.1073/pnas.0810059106

72. Himoudi N, Morgenstern DA, Yan M, Vernay B, Saraiva L, Wu Y, et al. Human Γδ T lymphocytes are licensed for professional antigen presentation by interaction with opsonized target cells. *J Immunol*. (2012) 188:1708–16. doi: 10.4049/jimmunol.1102654

73. Mao C, Mou X, Zhou Y, Yuan G, Xu C, Liu H, et al. Tumor-activated tcrγδ T cells from gastric cancer patients induce the antitumor immune response of tcrαβ T cells via their antigen-presenting cell-like effects. *J Immunol Res*. (2014) 2014:593562. doi: 10.1155/2014/593562

74. Lafont V, Liautard J, Liautard JP, Favero J. Production of tnf-α by human Vγ9vδ2 T cells via engagement of fcγriiia, the low affinity type 3 receptor for the fc portion of igg, expressed upon tcr activation by nonpeptidic antigen1. *J Immunol*. (2001) 166:7190–9. doi: 10.4049/jimmunol.166.12.7190

75. Alnaggar M, Xu Y, Li J, He J, Chen J, Li M, et al. Allogenic Vγ9vδ2 T cell as new potential immunotherapy drug for solid tumor: A case study for cholangiocarcinoma. *J Immunother Cancer*. (2019) 7:36. doi: 10.1186/s40425-019-0501-8

76. Kierkels GJJ, Scheper W, Meringa AD, Johanna I, Beringer DX, Janssen A, et al. Identification of a tumor-specific allo-hla-restricted Γδtcr. *Blood Adv*. (2019) 3:2870–82. doi: 10.1182/bloodadvances.2019032409

77. Scheper W, van Dorp S, Kersting S, Pietersma F, Lindemans C, Hol S, et al. Γδt cells elicited by cmv reactivation after allo-sct cross-recognize cmv and leukemia. *Leukemia*. (2013) 27:1328–38. doi: 10.1038/leu.2012.374

78. Willcox CR, Pitard V, Netzer S, Couzi L, Salim M, Silberzahn T, et al. Cytomegalovirus and tumor stress surveillance by binding of a human Γδ T cell antigen receptor to endothelial protein C receptor. *Nat Immunol*. (2012) 13:872–9. doi: 10.1038/ni.2394

79. Gaballa A, Alagrafi F, Uhlin M, Stikvoort A. Revisiting the role of Γδ T cells in anti-cmv immune response after transplantation. *Viruses*. (2021) 13:1031. doi: 10.3390/v13061031

80. Kalyan S, Kabelitz D. Defining the nature of human Γδ T cells: A biographical sketch of the highly empathetic. *Cell Mol Immunol*. (2013) 10:21–9. doi: 10.1038/cmi.2012.44

81. Berglund S, Gaballa A, Sawaisorn P, Sundberg B, Uhlin M. Expansion of gammadelta T cells from cord blood: A therapeutical possibility. *Stem Cells Int*. (2018) 2018:8529104. doi: 10.1155/2018/8529104

82. Benveniste PM, Roy S, Nakatsugawa M, Chen ELY, Nguyen L, Millar DG, et al. Generation and molecular recognition of melanoma-associated antigen-specific human Γδ T cells. *Sci Immunol*. (2018) 3:eaav4036. doi: 10.1126/sciimmunol.aav4036

83. Hur G, Choi H, Lee Y, Sohn H-J, Kim S-Y, Kim T-G. *In vitro* expansion of VΔ1+ T cells from cord blood by using artificial antigen-presenting cells and anti-cd3 antibody. *Vaccines*. (2023) 11:406.

84. Khan MWA, Otaibi AA, Sherwani S, Alshammari EM, Al-Zahrani SA, Khan WA, et al. Optimization of methods for peripheral blood mononuclear cells isolation and expansion of human gamma delta T cells. *Bioinformation*. (2021) 17:460–9. doi: 10.6026/97320630017460

85. Cruz MS, Diamond A, Russell A, Jameson JM. Human αβ and Γδ T cells in skin immunity and disease. *Front Immunol*. (2018) 9:1304. doi: 10.3389/fimmu.2018.01304

86. Cai Y, Shen X, Ding C, Qi C, Li K, Li X, et al. Pivotal role of dermal il-17-producing Γδ T cells in skin inflammation. *Immunity*. (2011) 35:649. doi: 10.1016/j.immuni.2011.10.006

87. Castillo-González R, Cibrian D, Sánchez-Madrid F. Dissecting the complexity of Γδ T-cell subsets in skin homeostasis, inflammation, and Malignancy. *J Allergy Clin Immunol*. (2021) 147:2030–42. doi: 10.1016/j.jaci.2020.11.023

88. Guo R, Li W, Li Y, Li Y, Jiang Z, Song Y. Generation and clinical potential of functional T lymphocytes from gene-edited pluripotent stem cells. *Exp Hematol Oncol*. (2022) 11:27. doi: 10.1186/s40164-022-00285-y

89. Themeli M, Kloss CC, Ciriello G, Fedorov VD, Perna F, Gonen M, et al. Generation of tumor-targeted human T lymphocytes from induced pluripotent stem cells for cancer therapy. *Nat Biotechnol*. (2013) 31:928–33. doi: 10.1038/nbt.2678

90. Wallet MA, Nishimura T, Del Casale C, Lebid A, Salantes B, Santostefano K, et al. Induced pluripotent stem cell-derived gamma delta car-T cells for cancer immunotherapy. *Blood*. (2021) 138:2771. doi: 10.1182/blood-2021-149095

91. Available online at: https://investor.adicetbio.com/news-releases/news-release-details/adicet-bio-reports-positive-data-ongoing-adi-001-phase-1-trial-0.

92. Murai N, Koyanagi-Aoi M, Terashi H, Aoi T. Re-generation of cytotoxic Γδt cells with distinctive signatures from human Γδt-derived ipscs. *Stem Cell Rep*. (2023) 18:853–68. doi: 10.1016/j.stemcr.2023.02.010

93. Wu D, Wu P, Wu X, Ye J, Wang Z, Zhao S, et al. Ex vivo expanded human circulating Vδ1 Γδt cells exhibit favorable therapeutic potential for colon cancer. *Oncoimmunology*. (2015) 4:e992749. doi: 10.4161/2162402x.2014.992749

94. Almeida AR, Correia DV, Fernandes-Platzgummer A, da Silva CL, da Silva MG, Anjos DR, et al. Delta one T cells for immunotherapy of chronic lymphocytic leukemia: clinical-grade expansion/differentiation and preclinical proof of concept. *Clin Cancer Res*. (2016) 22:5795–804. doi: 10.1158/1078-0432.Ccr-16-0597

95. Lee SJ, Kim YH, Hwang SH, Kim YI, Han IS, Vinay DS, et al. 4–1bb signal stimulates the activation, expansion, and effector functions of Γδ T cells in mice and humans. *Eur J Immunol*. (2013) 43:1839–48. doi: 10.1002/eji.201242842

96. Siegers GM, Dhamko H, Wang X-H, Mathieson AM, Kosaka Y, Felizardo TC, et al. Human Vδ1 Γδ T cells expanded from peripheral blood exhibit specific cytotoxicity against B-cell chronic lymphocytic leukemia-derived cells. *Cytotherapy*. (2011) 13:753–64. doi: 10.3109/14653249.2011.553595

97. Ferry GM, Agbuduwe C, Forrester M, Dunlop S, Chester K, Fisher J, et al. A simple and robust single-step method for car-Vδ1 Γδt cell expansion and transduction for cancer immunotherapy. *Front Immunol*. (2022) 13:863155. doi: 10.3389/fimmu.2022.863155

98. Chargui J, Combaret V, Scaglione V, Iacono I, Péri V, Valteau-Couanet D, et al. Bromohydrin pyrophosphate-stimulated Vγ9δ2 T cells expanded ex vivo from patients with poor-prognosis neuroblastoma lyse autologous primary tumor cells. *J Immunother*. (2010) 33:591–8. doi: 10.1097CJI.0b013e3181dda207

99. Okuno D, Sugiura Y, Sakamoto N, Tagod MSO, Iwasaki M, Noda S, et al. Comparison of a novel bisphosphonate prodrug and zoledronic acid in the induction of cytotoxicity in human Vγ2vδ2 T cells. *Front Immunol*. (2020) 11:1405. doi: 10.3389/fimmu.2020.01405

100. Wang Y, Wang L, Seo N, Okumura S, Hayashi T, Akahori Y, et al. Car-modified VΓ9vΔ2 T cells propagated using a novel bisphosphonate prodrug for allogeneic adoptive immunotherapy. *Int J Mol Sci*. (2023) 24:10873.

101. Rincon-Orozco B, Kunzmann V, Wrobel P, Kabelitz D, Steinle A, Herrmann T. Activation of Vγ9vδ2 T cells by nkg2d1. *J Immunol*. (2005) 175:2144–51. doi: 10.4049/jimmunol.175.4.2144

102. Wang H, Sarikonda G, Puan K-J, Tanaka Y, Feng J, Giner J-L, et al. Indirect stimulation of human Vγ2vδ2 T cells through alterations in isoprenoid metabolism. *J Immunol*. (2011) 187:5099–113. doi: 10.4049/jimmunol.1002697

103. Peters C, Meyer A, Kouakanou L, Feder J, Schricker T, Lettau M, et al. Tgf-β Enhances the cytotoxic activity of Vδ2 T cells. *OncoImmunology*. (2019) 8:e1522471. doi: 10.1080/2162402X.2018.1522471

104. Boucher JC, Yu B, Li G, Shrestha B, Sallman D, Landin AM, et al. Large scale ex vivo expansion of Γδ T cells using artificial antigen-presenting cells. *J Immunother*. (2023) 46:5–13. doi: 10.1097/cji.0000000000000445

105. Choi H, Lee Y, Hur G, Lee S-E, Cho H-I, Sohn H-J, et al. Γδ T cells cultured with artificial antigen-presenting cells and il-2 show long-term proliferation and enhanced effector functions compared with Γδ T cells cultured with only il-2 after stimulation with zoledronic acid. *Cytotherapy*. (2021) 23:908–17. doi: 10.1016/j.jcyt.2021.06.002

106. Kouakanou L, Xu Y, Peters C, He J, Wu Y, Yin Z, et al. Vitamin C promotes the proliferation and effector functions of human Γδ T cells. *Cell Mol Immunol*. (2020) 17:462–73. doi: 10.1038/s41423-019-0247-8

107. Polito VA, Cristantielli R, Weber G, Del Bufalo F, Belardinilli T, Arnone CM, et al. Universal ready-to-use immunotherapeutic approach for the treatment of cancer: expanded and activated polyclonal Γδ Memory T cells. *Front Immunol*. (2019) 10:2717. doi: 10.3389/fimmu.2019.02717

108. Deniger DC, Maiti SN, Mi T, Switzer KC, Ramachandran V, Hurton LV, et al. Activating and propagating polyclonal gamma delta T cells with broad specificity for Malignancies. *Clin Cancer Res*. (2014) 20:5708–19. doi: 10.1158/1078-0432.Ccr-13-3451

109. Landin AM, Cox C, Yu B, Bejanyan N, Davila M, Kelley L. Expansion and enrichment of gamma-delta (Γδ) T cells from apheresed human product. *J Vis Exp*. (2021) 175:e62622. doi: 10.3791/62622

110. Dokouhaki P, Han M, Joe B, Li M, Johnston MR, Tsao M-S, et al. Adoptive immunotherapy of cancer using ex vivo expanded human Γδ T cells: A new approach. *Cancer Lett*. (2010) 297:126–36. doi: 10.1016/j.canlet.2010.05.005

111. Kang N, Zhou J, Zhang T, Wang L, Lu F, Cui Y, et al. Adoptive immunotherapy of lung cancer with immobilized anti-tcrγδ Antibody-expanded human Γδ T cells in peripheral blood. *Cancer Biol Ther*. (2009) 8:1540–9. doi: 10.4161/cbt.8.16.8950

112. Zhou J, Kang N, Cui L, Ba D, He W. Anti-Γδ Tcr antibody-expanded Γδ T cells: A better choice for the adoptive immunotherapy of lymphoid Malignancies. *Cell Mol Immunol*. (2012) 9:34–44. doi: 10.1038/cmi.2011.16

113. Kondo M, Izumi T, Fujieda N, Kondo A, Morishita T, Matsushita H, et al. Expansion of human peripheral blood Γδ T cells using zoledronate. *J Vis Exp*. (2011) 55:e3182. doi: 10.3791/3182

114. Li W, Kubo S, Okuda A, Yamamoto H, Ueda H, Tanaka T, et al. Effect of il-18 on expansion of Γδ T cells stimulated by zoledronate and il-2. *J Immunother*. (2010) 33:287–96. doi: 10.1097/CJI.0b013e3181c80ffa

115. Holmen Olofsson G, Idorn M, Carnaz Simões AM, Aehnlich P, Skadborg SK, Noessner E, et al. Vγ9vδ2 T cells concurrently kill cancer cells and cross-present tumor antigens. *Front Immunol*. (2021) 12:645131. doi: 10.3389/fimmu.2021.645131

116. Kondo M, Sakuta K, Noguchi A, Ariyoshi N, Sato K, Sato S, et al. Zoledronate facilitates large-scale ex vivo expansion of functional gammadelta T cells from cancer patients for use in adoptive immunotherapy. *Cytotherapy*. (2008) 10:842–56. doi: 10.1080/14653240802419328

117. Siegers GM, Ribot EJ, Keating A, Foster PJ. Extensive expansion of primary human gamma delta T cells generates cytotoxic effector memory cells that can be labeled with feraheme for cellular mri. *Cancer Immunol Immunother*. (2013) 62:571–83. doi: 10.1007/s00262-012-1353-y

118. Tan W-K, Tay JC, Zeng J, Zheng M, Wang S, Therapeutics T, et al. Expansion of Gamma Delta T Cells - a Short Review on Bisphosphonate and K562-Based Methods. *J Immunol Sci*. (2018) 2:6–12. doi: 10.29245/2578-3009/2018/3.1133

119. Bold A, Gross H, Holzmann E, Knop S, Hoeres T, Wilhelm M. An optimized cultivation method for future in vivo application of Γδ T cells. *Front Immunol*. (2023) 14:1185564. doi: 10.3389/fimmu.2023.1185564

120. Makkouk A, Yang X, Barca T, Lucas A, Turkoz M, Wong J, et al. 119 adi-002: an il-15 armored allogeneic 'Off-the-shelf' Vδ1 gamma delta car T cell therapy for solid tumors targeting glypican-3 (Gpc3). *J ImmunoTher Cancer*. (2021) 9:A128–A. doi: 10.1136/jitc-2021-SITC2021.119

121. Herrman M, Barca T, Yang X, Tabrizizad M, Smith-Boeck M, Kiru L, et al. 198 innate-enhanced chimeric adaptors (Cad): A newly-described approach for augmenting potency of Γδ T cell immunotherapy. *J ImmunoTher Cancer*. (2022) 10:A211–A. doi: 10.1136/jitc-2022-SITC2022.0198

122. Ang WX, Ng YY, Xiao L, Chen C, Li Z, Chi Z, et al. Electroporation of Nkg2d Rna Car Improves Vγ9vδ2 t Cell Responses against Human Solid Tumor Xenografts. *Mol Ther Oncolytics*. (2020) 17:421–30. doi: 10.1016/j.omto.2020.04.013

123. Ding L, Li Y, Haak MT, Lamb L. Abstract 1777: A non-signaling car for gamma-delta (Γδ) T cells to preserve healthy tissues. *Cancer Res*. (2023) 83:1777–. doi: 10.1158/1538-7445.Am2023-1777

124. Lamb LS, Pereboeva L, Youngblood S, Gillespie GY, Nabors LB, Markert JM, et al. A combined treatment regimen of mgmt-modified Γδ T cells and temozolomide chemotherapy is effective against primary high grade gliomas. *Sci Rep*. (2021) 11:21133. doi: 10.1038/s41598-021-00536-8

125. Rozenbaum M, Meir A, Aharony Y, Itzhaki O, Schachter J, Bank I, et al. Gamma-delta car-T cells show car-directed and independent activity against leukemia. *Front Immunol*. (2020) 11:1347. doi: 10.3389/fimmu.2020.01347

126. Zhang X, Ng YY, Du Z, Li Z, Chen C, Xiao L, et al. Vγ9vδ2 T cells expressing a bcma—Specific chimeric antigen receptor inhibit multiple myeloma xenograft growth. *PloS One*. (2022) 17:e0267475. doi: 10.1371/journal.pone.0267475

127. Zhai X, You F, Xiang S, Jiang L, Chen D, Li Y, et al. Muc1-tn-targeting chimeric antigen receptor-modified Vγ9vδ2 T cells with enhanced antigen-specific anti-tumor activity. *Am J Cancer Res*. (2021) 11:79–91.

128. Makkouk A, Yang XC, Barca T, Lucas A, Turkoz M, Wong JTS, et al. Off-the-shelf Vδ1 gamma delta T cells engineered with glypican-3 (Gpc-3)-specific chimeric antigen receptor (Car) and soluble il-15 display robust antitumor efficacy against

hepatocellular carcinoma. *J Immunother Cancer*. (2021) 9:e003441. doi: 10.1136/jitc-2021-003441

129. Fleischer LC, Becker SA, Ryan RE, Fedanov A, Doering CB, Spencer HT. Non-signaling chimeric antigen receptors enhance antigen-directed killing by Γδ T cells in contrast to αβ T cells. *Mol Ther Oncolytics*. (2020) 18:149–60. doi: 10.1016/j.omto.2020.06.003

130. Fisher J, Abramowski P, Wisidagamage Don ND, Flutter B, Capsomidis A, Cheung GW-K, et al. Avoidance of on-target off-tumor activation using a co-stimulation-only chimeric antigen receptor. *Mol Ther*. (2017) 25:1234–47. doi: 10.1016/j.ymthe.2017.03.002

131. Zhang X, Ang WX, Du Z, Ng YY, Zha S, Chen C, et al. A cd123-specific chimeric antigen receptor augments anti-acute myeloid leukemia activity of Vγ9vδ2 T cells. *Immunotherapy*. (2022) 14:321–36. doi: 10.2217/imt-2021-0143

132. de Weerdt I, Lameris R, Scheffer GL, Vree J, de Boer R, Stam AG, et al. A bispecific antibody antagonizes prosurvival cd40 signaling and promotes Vγ9vδ2 T cell–mediated antitumor responses in human B-cell Malignancies. *Cancer Immunol Res*. (2021) 9:50–61. doi: 10.1158/2326-6066.Cir-20-0138

133. de Weerdt I, Lameris R, Ruben JM, de Boer R, Kloosterman J, King LA, et al. A bispecific single-domain antibody boosts autologous Vγ9vδ2-T cell responses toward cd1d in chronic lymphocytic leukemia. *Clin Cancer Res*. (2021) 27:1744–55. doi: 10.1158/1078-0432.Ccr-20-4576

134. Yang R, He Q, Zhou H, Gong C, Wang X, Song X, et al. Vγ2 X pd-L1, a bispecific antibody targeting both the Vγ2 tcr and pd-L1, improves the anti-tumor response of Vγ2vδ2 T cell. *Front Immunol*. (2022) 13:923969. doi: 10.3389/fimmu.2022.923969

135. Oberg H-H, Peipp M, Kellner C, Sebens S, Krause S, Petrick D, et al. Novel bispecific antibodies increase Γδ T-cell cytotoxicity against pancreatic cancer cells. *Cancer Res*. (2014) 74:1349–60. doi: 10.1158/0008-5472.Can-13-0675

136. Ganesan R, Chennupati V, Ramachandran B, Hansen MR, Singh S, Grewal IS. Selective recruitment of Γδ T cells by a bispecific antibody for the treatment of acute myeloid leukemia. *Leukemia*. (2021) 35:2274–84. doi: 10.1038/s41375-021-01122-7

137. King LA, Toffoli EC, Veth M, Iglesias-Guimarais V, Slot MC, Amsen D, et al. A bispecific Γδ T-cell engager targeting egfr activates a potent Vγ9vδ2 T cell-mediated immune response against egfr-expressing tumors. *Cancer Immunol Res*. (2023) 11 (9):1237–52. doi: 10.1158/2326-6066.Cir-23-0189

138. Hiasa A, Nishikawa H, Hirayama M, Kitano S, Okamoto S, Chono H, et al. Rapid αβ Tcr-mediated responses in Γδ T cells transduced with cancer-specific tcr genes. *Gene Ther*. (2009) 16:620–8. doi: 10.1038/gt.2009.6

139. van der Veken LT, Hagedoorn RS, van Loenen MM, Willemze R, Falkenburg JHF, Heemskerk MHM. αβ T-cell receptor engineered Γδ T cells mediate effective antileukemic reactivity. *Cancer Res*. (2006) 66:3331–7. doi: 10.1158/0008-5472.Can-05-4190

140. Ishihara M, Miwa H, Fujiwara H, Akahori Y, Kato T, Tanaka Y, et al. αβ-T cell receptor transduction gives superior mitochondrial function to Γδ-T cells with promising persistence. *iScience*. (2023) 26:107802. doi: 10.1016/j.isci.2023.107802

141. Legut M, Dolton G, Mian AA, Ottmann OG, Sewell AK. Crispr-mediated tcr replacement generates superior anticancer transgenic T cells. *Blood*. (2018) 131:311–22. doi: 10.1182/blood-2017-05-787598

142. Ichiki Y, Shigematsu Y, Baba T, Shiota H, Fukuyama T, Nagata Y, et al. Development of adoptive immunotherapy with kk-lc-1-specific tcr-transduced Γδt cells against lung cancer cells. *Cancer Sci*. (2020) 111:4021–30. doi: 10.1111/cas.14612

143. Shimizu K, Shinga J, Yamasaki S, Kawamura M, Dörrie J, Schaft N, et al. Transfer of mrna encoding invariant nkt cell receptors imparts glycolipid specific responses to T cells and Γδt cells. *PloS One*. (2015) 10:e0131477. doi: 10.1371/journal.pone.0131477

144. Neelapu SS, Hamadani M, Miklos DB, Holmes H, Hinkle J, Kennedy-Wilde J, et al. A phase 1 study of adi-001: anti-cd20 car-engineered allogeneic gamma delta (Γδ) T cells in adults with B-cell Malignancies. *J Clin Oncol*. (2022) 40:7509–. doi: 10.1200/JCO.2022.40.16_suppl.7509

145. Broijl A, Donk N, Bosch F, Mateos M-V, Rodríguez-Otero P, Tucci A, et al. Phase I dose escalation of lava-051, a novel bispecific gamma-delta T-cell engager (Gammabody), in relapsed/refractory hematological Malignancies. *J Clin Oncol*. (2022) 40:2577–. doi: 10.1200/JCO.2022.40.16_suppl.2577

146. Mehra N, Robbrecht D, Voortman J, Parren PWHI, Macia S, Veeneman J, et al. Early dose escalation of lava-1207, a novel bispecific gamma-delta T-cell engager (Gammabody), in patients with metastatic castration-resistant prostate cancer (Mcrpc). *J Clin Oncol*. (2023) 41:153–. doi: 10.1200/JCO.2023.41.6_suppl.153

147. He P, Liu H, Zimdahl B, Wang J, Luo M, Chang Q, et al. A novel antibody-tcr (Abtcr) T-cell therapy is safe and effective against cd19-positive relapsed/refractory B-cell lymphoma. *J Cancer Res Clin Oncol*. (2023) 149:2757–69. doi: 10.1007/s00432-022-04132-9

148. Li H-K, Wu T-S, Kuo Y-C, Hsiao C-W, Yang H-P, Lee C-Y, et al. 251 application of antibody-cell conjugation technology in a novel off-the-shelf cd20-targeting gamma delta T cell therapy ace1831. *J ImmunoTher Cancer*. (2022) 10:A266–A. doi: 10.1136/jitc-2022-SITC2022.0251

149. Nabors LB, Lamb LS, Beelen MJ, Pillay T, Haak MT, Youngblood S, et al. Phase 1 trial of drug resistant immunotherapy: A first-in-class combination of mgmt-modified Γδ T cells and temozolomide chemotherapy in newly diagnosed glioblastoma. *J Clin Oncol*. (2021) 39:2057–. doi: 10.1200/JCO.2021.39.15_suppl.2057

150. Sterner RC, Sterner RM. Car-T cell therapy: current limitations and potential strategies. *Blood Cancer J*. (2021) 11:69. doi: 10.1038/s41408-021-00459-7

151. Frieling JS, Tordesillas L, Bustos XE, Ramello MC, Bishop RT, Cianne JE, et al. Γδ-enriched car-T cell therapy for bone metastatic castrate-resistant prostate cancer. *Sci Adv*. (2023) 9:eadf0108. doi: 10.1126/sciadv.adf0108

152. June CH, Sadelain M. Chimeric antigen receptor therapy. *New Engl J Med*. (2018) 379:64–73. doi: 10.1056/NEJMra1706169

153. Shah NN, Lee DW, Yates B, Yuan CM, Shalabi H, Martin S, et al. Long-term follow-up of cd19-car T-cell therapy in children and young adults with B-all. *J Clin Oncol*. (2021) 39:1650–9. doi: 10.1200/jco.20.02262

154. Becker SA, Petrich BG, Yu B, Knight KA, Brown HC, Raikar SS, et al. Enhancing the Effectiveness of Γδ T cells by Mrna Transfection of Chimeric Antigen Receptors or Bispecific T cell Engagers. *Mol Ther Oncolytics*. (2023) 29:145–57. doi: 10.1016/j.omto.2023.05.007

155. Rischer M, Pscherer S, Duwe S, Vormoor J, Jürgens H, Rossig C. Human Γδ T cells as mediators of chimaeric-receptor redirected anti-tumour immunity. *Br J Haematol*. (2004) 126:583–92. doi: 10.1111/j.1365-2141.2004.05077.x

156. Cummins KD, Frey N, Nelson AM, Schmidt A, Luger S, Isaacs RE, et al. Treating relapsed/refractory (Rr) aml with biodegradable anti-cd123 car modified T cells. *Blood*. (2017) 130:1359–. doi: 10.1182/blood.V130.Suppl_1.1359.1359

157. Wang Y, Ji N, Zhang Y, Chu J, Pan C, Zhang P, et al. B7h3-targeting chimeric antigen receptor modification enhances antitumor effect of Vγ9vδ2 T cells in glioblastoma. *J Trans Med*. (2023) 21:672. doi: 10.1186/s12967-023-04514-8

158. Fedorov VD, Themeli M, Sadelain M. Pd-1- and ctla-4-based inhibitory chimeric antigen receptors (Icars) divert off-target immunotherapy responses. *Sci Transl Med*. (2013) 5:215ra172. doi: 10.1126/scitranslmed.3006597

159. Helsen CW, Hammill JA, Lau VWC, Mwawasi KA, Afsahi A, Bezverbnaya K, et al. The chimeric tac receptor co-opts the T cell receptor yielding robust anti-tumor activity without toxicity. *Nat Commun*. (2018) 9:3049. doi: 10.1038/s41467-018-05395-y

160. Asbury S, Yoo SM, Bramson J. 101 engineering gamma/delta T cells with the T-cell antigen coupler receptor effectively induces antigen-specific tumor cytotoxicity in vitro and in vivo. *J ImmunoTher Cancer*. (2020) 8:A63–A4. doi: 10.1136/jitc-2020-SITC2020.0101

161. Hirabayashi K, Du H, Xu Y, Shou P, Zhou X, Fucá G, et al. Dual-targeting car-T cells with optimal co-stimulation and metabolic fitness enhance antitumor activity and prevent escape in solid tumors. *Nat Cancer*. (2021) 2:904–18. doi: 10.1038/s43018-021-00244-2

162. Han X, Bryson PD, Zhao Y, Cinay GE, Li S, Guo Y, et al. Masked chimeric antigen receptor for tumor-specific activation. *Mol Ther*. (2017) 25:274–84. doi: 10.1016/j.ymthe.2016.10.011

163. Zhang C, Liu J, Zhong JF, Zhang X. Engineering car-T cells. *biomark Res*. (2017) 5:22. doi: 10.1186/s40364-017-0102-y

164. Fisher J, Sharma R, Don DW, Barisa M, Hurtado MO, Abramowski P, et al. Engineering Γδt cells limits tonic signaling associated with chimeric antigen receptors. *Sci Signaling*. (2019) 12:eaax1872. doi: 10.1126/scisignal.aax1872

165. Jonus HC, Lee JY, Silva JA, Spencer HT, Goldsmith KC. Abstract 4093: dual targeted car immunotherapy for neuroblastoma using Γδ T cells. *Cancer Res*. (2023) 83:4093–. doi: 10.1158/1538-7445.Am2023-4093

166. Zah E, Lin MY, Silva-Benedict A, Jensen MC, Chen YY. T cells expressing cd19/cd20 bispecific chimeric antigen receptors prevent antigen escape by Malignant B cells. *Cancer Immunol Res*. (2016) 4:498–508. doi: 10.1158/2326-6066.Cir-15-0231

167. Supimon K, Sangsuwannukul T, Sujjitjoon J, Chieochansin T, Junking M, Yenchitsomanus P-t. Cytotoxic activity of anti-mucin 1 chimeric antigen receptor T cells expressing pd-1-cd28 switch receptor against cholangiocarcinoma cells. *Cytotherapy*. (2023) 25:148–61. doi: 10.1016/j.jcyt.2022.10.006

168. Liao Q, Mao Y, He H, Ding X, Zhang X, Xu J. Pd-L1 chimeric costimulatory receptor improves the efficacy of car-T cells for pd-L1-positive solid tumors and reduces toxicity in vivo. *biomark Res*. (2020) 8:57. doi: 10.1186/s40364-020-00237-w

169. Roybal Kole T, Rupp Levi J, Morsut L, Walker Whitney J, McNally Krista A, Park Jason S, et al. Precision tumor recognition by T cells with combinatorial antigen-sensing circuits. *Cell*. (2016) 164:770–9. doi: 10.1016/j.cell.2016.01.011

170. Moretti A, Ponzo M, Nicolette CA, Tcherepanova IY, Biondi A, Magnani CF. The past, present, and future of non-viral car T cells. *Front Immunol*. (2022) 13:867013. doi: 10.3389/fimmu.2022.867013

171. Scholler J, Brady TL, Binder-Scholl G, Hwang W-T, Plesa G, Hege KM, et al. Decade-long safety and function of retroviral-modified chimeric antigen receptor T cells. *Sci Trans Med*. (2012) 4:132ra53–ra53. doi: 10.1126/scitranslmed.3003761

172. Fisher J, Anderson J. Engineering approaches in human gamma delta T cells for cancer immunotherapy. *Front Immunol*. (2018) 9:1409. doi: 10.3389/fimmu.2018.01409

173. Anderson J, Barisa M. Enhancing the Effectiveness of Γδ T cells by Mrna Transfection of Chimeric Antigen Receptors or Bispecific T cell Engagers. *Mol Ther Oncolytics*. (2023) 30:151–2. doi: 10.1016/j.omto.2023.08.003

174. Deniger DC, Switzer K, Mi T, Maiti S, Hurton L, Singh H, et al. Bispecific T-cells expressing polyclonal repertoire of endogenous Γδ T-cell receptors and introduced cd19-specific chimeric antigen receptor. *Mol Ther*. (2013) 21:638–47. doi: 10.1038/mt.2012.267

175. Harrer DC, Simon B, Fujii S-i, Shimizu K, Uslu U, Schuler G, et al. Rna-transfection of Γ/Δ T cells with a chimeric antigen receptor or an α/β T-cell receptor: A safer alternative to genetically engineered α/β T cells for the immunotherapy of melanoma. *BMC Cancer*. (2017) 17:551. doi: 10.1186/s12885-017-3539-3

176. Lameris R, Ruben JM, Iglesias-Guimarais V, de Jong M, Veth M, van de Bovenkamp FS, et al. A bispecific T cell engager recruits both type 1 nkt and Vγ9vδ2-T cells for the treatment of cd1d-expressing hematological Malignancies. *Cell Rep Med*. (2023) 4:100961. doi: 10.1016/j.xcrm.2023.100961

177. Goebeler M-E, Bargou RC. T cell-engaging therapies — Bites and beyond. *Nat Rev Clin Oncol*. (2020) 17:418–34. doi: 10.1038/s41571-020-0347-5

178. Lai AY, Patel A, Brewer F, Evans K, Johannes K, González LE, et al. Cutting edge: bispecific Γδ T cell engager containing heterodimeric btn2a1 and btn3a1 promotes targeted activation of Vγ9vδ2(+) T cells in the presence of costimulation by cd28 or nkg2d. *J Immunol*. (2022) 209:1475–80. doi: 10.4049/jimmunol.2200185

179. Arbabi-Ghahroudi M. Camelid single-domain antibodies: historical perspective and future outlook. *Front Immunol*. (2017) 8:1589. doi: 10.3389/fimmu.2017.01589

180. Nathan P, Hassel JC, Rutkowski P, Baurain JF, Butler MO, Schlaak M, et al. Overall survival benefit with tebentafusp in metastatic uveal melanoma. *N Engl J Med*. (2021) 385:1196–206. doi: 10.1056/NEJMoa2103485

181. Ma J, Mo Y, Tang M, Shen J, Qi Y, Zhao W, et al. Bispecific antibodies: from research to clinical application. *Front Immunol*. (2021) 12:626616. doi: 10.3389/fimmu.2021.626616

182. De Gassart A, Le K-S, Brune P, Agaugué S, Sims J, Goubard A, et al. Development of ict01, a first-in-class, anti-btn3a antibody for activating Vγ9vδ2 T cell–mediated antitumor immune response. *Sci Trans Med*. (2021) 13:eabj0835. doi: 10.1126/scitranslmed.abj0835

183. Li H-K, Wu T-S, Leng P-R, Kuo Y-C, Cheng Z-F, Lee C-Y, et al. Abstract lb089: ace2016: an off-the-shelf egfr-targeting Γδ2 T cell therapy against egfr-expressing solid tumors. *Cancer Res*. (2023) 83:LB089–LB. doi: 10.1158/1538-7445.Am2023-lb089

184. van der Veken LT, Coccoris M, Swart E, Falkenburg JHF, Schumacher TN, Heemskerk MHM. αβ T cell receptor transfer to Γδ T cells generates functional effector cells without mixed tcr dimers in vivo1. *J Immunol*. (2009) 182:164–70. doi: 10.4049/jimmunol.182.1.164

185. Drent E, Bisso A, Baardman S, Verweij D, Salcedo E, Coomans C, et al. Abstract 2818: targeting solid tumors with gdt002, a first-in-class Γδtcr-based T cell therapy. *Cancer Res*. (2022) 82:2818–. doi: 10.1158/1538-7445.Am2022-2818

186. Chen Z, Lin C, Pei H, Yuan X, Xu J, Zou M, et al. Antibody-based binding domain fused to tcrγ Chain facilitates T cell cytotoxicity for potent anti-tumor response. *Oncogenesis*. (2023) 12:33. doi: 10.1038/s41389-023-00480-4

187. Xu Y, Yang Z, Horan LH, Zhang P, Liu L, Zimdahl B, et al. A novel antibody-tcr (Abtcr) platform combines fab-based antigen recognition with gamma/delta-tcr signaling to facilitate T-cell cytotoxicity with low cytokine release. *Cell Discovery*. (2018) 4:62. doi: 10.1038/s41421-018-0066-6

188. Li C, Zhou F, Wang J, Chang Q, Du M, Luo W, et al. Novel cd19-specific Γ/Δ Tcr-T cells in relapsed or refractory diffuse large B-cell lymphoma. *J Hematol Oncol*. (2023) 16:5. doi: 10.1186/s13045-023-01402-y

189. Moon EK, Wang LC, Dolfi DV, Wilson CB, Ranganathan R, Sun J, et al. Multifactorial T-cell hypofunction that is reversible can limit the efficacy of chimeric antigen receptor-transduced human T cells in solid tumors. *Clin Cancer Res*. (2014) 20:4262–73. doi: 10.1158/1078-0432.Ccr-13-2627

190. Menon H, Chen D, Ramapriyan R, Verma V, Barsoumian HB, Cushman TR, et al. Influence of low-dose radiation on abscopal responses in patients receiving high-dose radiation and immunotherapy. *J Immunother Cancer*. (2019) 7:237. doi: 10.1186/s40425-019-0718-6

191. Lu L, Zhan M, Li XY, Zhang H, Dauphars DJ, Jiang J, et al. Clinically approved combination immunotherapy: current status, limitations, and future perspective. *Curr Res Immunol*. (2022) 3:118–27. doi: 10.1016/j.crimmu.2022.05.003

192. Park JH, Lee HK. Function of gammadelta T cells in tumor immunology and their application to cancer therapy. *Exp Mol Med*. (2021) 53:318–27. doi: 10.1038/s12276-021-00576-0

193. Lino CA, Harper JC, Carney JP, Timlin JA. Delivering crispr: A review of the challenges and approaches. *Drug Delivery*. (2018) 25:1234–57. doi: 10.1080/10717544.2018.1474964

194. Zhang P, Zhang G, Wan X. Challenges and new technologies in adoptive cell therapy. *J Hematol Oncol*. (2023) 16:97. doi: 10.1186/s13045-023-01492-8

195. Wang RN, Wen Q, He WT, Yang JH, Zhou CY, Xiong WJ, et al. Optimized protocols for Γδ T cell expansion and lentiviral transduction. *Mol Med Rep*. (2019) 19:1471–80. doi: 10.3892/mmr.2019.9831

196. Gustafsson K, Herrmann T, Dieli F. Editorial: understanding gamma delta T cell multifunctionality - towards immunotherapeutic applications. *Front Immunol*. (2020) 11:921. doi: 10.3389/fimmu.2020.00921

197. Hamieh M, Dobrin A, Cabriolu A, van der Stegen SJC, Giavridis T, Mansilla-Soto J, et al. Car T cell trogocytosis and cooperative killing regulate tumour antigen escape. *Nature*. (2019) 568:112–6. doi: 10.1038/s41586-019-1054-1

198. Huang SW, Pan CM, Lin YC, Chen MC, Chen Y, Jan CI, et al. Bite-secreting car-gammadeltat as a dual targeting strategy for the treatment of solid tumors. *Adv Sci (Weinh)*. (2023) 10:e2206856. doi: 10.1002/advs.202206856

199. Jin C, Lagoudas GK, Zhao C, Bullman S, Bhutkar A, Hu B, et al. Commensal microbiota promote lung cancer development via gammadelta T cells. *Cell*. (2019) 176:998–1013 e16. doi: 10.1016/j.cell.2018.12.040

200. Coffelt SB, Kersten K, Doornebal CW, Weiden J, Vrijland K, Hau CS, et al. Il-17-producing gammadelta T cells and neutrophils conspire to promote breast cancer metastasis. *Nature*. (2015) 522:345–8. doi: 10.1038/nature14282

201. Lopes N, McIntyre C, Martin S, Raverdeau M, Sumaria N, Kohlgruber AC, et al. Distinct metabolic programs established in the thymus control effector functions of gammadelta T cell subsets in tumor microenvironments. *Nat Immunol*. (2021) 22:179–92. doi: 10.1038/s41590-020-00848-3

202. Wu P, Wu D, Ni C, Ye J, Chen W, Hu G, et al. Gammadeltat17 cells promote the accumulation and expansion of myeloid-derived suppressor cells in human colorectal cancer. *Immunity*. (2014) 40:785–800. doi: 10.1016/j.immuni.2014.03.013

203. Ganapathy T, Radhakrishnan R, Sakshi S, Martin S. Car gammadelta T cells for cancer immunotherapy. Is the field more yellow than green? *Cancer Immunol Immunother*. (2023) 72:277–86. doi: 10.1007/s00262-022-03260-y

204. Burnham RE, Zoine JT, Story JY, Garimalla SN, Gibson G, Rae A, et al. Characterization of donor variability for Γδ T cell ex vivo expansion and development of an allogeneic Γδ T cell immunotherapy. *Front Med*. (2020) 7:588453. doi: 10.3389/fmed.2020.588453

Frontiers in Immunology

Explores novel approaches and diagnoses to treat immune disorders.

The official journal of the International Union of Immunological Societies (IUIS) and the most cited in its field, leading the way for research across basic, translational and clinical immunology.

Discover the latest Research Topics

See more →

Frontiers

Avenue du Tribunal-Fédéral 34
1005 Lausanne, Switzerland
frontiersin.org

Contact us

+41 (0)21 510 17 00
frontiersin.org/about/contact